frontiers | Research Topics

Integrative pharmacological approaches for regenerating cartilage and bone tissue

Edited by
Jie Fang, Lufei Wang, Wen Liao, Yoshitomo Honda and Yoshiya Hashimoto

Published in
Frontiers in Pharmacology

ISSN 1664-8714
ISBN 978-2-8325-7271-9
DOI 10.3389/978-2-8325-7271-9

Generative AI statement
Any alternative text (Alt text) provided alongside figures in the articles in this ebook has been generated by Frontiers with the support of artificial intelligence and reasonable efforts have been made to ensure accuracy, including review by the authors wherever possible. If you identify any issues, please contact us.

About Frontiers

Frontiers is more than just an open access publisher of scholarly articles: it is a pioneering approach to the world of academia, radically improving the way scholarly research is managed. The grand vision of Frontiers is a world where all people have an equal opportunity to seek, share and generate knowledge. Frontiers provides immediate and permanent online open access to all its publications, but this alone is not enough to realize our grand goals.

Frontiers journal series

The Frontiers journal series is a multi-tier and interdisciplinary set of open-access, online journals, promising a paradigm shift from the current review, selection and dissemination processes in academic publishing. All Frontiers journals are driven by researchers for researchers; therefore, they constitute a service to the scholarly community. At the same time, the *Frontiers journal series* operates on a revolutionary invention, the tiered publishing system, initially addressing specific communities of scholars, and gradually climbing up to broader public understanding, thus serving the interests of the lay society, too.

Dedication to quality

Each Frontiers article is a landmark of the highest quality, thanks to genuinely collaborative interactions between authors and review editors, who include some of the world's best academicians. Research must be certified by peers before entering a stream of knowledge that may eventually reach the public - and shape society; therefore, Frontiers only applies the most rigorous and unbiased reviews. Frontiers revolutionizes research publishing by freely delivering the most outstanding research, evaluated with no bias from both the academic and social point of view. By applying the most advanced information technologies, Frontiers is catapulting scholarly publishing into a new generation.

What are Frontiers Research Topics?

Frontiers Research Topics are very popular trademarks of the *Frontiers journals series*: they are collections of at least ten articles, all centered on a particular subject. With their unique mix of varied contributions from Original Research to Review Articles, Frontiers Research Topics unify the most influential researchers, the latest key findings and historical advances in a hot research area.

Find out more on how to host your own Frontiers Research Topic or contribute to one as an author by contacting the Frontiers editorial office: frontiersin.org/about/contact

Integrative pharmacological approaches for regenerating cartilage and bone tissue

Topic editors

Jie Fang — Sichuan University, China
Lufei Wang — Guangxi Medical University, China
Wen Liao — Sichuan University, China
Yoshitomo Honda — Osaka Dental University, Japan
Yoshiya Hashimoto — Osaka Dental University, Japan

Citation

Fang, J., Wang, L., Liao, W., Honda, Y., Hashimoto, Y., eds. (2025). *Integrative pharmacological approaches for regenerating cartilage and bone tissue*. Lausanne: Frontiers Media SA. doi: 10.3389/978-2-8325-7271-9

Table of contents

frontiers | Frontiers in Pharmacology

TYPE Editorial
PUBLISHED 30 April 2025
DOI 10.3389/fphar.2025.1613512

OPEN ACCESS

EDITED AND REVIEWED BY
Heike Wulff,
University of California, Davis, United States

*CORRESPONDENCE
Lufei Wang,
wlfdentist@outlook.com

RECEIVED 17 April 2025
ACCEPTED 18 April 2025
PUBLISHED 30 April 2025

CITATION
Tan J, Fang J, Liao W and Wang L (2025) Editorial: Integrative pharmacological approaches for regenerating cartilage and bone tissue.
Front. Pharmacol. 16:1613512.
doi: 10.3389/fphar.2025.1613512

Editorial: Integrative pharmacological approaches for regenerating cartilage and bone tissue

Jiahui Tan[1], Jie Fang[2], Wen Liao[2] and Lufei Wang[1]*

[1]Guangxi Key Laboratory of Oral and Maxillofacial Rehabilitation and Reconstruction & College and Hospital of Stomatology, Guangxi Medical University, Nanning, China, [2]State Key Laboratory of Oral Diseases and National Clinical Research Center for Oral Diseases, West China Hospital of Stomatology, Sichuan University, Chengdu, China

KEYWORDS

bone regeneration, cartilage regeneration, pharmacological interventions, biomaterials, stem cell therapy

Editorial on the Research Topic
Integrative pharmacological approaches for regenerating cartilage and bone tissue

Introduction

The destruction of cartilage and bone tissue—whether due to injury, degeneration, or disease—presents a significant clinical challenge that can severely impact mobility, function, and overall quality of life (Guo et al., 2023; Diaz-Solano et al., 2024). Conditions such as osteoarthritis (OA), osteoporosis, and fractures pose formidable obstacles due to the inherent limitations in the self-repair mechanisms of these tissues. Cartilage, being avascular, has a limited capacity for nutrient delivery and immune cell mobilization, which significantly diminishes its regenerative potential. While bone tissue is more metabolically active, its integration with surrounding tissues may be compromised by limited vascularization and slow healing.

To address these challenges, researchers have increasingly turned to integrative pharmacological approaches that include bioactive agents, growth factors, and stem cells to boost tissue regeneration (Adamička et al., 2021; Liao et al., 2024). These strategies aim to enhance healing by stimulating cellular activity, promoting repair, and improving tissue integration. Additionally, advances in tissue engineering and 3D printing are helping to create scaffolds and implants that support the regeneration of cartilage and bone (Gugliandolo et al., 2021; Wang et al., 2024). These developments offer promising avenues for more effective treatment options.

This Research Topic on "Integrative Pharmacological Approaches for Regenerating Cartilage and Bone Tissue" features 10 impactful studies, which consist of 4 original research articles, 3 critical reviews, 2 bibliometric analyses, and 1 meta-analysis, providing a comprehensive overview of diverse therapeutic strategies for regenerating cartilage or bone

tissue. The contributions cover pharmacological interventions, innovative biomaterials, and advancements in stem cell therapy.

Pathogenesis and treatment of osteoarthritis

Four studies within this topic focus on osteoarthritis (OA). Gao et al. demonstrated that age-related endoplasmic reticulum stress triggers YAP overexpression, which in turn leads to chondrocyte phenotype loss and OA progression. Their findings further revealed that treatment with pamrevlumab can alleviate these deleterious effects in cartilage-specific YAP overexpression transgenic mice, suggesting the therapeutic potential of targeting the endoplasmic reticulum stress–YAP–CTGF signaling pathway.

In another study, a bibliometric analysis conducted by Zhang et al. highlighted the growing importance of extracellular vesicles in OA research. The analysis revealed significant contributions from China, the United States of America, and Italy. The most frequently occurring keywords were "exosome," "expression," "knee OA," "extracellular vesicle," "mesenchymal stem cell," and "inflammation." These insights point toward the potential of extracellular vesicles as novel agents for OA treatment.

Liu et al. comprehensively summarized the roles of metal-organic frameworks (MOFs) as drug carriers and therapeutic agents in OA management and bone regeneration. The controlled drug release properties and tissue engineering capabilities of MOFs present long-term benefits, offering a new dimension in managing OA.

Hyaluronic acid (HA) intraarticular injection is a treatment used worldwide for knee OA. Tranexamic acid (TXA), a plasminogen activator inhibitor, inhibits fibrinolysis and matrix metalloproteases, which are key players in OA pathophysiology. According to Brochard et al., in a monosodium iodoacetate-induced murine model of knee OA, a single intraarticular injection of HA/TXA conjugate was shown to alleviate pain, slow OA progression, and provide chondroprotective effects—demonstrating its superiority over HA alone.

Novel biomaterials for bone regeneration

Li et al. introduced a functionally graded bilayer membrane composed of poly (lactic-co-glycolic acid), nano-hydroxyapatite, and gelatin, developed by combining phase inversion with electrospinning techniques. This novel membrane not only provides enhanced barrier function and mechanical properties but also exhibits pronounced osteogenic bioactivity in both *in vitro* and *in vivo* models, offering fresh insights into barrier membrane fabrication for guided bone regeneration.

Another bibliometric study by Zhang et al. investigated research trends related to bioprinted hydrogels for bone regeneration. The findings reveal a rapidly growing field, with a strong emphasis on 3D printing technologies, scaffolds, and hydrogels. China emerged as the leader in terms of publication output, and future research appears to be oriented toward the utilization of gelatin, additive manufacturing techniques, and growth factors.

Yang et al. reviewed the properties of stimuli-responsive biomaterials, which can alter their mechanical characteristics, shape, or drug release profile in response to external or internal triggers. These materials have become increasingly significant in bone regeneration applications, representing a transformative approach to biomedical engineering that holds promise for future clinical innovations.

Cell therapy in regenerative medicine

Liu et al. reviewed the effects of metformin—a widely used anti-diabetic drug—on mesenchymal stem cells (MSCs). The drug was found to promote MSC proliferation, differentiation, and resistance to aging, suggesting that metformin could enhance the therapeutic potential of MSCs in various regenerative contexts. This study highlights the pivotal role of cell therapy in the field of regenerative medicine.

In a comparative study, Li et al. evaluated MSCs derived from dental pulp, adipose tissue, placental amniotic membrane, and umbilical cord in an ovariectomy-induced mouse model of osteoporosis. The results indicated that dental pulp-derived MSCs not only maintained trabecular bone mass more efficiently but also exhibited superior immunoregulatory properties. These findings support the use of dental pulp-derived MSCs as the optimal cell source for cell therapy in postmenopausal osteoporosis.

Core decompression (CD) is a surgical operation commonly used for osteonecrosis of the femoral head (ONFH). Tang et al. contributed a meta-analysis that examined the combination of CD with regenerative therapies, such as bone marrow aspirate concentrate and bone-derived MSCs, in managing ONFH. Their analysis revealed that combining CD with regenerative approaches resulted in better outcomes for pain reduction and functional improvement compared to CD alone.

Conclusion

This Research Topic of studies highlights emerging strategies in cartilage and bone regeneration, emphasizing novel biomaterials, stem cell therapies, and pharmacological interventions. These integrative approaches offer new avenues for improving therapeutic outcomes in osteoarthritis, osteoporosis, and bone defects, paving the way for future research and clinical applications. Strengthening interdisciplinary collaboration and clinical trials will be essential in translating these innovations into effective therapies, ultimately enhancing patient quality of life.

Author contributions

JT: Writing – original draft, Writing – review and editing. JF: Writing – review and editing. WL: Writing – review and editing. LW: Writing – review and editing.

Funding

The author(s) declare that financial support was received for the research and/or publication of this article. This work was supported by National Natural Science Foundation of China (No. 82360191); Joint Project on Regional High-Incidence Diseases Research of Guangxi Natural Science Foundation (No. 2023GXNSFBA026125); First-class discipline innovation-driven talent program of Guangxi Medical University.

Conflict of interest

The authors declare that the research was conducted in the absence of any commercial or financial relationships that could be construed as a potential conflict of interest.

Generative AI statement

The authors declare that Generative AI was used in the creation of this manuscript. The authors declare that Generative AI was used in the creation of this manuscript for refining language.

Publisher's note

References

Adamička, M., Adamičková, A., Danišovič, L., Gažová, A., and Kyselovič, J. (2021). Pharmacological approaches and regeneration of bone defects with dental pulp stem cells. *Stem Cells Int.* 2021, 4593322. doi:10.1155/2021/4593322

Diaz-Solano, D., Sadri, B., Peshkova, M., Shpichka, A., Smirnova, O., Shams, R., et al. (2024). Advanced therapeutic medicinal products in bone and cartilage defects. *Curr. Rev. Clin. Exp. Pharmacol.* 19, 355–369. doi:10.2174/0127724328274436231207062008

Gugliandolo, A., Fonticoli, L., Trubiani, O., Rajan, T. S., Marconi, G. D., Bramanti, P., et al. (2021). Oral bone tissue regeneration: mesenchymal stem cells, secretome, and biomaterials. *Int. J. Mol. Sci.* 22, 5236. doi:10.3390/ijms22105236

Guo, X., Xi, L., Yu, M., Fan, Z., Wang, W., Ju, A., et al. (2023). Regeneration of articular cartilage defects: therapeutic strategies and perspectives. *J. Tissue Eng.* 14, 20417314231164765. doi:10.1177/20417314231164765

Liao, H., Ma, H., Meng, H., Kang, N., and Wang, L. (2024). Ropinirole suppresses LPS-induced periodontal inflammation by inhibiting the NAT10 in an ac4C-dependent manner. *BMC Oral Health* 24, 510. doi:10.1186/s12903-024-04250-5

Wang, L., Hu, H., and Ko, C.-C. (2024). Osteoclast-driven polydopamine-to-dopamine release: an upgrade patch for polydopamine-functionalized tissue engineering scaffolds. *J. Funct. Biomater* 15, 211. doi:10.3390/jfb15080211

frontiers | Frontiers in Pharmacology

TYPE Original Research
PUBLISHED 27 March 2024
DOI 10.3389/fphar.2024.1349199

OPEN ACCESS

EDITED BY
Rain L. Wong,
University of North Carolina at Chapel Hill, United States

REVIEWED BY
Zhi Hui Wang,
Shandong First Medical University, China
Haisen Huang,
Sichuan University, China

*CORRESPONDENCE
Yuling Zuo,
zuoyl@cdutcm.edu.cn
Chongyang Shen,
scylc@163.com
Yichao Wang,
xiaohonghuman@163.com

†These authors have contributed equally to this work

RECEIVED 04 December 2023
ACCEPTED 18 March 2024
PUBLISHED 27 March 2024

CITATION
Li C, Liu Y, Deng M, Li J, Li S, Li X, Zuo Y, Shen C and Wang Y (2024), Comparison of the therapeutic effects of mesenchymal stem cells derived from human dental pulp (DP), adipose tissue (AD), placental amniotic membrane (PM), and umbilical cord (UC) on postmenopausal osteoporosis.
Front. Pharmacol. 15:1349199.
doi: 10.3389/fphar.2024.1349199

Comparison of the therapeutic effects of mesenchymal stem cells derived from human dental pulp (DP), adipose tissue (AD), placental amniotic membrane (PM), and umbilical cord (UC) on postmenopausal osteoporosis

Chuncai Li[1,2†], Yincong Liu[1†], Mingxing Deng[1], Jun Li[3], Shengqi Li[3], Xiaoyu Li[1], Yuling Zuo[1,2*], Chongyang Shen[1*] and Yichao Wang[4*]

[1]Stem Cells Research Center, Chengdu University of Traditional Chinese Medicine, Chengdu, China, [2]TCM Hospital of Sichuan Province, Chengdu University of Traditional Chinese Medicine, Chengdu, China, [3]Sichuan Provincial Cells Tissue Bank, Chengdu, China, [4]Department of Thyroid Surgery, West China Hospital, Sichuan University, Chengdu, China

Background: Osteoporosis is a systemic bone disease characterized by bone loss and microstructural degeneration. Recent preclinical and clinical trials have further demonstrated that the transplantation of mesenchymal stem cells (MSCs) derived from human adipose tissue (AD), dental pulp (DP), placental amniotic membrane (AM), and umbilical cord (UC) tissues can serve as an effective form of cell therapy for osteoporosis. However, MSC-mediated osteoimmunology and the ability of these cells to regulate osteoclast-osteoblast differentiation varies markedly among different types of MSCs.

Methods: In this study, we investigated whether transplanted allogeneic MSCs derived from AD, DP, AM, and UC tissues were able to prevent osteoporosis in an ovariectomy (OVX)-induced mouse model of osteoporosis. The homing and immunomodulatory ability of these cells as well as their effects on osteoblastogenesis and the maintenance of bone formation were compared for four types of MSCs to determine the ideal source of MSCs for the cell therapy-based treatment of OVX-induced osteoporosis. The bone formation and bone resorption ability of these four types of MSCs were analyzed using micro-computed tomography analyses and histological staining. In addition, cytokine array-based analyses of serological markers and bioluminescence imaging assays were employed to evaluate cell survival and homing efficiency. Immune regulation was determined by flow cytometer assay to reflect the mechanisms of osteoporosis treatment.

Conclusion: These analyses demonstrated that MSCs isolated from different tissues have the capacity to treat osteoporosis when transplanted *in vivo*. Importantly, DP-MSCs infusion was able to maintain trabecular bone mass

Abbreviations: AD, adipose tissue; DP, dental pulp; AM, amniotic membrane; UC, umbilical cord; MSCs, mesenchymal stem cells; ECM, extracellular matrix.

more efficiently with corresponding improvements in trabecular bone volume, mineral density, number, and separation. Among the tested MSC types, DP-MSCs were also found to exhibit greater immunoregulatory capabilities, regulating the Th17/Treg and M1/M2 ratios. These data thus suggest that DP-MSCs may represent an effective tool for the treatment of osteoporosis.

KEYWORDS

osteoporosis, mesenchymal stem cells, Th17/Treg, macrophage polarization, immunoregulatory activity

Introduction

Osteoporosis is characterized by the progressive loss of bone mass and skeletal microarchitecture, resulting in increased bone fragility and a higher risk of fractures (Hurley and Khosla, 1997). Women with postmenopausal osteoporosis are particularly prone to fractures, contributing to worse quality of life and imposing a substantial financial burden on affected patients. While osteoporosis is already regarded as a major public health problem in many countries (Lindsay, 1993), its incidence continues to rise with the progressive aging of the global population. It has been reported that approximately 50% of postmenopausal women worldwide are affected by osteoporosis, and the prevalence of fractures among osteoporosis patients is as high as 40% (Rachner et al., 2011). The disruption of the homeostatic balance between bone formation and bone resorption is considered to be the direct cause of osteoporosis. The relative magnitudes of bone formation and bone resorption vary at different stages of osteoporosis development, with osteoclast-mediated increases in bone resorption predominating in the early stage (Eriksen et al., 1990) whereas osteoblast-mediated reductions in bone formation are evident in the later stages (Avioli, 1976). Immunomodulation plays an important role in bone homeostasis, as the overactivation of immune responses results in the production of inflammatory cytokines that promote osteoclast differentiation and accelerate bone resorption, while also inducing osteoblast apoptosis and suppressing bone formation (Fischer and Haffner-Luntzer, 2022). Given these effects, a growing number of studies have suggested that efforts to regulate the immune system may represent a more effective means of treating osteoporosis (Yang X. et al., 2021; Wang et al., 2021).

Recently, mesenchymal stem cells (MSCs) have attracted substantial attention owing to their immunomodulatory activity and ability to undergo osteogenic differentiation such that they are thought to offer potential value as a treatment for osteoporosis (Chen et al., 2021). To date there have been many clinical trials and studies exploring the therapeutic utility of various types of MSCs in the context of osteoporosis, revealing a range of effects mediated by diverse mechanisms. Commonly used types of MSCs in these prior studies include those derived from adipose tissue (AD-MSCs), dental pulp (DP-MSCs), placental amniotic membranes (AM-MSCs), and umbilical cord tissue (UC-MSC), with these cells exhibiting varying levels of efficacy. Prior mechanistic studies have demonstrated that AD-MSCs secrete a variety of bone cell-activating factors, including hepatocyte growth factor and extracellular matrix proteins (Lee et al., 2011), while also promoting osteogenesis and inhibiting lipogenesis in osteoporotic bone marrow MSCs (BM-MSCs) through the activation of the BMP-2 and BMPR-IB signaling pathways (Ye et al., 2014). DP-MSCs attenuate bone resorption by inhibiting interferon (IFN)-γ and interleukin (IL)-17 through the enhancement of M2 macrophage polarization (Maeda et al., 2022) and promote increased bone formation by secreting RNAs that target the telomerase activity of recipient BM-MSCs (Sonoda et al., 2020). AM-MSCs can reportedly ameliorate osteoporosis by stimulating osteoclastic bone formation and inhibiting osteoclastic bone resorption (Yin et al., 2022). UC-MSC can transfer the potently pro-osteogenic CLEC11A (C-type lectin domain family 11, member A) protein to inhibit osteoclast formation and enhance the transitioning of BM-MSCs from lipogenic to osteogenic differentiation (Hu et al., 2020a). With respect to the osteogenic ability of these different cell populations, DP-MSCs have been shown to exhibit a superior osteogenic capacity but a weaker lipogenic potential than that of BM-MSCs (Kumar et al., 2018). BM-MSCs have a higher propensity for osteogenesis than AD-MSCs (Mohamed-Ahmed et al., 2018), AM-MSCs (Barlow et al., 2008), and UC-MSC (Heo et al., 2016), however invasive procedures to obtained BM-MSCs and low abundance in bone marrow (approximately 0.01%) limited its clinical application. This suggests that DP-MSCs may offer superior therapeutic efficacy in osteoporosis. However, no studies to date have compared the relative efficacy of these MSC types for the cell therapy-based treatment of osteoporosis.

To address this gap in knowledge, it is important to explore the effects of different MSC populations on osteoporotic phenotypes in order to identify the most suitable cell type for the treatment of this debilitating condition. Accordingly, this study was developed with the goal of determining which MSC type can provide the greatest benefit when used for the treatment of osteoporosis while also clarifying the key mechanisms underlying the therapeutic effects of these cells.

Materials and methods

Cell culture

Human AD-MSCs, DP-MSCs, AM-MSCs, and UC-MSC were provided by Sichuan Provincial Cells Tissue Bank. Cells were cultured in α-MEM (Invitrogen, Carlsbad, CA, USA) supplemented with 10% heat-inactivated FBS (Gibco, Carlsbad CA, USA), 2 mM L-glutamine (Gibco), 100 U/mL penicillin, and 100 μg/mL streptomycin (Gibco), in a 37°C, 5% CO_2 incubator (Sanyo, Osaka, Japan). Cell growth medium was changed every 3 days. Cells were passaged with 0.125% trypsin (Gibco) at 75%

confluence. To generate lines stably expressing luciferase, AD-MSCs, DP-MSCs, AM-MSCs, and UC-MSC were transduced with an appropriate virus (Lenti-EF1-Luc-Puro) and selected with 1 μg/mL puromycin for 2 weeks.

Osteoclast differentiation of RAW264 cells

For osteoclast induction, different kinds of MSCs and RAW264.7 cells were co-cultured in a transwell insert 6-well plates, 50 ng/mL RANKL (R&D) was added to the culture medium. TRAP staining solution was added, and incubated for 40 min at 37°C. TRAP-positive cells containing three or more nuclei were considered osteoblasts.

Animals

Eight-week-old female C57BL/6 mice were purchased from Huafukang Company (Beijing, China) and were adaptively fed for 1 week. All mice were randomly divided into six groups (n = 12 per group). Referring to previous reports (Sophocleous and Idris, 2019), mice in five groups were anesthetized via the intraperitoneal injection of sodium pentobarbital and underwent ovariectomy (OVX), while the remaining group underwent sham surgery (a small amount of fat tissue was removed from the abdominal opening, but the ovaries were not removed). These five groups of OVX mice were then subjected to different interventional conditions, including blank control treatment or treatment with AD-MSCs, DP-MSCs, AM-MSCs, or UC-MSC. At 1 week post-OVX, 1×10^6 stem cells in 200 μL of saline were injected into the corresponding cell treatment groups via the tail vein, while blank control mice were injected with an equal amount of saline. Injections once a month for 2 months. All mice were housed in the same room with access to the same food and water. These animals were maintained at 23°C (±1°C) in a facility with 50% relative humidity and a 12 h light/dark cycle. Mice were euthanized after 2 months and appropriate tissues or organs were harvested according to the experimental requirements. All animal experiments were carried out in accordance with ethical standards and approved by the Institutional Animal Care and Use Committee of Chengdu University of Traditional Chinese Medicine (IBD2023000).

Micro-computed tomography (μCT) analyses

The femurs isolated from the mice were scanned following the recommendations by the American Society for Bone and Mineral Research. Briefly, dissected mouse femurs were fixed in 4% paraformaldehyde for 48 h and analyzed by high-resolution μCT (Skyscan1276, Bruker, Belgium). The scanner was set to 85 kV and 200 μA with a resolution of 10 μm, and two-thirds of each femur was scanned. A fixed threshold of 180 was used to manually contour the trabecular bone in the region of interest. For subsequent analysis, 200–500 layers below the growth plate were defined as the region of interest (ROI). The whole trabecular bone was isolated for three-dimensional reconstruction to quantitative μCT analysis.

Histological analyses

Femurs were decalcified with 10% EDTA for 4 weeks and paraffin embedded. Femur sections were then subjected to staining with hematoxylin and eosin (H&E) and tartrate-resistant acid phosphatase (TRAP). Images were captured with a Digital triocular camera microscope (Motic, China).

Bioluminescent imaging

Ten minutes before imaging, mice were intraperitoneally injected with 10 mL/kg of fluorescein (Cat#MX4603, MK, China) and anesthetized with inhaled isoflurane. Bioluminescent images were obtained using an *In Vivo* Imaging System (IVIS) Spectrum (PerkinElmer), and image reconstruction and analysis were performed with the IVIS imaging software (PerkinElmer).

Cytokine antibody array

The Mouse Cytokine Array C2 (Raybiotech, USA) was used to evaluate murine serum protein content after 8 weeks cells injection, using the protocols provided by the manufacturer. Immunoblotting results were detected via chemiluminescence (Touch Imager XL, China), and the intensity of each spot was quantified using the ImageJ software.

Flow cytometry analysis

Flow cytometry was performed on a CytoFLEX (Beckman), and data were analyzed by FlowJo software. The live cells were observed by the Fixable Viability Stain 780 (Cat#565388, BD Pharmingen). For cell-surface staining, cells were stained with BV510 Rat Anti-Mouse CD45(Cat#563891, BD Pharmingen), FITC Hamster Anti-Mouse CD3e (Cat#553061, BD Pharmingen), PE-Cy7 Rat Anti-Mouse CD4 (Cat#552775, BD Pharmingen), BV421 Rat Anti-Mouse CD25 (Cat#562606, BD Pharmingen), FITC Rat Anti-CD11b (Cat#557396, BD Pharmingen), BV421 Rat Anti-Mouse F4/80 (Cat#565411, BD Pharmingen), PE Rat Anti-Mouse CD86(Cat#561963 BD Pharmingen), Alexa Fluor 647 Rat Anti-Mouse CD206 (Cat#565250 BD Pharmingen). For intracellular staining, cells were stained with PE Rat Anti-Mouse IL-17A (Cat#561020 BD Pharmingen), Alexa Fluor 647 Rat anti-Mouse Foxp3(Cat#560402 BD Pharmingen). According to the reagent vendor's instructions, Purified Rat Anti-Mouse CD16/CD32 is used to exclude background fluorescent signal interference, Cells fixation and permeabilization Fixation/Permeablization Kit (Cat#554714 BD Pharmingen) and Transcription Factor Buffer Set (Cat#562574 BD Pharmingen) were used for cell fixation and permeabilization.

10.3389/fphar.2024.1349199

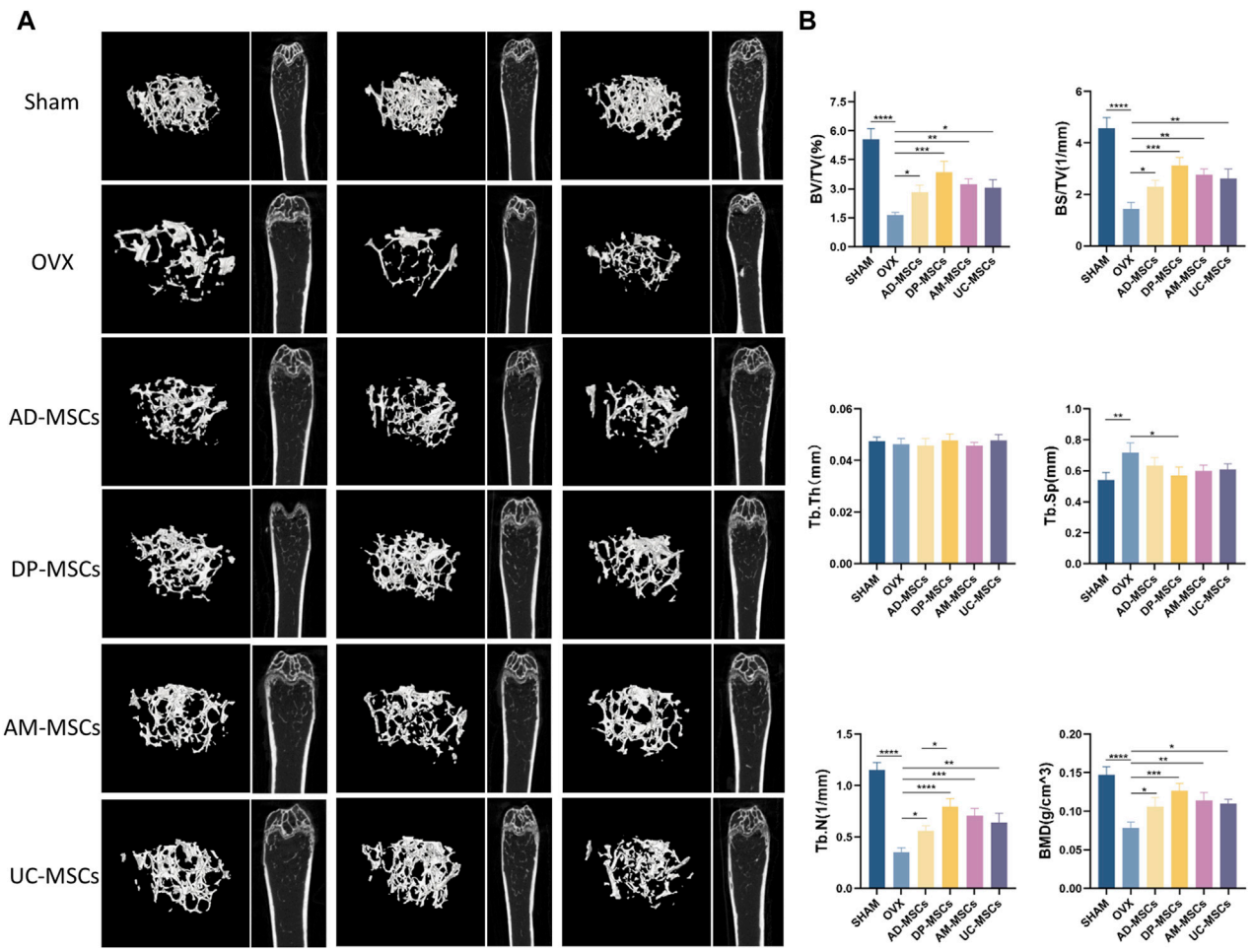

FIGURE 1
MSCs transplantation prevents bone loss in mice with osteoporosis. **(A)** Images of μCT reconstructions of distal femurs (n = 3). **(B)** Quantitative μCT analyses of the distal metaphyseal region of femurs (n = 3).

Statistical analysis

GraphPad Prism software (v7) was used to conduct statistical analysis (GraphPad Software). All data were expressed as the mean ± SD. Differences between the two experimental groups were determined by means of an unpaired two-tailed Student's t-test. One-way ANOVA was used to compare more than three groups. The results were statistically significant with p values: $^{***}p < 0.001$; $^{**}p < 0.01$; $^{*}p < 0.05$.

Results

MSC-based cell therapy prevents OVX-induced bone loss

The therapeutic effects of AD-MSCs, DP-MSCs, AM-MSCs, and UC-MSC were investigated by transplanting these cells into the OVX mice via the tail vein. The mice were randomly divided into six groups (n = 12 per group). Each injection was performed 8 weeks after the induction of the OVX model. Observations were made 8 weeks after cell injection. The right femur and the distal femoral epiphysis were separated and analyzed qualitatively through μCT scanning, as this is the area most sensitive to estrogen deficiency according to previous reports (Jee and Yao, 2001). Three-dimensional imaging results showed that OVX mice had much less bone mass than normal mice. In comparison to the OVX model group, trabecular bone structure and bone mass recovery were evident in the treatment groups (Figure 1A), suggesting MSCs were able to protect against the bone loss caused by ovarian resection. However, no significant changes in bone mineral density (BMD) were observed in OVX model mice over this same period. All four types of MSCs transplantation significantly improved trabecular bone volume/total volume (BV/TV), bone surface/total volume (BS/TV), BMD, and trabecular number (Tb.N). A significant decrease in trabecular space (Tb.Sp) was evident in the DP-MSCs and AM-MSCs transplantation groups compared to the OVX model group. In contrast, cellular therapy had little effect on trabecular thickness (Tb.Th) (Figure 1B). Notably, in comparison to the other groups, the DP-MSCs group exhibited the strongest therapeutic response, highlighting the promise of this approach to treating osteoporosis (Figure 1B).

10.3389/fphar.2024.1349199

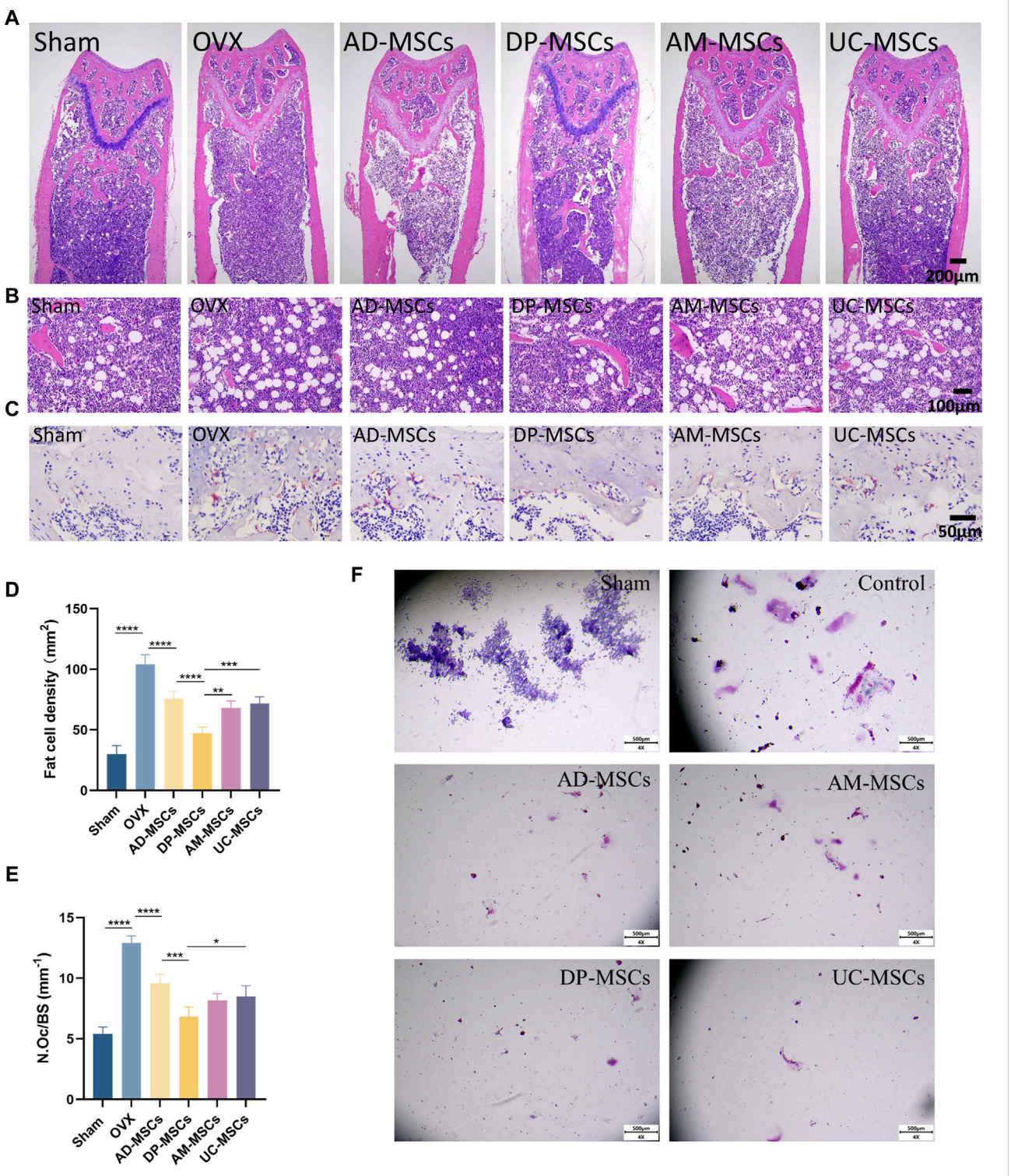

FIGURE 2
MSCs decrease the number of osteoclast and adipocytes. **(A)** Representative H&E staining of femur sections from these different MSCs treatment and control groups. **(B)** Exhibiting the marrow adipocytes. **(C)** TRAP staining of femur sections. Scale bar, 50 μm.**(D)** The numbers and area of adipocytes in the distal marrow per tissue area. **(E)** Quantification of osteoclasts in different experimental groups (n = 3). **(F)** Effect of MSC co-culture on osteoclast differentiation of RAW264 cells. Scale bar, 50 μm. Data are expressed as mean s± SD. *$p < 0.05$; **$p < 0.001$; ***$p < 0.0001$.

10.3389/fphar.2024.1349199

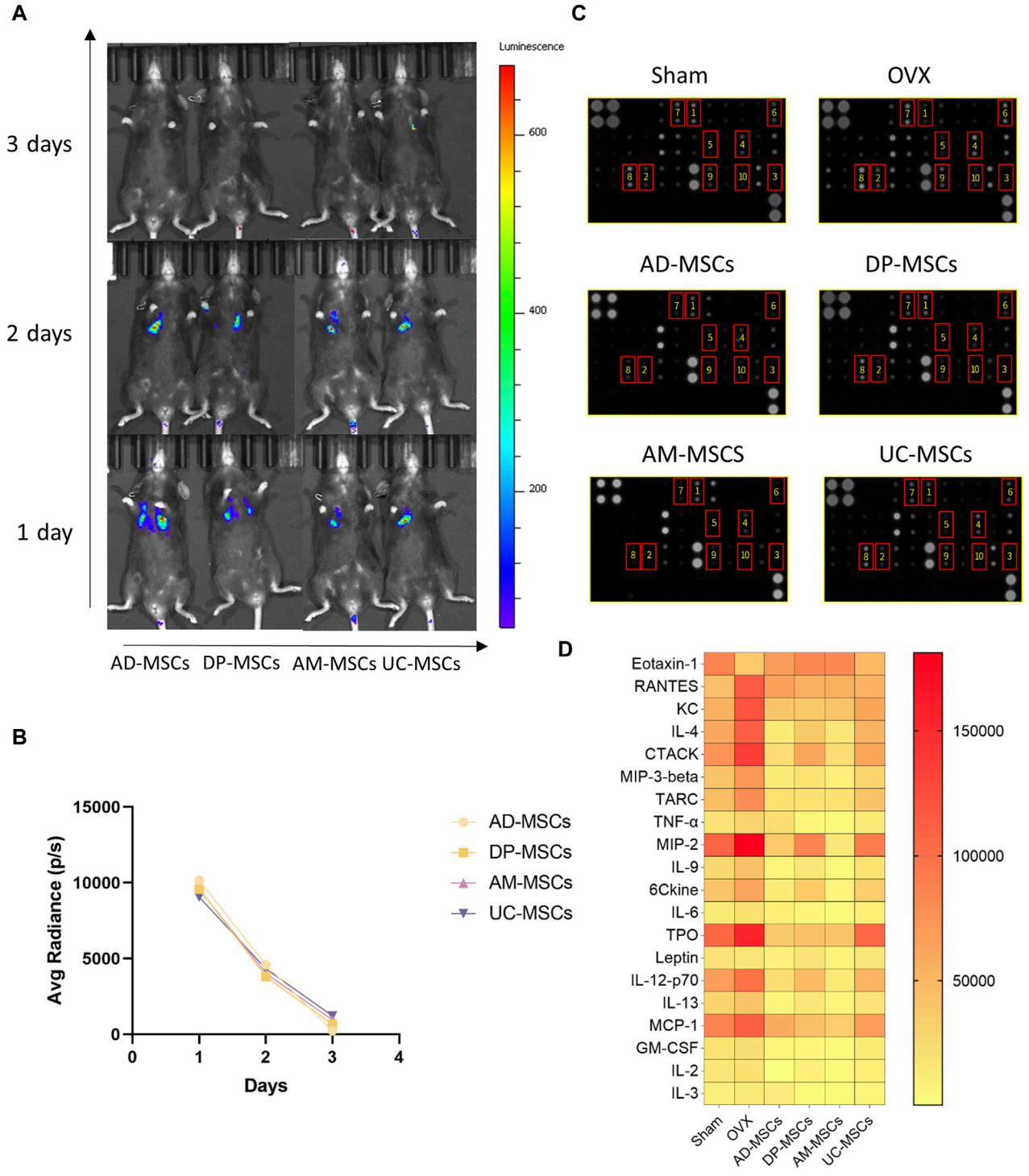

FIGURE 3
MSCs regulate peripheral serum cytokine levels through paracrine effects. **(A)** The distribution of MSCs in OVX model mice was determined via bioluminescent imaging. **(B)** The results of average radiance value analyses. **(C)** Images of the membranes used in serum cytokine antibody array analyses. Serum was separated from these different MSCs treatment and control groups. **(D)** Heatmap data demonstrating the results of comparative analyses of the same serum cytokine levels in mice in the sham, OVX, AD-MSCs, DP-MSCs, AM-MSCs, and UC-MSC groups (n = 2).

MSC-based cell therapy reduced OVX-induced increases in bone marrow osteoclast and adipocyte counts

To further determine the therapeutic effect of MSCs on bone loss in OVX mice, we observed adipocytes and osteoclasts in the bone marrow cavity. H&E staining revealed that bone marrow adipocyte density increased after OVX, whereas this cell density was decreased in the AD-MSCs, DP-MSCs AM-MSCs, and UC-MSC groups compared with the OVX model group (Figures 2A, B, D), suggesting that MSCs may reduce bone loss due to OVX by reducing bone marrow adipocyte generation. TRAP staining showed that bone marrow osteoclast abundance increased after OVX, whereas there were fewer osteoclasts shown in the AD-MSCs, DP-MSCs AM-MSCs, and UC-MSC groups (Figures 2C, E), suggesting that MSCs may prevent bone loss by reducing bone marrow osteoclast production. Accordingly, DP-MSCs had the best regulatory effect on adipocytes and osteoclasts. DP-MSCs thus presented with markedly higher osteogenic ability owing to their ability to inhibit adipocyte differentiation and suppress osteoclast formation, outperforming other types of tested MSCs. These results further support the potential value of DP-MSCs as an option for the treatment of osteoporosis.

To study the impact of mesenchymal stem cells (MSCs) on the differentiation of osteoclast cells *in vitro*, we conducted transwell cultures using MSCs and RAW264.7 cells (Figure 2F). demonstrates that in the control group, osteoclasts were differentiated from RAW264.7 cells following stimulation with RANK-L, leading to a considerable increase in both the number and size of osteoclasts. Conversely, in the indirect co-culture with MSCs, the number of differentiated osteoclasts substantially decreased, and there was hardly any observed osteoclast differentiation. All four types of MSCs exhibited the ability to inhibit osteoclast differentiation, yet there were no significant differences among them.

MSCs are short-lived *in vivo* following intravenous administration

MSCs are capable of migrating to the bone marrow and playing a local role in the induction of bone formation, exerting therapeutic effects by inducing peripheral tolerance and migrating to bone marrow after *in vivo* administration (Uccelli et al., 2008). In an effort to explore the homing efficiency and survival of MSCs following systemic transplantation, we tracked these four types of MSCs transduced with luciferase genes in each treatment group to observe their *in vivo* retention and distributions. Cells were detected via bioluminescent imaging on days 1, 2, and 3 after infusion, revealing that most of these MSCs migrated to the lungs after transplantation, with the cell signal having markedly decreased by day 3 (Figure 3A). On day 1 after cell infusion, all mice exhibited comparable levels of luminescence intensity (average radiance: 1×10^4 P/S). After 3 days, luminescence was largely absent in these animals, demonstrating that these MSCs cannot survive *in vivo* for extended periods such that their ability to improve OVX-induced osteoporosis may primarily be mediated through paracrine and immunoregulatory mechanisms (Figure 3B).

MSCs regulate bone metabolism through paracrine effects

Given the short lifespan of MSCs following their *in vivo* delivery, paracrine effects are likely to play an important role in their therapeutic benefits. As such, we compared peripheral blood cytokine expression profiles in these different treatment groups, as cytokines can regulate bone remodeling and play a vital role in bone homeostasis (Li et al., 2020). We measured the levels of chemokines and inflammatory cytokines in serum using an antibody array, as they play important roles in the incidence of osteoporosis (Brylka and Schinke, 2019; Damani et al., 2022). Compared to the sham-operated group, the serum levels of inflammatory cytokines and chemokines were significantly altered in osteoporotic mice, including Eotaxin-1 (CCL11), RANTES (CCL5), KC (CXCL1), IL-4, CTACK (CCL27), MIP-3β (CCL19), TARC (CCL17), MIP-2 (CXCL2), TPO, IL-12-p70, and MCP-1 (CCL2), (Figures 3C, D). In contrast, MSCs-transplanted mice exhibited elevated levels of serum cytokines associated with repressing adipogenesis and activating osteogenesis as compared to OVX-induced osteoporosis model mice (Figures 3C, D). These results suggest that MSCs prevent bone loss in OVX mice through paracrine functions.

Eotaxin-1, RANTES, and CXCL1 may be the key cytokines underlying the superior efficacy of DP-MSCs

To explore the mechanisms underlying the paracrine effects of MSC infusion in OVX-induced osteoporosis model mice, we next compared the levels of serum cytokines related to bone remodeling in different treatment groups. The cytokines exhibiting the most significant changes were Eotaxin-1, RANTES, and CXCL1 (Figure 4A). CXCL1 and Eotaxin-1 were significantly associated with a reduction in BMD. Serum levels of CXCL1 and Eotaxin-1 were correlated with bone mass. RANTES plays a role as an inflammatory factor, associated with massive bone resorption (Lechner et al., 2018; Ahmadi et al., 2020; Korbecki et al., 2022). We then compared the effects of each type of stem cell on these three indicators and found that DP-MSCs provided a significant increase in Eotaxin-1 and dramatic decreases in the levels of CXCL1, with RANTES levels also declining to the levels observed in healthy controls (Figure 4B). Other MSCs were also associated with changes in serum cytokine levels. More specifically, AD-MSCs downregulated IL-4, CTACK, TPO, and IL-13 (Figure 4C), while DP-MSCs downregulated CXCL1 and TRAC and upregulated Eotaxin-1 and Leptin, which are also linked to bone metabolism (Figure 4D). AM-MSCs downregulated IL-17, MIP-3β, TNF-α, MIP-2, IL-9, CCL21, IL-6, IL-12-p70, MCP-1, GM-CSF, IL-3 (Figure 4E), and UC-MSCS downregulated RANTES (Figure 4B). Taken together, our findings suggest that DP-MSCs may exhibit optimal anti-osteoporotic therapeutic effects by modulating the levels of Eotaxin-1, RANTES, and CXCL1, which are associated with bone metabolism.

10.3389/fphar.2024.1349199

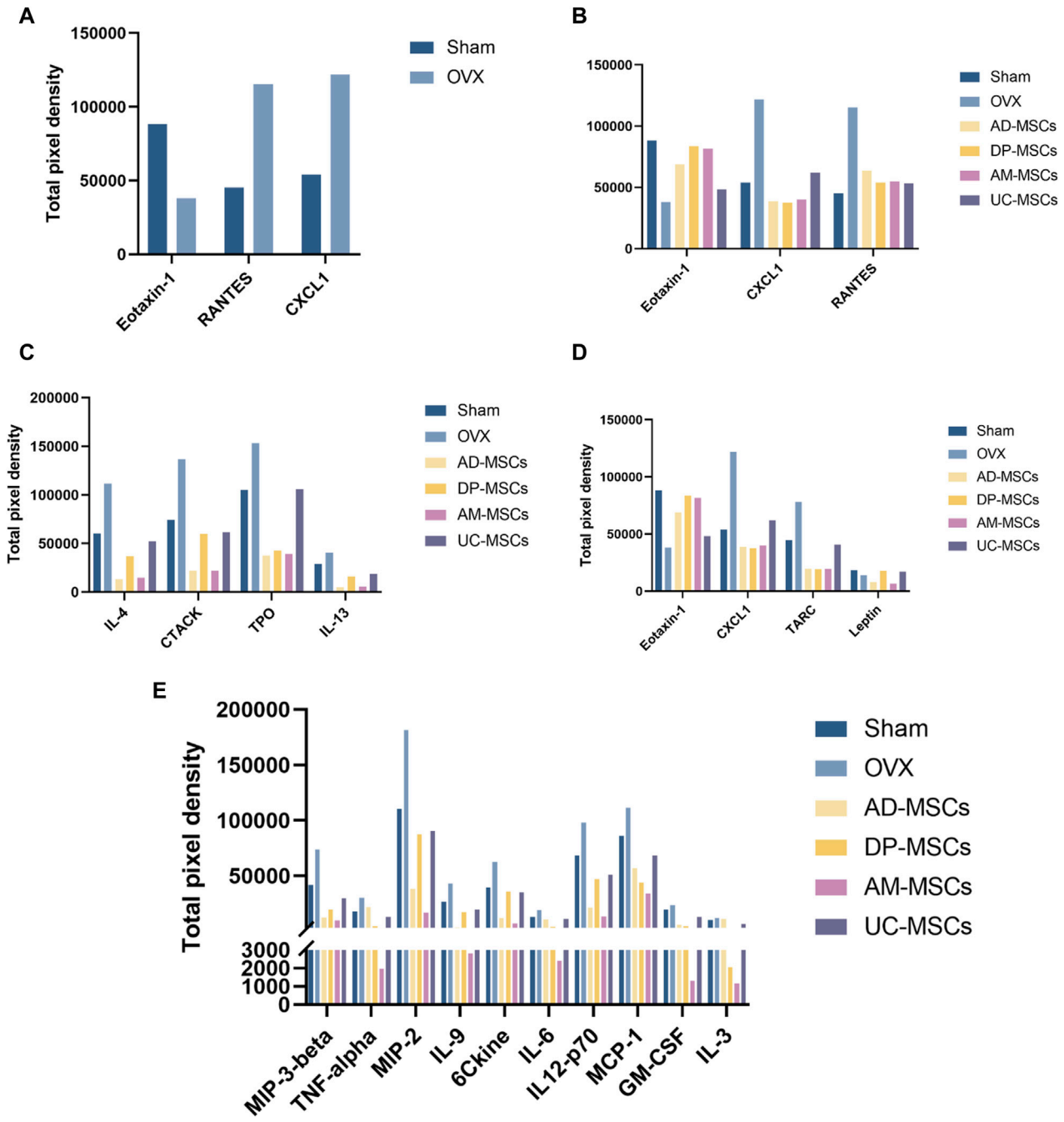

FIGURE 4
MSCs regulate serum cytokines. **(A)** Cytokines associated with significantly altered abundance when comparing the serum of normal and osteoporotic mice. **(B)** Analyses of the ability of MSCs to regulate Eotaxin-1, RANTES, and CXCL1. **(C–E)** The serum cytokines associated with the most significant improvements in the AD-MSCs **(C)**, DP-MSCs **(D)**, AM-MSCs **(E)** groups.

DP-MSCs regulate Th17/Treg cell homeostasis and macrophage polarization

MSC therapy has been extensively investigated in the context of the regulation of bone metabolism and the immune system. As such, we next assessed the ratio of splenic Th17/Treg cells and femoral macrophage polarization in our experimental mice. Th17/Treg cell homeostasis and appropriate macrophage polarization have both been shown to have a profound effect on osteoporosis (Muñoz et al., 2020; Zhu et al., 2020). Accordingly, we observed a slight decline in splenic Treg cells and an increase in Th17 cell abundance following OVX, while these changes were reversed after MSC transplantation (Figure 5A), suggesting that DP-MSCs improve OVX-induced osteoporosis through paracrine effects and immune regulation. Macrophages also participate in osteoclastogenesis by regulating the subtype M1/M2 balance and activity through cytokine signaling. MSC transplantation

10.3389/fphar.2024.1349199

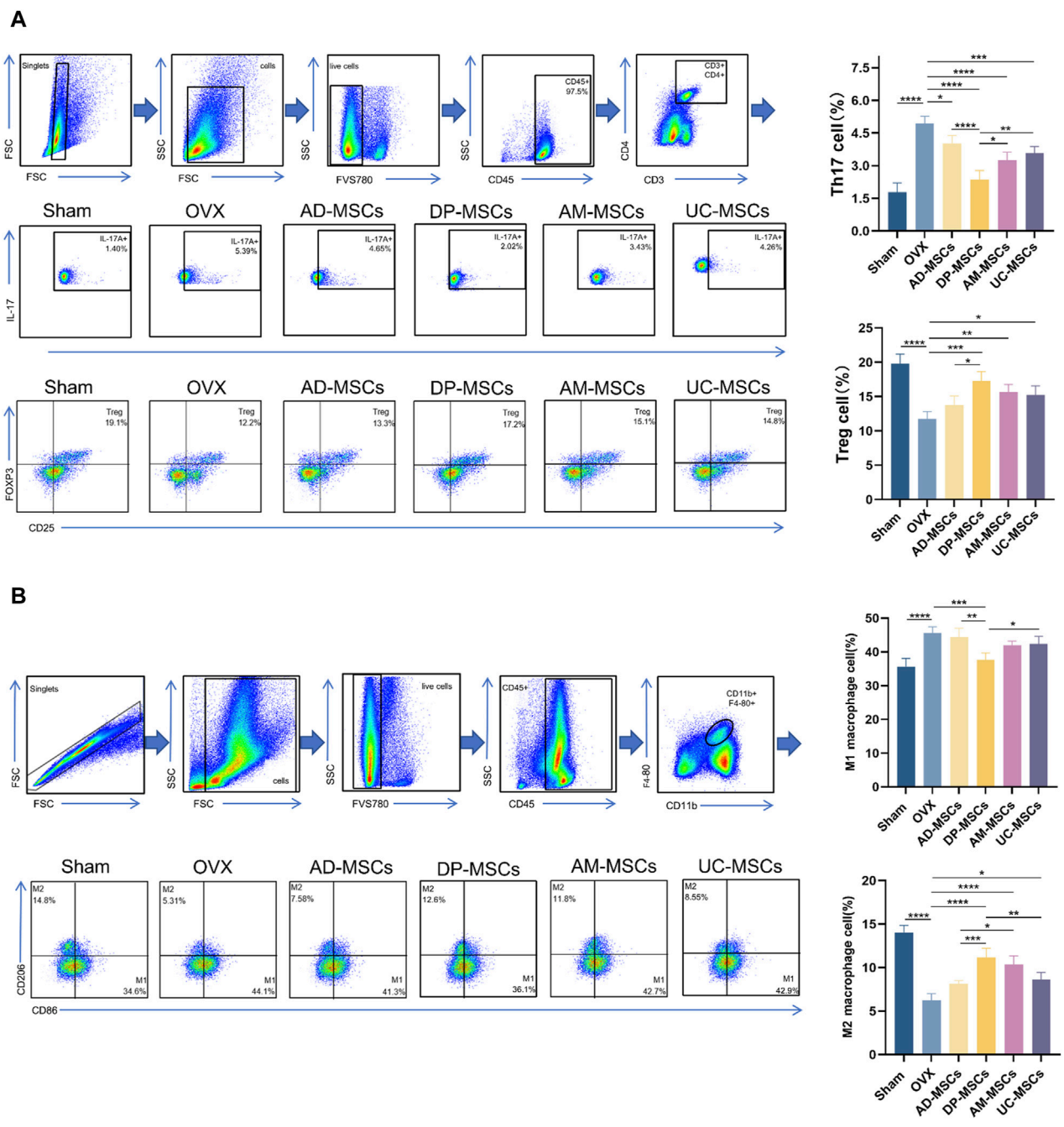

FIGURE 5
MSCs regulate splenicTh17/Treg cell balance and bone marrow macrophage polarization. **(A)** Representative flow plots and corresponding quantification of IL-17$^+$ and Foxp3$^+$ cell abundance in spleen (n = 4). **(B)** Representative flow plots and corresponding quantification of CD86$^+$ and CD206$^+$ cells in bone marrow (n = 4). Data are expressed as means ± SD. *$p < 0.05$; **$p < 0.001$; ***$p < 0.0001$.

can also modulate the polarization of macrophages in the bone marrow. Specifically, DP-MSCs decreased the abundance of M1 macrophages and decreased the abundance of M2 macrophages more efficiently than other MSCs (Figure 5B). These results suggest that the mechanism through which MSC infusion improves OVX-induced osteoporosis entails the regulation of Th17/Treg cells homeostasis and macrophage polarization.

Discussion

Early studies on the cell therapy-based treatment of osteoporosis have focused on how to apply MSC transplantation to improve OVX-induced osteoporosis in rodent model systems. MSCs like AD-MSCs, DP-MSCs, AM-MSCs, and UC-MSC have been widely used and their effects on immune regulation and the induction of osteogenic differentiation have been verified repeatedly. These

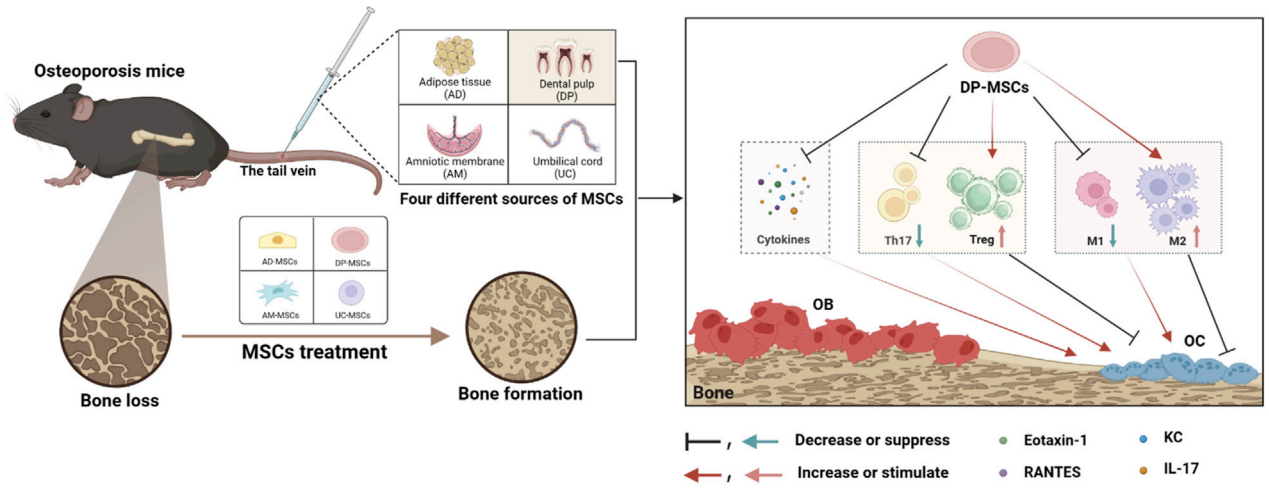

FIGURE 6
MSCs from different sources regulate the splenic Th17/Treg balance and bone marrow macrophage polarization through paracrine effects to treat osteoporosis, with DP-MSCs exhibiting the best therapeutic efficacy in this regard.

past studies have demonstrated that mechanisms underlying MSC-based anti-osteoporotic therapy are mainly reflected by the promotion of osteoblast activity and the downregulation of osteoclast activity. MSCs have also exhibited promise as tools for the treatment of osteoporosis in many studies (Jiang et al., 2021).

Ideal candidate stem cell type for anti-osteoporotic therapy requires several characteristics, including (1) the ability to home to damaged sites to exert a local functional role, which MSCs can achieve by differentiating into bone-forming cells or acting in a paracrine manner through the secretion of cytokines to remodel the local microenvironment so as to improve bone formation; (2) immunoregulatory properties, with MSCs and immune cells being able to interact to affect the differentiation and activity of immune cells and the secretion of various immune factors; and (3) the ability to balance bone metabolism, favoring osteogenic differentiation by regulating the development of osteoclasts and osteoblasts. Recently, several studies have focused on different cell populations for the cell therapy-based treatment of osteoporosis. In particular, AD-MSCs transplantation was reported to improve bone formation and prevent OVX-induced bone loss via the secretion of various osteogenic growth factors (Jiang et al., 2021). Another study demonstrated that after transplantation, UC-MSC exhibited significant inhibitory effects on T cell proliferation, with decreases in TNF-α levels, suggesting that UC-MSC may play an immunoregulatory role. In addition, DP-MSCs have been reported to have a higher osteogenic capability and low adipogenic potential. Furthermore, Sanvoranart et al. observed that the long-term engraftment of AM-MSCs long-term was associated with significantly increased bone formation (Sanvoranart et al., 2014). However, no study to date has evaluated differences in the therapeutic potential of DP-MSCs, AD-MSCs, AM-MSCs, and UC-MSC for the treatment of OVX-induced osteoporosis. In this study, we found that MSCs isolated from different tissues exhibited varying levels of cell therapy-based efficacy.

We first evaluated the ability of four MSCs types to protect the femoral bone in OVX mice. Different types of MSCs exhibited different therapeutic effects on osteoporosis. Notably, compared with AM-MSCs, UC-MSC, and AD-MSCs, DP-MSCs exhibited superior protective effects on OVX mice, and these data indicated that the systemic infusion of DP-MSCs restored trabecular bone mass with corresponding increases in trabecular bone volume, trabecular separation, trabecular number, and BMD, although they did not prevent changes in trabecular thickness. Additional analysis revealed that DP-MSCs therapy significantly increased bone volume while decreasing marrow adipocyte and osteoclast abundance. In addition, although the transplantation of MSCs was able to protect against bone volume changes and trabecular bone loss, its effects on Tb.Th were minimal. As such, MSC transplantation may best be deployed in combination with other therapeutic modalities, such as herbal remedies (Lin et al., 2020).

Bone is a dynamic organ that undergoes continuous remodeling via coordinated synergism between osteoclasts and osteoblasts. Osteoblasts originate from MSCs in the bone marrow, and dysregulated osteoblastic differentiation of MSCs has been tied to the initiation of osteoporosis. Accordingly, transplanted MSCs rescue bone loss either by homing to the bone marrow and/or promoting osteoblastic differentiation or immunomodulatory effects. As osteogenic differentiation and immunomodulatory activity are the main mechanisms whereby MSCs can treat osteoporosis, we therefore monitored the distribution and survival of MSCs transplanted *in vitro*. Our results are consistent with previous reports that MSCs transplanted *in vivo* do not survive for extended periods and that they rarely home to the bone marrow, suggesting that paracrine effects through the secretion of certain growth factors panel with immunomodulatory properties may be the primary mechanism through which these cells function (Kong et al., 2018). In our study, we found that most engrafted MSCs were retained in the lungs, less than 50% of infused MSCs survived for

48 h, and almost none remained alive after 72 h, suggesting that MSCs in this model system mediate their effects through a paracrine role, rather than through sustained engraftment in the bone marrow. The underlying mechanism behind the limited lifespan of MSCs and its impact on their efficacy remains uncertain. Nonetheless, a study conducted by MJ Hoogduijn revealed that when MSCs were infused, they were swiftly eliminated by monocytes through phagocytosis. This process further prompted the monocytes to adopt an immunosuppressive phenotype (de Witte et al., 2018).

The loss of appropriate homeostatic balance between the bone and the immune system compartments can arise under inflammatory conditions, leading to enhanced bone loss (Fischer and Haffner-Luntzer, 2022). Immune cells can regulate bone-related cells by secreting various immune factors (Saxena et al., 2021). Given the role of the immune system in this context, it is important to clearly define the relationship between various subsets of immune cells including Th17/Treg and M1/M2 cells, the progression of osteoporosis, and the therapeutic effects of MSCs.

Macrophages are key players in the regulation of bone homeostasis. Macrophages undergo microenvironment-specific polarization, which can lead to the development of populations including classically activated (M1) and alternatively activated (M2) macrophages. Under osteoporotic conditions, macrophages display mainly a pro-inflammatory M1 phenotype and release inflammatory cytokines such as IL-1, IL-6, IL-17, and RANTES, which are closely related to increased bone resorption and osteoclast activity (Souza and Lerner, 2013; Zhang et al., 2017). Macrophage inflammatory protein-1α (MCP-1α) has been reported to induce osteoclast formation via the activation of the MEK/ERK/c-Fos pathway (Tsubaki et al., 2010). We found that MIP-2 is also likely to play a role in bone resorption. AD-MSCs (Yang CY. et al., 2021), DP-MSCs (Tian et al., 2023), AM-MSCs (Cao et al., 2020), and UC-MSC (Li et al., 2022) can all regulate macrophage polarization to ameliorate disease. However, there have been no prior comparisons of their relative ability to regulate macrophage polarization in the context of osteoporosis. Our results show that M1 macrophage abundance rose significantly following OVX in mice, while MSC transplantation was able to partially abrogate increases in these M1 macrophage levels. In contrast, transplantation of MSCs in a porcine model reportedly led to not only an increase in M2 macrophage abundance, but also to reduced levels of inflammatory cytokines such as MCP-1, TARC, CXCL1, RANTES, and CTACK. Observational studies have reported associations between levels of MCP-1 and osteoporosis, in line with its ability to regulate osteoclast differentiation and maturation (Mulholland et al., 2019). RANTES is released by human adipose tissue that induces leukocyte migration (Appay and Rowland-Jones, 2001). RANTES is overexpressed in osteoporosis (Lechner et al., 2018) and promotes osteoclast formation and bone resorption (Feng et al., 2020). CXCL1 is a CXC family chemokine that may offer value as a new predictor of early bone loss (Hu et al., 2020b). Serum CXCL1 levels are positively associated with human osteoporosis (Hardaway et al., 2015) and may cause osteoporosis by accelerating cell senescence (Korbecki et al., 2022), mediating chronic inflammation (Shi et al., 2018), and promoting the migration and maturation of osteoclast progenitors (Govey et al., 2014; Hardaway et al., 2015). TARC and CTACK mediate the migration of T cells (Hijnen et al., 2004).

IL-17 is a pro-inflammatory cytokine (Yao et al., 1995), and is regarded as a catalyst for the development of osteoporosis (Molnár et al., 2014; Zhao et al., 2016; Tang et al., 2020), acting primarily by indirectly promoting osteoclast formation (Amarasekara et al., 2018). Both Th17 and Treg cells play key roles in the maintenance of bone homeostasis (Zhu et al., 2020). Th17 cells increase osteoclast formation by promoting inflammation, whereas Tregs suppress osteoclastogenesis by suppressing the inflammatory response. MSCs can regulate the Th17/Treg balance (Zhang et al., 2021; Hua et al., 2022). Interestingly, the abundance of Th17 cells in the spleens of mice in this increased after OVX, while MSC transplantation abrogated this increase, with DP-MSCs exhibiting the greatest efficacy as compared to other tested MSC populations, indicating that these cells are the strongest inhibitors of T cell proliferation with less immunogenicity. However, UC-MSC have been reported to exhibit the poorest osteogenic potential (Li et al., 2014). We observed that splenic Treg cell abundance was markedly increased in response to DP-MSCs transplantation, suggesting that DP-MSCs exhibit superior immunomodulatory capabilities.

Conclusion

In this study, the relative performance of four different MSC types (AD-MSCs, DP-MSCs, AM-MSCs, and UC-MSC) was compared to better clarify which of these cells are best able to protect against bone loss in OVX mice through the modulation of the immune microenvironment DP-MSCs infusion restored trabecular bone mass more efficiently than other treatments, with corresponding improvements in trabecular bone volume, mineral density, number, and separation. Of these different types of MSCs, DP-MSCs were also found to exhibit a higher immunoregulatory capacity by regulating the Th17/Treg and M1/M2 ratios (Figure 6). Therefore, these results indicate that DP-MSCs may represent an effective cell population for use in the cell therapy-based treatment of osteoporosis.

Data availability statement

The raw data supporting the conclusion of this article will be made available by the authors, without undue reservation.

Ethics statement

The animal study was approved by the ethics committee of Chengdu University of Traditional Chinese Medicine. The study was conducted in accordance with the local legislation and institutional requirements.

Author contributions

CL: Conceptualization, Data curation, Formal Analysis, Investigation, Methodology, Writing–original draft. YL: Conceptualization, Data curation, Investigation, Methodology,

Validation, Writing–original draft, Writing–review and editing. MD: Data curation, Investigation, Methodology, Writing–original draft. JL: Project administration, Resources, Writing–review and editing. SL: Data curation, Resources, Writing–review and editing. XL: Investigation, Methodology, Project administration, Writing–original draft. YZ: Investigation, Methodology, Project administration, Writing–review and editing. CS: Conceptualization, Funding acquisition, Investigation, Writing–review and editing. YW: Data curation, Investigation, Methodology, Project administration, Validation, Writing–original draft, Writing–review and editing.

Funding

The author(s) declare financial support was received for the research, authorship, and/or publication of this article. This work was supported by the National Natural Science Foundation of China (No. 82174226), Xinglin talent Foundation of Chengdu University of TCM (XSGG2020002).

Acknowledgments

We would like to thank LetPub for its linguistic assistance during the preparation of this manuscript.

Conflict of interest

The authors declare that the research was conducted in the absence of any commercial or financial relationships that could be construed as a potential conflict of interest.

Publisher's note

References

Ahmadi, H., Khorramdelazad, H., Hassanshahi, G., Abbasi Fard, M., Ahmadi, Z., Noroozi Karimabad, M., et al. (2020). Involvement of eotaxins (CCL11, CCL24, CCL26) in pathogenesis of osteopenia and osteoporosis. *Iran. J. Public Health* 49 (9), 1769–1775. doi:10.18502/ijph.v49i9.4098

Amarasekara, D. S., Yun, H., Kim, S., Lee, N., and Rho, J. (2018). Regulation of osteoclast differentiation by cytokine networks. *Immune Netw.* 18 (1), e8. doi:10.4110/in.2018.18.e8

Appay, V., and Rowland-Jones, S. L. (2001). RANTES: a versatile and controversial chemokine. *Trends Immunol.* 22 (2), 83–87. doi:10.1016/s1471-4906(00)01812-3

Avioli, L. V. (1976). Senile and postmenopausal osteoporosis. *Adv. Intern Med.* 21, 391–415.

Barlow, S., Brooke, G., Chatterjee, K., Price, G., Pelekanos, R., Rossetti, T., et al. (2008). Comparison of human placenta- and bone marrow-derived multipotent mesenchymal stem cells. *Stem Cells Dev.* 17 (6), 1095–1107. doi:10.1089/scd.2007.0154

Brylka, L. J., and Schinke, T. (2019). Chemokines in physiological and pathological bone remodeling. *Front. Immunol.* 10, 2182. doi:10.3389/fimmu.2019.02182

Cao, X., Duan, L., Hou, H., Liu, Y., Chen, S., Zhang, S., et al. (2020). IGF-1C hydrogel improves the therapeutic effects of MSCs on colitis in mice through PGE(2)-mediated M2 macrophage polarization. *Theranostics* 10 (17), 7697–7709. doi:10.7150/thno.45434

Chen, T., Yang, T., Zhang, W., and Shao, J. (2021). The therapeutic potential of mesenchymal stem cells in treating osteoporosis. *Biol. Res.* 54 (1), 42. doi:10.1186/s40659-021-00366-y

Damani, J. J., De Souza, M. J., VanEvery, H. L., Strock, N. C. A., and Rogers, C. J. (2022). The role of prunes in modulating inflammatory pathways to improve bone health in postmenopausal women. *Adv. Nutr.* 13 (5), 1476–1492. doi:10.1093/advances/nmab162

de Witte, S. F. H., Luk, F., Sierra Parraga, J. M., Gargesha, M., Merino, A., Korevaar, S. S., et al. (2018). Immunomodulation by therapeutic mesenchymal stromal cells (MSC) is triggered through phagocytosis of MSC by monocytic cells. *Stem Cells* 36 (4), 602–615. doi:10.1002/stem.2779

Eriksen, E. F., Hodgson, S. F., Eastell, R., Cedel, S. L., O'Fallon, W. M., and Riggs, B. L. (1990). Cancellous bone remodeling in type I (postmenopausal) osteoporosis: quantitative assessment of rates of formation, resorption, and bone loss at tissue and cellular levels. *J. Bone Min. Res.* 5 (4), 311–319. doi:10.1002/jbmr.5650050402

Feng, S. Y., Lei, J., Chen, H. M., Wang, Y. X., Yap, A. U. J., and Fu, K. Y. (2020). Increased chemokine RANTES in synovial fluid and its role in early-stage degenerative temporomandibular joint disease. *J. Oral Rehabil.* 47 (9), 1150–1160. doi:10.1111/joor.13041

Fischer, V., and Haffner-Luntzer, M. (2022). Interaction between bone and immune cells: implications for postmenopausal osteoporosis. *Semin. Cell Dev. Biol.* 123, 14–21. doi:10.1016/j.semcdb.2021.05.014

Govey, P. M., Jacobs, J. M., Tilton, S. C., Loiselle, A. E., Zhang, Y., Freeman, W. M., et al. (2014). Integrative transcriptomic and proteomic analysis of osteocytic cells exposed to fluid flow reveals novel mechano-sensitive signaling pathways. *J. Biomech.* 47 (8), 1838–1845. doi:10.1016/j.jbiomech.2014.03.022

Hardaway, A. L., Herroon, M. K., Rajagurubandara, E., and Podgorski, I. (2015). Marrow adipocyte-derived CXCL1 and CXCL2 contribute to osteolysis in metastatic prostate cancer. *Clin. Exp. Metastasis* 32 (4), 353–368. doi:10.1007/s10585-015-9714-5

Heo, J. S., Choi, Y., Kim, H. S., Kim, H. O., et al. (2016). Comparison of molecular profiles of human mesenchymal stem cells derived from bone marrow, umbilical cord blood, placenta and adipose tissue. *Int. J. Mol. Med.* 37 (1), 115–125. doi:10.3892/ijmm.2015.2413

Hijnen, D., De Bruin-Weller, M., Oosting, B., Lebre, C., De Jong, E., Bruijnzeel-Koomen, C., et al. (2004). Serum thymus and activation-regulated chemokine (TARC) and cutaneous T cell-attracting chemokine (CTACK) levels in allergic diseases: TARC and CTACK are disease-specific markers for atopic dermatitis. *J. Allergy Clin. Immunol.* 113 (2), 334–340. doi:10.1016/j.jaci.2003.12.007

Hu, Y., Wang, L., Zhao, Z., Lu, W., Fan, J., Gao, B., et al. (2020b). Cytokines CCL2 and CXCL1 may be potential novel predictors of early bone loss. *Mol. Med. Rep.* 22 (6), 4716–4724. doi:10.3892/mmr.2020.11543

Hu, Y., Zhang, Y., Ni, C. Y., Chen, C. Y., Rao, S. S., Yin, H., et al. (2020a). Human umbilical cord mesenchymal stromal cells-derived extracellular vesicles exert potent bone protective effects by CLEC11A-mediated regulation of bone metabolism. *Theranostics* 10 (5), 2293–2308. doi:10.7150/thno.39238

Hua, Q., Zhang, Y., Li, H., Li, H., Jin, R., Li, L., et al. (2022). Human umbilical cord blood-derived MSCs trans-differentiate into endometrial cells and regulate Th17/Treg balance through NF-κB signaling in rabbit intrauterine adhesions endometrium. *Stem Cell Res. Ther.* 13 (1), 301. doi:10.1186/s13287-022-02990-1

Hurley, D. L., and Khosla, S. (1997). Update on primary osteoporosis. *Mayo Clin. Proc.* 72 (10), 943–949. doi:10.1016/S0025-6196(11)63367-3

Jee, W. S., and Yao, W. (2001). Overview: animal models of osteopenia and osteoporosis. *J. Musculoskelet. Neuronal Interact.* 1 (3), 193–207.

Jiang, Y., Zhang, P., Zhang, X., Lv, L., and Zhou, Y. (2021). Advances in mesenchymal stem cell transplantation for the treatment of osteoporosis. *Cell Prolif.* 54 (1), e12956. doi:10.1111/cpr.12956

Kong, F., Shi, X., Xiao, F., Yang, Y., Zhang, X., Wang, L. S., et al. (2018). Transplantation of hepatocyte growth factor-modified dental pulp stem cells prevents bone loss in the early phase of ovariectomy-induced osteoporosis. *Hum. Gene Ther.* 29 (2), 271–282. doi:10.1089/hum.2017.091

Korbecki, J., Gąssowska-Dobrowolska, M., Wójcik, J., Szatkowska, I., Barczak, K., Chlubek, M., et al. (2022). The importance of CXCL1 in physiology and noncancerous diseases of bone, bone marrow, muscle and the nervous system. *Int. J. Mol. Sci.* 23 (8), 4205. doi:10.3390/ijms23084205

Kumar, A., Kumar, V., Rattan, V., Jha, V., and Bhattacharyya, S. (2018). Secretome proteins regulate comparative osteogenic and adipogenic potential in bone marrow and dental stem cells. *Biochimie* 155, 129–139. doi:10.1016/j.biochi.2018.10.014

Lechner, J., Rudi, T., and von Baehr, V. (2018). Osteoimmunology of tumor necrosis factor-alpha, IL-6, and RANTES/CCL5: a review of known and poorly understood

inflammatory patterns in osteonecrosis. *Clin. Cosmet. Investig. Dent.* 10, 251–262. doi:10.2147/CCIDE.S184498

Lee, K., Kim, H., Kim, J. M., Kim, J. R., Kim, J. K., Kim, Y. Y., et al. (2011). Systemic transplantation of human adipose-derived stem cells stimulates bone repair by promoting osteoblast and osteoclast function. *J. Cell Mol. Med.* 15 (10), 2082–2094. doi:10.1111/j.1582-4934.2010.01230.x

Li, J., Chen, X., Lu, L., and Yu, X. (2020). The relationship between bone marrow adipose tissue and bone metabolism in postmenopausal osteoporosis. *Cytokine Growth Factor Rev.* 52, 88–98. doi:10.1016/j.cytogfr.2020.02.003

Li, K., Yan, G., Huang, H., Zheng, M., Ma, K., Cui, X., et al. (2022). Anti-inflammatory and immunomodulatory effects of the extracellular vesicles derived from human umbilical cord mesenchymal stem cells on osteoarthritis via M2 macrophages. *J. Nanobiotechnology* 20 (1), 38. doi:10.1186/s12951-021-01236-1

Li, X., Bai, J., Ji, X., Xuan, Y., and Wang, Y. (2014). Comprehensive characterization of four different populations of human mesenchymal stem cells as regards their immune properties, proliferation and differentiation. *Int. J. Mol. Med.* 34 (3), 695–704. doi:10.3892/ijmm.2014.1821

Lin, W. L., Lin, P. Y., Hung, Y. C., and Hsueh, T. P. (2020). Benefits of herbal medicine on bone mineral density in osteoporosis: a meta-analysis of randomized controlled trials. *Am. J. Chin. Med.* 48 (8), 1749–1768. doi:10.1142/S0192415X20500871

Lindsay, R. (1993). Pathogenesis of postmenopausal osteoporosis. *Baillieres Clin. Rheumatol.* 7 (3), 499–513. doi:10.1016/s0950-3579(05)80075-5

Maeda, A., Kikuiri, T., Yoshimura, Y., Yawaka, Y., and Shirakawa, T. (2022). Bone resorption improvement by conditioned medium of stem cells from human exfoliated deciduous teeth in ovariectomized mice. *Exp. Ther. Med.* 23 (4), 299. doi:10.3892/etm.2022.11228

Mohamed-Ahmed, S., Fristad, I., Lie, S. A., Suliman, S., Mustafa, K., Vindenes, H., et al. (2018). Adipose-derived and bone marrow mesenchymal stem cells: a donor-matched comparison. *Stem Cell Res. Ther.* 9 (1), 168. doi:10.1186/s13287-018-0914-1

Molnár, I., Bohaty, I., and Somogyiné-Vári, É. (2014). IL-17A-mediated sRANK ligand elevation involved in postmenopausal osteoporosis. *Osteoporos. Int.* 25 (2), 783–786. doi:10.1007/s00198-013-2548-6

Mulholland, B. S., Forwood, M. R., and Morrison, N. A. (2019). Monocyte chemoattractant protein-1 (MCP-1/CCL2) drives activation of bone remodelling and skeletal metastasis. *Curr. Osteoporos. Rep.* 17 (6), 538–547. doi:10.1007/s11914-019-00545-7

Muñoz, J., Akhavan, N. S., Mullins, A. P., and Arjmandi, B. H. (2020). Macrophage polarization and osteoporosis: a review. *Nutrients* 12 (10), 2999. doi:10.3390/nu12102999

Rachner, T. D., Khosla, S., and Hofbauer, L. C. (2011). Osteoporosis: now and the future. *Lancet* 377 (9773), 1276–1287. doi:10.1016/S0140-6736(10)62349-5

Sanvoranart, T., Supokawej, A., Kheolamai, P., U-Pratya, Y., Klincumhom, N., Manochantr, S., et al. (2014). Bortezomib enhances the osteogenic differentiation capacity of human mesenchymal stromal cells derived from bone marrow and placental tissues. *Biochem. Biophys. Res. Commun.* 447 (4), 580–585. doi:10.1016/j.bbrc.2014.04.044

Saxena, Y., Routh, S., and Mukhopadhaya, A. (2021). Immunoporosis: role of innate immune cells in osteoporosis. *Front. Immunol.* 12, 687037. doi:10.3389/fimmu.2021.687037

Shi, H., Han, X., Sun, Y., Shang, C., Wei, M., Ba, X., et al. (2018). Chemokine (C-X-C motif) ligand 1 and CXCL2 produced by tumor promote the generation of monocytic myeloid-derived suppressor cells. *Cancer Sci.* 109 (12), 3826–3839. doi:10.1111/cas.13809

Sonoda, S., Murata, S., Nishida, K., Kato, H., Uehara, N., Kyumoto, Y. N., et al. (2020). Extracellular vesicles from deciduous pulp stem cells recover bone loss by regulating telomerase activity in an osteoporosis mouse model. *Stem Cell Res. Ther.* 11 (1), 296. doi:10.1186/s13287-020-01818-0

Sophocleous, A., and Idris, A. I. (2019). Ovariectomy/orchiectomy in rodents. *Methods Mol. Biol.* 1914, 261–267. doi:10.1007/978-1-4939-8997-3_13

Souza, P. P., and Lerner, U. H. (2013). The role of cytokines in inflammatory bone loss. *Immunol. Invest.* 42 (7), 555–622. doi:10.3109/08820139.2013.822766

Tang, M., Lu, L., and Yu, X. (2020). Interleukin-17A interweaves the skeletal and immune systems. *Front. Immunol.* 11, 625034. doi:10.3389/fimmu.2020.625034

Tian, J., Chen, W., Xiong, Y., Li, Q., Kong, S., Li, M., et al. (2023). Small extracellular vesicles derived from hypoxic preconditioned dental pulp stem cells ameliorate inflammatory osteolysis by modulating macrophage polarization and osteoclastogenesis. *Bioact. Mater* 22, 326–342. doi:10.1016/j.bioactmat.2022.10.001

Tsubaki, M., Kato, C., Isono, A., Kaneko, J., Isozaki, M., Satou, T., et al. (2010). Macrophage inflammatory protein-1α induces osteoclast formation by activation of the MEK/ERK/c-Fos pathway and inhibition of the p38MAPK/IRF-3/IFN-β pathway. *J. Cell Biochem.* 111 (6), 1661–1672. doi:10.1002/jcb.22907

Uccelli, A., Moretta, L., and Pistoia, V. (2008). Mesenchymal stem cells in health and disease. *Nat. Rev. Immunol.* 8 (9), 726–736. doi:10.1038/nri2395

Wang, X., Ji, Q., Hu, W., Zhang, Z., Hu, F., Cao, S., et al. (2021). Isobavachalcone prevents osteoporosis by suppressing activation of ERK and NF-κB pathways and M1 polarization of macrophages. *Int. Immunopharmacol.* 94, 107370. doi:10.1016/j.intimp.2021.107370

Yang, C. Y., Chang, P. Y., Chen, J. Y., Wu, B. S., Yang, A. H., and Lee, O. K. S. (2021b). Adipose-derived mesenchymal stem cells attenuate dialysis-induced peritoneal fibrosis by modulating macrophage polarization via interleukin-6. *Stem Cell Res. Ther.* 12 (1), 193. doi:10.1186/s13287-021-02270-4

Yang, X., Zhou, F., Yuan, P., Dou, G., Liu, X., Liu, S., et al. (2021a). T cell-depleting nanoparticles ameliorate bone loss by reducing activated T cells and regulating the Treg/Th17 balance. *Bioact. Mater* 6 (10), 3150–3163. doi:10.1016/j.bioactmat.2021.02.034

Yao, Z., Painter, S. L., Fanslow, W. C., Ulrich, D., Macduff, B. M., Spriggs, M. K., et al. (1995). Human IL-17: a novel cytokine derived from T cells. *J. Immunol.* 155 (12), 5483–5486. doi:10.4049/jimmunol.155.12.5483

Ye, X., Zhang, P., Xue, S., Xu, Y., Tan, J., and Liu, G. (2014). Adipose-derived stem cells alleviate osteoporosis by enhancing osteogenesis and inhibiting adipogenesis in a rabbit model. *Cytotherapy* 16 (12), 1643–1655. doi:10.1016/j.jcyt.2014.07.009

Yin, Y., Wang, Q., Xie, C., Chen, H., Jin, J., and Miao, D. (2022). Amniotic membrane mesenchymal stem cells-based therapy improves Bmi-1-deficient mandible osteoporosis through stimulating osteoblastic bone formation and inhibiting osteoclastic bone resorption. *J. Tissue Eng. Regen. Med.* 16 (6), 538–549. doi:10.1002/term.3300

Zhang, Y., Böse, T., Unger, R. E., Jansen, J. A., Kirkpatrick, C. J., and van den Beucken, J. J. J. P. (2017). Macrophage type modulates osteogenic differentiation of adipose tissue MSCs. *Cell Tissue Res.* 369 (2), 273–286. doi:10.1007/s00441-017-2598-8

Zhang, Y., Chen, J., Fu, H., Kuang, S., He, F., Zhang, M., et al. (2021). Exosomes derived from 3D-cultured MSCs improve therapeutic effects in periodontitis and experimental colitis and restore the Th17 cell/Treg balance in inflamed periodontium. *Int. J. Oral Sci.* 13 (1), 43. doi:10.1038/s41368-021-00150-4

Zhao, R., Wang, X., and Feng, F. (2016). Upregulated cellular expression of IL-17 by CD4+ T-cells in osteoporotic postmenopausal women. *Ann. Nutr. Metab.* 68 (2), 113–118. doi:10.1159/000443531

Zhu, L., Hua, F., Ding, W., Ding, K., Zhang, Y., and Xu, C. (2020). The correlation between the Th17/Treg cell balance and bone health. *Immun. Ageing* 17 (30), 30. doi:10.1186/s12979-020-00202-z

frontiers | Frontiers in Pharmacology

TYPE Review
PUBLISHED 31 July 2024
DOI 10.3389/fphar.2024.1437457

OPEN ACCESS

EDITED BY
Jie Fang,
Sichuan University, China

REVIEWED BY
Wei Huang,
Huazhong University of Science and Technology, China
Zhenting Xiang,
University of Pennsylvania, United States
Xiong Xiong,
Southwest Jiaotong University, China

*CORRESPONDENCE
Xiaojing Huang,
hxiaoj@163.com
Wen Zhou,
zhouwendentist@139.com

RECEIVED 23 May 2024
ACCEPTED 18 July 2024
PUBLISHED 31 July 2024

CITATION
Yang K, Wu Z, Zhang K, Weir MD, Xu HHK, Cheng L, Huang X and Zhou W (2024), Unlocking the potential of stimuli-responsive biomaterials for bone regeneration. *Front. Pharmacol.* 15:1437457. doi: 10.3389/fphar.2024.1437457

Unlocking the potential of stimuli-responsive biomaterials for bone regeneration

Ke Yang[1,2], Zhuoshu Wu[1,2], Keke Zhang[3], Michael D. Weir[4], Hockin H. K. Xu[4], Lei Cheng[5], Xiaojing Huang[1,2]* and Wen Zhou[1,2]*

[1]Fujian Key Laboratory of Oral Diseases & Fujian Provincial Engineering Research Center of Oral Biomaterial & Stomatological Key Lab of Fujian College and University, School and Hospital of Stomatology, Fujian Medical University, Fuzhou, China, [2]Clinical Research Center for Oral Tissue Deficiency Diseases of Fujian Province, School and Hospital of Stomatology, Fujian Medical University, Fuzhou, China, [3]School and Hospital of Stomatology, Wenzhou Medical University, Wenzhou, China, [4]Department of Biomaterials and Regenerative Dental Medicine, University of Maryland School of Dentistry, Baltimore, MD, United States, [5]State Key Laboratory of Oral Diseases & National Clinical Research Center for Oral Diseases, West China School of Stomatology & Department of Operative Dentistry and Endodontics, West China Hospital of Stomatology, Sichuan University, Chengdu, China

Bone defects caused by tumors, osteoarthritis, and osteoporosis attract great attention. Because of outstanding biocompatibility, osteogenesis promotion, and less secondary infection incidence ratio, stimuli-responsive biomaterials are increasingly used to manage this issue. These biomaterials respond to certain stimuli, changing their mechanical properties, shape, or drug release rate accordingly. Thereafter, the activated materials exert instructive or triggering effects on cells and tissues, match the properties of the original bone tissues, establish tight connection with ambient hard tissue, and provide suitable mechanical strength. In this review, basic definitions of different categories of stimuli-responsive biomaterials are presented. Moreover, possible mechanisms, advanced studies, and pros and cons of each classification are discussed and analyzed. This review aims to provide an outlook on the future developments in stimuli-responsive biomaterials.

KEYWORDS

bone regeneration, stimuli-responsive biomaterials, scaffolds, implants, composites, hydrogels

1 Introduction

Worldwide incidences of bone defects and other bone-related complications, including bone infection, bone tumor, and bone loss, have increased owing to the growing life expectancy and the aging population (Bose et al., 2023). Among all clinical available bone grafts, autogenous ones are the gold standard (Wang and Yeung, 2017). However, deficient blood supply and morbidity of donor site complications are the main limitations. Though allografts take up the second higher option, they also have several drawbacks, including secondary injury, limited resources, risk of infectious disease, and immunological rejection (De Long et al., 2007; Wei et al., 2022a). Moreover, various new bone restorative strategies have emerged, which comprise

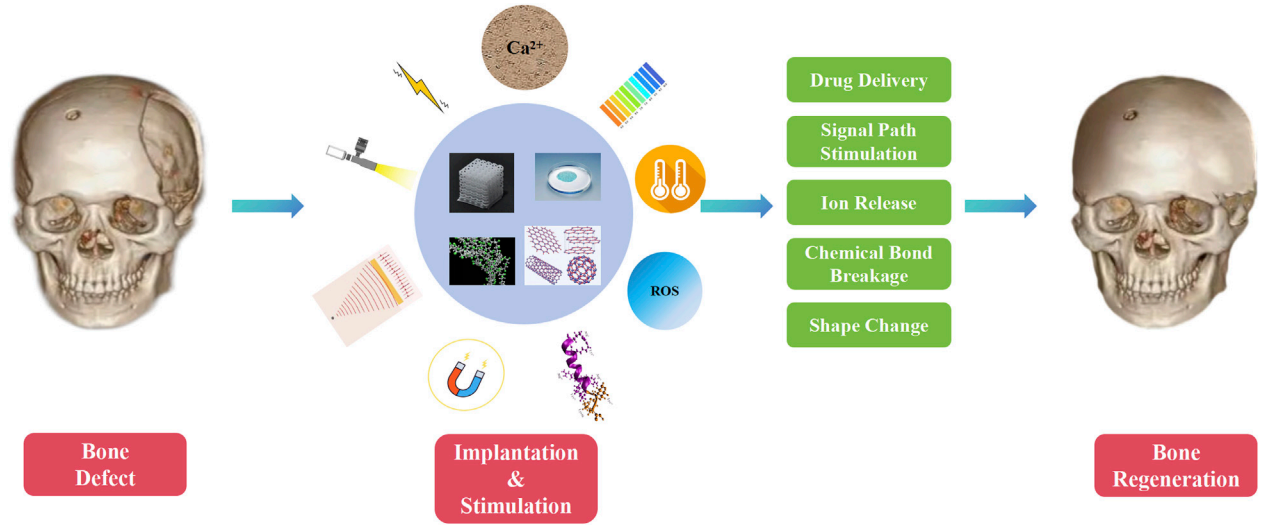

GRAPHICAL ABSTRACT

tissue-engineered periosteum and platelet-rich plasma (Fang et al., 2020; Zhang et al. (2022b). Nevertheless, because of the inadequate clinical application, their capacity for hard-tissue regeneration and drug delivery precision should be further verified (Bose et al., 2019; Fan et al., 2021; Losic, 2021). Hence, investigations on more intelligent bone grafting materials for treating bone disorders and reconstructing bone defects have radically become the focus in this field.

Bone tissue engineering (BTE) is a novel tactic for promoting bone regeneration by combining biomaterials and bioactive factors to encourage cells to migrate, attach and proliferate (Shang et al., 2021). Consequently, ideal restorative biomaterials should perform good mechanical strength, biocompatibility and steadily controllable drug release ability (Handa et al., 2022; Ni et al., 2023). Stimuli-responsive biomaterials are newly developed alternative materials for BTE, opening new frontiers in the development of scaffolds and implants. These biomaterials can mimic the dynamic nature of the native extracellular matrix, providing a more conducive environment for cell growth, differentiation, and bone regeneration. Therefore, stimuli-responsive biomaterials occupy a critical position in the development of restorative bone grafts.

Stimuli-responsive biomaterials for BTE include scaffolds, nanoparticles, biopolymers, hydrogel and so on. When these materials are exposed to certain stimuli, their mechanical properties, shape, form or drug-releasing rate may change accordingly to match the properties of the original bone tissues, establish tight connection with ambient hard tissue, and provide adequate mechanical strength (Lin et al., 2013; Islam et al., 2020; Sadowska and Ginebra, 2020; Wang et al., 2020; Shang et al., 2021). These materials are promising in clinical application. For instance, stimuli-responsive biomaterials like pH-responsive chitosan (CS) have been widely utilized in bone regeneration (Arora et al., 2023).

Stimuli-responsive biomaterials can be categorized into two main types: 1) external stimuli-responsive biomaterials; 2) internal stimuli-responsive biomaterials (Figure 1) (Wei et al., 2022a). External stimuli-responsive biomaterials include implants that can change their properties after being activated by external stimuli. The activated materials can affect the cell fate and enhance bone tissue regeneration by altering the mechanical characteristics, breaking chemical bonds, or causing other transformations (Lui et al., 2019). On the contrary, internal stimuli-responsive biomaterials are the ones that can respond to specific microenvironmental changes surrounding the lesion, such as decrease in pH, alteration of temperature, increase in reactive oxygen species (ROS), and fluctuation in enzyme levels (Du et al., 2019). Recently, stimuli-responsive biomaterials have been widely studied in controlling the release of loaded drugs (Yadav et al., 2023). By specific stimuli activating, changes are triggered in the stimuli-responsive biomaterials, which include self-assembly of peptides, breakage of chemical bonds, and alteration in release behaviors (Li et al., 2024; Mu et al., 2024). Thus, the activated materials can modulate certain cellular pathways related to the induction of bone regeneration.

In this review, recent studies on the development and mechanism of stimuli-responsive biomaterials in bone regeneration are summarized. An outlook on future advancements in stimuli-responsive biomaterials has also been provided.

2 Biomaterials responding to external stimuli

External or out-body stimuli are signals or irradiations applied outside the body (Fang et al., 2021; Montoya et al., 2021). External stimuli include electricity, light, ultrasound, and magnetic field. External stimuli-responsive biomaterials undergoes conformational changes, reversible microphase separation, or self-assembly according to the stimulus (Figure 2) (Montoya et al., 2021). Subsequently, the activated materials can affect cell

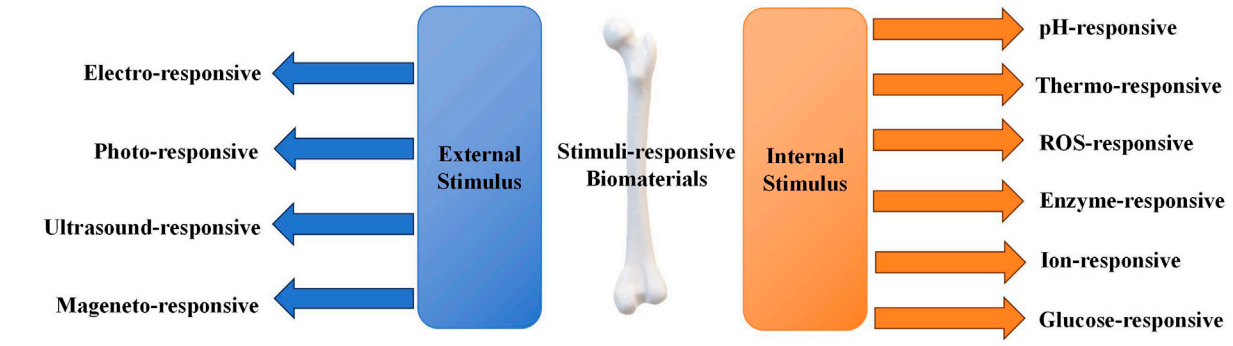

FIGURE 1
Categories of stimuli-responsive biomaterials.

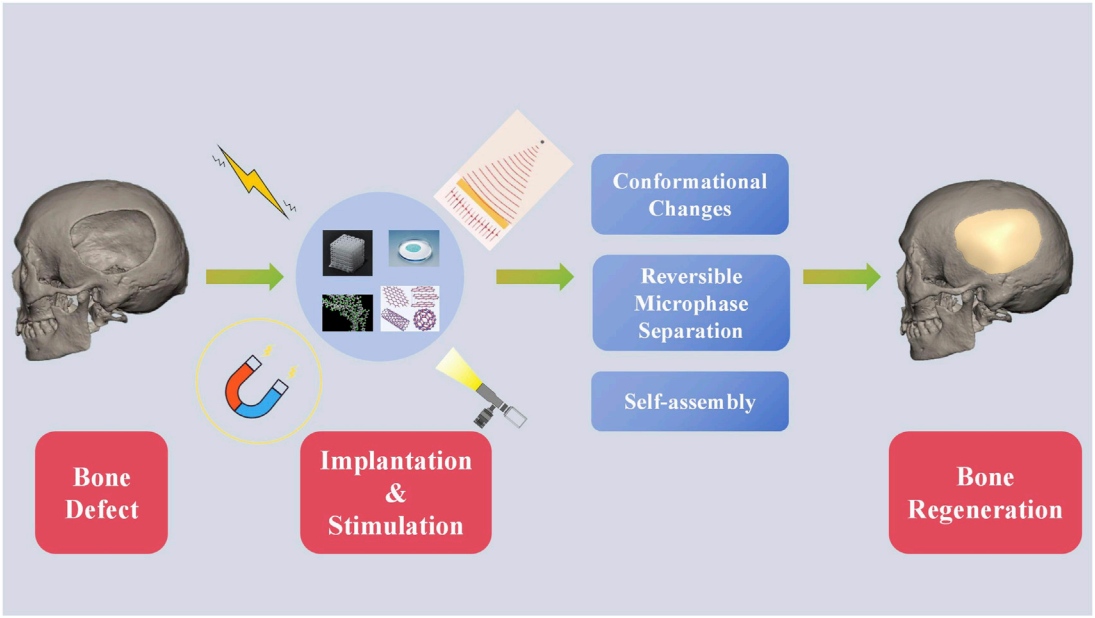

FIGURE 2
Schematics of external stimuli-responsive biomaterials for bone regeneration.

attachment, migration, and proliferation to enhance osteogenesis (Wei et al., 2022a).

2.1 Electro-responsive composites

Electrical stimulation (EStim) can improve bone regeneration by promoting bone-forming stem cells activities like migration, proliferation, differentiation, mineralization, extracellular matrix deposition, and attachment to scaffold materials (George et al., 2017; Leppik et al., 2020). Generally, there are two kinds of EStim, direct (external electric field) and indirect ones (piezoelectrical field) (Zhu et al., 2023).

When exposed to the certain external electric stimulator, electro-responsive composites can deliver localized electrical signals (Wei et al., 2022b). Followingly, these signals can stimulate the calcium–calmodulin pathway or induce the transformation of other cytokines, which form the basis of osteogenesis (Wei et al., 2022b). Under exogenous electrical stimulation, the delivered electrical signals can contribute to upregulating level of transforming growth factor-β (TGF-β), bone morphogenetic proteins-2 (BMP-2) and the expression of Runt-related transcription factor 2 (Runx2), Osteocalcin (OCN), and Osteopontin (OPN) (Fu et al., 2019; Khare et al., 2020; Wei et al., 2022b).

Zhang et al. prepared polypyrrole (PPY) nanoparticles dispersed in a chitosan matrix with BMP-2 covalently immobilized on the surface (PPY/chitosan films) (Zhang et al., 2013). When osteoblasts cultured on the electrical stimulated PPY/chitosan film, greater increasing in cellular metabolic activity, ALP activity and

mineralization over control group were observed (Zhang et al., 2013). Moreover, osteogenic gene expression analysis showed that releasing of BMP-2 and exogenous electrical stimulation did have synergistic effects on osteoblast differentiation and maturation (Zhang et al., 2013).

Piezoelectric scaffolds are biomaterials with a uniquely porous morphology (Sultana et al., 2017; Chorsi et al., 2019; Liu et al., 2023). Under mechanical stress, transient deformation of piezoelectric scaffold occurs, leading to an atomic position shift (Mao et al., 2022). This phenomenon results in the loss of the center of symmetry and induces the accumulation of charge through an ordered dipole distribution (Mao et al., 2022). Therefore, piezoelectric scaffolds can generate electrical charges in response to applied mechanical stress or deformation (Turner et al., 2001; Halperin et al., 2004; Minary-Jolandan and Yu, 2010). The stress-generated electrical signal can activate voltage-gated Ca^{2+} channels, promote displacement of C=O bonds, and favor the M2 phenotype of macrophages, leading to charge alteration on the cell membrane (Balint et al., 2014; Ud-Din and Bayat, 2014; More and Kapusetti, 2017; Murillo et al., 2017). Charge transfer promotes regenerative activities by modulating cellular behavior through molecular pathways, such as phosphatidylinositol 3-kinase (PI3K) and phosphatase and tensin homolog (Balint et al., 2014; Ud-Din and Bayat, 2014; More and Kapusetti, 2017; Murillo et al., 2017).

Representative piezoelectric scaffolds for efficient osteogenesis, including piezo-bioceramics (e.g., barium titanate ($BaTiO_3$), magnesium silicate, zinc oxide) and some piezo-biopolymers (e.g., polyvinylidene fluoride, polyhydroxybutyrate, collagen, etc.), have been extensively studied (Jacob et al., 2018; Khare et al., 2020). For example, piezoelectric $BaTiO_3$ was integrated into bioactive nano-titania ceramics as TiO_2/$BaTiO_3$ composite ceramics scaffolds (Li et al., 2009). $BaTiO_3$ could adjust the elastic modulus of the scaffolds analogous to that of human bone (Li et al., 2009). Meanwhile, the piezoelectric properties of $BaTiO_3$ also showed the enhancing effects on the bioactivity, which made the osteoblasts proliferate faster on the scaffolds *in vitro* (Li et al., 2009). Moreover, Wang's team developed a piezoelectric poly (vinylidene fluoride-trifluoroethylene) (PVDF-TrFE) scaffold (Wang et al., 2018). Under physiological loads, the scaffold in the defect area can generate electrical potential (Wang et al., 2018). Once the osteoblasts were stimulated by the scaffold surface charges, osteoblastic proliferation would be enhanced, which promoted bone regeneration in the defect area (Wang et al., 2018). Furthermore, via electrospinning, Barbosa et al. filled PVDF-TrFE scaffolds with hydroxyapatite (HAp) (PVDF-TrFE/HAp) (Barbosa et al., 2023). Besides cell proliferation enhancement, PVDF-TrFE/HAp can boost bone tissue mineralization process and enhance the osteogenic differentiation (Barbosa et al., 2023). Also, the collagen-based composite scaffolds have been reported for efficient hard tissue engineering (Zhang et al., 2023). The compressive force on collagen triggered the re-organization of dipole moment and generated negative charges, which prompted the electrical stimulation to the cells and leads to the opening of voltage-gated Ca^{2+} channels (Zhang et al., 2023). This activity can subsequently activate the expression of osteogenesis related genes like TGFβ, BMP-2 (Zhang et al., 2023).

2.2 Photo-responsive composites

Photo-responsive composites are stimuli-responsive materials with minimal damage toward normal tissues and easily remote-control properties (Zhao et al., 2019a; Jamnongpak et al., 2024). When exposed to certain wavelength of light, the drug delivery ratio, shape or surface charges of photo-responsive composites may be altered in response to different categories of light (Xing et al., 2023). Lights that are commonly used for photo-responsive therapy comprise 1) visible and 2) near-infrared (NIR) lights; their wavelengths fall between 400–700 nm and 700–1,300 nm, respectively, and can penetrate most tissues to reach the target area (Escudero et al., 2019; Wan et al., 2020). For example, *in vivo* studies verified that when an 810-nm NIR light was applied to a rat's head, 51% of the laser could transmit through the skull and 40% through the scalp and skull in the prefrontal regions (Salehpour et al., 2019).

In Zhang's work, an NIR light-responsive scaffold that contained shape memory polyurethane (SMPU) as an SMPU/Mg composite porous scaffold was utilized (Zhang et al., 2022b). Before being implanted into the defect area, shape memory composites were programmed to a certain size (Zhang et al., 2022b). Upon exposure to NIR light, the form-programmed shape memory composites recovered, achieving tight connection with the surrounding hard tissue (Figure 3) (Zhang et al., 2022b). Accordingly, the shape memory composites precisely repaired the defective bone tissue (Zhang et al., 2022b). Moreover, Yan et al. combined graphitic carbon nitride (g-C_3N_4), reduced graphene oxide (rGO) with Ti-based orthopedic implant (rGO/CN/TO) (Yan et al., 2022). Under blue LED exposure, the rGO/CN/TO ternary nanocoating exhibited higher open circuit potential and transient photocurrent density (Yan et al., 2022). This exerted greater effects on enhancing osteogenic differentiation of MC3T3-E1 cells through increasing Ca^{2+} influx under visible-light stimulation (Yan et al., 2022). Therefore, the implant was proved to be able to stimulate the regeneration of bone and nerves.

2.3 Ultrasound-responsive composites

Ultrasound-responsive composites represent a category of stimuli-responsive biomaterials with the capacity to regulate protein release, electric charges level, structure alternation, etc., by reacting to external ultrasound radiation (Brudno and Mooney, 2015). When induced by intensity-elevated ultrasound, certain chemical linkage breaks occur, such as Diels-Alder linker, fatty acid ester bonds, and phosphoester bonds (Suslick, 2013). Thereafter, the loaded bone formation-related components are released, such as cyclooxygenase 2, prostaglandin E2, short-chain fatty acid, and dopamine-functionalized hyaluronic acid ions, which can facilitate stem cells proliferation and differentiation (Veronick et al., 2018; An et al., 2021; Arrizabalaga et al., 2022; Zhou et al., 2024). Thus, combining and modulating composites with ultrasound can enhance osteoblastic response considerably and expedite the mineralization of hard issues (Moonga and Qin, 2018; Veronick et al., 2018; Fan et al., 2020).

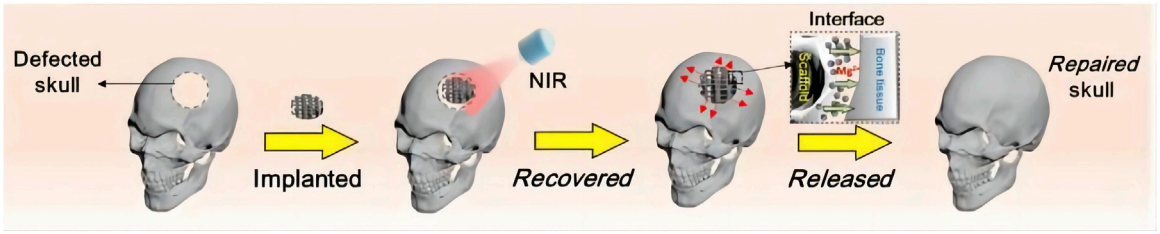

FIGURE 3
Procedure for bone regeneration using shape memory biomaterials (Reproduced with permission., Zhang et al. (2022b), Bioactive Materials).

A myriad of multifunctional biomaterials that utilize ultrasound as stimulation to enhance osteogenesis expression were fabricated recently. Among these biomaterials, the ultrasound-responsive nanofiber hydrogel (UPN@hydrogel) has provided a novel strategy for bone repair (Zhang et al., 2024). These nanofibers can be released from hydrogel in a time-dependent manner upon ultrasound stimulation (Zhang et al., 2024). Then, nanofibers could activate M2 macrophages to secrete BMP-2 and insulin-like growth factor 1, accelerating the osteogenic differentiation of BMSCs (Zhang et al., 2024). Similarly, when targeted with focused ultrasound, crosslinking chitosan also show ability in regulating BMSCs differentiation via the breakage of innate two distinct Diels-Alder linkers and the release entrapped cytokines (Pajarinen et al., 2019; Arrizabalaga et al., 2022). Moreover, combination of ultrasound irradiation and gene-activated matrix-based therapeutics also showed promising outcomes by responsively releasing osteogenesis-related peptides, such as BMP-2/7 (Nomikou et al., 2018). In addition, with assistance of ultrasound, piezoelectric nylon-11 nanoparticles (nylon-11 NPs) could promote the osteogenic differentiation of dental pulp stem cells efficiently in a noninvasive way (Ma et al., 2019). Therefore, nylon-11 NPs are promising to be used in BTE.

2.4 Magneto-responsive composites

Lately, researchers have integrated magnetic nanoparticles, such as Co_3O_4, Fe_3O_4 or $MnFe_3O_4$ nanoparticles, into various matrices to fabricate magnetic composites, exploring the potential for application as bone scaffolds or substitutes (Xu and Gu, 2014; Lui et al., 2019). When subjected to an external magnetic field, magneto-responsive nanocomposites exhibit magnetic twisting or clustering responsiveness and can function as carriers for biologically or chemically active agents via magneto-driven delivery (Cojocaru et al., 2022). By delivering bone-forming substances, such as BMP-2 and dexamethasone acetate, magneto-responsive nanocomposites are conducive for bone regeneration (Butoescu et al., 2009; Wang et al., 2012).

Magneto-responsive nanocomposites allow several processing options. Tang et al. designed a magneto-responsive $CoFe_2O_4$/P(VDF-TrFE) nanocomposite (Tang et al., 2021). Cellular osteogenic differentiation can be enhanced when the nanocomposite is exposed to magnetic field. Moreover, this material can significantly upregulate the expression level of α2β1 integrin and p-ERK, which exhibited promising potential in bone tissue repair and regeneration. Meanwhile, Wu et al. fabricated a ceramic composite containing super-paramagnetic nanoparticles (Wu et al., 2010). *In vivo* experiments demonstrated that the super-paramagnetic nanoparticles integrated in the composites accelerated new bone-like tissue formation (Wu et al., 2010).

Magnetic Resonance Imaging (MRI) is widely used for clinical examinations. It is a common intermittent pulsing electromagnetic field. When magneto-responsive nanocomposites are exposed to MRI, the stiffness of magneto-responsive nanocomposites increases due to the rearrangement of magnetic particles (Li et al., 2020). Then, integrins on the stem cell membrane transferred information about the mechanical state of the extracellular matrix into cells (Li et al., 2020). Activating osteogenic differentiation signal pathways, such as the PI3K/Akt pathway, enhances stiffness, increases the number of mitochondria, and changes cell morphology (Yan et al., 1998; Lambertini et al., 2015; Androjna et al., 2021). These results suggest that stem cell osteogenic differentiation can be regulated; MRI appears to positively affect magneto-responsive nanocomposites when used for patient examinations.

External stimuli-responsive biomaterials permit noninvasive activation and remote control (Yang et al., 2018; Lin et al., 2020; Wan et al., 2020; Zhao et al., 2020). In addition, targeted drug delivery to specific sites within the body can be achieved via out-body stimulation such as magnetic guidance (Lu et al., 2018; Lui et al., 2019). However, it is challenging to achieve optimal performance and responses. Moreover, external stimuli, such as NIR light and ultrasound, may generate heat in the tissue, leading to thermal damage (Sun D. et al., 2020; Arrizabalaga et al., 2022). Therefore, further studies are needed to improve this type of biomaterials. More details on the advantages and disadvantages of stimuli-responsive biomaterials are listed in Table 1.

3 Biomaterials responding to internal stimuli

Internal or in-body stimulus refers to signals in the microenvironment inside the body around the biomaterial (Lee et al., 2018a; Nguyen et al., 2018; Yao et al., 2019; Ding et al., 2022). These stimuli comprise of pH, temperature, ROS, enzyme ion concentration and etc. Drug carriers of internal stimulus-responsive biomaterials can be designed to respond to specific triggers, such as pH changes, ROS fluctuations, or the presence of

TABLE 1 Advantages and disadvantages of different stimuli-responsive biomaterials.

	Biomaterial	Advantages	Disadvantages	References
External stimuli-responsive biomaterials	Piezoelectricity-responsive scaffolds	1) Mechano-electrical coupling can mimic natural processes in the body where mechanical stimuli influence cellular behavior 2) The dual functionality of stress responsiveness and piezoelectricity may enhance cellular response to the scaffold	1) It is challenging to achieve optimal performance and responses 2) Studies on piezoelectric biomaterials in the repair and regeneration of hard tissues remain limited	Jacob et al. (2018), Tandon et al. (2018), Ghosh et al. (2022)
	NIR light-responsive 3D-printed shape memory composites	1) NIR light permits the noninvasive activation of the scaffold within the body 2) NIR light-responsive scaffolds can be engineered with various functionalities, such as drug release, photothermal effects, or changes in material properties, offering versatility in their applications	1) Prolonged exposure to NIR light can lead to photobleaching of the photosensitive components in the scaffold, potentially reducing their responsiveness over time 2) The depth of penetration remains limited	Yang et al. (2018), Lin et al. (2020), Wan et al. (2020), Zhao et al. (2020)
	Ultrasound-responsive hydrogels	1) Ultrasound allows for precise control over the location and timing of hydrogel activation 2) Ultrasound can be applied externally, providing remote control for activating the hydrogels	1) High-intensity ultrasound may generate heat in tissues, potentially leading to thermal damage 2) The depth of penetration is limited	Sun et al. (2020a), Arrizabalaga et al. (2022)
	Magneto-responsive nanocomposites	Targeted drug delivery to specific sites within the body can be achieved via magnetic guidance	May present biocompatibility challenges	Lu et al. (2018), Lui et al. (2019)
Internal stimuli-responsive biomaterials	pH-responsive hydrogels	1) The release of drugs or therapeutic agents from pH-responsive hydrogels can be finely controlled by pH levels 2) Can be engineered to respond to a wide range of pH values	pH changes in the body may occur in response to various factors, and unintended activation of pH-responsive hydrogels could lead to undesirable consequences	Chen et al. (2019), Zhang et al. (2020), Montoya et al. (2021)
	Thermo-responsivehydrogels	1) The state of hydrogel can be altered and easy to be injected 2) Injectable thermo-responsive hydrogels can fit into the shape of bone defect integrally	Temperature alteration cannot be controlled precisely	Yu et al. (2021), Kim et al. (2023)
	ROS-responsive scaffolds	1) Can be tailored for disease-specific activation and intervention 2) Can deliver therapeutic agents precisely in response to the pathological conditions	Reactive oxygen species generation or consumption by the scaffold may result in oxidative stress	Hayyan et al. (2016), Sun et al. (2020b), Ren et al. (2022)
	Enzyme-responsive scaffolds	1) Enable precise control over the release of therapeutic agents 2) Can be designed to mimic and interact with natural biological processes, which facilitate integration with the body's existing systems and enhances compatibility	1) Achieving a balance between sufficient stability for the scaffold and appropriate biodegradability can be challenging 2) The response to an enzymatic stimulus can in some cases depend on the age of the host	Boskey and Coleman (2010), Nguyen et al. (2018), Berillo et al. (2021)
	Ion-responsive scaffolds	Possess stable structure, low cytotoxicity, great specific surface area and versatile usage	Relating researches are limited	Simon-Yarza et al. (2018), Gao et al. (2019), Kumar et al. (2021)
	Glucose-responsive biomaterials	Effectively utilize superfluous glucose in blood to renovate the oppressed bone remodeling.	The effectiveness of osteogenesis promotion via blood sugar is not yet clear.	(Mohanty et al., 2022)

specific biomolecules. Thus, internal stimulus-responsive biomaterials are able to deliver the loaded medicine to the target area or release certain ions when the concentration of the chemical substance changes (Figure 4) (Hein et al., 2008; Lallana et al., 2012; McKay and Finn, 2014; Gregoritza and Brandl, 2015). Furthermore, the released medicine can exert an impact on the metabolism of a series of osteocytes. This level of precision minimizes the side effects and enhances the overall efficacy of the treatment. To develop a direct approach for bone regeneration, various studies focusing on internal-responsive biomaterials have been performed.

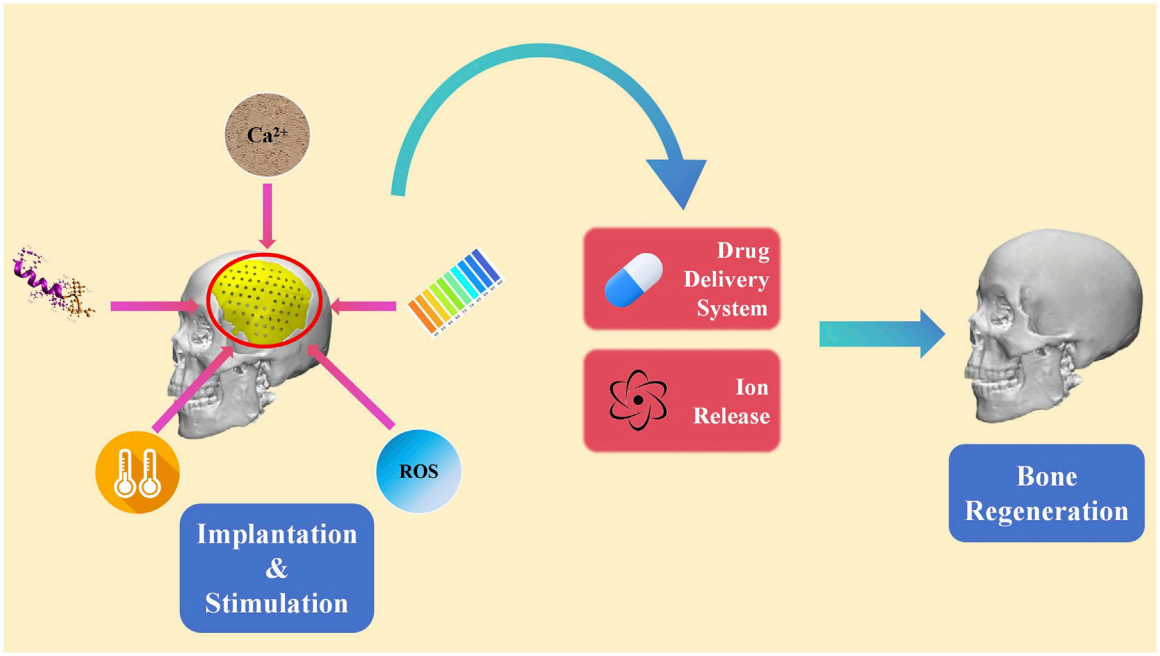

FIGURE 4
Schematics of internal stimuli-responsive biomaterials.

3.1 pH-responsive composites

The pathological circumstance, such as tumor or inflammation, is mildly acidic, whereas the physiological pH is neutral (7.0-7.4) (Swietach et al., 2014). pH-responsive composites have the capacity of reacting to specific pH levels in physiological and pathological environments (Li et al., 2023; Xu et al., 2023; Zheng et al., 2023). The composites have pH-sensitive coordination bonds, such as catechins, ferric irons, citraconic amide bonds, and Schiff base bonds. These bonds can change with the fluctuation in pH levels (Liang et al., 2021; Jo et al., 2023). Therefore, the state of composites can alter accordingly (Kocak et al., 2020; Zhu et al., 2021). Drugs related to BTE can be delivered by alteration between different states (Zhu et al., 2018; Constantin et al., 2020; Ding et al., 2022). When sensing the change in pH levels, these composites can set up targeted and localized drug delivery (Liu et al., 2017). Finally, certain drugs are able to upregulate the expression of Runx2, osterix, OCN, and OPN and support mesenchymal stem cells proliferation, adhesion, osteoinduction, and biocompatibility, which are essential to regenerate bone tissues (Lavanya et al., 2020).

To fabricate composites with pH-responsive drug release property, Tang et al. designed a hydrogel with a alendronate-modified oxidized alginate network (GelMA-OSA@ALNDN hydrogel) in which Schiff base bonds were distributed uniformly (Tang et al., 2022). Alendronate (ALN) is a type of bisphosphonate with promising hard tissue repair functions (Wang et al., 2021). Therefore, by reacting to changing pH level, GelMA-OSA@ALNDN hydrogel can maintain a stable drug concentration to activate the repair process in the defective bone area (Tang et al., 2022). Besides, an asymmetric microfluidic/chitosan hydrogel, poly [2-(dimethylamino) ethyl methacrylate] (PDMAEMA) hydrogel, was successfully fabricated (Chen et al., 2023). The hydrogel was demonstrated with the ability of achieving pH-responsive drug release to promote osteoblast proliferation and combating with bacterial infection simultaneously (Figure 5) (Chen et al., 2023).

Currently, researchers tend to synthetize CS-based biomaterials, which are natural polymers with enzymatic biodegradability, pH sensitivity, polycationic nature, extensive application, etc. (Almajidi et al., 2023). For example, pH-responsive carboxymethyl chitosan/amorphous calcium phosphate (CMC-ACP) hydrogel system was designed (Zhao et al., 2019b). This hydrogel system was found to significantly upregulate the expression of bone markers, such as Runx2, osterix, OCN, and OPN (Zhao et al., 2019b). *In vivo* findings also showed that the injectable hydrogel strongly enhances the efficiency and maturity of the bone regeneration while suppressing the bone resorption (Zhao et al., 2019b). Furthermore, Ressler et al. synthesized a pH-responsive chitosan-hydroxyapatite hydrogel (CS/HAp/$NaHCO_3$) (Ressler et al., 2018). Activating by acidic microenvironment, CS/HAp/$NaHCO_3$ can improve stability, homogenous dispersion of mesenchymal stem cell (MSCs) and promote calcium phosphate deposits and extracellular matrix (ECM) mineralization (Ressler et al., 2018).

3.2 Thermo-responsive composites

Phase transition temperature refers to the temperature required to induce a change between phases, such as solid and liquid, sol and gel (Scott, 1974). Thermo-responsive composites exhibit reversible phase transition effect in response to change in temperature (Kim and Matsunaga, 2017). The rapid shift from a sol to a gel state at physiologic temperature can optimize the release of loaded TGF-β, drugs or ions, which has positive effect in boosting osteoblasts adherence, differentiation and proliferation (Duan et al., 2020; Khan et al., 2022).

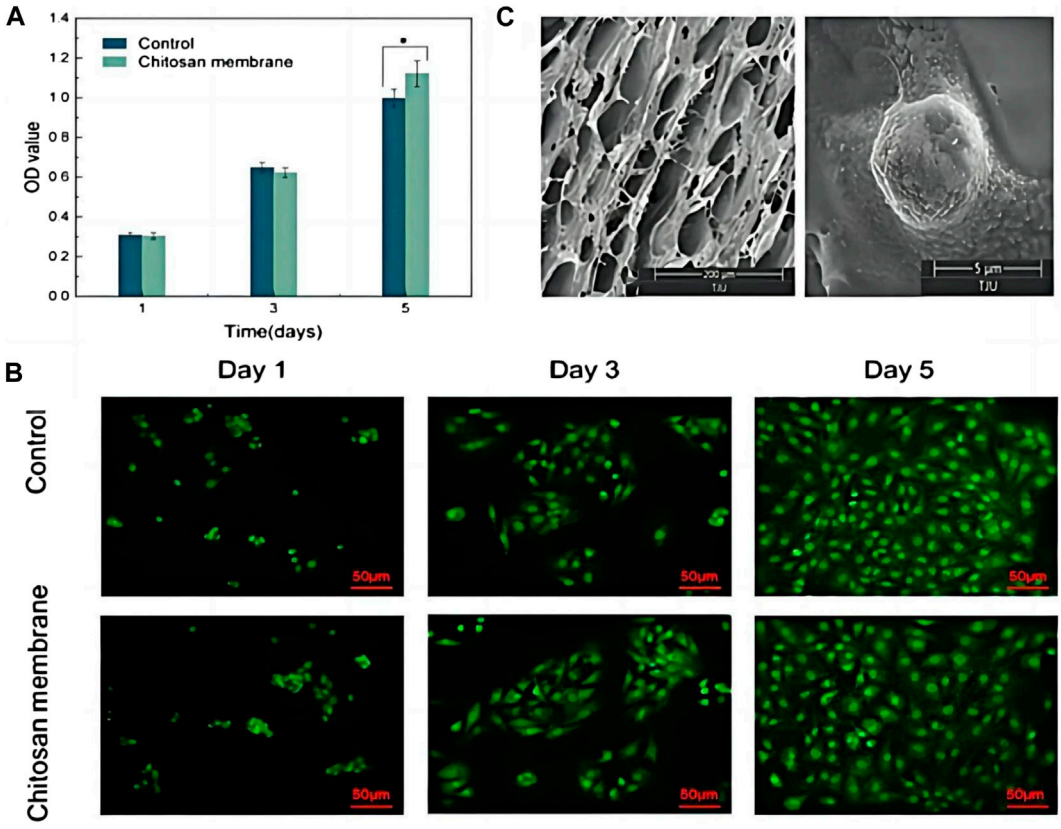

FIGURE 5
(A) CCK-8 assay of osteoblasts seeded into wells (Control) and on the surface of the chitosan membrane. *$p < 0.05$. **(B)** LSCM images of osteoblasts in wells and attached to the chitosan surface. Scale bar in LSCM images is 50 μm. **(C)** SEM images of the surface of chitosan membrane in 200 μm scale (left), and osteoblasts attached on the chitosan surface after 5 days culturing in 5 μm scale (right). Reproduced with permission., Chen et al. (2023), MDPI.

To address the issue of the efficient local delivery of BMP-2 to complex bone fracture sites, BMP-2-functionalized MgFe-layered double hydroxide nanosheets were integrated into chitosan/silk fibroin hydrogels (CSP-LB hydrogel) (Lv et al., 2023). This thermo-responsive hydrogel solution can be injected to fit the defects precisely and then solidify quickly under 37°C condition (Lv et al., 2023). The solidified hydrogel showed 4.5-fold bone volume and 3.6-fold bone mineral density increment compared with that of the control group (Lv et al., 2023). Simultaneously, CS thermogels, supported with demineralized bone matrix, could retain more cells and provide better strength for efficient chondrogenesis in both *in vitro* and *in vivo* (Huang et al., 2014). Wu et al. constructed a thermo-sensitive N-isopropylacrylamide-chitosan hydrogel (Wu et al., 2018). This hydrogel ensured osteoinduction and biocompatibility (Wu et al., 2018). And these properties were proved by *in vitro* tests with infrapatellar fat pad-derived mesenchymal stem cells (IFP-MSCs), fibroblasts (NIH-3T3), and osteoblasts (MC3T3-E1) (Wu et al., 2018).

3.3 ROS-responsive composites

ROS are a family of reactive chemical species that contain oxygen (Zorov et al., 2014). ROS have been considered pivotal signaling molecules in many physiological processes and are usually overproduced in various inflammatory tissues (Yao et al., 2019). These molecules can influence the differentiation of osteoclasts (Badila et al., 2022). ROS-responsive composites are a series of biomaterials that can target the high-level ROS in bone-related diseases (Ren et al., 2022). These scaffolds possess unique features under oxidative conditions (Figure 6) and can fit in different bone defects to achieve bone regeneration (Lee et al., 2013; Xu et al., 2016; Ren et al., 2022). Moreover, these materials can support osteocyte adhesion and growth owing to their porous structures to boost the BTE (Yao et al., 2019).

In order to renovate the adverse effect of ROS stimulation to bone regeneration, Martin et al. synthesized a layer-by-layer-compatible polycation (Yamaguchi et al., 1991). This polycation presented an ROS dose-dependent delivery of the preloaded BMP-2 and promoted the cellular proliferation of progenitor cells and spurred stem cell differentiation into bone-forming osteoblasts (Yamaguchi et al., 1991; Tian et al., 2022). Moreover, a 3D-printed ROS-responsive molybdenum (Mo)-containing bioactive glass ceramic scaffold was developed recently (Lee et al., 2018b). The scaffold decreased mitochondrial ROS produced by osteoclasts and increased the expressions of certain genes related to osteogenesis, such as matrix metalloprotein (MMP), NFATc1, and RANKL (Lee et al., 2018b). In the study by Lee et al., 3-dimension

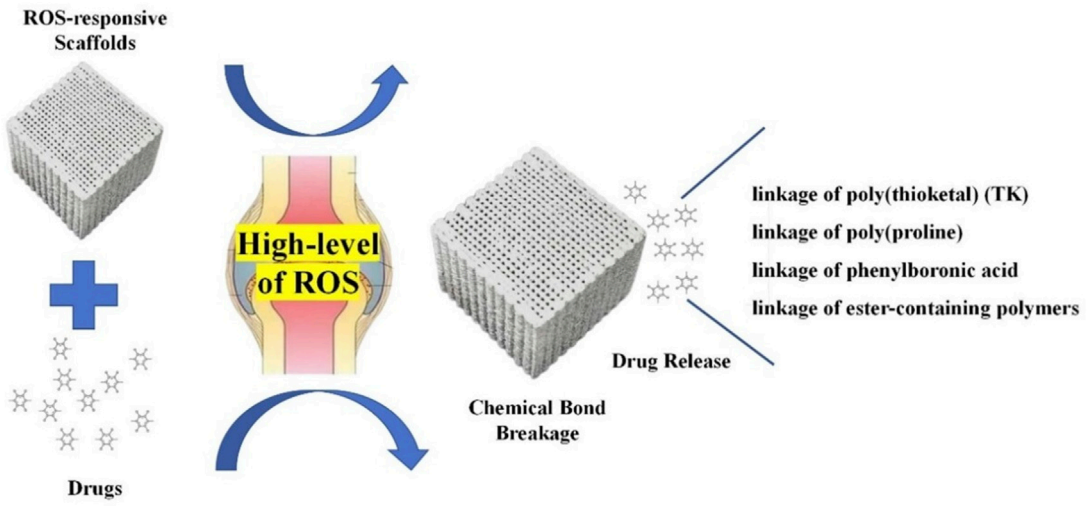

FIGURE 6
Unique features of ROS-responsive biomaterials under oxidative conditions.

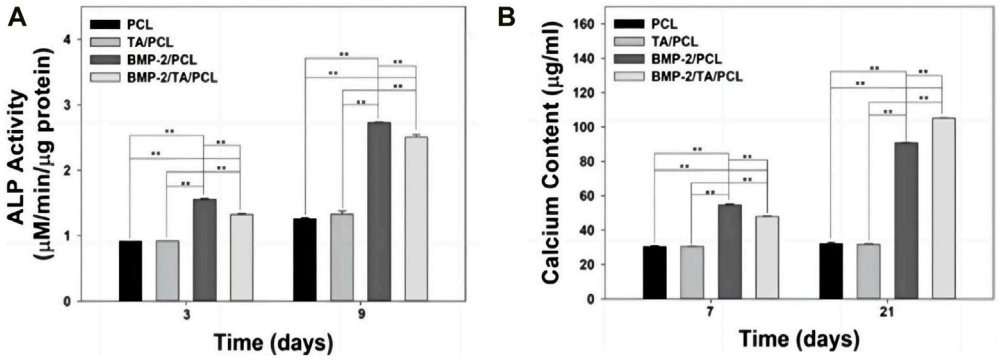

FIGURE 7
(A) Alkaline phosphatase activity and **(B)** calcium deposition of MC3T3-E1 cells cultured on PCL, TA/PCL, BMP-2/PCL, and BMP-2/TA/PCL scaffolds. Error bars represent mean ± SD. Reproduced with permission., Yang et al. (2020), MDPI.

polycaprolactone (PCL) scaffold with tannic acid (TA) and BMP-2 (BMP-2/TA/PCL) was fabricated (Yang et al., 2020). In the ROS-overproduction environment, the BMP-2/TA/PCL scaffold maintained the sustained and controlled release of BMP-2, which stimulated the osteogenic differentiation of MC3T3-E1 cells by increasing ALP activity and calcium deposition (Figure 7) (Yang et al., 2020).

3.4 Enzyme-responsive composites

Enzymes play pivotal roles in growth, blood coagulation, wound healing, respiration, digestion, and various other physiological processes (Yang et al., 2020). Disruptions in the expressions or activities of enzymes lead to severe pathological conditions, including but not limited to cancer, cardiovascular disorders, inflammation, and degenerative arthritis (Hu et al., 2014). Composites responsive to enzymes are activated by the selective catalytic activities of specific enzymes (Zhang et al., 2016). For example, type II collagen forms the base for the formation of cartilage and bone (Anjum et al., 2016; Ding et al., 2020; Fischer et al., 2021). Local gene expression and the secretion of type II collagen can be regulated by the overexpression of enzymes such as polygalacturonase, BMPs, and matrix metalloprotein (Anjum et al., 2016; Ding et al., 2020; Fischer et al., 2021).

Blood coagulation factor XIII (FXIIIa) is closely related to bone tissue repair. This enzyme can regulate the RANKL/RANK system in MSCs, augmenting osteoblast differentiation and mineralization (Ikebuchi et al., 2018; Dang et al., 2023). Therefore, Anjum et al. built an enzymatically formed chondroitin sulfate and poly (ethylene glycol) (PEG)-based hybrid hydrogel scaffold system (Anjum et al., 2016). Induced by FXIIIa-catalyzed glutaminating reaction, the degraded hydrogel released BMP-2, facilitating the integration of the newly formed bone tissue (Anjum et al., 2016).

3.5 Ion-responsive scaffolds

Inbody ion level may shift in some physiological and pathological environment (Mészáros et al., 2022; Ye et al., 2022; Adella and de Baaij, 2023). Therefore, the fluctuation of ions concentration like Na^+, K^+, Ca^{2+} can be used as the internal stimulation to activate the ion-responsive scaffolds (Zhou et al., 2013; Xu et al., 2015). Certain ions loaded on the porous surface of the ion-responsive scaffolds would be displaced when the materials were activated. The released ions could automatically combine with hydroxy phosphates (Wang et al., 2023). The self-combination results in large hydroxyapatite-like crystals *in vivo*, accelerating bone remineralization and regeneration (Zhou et al., 2013; Gao et al., 2021; Wang et al., 2023).

Sun et al. used melt electrowritten printing technology to design a mineralized zeolitic imidazolate framework-8/polycaprolactone (ZIF-8/PCL) scaffold (Wang et al., 2023). In a simulated body fluid solution, Zn-N bonds and hydrogen bonds in ZIF-8 slightly decomposed because of the competitive binding of Ca ions, forming excess insoluble zinc hydroxy phosphates (Wang et al., 2023). Apatite and zinc positively promote bone regeneration by rising the biocompatibility of biomaterials and promoting tissue integration (Su et al., 2019; Gao et al., 2021). Accordingly, ZIF-8 showed a favorable impact on promoting osteogenesis. Moreover, by mixing ZIF-8 and PCL, the scaffold presented low inflammatory responses and increased biocompatibility (Wang et al., 2023).

3.6 Glucose-responsive biomaterials

Diabetes mellitus (DM) is an intricate disorder of glucose metabolism. The incidence of DM is projected to reach 10.2% by 2030 and 10.9% by 2045 (Saeedi et al., 2019). The irregular hyperglycemic environment makes the cells and tissues in dysfunction and hinder the osseointegration process (Khosla et al., 2021). Hence, biomaterials can effectively utilize superfluous glucose in blood to renovate the oppressed bone remodeling are fairly in need. And series glucose-responsive biomaterials have emerged. For instance, a functional glucose-responsive immunomodulation-assisted periosteal regeneration composite material, Polylactic Acid/Collagen I/Liposome-APY29 (PCLA), was constructed (Qiao et al., 2023). In the DM microenvironment, the high glucose can promote the combination of hydroxyl groups grafted in the glucose-responsive composites (Mohanty et al., 2022; Qiao et al., 2023). This makes the composite surface changes from hydrophobic to hydrophilic, which is beneficial to promote cell adhesion and proliferation (Mohanty et al., 2022; Qiao et al., 2023). Meanwhile, by blocking the IREα/NOD-like/NF-κB signaling pathway, PCLA can remodel the pathologic diabetic microenvironment into a regenerative microenvironment (Qiao et al., 2023). Moreover, He et al. devised a glucose-primed orthopedic polyetheretherketone (PEEK) implant (sP-P@C-G) composed of Cu-chelated metal-polyphenol network (hauberk coating) and glucose oxidase (GOx) (He et al., 2023). In hyperglycemic microenvironment, glucose-responsive enzymatic cascade can be activated by GOx to produce endogenous H_2O_2 (He et al., 2023). Then, dopamine (DA) anchor onto PEEK implant surfaces in the alkaline environment via self-polymerization (He et al., 2023). DA shows promising ability on facilitating cell attachment, which endows sP-P@C-G with appealing biocompatibility and outstanding osteogenicity (Chen et al., 2017; He et al., 2023).

When compared with external stimuli-responsive biomaterials, the primary benefit of internal stimuli-responsive biomaterials lies in their capacity for activation without external stimuli (Berillo et al., 2021). These materials may lower the cost of purchasing certain external machines and alleviate the workload of treatment (Boskey and Coleman, 2010). However, changes in the specific stimuli may happen under various conditions and may lead to the unintended activation of the materials (Chen et al., 2019; Zhang et al., 2020; Montoya et al., 2021). In addition, achieving a balance between sufficient stability of the materials and appropriate biodegradability can be challenging (Boskey and Coleman, 2010; Nguyen et al., 2018; Berillo et al., 2021).

4 Conclusion

Stimuli-responsive biomaterials have been considerably explored and have garnered substantial attention. As the interdisciplinary collaboration among materials science, biology, and medicine continues to flourish, the future holds exciting prospects for stimuli-responsive biomaterials. Nonetheless, despite the promising bone regeneration effect, stimuli-responsive biomaterials are still in infancy with challenges need to be settled:

1) Due to insufficient sample size, inadequate simulated conditions and deficient number of experiments, the clinical application evidence for most stimuli-responsive biomaterials is still limited. Therefore, more high-quality studies and preclinical studies are needed.
2) More and more studies tend to design multiple stimulation-responsive biomaterials. However, it remains to be discussed that whether applying two or more stimulus would obtain better bone regeneration effect than single one.
3) Proper application conditions for valid osteogenesis need to be verified. For example, feasible pH stimulation range for optimal bone regeneration effect, suitable magnetic field strength for BTE, etc.
4) Current synthetic processes of stimuli-responsive biomaterials are generally time-consuming and complicated. Thus, the exploration of safer and more efficient synthetic processes is necessary.

In a nutshell, although certain challenges persist and clinical translation remains a formidable task, it is conceivable that the integration of intelligent stimuli-responsive materials holds considerable promise for transformative biomedical applications in the future. Consequently, there is still a long way to go to reach the optimum of ideal stimuli-responsive biomaterials for bone regeneration.

Author contributions

KY: Investigation, Methodology, Writing–original draft, Writing–review and editing. ZW: Writing–original draft. KZ: Writing–original draft, Writing–review and editing. MW: Conceptualization, Writing–review and editing. HX: Writing–original draft, Writing–review and editing. LC: Writing–original draft, Writing–review and editing. XH:

Conceptualization, Funding acquisition, Project administration, Writing–review and editing, Writing–original draft. WZ: Conceptualization, Funding acquisition, Project administration, Writing–original draft, Writing–review and editing.

Funding

The author(s) declare that financial support was received for the research, authorship, and/or publication of this article. This work was supported by the Joint Funds for the innovation of science and Technology, Fujian province (Grant number: 2021Y9026), Introduced Talents Grant of School and Hospital of Stomatology Fujian Medical University (Grant number: 2023KQYJ01), and Joint Funds for the innovation of science and Technology, Fujian province (Grant number: 2023Y9223).

Conflict of interest

The authors declare that the research was conducted in the absence of any commercial or financial relationships that could be construed as a potential conflict of interest.

The handling editor JF declared a shared parent affiliation with the author LC at the time of review.

Publisher's note

References

Adella, A., and de Baaij, J. H. F. (2023). Mtor signaling in renal ion transport. *Acta Physiol. (Oxf)* 238, e13960. doi:10.1111/apha.13960

Almajidi, Y. Q., Gupta, J., Sheri, F. S., Zabibah, R. S., Faisal, A., Ruzibayev, A., et al. (2023). Advances in chitosan-based hydrogels for pharmaceutical and biomedical applications: a comprehensive review. *Int. J. Biol. Macromol.* 253, 127278. doi:10.1016/j.ijbiomac.2023.127278

An, J. Y., Um, W., You, D. G., Song, Y., Lee, J., Van Quy, N., et al. (2021). Gold-installed hyaluronic acid hydrogel for ultrasound-triggered thermal elevation and on-demand cargo release. *Int. J. Biol. Macromol.* 193, 553–561. doi:10.1016/j.ijbiomac.2021.10.071

Androjna, C., Yee, C. S., White, C. R., Waldorff, E. I., Ryaby, J. T., Zborowski, M., et al. (2021). A comparison of alendronate to varying magnitude pemf in mitigating bone loss and altering bone remodeling in skeletally mature osteoporotic rats. *Bone* 143, 115761. doi:10.1016/j.bone.2020.115761

Anjum, F., Lienemann, P. S., Metzger, S., Biernaskie, J., Kallos, M. S., and Ehrbar, M. (2016). Enzyme responsive gag-based natural-synthetic hybrid hydrogel for tunable growth factor delivery and stem cell differentiation. *Biomaterials* 87, 104–117. doi:10.1016/j.biomaterials.2016.01.050

Arora, S., Das, G., Alqarni, M., Grover, V., Manzoor Baba, S., Saluja, P., et al. (2023). Role of chitosan hydrogels in clinical dentistry. *Gels* 9, 698. doi:10.3390/gels9090698

Arrizabalaga, J. H., Smallcomb, M., Abu-Laban, M., Liu, Y., Yeingst, T. J., Dhawan, A., et al. (2022). Ultrasound-responsive hydrogels for on-demand protein release. *ACS Appl. Bio Mater* 5, 3212–3218. doi:10.1021/acsabm.2c00192

Badila, A. E., Radulescu, D. M., Ilie, A., Niculescu, A. G., Grumezescu, A. M., and Radulescu, A. R. (2022). Bone regeneration and oxidative stress: an updated overview. *Antioxidants (Basel)* 11, 318. doi:10.3390/antiox11020318

Balint, R., Cassidy, N. J., and Cartmell, S. H. (2014). Conductive polymers: towards a smart biomaterial for tissue engineering. *Acta Biomater.* 10, 2341–2353. doi:10.1016/j.actbio.2014.02.015

Barbosa, F., Garrudo, F. F. F., Alberte, P. S., Resina, L., Carvalho, M. S., Jain, A., et al. (2023). Hydroxyapatite-filled osteoinductive and piezoelectric nanofibers for bone tissue engineering. *Sci. Technol. Adv. Mater* 24, 2242242. doi:10.1080/14686996.2023.2242242

Berillo, D., Yeskendir, A., Zharkinbekov, Z., Raziyeva, K., and Saparov, A. (2021). Peptide-based drug delivery systems. *Med. Kaunas.* 57, 1209. doi:10.3390/medicina57111209

Bose, S., Sarkar, N., and Jo, Y. (2023). Natural medicine delivery from 3d printed bone substitutes. *J. Control Release* 365, 848–875. doi:10.1016/j.jconrel.2023.09.025

Bose, S., Traxel, K. D., Vu, A. A., and Bandyopadhyay, A. (2019). Clinical significance of three-dimensional printed biomaterials and biomedical devices. *MRS Bull.* 44, 494–504. doi:10.1557/mrs.2019.121

Boskey, A. L., and Coleman, R. (2010). Aging and bone. *J. Dent. Res.* 89, 1333–1348. doi:10.1177/0022034510377791

Brudno, Y., and Mooney, D. J. (2015). On-demand drug delivery from local depots. *J. Control Release* 219, 8–17. doi:10.1016/j.jconrel.2015.09.011

Butoescu, N., Seemayer, C. A., Foti, M., Jordan, O., and Doelker, E. (2009). Dexamethasone-containing plga superparamagnetic microparticles as carriers for the local treatment of arthritis. *Biomaterials* 30, 1772–1780. doi:10.1016/j.biomaterials.2008.12.017

Chen, H., Qin, Z., Zhao, J., He, Y., Ren, E., Zhu, Y., et al. (2019). Cartilage-targeting and dual mmp-13/ph responsive theranostic nanoprobes for osteoarthritis imaging and precision therapy. *Biomaterials* 225, 119520. doi:10.1016/j.biomaterials.2019.119520

Chen, H., Tan, W., Tong, T., Shi, X., Ma, S., and Zhu, G. (2023). A ph-responsive asymmetric microfluidic/chitosan device for drug release in infective bone defect treatment. *Int. J. Mol. Sci.* 24, 4616. doi:10.3390/ijms24054616

Chen, X., Cortez-Jugo, C., Choi, G. H., Björnmalm, M., Dai, Y., Yoo, P. J., et al. (2017). Patterned poly(dopamine) films for enhanced cell adhesion. *Bioconjug Chem.* 28, 75–80. doi:10.1021/acs.bioconjchem.6b00544

Chorsi, M. T., Curry, E. J., Chorsi, H. T., Das, R., Baroody, J., Purohit, P. K., et al. (2019). Piezoelectric biomaterials for sensors and actuators. *Adv. Mater* 31, e1802084. doi:10.1002/adma.201802084

Cojocaru, F.-D., Balan, V., and Verestiuc, L. (2022). Advanced 3d magnetic scaffolds for tumor-related bone defects. *Int. J. Mol. Sci.* 23, 16190. doi:10.3390/ijms232416190

Constantin, M., Bucatariu, S., Ascenzi, P., Butnaru, M., and Fundueanu, G. (2020). Smart drug delivery system activated by specific biomolecules. *Mater Sci. Eng. C Mater Biol. Appl.* 108, 110466. doi:10.1016/j.msec.2019.110466

Dang, Y., Zhang, Y., Jian, M., Luo, P., Anwar, N., Ma, Y., et al. (2023). Advances of blood coagulation factor xiii in bone healing. *Tissue Eng. Part B Rev.* 29, 591–604. doi:10.1089/ten.TEB.2023.0016

De Long, W. G., Jr., Einhorn, T. A., Koval, K., McKee, M., Smith, W., Sanders, R., et al. (2007). Bone grafts and bone graft substitutes in orthopaedic trauma surgery. A critical analysis. *J. Bone Jt. Surg. Am.* 89, 649–658. doi:10.2106/jbjs.F.00465

Ding, H., Tan, P., Fu, S., Tian, X., Zhang, H., Ma, X., et al. (2022). Preparation and application of ph-responsive drug delivery systems. *J. Control Release* 348, 206–238. doi:10.1016/j.jconrel.2022.05.056

Ding, Y., Hao, Y., Yuan, Z., Tao, B., Chen, M., Lin, C., et al. (2020). A dual-functional implant with an enzyme-responsive effect for bacterial infection therapy and tissue regeneration. *Biomater. Sci.* 8, 1840–1854. doi:10.1039/c9bm01924c

Du, Y., Guo, J. L., Wang, J., Mikos, A. G., and Zhang, S. (2019). Hierarchically designed bone scaffolds: from internal cues to external stimuli. *Biomaterials* 218, 119334. doi:10.1016/j.biomaterials.2019.119334

Duan, J., Huang, Y., Zong, S., and Jiang, J. (2020). Preparation and drug release properties of a thermo sensitive Ga hydrogel. *Polym. (Basel)* 13, 119. doi:10.3390/polym13010119

Escudero, J. S. B., Perez, M. G. B., de Oliveira Rosso, M. P., Buchaim, D. V., Pomini, K. T., Campos, L. M. G., et al. (2019). Photobiomodulation therapy (pbmt) in bone repair: a systematic review. *Injury* 50, 1853–1867. doi:10.1016/j.injury.2019.09.031

Fan, B., Guo, Z., Li, X., Li, S., Gao, P., Xiao, X., et al. (2020). Electroactive barium titanate coated titanium scaffold improves osteogenesis and osseointegration with low-intensity pulsed ultrasound for large segmental bone defects. *Bioact. Mater* 5, 1087–1101. doi:10.1016/j.bioactmat.2020.07.001

Fan, L., Guan, P., Xiao, C., Wen, H., Wang, Q., Liu, C., et al. (2021). Exosome-functionalized polyetheretherketone-based implant with immunomodulatory property for enhancing osseointegration. *Bioact. Mater* 6, 2754–2766. doi:10.1016/j.bioactmat.2021.02.005

Fang, J., Wang, X., Jiang, W., Zhu, Y., Hu, Y., Zhao, Y., et al. (2020). Platelet-rich plasma therapy in the treatment of diseases associated with orthopedic injuries. *Tissue Eng. Part B Rev.* 26, 571–585. doi:10.1089/ten.TEB.2019.0292

Fang, R., Pi, J., Wei, T., Ali, A., and Guo, L. (2021). Stimulus-responsive polymers based on polypeptoid skeletons. *Polymers* 13, 2089. doi:10.3390/polym13132089

Fischer, N. G., Chen, X., Astleford-Hopper, K., He, J., Mullikin, A. F., Mansky, K. C., et al. (2021). Antimicrobial and enzyme-responsive multi-peptide surfaces for bone-anchored devices. *Mater Sci. Eng. C Mater Biol. Appl.* 125, 112108. doi:10.1016/j.msec.2021.112108

Fu, J., Liu, X., Tan, L., Cui, Z., Zheng, Y., Liang, Y., et al. (2019). Photoelectric-responsive extracellular matrix for bone engineering. *ACS Nano* 13, 13581–13594. doi:10.1021/acsnano.9b08115

Gao, L., Chen, Q., Gong, T., Liu, J., and Li, C. (2019). Recent advancement of imidazolate framework (Zif-8) based nanoformulations for synergistic tumor therapy. *Nanoscale.* 11, 21030–21045. doi:10.1039/c9nr06558j

Gao, X., Xue, Y., Zhu, Z., Chen, J., Liu, Y., Cheng, X., et al. (2021). Nanoscale zeolitic imidazolate framework-8 activator of canonical mapk signaling for bone repair. *ACS Appl. Mater Interfaces* 13, 97–111. doi:10.1021/acsami.0c15945

George, P. M., Bliss, T. M., Hua, T., Lee, A., Oh, B., Levinson, A., et al. (2017). Electrical preconditioning of stem cells with a conductive polymer scaffold enhances stroke recovery. *Biomaterials* 142, 31–40. doi:10.1016/j.biomaterials.2017.07.020

Ghosh, S., Qiao, W., Yang, Z., Orrego, S., and Neelakantan, P. (2022). Engineering dental tissues using biomaterials with piezoelectric effect: current progress and future perspectives. *J. Funct. Biomater.* 14, 8. doi:10.3390/jfb14010008

Gregoritza, M., and Brandl, F. P. (2015). The diels-alder reaction: a powerful tool for the design of drug delivery systems and biomaterials. *Eur. J. Pharm. Biopharm.* 97, 438–453. doi:10.1016/j.ejpb.2015.06.007

Halperin, C., Mutchnik, S., Agronin, A., Molotskii, M., Urenski, P., Salai, M., et al. (2004). Piezoelectric effect in human bones studied in nanometer scale. *Nano Lett.* 4 (7), 1253–1256. doi:10.1021/nl049453i

Handa, M., Singh, A., Flora, S. J. S., and Shukla, R. (2022). Stimuli-responsive polymeric nanosystems for therapeutic applications. *Curr. Pharm. Des.* 28, 910–921. doi:10.2174/1381612827666211208150210

Hayyan, M., Hashim, M. A., and AlNashef, I. M. (2016). Superoxide ion: generation and chemical implications. *Chem. Rev.* 116, 3029–3085. doi:10.1021/acs.chemrev.5b00407

He, M., Wang, H., Han, Q., Shi, X., He, S., Sun, J., et al. (2023). Glucose-primed peek orthopedic implants for antibacterial therapy and safeguarding diabetic osseointegration. *Biomaterials* 303, 122355. doi:10.1016/j.biomaterials.2023.122355

Hein, C. D., Liu, X. M., and Wang, D. (2008). Click chemistry, a powerful tool for pharmaceutical sciences. *Pharm. Res.* 25, 2216–2230. doi:10.1007/s11095-008-9616-1

Hu, Q., Katti, P. S., and Gu, Z. (2014). Enzyme-responsive nanomaterials for controlled drug delivery. *Nanoscale* 6, 12273–12286. doi:10.1039/c4nr04249b

Huang, H., Zhang, X., Hu, X., Shao, Z., Zhu, J., Dai, L., et al. (2014). A functional biphasic biomaterial homing mesenchymal stem cells for *in vivo* cartilage regeneration. *Biomaterials* 35, 9608–9619. doi:10.1016/j.biomaterials.2014.08.020

Ikebuchi, Y., Aoki, S., Honma, M., Hayashi, M., Sugamori, Y., Khan, M., et al. (2018). Coupling of bone resorption and formation by rankl reverse signalling. *Nature* 561, 195–200. doi:10.1038/s41586-018-0482-7

Islam, M. M., Shahruzzaman, M., Biswas, S., Nurus Sakib, M., and Rashid, T. U. (2020). Chitosan based bioactive materials in tissue engineering applications-a review. *Bioact. Mater* 5, 164–183. doi:10.1016/j.bioactmat.2020.01.012

Jacob, J., More, N., Kalia, K., and Kapusetti, G. (2018). Piezoelectric smart biomaterials for bone and cartilage tissue engineering. *Inflamm. Regen.* 38, 2. doi:10.1186/s41232-018-0059-8

Jamnongpak, W., Tiptipakorn, S., Arumugam, H., Charoensuk, K., Karagiannidis, P., and Rimdusit, S. (2024). Development of nir light-responsive shape memory composites based on bio-benzoxazine/bio-urethane copolymers reinforced with graphene. *Nanoscale Adv.* 6, 499–510. doi:10.1039/d3na00647f

Jo, M. J., Shin, H. J., Yoon, M. S., Kim, S. Y., Jin, C. E., Park, C. W., et al. (2023). Physicochemical, pharmacokinetic, and toxicity evaluation of Soluplus® polymeric micelles encapsulating fenbendazole. *Pharmaceutics* 12, 1000. doi:10.3390/pharmaceutics12101000

Khan, M. U. A., Al-Arjan, W. S., Ashammakhi, N., Haider, S., Amin, R., and Hasan, A. (2022). Multifunctional bioactive scaffolds from arx-G-(Zn@Rgo)-Hap for bone tissue engineering: *in vitro* antibacterial, antitumor, and biocompatibility evaluations. *ACS Appl. Bio Mater* 5, 5445–5456. doi:10.1021/acsabm.2c00777

Khare, D., Basu, B., and Dubey, A. K. (2020). Electrical stimulation and piezoelectric biomaterials for bone tissue engineering applications. *Biomaterials* 258, 120280. doi:10.1016/j.biomaterials.2020.120280

Khosla, S., Samakkarnthai, P., Monroe, D. G., and Farr, J. N. (2021). Update on the pathogenesis and treatment of skeletal fragility in type 2 diabetes mellitus. *Nat. Rev. Endocrinol.* 17, 685–697. doi:10.1038/s41574-021-00555-5

Kim, J., Choi, H. S., Kim, Y. M., and Song, S. C. (2023). Thermo-responsive nanocomposite bioink with growth-factor holding and its application to bone regeneration. *Small* 19, e2203464. doi:10.1002/smll.202203464

Kim, Y.-J., and Matsunaga, Y. T. (2017). Thermo-responsive polymers and their application as smart biomaterials. *J. Mater. Chem. B* 5, 4307–4321. doi:10.1039/c7tb00157f

Kocak, F. Z., Talari, A. C. S., Yar, M., and Rehman, I. U. (2020). *In-situ* forming ph and thermosensitive injectable hydrogels to stimulate angiogenesis: potential candidates for fast bone regeneration applications. *Int. J. Mol. Sci.* 21, 1633. doi:10.3390/ijms21051633

Kumar, A., Sharma, A., Chen, Y., Jones, M. M., Vanyo, S. T., Li, C., et al. (2021). Copper@Zif-8 core-shell nanowires for reusable antimicrobial face masks. *Adv. Funct. Mater* 31, 2008054. doi:10.1002/adfm.202008054

Lallana, E., Fernandez-Trillo, F., Sousa-Herves, A., Riguera, R., and Fernandez-Megia, E. (2012). Click chemistry with polymers, dendrimers, and hydrogels for drug delivery. *Pharm. Res.* 29, 902–921. doi:10.1007/s11095-012-0683-y

Lambertini, E., Penolazzi, L., Morganti, C., Lisignoli, G., Zini, N., Angelozzi, M., et al. (2015). Osteogenic differentiation of human mscs: specific occupancy of the mitochondrial DNA by Nfatc1 transcription factor. *Int. J. Biochem. Cell. Biol.* 64, 212–219. doi:10.1016/j.biocel.2015.04.011

Lavanya, K., Chandran, S. V., Balagangadharan, K., and Selvamurugan, N. (2020). Temperature- and ph-responsive chitosan-based injectable hydrogels for bone tissue engineering. *Mater Sci. Eng. C Mater Biol. Appl.* 111, 110862. doi:10.1016/j.msec.2020.110862

Lee, J., Byun, H., Madhurakkat Perikamana, S. K., Lee, S., and Shin, H. (2018a). Current advances in immunomodulatory biomaterials for bone regeneration. *Adv. Healthc. Mater.* 8, e1801106. doi:10.1002/adhm.201801106

Lee, J. Y., Lim, H., Ahn, J. W., Jang, D., Lee, S. H., Park, K., et al. (2018b). Design of a 3d bmp-2-delivering tannylated pcl scaffold and its anti-oxidant, anti-inflammatory, and osteogenic effects *in vitro*. *Int. J. Mol. Sci.* 19, 3602. doi:10.3390/ijms19113602

Lee, S. H., Gupta, M. K., Bang, J. B., Bae, H., and Sung, H. J. (2013). Current progress in reactive oxygen species (Ros)-Responsive materials for biomedical applications. *Adv. Healthc. Mater* 2, 908–915. doi:10.1002/adhm.201200423

Leppik, L., Oliveira, K. M. C., Bhavsar, M. B., and Barker, J. H. (2020). Electrical stimulation in bone tissue engineering treatments. *Eur. J. Trauma Emerg. Surg.* 46, 231–244. doi:10.1007/s00068-020-01324-1

Li, P., Li, Y., Fu, R., Duan, Z., Zhu, C., and Fan, D. (2023). Nir- and ph-responsive injectable nanocomposite alginate-graft-dopamine hydrogel for melanoma suppression and wound repair. *Carbohydr. Polym.* 314, 120899. doi:10.1016/j.carbpol.2023.120899

Li, S., Wei, C., and Lv, Y. (2020). Preparation and application of magnetic responsive materials in bone tissue engineering. *Curr. Stem Cell. Res. Ther.* 15, 428–440. doi:10.2174/1574888X15666200101122505

Li, X., Shen, M., Yang, J., Liu, L., and Yang, Y. W. (2024). Pillararene-based stimuli-responsive supramolecular delivery systems for cancer therapy. *Adv. Mater* 36, e2313317. doi:10.1002/adma.202313317

Li, Z., Qu, Y., Zhang, X., and Yang, B. (2009). Bioactive nano-titania ceramics with biomechanical compatibility prepared by doping with piezoelectric batio(3). *Acta Biomater.* 5, 2189–2195. doi:10.1016/j.actbio.2009.02.013

Liang, Y., Li, Z., Huang, Y., Yu, R., and Guo, B. (2021). Dual-dynamic-bond cross-linked antibacterial adhesive hydrogel sealants with on-demand removability for post-wound-closure and infected wound healing. *ACS Nano* 15, 7078–7093. doi:10.1021/acsnano.1c00204

Lin, C., Hao, H., Mei, L., and Wu, M. (2020). Metal-free two-dimensional nanomaterial-mediated photothermal tumor therapy. *Smart Mater. Med.* 1, 150–167. doi:10.1016/j.smaim.2020.09.001

Lin, K., Xia, L., Li, H., Jiang, X., Pan, H., Xu, Y., et al. (2013). Enhanced osteoporotic bone regeneration by strontium-substituted calcium silicate bioactive ceramics. *Biomaterials* 34, 10028–10042. doi:10.1016/j.biomaterials.2013.09.056

Liu, H., Shi, Y., Zhu, Y., Wu, P., Deng, Z., Dong, Q., et al. (2023). Bioinspired piezoelectric periosteum to augment bone regeneration via synergistic immunomodulation and osteogenesis. *ACS Appl. Mater Interfaces* 15, 12273–12293. doi:10.1021/acsami.2c19767

Liu, M., Du, H., Zhang, W., and Zhai, G. (2017). Internal stimuli-responsive nanocarriers for drug delivery: design strategies and applications. *Mater Sci. Eng. C Mater Biol. Appl.* 71, 1267–1280. doi:10.1016/j.msec.2016.11.030

Losic, D. (2021). Advancing of titanium medical implants by surface engineering: recent progress and challenges. *Expert Opin. Drug Deliv.* 18, 1355–1378. doi:10.1080/17425247.2021.1928071

Lu, J. W., Yang, F., Ke, Q. F., Xie, X. T., and Guo, Y. P. (2018). Magnetic nanoparticles modified-porous scaffolds for bone regeneration and photothermal therapy against tumors. *Nanomedicine.* 14, 811–822. doi:10.1016/j.nano.2017.12.025

Lui, Y. S., Sow, W. T., Tan, L. P., Wu, Y., Lai, Y., and Li, H. (2019). 4d printing and stimuli-responsive materials in biomedical aspects. *Acta Biomater.* 92, 19–36. doi:10.1016/j.actbio.2019.05.005

Lv, Z., Hu, T., Bian, Y., Wang, G., Wu, Z., Li, H., et al. (2023). A mgfe-ldh nanosheet-incorporated smart thermo-responsive hydrogel with controllable growth factor releasing capability for bone regeneration. *Adv. Mater* 35, e2206545. doi:10.1002/adma.202206545

Ma, B., Liu, F., Li, Z., Duan, J., Kong, Y., Hao, M., et al. (2019). Piezoelectric nylon-11 nanoparticles with ultrasound assistance for high-efficiency promotion of stem cell osteogenic differentiation. *J. Mater Chem. B* 7, 1847–1854. doi:10.1039/c8tb03321h

Mao, L., Bai, L., Wang, X., Chen, X., Zhang, D., Chen, F., et al. (2022). Enhanced cell osteogenesis and osteoimmunology regulated by piezoelectric biomaterials with controllable surface potential and charges. *ACS Appl. Mater Interfaces* 14, 44111–44124. doi:10.1021/acsami.2c11131

McKay, C. S., and Finn, M. G. (2014). Click chemistry in complex mixtures: bioorthogonal bioconjugation. *Chem. Biol.* 21, 1075–1101. doi:10.1016/j.chembiol.2014.09.002

Mészáros, B., Csoti, A., Szanto, T. G., Telek, A., Kovács, K., Toth, A., et al. (2022). The heag1 K(+) channel inhibitor astemizole stimulates Ca(2+) deposition in saos-2 and Mg-63 osteosarcoma cultures. *Int. J. Mol. Sci.* 23, 10533. doi:10.3390/ijms231810533

Minary-Jolandan, M., and Yu, M.-F. (2010). Shear piezoelectricity in bone at the nanoscale. *Appl. Phys. Lett.* 97, 97. doi:10.1063/1.3503965

Mohanty, A. R., Ravikumar, A., and Peppas, N. A. (2022). Recent advances in glucose-responsive insulin delivery systems: novel hydrogels and future applications. *Regen. Biomater.* 9, rbac056. doi:10.1093/rb/rbac056

Montoya, C., Du, Y., Gianforcaro, A. L., Orrego, S., Yang, M., and Lelkes, P. I. (2021). On the road to smart biomaterials for bone research: definitions, concepts, advances, and outlook. *Bone Res.* 9, 12. doi:10.1038/s41413-020-00131-z

Moonga, S. S., and Qin, Y. X. (2018). Mc3t3 infiltration and proliferation in bovine trabecular scaffold regulated by dynamic flow bioreactor and augmented by low-intensity pulsed ultrasound. *J. Orthop. Transl.* 14, 16–22. doi:10.1016/j.jot.2018.02.002

More, N., and Kapusetti, G. (2017). Piezoelectric material - a promising approach for bone and cartilage regeneration. *Med. Hypotheses* 108, 10–16. doi:10.1016/j.mehy.2017.07.021

Mu, R., Zhu, D., Abdulmalik, S., Wijekoon, S., Wei, G., and Kumbar, S. G. (2024). Stimuli-responsive peptide assemblies: design, self-assembly, modulation, and biomedical applications. *Bioact. Mater* 35, 181–207. doi:10.1016/j.bioactmat.2024.01.023

Murillo, G., Blanquer, A., Vargas-Estevez, C., Barrios, L., Ibanez, E., Nogues, C., et al. (2017). Electromechanical nanogenerator-cell interaction modulates cell activity. *Adv. Mater* 29, 29. doi:10.1002/adma.201605048

Nguyen, H. T., Ono, M., Oida, Y., Hara, E. S., Komori, T., Akiyama, K., et al. (2018). Bone marrow cells inhibit bmp-2-induced osteoblast activity in the marrow environment. *J. Bone Mineral Res.* 34, 327–332. doi:10.1002/jbmr.3598

Ni, X., Xing, X., Deng, Y., and Li, Z. (2023). Applications of stimuli-responsive hydrogels in bone and cartilage regeneration. *Pharmaceutics* 15, 982. doi:10.3390/pharmaceutics15030982

Nomikou, N., Feichtinger, G. A., Saha, S., Nuernberger, S., Heimel, P., Redl, H., et al. (2018). Ultrasound-responsive gene-activated matrices for osteogenic gene therapy using matrix-assisted sonoporation. *J. Tissue Eng. Regen. Med.* 12, e250–e260. doi:10.1002/term.2406

Pajarinen, J., Lin, T., Gibon, E., Kohno, Y., Maruyama, M., Nathan, K., et al. (2019). Mesenchymal stem cell-macrophage crosstalk and bone healing. *Biomaterials* 196, 80–89. doi:10.1016/j.biomaterials.2017.12.025

Qiao, Y., Yu, L., Yang, P., Chen, M., Sun, H., Wang, L., et al. (2023). Spatiotemporal immunomodulation and biphasic osteo-vascular aligned electrospun membrane for diabetic periosteum regeneration. *Adv. Sci. (Weinh)* 10, e2302874. doi:10.1002/advs.202302874

Ren, X., Liu, H., Wu, X., Weng, W., Wang, X., and Su, J. (2022). Reactive oxygen species (Ros)-Responsive biomaterials for the treatment of bone-related diseases. *Front. Bioeng. Biotechnol.* 9, 820468. doi:10.3389/fbioe.2021.820468

Ressler, A., Ródenas-Rochina, J., Ivanković, M., Ivanković, H., Rogina, A., and Gallego Ferrer, G. (2018). Injectable chitosan-hydroxyapatite hydrogels promote the osteogenic differentiation of mesenchymal stem cells. *Carbohydr. Polym.* 197, 469–477. doi:10.1016/j.carbpol.2018.06.029

Sadowska, J. M., and Ginebra, M. P. (2020). Inflammation and biomaterials: role of the immune response in bone regeneration by inorganic scaffolds. *J. Mater Chem. B* 8, 9404–9427. doi:10.1039/d0tb01379j

Saeedi, P., Petersohn, I., Salpea, P., Malanda, B., Karuranga, S., Unwin, N., et al. (2019). Global and regional diabetes prevalence estimates for 2019 and projections for 2030 and 2045: results from the international diabetes federation diabetes atlas, 9(Th) edition. *Diabetes Res. Clin. Pract.* 157, 107843. doi:10.1016/j.diabres.2019.107843

Salehpour, F., Cassano, P., Rouhi, N., Hamblin, M. R., De Taboada, L., Farajdokht, F., et al. (2019). Penetration profiles of visible and near-infrared lasers and light-emitting diode light through the head tissues in animal and human species: a review of literature. *Photobiomodul Photomed. Laser Surg.* 37, 581–595. doi:10.1089/photob.2019.4676

Scott, J. F. (1974). Soft-mode spectroscopy: experimental studies of structural phase transitions. *Rev. Mod. Phys.* 46, 83–128. doi:10.1103/RevModPhys.46.83

Shang, F., Yu, Y., Liu, S., Ming, L., Zhang, Y., Zhou, Z., et al. (2021). Advancing application of mesenchymal stem cell-based bone tissue regeneration. *Bioact. Mater* 6, 666–683. doi:10.1016/j.bioactmat.2020.08.014

Simon-Yarza, T., Mielcarek, A., Couvreur, P., and Serre, C. (2018). Nanoparticles of metal-organic frameworks: on the road to *in vivo* efficacy in biomedicine. *Adv. Mat.* 30, e1707365. doi:10.1002/adma.201707365

Su, Y., Yang, H., Gao, J., Qin, Y. X., Zheng, Y., and Zhu, D. (2019). Interfacial zinc phosphate is the key to controlling biocompatibility of metallic zinc implants. *Adv. Sci. (Weinh)* 6, 1900112. doi:10.1002/advs.201900112

Sultana, A., Ghosh, S. K., Sencadas, V., Zheng, T., Higgins, M. J., Middya, T. R., et al. (2017). Human skin interactive self-powered wearable piezoelectric bio-E-skin by electrospun poly-L-lactic acid nanofibers for non-invasive physiological signal monitoring. *J. Mater Chem. B* 5, 7352–7359. doi:10.1039/c7tb01439b

Sun, C., Wang, Z., Yue, L., Huang, Q., Lu, S., and Wang, R. (2020b). Ros-initiated chemiluminescence-driven payload release from macrocycle-based azo-containing polymer nanocapsules. *J. Mater Chem. B* 8, 8878–8883. doi:10.1039/d0tb01475c

Sun, D., Zhang, Z., Chen, M., Zhang, Y., Amagat, J., Kang, S., et al. (2020a). Co-immobilization of Ce6 sono/photosensitizer and protonated graphitic carbon nitride on pcl/gelation fibrous scaffolds for combined sono-photodynamic cancer therapy. *ACS Appl. Mater Interfaces* 12, 40728–40739. doi:10.1021/acsami.0c08446

Suslick, K. S. (2013). Applications of ultrasound to materials chemistry. *MRS Bull.* 20, 29–34. doi:10.1557/s088376940004464x

Swietach, P., Vaughan-Jones, R. D., Harris, A. L., and Hulikova, A. (2014). The chemistry, physiology and pathology of ph in cancer. *Philos. Trans. R. Soc. Lond B Biol. Sci.* 369, 20130099. doi:10.1098/rstb.2013.0099

Tandon, B., Blaker, J. J., and Cartmell, S. H. (2018). Piezoelectric materials as stimulatory biomedical materials and scaffolds for bone repair. *Acta Biomater.* 73, 1–20. doi:10.1016/j.actbio.2018.04.026

Tang, B., Shen, X., Yang, Y., Xu, Z., Yi, J., Yao, Y., et al. (2021). Enhanced cellular osteogenic differentiation on cofe(2)O(4)/P(Vdf-Trfe) nanocomposite coatings under static magnetic field. *Colloids Surf. B Biointerfaces* 198, 111473. doi:10.1016/j.colsurfb.2020.111473

Tang, G., Zhu, L., Wang, W., Zuo, D., Shi, C., Yu, X., et al. (2022). Alendronate-functionalized double network hydrogel scaffolds for effective osteogenesis. *Front. Chem.* 10, 977419. doi:10.3389/fchem.2022.977419

Tian, B., Li, X., Zhang, J., Zhang, M., Gan, D., Deng, D., et al. (2022). A 3d-printed molybdenum-containing scaffold exerts dual pro-osteogenic and anti-osteoclastogenic effects to facilitate alveolar bone repair. *Int. J. Oral Sci.* 14, 45. doi:10.1038/s41368-022-00195-z

Turner, C. H., Wang, T., and Burr, D. B. (2001). Shear strength and fatigue properties of human cortical bone determined from pure shear tests. *Calcif. Tissue Int.* 69, 373–378. doi:10.1007/s00223-001-1006-1

Ud-Din, S., and Bayat, A. (2014). Electrical stimulation and cutaneous wound healing: a review of clinical evidence. *Healthc. (Basel)* 2 (2), 445–467. doi:10.3390/healthcare2040445

Veronick, J. A., Assanah, F., Piscopo, N., Kutes, Y., Vyas, V., Nair, L. S., et al. (2018). Mechanically loading cell/hydrogel constructs with low-intensity pulsed ultrasound for bone repair. *Tissue Eng. Part A* 24, 254–263. doi:10.1089/ten.TEA.2016.0547

Wan, Z., Zhang, P., Lv, L., and Zhou, Y. (2020). Nir light-assisted phototherapies for bone-related diseases and bone tissue regeneration: a systematic review. *Theranostics* 10, 11837–11861. doi:10.7150/thno.49784

Wang, A., Liu, Z., Hu, M., Wang, C., Zhang, X., Shi, B., et al. (2018). Piezoelectric nanofibrous scaffolds as *in vivo* energy harvesters for modifying fibroblast alignment and proliferation in wound healing. *Nano Energy* 43, 63–71. doi:10.1016/j.nanoen.2017.11.023

Wang, B., Zeng, Y., Liu, S., Zhou, M., Fang, H., Wang, Z., et al. (2023). Zif-8 induced hydroxyapatite-like crystals enabled superior osteogenic ability of mew printing pcl scaffolds. *J. Nanobiotechnology* 21, 264. doi:10.1186/s12951-023-02007-w

Wang, C., Huang, W., Zhou, Y., He, L., He, Z., Chen, Z., et al. (2020). 3d printing of bone tissue engineering scaffolds. *Bioact. Mater* 5, 82–91. doi:10.1016/j.bioactmat.2020.01.004

Wang, H., Leeuwenburgh, S. C., Li, Y., and Jansen, J. A. (2012). The use of micro- and nanospheres as functional components for bone tissue regeneration. *Tissue Eng. Part B Rev.* 18, 24–39. doi:10.1089/ten.TEB.2011.0184

Wang, L., Mi, B., Zhang, Y., Yan, H., and Zhu, H. (2021). Alendronate promotes the gene expression of extracellular matrix mediated by sp-1/sox-9. *Hum. Exp. Toxicol.* 40, 1173–1182. doi:10.1177/0960327120988875

Wang, W., and Yeung, K. W. K. (2017). Bone grafts and biomaterials substitutes for bone defect repair: a review. *Bioact. Mater* 2, 224–247. doi:10.1016/j.bioactmat.2017.05.007

Wei, H., Cui, J., Lin, K., Xie, J., and Wang, X. (2022a). Recent advances in smart stimuli-responsive biomaterials for bone therapeutics and regeneration. *Bone Res.* 10, 17. doi:10.1038/s41413-021-00180-y

Wei, H., Cui, J., Lin, K., Xie, J., and Wang, X. (2022b). Recent advances in smart stimuli-responsive biomaterials for bone therapeutics and regeneration. *Bone Res.* 10, 17. doi:10.1038/s41413-021-00180-y

Wu, S. W., Liu, X., Miller, A. L., 2nd, Cheng, Y. S., Yeh, M. L., and Lu, L. (2018). Strengthening injectable thermo-sensitive nipaam-G-chitosan hydrogels using chemical

cross-linking of disulfide bonds as scaffolds for tissue engineering. *Carbohydr. Polym.* 192, 308–316. doi:10.1016/j.carbpol.2018.03.047

Wu, Y., Jiang, W., Wen, X., He, B., Zeng, X., Wang, G., et al. (2010). A novel calcium phosphate ceramic-magnetic nanoparticle composite as a potential bone substitute. *Biomed. Mater* 5, 15001. doi:10.1088/1748-6041/5/1/015001

Xing, Y., Qiu, L., Liu, D., Dai, S., and Sheu, C. L. (2023). The role of smart polymeric biomaterials in bone regeneration: a review. *Front. Bioeng. Biotechnol.* 11, 1240861. doi:10.3389/fbioe.2023.1240861

Xu, B., Li, Y., Gao, F., Zhai, X., Sun, M., Lu, W., et al. (2015). High strength multifunctional multiwalled hydrogel tubes: ion-triggered shape memory, antibacterial, and anti-inflammatory efficacies. *ACS Appl. Mater Interfaces* 7, 16865–16872. doi:10.1021/acsami.5b05074

Xu, H.-Y., and Gu, N. (2014). Magnetic responsive scaffolds and magnetic fields in bone repair and regeneration. *Front. Mater. Sci.* 8, 20–31. doi:10.1007/s11706-014-0232-1

Xu, L., Bai, E., Zhu, Y., Qin, J., Du, X., and Huang, H. (2023). Ph-responsive hydrogel as a potential oral delivery system of baicalin for prolonging gastroprotective activity. *Pharmaceutics* 15, 257. doi:10.3390/pharmaceutics15010257

Xu, Q., He, C., Xiao, C., and Chen, X. (2016). Reactive oxygen species (ros) responsive polymers for biomedical applications. *Macromol. Biosci.* 16, 635–646. doi:10.1002/mabi.201500440

Yadav, D., Sharma, P. K., Malviya, R., Mishra, P. S., Surendra, A. V., Rao, G. K., et al. (2023). Stimuli-responsive biomaterials for tissue engineering applications. *Curr. Pharm. Biotechnol.* 25, 981–999. doi:10.2174/1389201024666230818121821

Yamaguchi, A., Katagiri, T., Ikeda, T., Wozney, J. M., Rosen, V., Wang, E. A., et al. (1991). Recombinant human bone morphogenetic protein-2 stimulates osteoblastic maturation and inhibits myogenic differentiation *in vitro*. *J. Cell. Biol.* 113 (3), 681–687. doi:10.1083/jcb.113.3.681

Yan, Q. C., Tomita, N., and Ikada, Y. (1998). Effects of static magnetic field on bone formation of rat femurs. *Med. Eng. Phys.* 20, 397–402. doi:10.1016/s1350-4533(98)00051-4

Yan, Z., Li, K., Shao, D., Shen, Q., Ding, Y., Huang, S., et al. (2022). Visible-light-responsive reduced graphene oxide/G-C(3)N(4)/tio(2) composite nanocoating for photoelectric stimulation of neuronal and osteoblastic differentiation. *RSC Adv.* 12, 8878–8888. doi:10.1039/d2ra00282e

Yang, B., Yin, J., Chen, Y., Pan, S., Yao, H., Gao, Y., et al. (2018). 2d-Black-Phosphorus-Reinforced 3d-printed scaffolds:A stepwise countermeasure for osteosarcoma. *Adv. Mater* 30, 30. doi:10.1002/adma.201705611

Yang, G., Miton, C. M., and Tokuriki, N. (2020). A mechanistic view of enzyme evolution. *Protein Sci.* 29, 1724–1747. doi:10.1002/pro.3901

Yao, Y., Zhang, H., Wang, Z., Ding, J., Wang, S., Huang, B., et al. (2019). Reactive oxygen species (Ros)-Responsive biomaterials mediate tissue microenvironments and tissue regeneration. *J. Mater. Chem. B* 7, 5019–5037. doi:10.1039/c9tb00847k

Ye, J., Zhuang, X., Li, X., Gong, X., Sun, Y., Wang, W., et al. (2022). Novel metabolic classification for extrahepatic complication of metabolic associated fatty liver disease: a data-driven cluster analysis with international validation. *Metabolism* 136, 155294. doi:10.1016/j.metabol.2022.155294

Yu, Y., Yu, X., Tian, D., Yu, A., and Wan, Y. (2021). Thermo-responsive chitosan/silk fibroin/amino-functionalized mesoporous silica hydrogels with strong and elastic characteristics for bone tissue engineering. *Int. J. Biol. Macromol.* 182, 1746–1758. doi:10.1016/j.ijbiomac.2021.05.166

Zhang, F., Lv, M., Wang, S., Li, M., Wang, Y., Hu, C., et al. (2024). Ultrasound-triggered biomimetic ultrashort peptide nanofiber hydrogels promote bone regeneration by modulating macrophage and the osteogenic immune microenvironment. *Bioact. Mater* 31, 231–246. doi:10.1016/j.bioactmat.2023.08.008

Zhang, J., Liu, L., Wang, L., Zhu, W., Wang, H., and Ph, (2020). pH responsive zwitterionic-to-cationic transition for safe self-defensive antibacterial application. *J. Mater Chem. B* 8, 8908–8913. doi:10.1039/d0tb01717e

Zhang, J., Neoh, K. G., Hu, X., Kang, E. T., and Wang, W. (2013). Combined effects of direct current stimulation and immobilized bmp-2 for enhancement of osteogenesis. *Biotechnol. Bioeng.* 110, 1466–1475. doi:10.1002/bit.24796

Zhang, W., Wang, N., Yang, M., Sun, T., Zhang, J., Zhao, Y., et al. (2022a). Periosteum and development of the tissue-engineered periosteum for guided bone regeneration. *J. Orthop. Transl.* 33, 41–54. doi:10.1016/j.jot.2022.01.002

Zhang, X., Li, Y., Chen, Y. E., Chen, J., and Ma, P. X. (2016). Cell-free 3d scaffold with two-stage delivery of mirna-26a to regenerate critical-sized bone defects. *Nat. Commun.* 7, 10376. doi:10.1038/ncomms10376

Zhang, Y., Li, C., Zhang, W., Deng, J., Nie, Y., Du, X., et al. (2022b). 3d-Printed nir-responsive shape memory polyurethane/magnesium scaffolds with tight-contact for robust bone regeneration. *Bioact. Mater* 16, 218–231. doi:10.1016/j.bioactmat.2021.12.032

Zhang, Z. M., Yu, P., Zhou, K., Yu, F. Y., Bao, R. Y., Yang, M. B., et al. (2023). Hierarchically porous implants orchestrating a physiological viscoelastic and piezoelectric microenvironment for bone regeneration. *Adv. Healthc. Mater* 12, e2300713. doi:10.1002/adhm.202300713

Zhao, C., Qazvini, N. T., Sadati, M., Zeng, Z., Huang, S., De La Lastra, A. L., et al. (2019b). A ph-triggered, self-assembled, and bioprintable hybrid hydrogel scaffold for mesenchymal stem cell based bone tissue engineering. *ACS Appl. Mater Interfaces* 11, 8749–8762. doi:10.1021/acsami.8b19094

Zhao, P.-P., Ge, Y.-W., Liu, X.-L., Ke, Q.-F., Zhang, J.-W., Zhu, Z.-A., et al. (2020). Ordered arrangement of hydrated Gdpo4 nanorods in magnetic chitosan matrix promotes tumor photothermal therapy and bone regeneration against breast cancer bone metastases. *Chem. Eng. J.* 381, 122694. doi:10.1016/j.cej.2019.122694

Zhao, W., Zhao, Y., Wang, Q., Liu, T., Sun, J., and Zhang, R. (2019a). Remote light-responsive nanocarriers for controlled drug delivery: advances and perspectives. *Small* 15, e1903060. doi:10.1002/smll.201903060

Zheng, Z., Yang, X., Zhang, Y., Zu, W., Wen, M., Liu, T., et al. (2023). An injectable and ph-responsive hyaluronic acid hydrogel as metformin carrier for prevention of breast cancer recurrence. *Carbohydr. Polym.* 304, 120493. doi:10.1016/j.carbpol.2022.120493

Zhou, S., Bismarck, A., and Steinke, J. H. G. (2013). Ion-responsive alginate based macroporous injectable hydrogel scaffolds prepared by emulsion templating. *J. Mater Chem. B* 1, 4736–4745. doi:10.1039/c3tb20888e

Zhou, S., Xiao, C., Fan, L., Yang, J., Ge, R., Cai, M., et al. (2024). Injectable ultrasound-powered bone-adhesive nanocomposite hydrogel for electrically accelerated irregular bone defect healing. *J. Nanobiotechnology* 22, 54. doi:10.1186/s12951-024-02320-y

Zhu, C., Tang, N., Gan, J., Zhang, X., Li, Y., Jia, X., et al. (2021). A ph-sensitive semi-interpenetrating polymer network hydrogels constructed by konjac glucomannan and poly (Gamma-Glutamic acid): synthesis, characterization and swelling behavior. *Int. J. Biol. Macromol.* 185, 229–239. doi:10.1016/j.ijbiomac.2021.06.046

Zhu, F., Liu, W., Li, P., Zhao, H., Deng, X., and Wang, H. L. (2023). Electric/magnetic intervention for bone regeneration: a systematic review and network meta-analysis. *Tissue Eng. Part B Rev.* 29, 217–231. doi:10.1089/ten.TEB.2022.0127

Zhu, J., Han, H., Ye, T. T., Li, F. X., Wang, X. L., Yu, J. Y., et al. (2018). Biodegradable and ph sensitive peptide based hydrogel as controlled release system for antibacterial wound dressing application. *Molecules* 23, 3383. doi:10.3390/molecules23123383

Zorov, D. B., Juhaszova, M., and Sollott, S. J. (2014). Mitochondrial reactive oxygen species (ros) and ros-induced ros release. *Physiol. Rev.* 94, 909–950. doi:10.1152/physrev.00026.2013

frontiers | Frontiers in Pharmacology

TYPE Review
PUBLISHED 13 August 2024
DOI 10.3389/fphar.2024.1465697

OPEN ACCESS

EDITED BY
Wen Liao,
Sichuan University, China

REVIEWED BY
Xingfu Bao,
Jilin University, China
Yunfeng Lin,
Sichuan University, China

*CORRESPONDENCE
Gang Ding,
dinggang@sdsmu.edu.cn

RECEIVED 16 July 2024
ACCEPTED 01 August 2024
PUBLISHED 13 August 2024

CITATION
Liu X, Li Z, Liu L, Zhang P, Wang Y and Ding G (2024) Metformin-mediated effects on mesenchymal stem cells and mechanisms: proliferation, differentiation and aging. *Front. Pharmacol.* 15:1465697. doi: 10.3389/fphar.2024.1465697

Metformin-mediated effects on mesenchymal stem cells and mechanisms: proliferation, differentiation and aging

Xinjuan Liu, Zekun Li, Luyun Liu, Ping Zhang, Yue Wang and Gang Ding*

School of Stomatology, Shandong Second Medical University, Weifang, Shandong, China

Mesenchymal stem cells (MSCs) are a type of pluripotent adult stem cell with strong self-renewal and multi-differentiation abilities. Their excellent biological traits, minimal immunogenicity, and abundant availability have made them the perfect seed cells for treating a wide range of diseases. After more than 60 years of clinical practice, metformin is currently one of the most commonly used hypoglycaemic drugs for type 2 diabetes in clinical practice. In addition, metformin has shown great potential in the treatment of various systemic diseases except for type 2 diabetes in recent years, and the mechanisms are involved with antioxidant stress, anti-inflammatory, and induced autophagy, etc. This article reviews the effects and the underlying mechanisms of metformin on the biological properties, including proliferation, multi-differentiation, and aging, of MSCs *in vitro* and *in vivo* with the aim of providing theoretical support for in-depth scientific research and clinical applications in MSCs-mediated disease treatment.

KEYWORDS

mesenchymal stem cells, metformin, proliferation, differentiation, aging

1 Introduction

First isolated in mouse bone marrow by Friedenstein et al. in 1968, mesenchymal stem cells (MSCs) are nonhematopoietic stem cells derived from various postnatal tissues such as umbilical cord blood, fat, liver, skin, dental pulp, etc (Gronthos et al., 2000; Campagnoli et al., 2001; Keating, 2012), with the morphology similar to that of fibroblasts. MSCs possess profound multi-directional differentiation potentials and could differentiate into chondrocytes, osteoblasts, adipocytes under certain induced conditions (Longobardi et al., 2006). When flow cytometry is used to detect MSCs, it is found that the expression rates of CD105, CD90, and CD73 are above 95%, and the expression rates of CD45 and CD34 are below 5%. At the same time, if they meet the standard culture conditions for plastic adhesion and have the potential for multi-directional differentiation as mentioned above, the obtained sample can be considered as MSCs(Pittenger et al., 1999). MSCs are the most widely used postnatal tissue-specific stem cells used in clinical practice, and transplanting MSCs to replace damaged tissues can restore tissue structure and function (Keshavarz et al., 2023). In addition, MSCs were capable of secreting a large number of cytokines and growth factors, and playing multiple roles in immune regulation. Due to its characteristics of self-renewal, multi-directional differentiation potential, and low immunogenicity, MSCs have been considered as an excellent seed cells for regenerative

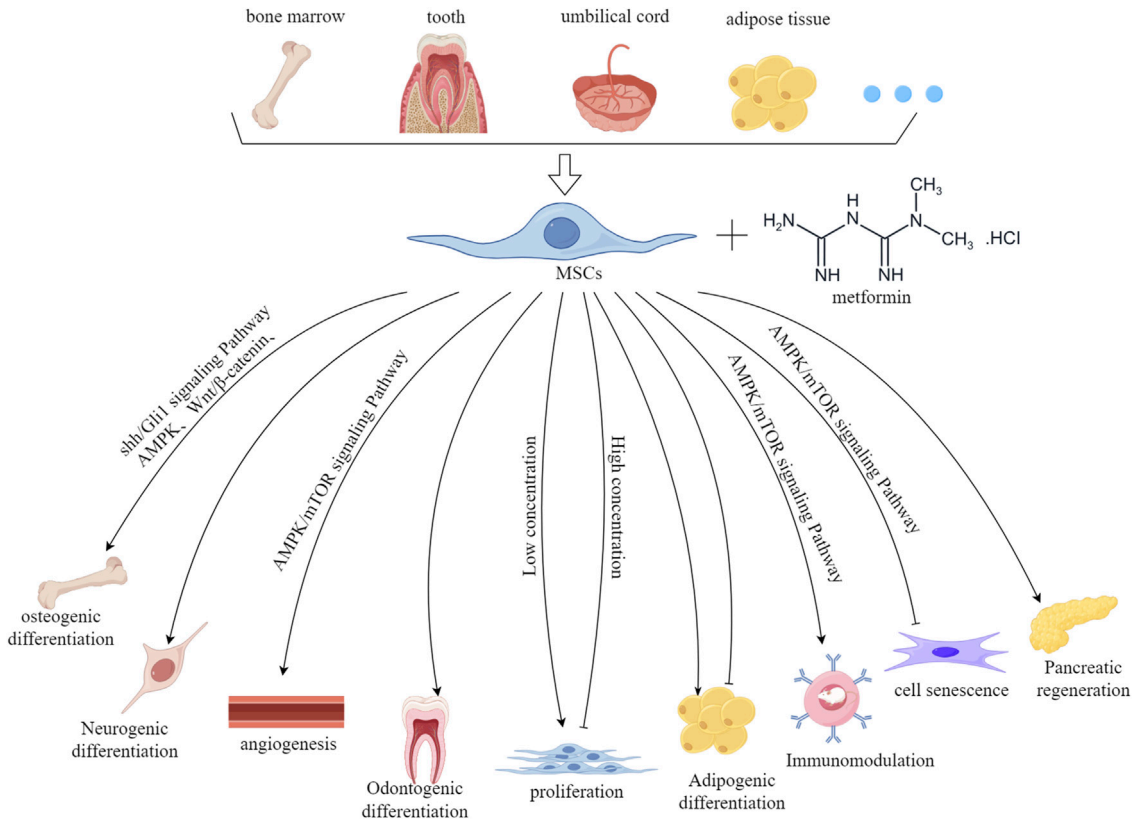

FIGURE 1
The effect and mechanism of metformin on the biological characteristics of MSCs derived from various tissue sources. This figure was generated by figdraw.

medicine and tissue engineering and have been used in the research and treatment of various diseases (Sherman et al., 2019; Meng et al., 2020; Zheng et al., 2020; Hoang et al., 2022; Huang et al., 2023).

Metformin is orally administered, with a bio-availability of 50%–60%, and the plasma half-life has been calculated to be 1.5–4 h. It is absorbed through the intestine, enters the portal vein, and accumulates in the liver, while the remaining portion is excreted through urine and feces. In recent years, the efficacy and mechanism of metformin have been gradually elucidated, including but not limited to, improving blood glucose and insulin resistance, inhibiting the synthesis of insulin-like growth factor and aspartic acid, and affecting immune cells (Marcucci et al., 2020; LaMoia and Shulman, 2021; Veeramachaneni et al., 2021). As the most widely used anti-diabetic drug currently, metformin's main role is to regulate blood glucose homeostasis and reduce insulin resistance by up-regulating adenosine 5′-monophosphate activated protein kinase (AMPK) to maintain cellular energy homeostasis and activate glucose uptake, thus being recommended as the first choice for treatment of type 2 diabetes patients (Wróbel et al., 2017). In addition to its anti-diabetes effect, more and more studies have also reported that metformin has unexpected efficacy in a variety of pathological and physiological processes, including but not limited to, alleviating oxidative stress and inflammatory reactions, treating several diseases, such as cancer, polycystic ovary syndrome, cardiovascular diseases, etc., with the potential to become a comprehensive therapeutic drug (Soldat-Stanković et al., 2021; Chaudhary and Kulkarni, 2024).

In recent years, a growing number of studies have shown that metformin has a significant effect on the biological properties of MSCs, including proliferation, multi-directional differentiation, and cell aging. Thus, it is necessary to explore the effects of metformin on MSCs in depth, therefore promoting their application in regenerative medicine. This article reviews the effects and possible mechanisms of metformin on the biological characteristics of MSCs (Figure 1).

2 The effect of metformin on the biological characteristics of MSCs *in vitro*

At present, *in vitro* studies on the biological functions of MSCs mainly focus on their proliferation, differentiation, and aging. In order to obtain sufficient numbers of MSCs for stem cell-based therapies, continuous cell culture and frequent passages are required (Liu, 2022). However, the number of cells obtained from conventional culture is insufficient for pre-clinical research and regenerative medicine applications, and repeated passages can also accelerate the aging of stem cells (Saei Arezoumand et al., 2016). It is therefore crucial to find effective methods to promote cell proliferation and differentiation and to inhibit aging.

TABLE 1 The effects of metformin on the proliferation of MSCs.

Cell sources	Metformin concentration	Action time	Effects	References
UCMSCs	0–500 μM	24 h	Promoted cell proliferation	Lei et al. (2021)
	>1000 μM		Inhibited cell proliferation	
UCMSCs	0.1–50 mM	48 h	Inhibited cell proliferation	Bajetto et al. (2023)
UCMSCs	10 μM	7 d	No significant influence	Al Jofi et al. (2018)
BMSCs	0.5–500 μM	14 d	Inhibited cell proliferation	Montazersaheb et al. (2018)
PDLSCs	≤1000 μM	5 d	No significant influence	Jia et al. (2020)
	2500 μM		Inhibited cell proliferation	
PDLSCs	10 μM	7 d	No significant influence	Zhang et al. (2019)
	50μM/100 μM	5d/7 d	Promoted cell proliferation	
SHEDs	10–200 μM	7 d	No significant influence	Zhao et al. (2020)
DPSCs	≤50 μM	7 d	No significant influence	Qin et al. (2018b)

2.1 The effect of metformin on the proliferation of MSCs

The effect of metformin on the proliferation of MSCs shows a double-edged sword phenomenon. Specifically, low concentrations of metformin promote the proliferation of MSCs, while high concentrations of metformin inhibit it (Table 1). The experimental results of Lei et al. indicated that 0–500 μM metformin has a promoting effect on the proliferation of human umbilical cord MSCs (UCMSCs), while high concentrations of metformin (1,000 μM) have inhibitory effects (Lei et al., 2021). However, in other experiments, when UCMSCs were treated with a higher concentration (0.1–50 mM) for 48 h, cell viability analysis showed that metformin caused a dose-dependent decrease in cell growth in all UCMSCs samples, reaching statistical significance from 3 mM and maximum efficacy at 50 mM (Bajetto et al., 2023). In another low concentration gradient experiment, metformin (10–200 μM) did not affect the viability and proliferation of MSCs from human exfoliated deciduous teeth (SHED) (Zhao et al., 2020), 10 μM metformin treatment had no significant effect on the proliferation of periodontal ligament stem cells (PDLSCs), while 50 μM and 100 μM metformin treatments significantly promoted the proliferation of PDLSCs on days 5 and 7 (Zhang et al., 2019). In addition, low concentrations of metformin (≤1,000 μM) was shown to have no significant influence on the proliferation of PDLSCs (Jia et al., 2020). This phenomenon may be due to different types of stem cells, different experimental conditions, and different observation times. In order to investigate the effect of processing time on MSCs, researchers have used different doses of metformin (0.5, 1, 10, 50, 100, 200, and 500 μM) to process bone marrow MSCs (BMSCs) for 14 days, and the results showed a dose-dependent decrease in cell survival rate, which may be due to the prolonged incubation time of metformin, leading to a decrease in the synthesis of factors such as insulin-like growth factor-2 (Montazersaheb et al., 2018). Under high sugar conditions, cell proliferation was significantly inhibited (Raghavan et al., 2020). However, it is worth noting that the addition of metformin reversed the inhibitory effect of high glucose levels on cell proliferation, mainly because metformin significantly cleared high glucose induced reactive oxygen species (ROS) (Dong et al., 2022) and regulated the ROS-AKT (protein kinase B)-mTOR (rapamycin target protein) axis inhibited by high glucose levels (Zhou et al., 2020). Previous studies have shown that biomaterials can be used to load metformin to further enhance its promoting effect on the proliferation of MSCs. Somayeh Ahmadi et al. encapsulated hyaluronic acid/gelatin with metformin loaded mesoporous silica nanoparticles, which resulted in a sustained release of metformin for 15 days. The authors co-cultured it with BMSCs and found that cell proliferation rate and metformin metabolic activity were improved through PicoGreen and 3 (4,5-dimethyl thiazol2-yl) 2, 5-diphenyl-tetrazolium bromide tests (Ahmadi et al., 2023).

Based on the studies conducted by the above researchers, it is possible to conclude that the proliferation of MSCs could be stimulated by a certain concentration of metformin. Further research is needed since the effects and mechanisms of metformin on cell proliferation are very complex, and different types of MSCs may respond differently to the drug. In addition, the response of these cells to metformin is closely tied to the duration of treatment.

2.2 The effect of metformin on multi-directional differentiation of MSCs

MSCs have the potential for multi-directional differentiation, and are capable of differentiating into chondrocytes, osteoblasts, adipocytes, neurons, and muscle cells under different induction conditions. Many researchers have demonstrated that metformin could promote or inhibit the multi-directional differentiation potential of MSCs to a certain extent and also explored possible mechanisms (Table 2).

2.2.1 Osteogenic differentiation

Bone regeneration and repair are major challenges in clinical medicine, such as bone resorption caused by periodontitis and

TABLE 2 The effects of metformin on the differentiation of MSCs.

Cells	Biomaterial	*In vitro*	Dose of metformin	Results	*In vivo*	Dose of metformin	Animal models	Administration methods	Results	Mechanisms	References
rASCs	—	√	500 μM	Enhanced the odontogenic differentiation	√	250 mg/kg	Rat bilateral cranial defect mode	Drinking water	Promotes trabecular bone formation	Activating AMPK signaling pathway	Śmieszek et al. (2018)
iPSC-MSCs	—	√	10 μM	Enhanced the odontogenic differentiation	—	—	—	—	—	Activating LKB/AMPK signaling pathway	Wang et al. (2017)
rBMSCs	Metformin hydrochloride and citric acid	√	—	Enhanced the odontogenic differentiation	√	20 mg/kg	A periodontitis model of Wistar rats	The local injection	MCDs could more effectively enhance the periodontal bone regeneration than the raw material metformin	Activating ERK/AMPK signaling pathway	Ren et al. (2021)
N-BMSCs	—	√	50, 100 μM	Enhanced the odontogenic differentiation	√	50 mg/kg	Wistar rats femur defect model	Drinking water	Increase bone regeneration around implants	Activating AMPK/BMP/Smad signaling pathway	Sun et al. (2021)
DM-BMSCs	—		<200 μM	Enhanced the odontogenic differentiation (the maximum effective concentration is 125 μM)							
			≥200 μM	Inhibited osteogenic differentiation							
DPSCs	Demineralized dentin matrix	√	—	Increased mineralization and upregulated osteogenesis-related genes	—	—	—	—	—	Activating the AMPK pathway	Gao et al. (2020)
DPSCs	Calcium phosphate cement	√	50 μg/mL	Enhanced the odontogenic differentiation elevated expression of odontoblastic markers and strong mineral deposition	—	—	—	—	—	—	Qin et al. (2018b)
DPSCs	Freezedried bone allograft (FDBA)	√	100 μM	Enhanced the adhesion increase cell proliferation/viability Enhanced the osteogenic capability	—	—	—	—	—	—	Kouhestani et al. (2021)

(Continued on following page)

10.3389/fphar.2024.1465697

TABLE 2 (*Continued*) The effects of metformin on the differentiation of MSCs.

Cells	Biomaterial	*In vitro*	Dose of metformin	Results	*In vivo*	Dose of metformin	Animal models	Administration methods	Results	Mechanisms	References
DPSCs	Resin	√	20%	Enhanced odontoblastic differentiation Mineral synthesis	—	—	—	—	—	—	Wang et al. (2018)
PDLSCs	Polydopamine-templated hydroxyapatite (tHA)	√	100 μM	Promote osteogenic differentiation	—	—	—	—	—	Via the AMPK/mTOR signaling pathway by regulating autophagy	Yang et al. (2019)
			100 μM, 500 μM, 1 mM	Promote proliferation reduce cell apoptosis							
PDLSCs	Novel alginate-fibrin fibers	√	50 μM	Enhanced the odontogenic differentiation	—	—	—	—	—	Activating the Shh/Gli1 signaling pathway	Yin et al. (2023)
PDLSCs	—	√	10, 100, 500 μM	Promoted the osteogenic differentiation Inhibited the adipogenic differentiation	—	—	—	—	—	Activating of the Akt/Nrf2 signaling pathway	Jia et al. (2020)
PDLSCs	—	√	100 μM	Osteogenic differentiation under high glucose was decreased, and metformin addition enhanced it	—	—	—	—	—	Downregulation of NPR3 and inhibition of its downstream MAPK pathway	Zhang et al. (2022)
GMSCs	chitosan hydrogel	√	—	Powerful osteogenic, adipogenic and chondrogenic abilities in the induction medium supplemented with metformin	—	—	—	—	—	—	Cai et al. (2022)
SHEDs	—	√	100 μM	Promoted proliferation as well as osteogenic, adipogenic and chondrogenic differentiation Significantly improved the migration and angiogenesis of human umbilical vein endothelial cells	√	10 nM	Nude mice	The local injection	SHED pre-treated with metformin promotes angiogenesis	—	Deng et al. (2022)

(Continued on following page)

10.3389/fphar.2024.1465697

TABLE 2 (*Continued*) The effects of metformin on the differentiation of MSCs.

Cells	Biomaterial	*In vitro*	Dose of metformin	Results	*In vivo*	Dose of metformin	Animal models	Administration methods	Results	Mechanisms	References
BMSCs	—	√	100 μM	Enhanced the odontogenic differentiation	—	—	—	—	—	Inhibiting GSK3β activity Activating Wnt/β-catenin signaling	Ma et al. (2018)
UCMSCs	—	√	100 μM	Promotion of osteogenesis inhibition of adipogenesis Exhibited stronger angiogenesis	√	UCMSCs + metformin (100 μM)+ HUVEC	Male BALB/c nude mice	The local injection	Enhances the ability of angiogenesis	—	Lei et al. (2021)
UCMSCs	—	√	0.03–5 mM	A significant increase in lipid-rich vacuole formation No significant effect on osteogenesis	—	—	—	—	—	Activating the AMPK pathway	Bajetto et al. (2023)
ADMSCs	vitamin D3 (1nM and 2 nM)	√	25 mM	The combination of vitamin D3 and metformin accelerated the osteogenic differentiation of ADMSCs under high glucose concentrations	—	—	—	—	—	—	Ha et al. (2023)

10.3389/fphar.2024.1465697

insufficient bone mass in implant repair in dentistry (Zhu et al., 2022). The use of metformin can reduce the risk of fractures in patients with type 2 diabetes, and is considered to play a direct role in promoting bone formation (Hidayat et al., 2019; Lee et al., 2019). Several studies investigated the effects of metformin on the osteogenic differentiation, detected the osteogenic markers, including alkaline phosphatase (ALP), osteocalcin and type I collagen after incubation of MSCs and metformin, and found the increased expression of these markers (Gao et al., 2008). However, the mechanism by which metformin promotes osteogenesis is not very clear. At present, many scientists believe that metformin mainly promotes osteogenic differentiation of MSCs through AMPK pathway.

Agnieszka et al. found that metformin significantly stimulated ALP activity and osteocalcin production, and promoted osteogenic differentiation of rat adipose tissue derived MSCs (ADMSCs) by activating AMPK signaling pathway. *In vivo*, using the rat bilateral skull defect model, the authors further observed that the amount of new bone and bone volume were significantly higher in the metformin group than in the control group (Śmieszek et al., 2018). Meanwhile, metformin at a concentration of 10 μM can induce osteogenic differentiation of pluripotent stem cell-derived MSCs (iPSC-MSCs), as shown by the significantly stimulated ALP activity, the increased expression of Runt-related transcription factor 2 (Runx2), and late-stage markers of osteoblasts, osterix. Functional organic cation transporter expressing iPSC-MSCs responded to metformin by inducing an osteogenic effect in part mediated by the LKB1/AMPK pathway (Wang et al., 2017), with the same pathway also found in another study on UCMSCs (Al Jofi et al., 2018). Nanomaterials have been widely used in various fields due to their outstanding advantages such as large surface area to volume ratio, high reactivity, and easy surface modification. Therefore, researchers have incorporated metformin into nanomaterials and investigated its effects on MSCs. Metformin carbon dots (MCDs) are prepared from metformin hydrochloride and urban acid via a hydraulic method. The experimental results showed that MCDs can activate the extracellular signal regulated kinase (ERK)/AMPK pathway, enhance the osteogenic potential of BMSCs, and their effect is superior to that of metformin. In a rat model of periodontitis, it was further observed that MCDs can effectively guide alveolar bone regeneration, while metformin cannot. Nevertheless, as a novel material, MCD has not been extensively studied in the field of MSCs, needing in-depth study to explore the effects and mechanisms (Ren et al., 2021).

Because metformin is a common drug used to treat type 2 diabetes, and type 2 diabetes patients are more likely to develop osteoporosis than non-diabetics, studies on how metformin promotes the osteogenic differentiation of MSCs are mostly conducted in diabetes models. When BMSCs from diabetic mice were treated with metformin, their osteogenic differentiation potential was enhanced, and when the metformin-treated cells were re-implanted into type 2 diabetic mice, their osteogenic effect was still good (Guo et al., 2023). Sun et al. treated BMSCs from alveolar bone of normal humans (N-BMSCs) and diabetes patients (DM-BMSCs) with different concentrations of metformin, and the results showed that the 50 and 100 μM groups significantly promoted osteogenesis of N-BMSCs, while in DM-BMSCs, metformin promoted ALP activity in a dose-dependent manner, with a maximum effective concentration of 125 μM. When the concentration exceeded 200 μM, metformin exhibited inhibitory effects on DM-BMSCs, owing to the lack of effective drug metabolism pathways in the cultured cell type and resulting in an inability to degrade metformin and subsequent drug accumulation and increased cytotoxicity, which is also the first evidence that high concentrations (>200 μM) of metformin can inhibit the osteogenic performance of DM-BMSCs. At the same time, *in vivo* experiments can observe that 50 and 100 μM metformin is able to promote bone integration indicators in rat bones and implants. In addition, metformin increased the expression of phosphorylated AMPK (p-AMPK) and Runx2, while compound C, a specific AMPK inhibitor, downregulated the expression of these proteins induced by metformin. Mechanism research suggested the AMPK/BMP/Smad pathway was responsible for metformin-promoted bone formation (Sun et al., 2021), which was also shown in Liang's data (Liang et al., 2020).

Compared to other sources of MSCs, dental stem cells (DSCs) have the advantage of being easier to obtain and have a higher proliferation rate. Obtaining from discarded tissue also reduces ethical issues (Miura et al., 2003). Many researchers have also demonstrated that metformin promotes osteogenesis of DSCs (Qin et al., 2018a; Kuang et al., 2019; Zhang et al., 2019; Zhao et al., 2020). However, there is a phenomenon of rapid dilution when metformin is used alone, and more studies tend to combine metformin with other scaffold materials to develop a drug delivery system with controlled release of metformin, which has broader application prospects in clinical practice. Although as a nanobiomaterial that promotes bone tissue engineering and osteogenesis, high concentrations of polydopamine template hydroxyapatite (tHA) stimulate the production of ROS, leading to cell damage and apoptosis. Metformin can remove ROS and reduce its damage to cells. After the co-culture of PDLSCs + tHA + metformin, the expression of phosphorylated AMPK increased and the expression of phosphorylated mTOR decreased, indicating that the combination of tHA and metformin regulates autophagy through the AMPK/mTOR signaling pathway and thereby improving the survival ability of PDLSCs and further enhancing the osteogenic effect (Yang et al., 2019). When metformin was incorporated into a resin at 20% by mass as a model system, the gene expression levels of dentin sialophosphoprotein, dentin matrix hosphoprotein1, ALP, and Runx2 of dental pulp stem cells (DPSCs) were significantly increased compared to the group without metformin, which provides ideas for subsequent deep caries filling, pulp hole repair, and periodontal tissue regeneration (Wang et al., 2018). In addition, after loading metformin onto de-mineralized dentin matrix and co-culturing with DPSCs, an appropriate concentration of metformin could release regularly, and upregulation of osteogenic genes and increased mineralisation can be observed (Gao et al., 2020).

In addition to the AMPK pathway, other pathways also have been shown to promote osteogenesis in MSCs by metformin. The Wnt/β-catenin signaling pathway is involved in the regulation of various biological processes of life and has been proven to be a key signaling pathway in the osteogenic differentiation of BMSCs. Ma et al. showed that metformin (at a dose of 100 μM is the best) can increase the phosphorylation of GSK3β at serine 9 residue and promote the activation of β-catenin and the activity of TOPFlash, an

effective tool to investigate the activation of Wnt signaling, therefore enhancing the metformin-mediated osteogenic differentiation of BMSCs (Ma et al., 2018). The same effects at the same concentration of metformin were also demonstrated in other studies (Jia et al., 2020; Zhao et al., 2020). In addition, inhibition of GSK-3β phosphorylation abolished metformin-induced osteogenic differentiation of BMSCs (Ma et al., 2018).

Metformin and PDLSCs were encapsulated in alginate fibrinogen solution to form alginate fibrinogen fibers, and 50 μM metformin promotes osteogenic differentiation of PDLSCs by up-regulating the Shh/Gli1 signaling pathway, while inhibiting the Shh/Gli1 signaling pathway significantly reduces the osteogenic differentiation ability of PDLSCs, which is the first evidence showing that the Shh/Gli1 signaling pathway is involved in metformin-enhanced osteogenic differentiation of PDLSCs. At the same time, it has been demonstrated that alginate fibrin embedded PDLSCs and metformin have great potential in the treatment of maxillofacial bone defects caused by trauma, tumors, etc (Yin et al., 2023).

The formation of bone tissue is influenced by various factors, among which the immune system is an important influencing part. Shen et al. co-cultured metformin-treated macrophages with UCMSCs and demonstrated that metformin plays a regulatory role in the conversion of M1 macrophages into M2 macrophages, and further enhanced M2 macrophages promote osteogenesis of UCMSCs by activating the PI3K/AKT/mTOR signaling pathway (Shen et al., 2022). In addition, the effect of metformin in promoting osteogenic differentiation of MSCs may also be related to treatment time. Experiments have shown that although 100 μM metformin can promote osteogenic differentiation of PDLSCs for 7 and 14 days, metformin significantly promoted the phosphorylation of AKT (p-AKT) at 10 min, and the degree of phosphorylation decreased with time up to 120 min. When the positive effect of metformin on p-AKT was inhibited, the expression of various osteogenic markers of PDLSCs was also reduced (Jia et al., 2020).

Although numerous studies have been conducted on the promotion of MSCs osteogenesis by metformin, and researchers have also proposed and tested its clinical application, it is currently limited to cell experiments and animal models. There is, therefore, a considerable way to go for further research.

2.2.2 Lipogenic differentiation

It is generally accepted that osteogenesis and adipogenic differentiation are mutually exclusive processes. Following incubation of PDLSCs with metformin, the number of lipid droplets in the metformin group was found to be significantly reduced in comparison to the control group. The qRT-PCR results demonstrated that metformin treatment resulted in a reduction in the mRNA levels of the lipid production markers, including peroxisome proliferator-activated receptor γ (PPARγ) and the lipoprotein lipase, in a dose-dependent manner, which indicates that metformin inhibited the adipogenic differentiation of PDLSCs (Jia et al., 2020). Another *in vitro* experiment showed that 1 mM of metformin inhibited fat formation of BMSCs, which may be due to metformin-induced apoptosis of BMSCs and the filling of mouse tibial adipose tissue (Duan et al., 2022). However, Lei et al. have demonstrated that metformin at 3 and 5 mM enhances adipogenic differentiation in UCMSCs, leading to the upregulation of PPARγ mRNA and the downregulation of fatty acid binding protein 4 (Bajetto et al., 2023). Interestingly, similar results were also observed in an *in vivo* study, which showed that after 4 weeks of treatment, 200 mg/kg of metformin increased bone marrow adipose tissue in normal mice and ob/ob mice (a class T2DM model), and interfered with the proliferation of BMSCs and the expression of PPARγ mRNA in BMSCs.

2.2.3 Neurogenic differentiation

Previous studies have shown that metformin activates an atypical protein kinase C- binding protein pathway, which promotes neurogenesis both in cells derived from the bodies of rodents and humans and in adult mouse brains in a CREB binding protein dependent manner (Wang et al., 2012). Although a number of experiments have demonstrated that MSCs exhibit a neural differentiation effect (Lai et al., 2022; Jaiswal and Dhayal, 2023; Romano et al., 2024), there is a paucity of studies investigating the effects of metformin on the neural differentiation of MSCs, and the majority of studies have focused on neural stem cells. Due to the origination from the cranial neural crest, DSCs are considered to have stronger neural differentiation potential than other MSCs, and are also commonly used in the research of neurodegeneration. A combination of chitosan hydrogel and metformin has been employed to enable metformin to function in a three-dimensional environment, significantly enhancing the expression of neural-related markers in human gingival MSCs, including nestin and β-microtubulin, and promoting the upregulation of nerve regeneration related proteins, including ATP5F1, ATP5J, NADH dehydrogenase Fe-S protein 3 and glutamate dehydrogenase 1, which proves the potential of human gingival MSCs-mediated treatment for neurological injury diseases (Cai et al., 2022).

2.2.4 Odontogenic differentiation

Treatment of DPSCs with metformin has been demonstrated to increase the expression of dental cell markers, including dentin sialophosphoprotein and dentin matrix protein 1. Conversely, pre-treatment with compound C resulted in a significant reversal of odontogenic differentiation of DPSCs induced by metformin, indicating that an AMPK-dependent manner was involved in this process (Qin et al., 2018b). Furthermore, MCDs have been demonstrated to activate autophagy and enhance the odontogenic differentiation of DPSCs by up-regulating odontoblast gene marker and protein expression (Lu et al., 2022). When metformin is incorporated into dental resin, which is commonly employed in dental clinical practice, there is no discernible difference in the proliferation of DPSCs compared to resins without metformin. However, odontoblastic differentiation and mineral synthesis of DPSCs are greatly increased. Metformin resin exhibits no cytotoxicity and has the potential to stimulate pulp cells to synthesize new dentin and form dental bridges, demonstrating that the novel resin formulation comprising metformin and lining resin is anticipated to be employed in deep cavities and pulp capping, markedly enhancing the formation of tertiary dentin, facilitating pulp repair, and safeguarding the pulp (Wang et al., 2018). In addition, the combined application of calcium phosphate cement and DPSCs (Qin et al., 2018a), as well as that of novel alginate-fibrin fibers and PDLSCs (Yin et al., 2023), has also yielded an improvement in odontoblastic differentiation.

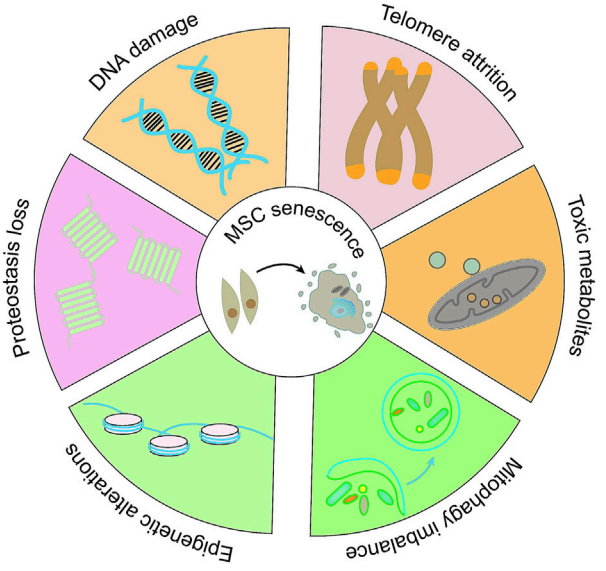

FIGURE 2
The molecular alterations in MSCs senescence. Adapted from (Zhao et al., 2024).

2.2.5 Vascular differentiation

UCMSCs can facilitate the formation of blood vessels in the body by promoting the activity of human umbilical vein endothelial cells (HUVECs), and metformin can enhance this effect. In the experiment conducted by Lei et al., it was observed that UCMSCs treated with metformin exhibited a significantly enhanced angiogenic potential when co-cultured with HUVECs, which was evidenced by an increase in the expression of angiogenesis-related genes including stem cell factor, vascular endothelial growth factor receptor 2, and angiopoietin-2 in UCMSCs. Additionally, *in vivo* experiments using nude mice showed that metformin enhances the promotion of HUVECs angiogenesis by UCMSCs (Lei et al., 2021). BMSCs were incubated on fibrin scaffolds and implanted into the wound model of diabetes rats, and angiogenesis was promoted at the wound through the AKT/mTOR pathway. Moreover, the addition of metformin at an anti-diabetes dose resulted in a significant increase in the levels of p-AKT and p-mTOR in local diabetes wounds, therefore promoting the angiogenic potential of BMSCs (Du et al., 2023). Different concentrations of metformin (5, 10, 20 μM) were used to treat DPSCs, and a dose-dependent manner angiogenic potential of DPSCs was shown, thereby promoting the tissue regeneration mediated by DPSCs (Boreak et al., 2021). However, after long-term cultivation with metformin, the angiogenic potential of MSCs may decrease. Following 14 days of co-culture with BMSCs, the angiogenic potential of BMSCs is observed to decline, and suppression of BMSCs' differentiating into the endothelial lineage by the overly active autophagy pathway was responsible for this phenomenon (Montazersaheb et al., 2018).

2.3 The effect of metformin on the aging of MSCs

Cellular aging is a complex cellular state in which cells respond to various stressors, including changes in function and replication ability, ultimately leading to cessation of cell proliferation, lack of tissue recovery ability, and increased susceptibility to certain diseases (Figure 2) (Fasching, 2018; Zhao et al., 2024). Long term *in vitro* passage culture of MSCs could lead to replicative aging, weakened proliferation and differentiation ability, loss of surface antigen expression of MSCs, seriously affecting the function of MSCs(Wang et al., 2013). In addition, some exogenous stimuli can also induce premature aging of cells (Yu et al., 2021), resulting in decreased regenerative potential and affecting their application in regenerative medicine. It is of great importance for regenerative medicine to re-vitalize MSCs through various methods, in order that they could be re-used for possible treatments. Multiple experimental studies and epidemiological data have shown that metformin has great potential in the prevention and treatment of age-related diseases. Long term use can reduce many pathological risks associated with aging, including cardiovascular diseases, neurodegenerative diseases, and cancers (Porter et al., 2019; Schernthaner et al., 2022). Currently, research on the anti-aging effects of metformin is receiving increasing attention, and its impact on aging MSCs has also been extensively studied (Table 3).

2.3.1 BMSCs

In a model of aging induced by D-galactose in BMSCs, metformin in a low concentration range (10–500 μM) has anti-aging effects on BMSCs, while the opposite is true in high concentrations (200 μM). The specific manifestation is that after treatment with metformin, the production of ROS, loss of mitochondrial membrane potential, and cell cycle arrest in aging cells are reversed, and further investigation revealed that activation of AMPK enhanced autophagy in aged BMSCs and inhibited the aging process (Ye et al., 2023). Compared with BMSCs extracted from normal rats, the ROS level of BMSCs extracted from diabetes rats was significantly higher, and the SA-β-gal staining results showed significant cellular aging. However, after the addition of 200 μM metformin, the intracellular ROS levels and cellular aging were significantly reduced, whereas addition of H_2O_2 inhibited the effect of metformin, indicating that metformin can inhibit cellular aging caused by oxidative stress (Dong et al., 2022). Furthermore, the combined application with biomaterials can achieve sustained release of metformin, thereby promoting the proliferation of BMSCs, and it has also been found that it could neutralize cell aging and attain adequate quantities of fresh BMSCs for tissue engineering applications (Ahmadi et al., 2023).

2.3.2 DSCs

Following the treatment of PDLSCs with H_2O_2, a reduction in proliferation potential was observed, accompanied by an increase in lysosomal β-galactosidase activity, ROS accumulation and the expression of the senescence-associated secretory phenotype (SASP). Metformin pre-treatment has been demonstrated to stimulate autophagy of PDLSCs, partially reverse the harmful effects of H_2O_2 on PDLSCs. In addition, inhibiting autophagy with 3-methyladenosine has been shown to reverse the anti-aging effect of metformin (Kuang et al., 2019). When DPSCs were isolated from elderly donors, metformin was capable of down-regulating miR-34a-3p and up-regulating CAB39 via autophagy related AMPK/mTOR signaling pathway, thereby alleviating the aging of DPSCs (Zhang et al., 2021). However, another study showed that

TABLE 3 The effects of metformin on the aging of MSCs.

Cells	Model building	*In vitro*/ *In vivo*	Dose of metformin	Treatment time	Conclusions	Mechanisms	References
BMSCs	20 g/L of D-gal following 24 h treatment	*in vitro*	10–500 μM 1, 2 mM	72 h	500 μM metformin exerted the best antiaging effect by targeting autophagy	—	Ye et al. (2023)
PDLSCs	exposed to 100 μM H_2O_2 for 2 h	*in vivo*	100 μM	24 h	Metformin could alleviate oxidative stress-induced senescence via stimulating autophagy	—	Kuang et al. (2019)
DPSCs	Aging donors	*in vitro*	100 μM	24 h	—	Upregulate CAB39 and activate the AMPK/mTOR signaling pathway by downregulating miR-34a-3p	Zhang et al. (2021)
rBMSCs	CKD mice	*in vitro*	10 μM	72 h	Metformin preconditioning may exhibit a therapeutic benefit to target accelerated senescence of CKD MSCs	—	Kim et al. (2021)
ADMSCs	Patients with CKD stage 5		Similar to that detected in the serum of patients with type 2 diabetes	—			
ADMSCs	Exposed to 200 μM H_2O_2 for 2 h	*in vitro*	100 μM	24 h	—	Conferred protection against H_2O_2-induced senescence by repressing the mTOR signaling pathway in an AMPK-mediated manner	Li et al. (2022)
		in vivo	—	—	Injection of metformin preconditioned ADSCs slowed osteoarthritis progression and reduced pain in mice		

metformin could result in a significant increase in the number of senescent dental follicle cells. Concurrently, the ratio of NAD to NADH, an indicator of mitochondrial dysfunction and associated with the process of aging, was observed to decrease. These data demonstrated the complexity and uncertainty of metformin's role in cellular aging (Morsczeck et al., 2023).

2.3.3 Adipose derived MSCs

After pre-treatment with metformin in H_2O_2 induced mouse ADMSCs aging model, the levels of ROS were significantly reduced, and the fluorescence intensity of DNA damage markers, including γH2A.X and Rad51, was also observed to be significantly decreased. In addition, the metformin-pretreated-ADMSCs group showed a significant increase in autophagic vacuoles, whereas the addition of 3-MA, an autophagy inhibitor, resulted in a decrease in the number of autophagic vacuoles (Figure 3). The same results were obtained by detecting protein expression levels. In addition, pre-treatment of ADMSCs with compound C resulted in increased levels of p21, p16, and p-mTOR, clearly displayed that metformin stimulates autophagy by activating the AMPK/mTOR pathway, alleviating H_2O_2 induced aging of ADMSCs (Li et al., 2022). Due to the high levels of chronic inflammation and oxidative stress in patients with chronic kidney disease (CKD), which can lead to the accumulation of aging cells, researchers isolated BMSCs from CKD mice and detected DNA damage and cell aging, and found that the expression of the LMNA gene and prelamin A increased, whereas metformin treatment for 72 h resulted in a reduction in their expression, shown by the upregulation of CDKN2A expression and SASP. Additionally, the same results were obtained by ADMSCs from CKD patients, proving that metformin treatment significantly weakened the effects of CKD on cell proliferation and aging. However, further research is required to elucidate the potential relationship and mechanism between aging, autophagy, ROS, and DNA damage (Kim et al., 2021).

3 The effect of metformin on the *in vivo* performance of MSCs

The *in vivo* function of MSCs is mainly manifested in two principal aspects: immunity and regeneration. MSCs have a broad-spectrum immune regulatory ability, which can affect both acquired and innate immunity (Figure 4). It can promote inflammation when the immune system is under-activated, suppress inflammation when the immune system is over-activated to avoid self aggression (Aggarwal and Pittenger, 2005; Chen et al., 2023), and at the same time, MSCs secrete cytokines to promote or suppress immune responses and maintain immune balance according to the type or intensity of inflammation related signals (Jiang and Xu, 2019). In the context of an inflammatory microenvironment, MSCs can influence the proliferation, differentiation, and other functions of immune cells through cell-cell contact or the production of soluble factors, thereby facilitating the repair of damaged tissue, exerting anti-oxidant, immune regulatory, and anti-inflammatory effects, thus been widely used in the treatment of various autoimmune diseases (Lopez-Santalla et al., 2020; Gan et al., 2023). Meanwhile, MSCs can be safely harvested without major ethical issues, have low immunogenicity, and can diminish the risk of transplant rejection and complications, being of greater research value and regarded as an efficacious and reliable cell source for stem cell therapy (Wang et al., 2014). Metformin has been demonstrated to possess profound immune regulatory and anti-

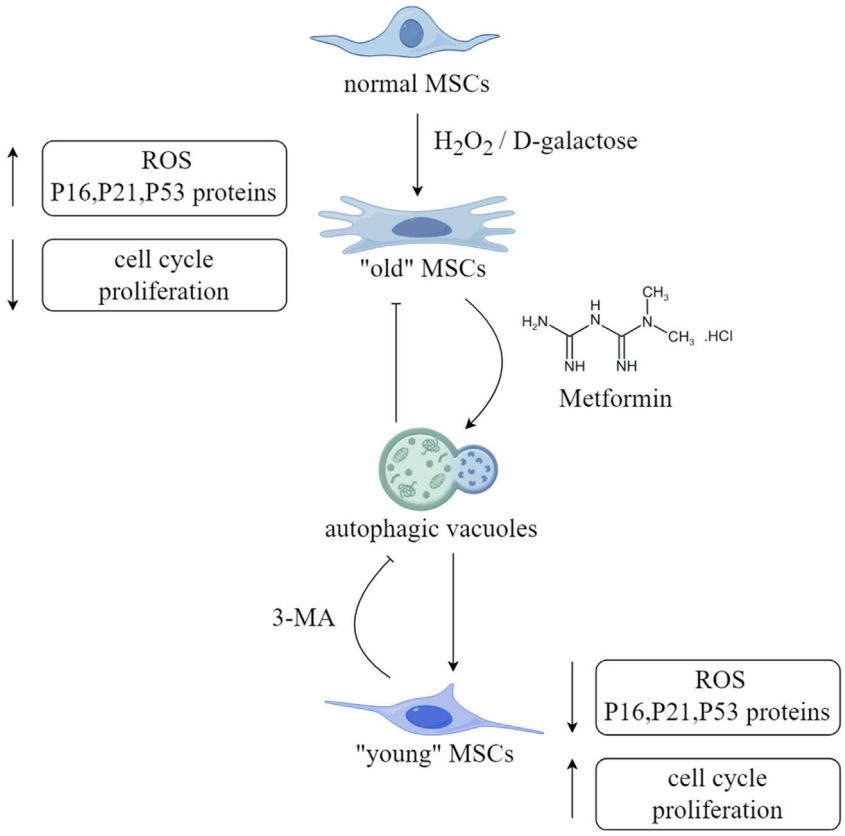

FIGURE 3
Schematic diagram of the anti-aging effect of metformin on MSCs. (ROS,reactive oxyge species). This figure was generated by figdraw.

inflammatory effects *in vitro*, and has shown good therapeutic effects in the treatment of diseases such as cancer, inflammation, and endocrine disorders. In the microenvironment of the body, it can regulate mitochondrial function, autophagy, and immunity, significantly affecting the inflammatory state and health of the body (Cameron et al., 2016). Injury or aging may result in a decline in the body's self-repair function (Notari et al., 2018). MSCs, when used alone or in conjunction with tissue engineering scaffolds, can facilitate tissue repair and play a pivotal role in regenerative medicine. Some progress has been made in regenerating human tissues using autologous MSCs(Lei et al., 2021; Zayed et al., 2021) (Table 4).

3.1 Metformin enhances the immunomodulatory properties of MSCs

Metformin has been demonstrated to regulate metabolism, with the potential to treat autoimmune diseases such as systemic lupus erythematosus (Titov et al., 2019), chronic colitis (Takahara et al., 2022), Sjogren's syndrome (Kim et al., 2019), and others. Metformin pre-treatment resulted in an increase in indoleamine 2, 3-dioxygenase and IL-10 mRNA levels in the culture supernatant of ADMSCs, which suggested that it could upregulate the immune regulatory properties of ADMSCs. In addition, metformin exposure to ADMSCs can lead to the appearance of autophagic vacuoles, and an increase in mitochondrial cristae and density, indicating that metformin pre-treatment stimulated the immune regulatory properties of ADMSCs, which is related to autophagy induction and improved mitochondrial function. Concomitantly, the expression of p-AMPK and p-STAT1 is upregulated, while that of p-STAT3 and p-mTOR is inhibited, demonstrating that metformin promotes the immunomodulatory capacity of ADMSCs by enhancing the expression of STAT1, which depends on the AMPK/mTOR pathway. Subsequently, researchers used lupus animal models to study the *in vivo* effects of metformin on ADMSCs, and the results demonstrated that metformin significantly mitigated the clinical features of lupus, nephritis, and immune cell dysfunction in mice by regulating $CD90.2^{+}CD4^{-}CD8^{-}$ double-negative T cells, $CD4^{+}IL\text{-}17^{+}$ T cells, and $CD4^{+}CD25^{+}Foxp3^{+}$ regulatory T cells, indicating that ADMSCs treated with metformin possess a comprehensive immune regulatory capacity, which may have potential in the clinical application of MSCs for lupus cell therapy (Park et al., 2020). Furthermore, metformin has been shown to significantly enhance the immune regulatory ability of UCMSCs on $CD3^{+}$ and $CD8^{+}$ T cells. Nevertheless, the conditioned medium of UCMSCs treated with metformin is ineffective against $CD4^{+}$ cells, as these cells require different inflammatory cytokines to provide a stimulating response, suggesting that the effect of metformin on the immunoregulatory capabilities of MSCs is closely related to the pro-inflammatory factors (Bajetto et al., 2023).

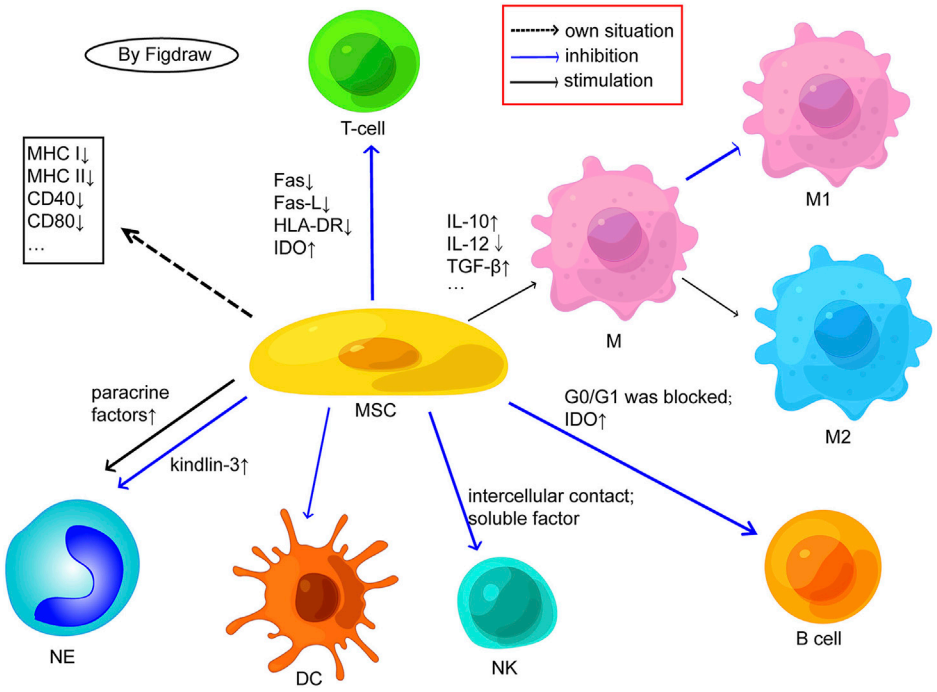

FIGURE 4
Possible cellular mechanisms related to the immunogenicity of MSCs. (M, macrophage; NK, natural killer cell; NE, neutrophil; DC, dendritic cells; Fas-L, fas ligand; IDO, indoleamine 2,3-dioxygenase; HLA, human leukocyte antigen; IL, interleukin; TGF, transforming growth factor). MSCs express low MHC/HLA class I and almost no MHC/HLA class II or costimulatory molecules. MSCs inhibit T cell proliferation by negatively regulating Fas ligand/Fas receptor, downregulating HLA-DR, and activating IDO; MSCs can also inhibit the differentiation of T cells into TH1 and TH17 and enhance the production of Tregs. MSCs facilitate the transition from M1 proinflammatory phenotype macrophages to anti-inflammatory phenotype M2 by promoting the secretion of anti-inflammatory factors and inhibiting the secretion of anti-inflammatory factors. MSCs may inhibit B cell proliferation by blocking G0/G1 phase and activating IDO. E, MSCs inhibit the proliferation of NK cells through intercellular contact and soluble factor mediation. MSCs have an inhibitory effect on the differentiation, maturation, and function of DCs. MSCs may maintain the viability and activity of neutrophils through paracrine factors and may also inhibit the release of NETs from neutrophils by upregulating kindlin-3 signalling. Adapted from (Chen et al., 2023).

Nucleosome assembly protein 1-like 2(Nap1l2) significantly impairs the migration and immune regulatory ability of BMSCs. Transplanting Nap1l2 over-expressing BMSCs into mice reduces the therapeutic effect on autoimmune diseases, including inflammatory bowel disease and experimental allergic encephalomyelitis. However, metformin has been shown to increase the AMP/ATP ratio, activate the AMPK signaling pathway, affect the metabolism of OE-Nap1l2 BMSCs, and enhance their immune regulatory ability (Liu et al., 2024).

3.2 Metformin enhances the regenerative properties of MSCs

MSCs are considered a potential therapeutic agent in regenerative medicine, and the formation of regenerative tissues is dependent upon the presence of blood vessels (Hou et al., 2015). As previously stated, UCMSCs can facilitate HUVECs angiogenesis *in vivo*, and metformin can augment this effect (Lei et al., 2021). Prajakta Kamble et al. conducted an experiment to test the efficacy of metformin-pretreated buccal fat pad-MSCs (BFPMSCs) in reversing hyperglycaemia. In the animal experiment with diabetic rats as the model, it was found that the blood sugar of the rats in the stem cell group, following pre-treatment with metformin, was reduced in comparison to the rats in other groups. Additionally, the pancreatic and serum insulin levels were also normal. The histological results demonstrated that pancreatic cells increased, and the pancreatic regeneration ability was reversed, indicating that the BFPMSCs pre-treated with metformin could regenerate pancreatic cells (Kamble et al., 2023). In comparison to the control group, HUVECs co-cultured with SHED that had been pre-treated with metformin demonstrated the capacity to form more capillary-like structures, showing a higher anti-CD31-positive capillary density (Deng et al., 2022). Nevertheless, it should be noted that not all metformin pre-treated MSCs demonstrate beneficial effects in disease models. Transplantation of BMSCs can prevent cardiac fibrosis and promote angiogenesis in diabetic rats. However, adding metformin could downregulate the cardiac protection mediated by BMSCs. Interestingly, both BMSCs and metformin alone can improve heart function, while the combination of metformin and BMSCs does not have a synergistic effect. As for the underlying mechanisms, metformin treatment was shown to impair the homing of transplanted BMSCs in the heart and lead to a decrease in the survival rate of transplanted cells, which is caused by AMPK activation (Ammar et al., 2021).

4 Existing problems and future direction

MSCs are a promising tool in the field of regenerative medicine due to their ability to proliferate, differentiate into multiple cell types,

TABLE 4 The effects of metformin on the *in vivo* characteristics of MSCs.

Cells	*In vitro*	Dose and time of metformin	Gene expression	*In vivo*	Animals	Model induction	Concentration and time	Administration method	Results	Mechanisms	References
ADMSCs	√	5 mM 72 h	Enhanced IDO, IL-10 and TGF-β Inhibited $CD4^-$ $CD8^-$ T-cell expansion and Th17/Treg cell ratio	√	Female MRL/lpr mice	—	ADMSCs were pretreated with 5 mM metformin for 3 d	I.v.injection once weekly for 8 weeks	Significant disease activity improvement including inflammatory phenotype, glomerulonephritis, proteinuria and anti-dsDNA IgG antibody production	Metformin enhanced the immunomodulatory properties of Ad-MSCs through STAT1	Park et al. (2020)
UCMSCs	√	3 mM 72 h	Reduce the expression of IL-6, MCP-1, and COX-2	—	—		—	—	Reduce the production of inflammatory mediators, enhancing UCMSC immunoregulatory capacity on $CD3^+$ and $CD8^+$ T cells	—	Bajetto et al. (2023)
ADMSCs	√	1 mM 48 h	Increased IDO and IL-10 mRNA levels	√	Six-week-old male Wistar rats	Injected with 3 mg of monosodium iodoacetate to form osteoarthritis	—	ADMSCs or metformin stimulated ADMSCs were administered i.v. twice: at 0 and 4 days	Metformin pretreatment stimulated the immunoregulatory properties of ADMSCs and that this was associated with autophagy induction and improved mitochondrial function	—	Park et al. (2019)
BMSCs	√	—	IL-6 and IL-1 expression downregulated and Tgfβ and IL-10 expression upregulated in a dose-dependent manner	√	Male C57BL/6 mice	3% DSS in drinking water was provided *ad libitum* for 7 days	—	The tail vein injection	Metformin could improve the impaired therapeutic efficacy of OE-Nap1l2 BMSCs in the treatment of colitis and experimental autoimmune encephalomyelitis in mice	Metformin treatment could rescue the immunomodulation capacities of BMSCs by activating the AMPK signalling pathway	Liu et al. (2024)
BFPMSCs	—	—	—	√	Male and female Wistar rats with weights 200–250 g and ages 3–4 months	Injecting streptozotocin intravenously with a dose of 45 mg/kg of body weight	BFPMSCs were pre-treated with 1 mM metformin for 24 h	Injected intramuscularly into rats at 0.5 millioncells/animal	Metformin preconditioned BFPMSCs can regenerate pancreatic cells	—	Kamble et al. (2023)

(Continued on following page)

10.3389/fphar.2024.1465697

TABLE 4 (*Continued*) The effects of metformin on the *in vivo* characteristics of MSCs.

Cells	*In vitro*	Dose and time of metformin	Gene expression	*In vivo*	Animals	Model induction	Concentration and time	Administration method	Results	Mechanisms	References
SHED	√	100 μM 24 h	SHED pre-treated with metformin improves migration and angiogenesis of HUVECs *in vitro*	√	Nude mice	—	—	Injected into the lower dorsal region of the nude mice	SHED pre-treated with metformin exhibits a strong capacity for promoting angiogenesis	—	Deng et al. (2022)
BMSCs	—	—	—	√	Male adult Wistar rats (150–170 g)	Injected with streptozotocin (52.5 mg/kg) to Induce diabetes	300 mg/kg/d after diabetes con-firmation at day 3 and continued till the end of the study	Oral gavage	Metformin impairs homing and engraftment of transplanted BMSCs in the heart	Metformin treatment led to activation of AMPK that further was responsible for poor homing and survival of transplanted BMSCs in the heart	Ammar et al. (2021)
BMSCs	√	50 and 100 μM 14 d	The angiogenic potential of MSCs was shown to decrease after prolonged incubation with metformin	—	—	—	—	—	—	—	Montazersaheb et al. (2018)

10.3389/fphar.2024.1465697

regulate the immune system, and exhibit other beneficial characteristics. Their versatility and therapeutic potential have led to their extensive use in various disease models. Nevertheless, in the treatment of certain pre-clinical models, the requisite characteristics are not consistently expressed, necessitating the optimization of MSCs applications to ensure optimal outcomes. Metformin has good bio-safety and relatively low cost, and has been widely used in clinical diagnosis and treatment for many years. Recent studies have demonstrated that its effects extend beyond the regulation of blood sugar. A review of existing clinical and experimental studies indicates that metformin has excellent bone promoting effects, inhibits cell aging, and has anti-tumor effects. Nevertheless, the study of metformin based on its non-antidiabetic functions is still in its infancy, which suggests that metformin still has considerable scope for further investigation in this field. The current studies are mainly limited to pre-clinical cell and animal research models. Following the demonstration of numerous positive effects *in vitro* and in animal studies, it is recommended that human clinical trials be conducted in order to evaluate the extent to which metformin has beneficial effects on human participants. Meanwhile, compared to single drug therapy, the combination of drugs using stem cells may have better therapeutic effects. However, it is worth noting that the optimal concentration of metformin varies greatly among different cell types. Exploring the appropriate concentration of metformin for different cells is of great significance for its application in tissue engineering. Metformin exerts its effects on MSCs through a multitude of molecular mechanisms and signaling pathways, which may vary depending on the source of the stem cells. Furthermore, the sustained effect of metformin in applications is also a significant issue that requires further investigation, and the combined use of scaffold materials may be a good choice. Anyway, the positive effects of metformin on tissue regeneration of MSCs still require more *in vivo* experiments to verify, which is a key area of future research.

5 Conclusion

Metformin, a commonly used drug, has many potential applications and considerable benefits on the biological characteristics of MSCs, providing broader insights for MSCs-mediated immunomodulation and tissue regeneration. However, there is still a long way to go before the application in clinics.

Author contributions

XL: Conceptualization, Formal Analysis, Investigation, Methodology, Writing–original draft. ZL: Formal Analysis, Investigation, Methodology, Writing–original draft. LL: Formal Analysis, Investigation, Methodology, Writing–original draft. PZ: Formal Analysis, Investigation, Methodology, Writing–original draft. YW: Data curation, Formal Analysis, Investigation, Writing–original draft. GD: Conceptualization, Funding acquisition, Supervision, Writing–review and editing.

Funding

The author(s) declare that financial support was received for the research, authorship, and/or publication of this article. This work was supported by grants from the Natural Science Foundation of Shandong Province (No.ZR2021MH051 to GD), the National Natural Science Foundation of China (No.81570945 to GD), and the Kite Capital Scholars Programme (NO.ydxz2023002 to GD). The funding source was not involved in study design, in collection, analysis and interpretation of data, in the writing of the manuscript, or in the decision to submit the article for publication.

Conflict of interest

The authors declare that the research was conducted in the absence of any commercial or financial relationships that could be construed as a potential conflict of interest.

Publisher's note

References

Aggarwal, S., and Pittenger, M. F. (2005). Human mesenchymal stem cells modulate allogeneic immune cell responses. *Blood* 105 (4), 1815–1822. doi:10.1182/blood-2004-04-1559

Ahmadi, S., Dadashpour, M., Abri, A., and Zarghami, N. (2023). Long-term proliferation and delayed senescence of bone marrow-derived human mesenchymal stem cells on metformin co-embedded HA/Gel electrospun composite nanofibers. *J. Drug Deliv. Sci. Technol.* 80, 104071. doi:10.1016/j.jddst.2022.104071

Al Jofi, F. E., Ma, T., Guo, D., Schneider, M. P., Shu, Y., Xu, H. H. K., et al. (2018). Functional organic cation transporters mediate osteogenic response to metformin in human umbilical cord mesenchymal stromal cells. *Cytotherapy* 20 (5), 650–659. doi:10.1016/j.jcyt.2018.02.369

Ammar, H. I., Shamseldeen, A. M., Shoukry, H. S., Ashour, H., Kamar, S. S., Rashed, L. A., et al. (2021). Metformin impairs homing ability and efficacy of mesenchymal stem cells for cardiac repair in streptozotocin-induced diabetic cardiomyopathy in rats. *Am. J. Physiol. Heart Circ. Physiol.* 320 (4), H1290–H1302. doi:10.1152/ajpheart.00317.2020

Bajetto, A., Pattarozzi, A., Sirito, R., Barbieri, F., and Florio, T. (2023). Metformin potentiates immunosuppressant activity and adipogenic differentiation of human umbilical cord-mesenchymal stem cells. *Int. Immunopharmacol.* 124, 111078. doi:10.1016/j.intimp.2023.111078

Boreak, N., Khayrat, N. M. A., Shami, A. O., Zaylaee, H. J. M., Hanbashi, A. A., Souri, S. A., et al. (2021). Metformin pre-conditioning enhances the angiogenic ability of the secretome of dental pulp stem cells. *Saudi Pharm. J.* 29 (8), 908–913. doi:10.1016/j.jsps.2021.07.004

Cai, S., Lei, T., Bi, W., Sun, S., Deng, S., Zhang, X., et al. (2022). Chitosan hydrogel supplemented with metformin promotes neuron-like cell differentiation of gingival mesenchymal stem cells. *Int. J. Mol. Sci.* 23 (6), 3276. doi:10.3390/ijms23063276

Cameron, A. R., Morrison, V. L., Levin, D., Mohan, M., Forteath, C., Beall, C., et al. (2016). Anti-inflammatory effects of metformin irrespective of diabetes status. *Circ. Res.* 119 (5), 652–665. doi:10.1161/circresaha.116.308445

Campagnoli, C., Roberts, I. A., Kumar, S., Bennett, P. R., Bellantuono, I., and Fisk, N. M. (2001). Identification of mesenchymal stem/progenitor cells in human first-trimester fetal blood, liver, and bone marrow. *Blood* 98 (8), 2396–2402. doi:10.1182/blood.v98.8.2396

Chaudhary, S., and Kulkarni, A. (2024). Metformin: past, present, and future. *Curr. Diab. Rep.* 24 (6), 119–130. doi:10.1007/s11892-024-01539-1

Chen, W., Lv, L., Chen, N., and Cui, E. (2023). Immunogenicity of mesenchymal stromal/stem cells. *Scand. J. Immunol.* 97 (6), e13267. doi:10.1111/sji.13267

Deng, S., Lei, T., Chen, H., Zheng, H., Xiao, Z., Cai, S., et al. (2022). Metformin pre-treatment of stem cells from human exfoliated deciduous teeth promotes migration and angiogenesis of human umbilical vein endothelial cells for tissue engineering. *Cytotherapy* 24 (11), 1095–1104. doi:10.1016/j.jcyt.2022.07.003

Dong, K., Zhou, W.-J., and Liu, Z.-H. (2022). Metformin enhances the osteogenic activity of rat bone marrow mesenchymal stem cells by inhibiting oxidative stress induced by diabetes mellitus: an *in vitro* and *in vivo* study. *J. Periodontal Implant Sci.* 53 (1), 54–68. doi:10.5051/jpis.2106240312

Du, F., Liu, M., Wang, J., Hu, L., Zeng, D., Zhou, S., et al. (2023). Metformin coordinates with mesenchymal cells to promote VEGF-mediated angiogenesis in diabetic wound healing through Akt/mTOR activation. *Metabolism* 140, 155398. doi:10.1016/j.metabol.2023.155398

Duan, W., Zou, H., Zang, N., Ma, D., Yang, B., and Zhu, L. (2022). Metformin increases bone marrow adipose tissue by promoting mesenchymal stromal cells apoptosis. *Aging-US* 15 (2), 542–552. doi:10.18632/aging.204486

Fasching, C. L. (2018). Telomere length measurement as a clinical biomarker of aging and disease. *Crit. Rev. Clin. Lab. Sci.* 55 (7), 443–465. doi:10.1080/10408363.2018.1504274

Gan, J., Zhang, X., Chen, G., Hao, X., Zhao, Y., and Sun, L. (2023). CXCR4-expressing mesenchymal stem cells derived nanovesicles for rheumatoid arthritis treatment. *Adv. Healthc. Mat.* 13 (9), 2303300. doi:10.1002/adhm.202303300

Gao, X., Qin, W., Chen, L., Fan, W., Ma, T., Schneider, A., et al. (2020). Effects of targeted delivery of metformin and dental pulp stem cells on osteogenesis via demineralized dentin matrix under high glucose conditions. *ACS Biomater. Sci. Eng.* 6 (4), 2346–2356. doi:10.1021/acsbiomaterials.0c00124

Gao, Y., Xue, J., Li, X., Jia, Y., and Hu, J. (2008). Metformin regulates osteoblast and adipocyte differentiation of rat mesenchymal stem cells. *J. Pharm. Pharmacol.* 60 (12), 1695–1700. doi:10.1211/jpp.60.12.0017

Gronthos, S., Mankani, M., Brahim, J., Robey, P. G., and Shi, S. (2000). Postnatal human dental pulp stem cells (DPSCs) *in vitro* and *in vivo*. *Proc. Natl. Acad. Sci. U. S. A.* 97 (25), 13625–13630. doi:10.1073/pnas.240309797

Guo, Y., Wei, J., Liu, C., Li, X., and Yan, W. (2023). Metformin regulates bone marrow stromal cells to accelerate bone healing in diabetic mice. *eLife* 12, e88310. doi:10.7554/eLife.88310

Ha, N.N.-Y., Huynh, T. K. T., Phan, N. U. P., Nguyen, T.-H., Vong, L. B., and Trinh, N.-T. (2023). Synergistic effect of metformin and vitamin D3 on osteogenic differentiation of human adipose tissue-derived mesenchymal stem cells under high d-glucose conditions. *Regen. Ther.* 25, 147–156. doi:10.1016/j.reth.2023.12.003

Hidayat, K., Du, X., Wu, M. J., and Shi, B. M. (2019). The use of metformin, insulin, sulphonylureas, and thiazolidinediones and the risk of fracture: systematic review and meta-analysis of observational studies. *Obes. Rev.* 20 (10), 1494–1503. doi:10.1111/obr.12885

Hoang, D. M., Pham, P. T., Bach, T. Q., Ngo, A. T. L., Nguyen, Q. T., Phan, T. T. K., et al. (2022). Stem cell-based therapy for human diseases. *Signal Transduct. Target. Ther.* 7 (1), 272. doi:10.1038/s41392-022-01134-4

Hou, L., Kim, J. J., Woo, Y. J., and Huang, N. F. (2015). Stem cell-based therapies to promote angiogenesis in ischemic cardiovascular disease. *Am. J. Physiol. Heart Circ. Physiol.* 310 (4), H455–H465. doi:10.1152/ajpheart.00726.2015

Huang, H., Liu, X., Wang, J., Suo, M., Zhang, J., Sun, T., et al. (2023). Umbilical cord mesenchymal stem cells for regenerative treatment of intervertebral disc degeneration. *Front. Cell Dev. Biol.* 11, 1215698. doi:10.3389/fcell.2023.1215698

Jaiswal, J., and Dhayal, M. (2023). Rapid neurogenic differentiation of human mesenchymal stem cells through electrochemical stimulation. *Bioelectrochemistry* 153, 108468. doi:10.1016/j.bioelechem.2023.108468

Jia, L., Xiong, Y., Zhang, W., Ma, X., and Xu, X. (2020). Metformin promotes osteogenic differentiation and protects against oxidative stress-induced damage in periodontal ligament stem cells via activation of the Akt/Nrf2 signaling pathway. *Exp. Cell Res.* 386 (2), 111717. doi:10.1016/j.yexcr.2019.111717

Jiang, W., and Xu, J. (2019). Immune modulation by mesenchymal stem cells. *Cell Prolif.* 312 (12), 127122–e22179. doi:10.1111/cpr.12712

Kamble, P., Desai, S., Bhonde, R., Sanap, A., Shimpi, J., Kumbhar, R., et al. (2023). Therapeutic potential of metformin-preconditioned mesenchymal stem cells for pancreatic regeneration. *Curr. Drug Discov. Technol.* 20 (3), e090323214492. doi:10.2174/1570163820666230309094233

Keating, A. (2012). Mesenchymal stromal cells: new directions. *Cell Stem Cell* 10 (6), 709–716. doi:10.1016/j.stem.2012.05.015

Keshavarz, R., Olsen, S., and Almeida, B. (2023). Using biomaterials to improve mesenchymal stem cell therapies for chronic, nonhealing wounds. *Bioeng. Transl. Med.* 9 (1), e10598. doi:10.1002/btm2.10598

Kim, H., Yu, M. R., Lee, H., Kwon, S. H., Jeon, J. S., Han, D. C., et al. (2021). Metformin inhibits chronic kidney disease-induced DNA damage and senescence of mesenchymal stem cells. *Aging Cell* 20 (2), e13317. doi:10.1111/acel.13317

Kim, J.-W., Kim, S.-M., Park, J.-S., Hwang, S.-H., Choi, J., Jung, K.-A., et al. (2019). Metformin improves salivary gland inflammation and hypofunction in murine Sjögren's syndrome. *Arthritis Res. Ther.* 21 (1), 136. doi:10.1186/s13075-019-1904-0

Kouhestani, F., Rezai Rad, M., Mohaghegh, S., and Motamedian, S. R. (2021). Effect of metformin on the behavior of dental pulp stem cells cultured on freeze-dried bone allografts. *Dent. Med. Probl.* 58 (3), 343–349. doi:10.17219/dmp/131988

Kuang, Y., Hu, B., Feng, G., Xiang, M., Deng, Y., Tan, M., et al. (2019). Metformin prevents against oxidative stress-induced senescence in human periodontal ligament cells. *Biogerontology* 21 (1), 13–27. doi:10.1007/s10522-019-09838-x

Lai, C. F., Shen, J., Balic, A., Pagella, P., Schwab, M. E., and Mitsiadis, T. A. (2022). Nogo-A regulates the fate of human dental pulp stem cells toward osteogenic, adipogenic, and neurogenic differentiation. *Cells* 11 (21), 3415. doi:10.3390/cells11213415

LaMoia, T. E., and Shulman, G. I. (2021). Cellular and molecular mechanisms of metformin action. *Endocr. Rev.* 42 (1), 77–96. doi:10.1210/endrev/bnaa023

Lee, R. H., Sloane, R., Pieper, C., Lyles, K. W., Adler, R. A., Van Houtven, C., et al. (2019). Glycemic control and insulin treatment alter fracture risk in older men with type 2 diabetes mellitus. *J. Bone Min. Res.* 34 (11), 2045–2051. doi:10.1002/jbmr.3826

Lei, T., Deng, S., Chen, P., Xiao, Z., Cai, S., Hang, Z., et al. (2021). Metformin enhances the osteogenesis and angiogenesis of human umbilical cord mesenchymal stem cells for tissue regeneration engineering. *Int. J. Biochem. Cell Biol.* 141, 106086. doi:10.1016/j.biocel.2021.106086

Li, Z., Liu, L., Yang, Y., Zheng, H., Cai, Y., Ma, Y., et al. (2022). Metformin ameliorates senescence of adipose-derived mesenchymal stem cells and attenuates osteoarthritis progression via the AMPK-dependent autophagy pathway. *Oxid. Med. Cell. Longev.* 2022, 4620254. doi:10.1155/2022/4620254

Liang, C., Sun, R., Xu, Y., Geng, W., and Li, J. (2020). Effect of the abnormal expression of BMP-4 in the blood of diabetic patients on the osteogenic differentiation potential of alveolar BMSCs and the rescue effect of metformin: a bioinformatics-based study. *Biomed. Res. Int.* 2020, 7626215. doi:10.1155/2020/7626215

Liu, F., Han, R., Nie, S., Cao, Y., Zhang, X., Gao, F., et al. (2024). Metformin rejuvenates Nap1l2-impaired immunomodulation of bone marrow mesenchymal stem cells via metabolic reprogramming. *Cell Prolif.* 57 (7), e13612. doi:10.1111/cpr.13612

Liu, T.-M. (2022). Application of mesenchymal stem cells derived from human pluripotent stem cells in regenerative medicine. *World J. Stem Cells* 13 (12), 1826–1844. doi:10.4252/wjsc.v13.i12.1826

Longobardi, L., O'Rear, L., Aakula, S., Johnstone, B., Shimer, K., Chytil, A., et al. (2006). Effect of IGF-I in the chondrogenesis of bone marrow mesenchymal stem cells in the presence or absence of TGF-beta signaling. *J. Bone Min. Res.* 21 (4), 626–636. doi:10.1359/jbmr.051213

Lopez-Santalla, M., Hervas-Salcedo, R., Fernandez-Garcia, M., Bueren, J. A., and Garin, M. I. (2020). Cell therapy with mesenchymal stem cells induces an innate immune memory response that attenuates experimental colitis in the long term. *J. Crohns Colitis* 14 (10), 1424–1435. doi:10.1093/ecco-jcc/jjaa079

Lu, J., Li, R., Ni, S., Xie, Y., Liu, X., Zhang, K., et al. (2022). Metformin carbon nanodots promote odontoblastic differentiation of dental pulp stem cells by pathway of autophagy. *Front. Bioeng. Biotechnol.* 10, 1002291. doi:10.3389/fbioe.2022.1002291

Ma, J., Zhang, Z. L., Hu, X. T., Wang, X. T., and Chen, A. M. (2018). Metformin promotes differentiation of human bone marrow derived mesenchymal stem cells into osteoblast via GSK3β inhibition. *Eur. Rev. Med. Pharmacol. Sci.* 22 (22), 7962–7968. doi:10.26355/eurrev_201811_16424

Marcucci, F., Romeo, E., Caserta, C. A., Rumio, C., and Lefoulon, F. (2020). Context-dependent pharmacological effects of metformin on the immune system. *Trends Pharmacol. Sci.* 41 (3), 162–171. doi:10.1016/j.tips.2020.01.003

Meng, F., Xu, R., Wang, S., Xu, Z., Zhang, C., and Li, Y. (2020). Human umbilical cord-derived mesenchymal stem cell therapy in patients with COVID-19: a phase 1 clinical trial. *Signal Transduct. Target Ther.* 5 (1), 172. doi:10.1038/s41392-020-00286-5

Miura, S. G., Zhao, M., Lu, B., Fisher, L. W., Robey, P. G., et al. (2003). SHED Stem cells from human exfoliated deciduous teeth. *Proc. Natl. Acad. Sci. U. S. A.* 100 (10), 5807–5812. doi:10.1073/pnas.0937635100

Montazersaheb, S., Kabiri, F., Saliani, N., Nourazarian, A., Avci, Ç. B., Rahbarghazi, R., et al. (2018). Prolonged incubation with metformin decreased angiogenic potential in human bone marrow mesenchymal stem cells. *Biomed. Pharmacother.* 108, 1328–1337. doi:10.1016/j.biopha.2018.09.135

Morsczeck, C., Reck, A., and Reichert, T. E. (2023). Changes in AMPK activity induces cellular senescence in human dental follicle cells. *Exp. Gerontol.* 172, 112071. doi:10.1016/j.exger.2022.112071

Notari, M., Ventura-Rubio, A., Bedford-Guaus, S. J., Jorba, I., Mulero, L., Navajas, D., et al. (2018). The local microenvironment limits the regenerative potential of the mouse neonatal heart. *Sci. Adv.* 4 (5), eaao5553. doi:10.1126/sciadv.aao5553

Park, M.-J., Moon, S.-J., Baek, J.-A., Lee, E.-J., Jung, K.-A., Kim, E.-K., et al. (2019). Metformin augments anti-inflammatory and chondroprotective properties of mesenchymal stem cells in experimental osteoarthritis. *J. Immunol.* 203 (1), 127–136. doi:10.4049/jimmunol.1800006

Park, S.-H., Cho, M.-L., Kwok, S.-K., Hong, S.-M., Lee, J., and Jang, S. G. (2020). Metformin enhances the immunomodulatory potential of adipose-derived mesenchymal stem cells through STAT1 in an animal model of lupus. *Rheumatology* 59 (6), 1426–1438. doi:10.1093/rheumatology/kez631

Pittenger, M. F., Mackay, A. M., Beck, S. C., Jaiswal, R. K., Douglas, R., Mosca, J. D., et al. (1999). Multilineage potential of adult human mesenchymal stem cells. *Science* 284 (5411), 143–147. doi:10.1126/science.284.5411.143

Porter, K. M., Ward, M., Hughes, C. F., O'Kane, M., Hoey, L., McCann, A., et al. (2019). Hyperglycemia and metformin use are associated with B vitamin deficiency and cognitive dysfunction in older adults. *J. Clin. Endocrinol. Metab.* 104 (10), 4837–4847. doi:10.1210/jc.2018-01791

Qin, W., Chen, J.-Y., Guo, J., Ma, T., Weir, M. D., Guo, D., et al. (2018a). Novel calcium phosphate cement with metformin-loaded chitosan for odontogenic differentiation of human dental pulp cells. *Stem Cells Int.* 2018 (1), 7173481–7173510. doi:10.1155/2018/7173481

Qin, W., Gao, X., Ma, T., Weir, M. D., Zou, J., Song, B., et al. (2018b). Metformin enhances the differentiation of dental pulp cells into odontoblasts by activating AMPK signaling. *J. Endod.* 44 (4), 576–584. doi:10.1016/j.joen.2017.11.017

Raghavan, S., Malayaperumal, S., Mohan, V., and Balasubramanyam, M. (2020). A comparative study on the cellular stressors in mesenchymal stem cells (MSCs) and pancreatic β-cells under hyperglycemic milieu. *Mol. Cell. Biochem.* 476 (1), 457–469. doi:10.1007/s11010-020-03922-4

Ren, C., Hao, X., Wang, L., Hu, Y., Meng, L., Zheng, S., et al. (2021). Metformin carbon dots for promoting periodontal bone regeneration via activation of ERK/AMPK pathway. *Adv. Healthc. Mat.* 10 (12), e2100196. doi:10.1002/adhm.202100196

Romano, I. R., D'Angeli, F., Gili, E., Fruciano, M., Lombardo, G. A. G., Mannino, G., et al. (2024). Melatonin enhances neural differentiation of adipose-derived mesenchymal stem cells. *Int. J. Mol. Sci.* 25 (9), 4891. doi:10.3390/ijms25094891

Saei Arezoumand, K., Alizadeh, E., Pilehvar-Soltanahmadi, Y., Esmaeillou, M., and Zarghami, N. (2016). An overview on different strategies for the stemness maintenance of MSCs. *Artif. Cells Nanomed. Biotechnol.* 45 (7), 1255–1271. doi:10.1080/21691401.2016.1246452

Schernthaner, G., Brand, K., and Bailey, C. J. (2022). Metformin and the heart: update on mechanisms of cardiovascular protection with special reference to comorbid type 2 diabetes and heart failure. *Metabolism* 35 (7), 155160. doi:10.1016/j.metabol.2022.155160

Shen, M., Yu, H., Jin, Y., Mo, J., Sui, J., Qian, X., et al. (2022). Metformin facilitates osteoblastic differentiation and M2 macrophage polarization by PI3K/AKT/mTOR pathway in human umbilical cord mesenchymal stem cells. *Stem Cells Int.* 2022, 9498876. doi:10.1155/2022/9498876

Sherman, L. S., Romagano, M. P., Williams, S. F., and Rameshwar, P. (2019). Mesenchymal stem cell therapies in brain disease. *Semin. Cell Dev. Biol.* 95, 111–119. doi:10.1016/j.semcdb.2019.03.003

Śmieszek, A., Tomaszewski, K., Kornicka, K., and Marycz, K. (2018). Metformin promotes osteogenic differentiation of adipose-derived stromal cells and exerts pro-osteogenic effect stimulating bone regeneration. *J. Clin. Med.* 7 (12), 482. doi:10.3390/jcm7120482

Soldat-Stanković, V., Popović-Pejičić, S., Stanković, S., Prtina, A., Malešević, G., Bjekić-Macut, J., et al. (2021). The effect of metformin and myoinositol on metabolic outcomes in women with polycystic ovary syndrome: role of body mass and adiponectin in a randomized controlled trial. *J. Endocrinol. Inves.* 45 (3), 583–595. doi:10.1007/s40618-021-01691-5

Sun, R., Liang, C., Sun, Y., Xu, Y., Geng, W., and Li, J. (2021). Effects of metformin on the osteogenesis of alveolar BMSCs from diabetic patients and implant osseointegration in rats. *Oral Dis.* 28 (4), 1170–1180. doi:10.1111/odi.13808

Takahara, M., Takaki, A., Hiraoka, S., Takei, K., Yasutomi, E., Igawa, S., et al. (2022). Metformin ameliorates chronic colitis in a mouse model by regulating interferon-γ-producing lamina propria CD4+ T cells through AMPK activation. *FASEB J.* 36 (2), e22139. doi:10.1096/fj.202100831RR

Titov, A. A., Baker, H. V., Brusko, T. M., Sobel, E. S., and Morel, L. (2019). Metformin inhibits the type 1 IFN response in human CD4+ T cells. *J. Immunol.* 203 (2), 338–348. doi:10.4049/jimmunol.1801651

Veeramachaneni, R., Yu, W., Newton, J. M., Kemnade, J. O., Skinner, H. D., Sikora, A. G., et al. (2021). Metformin generates profound alterations in systemic and tumor immunity with associated antitumor effects. *J. Immunother. Cancer* 9 (7), e002773. doi:10.1136/jitc-2021-002773

Wang, J., Gallagher, D., DeVito, L. M., Cancino, G. I., Tsui, D., He, L., et al. (2012). Metformin activates an atypical PKC-CBP pathway to promote neurogenesis and enhance spatial memory formation. *Cell Stem Cell* 11 (1), 23–35. doi:10.1016/j.stem.2012.03.016

Wang, P., Ma, T., Guo, D., Hu, K., Shu, Y., Xu, H. H. K., et al. (2017). Metformin induces osteoblastic differentiation of human induced pluripotent stem cell-derived mesenchymal stem cells. *J. Tissue Eng. Regen. Med.* 12 (2), 437–446. doi:10.1002/term.2470

Wang, S., Xia, Y., Ma, T., Weir, M. D., Ren, K., Reynolds, M. A., et al. (2018). Novel metformin-containing resin promotes odontogenic differentiation and mineral synthesis of dental pulp stem cells. *Drug Deliv. Transl. Res.* 9 (1), 85–96. doi:10.1007/s13346-018-00600-3

Wang, Y., Chen, X., Cao, W., and Shi, Y. (2014). Plasticity of mesenchymal stem cells in immunomodulation: pathological and therapeutic implications. *Nat. Immunol.* 15 (11), 1009–1016. doi:10.1038/ni.3002

Wang, Y., Zhang, Z., Chi, Y., Zhang, Q., Xu, F., Yang, Z., et al. (2013). Long-term cultured mesenchymal stem cells frequently develop genomic mutations but do not undergo malignant transformation. *Cell Death Dis.* 4 (12), e950. doi:10.1038/cddis.2013.480

Wróbel, M. P., Marek, B., Kajdaniuk, D., Rokicka, D., Szymborska-Kajanek, A., and Strojek, K. (2017). Metformin - a new old drug. *Endokrynol. Pol.* 68 (4), 482–496. doi:10.5603/ep.2017.0050

Yang, Z., Gao, X., Zhou, M., Kuang, Y., Xiang, M., Li, J., et al. (2019). Effect of metformin on human periodontal ligament stem cells cultured with polydopamine-templated hydroxyapatite. *Eur. J. Oral Sci.* 127 (3), 210–221. doi:10.1111/eos.12616

Ye, P., Feng, L., Zhang, D., Li, R., Wen, Y., Tong, X., et al. (2023). Metformin ameliorates D-galactose-induced senescent human bone marrow-derived mesenchymal stem cells by enhancing autophagy. *Stem Cells Int.* 2023, 1429642. doi:10.1155/2023/1429642

Yin, J., Lei, Q., Luo, X., Jiang, T., Zou, X., Schneider, A., et al. (2023). Degradable hydrogel fibers encapsulate and deliver metformin and periodontal ligament stem cells for dental and periodontal regeneration. *J. Appl. Oral Sci.* 31, e20220447. doi:10.1590/1678-7757-2022-0447

Yu, C., Xiao, J.-H., and Rupasinghe, H. P. V. (2021). The Keap1-Nrf2 System: a mediator between oxidative stress and aging. *Oxid. Med. Cell. Longev.* 2021, 6635460. doi:10.1155/2021/6635460

Zayed, M., Iohara, K., Watanabe, H., Ishikawa, M., Tominaga, M., and Nakashima, M. (2021). Characterization of stable hypoxia-preconditioned dental pulp stem cells compared with mobilized dental pulp stem cells for application for pulp regenerative therapy. *Stem Cell Res. Ther.* 12 (1), 302. doi:10.1186/s13287-021-02240-w

Zhang, R., Liang, Q., Kang, W., and Ge, S. (2019). Metformin facilitates the proliferation, migration, and osteogenic differentiation of periodontal ligament stem cells *in vitro*. *Cell Biol. Int.* 44 (1), 70–79. doi:10.1002/cbin.11202

Zhang, S., Zhang, R., Qiao, P., Ma, X., Lu, R., Wang, F., et al. (2021). Metformin-induced microRNA-34a-3p downregulation alleviates senescence in human dental pulp stem cells by targeting CAB39 through the AMPK/mTOR signaling pathway. *Stem Cells Int.* 2021, 6616240. doi:10.1155/2021/6616240

Zhang, Y.-L., Liu, F., Li, Z.-B., He, X.-T., Li, X., Wu, R.-X., et al. (2022). Metformin combats high glucose-induced damage to the osteogenic differentiation of human periodontal ligament stem cells via inhibition of the NPR3-mediated MAPK pathway. *Stem Cell Res. Ther.* 13 (1), 305. doi:10.1186/s13287-022-02992-z

Zhao, H., Zhao, H., and Ji, S. (2024). A mesenchymal stem cell aging framework, from mechanisms to strategies. *Stem Cell Rev. Rep.* doi:10.1007/s12015-024-10732-4

Zhao, X., Pathak, J. L., Huang, W., Zhu, C., Li, Y., Guan, H., et al. (2020). Metformin enhances osteogenic differentiation of stem cells from human exfoliated deciduous teeth through AMPK pathway. *J. Tissue Eng. Regen. Med.* 14 (12), 1869–1879. doi:10.1002/term.3142

Zheng, J., Lu, T., Zhou, C., Cai, J., Zhang, X., Liang, J., et al. (2020). Extracellular vesicles derived from human umbilical cord mesenchymal stem cells protect liver ischemia/reperfusion injury by reducing CD154 expression on CD4+ T cells via CCT2. *Adv. Sci.* 7 (18), 1903746. doi:10.1002/advs.201903746

Zhou, R., Ma, Y., Qiu, S., Gong, Z., and Zhou, X. (2020). Metformin promotes cell proliferation and osteogenesis under high glucose condition by regulating the ROS-AKT-mTOR axis. *Mol. Med. Rep.* 22 (4), 3387–3395. doi:10.3892/mmr.2020.11391

Zhu, M., Zhao, Z., Xu, H. H. K., Dai, Z., Yu, K., Xiao, L., et al. (2022). Effects of metformin delivery via biomaterials on bone and dental tissue engineering. *Int. J. Mol. Sci.* 23 (24), 15905. doi:10.3390/ijms232415905

frontiers | Frontiers in Pharmacology

TYPE Original Research
PUBLISHED 11 September 2024
DOI 10.3389/fphar.2024.1456495

OPEN ACCESS

EDITED BY
Rain L. Wong,
University of North Carolina at Chapel Hill, United States

REVIEWED BY
Prabhat Upadhyay,
Harvard Medical School, United States
Shekher Mohan,
Liberty University, United States

*CORRESPONDENCE
Thierry Conrozier,
thierry_conrozier@hotmail.fr

RECEIVED 28 June 2024
ACCEPTED 26 August 2024
PUBLISHED 11 September 2024

CITATION
Brochard S, Boumédiene K, Mercier J, Agin V, Conrozier T and Baugé C (2024) A single intraarticular injection of a tranexamic acid-modified hyaluronic acid (HA/TXA) alleviates pain and reduces OA development in a murine model of monosodium iodoacetate-induced osteoarthritis.
Front. Pharmacol. 15:1456495.
doi: 10.3389/fphar.2024.1456495

A single intraarticular injection of a tranexamic acid-modified hyaluronic acid (HA/TXA) alleviates pain and reduces OA development in a murine model of monosodium iodoacetate-induced osteoarthritis

Sybille Brochard[1], Karim Boumédiene[1], Jéromine Mercier[2], Véronique Agin[3], Thierry Conrozier[4]* and Catherine Baugé[1]

[1]UR7451 Bioconnect, Université de Caen Normandie, Caen, France, [2]Laboratoire de Rhumatologie Appliquée, Lyon, France, [3]INSERM U1237, Physiopathology and Imaging of Neurological Disorders, Université de Caen Normandie, Caen, France, [4]Department of Rheumatology, Hôpital Nord Franche-Comté, Belfort, France

Rationale: Tranexamic acid (TXA) is a strong and specific plasminogen activator inhibitor with inhibitory effects on the matrix metalloproteases involved in the pathophysiology of osteoarthritis (OA) through targeting of the fibrinolysis pathway. In this study, we evaluated the analgesic and chondroprotective effects of a HA-tranexamic acid (HA/TXA) conjugate, compared to HA alone and placebo, in an animal model of knee OA.

Methods: Knee OA was induced in 15 C^{5}7 b l/6J mice by IA injection of 0.75 mg of Monosodium IodoAcetate (MIA). At day 28, the mice received 1 IA injection of 10 µL of saline (control-group), or of HA or of HA/TXA. Tactile sensitivity was assessed using von Frey filaments. Stimulations started at 1 g and increased until a response was obtained (up to 4 g). A response to the stimulus was counted if the animal withdrew its paw. If the animal responded to the 1 g stimulation, stimulation was reduced until the lack of response was observed (up to 0.2 g). At day 56, mice were euthanized for knee histological assessment. Cartilage degradation was assessed using the OARSI score. Statistical analysis was performed on GraphPad Prism 8.0.2 software. Kruskal–Wallis or Mann-Whitney tests were performed as appropriate.

Results: Just before treatment administration, no intergroup difference in paw withdrawal threshold was observed. Throughout the experiment animals given saline and HA had a lower paw withdrawal threshold than those treated with HA/TXA ($p < 0.01$). In the control group OARSI score was 5.5 $\pm$ 0.6. In HA and HA + TXA treated mice the OARSI score was 3.2 $\pm$ 0.8 and 3.1 $\pm$ 0.5 ($p < 0.01$) showing that both treatments were able to reduce OA progression.

Conclusion: In this animal model of MIA induced KOA, a single IA injection of a HA/TXA conjugate resulted in a greater efficacy on pain than both saline and HA. HA and HA/TXA exhibited chondroprotective effects compared to placebo.

KEYWORDS

hyaluronic acid, tranexamic acid, controlled trial, rodents, osteoarthritis

Introduction

Osteoarthritis (OA) is a leading cause of disability-adjusted life years (DALYs) (Cross et al., 2014). By 2050, it is estimated that there will be 642 million (95% CI 574–722) people suffering from knee OA (Steinmetz et al., 2023) resulting in an increased economic burden due to the growing number of joint arthroplasties (Jonsson et al., 2016). The etiology of OA is complex, involving advanced age and mechanical (i.e., excess weight, trauma), hereditary and environmental factors (Nicholls et al., 2017). Inflammation of the synovium plays a central role in the development and progression of OA. Multiple inflammatory mediators are involved, including interleukin (IL)-1β, IL-6, IL-17 and tumor necrosis factor α (TNF-α), the effects of which are mediated through the linkage with receptors, including CD44, HA-mediated motility receptor (RHAMM), and toll-like receptors (TLRs) (Dunn et al., 2009). IL-1β binds to receptors on articular cartilage chondrocytes and synovial cells and increases matrix metalloproteinases (MMPs) synthesis. Collagenases MMP-1 and MMP-13, by degrading type 2 collagen, play a major role in the hyaline cartilage extracellular matrix (ECM) breakdown. IL-1β also stimulates chondrocyte production of A Disintegrin And Metalloproteinase with Thrombospondin motifs (ADAMTS), a family of enzymes which degrade ECM aggrecans (Durigova et al., 2011; Massoud and Jian Q., 2008). The increased expression of MMPs in OA chondrocytes, and the better understanding of the pathways involved in their upregulation, has made MMPs interesting targets for OA treatment (Radwan et al., 2013). Non-proteolytic mechanisms of cartilage degradation can also contribute to the loss of ECM integrity. IL-1β also increases nitric oxide (NO) synthesis and decreases expression of superoxide dismutase and glutathione peroxidase, leading to an acceleration of the damaging effects of oxygen radicals on ECM (Kapoor et al., 2011). Lastly, it has recently been demonstrated that activation of fibrinolysis may promote OA development through multiple mechanisms, including the degradation of lubricin and cartilage proteoglycans and the induction of inflammatory and degradative mediators, suggesting that therapeutic targeting of the fibrinolysis pathway can prevent or slow development of OA. Indeed, in mice, genetic deficiency in the plasminogen gene *Plg* and pharmacological blockade of plasmin attenuate OA while genetic deficiency of plasminogen activator inhibitor (PAI) accelerates OA (Wang et al., 2024).

Currently, there is no effective treatment for this severe disease. The primary approach involves pain management and efforts to slow the disease's progression (Sukhikh et al., 2021). Clinical treatment typically includes oral medications like non-steroidal anti-inflammatory (NSAID) drugs or using bioactive compounds from natural sources which have shown their potential due to their anti-inflammatory and antioxidant properties (Lee et al., 2021; Lee et al., 2022). However, long-term use of these drugs can cause damage to various organs, particularly the kidneys, gastrointestinal tract, and cardiovascular system (Cabassi et al., 2020) and there is no rigorous clinical proof of their actual effectiveness of natural compounds (Liu et al., 2018). Therefore, there is an urgent need to develop a treatment strategy that can alleviate osteoarthritis symptoms over an extended period with minimal side effects in clinical practice.

Hyaluronic acid (HA) intra-articular (IA) injections, also named viscosupplementation, are a treatment used worldwide for knee OA for more than 30 years (Conrozier et al., 2023). The rational of the use of IA-HA for treating OA is based on the evidence that HA, beyond its viscoelastic properties, exhibits antinociceptive and anti-inflammatory actions and has demonstrated both *in vitro* and *in vivo* disease-modifying effects beneficial in the preservation of the extracellular matrix. The current literature supports that HA is not only a medical device used for joint lubrication but a biologically active molecule that can improve the physiology of articular cartilage (Nicholls et al., 2017). Although viscosupplementation has been used for more than 3 decades and is recommended in several guidelines for the management of OA (Sellam et al., 2020; Olivier et al., 2019; Jordan et al., 2003; Rillo et al., 2016; Trojian et al., 2016), the use of viscosupplementation in OA remains a topic for debate regarding treatment efficacy and safety and the best dosing regimen. These discrepancies may originate from differences between the marketed HA products that differ widely from one to another (Webner et al., 2021; Altman et al., 2016). Optimizing clinical effectiveness of viscosupplementation is an exciting challenge for manufacturers, who develop new formulations adding various active molecules (antioxidant (Conrozier, 2018), corticosteroid (Hangody et al., 2018), non-steroidal anti-inflammatory drugs (Badawi et al., 2013), gold particles (Rasmussen et al., 2024), bisphosphonate (Scanu et al., 2023)) to HA.

In the present study we assess the analgesic and chondroprotective effect of a HA-tranexamic acid conjugate (HA/TXA) in an animal model of knee OA. TXA (Trans-4-amino-methyl-cyclohexane-carboxylic acid) is a strong and specific inhibitor of the plasminogen activator (PA) with inhibiting effects on the proteolytic enzyme through targeting of the fibrinolysis pathway (Vignon et al., 1991).

Methods

Material

The studied medical device (PANDORA®, LABRHA SAS, Lyon, France) is a sterile, non-pyrogenic solution of high molecular weight HA (3.5 MDa), of *streptococcus* equi biofermentative origin, (HTL-BIOTECHNOLOGY, Javene, France) and tranexamic acid (TXA)

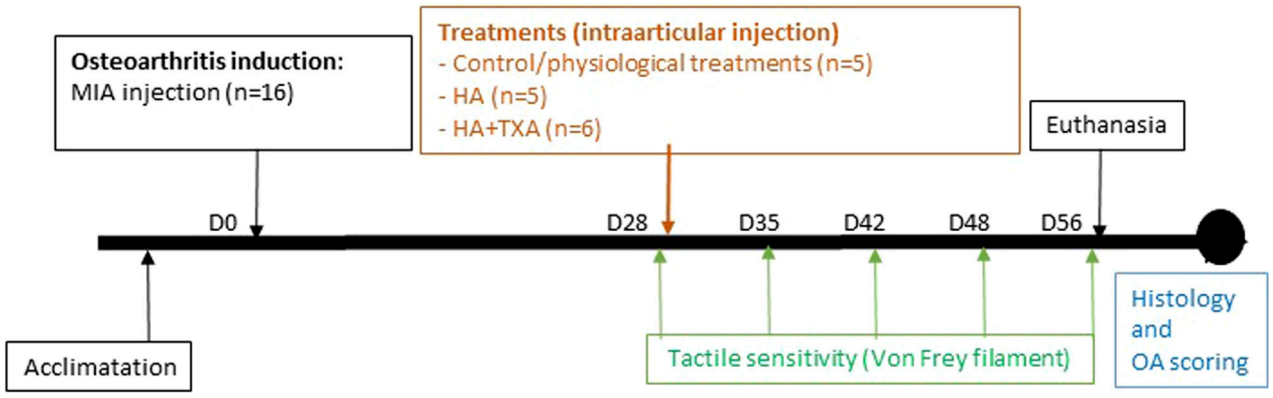

FIGURE 1
Timeline of the experimental procedure.

(SPECTRUM CHEMICAL, New Brunswick, New Jersey, USA) in a phosphate buffer of purified water, sodium chloride (NaCl), disodium phosphate (DSP, Na2HPO4) and monopotassium phosphate (MKP, KH2PO4) (COOPER, Melun, France). One milliliter of PANDORA® contains 22 mg of HA and 15 mg of TXA. The PANDORA gel is indicated in the symptomatic treatment of knee OA and is the subject of a research program still in progress (clinicalTrials.gov Identifier NCT05414617 and NCT05978180).

The same HA, at the same concentration, diluted in the same phosphate buffer, was used as an active control.

Ethical considerations

The animal experiments were carried out in compliance with European directive 2010/63/EU in accordance with French legislation (decree 87/848) at the GIP CYCERON/CURB (Centre Universitaire de Ressources Biologiques, approval #D14118001). The procedures were approved by the Ministry of Education and Research and the committee of regional ethics (CENOMEXA, France, APAFIS number #16185).

The manipulations were carried out following the ARRIVE guidelines (Animal research: report of *in vivo* experiments; https://www.nc3rs.org.uk). All animals were handled in accordance with recognized international ethical principles for the use of laboratory animals and every effort was made to refine the experiments, reduce the number of animals used and replace the use of animals when this was possible, and the experimenters were aware of their responsibilities.

Animals

Fifteen C57bl/6J 8-week-old male mice from the Janvier Labs laboratory were used. The animals were housed in a room with controlled temperature and light (temperature 23°C ± 2°C, 12-h day/night cycle in reverse cycle) at CURB, University of Caen Normandy, France. The animals had access to food and water *ad libitum* and the cages were changed once a week. The experiments were performed between 8a.m. and 5p.m. in a room with dim illumination (6 lx). All the behavioral procedures were carried out within the HANDIFORM platform (UNICAEN, Caen, France).

Induction of osteoarthritis

The experiments were performed according to the timeline presented in Figure 1.

Osteoarthritis was induced at day 0 by intra-articular injection of 0.75 mg of Monosodium IodoAcetate (MIA, Sigma-aldrich) dissolved in 10 µL of sterile physiological serum. Alcohol was used to disinfect the bench and a field was laid down. Animals were anesthetized using 5% isoflurane mediated by 70% N_2O/30% O_2. then maintained at 3% isoflurane (70% N_2O/30% O_2). Anesthesia time was on average 10 min, including recovery and induction time. The animals were placed in dorsal recumbency, and the right knee disinfected with 2% alcoholic chlorhexidine (Gilbert, Hérouville-Saint-Clair, France). The knee was bent to 45° and the joint was identified by observing the patellar tendon through the skin of the animal; the injection of 10 µL was then performed in 1 min into the synovial capsule using a 30 G needle (microlance 3 30 G 1/2″0.3 × 13 mm; BD, Rungis, France) and a 25 µL syringe (Hamilton, Giarmata, Romania). After removal of the needle, the joint was mobilized to diffuse the product. The injection site was cleaned with physiological serum in order to remove potential traces of MIA which could create skin inflammations. Finally, the anesthesia was lifted, and the animals were kept in the hand until fully awakening to limit the drop in body temperature. The health of the animals was monitored for 1 h after the injection without ever observing any sign of discomfort.

Treatments

At day 28, according to the same protocol of MIA injection, the mice received a single intra-articular injection of one of the following treatments: Control-group (n = 5) received 10 µL of physiological serum, HA-group (n = 5) received 10 µL of hyaluronic acid, and HA/TXA-group (n = 6) received 10 µL of Pandora®.

Functional pain outcomes

Tactile sensitivity was assessed using von Frey filaments (Ugo Basile, Salon-de-Provence, France).

The mice were placed in isolation cages placed on a raised grid. An exploration time of 30 min is given to the animals so that they are as calm as possible. Using nylon filaments, a controlled weight pressure is exerted between the pads of the animals' hind legs. A response to the stimulus is counted if the animal withdraws its paw (snap, withdrawal or lick). A response is not counted if the animal moves accidentally at the time of stimulation. Both hind paws were tested 5 times in a random order and with a refractory period of 1 min between each trial. If three responses are counted over 5 trials, then the animal responds to the stimulus associated with the weight of the filament. Stimulations start at 1 g. If the animal does not respond to stimulation, the increase in stimulation applied will increase until a response is obtained (1.4 g, 2 g, 4 g). If the animal responds to the 1 g stimulation, the decrease in stimulation will be carried out until there is no response (0.6 g, 0.4 g, etc.). In the case of a reduction in stimulation, the filament retained is the last one to have provoked a series of three responses. To analyze these results, the ratio of responses to stimuli under the right paw is compared to responses under the left paw for each animal.

Before evaluation, the mice underwent 3 weeks of habituation to handling with one visit every 2 days, excluding cage changing days, in order to familiarize themselves with the handler and the handling and thus reduce their stress.

Histological examination

At day 56, the mice were euthanized by cervical dislocation after deep anesthesia (5% isoflurane, 70% N2O/30% O2). The knee joints were dissected, fixed for 3 days in 10% neutral buffered formalin (NBF), and decalcified in Osteosoft (Sigma Aldrich) for 72 h week at room temperature and then left, cryoprotected by a 15% sucrose bath, for 48 h at 4°C. Thereafter, the knees were embedded in OCT and sections with 10 µm thickness were prepared using a cryostat (CM3050 S, Leica). Sections were stained with Safranin O and counterstained with Fast Green.

Cartilage degradation was assessed using the OARSI score (Pritzker et al., 2006). This score is separated into 6 grades, including changes in the subchondral bone for the last two. The different grades of the OARSI score according to Pritzker make it possible to precisely quantify cartilage degradation, with a score ranging from 0 to 6.5.

Statistical analysis

Statistical analysis and graphs were performed on GraphPad Prism 8.0.2 software. The normality of all data was checked by the Shapiro-Wilk test and verified visually by a QQ plot. For non-parametric unpaired data, a Kruskal–Wallis test was performed as well as a *post hoc* test for two-by-two comparison of groups using the one-sided Mann-Whitney test. For unpaired parametric data, only two-group comparisons were performed and the t-test for unpaired data was used. The significance threshold was set at p-value <0.05.

Results

HA/TXA reduced OA pain

On day 28 after OA induction, just before treatment administration, we observed no differences between the three groups in paw withdrawal threshold. Throughout the experiment and on day 56, we observed that animals given saline had a lower paw withdrawal threshold for the OA paw (right) than for the non-OA paw (left). Mice injected with HA presented the same profile, suggesting the absence of a beneficial effect of HA on OA pain. Conversely, HA/TXA administration increased the paw withdrawal threshold, indicating a reduction in tactile sensitivity of the arthritic paw and therefore a reduction in joint pain induced by OA. The significant difference in the paw withdrawal threshold after HA/TXA administration shows that the beneficial effect lasts at least 4 weeks after HA/TXA injection (Figure 2).

Both HA and HA/TXA reduced OA progression

In the control group, we observed that MIA induced an OA of high grade (OARSI score = 5.5 ± 0.62). Interestingly, administration of HA and HA + TXA was able to reduce the OARSI score (score = 3.2 ± 0.84 and 3.15 ± 0.51, respectively), suggesting that both treatments are able to improve OA and reduce its progression (Figure3). Individual results are given in Figure 4.

Discussion

This animal study suggests that the addition of TXA to a high molecular weight HA makes it possible to obtain an analgesic effect greater than that of HA alone, without reducing its chondroprotective effect.

Tranexamic acid is a lysine analog that binds with high affinity to the lysine binding sites (LBS) of plasminogen. Hence TXA prevents plasminogen activator (PA) activation and therefore plasmin production. Fibrinolysis is one of the major pathological changes occurring in arthritic joints, in the pathophysiology of which the PA system plays a key role. The balance between PA and plasminogen activator inhibitor (PAI) determines the direction in which plasminogen is activated into plasmin, which in turn further promotes fibrinolysis by activating MMPs (Masuko et al., 2009). Several other anti-osteoarthritic drugs interact with the PA system. The Receptor for u-PA, which is expressed in the synovium in both OA and rheumatoid arthritis, has been shown to be attenuated by treatment with HA (Masuko et al., 2009). The anti-inflammatory and analgesic effect of hydrocortisone is due, a least in part, to the upregulation of PAI-1 expression along with downregulation of tissue PA activity as demonstrated in both normal and inflammatory conditions (Nonaka et al., 2000). Tranexamic acid, from sub micromolar concentrations, attenuates the activation of plasminogen and considerably reduces the production of plasmin (Wu et al., 2019). It is mainly for its anti-fibrinolytic effect that TXA is used as an antihemorrhagic agent in cases of trauma, as well as in major surgical procedures, such as

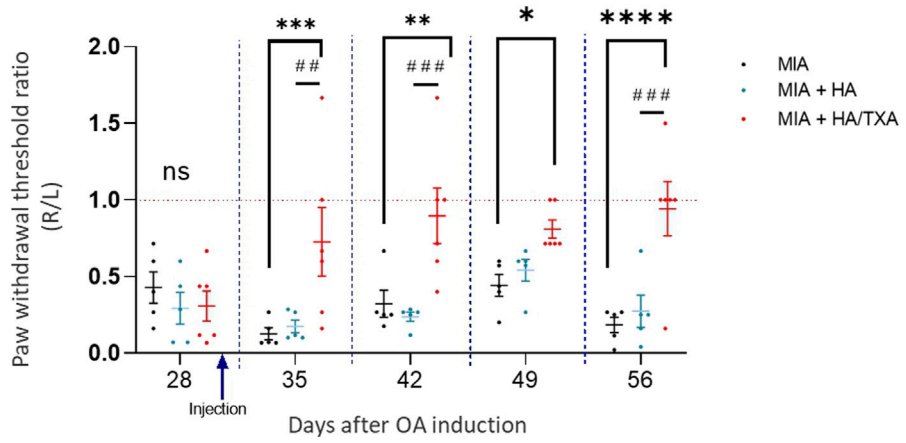

FIGURE 2
A single intraarticular injection of HA + TXA improved pain during osteoarthritis. Osteoarthritis (OA) was induced by intraarticular injection of MIA in the right knee of mice. Four weeks later, OA knees of mice were injected with physiological serum (n = 5), HA (n = 5) or HA + TXA (n = 5). Tactile sensitivity was evaluated in both paws at days 28 (before treatment injection), and then once a week for 4 weeks. Values are presented as ratio of withdrawal threshold between right and left paw (R/L). Data are expressed as means ± SEM. *p-value <0.05. **p-value <0.01.

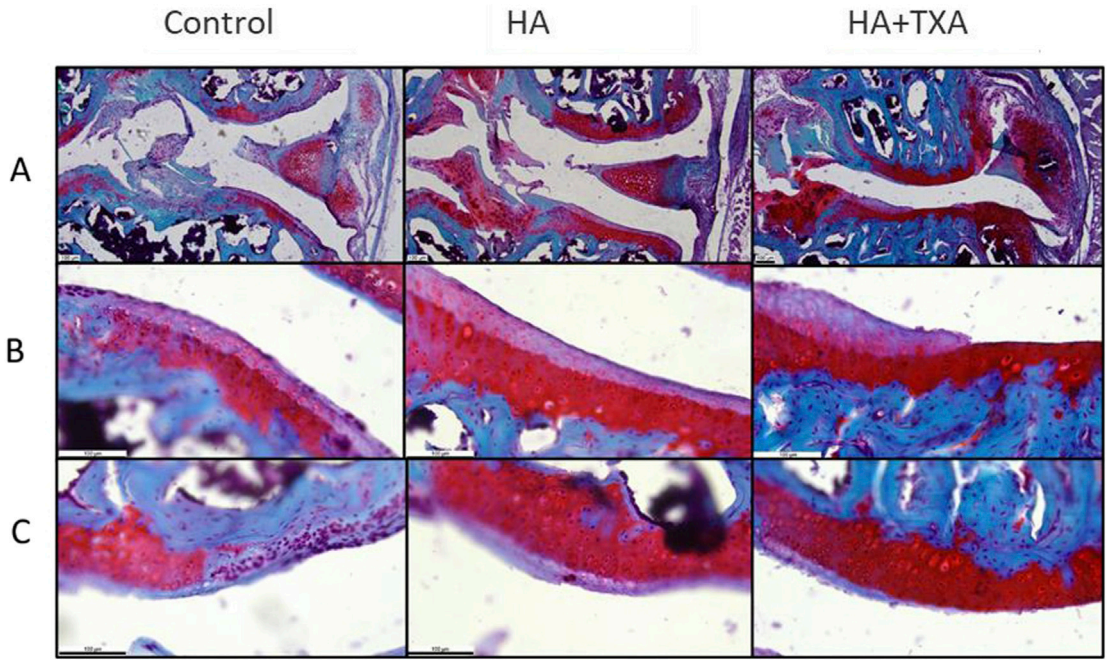

FIGURE 3
A single intraarticular injection of HA + TXA reduced OA progression in mice. Osteoarthritis (OA) was induced by intraarticular injection of MIA in the right knee of mice. Four weeks later, OA knees of mice were injected with physiological serum (n = 5), HA (n = 5) or HA + TXA (n = 6). Mice were euthanized 8 weeks after OA induction, and knee sections were stained with safranin O/fast green. **(A,B, C)** Representative images of knees. **(A)** Internal joint of the right knee of the mouse (where the lesions are located) **(B)** Cartilage of the internal tibial plateau, **(C)** Cartilage of the internal femoral condyle.

cardiac, orthopedic and hepatic surgeries (Pai et al., 2023). *In vitro* studies also suggested that plasmin may promote OA development through multiple mechanisms, including the degradation of proteoglycans and lubricin, and the stimulation of the synthesis of inflammatory and degradative mediators (Wang et al., 2024). The beneficial effect on pain of the TXA/HA combination is likely due to the anti-inflammatory properties of TXA. In patients treated with knee arthroscopic arthrolysis, the pain scores and the serum levels of proinflammatory mediators IL-6 and C Reactive-protein were shown to be significantly lower 1 week after surgery in patients who received topical administration of 500 mg of TXA at the end of the surgical procedure than that of those who did not (Li et al., 2023). Likewise, the TXA group underwent better post-operative range of motion and Lysholm knee scores (Nick and Deiary F., 2013).

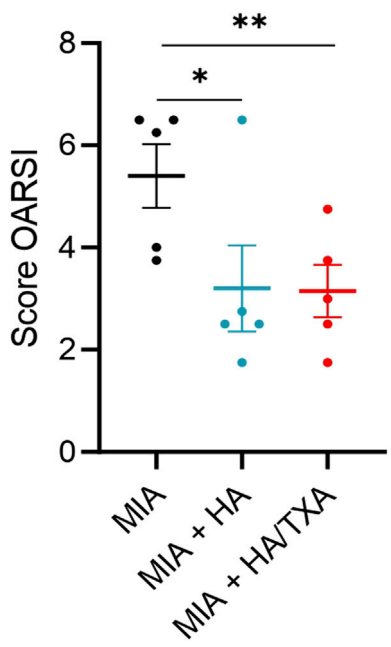

FIGURE 4
OARSI score at Day 56 after intra-articular injection of salie, HA or HA/TXA. Data are expressed as means ± SEM.
*p-value <0.05. **p-value <0.01.

In our experiment both HA and HA/TXA demonstrated a chondroprotective effect, as shown by the lower OARSI score compared to that of saline injection. The structure-modifying effect of HA has been widely evidenced (Henrotin et al., 2020). Exogenous HA increases the synthesis of extracellular matrix molecules, stimulates synovial fibroblasts to produce new HA, the amount of newly synthesized HA being dependent on both the concentration and molecular weight of the exogenous HA (Nicholls et al., 2017). Exogenous high molecular weight HAs have demonstrated a higher stimulating effect on HA synthesis than low molecular ones (Smith and Ghosh, 1987). HAs used in the present study were both of HMW with an average MW of 2 MDa. We were unable to demonstrate a greater chondroprotective effect thanks to the addition of TXA. However, several studies argue for an anti-osteoarthritic effect of TXA. In an animal model of OA, Wang et al. showed that the pharmacological inhibition of plasmin attenuated OA progression while injection of plasmin exacerbated OA (Wang et al., 2024). Many years ago, Vignon et al. assessed the effects of TXA in a rabbit model of OA induced by section of the knee anterior cruciate ligament. Prophylactic treatment administered intramuscularly thrice weekly for 3 and 6 months significantly inhibited stromelysin and collagenase activity and reduced cartilage destructive lesions (Vignon et al., 1991). Butler et al. showed, in rabbits subjected to partial lateral meniscectomy and section of the sesamoid and collateral fibular ligaments, that triamcinolone hexacetonide as well as TXA exhibited significant anti-osteoarthritic activity (Butler et al., 1983). Likewise, it has been demonstrated that TXA reduced urinary collagen cross-link excretion in both adjuvant-induced arthritis and rheumatoid arthritis (Ronday et al., 1998).

To demonstrate the benefit of TXA/HA treatment, we used monoiodoacetate to induce OA in the knees of mice. This chemical model is frequently used to exploring OA-related pain (Aüllo-Rasser et al., 2020; Upadhyay et al., 2023), which is the main reason OA patients seek medical help. Indeed, intraarticular injection of MIA induces rapid pain-like responses in the ipsilateral limb as well as morphological changes of the articular cartilage and bone disruption which are reflective of some aspects of patient pathology (Pitcher et al., 2016). Nonetheless, it does not recapitulate the natural onset of the human disease and does not reproduce entirely all symptoms of the disease (de Sousa Valente, 2019). In particular, the initiating events are not typical of OA. In addition, there are obvious limitations due to use of mice, particularly those related to differences in anatomy, gait, and cartilage characteristics compared to human joints. Thus, as all animal models, the murine MIA model only mimics parts or stages of the disease, but does not completely reproduce human OA complexity (de Sousa Valente, 2019). Nevertheless, it has been shown to have a pre-clinical value and has the advantage of generating robust and reproducible pain phenotypes associated with the alteration of joint tissues (Micheli et al., 2019; Bove et al., 2003).

Monoiodoacetate is a cysteine peptidase inhibitor that targets the glyceraldehyde-3-phosphate dehydrogenase (GAPDH), a key enzyme in the glycolysis pathway. The disruption of glycolysis in joint cells results in chondrocyte death, neovascularization, subchondral bone necrosis and collapse, as well as inflammation (de Sousa Valente, 2019). The death of chondrocytes makes it impossible to maintain the extracellular matrix, which deteriorates over time, leading to joint degeneration similar to that seen in osteoarthritis (Aüllo-Rasser et al., 2020).

Despite its artificial onset, MIA model offers several useful advantages compared to other murine models. For instance, this inflammatory chemical model is less invasive than surgical models (Alves-Simões, 2022) and consequently easier to induce and more reproducible, making it ideal for short-term trials. Furthermore, the MIA model offers a unique opportunity to study OA-related pain, whereas surgical methods, such as destabilization of medial meniscus or menisectomy are more useful for studying the onset and progression of posttraumatic osteoarthritis as well as the structural and biological processes throughout the progression of the pathology (Alves-Simões, 2022).

Because animals are nonverbal, assessment of pain is challenging. However, several methods have been proposed for monitoring pain in mice, including examining the animal directly and making a subjective assessment of animal comfort based upon hair coat, posture, general activity level, and degree of alertness (Turner et al., 2019). In the context of an experimental OA model, the manual Von Frey test, that we used in this study, is the most common method to quantify “pain-like” behaviors in mice (Drevet et al., 2022). This classical static test permits to identify mechanical/tactile allodynia. It can be used in the clinic to quantify tactile allodynia, and it can also be a useful diagnostic tool in preclinical animal experiments. In OA mice, the innocuous mechanical pressure is applied using nylon filaments on the hind paw as a measure of secondary mechanical hyperalgesia (Alves-Simões, 2022). Other tests exist; we can cite the static or dynamic weight-bearing assay to evaluate weight distribution asymmetry induced by pain; the rotarod to measure ambulatory pain, or the hot/cold plate

test to measure thermal hyperalgesia (Alves-Simões, 2022) but they are more difficult to perform or less reproducible. Interestingly, the MIA model associated to pain assays has been pharmacologically validated by commonly used therapeutic agents such as paracetamol, naproxen, or diclofenac, which alleviated pain following MIA injection. In addition, the MIA model has been used in several preclinical OA studies which are currently continuing with phase IIa clinical trials (Alves-Simões, 2022), making it the most adequate model for this preclinical study aiming to investigate the chondroprotective and antinociceptive effects of HA-TXA.

Data availability statement

The raw data supporting the conclusions of this article will be made available by the authors, without undue reservation.

Ethics statement

The animal study was approved by Ministry of Education and Research and the committee of regional ethics (CENOMEXA, France, APAFIS number #16185). The study was conducted in accordance with the local legislation and institutional requirements.

Author contributions

SB: Conceptualization, Data curation, Formal Analysis, Investigation, Methodology, Resources, Software, Validation, Writing–original draft, Writing–review and editing. KB: Conceptualization, Funding acquisition, Project administration, Supervision, Writing–review and editing. JM: Writing–original draft, Writing–review and editing. VA: Conceptualization, Data curation, Investigation, Resources, Writing–original draft, Writing–review and editing. TC: Conceptualization, Writing–original draft, Writing–review and editing. CB: Conceptualization, Formal Analysis, Funding acquisition, Methodology, Project administration, Supervision, Validation, Writing–original draft, Writing–review and editing.

Funding

The author(s) declare that financial support was received for the research, authorship, and/or publication of this article. The authors disclose receipt of the following financial or material support for the research, authorship, and/or publication of this article: this work was supported by the LABRHA SAS, 19 place Tolozan, Lyon, France.

Acknowledgments

We thank Palma PRO (CYCERON, UNICAEN, Caen, France) for advice for animal experiments, Elodie Bouvier (Unité de Recherche Clinique, HNFC, Trevenans, France) and ALPHATRAD (Besançon, France) for English proofreading.

Conflict of interest

Jeromine mercier is a employee of LABRHA TC received honoraria from LABRHA for scientific and consulting services.

The remaining authors declare that the research was conducted in the absence of any commercial or financial relationships that could be construed as a potential conflict of interest.

Publisher's note

References

Altman, R. D., Bedi, A., Karlsson, J., Sancheti, P., and Schemitsch, E. (2016). Product differences in intra-articular hyaluronic acids for osteoarthritis of the knee. *Am. J. Sports Med.* 44 (8), 2158–2165. doi:10.1177/0363546515609599

Alves-Simões, M. (2022). Rodent models of knee osteoarthritis for pain research. *juin* 30 (6), 802–814. doi:10.1016/j.joca.2022.01.010

Aüllo-Rasser, G., Dousset, E., Roffino, S., Zahouani, H., Lecurieux-Clerville, R., Argenson, J. N., et al. (2020). Early-stage knee OA induced by MIA and MMT compared in the murine model via histological and topographical approaches. *Sci. Rep. 22 Sept.* 10 (1), 15430. doi:10.1038/s41598-020-72350-7

Badawi, A. A., El-Laithy, H. M., Nesseem, D. I., and El-Husseney, S. S. (2013). Pharmaceutical and medical aspects of hyaluronic acid-ketorolac combination therapy in osteoarthritis treatment: radiographic imaging and bone mineral density. *J. Drug Target* 21 (6), 551–563. doi:10.3109/1061186X.2013.776054

Bove, S. E., Calcaterra, S. L., Brooker, R. M., Huber, C. M., Guzman, R. E., Juneau, P. L., et al. (2003). Weight bearing as a measure of disease progression and efficacy of anti-inflammatory compounds in a model of monosodium iodoacetate-induced osteoarthritis. *Osteoarthr. Cartil.* 11 (11), 821–830. doi:10.1016/s1063-4584(03)00163-8

Butler, M., Colombo, C., Hickman, L., O'Byrne, E., Steele, R., Steinetz, B., et al. (1983). A new model of osteoarthritis in rabbits. III. Evaluation of anti-osteoarthritic effects of selected drugs administered intraarticularly. *Arthritis and Rheumatism.* 26 (11), 1380–1386. doi:10.1002/art.1780261111

Cabassi, A., Tedeschi, S., Perlini, S., Verzicco, I., Volpi, R., Gonzi, G., et al. (2020). Non-steroidal anti-inflammatory drug effects on renal and cardiovascular function: from physiology to clinical practice. *Eur. J. Prev. Cardiol.* 27 (8), 850–867. doi:10.1177/2047487319848105

Conrozier, T. (2018). Is the addition of a polyol to hyaluronic acid a significant advance in the treatment of osteoarthritis? *Curr. Rheumatol. Rev.* 14 (3), 226–230. doi:10.2174/1573397113666170710115558

Conrozier, T., Diraçoglù, D., Monfort, J., Chevalier, X., Bard, H., Baron, D., et al. (2023). EUROVISCO good practice recommendations for a first viscosupplementation in patients with knee osteoarthritis. *juin* 14 (2), 125–135. doi:10.1177/19476035221138958

Cross, M., Smith, E., Hoy, D., Nolte, S., Ackerman, I., Fransen, M., et al. (2014). The global burden of hip and knee osteoarthritis: estimates from the global burden of disease 2010 study. *Ann. Rheum. Dis. juill* 73 (7), 1323–1330. doi:10.1136/annrheumdis-2013-204763

de Sousa Valente, J. (2019). The pharmacology of pain associated with the monoiodoacetate model of osteoarthritis. *Front. Pharmacol. 18 Sept.* 10, 974. doi:10.3389/fphar.2019.00974

Drevet, S., Favier, B., Brun, E., Gavazzi, G., and Lardy, B. (2022). Mouse models of osteoarthritis: a summary of models and outcomes assessment. *Comp. Med. févr* 72 (1), 3–13. doi:10.30802/AALAS-CM-21-000043

Dunn, S., Kolomytkin, O. V., Waddell, D. D., and Marino, A. A. (2009). Hyaluronan-binding receptors: possible involvement in osteoarthritis. *Mod. Rheumatol.* 19 (2), 151–155. doi:10.1007/s10165-008-0136-y

Durigova, M., Troeberg, L., Nagase, H., Roughley, P. J., and Mort, J. S. (2011). Involvement of adamts5 and hyaluronidase in aggrecan degradation and release from osm-stimulated cartilage. *Eur. Cell Mater. 12 janv* 21, 31–45. doi:10.22203/ecm.v021a03

Hangody, L., Szody, R., Lukasik, P., Zgadzaj, W., Lénárt, E., Dokoupilova, E., et al. (2018). Intraarticular injection of a cross-linked sodium hyaluronate combined with triamcinolone hexacetonide (cingal) to provide symptomatic relief of osteoarthritis of the knee: a randomized, double-blind, placebo-controlled multicenter clinical trial. *juill* 9 (3), 276–283. doi:10.1177/1947603517703732

Henrotin, Y., Chevalier, X., Raman, R., Richette, P., Montfort, J., Jerosch, J., et al. (2020). EUROVISCO guidelines for the design and conduct of clinical trials assessing the disease-modifying effect of knee viscosupplementation. *janv* 11 (1), 60–70. doi:10.1177/1947603518783521

Jonsson, H., Olafsdottir, S., Sigurdardottir, S., Aspelund, T., Eiriksdottir, G., Sigurdsson, S., et al. (2016). Incidence and prevalence of total joint replacements due to osteoarthritis in the elderly: risk factors and factors associated with late life prevalence in the AGES-Reykjavik Study. *BMC Musculoskelet. Disord.* 17, 14. doi:10.1186/s12891-016-0864-7

Jordan, K. M., Arden, N. K., Doherty, M., Bannwarth, B., Bijlsma, J. W. J., Dieppe, P., et al. (2003). EULAR recommendations 2003: an evidence based approach to the management of knee osteoarthritis: report of a task force of the standing committee for international clinical studies including therapeutic trials (ESCISIT). *Ann. Rheum. Dis. déc* 62 (12), 1145–1155. doi:10.1136/ard.2003.011742

Kapoor, M., Martel-Pelletier, J., Lajeunesse, D., Pelletier, J. P., and Fahmi, H. (2011). Role of proinflammatory cytokines in the pathophysiology of osteoarthritis. *Nat. Rev. Rheumatol. janv* 7 (1), 33–42. doi:10.1038/nrrheum.2010.196

Lee, H., Zhao, X., Son, Y. O., and Yang, S. (2021). Therapeutic single compounds for osteoarthritis treatment. *Pharm. (Basel)* 14 (2), 131. doi:10.3390/ph14020131

Lee, Y. T., Yunus, M. H. M., Ugusman, A., and Yazid, M. D. (2022). Natural compounds affecting inflammatory pathways of osteoarthritis. *Antioxidants (Basel)* 11 (9), 1722. doi:10.3390/antiox11091722

Li, J., You, M., Yao, L., Fu, W., Li, Q., Chen, G., et al. (2023). Topical administration of tranexamic acid reduces postoperative blood loss and inflammatory response in knee arthroscopic arthrolysis: a retrospective comparative study. *BMC Musculoskelet. Disord.* 24 (1), 269. doi:10.1186/s12891-023-06349-2

Liu, X., Machado, G. C., Eyles, J. P., Ravi, V., and Hunter, D. J. (2018). Dietary supplements for treating osteoarthritis: a systematic review and meta-analysis. *Br. J. Sports Med.* 52 (3), 167–175. doi:10.1136/bjsports-2016-097333

Massoud, D., and Jian Q., Y. (2008). The interleukin 1β pathway in the pathogenesis of osteoarthritis. *J. Rheumatology* 12, 2306–2312. doi:10.3899/jrheum.080346

Masuko, K., Murata, M., Yudoh, K., Kato, T., and Nakamura, H. (2009). Anti-inflammatory effects of hyaluronan in arthritis therapy: not just for viscosity. *IJGM. 30 avr* 2, 77–81. doi:10.2147/ijgm.s5495

Micheli, L., Ghelardini, C., Lucarini, E., Parisio, C., Trallori, E., Cinci, L., et al. (2019). Intra-articular mucilages: behavioural and histological evaluations for a new model of articular pain. *J. Pharm. Pharmacol. juin* 71 (6), 971–981. doi:10.1111/jphp.13078

Nicholls, M. A., Fierlinger, A., Niazi, F., and Bhandari, M. (2017). The disease-modifying effects of hyaluronan in the osteoarthritic disease state. *Clin. Med. Insights Arthritis Musculoskelet. Disord. 11 août* 10, 1179544117723611. doi:10.1177/1179544117723611

Nick, C., and Deiary F., K. (2013). Rating systems in the evaluation of knee ligament injuries. *Class. Pap. Orthop.*, 201–203. doi:10.1007/978-1-4471-5451-8_49

Nonaka, T., Kikuchi, H., Ikeda, T., Okamoto, Y., Hamanishi, C., and Tanaka, S. (2000). Hyaluronic acid inhibits the expression of u-PA, PAI-1, and u-PAR in human synovial fibroblasts of osteoarthritis and rheumatoid arthritis. *J. Rheumatol. 1 avr* 27 (4), 997–1004.

Olivier, B., Germain, H., Nicola, V., Nigel K, A., Jaime, B., Curtis, E. M., et al. (2019). An algorithm recommendation for the management of knee osteoarthritis in Europe and internationally: a report from a task force of the European Society for Clinical and Economic Aspects of Osteoporosis and Osteoarthritis. *Semin. Arthritis Rheum.* 49 (3), 337–350. doi:10.1016/j.semarthrit.2019.04.008

Pai, B. H. P., Patel, S., and Lai, Y. H. (2023). Updated clinical review: perioperative use of tranexamic acid in orthopedics and other surgeries. *Adv. Anesth. déc* 41 (1), 1–15. doi:10.1016/j.aan.2023.05.001

Pitcher, T., Sousa-Valente, J., and Malcangio, M. (2016). The monoiodoacetate model of osteoarthritis pain in the mouse. *J. Vis. Exp.* 16 (111), 53746. mai. doi:10.3791/53746

Pritzker, K. P. H., Gay, S., Jimenez, S. A., Ostergaard, K., Pelletier, J. P., Revell, P. A., et al. (2006). Osteoarthritis cartilage histopathology: grading and staging. *Osteoarthr. Cartil.* 14 (1), 13–29. doi:10.1016/j.joca.2005.07.014

Radwan, M., Gavriilidis, C., Robinson, J. H., Davidson, R., Clark, I. M., Rowan, A. D., et al. (2013). Matrix metalloproteinase 13 expression in response to double-stranded RNA in human chondrocytes. *Arthritis Rheum. mai* 65 (5), 1290–1301. doi:10.1002/art.37868

Rasmussen, S., Petersen, K. K., Aboo, C., Andersen, J. S., Skjoldemose, E., Jørgensen, N. K., et al. (2024). Intra-articular injection of gold micro-particles with hyaluronic acid for painful knee osteoarthritis. *BMC Musculoskelet. Disord.* 25 (1), 211. doi:10.1186/s12891-024-07321-4

Rillo, O., Riera, H., Acosta, C., Liendo, V., Bolaños, J., Monterola, L., et al. (2016). PANLAR consensus recommendations for the management in osteoarthritis of hand, hip, and knee. *J. Clin. Rheumatol.* 22 (7), 345–354. doi:10.1097/RHU.0000000000000449

Ronday, H. K., Te Koppele, J. M., Greenwald, R. A., Moak, S. A., De Roos, J. A., Dijkmans, B. A., et al. (1998). Tranexamic acid, an inhibitor of plasminogen activation, reduces urinary collagen cross-link excretion in both experimental and rheumatoid arthritis. *Br. J. Rheumatol. janv* 37 (1), 34–38. doi:10.1093/rheumatology/37.1.34

Scanu, A., Luisetto, R., Pavan, M., Guarise, C., Beninatto, R., Giraudo, C., et al. (2023). Effect of intra-articular injection of a hyaluronic acid-alendronate conjugate on post-traumatic osteoarthritis induced by destabilization of the medial meniscus in rats. *Sci. Rep.* 13 (1), 20692. doi:10.1038/s41598-023-46965-5

Sellam, J., Courties, A., Eymard, F., Ferrero, S., Latourte, A., Ornetti, P., et al. (2020). Recommendations of the French Society of Rheumatology on pharmacological treatment of knee osteoarthritis. *Jt. Bone Spine* 87 (6), 548–555. doi:10.1016/j.jbspin.2020.09.004

Smith, M. M., and Ghosh, P. (1987). The synthesis of hyaluronic acid by human synovial fibroblasts is influenced by the nature of the hyaluronate in the extracellular environment. *Rheumatol. Int.* 7 (3), 113–122. doi:10.1007/BF00270463

Steinmetz, J. D., Culbreth, G. T., Haile, L. M., Rafferty, Q., Lo, J., Fukutaki, K. G., et al. (2023). Global, regional, and national burden of osteoarthritis, 1990–2020 and projections to 2050: a systematic analysis for the Global Burden of Disease Study 2021. *Lancet Rheumatology. 1 sept* 5 (9), e508–e522. doi:10.1016/S2665-9913(23)00163-7

Sukhikh, S., Noskova, S., Ivanova, S., Ulrikh, E., Izgaryshev, A., and Babich, O. (2021). Chondroprotection and molecular mechanism of action of phytonutraceuticals on osteoarthritis. *Molecules* 26 (8), 2391. doi:10.3390/molecules26082391

Trojian, T. H., Concoff, A. L., Joy, S. M., Hatzenbuehler, J. R., Saulsberry, W. J., and Coleman, C. I. (2016). AMSSM scientific statement concerning viscosupplementation injections for knee osteoarthritis: importance for individual patient outcomes. *Br. J. Sports Med.* 50 (2), 84–92. doi:10.1136/bjsports-2015-095683

Turner, P. V., Pang, D. S., and Lofgren, J. L. (2019). A review of pain assessment methods in laboratory rodents. *Comp. Med. 1 déc* 69 (6), 451–467. doi:10.30802/AALAS-CM-19-000042

Upadhyay, P., Kalra, D., Nilakhe, A. S., Aggrawal, V., and Gupta, S. (2023). Polyherbal formulation PL02 alleviates pain, inflammation, and subchondral bone deterioration in an osteoarthritis rodent model. *Front. Nutr.* 10, 1217051. doi:10.3389/fnut.2023.1217051

Vignon, E., Mathieu, P., Bejui, J., Descotes, J., Hartmann, D., Patricot, L. M., et al. (1991). Study of an inhibitor of plasminogen activator (tranexamic acid) in the treatment of experimental osteoarthritis. *J. Rheumatol. Suppl. févr* 27, 131–133.

Wang, Q., Shao, G., Zhao, X., Wong, H. H., Chin, K., Zhao, M., et al. (2024). Dysregulated fibrinolysis and plasmin activation promote the pathogenesis of osteoarthritis. *JCI Insight* 9 (8), e173603. doi:10.1172/jci.insight.173603

Webner, D., Huang, Y., and Hummer, C. D. (2021). Intraarticular hyaluronic acid preparations for knee osteoarthritis: are some better than others? Cartilage. *déc* 13 (1_Suppl. l), 1619S–1636S. doi:10.1177/19476035211017320

Wu, G., Mazzitelli, B. A., Quek, A. J., Veldman, M. J., Conroy, P. J., Caradoc-Davies, T. T., et al. (2019). Tranexamic acid is an active site inhibitor of urokinase plasminogen activator. *Blood Adv. 27 févr* 3 (5), 729–733. doi:10.1182/bloodadvances.2018025429

frontiers | Frontiers in Pharmacology

TYPE Review
PUBLISHED 18 September 2024
DOI 10.3389/fphar.2024.1462368

OPEN ACCESS

EDITED BY
Wen Liao,
Sichuan University, China

REVIEWED BY
Xudong Li,
Sichuan University, China
Hegang Li,
Southern Medical University, China
Xu Chen,
Nanjing Medical University, China

*CORRESPONDENCE
Xingfu Bao,
baoxf@jlu.edu.cn

RECEIVED 10 July 2024
ACCEPTED 09 September 2024
PUBLISHED 18 September 2024

CITATION
Liu Y, Zhang H, Chen T, Xu C and Bao X (2024) Metal-organic frameworks (MOFs) and their derivatives as emerging biomaterials for the treatment of osteoarthritis.
Front. Pharmacol. 15:1462368.
doi: 10.3389/fphar.2024.1462368

Metal-organic frameworks (MOFs) and their derivatives as emerging biomaterials for the treatment of osteoarthritis

Yufu Liu, Hongwei Zhang, Tianyan Chen, Chang Xu and Xingfu Bao*

Jilin Provincial Key Laboratory of Tooth Development and Bone Remodeling, School and Hospital of Stomatology, Jilin University, Changchun, China

As a novel class of smart biomaterials with promising potentials, metal-organic frameworks (MOFs) are widely utilized in the field of biomedicine. Current researches indicate that the therapeutic strategies for osteoarthritis (OA) are highly limited to achieving symptom improvement and reducing both pain and inflammation. Together, the introduction of MOFs into the treatment of OA holds the potential to offer significant benefits. This is because MOFs not only have intrinsic biological activities, but also act as carriers to facilitate controlled drug delivery and prolong the duration in the management of OA. This paper presents a review of the recent studies that have explored the potential usage of MOFs as drugs or carriers in the treatment of OA, which also examines the progress of MOFs in tissue engineering for the treatment of OA. These studies are anticipated to not only enhance the comprehension of MOFs but also provide strong evidence in favor of their utilization in the treatment of OA.

KEYWORDS

metal-organic frameworks, osteoarthritis, biomaterials, scaffold, bone tissue engineering

1 Introduction

As a prevalent and destructive chronic disease, osteoarthritis (OA) has been considered as the primary cause of cartilage erosion. The etiology of OA mainly involves the following factors, such as age, weight, gender, genetic susceptibility, sports-related injury, and inflammation. It is well known that any joint in the body can be impacted along with the occurrence of OA, which can induce the patients to experience symptoms including pain, edema, stiffness, and restricted movement (Motta et al., 2023). According to recent studies, over 240 million worldwide individuals are believed to experience symptomatic OA, resulting in substantial physical and psychological strain on sufferers, especially among the elderly (Lv et al., 2024). More importantly, articular cartilage is composed of chondrocytes and an extracellular matrix (ECM) that surrounds the chondrocytes, which does not possess sufficient circulatory, neural, and lymphatic systems that are necessary for self-healing (Liu et al., 2021; Gao et al., 2022). Therefore, it has been proven to be a challenge that managing osteoarthritis through the regeneration of articular cartilage.

A series of medication including corticosteroids, non-steroidal anti-inflammatory drugs, and hyaluronic acid has been well developed to alleviate inflammation in OA. Compared with other alternative techniques, intra-articular injections are considered as the

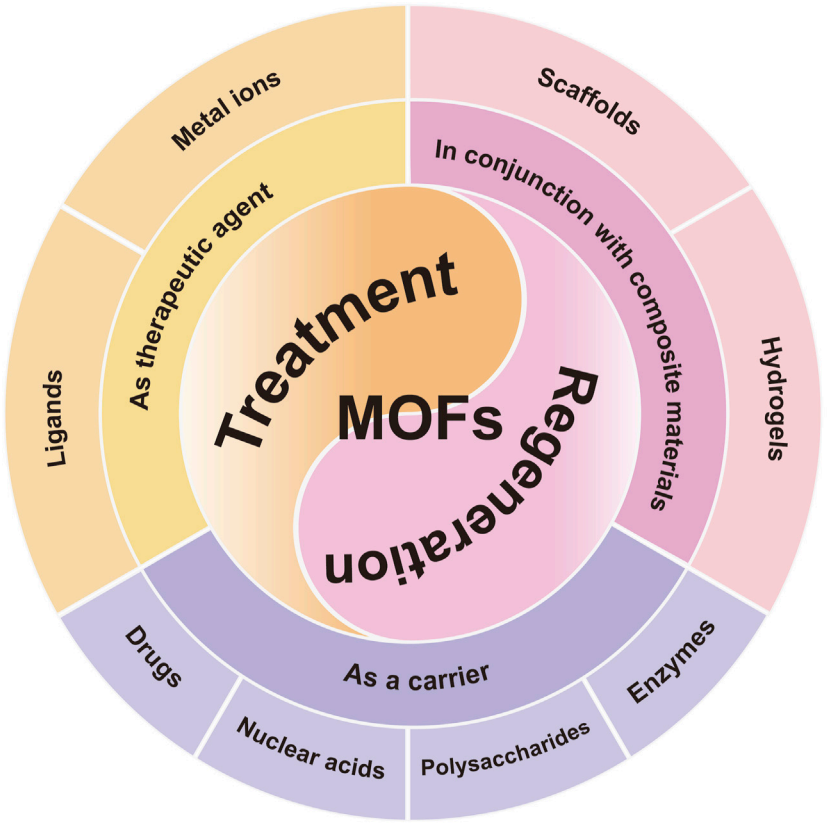

FIGURE 1
The summary of MOFs and their derivatives in the field of OA treatment. Schematic representation of the three pillars of MOFs application-therapeutic agents, carriers and compositions for scaffold materials.

most efficacious method for treating OA (Richard et al., 2023; Guo et al., 2022). Although promising, it is still difficult to ensure the controlled release of drug and its long-term release effectiveness. Currently, scientists are exploring innovative approaches to improve the delivery of drugs with the assistance of nanotechnology. As well known, nanomaterials possess the capacity to encapsulate drugs and accurately release them at the target sites (Sattar et al., 2022; Chamundeeswari et al., 2019). Moreover, nanoassemblies based on anti-inflammatory biomolecules possess the capability to reduce inflammation by themselves. Accordingly, the use of high-performance nanomaterials as emerging biomaterials for the treatment of OA is regarded as an urgent strategy.

Metal-organic frameworks (MOFs) are crystalline compounds composed of organic ligands and metal ions. Because of the intrinsic porous properties, thermal and chemical stability, easy surface modification, as well as high biosafety, metal-organic frameworks (MOFs) have been considered as promising nanocarriers in the field of biomedicine (Horcajada et al., 2008; Li L. et al., 2023; Li X. et al., 2023). It is worth noting that a variety of factors including internal stimuli such as redox, pH, and enzymes, as well as external stimuli such as light, temperature, magnetism, ultrasound, and mechanical force have been utilized to trigger the release of guest molecules from MOF-based nanosystems. Meanwhile, these aforementioned nanosystems usually exhibit the ability to react towards multiple stimuli, which can enable them to release chemicals at specified moments or spaces (Gu et al., 2023). More importantly, MOFs and their derivatives with inherent bioactivity can relieve localized inflammation in the treatment of inflammatory diseases (Li et al., 2024; Shyngys et al., 2021). This review article critically summarized the recent advances made in the development of MOFs and their derivatives, as well as their potentials for treating OA. As illustrated in Figure 1, the key emphasis of this review was to discuss the roles of MOFs and their derivatives for the OA treatment and bone regeneration. Moreover, the stability and biological activity of these biomaterials were well evaluated in the above-mentioned OA treatments. Last but not least, this review concluded with an overview of the challenges hindering further development of MOFs and their derivatives and a perspective on the future of the field before their clinical translation.

2 MOF as a therapeutic agent

Essential metal ions or clusters including Zn, Mg, Zr, Fe, Cu, and Mn usually held the ability to cure OA, which could also serve as the structure centers of MOFs and their derivatives. As illustrated in Figure 2A, Cheng and co-workers synthesized a novel MOF named as $\{[Zn(H_2O)(HL)]\cdot(DMF)_2(H_2O)_2\}_n$, which could regulate the inflammation associated with OA via reducing the activation of the PI3K/AKT signaling pathway (Cai et al., 2020; Sun et al., 2020). Tang and co-workers developed a new Mg/HCOOH-MOF, which could serve as a controlled-release drug for treating OA. The

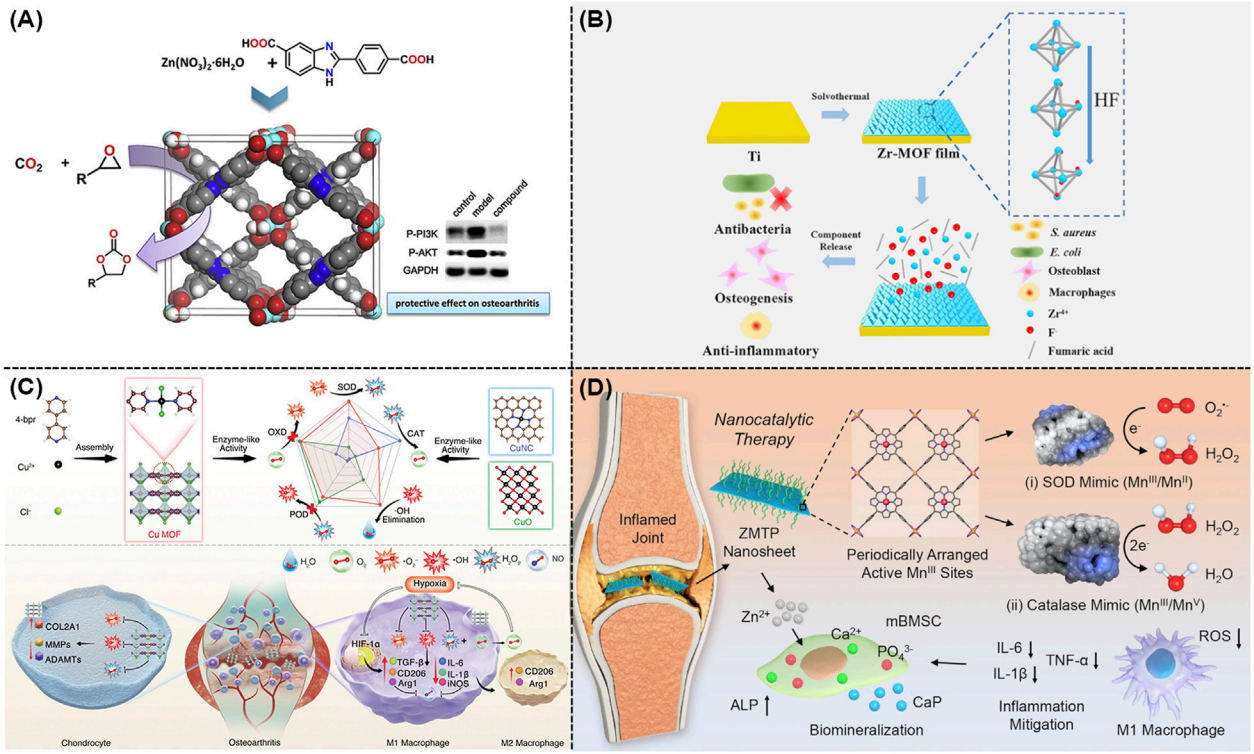

FIGURE 2
(A) Schematic representation of the preparation of Zn(II)-MOF and its effect on activation of the PI3K/AKT signaling pathway (Cai et al., 2020). **(B)** Preparation of Zr-MOF film and its antimicrobial, anti-inflammatory, and osteogenic capabilities (Yan et al., 2022). **(C)** Schematic illustration of Cu-MOF nanozymes for the treatment of OA by scavenging ROS and regulating macrophage phenotype (Yu et al., 2024). **(D)** Schematic illustration of the therapeutic mechanism of ZMTP nanosheets for nanocatalytic treatment of rheumatoid arthritis (Yang B. et al., 2022).

magnesium ions derived from Mg/HCOOH-MOF held both anti-inflammatory and osteogenic properties, promising their potentials in the anti-inflammatory therapy and further promotion of osteogenesis (Li et al., 2020b). As shown in Figure 2B, Yan and co-workers prepared a novel Zr-MOF-801 with admirable antimicrobial effect and enhanced osteogenic performance (Yan et al., 2022).

Reactive oxygen species (ROS) could significantly contribute to the development and exacerbation of OA, which emerged as a promising therapeutic target. As a famous nanozyme that came from Fe-based MOF family, Mil-88 with excellent peroxidase activity exhibited the ability to eliminate ROS both *in vitro* and *in vivo*. According to these findings, a very recent study revealed that a feasible Mil-88-based enzymatic healing process could be beneficial for treating OA (Lopez-Cantu et al., 2022). For instance, Mil-88 could enhance the bioactivity of genes related to tissue growth (such as Col-2) and reduce the activity of genes associated with OA tissue breakdown (such as MMP-13), promising its potential to be a novel and advantageous method for treating OA (Hu et al., 2023). Meanwhile, a well-defined Cu-MOF nanozymes were well developed for the treatment of OA using a straightforward self-assembly method, as shown in Figure 2C. According to the density functional theory (DFT), these Cu-MOF nanozymes with excellent superoxide dismutase (SOD) and catalase (CAT) mimicking characteristics had higher antioxidant activity in comparison to other Cu-based antioxidants. As expected, these Cu-MOF nanozymes could alleviate the low oxygen conditions in OA, transform macrophages into the M2 phenotype, prevent cartilage damage, as well as decrease the release of pro-inflammatory factors (Yu et al., 2024). Furthermore, a MOF named as Zn-Mn-TCPP-PVP (ZMTP) were well designed using the coordination effect between the benzoyloxy group of Mn-TCPP and Zn^{2+} (Yang B. et al., 2022). As shown in Figure 2D, these well-developed ZMTP with high SOD activity and CAT activity exhibited great anti-inflammatory and bio-mineralization performances in both *in vitro* and *in vivo* models.

3 MOF as a carrier

Considering that there were lots of drugs utilized for treating OA in daily clinic, a variety of carriers were highly required. In comparison to other nanoscale carriers, MOFs and their derivatives held several advantages including a substantial specific surface area for the attachment of cells, a high porosity for the encapsulation of biomolecules, a great feasibility for the surface modification with targeted and responsive molecules, and a high biocompatibility. Therefore, it is suitable for the delivery of various guest molecules, including drugs, proteins, nucleic acids and polysaccharides.

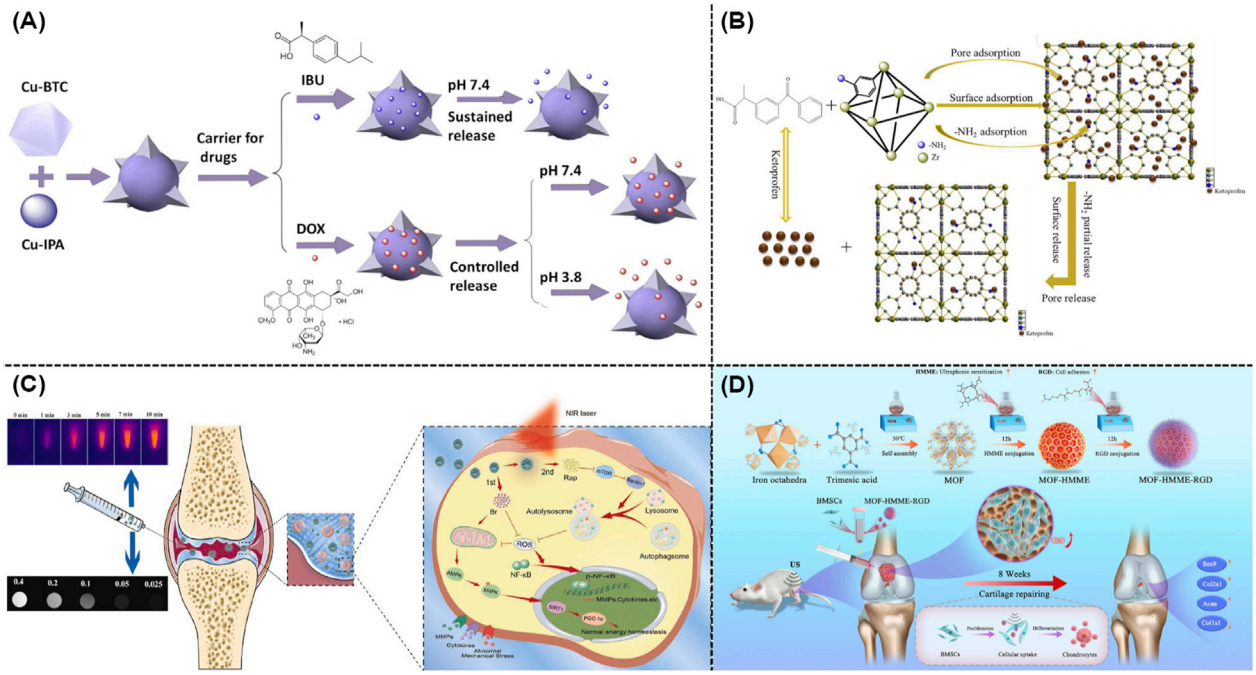

FIGURE 3
(A) Schematic illustration of the application of mixed ligand MOFs as efficient drug carriers for IBU and DOX (Sun et al., 2017). **(B)** Drug loading and release mechanism of UiO-66-NH_2 as a drug carrier (Li et al., 2019b). **(C)** Mechanisms of dual drug delivery nanoplatforms with cartilage-targeting effect and near-infrared laser response in OA therapy (Xue S. et al., 2021). **(D)** Schematic illustration of the synthesis of MOF-HMME-RGD and relative therapeutic mechanisms (Luo et al., 2024).

3.1 Loading drugs

According to recent clinical research, the predominant non-steroidal anti-inflammatory drugs (NSAIDs) for the symptomatic management of OA were mainly ibuprofen, ketoprofen, and diclofenac (Richard et al., 2023). Although the localized use of NSAIDs extremely enhanced their absorption, two factors might seriously lead to a decrease in their effectiveness. First, a periarticular microvascular system usually facilitated the rapid drug clearance from joints. Second, the skin played an active role in metabolizing medicines using the cytochrome P450 enzyme. In order to improve the medication usage and relative OA treatment efficacy, well-defined nanoscale carriers were highly needed (Patil et al., 2023). Previous studies demonstrated that MIL-101 (Cr) and MIL-100 could achieve the high loading of ibuprofen and its stimuli-responsive release (Silva et al., 2016). Figure 3A revealed that novel Cu-MOFs composed with multiple ligands were created as efficient carriers for delivering IBU and DOX (Sun et al., 2017). Furthermore, Tan and co-workers utilized zirconium-based MOF (UiO-66) as an efficient drug carrier (Li et al., 2019b). As shown in Figure 3B, by changing different functional groups, these well-developed nano-sized carriers could well response toward different stimulants. As expected, UiO-66-NH_2 held the best loading and release properties. Furthermore, a MOF-based drug delivery nanosystem based on Sr/PTA-MOF-ketoprofen could reduce inflammation, relieve pain, as well as maintain bone homeostasis (Li et al., 2019a; Li et al., 2020a).

Owing to the acidic nature of joint milieu, the acid-responsive release mechanism was well understood in various MOF-based delivery systems. Itaconic acid-contained ZIF-8 was well prepared as a pH-responsive drug-loaded nanocarrier in which itaconic acid could alleviate OA after the efficient cellular penetration and endocytosis (Yu et al., 2023). Meanwhile, the ZIF-8's pH-responsive characteristic was utilized to encapsulate neoflavone (NBIF), which could extremely reduce the poor solubility of NBIF and its rapid degradation (Jiang et al., 2023). As shown in Figure 3C, a nano-size hybrid nanocarrier based on mesoporous polydopamine and MOF was rationally developed as an efficient photothermal reagent to promote the OA treatment. The above mentioned nanosystem exhibited rapid responsiveness toward the irradiation of near infrared (NIR) light, leading to the enhanced drug release (Xue S. et al., 2021). Moreover, a zirconium-based MOF was modified with polyphenols and gold, which exhibited excellent photothermal outcomes for the treatment of OA (Xu S. et al., 2023). Recent studies indicated that sonodynamic therapy was utilized in the OA treatment. As shown in Figure 3D, a Fe-based MOF was well conjugated with hematoporphyrin monomethyl ether (HMME) and arginine-aspartate-glycine (RGD) peptides for repairing cartilage defects (Luo et al., 2024). According to the current design, the porous architecture of MOFs could effectively prevent organic acoustic molecules from their self-quenching while ROS could be rapidly generated through the linker-metal charge transfer pathway with high efficacy.

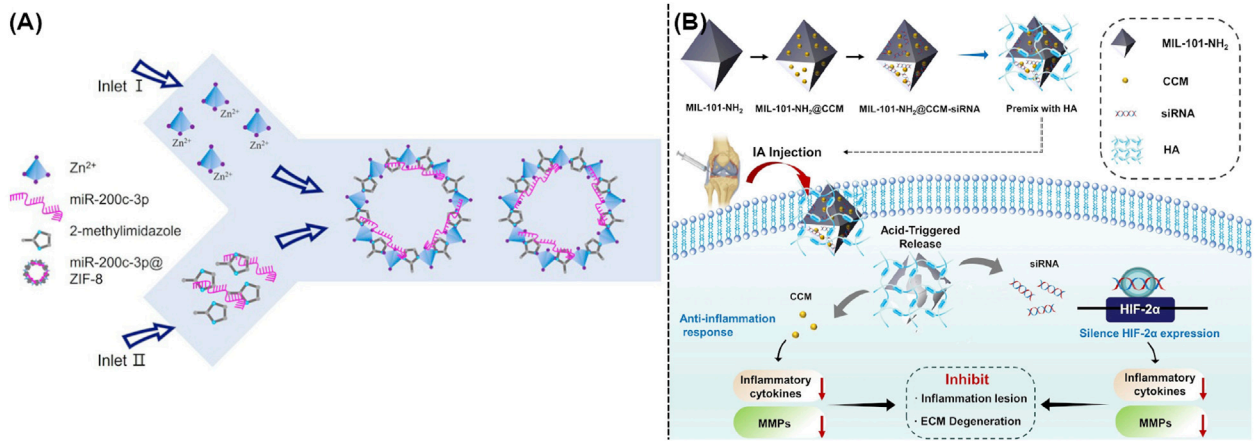

FIGURE 4
(A) Schematic illustration of a one-step microfluidic preparation of miR-200c-3p@ZIF-8 (Yang et al., 2023). **(B)** Synthesis of MIL-101-NH_2@CCM-siRNA and its usage in the OA treatment (Zhang et al., 2023a).

3.2 Loading nuclear acids

Recent studies indicated that RNA-based gene therapy was widely utilized to treat OA. This innovative method usually employed microRNAs and anti-miRNAs for polygenic regulation, small interfering RNAs (siRNAs) for gene silencing, and mRNAs for gene supplementation (DeJulius et al., 2024). Although promising, current systemic delivery of RNA usually failed because of the complicated environment of body and the biodegradability of nuclear acids, which also could lead to serious side effects including uncertain retention duration in body, immunological infection, and potential toxicity. Recent studies suggested the applications of MOFs and their derivatives as high-performance nanocarriers for the delivery of nuclear acid (He et al., 2023). The well-defined chemical structures of MOFs and their derivatives endowed them with the possibility of strong interaction with nucleic acid biomolecules, which could occur by encapsulation, physical adsorption, as well as chemical grafting (He et al., 2023). As illustrated in Figure 4A, some researchers utilized ZIF-8 to create miR-200c-3p@ZIF-8 using a facile one-step approach with the assistance of a Y-shape microfluidic chip. This approach allows for the exact manipulation of miR-200c-3p@ZIF-8 with ideal size, resulting in the admirable encapsulation efficacy and transport outcome. As expected, these well-developed miR-200c-3p@ZIF-8 hybrids could significantly lowered the expression of associated inflammatory factors during the OA treatment (Yang et al., 2023). Moreover, siRNA targeting the hypoxia-inducible factor-2α (HIF-2α) gene and the relative anti-inflammation therapy could be well achieved using MIL-101-NH_2 as efficient nanocarrier. Figure 4B demonstrated that gene and drug loaded MIL-101-NH_2 could efficiently release siRNA and curcumin in the acidic OA microenvironment, which thus silenced the HIF-2α gene, reduced the levels of pro-inflammatory factors, and avoided the relative cartilage degradation (Zhang et al., 2023a).

3.3 Loading polysaccharides

Due to their high biocompatibility and low systemic toxicity, polysaccharides and polysaccharide-based materials were ideal for the treatment of OA. Recent studies demonstrated that polysaccharides could be well utilized as raw materials for the synthesis of ECM, which served as efficient lubricants for lubricating joints. Moreover, polysaccharides could provide a suitable environment for chondrocyte repair, exert antioxidant activity to regulate the OA microenvironment, as well as interact with cell membrane receptors to avoid the attack of inflammatory factors (An et al., 2024; Alcaide-Ruggiero et al., 2023). Although promising, essential strategies were highly required to optimize the current delivery approach and therapeutic efficacy due to the high molecular weight and fragility of various polysaccharides.

Traditional carriers including silica, hydrogels, and polymer-based materials were highly limited by their non-biodegradability, low loading efficacy, as well as complicated synthesis. Recent studies indicated that the intrinsic porous structure of MOFs could efficiently adsorb and accommodate polysaccharides. Moreover, polysaccharides could be well loaded into the interior of MOFs via the electrostatic interaction in the mixture containing metal ions, organic ligands, and polysaccharides, which resulted in the direct synthesis of polysaccharide-loaded MOFs (Tong et al., 2021). As shown in Figure 5A, ZIF-8 could encapsulate heparin, fucoidan sulfate, and fucosylated chondroitin sulfate, and hyaluronic acid. The well-developed nanocomposites named as polysaccharide@ZIF-8 followed an acid-responsive property, which could release polysaccharide in the OA microenvironment (Zheng et al., 2021). Furthermore, several pH-responsive MOFs including ZIF-8, ZIF-90, and MAF-7 were rationally designed and utilized to provide the protection for glycosaminoglycans (GAG). As shown in Figure 5B, the above mentioned GAG-loaded nanocomposites could offer new avenues for the further therapy of OA (Velásquez-Hernández et al., 2020).

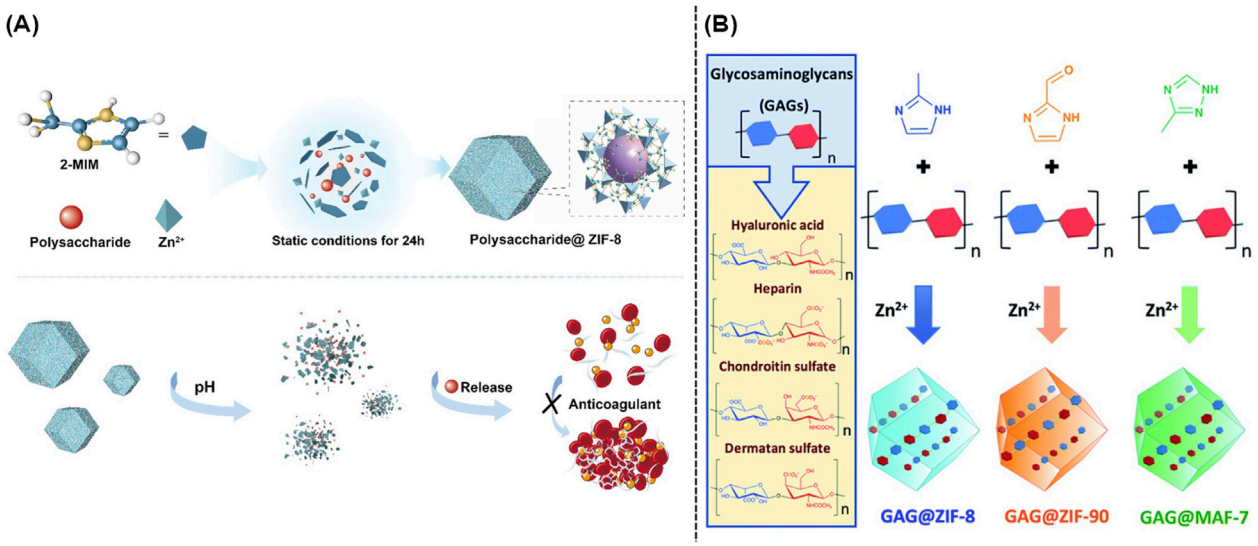

FIGURE 5
(A) Schematic illustration of the synthesis of polysaccharides@ZIF-8 (Zheng et al., 2021). **(B)** One-pot synthesis of GAG@MOFs originated from three different metallic nitrogen heterocyclic frameworks (Velásquez-Hernández et al., 2020).

3.4 Loading enzymes

Previous studies demonstrated that natural enzymes or artificial enzymes with antioxidant activity held great potentials in the OA therapy. Accordingly, MOFs were widely utilized to load these enzymes, which could extremely improve their stability and endurance under physiological conditions. For example, platinum (Pt) nanozymes with excellent ROS scavenging and anti-inflammatory activities were encapsulated in ZIF-8 while lantanum (La) as an osteogenic active element was well incorporated via ion exchange, which resulted in the formation of Pt@ZIF-8@La with a bimetallic-organic backbone. Both *in vitro* and *in vivo* results demonstrated that this well-developed multifunctional nanoplatform with high enzyme activity and great ability of ion release exhibited efficient synergistic therapeutic effects of immunomodulation and osteogenesis (Pan et al., 2023). In addition, Pt@PCN222-Mn with multifunctional active sites was involved in the treatment of temporomandibular joint (TMJ) osteoarthritis. This well-prepared nanocomposite could remodel the inflammatory microenvironment of TMJ OA and delay its development through regulating the ROS-NF-κB and p38/MAPK signaling pathways (Zhang et al., 2023).

4 MOF as a scaffold material composition

Besides many drugs and biomolecules were widely utilized for the inflammation control and cartilage repairing in clinic, tissue engineering still remained its necessity and specificity in the promotion of new cartilage formation. Combined with the use of MOFs and their derivatives, multifunctional platforms based on scaffolds or hydrogels could result in ideal therapeutic outcomes for OA. The addition of MOFs to scaffolds can endow these scaffold materials with special physicochemical properties and biological effects, so as to better assist the function of scaffold materials.

4.1 Scaffolds

Recently, approaches including electrostatic spinning, solvent casting, particle leaching, gas foaming and freeze drying, stereolithography, and 3D bioprinting were widely utilized to create artificial scaffolding (Wu et al., 2022). MOFs and other biomaterials were well integrated with the above mentioned artificial scaffolding to develop novel hybrid scaffolds for the OA therapy. As expected, these well-designed multifunctional platforms exhibited excellent anti-inflammatory and antioxidant activity, which could result in the ideal cartilage repairing. For example, poly(lactide-co-glycolide) (PLGA) and dimethyloxallyl glycine (DMOG) loaded iron-based MIL-88 were utilized to prepare novel nanofibrous scaffolds via electrostatic spinning technology, which could serve as artificial extracellular matrix for the promotion of osteogenesis and angiogenesis (Wu et al., 2022). Figure 6A illustrated the synthesis approach of hybrid scaffold and their mechanism in the OA treatment. Compared with the scaffold without any modification, the electrostatically spun mats became rougher upon the addition of MOFs, which thus made the gradual breakdown and absorption of hybrid scaffolds more easily and allowed for the ideal release of iron ions within the injury sites (Xu C. et al., 2023). Furthermore, another novel bioceramic scaffolds with good mechanical characteristics and bioactivity were involved into the field of bone tissue engineering. As well known, β-tricalcium phosphate (β-TCP) was widely utilized for the bone regeneration because it could gradually degrade into calcium and phosphate ions upon the acid microenvironment. Figure 6B

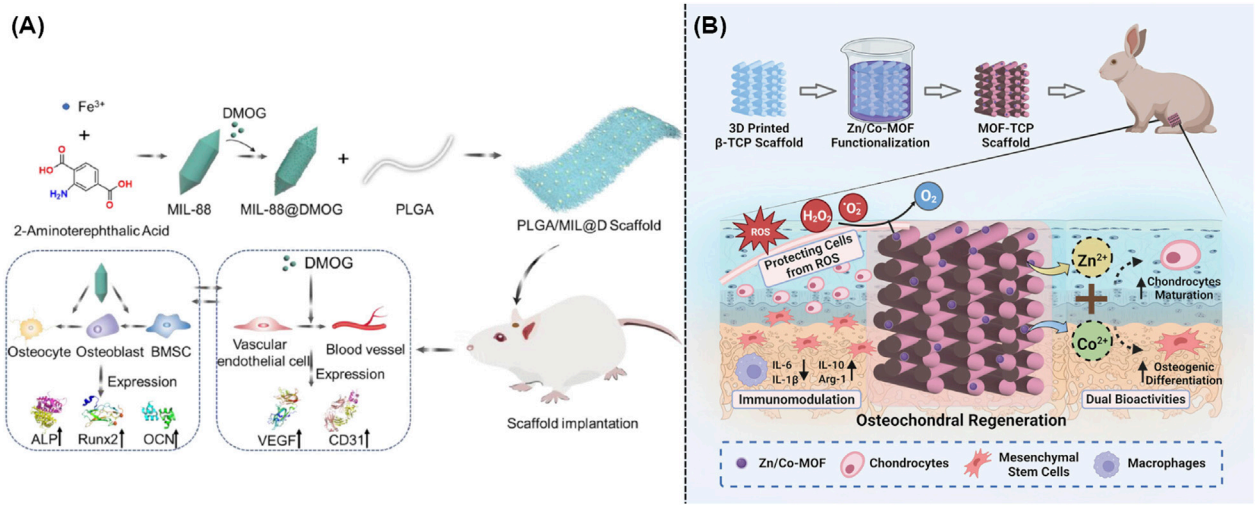

FIGURE 6
(A) Preparation and mechanism of the iron-based MOF-contained hybrid scaffolds for the repair of bone defects (Xu C. et al., 2023). **(B)** Synthesis and mechanism of the MOF-TCP-based scaffold for the treatment of osteoarthritis (Shu et al., 2023).

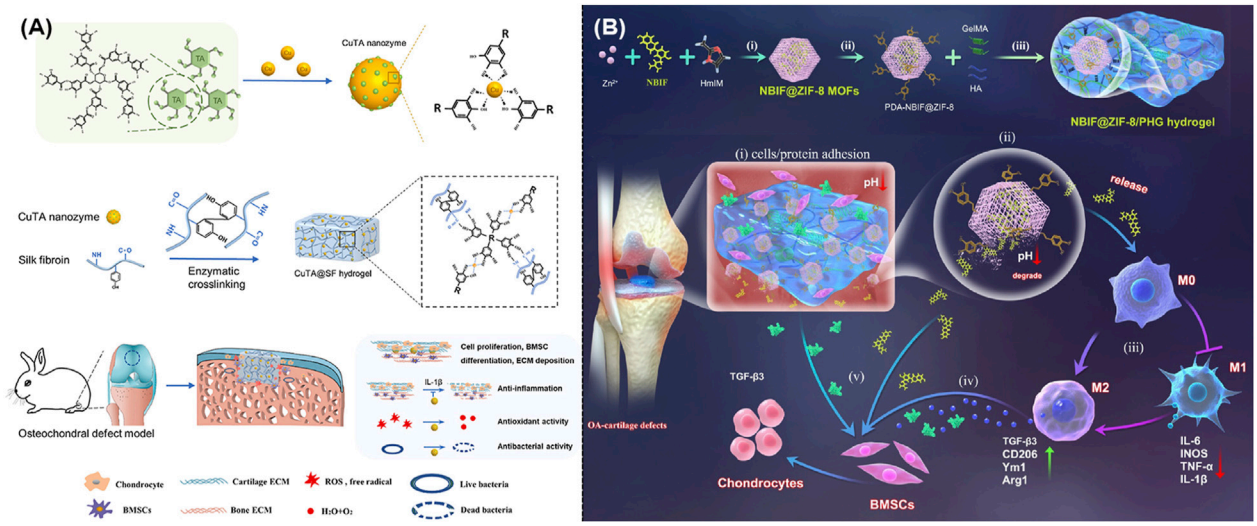

FIGURE 7
(A) Schematic illustration of the synthesis of CuTA nanozymes and CuTA@SF hydrogels, as well as their application in the repair of bone defects (Cao et al., 2023). **(B)** Schematic illustration of the design and usage of a MOF-based hydrogel to promote OA-induced cartilage defect repair (Jiang et al., 2023).

illustrated that the addition of Zn/Co-MOF into β-TCP could result in the formation of a novel hybrid scaffold, which could reduce localized inflammation and repair osteochondral tissue through the elimination of ROS and release of ions (Shu et al., 2023).

Electrospun fibrous membrane was a novel bionic flexible scaffold that could be utilized to repair tissue injuries, particularly gradient tissue damage that occurred at the interfaces of tendons and bones. Recently, a metal-organic framework-based bipolar metal flexible electrospun fibrous membrane was prepared as a new kind of biomimetic flexible scaffold with multiple layers using electrostatic spinning technology. If the fibers degraded, metal ions such as Zn^{2+} and Cu^{2+} might be released, which could regulate collagen formation, osteoclast differentiation, and angiogenesis (Yang R. et al., 2022). In addition, researchers also created an asymmetric bilayer PCL/Col membrane that was changed in the same way by ZIF-8 crystals. The composite membrane made of PCL/Col/ZIF-8 included two layers including a barrier layer and a crystal layer. Several admirable properties including increased tensile strength, low pH responsiveness, and controlled degradation rate endowed these well-developed composites with great performance in the bone regeneration both *in vitro* and *in vivo* (Xue Y. et al., 2021).

4.2 Hydrogels

It was well known that hydrogel held a striking structural similarity to the ECM of bone and cartilage, which could gradually build up a three-dimensional structure, well integrate with the surrounding tissues, and provide essential support and protection during the tissue repairing. Recent studies indicated that hydrogels held the ability to encapsulate medicines or growth factors that aided in the cartilage healing. As expected, Figure 7A illustrated the creation of CuTA@SF using MOFs, which could speed up the cell proliferation and extremely enhance the tissue regeneration (Cao et al., 2023). Meanwhile, IA-ZIF-8@HMs was effectively prepared using a one-step microfluidic approach. During the treatment of OA, IA-ZIF-8 could be released from hydrogel microspheres (HMs), further decreasing the localized inflammation (Yu et al., 2023). Moreover, researchers designed and created a hybrid hydrogel (G-GH/CL-CD-MOF) by mixing gelatin-glucosamine hydrochloride with cross-linked cyclodextrin MOF. The optimum porosity structure of this drug delivery system endowed it with a long-term, sustained release of ibuprofen and excellent anti-inflammation treatment of OA (Yang H. et al., 2022). On the other hand, researchers also mixed polycaprolactone and gelatin mats with different amounts of glucosamine loaded ZIF-8 nanoparticles with the ideal goal to achieve the growth of cartilage tissue (Ranjbar et al., 2023). As shown in Figure 7B, novel NBIF@ZIF-8/PHG hydrogels with robust mechanical characteristics and the ability to recover from deformation were well created as efficient alternatives in the cartilage repairing (Jiang et al., 2023). In addition, the tendon-targeting peptide and cartilage-targeting peptide were well loaded in ZIF-8 and Mg-MOF, respectively. Subsequently, these peptide-loaded MOFs were immobilized in methacrylate gelatin using UV-induced photopolymerization to produce LZIF-8/WMg-MOF@GEL, which could achieve a tailored ion delivery platform to both tendon and cartilage (Ma et al., 2024).

5 Conclusion and perspective

With the rapid development of medicine and material science, the use of smart MOFs and their derivatives as emerging biomaterials for the OA treatment has been one of the most important topic of biomedical engineering. In this review, we summarized the latest studies focused on the use of MOFs and their derivatives as ideal carriers for drugs and biomolecules or main composites of hybrid scaffolds and hydrogels in the treatment of OA. The greatest advantage of these well-designed MOFs and their derivatives for OA therapy were concluded as that they could significantly overcome some limitations of drugs and biomolecules such as poor solubility, short retention time, poor targeting capacity, and ease of biodegradability. Moreover, the essential role of MOFs and their derivatives in tissue engineering was well understood after that they were integrated with scaffolds and hydrogels to construct hybrid platforms. Although these MOFs held promising clinical potentials, their further clarification was still necessary on some certain issues. First, there was still a lack of knowledge regarding the drug delivery and release dynamics in MOFs. Second, the *in vivo* stability, organ distribution and metabolites of MOFs remain unknown, limiting further development and utilization. Third, how to promote tissue regeneration rather than just control inflammation, and the function of MOFs in this process need to be further explored. Accordingly, this review not only emphasizes the considerable potentials of MOFs and their derivatives in the OA treatment, but also anticipated an increase in the number of relevant studies applying MOFs to the treatment of OA in the future. Last but not least, we believed that it would be a transformative clinical achievement by using MOFs as efficient biomaterials to promote the treatment of OA and its related diseases.

Author contributions

YL: Writing–original draft, Writing–review and editing. HZ: Writing–review and editing. TC: Writing–review and editing. CX: Writing–review and editing. XB: Supervision, Validation, Writing–review and editing.

Funding

The author(s) declare that financial support was received for the research, authorship, and/or publication of this article. Financial support was provided by the Jilin Province Science and Technology Development Plan Project (JCSZ2023481-6), and the Bethune Plan of Jilin University (2024B15).

Conflict of interest

The authors declare that the research was conducted in the absence of any commercial or financial relationships that could be construed as a potential conflict of interest.

Publisher's note

References

Alcaide-Ruggiero, L., Cugat, R., and Domínguez, J. M. (2023). Proteoglycans in articular cartilage and their contribution to chondral injury and repair mechanisms. *Int. J. Mol. Sci.* 24 (13), 10824. doi:10.3390/ijms241310824

An, H., Zhang, M., Gu, Z., Jiao, X., Ma, Y., Huang, Z., et al. (2024). Advances in polysaccharides for cartilage tissue engineering repair: a review. *Biomacromolecules* 25 (4), 2243–2260. doi:10.1021/acs.biomac.3c01424

Cai, Z., Qian, J., Zhao, Y., and Cheng, Y. (2020). Microporous MOF with open metal sites for CO_2 fixation and protective effect on osteoarthritis by regulating the activation of PI3K/AKT pathway. *J. Solid State Chem.* 283, 121169. doi:10.1016/j.jssc.2019.121169

Cao, Z., Wang, H., Chen, J., Zhang, Y., Mo, Q., Zhang, P., et al. (2023). Silk-based hydrogel incorporated with metal-organic framework nanozymes for enhanced osteochondral regeneration. *Bioact. Mater.* 20, 221–242. doi:10.1016/j.bioactmat.2022.05.025

Chamundeeswari, M., Jeslin, J., and Verma, M. L. (2019). Nanocarriers for drug delivery applications. *Environ. Chem. Lett.* 17 (2), 849–865. doi:10.1007/s10311-018-00841-1

DeJulius, C. R., Walton, B. L., Colazo, J. M., d'Arcy, R., Francini, N., Brunger, J. M., et al. (2024). Engineering approaches for RNA-based and cell-based osteoarthritis therapies. *Nat. Rev. Rheumatol.* 20 (2), 81–100. doi:10.1038/s41584-023-01067-4

Gao, H., Pan, Q., Dong, W., and Yao, Y. (2022). Progress in osteochondral regeneration with engineering strategies. *Ann. Biomed. Eng.* 50 (10), 1232–1242. doi:10.1007/s10439-022-03060-6

Gu, Z., Wang, J., Fu, Y., Pan, H., He, H., Gan, Q., et al. (2023). Smart biomaterials for articular cartilage repair and regeneration. *Adv. Funct. Mater.* 33 (10), 2212561. doi:10.1002/adfm.202212561

Guo, L., Zhong, S., Liu, P., Guo, M., Ding, J., and Zhou, W. (2022). Radicals scavenging MOFs enabling targeting delivery of siRNA for rheumatoid arthritis therapy. *Small* 18 (27), 2202604. doi:10.1002/smll.202202604

He, Y., Li, D., Wu, L., Yin, X., Zhang, X., Patterson, L. H., et al. (2023). Metal-organic frameworks for gene therapy and detection. *Adv. Funct. Mater.* 33 (12), 2212277. doi:10.1002/adfm.202212277

Horcajada, P., Serre, C., Maurin, G., Ramsahye, N. A., Balas, F., Vallet-Regí, M., et al. (2008). Flexible porous metal-organic frameworks for a controlled drug delivery. *J. Am. Chem. Soc.* 130 (21), 6774–6780. doi:10.1021/ja710973k

Hu, H., Huang, X., Dai, Y., Zhu, K., Ye, X., Meng, S., et al. (2023). Organic metal matrix Mil-88a nano-enzyme for joint repair in the osteoarthritis mouse model. *Front. Bioeng. Biotechnol.* 11, 1164942. doi:10.3389/fbioe.2023.1164942

Jiang, Y., Liao, H., Yan, L., Jiang, S., Zheng, Y., Zhang, X., et al. (2023). A metal-organic framework-incorporated hydrogel for delivery of immunomodulatory neobavaisoflavone to promote cartilage regeneration in osteoarthritis. *ACS Appl. Mater. and Interfaces* 15 (40), 46598–46612. doi:10.1021/acsami.3c06706

Li, D., Yadav, A., Zhou, H., Roy, K., Thanasekaran, P., and Lee, C. (2024). Advances and applications of metal-organic frameworks (MOFs) in emerging technologies: a comprehensive review. *Glob. Challenges* 8 (2), 2300244. doi:10.1002/gch2.202300244

Li, L., Zhu, Y., Qi, Z., Li, X., Pan, H., Liu, B., et al. (2023a). GCMC simulations to study the potential of MOFs as drug delivery vehicles. *Appl. Organomet. Chem.* 37 (9), e7199. doi:10.1002/aoc.7199

Li, X., Shu, X., Shi, Y., Li, H., and Pei, X. (2023b). MOFs and bone: application of MOFs in bone tissue engineering and bone diseases. *Chin. Chem. Lett.* 34 (7), 107986. doi:10.1016/j.cclet.2022.107986

Li, Z., Li, Z., Li, S., Wang, K., Ma, F., and Tang, B. (2020a). Potential application development of Sr/HCOOH metal organic framework in osteoarthritis. *Microporous Mesoporous Mater.* 294, 109835. doi:10.1016/j.micromeso.2019.109835

Li, Z., Peng, Y., Pang, X., and Tang, B. (2020b). Potential therapeutic effects of Mg/HCOOH metal organic framework on relieving osteoarthritis. *ChemMedChem* 15 (1), 13–16. doi:10.1002/cmdc.201900546

Li, Z., Peng, Y., Xia, X., Cao, Z., Deng, Y., and Tang, B. (2019a). Sr/PTA metal organic framework as a drug delivery system for osteoarthritis treatment. *Sci. Rep.* 9 (1), 17570. doi:10.1038/s41598-019-54147-5

Li, Z., Zhao, S., Wang, H., Peng, Y., Tan, Z., and Tang, B. (2019b). Functional groups influence and mechanism research of UiO-66-type metal-organic frameworks for ketoprofen delivery. *Colloids Surfaces B Biointerfaces* 178, 1–7. doi:10.1016/j.colsurfb.2019.02.027

Liu, Y., Shah, K. M., and Luo, J. (2021). Strategies for articular cartilage repair and regeneration. *Front. Bioeng. Biotechnol.* 9, 770655. doi:10.3389/fbioe.2021.770655

Lopez-Cantu, D. O., González-González, R. B., Sharma, A., Bilal, M., Parra-Saldívar, R., and Iqbal, H. M. N. (2022). Bioactive material-based nanozymes with multifunctional attributes for biomedicine: expanding antioxidant therapeutics for neuroprotection, cancer, and anti-inflammatory pathologies. *Coord. Chem. Rev.* 469, 214685. doi:10.1016/j.ccr.2022.214685

Luo, S., Shang, Y., Qin, Z., Zhou, B., Lu, C., Qu, Y., et al. (2024). A novel cartilage-targeting MOF-HMME-RGD sonosensitizer combined with sonodynamic therapy to enhance chondrogenesis and cartilage regeneration. *Front. Bioeng. Biotechnol.* 12, 1339530. doi:10.3389/fbioe.2024.1339530

Lv, Z., Wang, Z., Chen, D., and Shi, D. (2024). Advances in osteoarthritis research: from diagnosis, treatment to mechanism studies. *J. Orthop. Transl.* 44, A4–A6. doi:10.1016/j.jot.2024.01.006

Ma, J., Yu, H., Zhang, X., Xu, Z., Hu, H., Liu, J., et al. (2024). Dual-targeted metal ion network hydrogel scaffold for promoting the integrated repair of tendon-bone interfaces. *ACS Appl. Mater. and Interfaces* 16 (5), 5582–5597. doi:10.1021/acsami.3c16544

Motta, F., Barone, E., Sica, A., and Selmi, C. (2023). Inflammaging and osteoarthritis. *Clin. Rev. Allergy and Immunol.* 64 (2), 222–238. doi:10.1007/s12016-022-08941-1

Pan, H., Miao, X., Deng, J., Pan, C., Cheng, X., and Wang, X. (2023). Bimetallic metal-organic framework for mitigating aseptic osteolysis. *ACS Appl. Mater. and Interfaces* 15 (4), 4935–4946. doi:10.1021/acsami.2c19449

Patil, P., Nene, S., Shah, S., Singh, S. B., and Srivastava, S. (2023). Exploration of novel drug delivery systems in topical management of osteoarthritis. *Drug Deliv. Transl. Res.* 13 (2), 531–546. doi:10.1007/s13346-022-01229-z

Ranjbar, N., Kolahdoozan, M., and Ebadi-Dehaghani, H. (2023). Electrospun polycaprolactone/gelatin mat incorporated with glucosamine-loaded zeolite imidazolate framework-8 nanoparticles for cartilage tissue engineering. *J. Polym. Res.* 31 (1), 9. doi:10.1007/s10965-023-03847-8

Richard, M. J., Driban, J. B., and McAlindon, T. E. (2023). Pharmaceutical treatment of osteoarthritis. *Osteoarthr. Cartil.* 31 (4), 458–466. doi:10.1016/j.joca.2022.11.005

Sattar, R., Shahzad, F., Ishaq, T., Mukhtar, R., and Naz, A. (2022). Nano-drug carriers: a potential approach towards drug delivery methods. *ChemistrySelect* 7 (22), e202200884. doi:10.1002/slct.202200884

Shu, C., Qin, C., Chen, L., Wang, Y., Shi, Z., Yu, J., et al. (2023). Metal-organic framework functionalized bioceramic scaffolds with antioxidative activity for enhanced osteochondral regeneration. *Adv. Sci.* 10 (13), 2206875. doi:10.1002/advs.202206875

Shyngys, M., Ren, J., Liang, X., Miao, J., Blocki, A., and Beyer, S. (2021). Metal-organic framework (MOF)-based biomaterials for tissue engineering and regenerative medicine. *Front. Bioeng. Biotechnol.* 9, 603608. doi:10.3389/fbioe.2021.603608

Silva, I., Carvalho, M., Oliveira, C., Profirio, D., Ferreira, R., Corbi, P., et al. (2016). Enhanced performance of a metal-organic framework analogue to MIL-101(Cr) containing amine groups for ibuprofen and nimesulide controlled release. *Inorg. Chem. Commun.* 70, 47–50. doi:10.1016/j.inoche.2016.05.020

Sun, K., Li, L., Yu, X., Liu, L., Meng, Q., Wang, F., et al. (2017). Functionalization of mixed ligand metal-organic frameworks as the transport vehicles for drugs. *J. Colloid Interface Sci.* 486, 128–135. doi:10.1016/j.jcis.2016.09.068

Sun, K., Luo, J., Guo, J., Yao, X., Jing, X., and Guo, F. (2020). The PI3K/AKT/mTOR signaling pathway in osteoarthritis: a narrative review. *Osteoarthr. Cartil.* 28 (4), 400–409. doi:10.1016/j.joca.2020.02.027

Tong, P.-H., Zhu, L., Zang, Y., Li, J., He, X.-P., and James, T. D. (2021). Metal-organic frameworks (MOFs) as host materials for the enhanced delivery of biomacromolecular therapeutics. *Chem. Commun.* 57 (91), 12098–12110. doi:10.1039/D1CC05157A

Velásquez-Hernández, M. d. J., Astria, E., Winkler, S., Liang, W., Wiltsche, H., Poddar, A., et al. (2020). Modulation of metal-azolate frameworks for the tunable release of encapsulated glycosaminoglycans. *Chem. Sci.* 11 (39), 10835–10843. doi:10.1039/D0SC01204A

Wu, J., Qin, Z., Jiang, X., Fang, D., Lu, Z., Zheng, L., et al. (2022). ROS-responsive PPGF nanofiber membrane as a drug delivery system for long-term drug release in attenuation of osteoarthritis. *NPG Regen. Med.* 7 (1), 66. doi:10.1038/s41536-022-00254-3

Xu, C., Kang, Y., Guan, S., Dong, X., Jiang, D., and Qi, M. (2023a). Iron-based metal-organic framework as a dual cooperative release system for enhanced vascularization and bone regeneration. *Chin. Chem. Lett.* 34 (5), 107825. doi:10.1016/j.cclet.2022.107825

Xu, S., Lin, Y., Zhao, X., Liang, Z., Hu, Y., Chen, Z., et al. (2023b). NIR triggered photocatalytic and photothermal bifunctional MOF nanozyme using for improving osteoarthritis microenvironment by repairing injured chondrocytes of mitochondria. *Chem. Eng. J.* 468, 143826. doi:10.1016/j.cej.2023.143826

Xue, S., Zhou, X., Sang, W., Wang, C., Lu, H., Xu, Y., et al. (2021a). Cartilage-targeting peptide-modified dual-drug delivery nanoplatform with NIR laser response for osteoarthritis therapy. *Bioact. Mater.* 6 (8), 2372–2389. doi:10.1016/j.bioactmat.2021.01.017

Xue, Y., Zhu, Z., Zhang, X., Chen, J., Yang, X., Gao, X., et al. (2021b). Accelerated bone regeneration by MOF modified multifunctional membranes through enhancement of osteogenic and angiogenic performance. *Adv. Healthc. Mater.* 10 (6), 2001369. doi:10.1002/adhm.202001369

Yan, B., Tan, J., Zhang, H., Liu, L., Chen, L., Qiao, Y., et al. (2022). Constructing fluorine-doped Zr-MOF films on titanium for antibacteria, anti-inflammation, and osteogenesis. *Biomater. Adv.* 134, 112699. doi:10.1016/j.msec.2022.112699

Yang, B., Yao, H., Yang, J., Chen, C., and Shi, J. (2022a). Construction of a two-dimensional artificial antioxidase for nanocatalytic rheumatoid arthritis treatment. *Nat. Commun.* 13 (1), 1988. doi:10.1038/s41467-022-29735-1

Yang, H., Hu, Y., Kang, M., Ding, H., Gong, Y., Yin, X., et al. (2022b). Gelatin-glucosamine hydrochloride/crosslinked-cyclodextrin metal-organic frameworks@IBU composite hydrogel long-term sustained drug delivery system for osteoarthritis treatment. *Biomed. Mater.* 17 (3), 035003. doi:10.1088/1748-605X/ac61fa

Yang, K., Ni, M., Xu, C., Wang, L., Han, L., Lv, S., et al. (2023). Microfluidic one-step synthesis of a metal-organic framework for osteoarthritis therapeutic micrornas delivery. *Front. Bioeng. Biotechnol.* 11, 1239364. doi:10.3389/fbioe.2023.1239364

Yang, R., Zheng, Y., Zhang, Y., Li, G., Xu, Y., Zhang, Y., et al. (2022c). Bipolar metal flexible electrospun fibrous membrane based on metal-organic framework for gradient

healing of tendon-to-bone interface regeneration. *Adv. Healthc. Mater.* 11 (12), 2200072. doi:10.1002/adhm.202200072

Yu, B., Sun, W., Lin, J., Fan, C., Wang, C., Zhang, Z., et al. (2024). Using Cu-based metal-organic framework as a comprehensive and powerful antioxidant nanozyme for efficient osteoarthritis treatment. *Adv. Sci.* 11 (13), 2307798. doi:10.1002/advs.202307798

Yu, H., Ren, P., Pan, X., Zhang, X., Ma, J., Chen, J., et al. (2023). Intracellular delivery of itaconate by metal-organic framework-anchored hydrogel microspheres for osteoarthritis therapy. *Pharmaceutics* 15 (3), 724. doi:10.3390/pharmaceutics15030724

Zhang, Z., Hou, Y., Chen, M., Yu, X., Chen, S., Yue, Y., et al. (2023a). A pH-responsive metal-organic framework for the co-delivery of HIF-2α siRNA and curcumin for enhanced therapy of osteoarthritis. *J. Nanobiotechnology* 21, 18. doi:10.1186/s12951-022-01758-2

Zhang, Z., Yuan, L., Liu, Y., Wang, R., Zhang, Y., Yang, Y., et al. (2023). Integrated cascade nanozyme remodels chondrocyte inflammatory microenvironment in temporomandibular joint osteoarthritis via inhibiting ROS-NF-κB and MAPK pathways. *Adv. Healthc. Mater.* 12 (10), 2203195. doi:10.1002/adhm.202203195

Zheng, J., Li, B., Ji, Y., Chen, Y., Lv, X., Zhang, X., et al. (2021). Prolonged release and shelf-life of anticoagulant sulfated polysaccharides encapsulated with ZIF-8. *Int. J. Biol. Macromol.* 183, 1174–1183. doi:10.1016/j.ijbiomac.2021.05.007

frontiers | Frontiers in Pharmacology

TYPE Original Research
PUBLISHED 27 September 2024
DOI 10.3389/fphar.2024.1453036

OPEN ACCESS

EDITED BY
Wen Liao,
Sichuan University, China

REVIEWED BY
Sandeep Kumar Mishra,
Yale University, United States
Li Xiao,
Sichuan Academy of Medical Sciences and Sichuan Provincial People's Hospital, China

*CORRESPONDENCE
Hanchi Wang,
whc23@jlu.edu.cn
Li Fu,
fuli1127@jlu.edu.cn

RECEIVED 22 June 2024
ACCEPTED 17 September 2024
PUBLISHED 27 September 2024

CITATION
Li J, Ding J, Zhou T, Li B, Wang J, Wang H and Fu L (2024) A novel functionally graded bilayer membrane with excellent barrier function and *in vivo* osteogenesis promotion for guided bone regeneration.
Front. Pharmacol. 15:1453036.
doi: 10.3389/fphar.2024.1453036

A novel functionally graded bilayer membrane with excellent barrier function and *in vivo* osteogenesis promotion for guided bone regeneration

Junxuan Li, Jiaxin Ding, Tao Zhou, Bolun Li, Jingjing Wang, Hanchi Wang* and Li Fu*

Department of Oral Implantology, Jilin Provincial Key Laboratory of Tooth Development and Bone Remodeling, Hospital of Stomatology, Jilin University, Changchun, China

Introduction: Guided bone regeneration (GBR) technology has been widely used as a reliable method to address alveolar bone defects. To improve the clinical effects of GBR approach, there have been attempts to develop barrier membranes with enhanced regenerative properties. However, modifying the material and structure of GBR membranes to integrate physicochemical properties and biological activity remains challenging. The aim of this study was to develop a novel functionally graded bilayer membrane (FGBM) with a gradient structure and composition, and to evaluate its osteogenesis promotion effect for GBR.

Methods: By combining the phase inversion method and electrospinning method, functionally graded bilayer membranes (FGBM) with gradient structure and composition of poly(lactic-co-glycolic acid) (PLGA), nano-hydroxyapatite (nHA), and gelatin were fabricated in this study. The physicochemical and biological properties of the prepared FGBM, including structural and morphological characterization, mechanical properties, *in vitro* biodegradation, cell behaviors, and *in vivo* osteogenic bioactivity, were comprehensively evaluated.

Results: The findings demonstrated the successful fabrication of PLGA/nHA/gelatin FGBM with an asymmetric structure, exhibiting enhanced hydrophilic, mechanical, and degradation properties. The incorporation of gelatin not only improved the biological integration, but also enhanced the binding affinity between electrospun fiber layer and phase inversion layer. The FGBM with a 30% nHA mass fraction and a PLGA/gelatin mass ratio of 1:1 exhibited excellent barrier function and osteogenic bioactivities *in vitro* and *in vivo*.

Discussion: This work demonstrated the potential of PLGA/nHA/gelatin FGBM in bone regeneration and provided valuable insight for the development of barrier membrane.

KEYWORDS

guided bone regeneration, poly(lactic-co-glycolic acid), nanohydroxyapatite, gelatin, osteogenesis

1 Introduction

Insufficient alveolar ridge bone volume poses a significant challenge to the successful placement of implants in the optimal three-dimensional position, leading to adverse effects on the delivery and aesthetic outcome of implant prostheses in the future (Testori et al., 2018; Shi et al., 2022). The guided bone regeneration (GBR) technique is a promising approach to alveolar ridge reconstruction based on the rationale that the regenerative potential of soft tissue exceeds that of bone tissue, and therefore advocates to mechanically prevent the growth of undesirable soft tissues into the bone defect area, thereby allowing only osteoblast clusters from the parent bone to refill (Dahlin et al., 1988; Retzepi and Donos, 2010; Sheikh et al., 2017). In that case, the key element of this technique, guided bone regeneration membrane (GBRM), serves as a biocompatible mechanical barrier that protects the defective area from non-osteoblasts and promotes selective proliferation of autologous osteoblasts, which results in the regeneration of new bone to reconstruct bone defect. The realization of these functions relies on the specific properties of GBRM. Consequently, the choice of GBRM is crucial (Retzepi and Donos, 2010; Elgali et al., 2017; Buser et al., 2023).

According to their degradation performance, GBRM commonly used in clinical practice can be categorized into resorbable and non-resorbable membranes. Non-resorbable membranes are typically composed of polytetrafluoroethylene-based materials or metallic materials with high biocompatibility and mechanical strength (Elgali et al., 2017; Omar et al., 2019; Bee and Hamid, 2022). However, this type of membrane requires a second surgical intervention to be removed, increasing the patients' therapeutical cost and the risks of wound healing complications (Zhang et al., 2019; Naenni et al., 2021). In comparison, the use of resorbable GBRM eliminates the risk of complications associated with secondary surgery that exists with the non-resorbable GBRM.

The material properties of GBRM are crucial in determining its physicochemical and biological characteristics to meet the requirements of an ideal GBRM (Liu and Li, 2019; Omar et al., 2019; Mizraji et al., 2023). Collagen and synthetic polymers such as polylactic acid (PLA), polyglycolic acid (PGA), poly(lactic-co-glycolic acid) (PLGA), are the most commonly used materials for resorbable GBRM. However, the unpredictable and uncontrolled resorption can lead to the loss of space maintenance of the membranes (Nahid et al., 2022; Patil et al., 2023). In reality, not only is the ideal biodegradation vital for resorbable GBRM, but sufficient mechanical strength may also be beneficial for bone regeneration (Rider et al., 2022). PLGA is an excellent scaffold component for bone tissue engineering materials due to its tunable mechanical strength and processing properties (Lian et al., 2019; Jin et al., 2021). Although its hydrophobic surface structure and lack of cellular recognition sites result in limited cytocompatibility. Additionally, the accumulation of acidic degradation products can cause local inflammation. Fortunately, these issues can be addressed through the implementation of appropriate design and modifications (Jin et al., 2021; Li et al., 2021; Xu et al., 2024). Gelatin is a partially denatured derivative of collagen, inheriting its advantageous properties of good biocompatibility and bioactivity while eliminating its antigenicity. Hydroxyapatite (HA) is the principal inorganic component of bone tissue, exhibiting high biocompatibility and osteoconductive properties (Lin et al., 2020; Zheng et al., 2021; Qin et al., 2023). The incorporation of gelatin and hydroxyapatite into PLGA-based composite scaffolds can compensate for their inherent deficiencies, markedly enhance the mechanical and degradation properties of the composite scaffolds, and augment the osteogenic activity and biocompatibility by mimicking the composition and structure of the ECM, as well as neutralizing the acidic microenvironment generated by PLGA degradation (Ji et al., 2012; Aldana and Abraham, 2017; Naik et al., 2017; Jin et al., 2019). Hence, to maximize the benefits of various biomaterials, researchers have combined gelatin with synthetic polyesters and bioceramic materials to create tissue-engineered nanocomposites with improved physicochemical and biological properties (Fu et al., 2017; Zhang et al., 2020; Gautam et al., 2021; Li et al., 2021; Xiang et al., 2022).

The morphology and structure of GBRM also play a crucial role in its performance and osteogenesis promotion effects. In recent years, a novel functional grade membrane (FGM), characterized by an asymmetric structure and composition, has been developed to further improve the properties (Shah et al., 2019; Abe et al., 2020; Lian et al., 2020). As demonstrated in our previous study (Fu et al., 2017), a functionally graded bilayer membrane (FGBM) with asymmetric bilayer structures, could be fabricated by the phase inversion method combined with electrospinning method, utilizing PLGA and nano-hydroxyapatite (nHA) as primary raw materials. On the one side of the FGBM was a hard and dense layer, which acted as a mechanical barrier to prevent undesirable soft tissues from growing in. On the other side was a porous fiber layer with high porosity and large specific surface area, similar to osteoblastic extracellular matrix (ECM), which could effectively facilitate bone regeneration. However, the hydrophilicity of the PLGA/nHA membrane necessitated improvement. In addition, the biocompatibility and osteogenic activity of the FGBM in animal models remain unexplored.

To address these gaps, further improve the physicochemical properties of FGBM and explore their osteogenesis promotion effects *in vivo*, the present study drew inspiration from bionics and further modified FGBM by mimicking the composition and structure of the osteoblastic ECM (Figure 1). As widely acknowledged, in the osteoblastic ECM of natural bone tissue, the deposition of calcium is deposited on collagen fibers as the form of hydroxyapatite (HA), which together provide structural support for bone tissue (Salhotra et al., 2020). In this study, using bioactive materials that are fully biocompatible as raw materials, we introduced gelatin into the primary PLGA/nHA nanofibers, which were then electrospun onto the bone-tissue interface of a PLGA/nHA phase inversion membrane, to fabricate a PLGA/nHA/Gelatin FGBM. nHA particles were uniformly doped into the individual nanofiber scaffolds composed of gelatin and PLGA as the main body. Such nanofibers were interwoven with each other to fully utilize the advantages of this strategic modification in terms of physical structure and chemical composition. This enhanced the mechanical strength of the whole membrane while facilitating osteoblast adhesion and growth by providing suitable carriers and stimulation signals, thereby promoting cell proliferation and differentiation. A series of *in vitro* and *in vivo* experiments were designed and performed to validate the dual effects of the good tissue barrier and bone-enhancing effects of PLGA/nHA/Gelatin FGBM. These results are encouraging, as they indicate a promising future for PLGA/nHA/Gelatin FGBM in the treatment of alveolar bone defects.

10.3389/fphar.2024.1453036

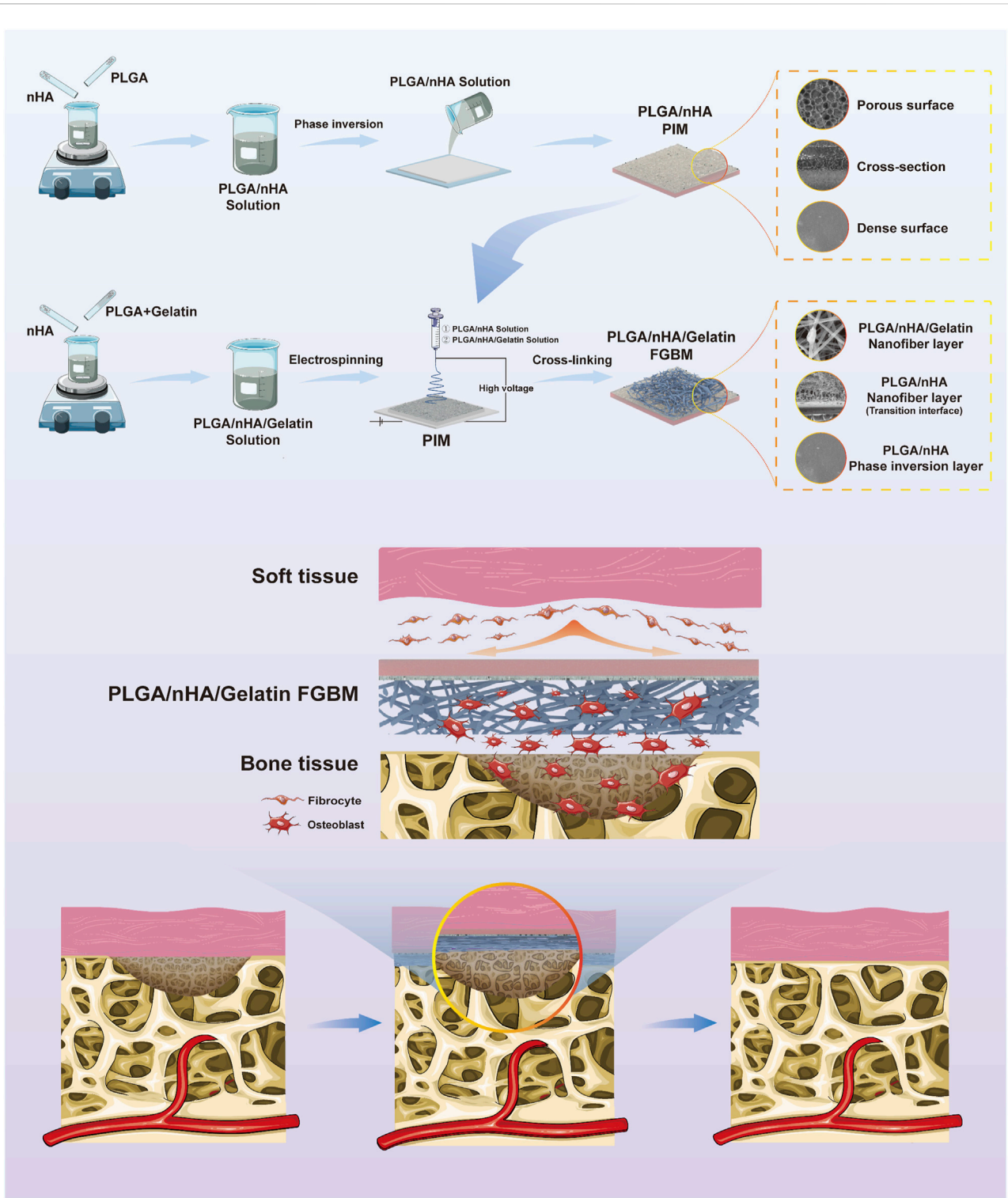

FIGURE 1
The schematic diagram of the fabrication process of PLGA/nHA/Gelatin functionally graded bilayer membrane and applied for guided bone regeneration.

2 Materials and methods

2.1 Materials

Nano-Hydroxyapatite (nHA, 50–100 nm in length and 20–30 nm in width), N, N-dimethylformamide (DMF), and 1,1,1,3,3,3-Hexafluoro-2-propanol (HFIP), were purchased from Aladdin (China). Gelatin, 3-(4,5 dimethylthiazol-2-yl)-2,5-diphenyl tetrazolium bromide (MTT), 4′,6-diamidino-2-phenylindole (DAPI), trypan blue solution, and cetylpyridinium chloride were purchased from Sigma-Aldrich (United States). Poly(Lactic-co-glycolic acid) (PLGA, LA: GA = 75:25, with a molecular weight of 100,000) was donated by the Changchun Institute of applied chemistry (Changchun, China). Dulbecco's Modified Eagle Medium (DMEM), 10% fetal bovine serum (FBS), and Penicillin streptomycin were purchased from Gibco (United States). Trypsin was purchased from Biotechs (China).

2.2 Fabrication of PLGA/nHA/gelatin functionally graded bilayer membrane

2.2.1 Fabrication of phase inversion membrane

The fabrication process of the phase inversion membrane closely followed the procedures outlined in our prior study (Fu et al., 2017). PLGA was dissolved in N,N-dimethylformamide (DMF) to prepare a 5% (w/v) homogeneous solution. nHA was added to the mixture in an nHA/(PLGA + nHA) mass fractions of 5%. The solution was then stirred vigorously for 2 h to ensure homogeneous dispersion of the nHA. Subsequently, the solution was casted onto a glass plate maintained at a constant temperature and scraped with a spatula. The glass plate was then submerged in a water bath at 25°C until the film was fully detached to obtain a phase inversion membrane (PLGA with 5 wt % nHA) (PIM).

2.2.2 Preparation of PLGA/nHA electrospinning solution

1 g PLGA was added in 6 mL HFIP and stirred magnetically until complete dissolution. Add 0.43 g nano-hydroxyapatite (nHA/(PLGA + nHA) = 30 wt%) into 4 mL HFIP and ultrasonically dispersed for 30 min to disperse nHA particles uniformly. Blend the above two solutions and stir continuously for 24 h to get PLGA/nHA electrospinning solution.

2.2.3 Preparation of PLGA/nHA/gelatin electrospinning solution

PLGA and Gelatin were dissolved in 2 mL HFIP and stirred until completely dissolved, respectively. Blended the two solutions, then added 12 μL acetic acid (CH_3COOH), and stirring was continued for 6 h. The ratios of PLGA/Gelatin (w/w) were set to 7/3 (0.42 g PLGA, 0.18 g Gelatin), 5/5 (0.3 g PLGA, 0.3 g Gelatin), and 3/7 (0.18 g PLGA, 0.42 g Gelatin). 0.25 g of nano-hydroxyapatite [nHA/(PLGA + Gelatin + nHA) = 30 wt%] was added into 2 mL HFIP and ultrasonically dispersed for 30 min. The above two solutions were blended and stirred for 24 h to obtain three types of PLGA/nHA/Gelatin electrospinning solutions.

2.2.4 Electrospinning

The phase inversion membrane was fixed on a 10 cm × 10 cm aluminum foil receiving screen with the rough surface facing upward. Electrospinning was performed at room temperature with a voltage of 20 kV, a spinneret diameter of 0.4 mm, a flow rate of 1 mL/h, and a receiving distance of 15 cm, utilizing a high-voltage Electrospinning machine. Initially, 1 mL of PLGA/nHA solution was electrospun onto the phase inversion membrane, followed by the immediate electrospinning of 6 mL of PLGA/nHA/Gelatin solution onto the PLGA/nHA layer. The electrospinning process was repeated three times to produce three distinct types of functionally graded bilayer membrane, FGBM PHG1, FGBM PHG2, and FGBM PHG3, each composed of different ratios (7/3, 5/5, and 3/7) of PLGA/Gelatin. These membranes underwent cross-linking in glutaraldehyde (GA) vapor for 1 h. In addition, the remaining 7 mL of PLGA/nHA solution was electrospun onto the phase inversion membrane alone, serving as a control group (FGBM PH). Subsequently, the four obtained FGBMs were dried in a vacuum oven (Jinghong, Shanghai, China) for 24 h to eliminate residual solvent.

2.3 Structural and morphological characterization methods

Structural and morphological characterizations of PLGA/nHA/Gelatin electrospun fiber layer of FGBMs (FGBM PH, FGBM PHG1, FGBM PHG2, and FGBM PHG3) and PIM were observed by environmental scanning electron microscope (ESEM; Model XL 30 ESEM FEG, Micro FEI Philips, Amsterdam, Netherlands) and transmission electron microscopy (TEM, JEM 200cx, Japan). The hydrophilicity of the electrospun fiber layer of FGBM was evaluated by a contact angle tester (Fangrui, Shanghai, China) at room temperature.

2.4 Mechanical tests

The mechanical properties of FGBM were evaluated by Instron 3,367 mechanical testing machine (Norwood, United States). Each type of membrane was cut into 20 mm × 15 mm rectangular samples. Measured the sample thickness with a spiral micrometer. Stretched the sample at a tensile strength of 100 N and a speed of 10 mm ·min^{-1}, at room temperature. The values of tensile strength were recorded.

2.5 *In vitro* biodegradation

To evaluate the *in vitro* biodegradation performance of FGBM, rectangular samples of 8.0 mm × 5.0 mm were prepared. Each sample's initial weight (W_0) was measured separately on an analytical balance. The samples were immersed in 10 mL phosphate-buffered saline (PBS) (0.1 M, pH = 7.4), and placed in a constant temperature oscillating incubator (100 rpm) at 37°C. Weekly, removed the samples, quickly absorbed surface water with filter paper, and then weighed on an analytical balance (W_t). Then placed the samples in a desiccator to dry completely, and weighed on

an analytical balance ($W_t^{'}$). The mass remaining (percentage) was calculated by Equation 1, and the water uptake (percentage) was calculated by Equation 2. Measured the mass retention, water uptake, and pH of the samples weekly for 8 weeks.

$$\text{Mass remaining}\ (\%) = W_t^{'} / W_0 \times 100\,\% \quad (1)$$

$$\text{Water uptake}\ (\%) = \left(W_t - W_t^{'}\right) / W_t \times 100\,\% \quad (2)$$

2.6 *In vitro* biocompatibility

2.6.1 Barrier function of phase inversion membrane to L929 cells

The barrier function of PIM was *in vitro* evaluated on L929 cells according to previously established method (Fu et al., 2017). To briefly summarize, the PIM was immobilized using a Cell Crown (Sigma-Aldrich, St. Louis, MO, United States), and a L929 cells suspension at a density of 4×10^3 cells·ml^{-1} was added to the Cell Crown and suspended in a 24-well plate spiked with 1 mL of cell-free medium liquid. The smooth surface of the membrane was kept in direct contact with the cells during the process (Supplementary Figure S4A). At 1 and 3 days after incubation, the smooth surface of the membrane and the bottom of the 24-well plate were stained with DAPI. Cell growth on the membrane and at the bottom of the well plate was observed using an inverted fluorescence microscope (TE2000-S, Nikon, United States).

2.6.2 MC3T3-E1 cells adhesion on the FGBM

The FGBM was cut to the size of the well of 24-well cell culture plate, and the UV light irradiated the front and back of the FGBM samples for 1 h, respectively. The sterilized sample was then placed inside the 24-well plate with the porous fiber layer facing upward, and a sterile iron ring with an inner diameter matching the diameter of the 24-well plate was pressed onto the sample to prevent it from floating up. MC3T3-E1 cells were inoculated on the fib surface at a density of 1.5×10^5 cell·cm^{-2} and cultured at 37°C with 5% CO_2, using CO_2 thermostat cell incubator (MCO-15AC, SANYO, Japan). To detect the early adhesion of cells, at 4 h after inoculation, stained the cells with DAPI, and then observed the cells cultured on the scaffold under inverted fluorescence microscope. The cell density (D) was calculated by $D_{cell} = N_{cell}/A$ (N_{cell} represented the number of cells in the observation area, and A represented the area of the observation area). Six parallel samples were tested in each group. Three observation areas were randomly selected for each sample for photograph and calculation.

2.6.3 MC3T3-E1 cells proliferation on the FGBM

Cell behaviors were evaluated by detecting the survival of Murine osteoblast-like cells (MC3T3-E1 cells) inoculated on FGBM. The cells were donated by the Medical Department of Jilin University (Changchun, China). MC3T3-E1 cells were inoculated on the fibrous surface of FGBM at a density of 1.5×10^5 cells/cm^2. The culture was terminated at 1, 4, and 7 days, separately, and the cells that failed to attach to the membrane were washed three times with PBS.

The integrity of the cytomembrane was examined using a live/dead cell staining assay to evaluate cell viability on the nanofiber membrane. Covered the surface of the samples with PBS which contained 4 μM ethidium homodimer^{-1} (EthD^{-1}) and 2 μM calcein-AM, and stained the cells for 20 min. The stained cells were observed under an inverted fluorescence microscope, in which live cells were excited by blue light fluorescing green and dead cells excited by green light fluorescing red. The percentage of live cells was calculated at each time point.

The MTT was used to detect cell proliferation on the nanofiber membrane. Added 20 μL of 5 mg mL^{-1} MTT solution to the well and incubated at 37°C for 4 h. Then carefully removed the supernatant, added 150 μL of LDMSO, shook it to dissolve the formed methanogenic crystals completely. The levels of MTT were determined by measuring the absorbance value at 490 nm with a Microplate Reader (SANYO, Japan).

2.6.4 MC3T3-E1 cells differentiation on the FGBM

The differentiation of MC3T3-E1 cells on the PLGA/nHA/Gelatin electrospun fiber layer was assessed through an alkaline phosphatase (ALP) activity assay. MC3T3-E1 cells were seeded onto the fibrous surface of the FGBM at a density of 1.5×10^5 cells/cm^2. The culture was terminated at two distinct time points, namely, 1 and 14 days. At each time point, cells were lysed, and the collected lysate was subjected to relative quantitative measurements of ALP using an ALP substrate reaction solution. The levels of ALP were determined by measuring the absorbance value at 405 nm with a Microplate Reader.

Alizarin red S (ARS) staining was used to assess the quality and quantity of the extracellular matrix secreted by MC3T3-E1 cells. At 1, 7, and 14 days of cell culture, the cell-laden scaffolds were fixed in 90% ice ethanol solution for 10 min, then washed 3 times with distilled water, to which the configured 0.1% ARS dye was added, stained in a 37°C water bath for 30 min, gently washed three times with deionized water, and photographed by a camera. Then the ARS on the specimen was dissolved with 10% cetylpyridinium chloride. The levels of ARS were determined by measuring the absorbance value at 540 nm with a Microplate Reader.

2.7 *In vivo* assessments with rat cranial bone defect model

2.7.1 Rat cranial bone defect model establishment

Twenty-four Wistar rats, aged 12 weeks and weighing between 250 and 300 g, were selected for the establishment of 5-mm cranial bone defects, assessing the bone-regenerating potential of the PLGA/nHA/Gelatin FGBM. Ethical guidelines were strictly observed in accordance with the approval of the Animal Experimentation Ethics Committee of the Stomatology School of Jilin University.

Cranial bone defects were induced using a trephine bar (Micro-Tech, Japan) in accordance with a previously described method (Yoshimoto et al., 2018). The rats were randomly divided into four groups based on the type of membrane used. The test group, which evaluated *in vivo* bone regeneration, featured the PLGA/nHA/Gelatin FGBM with PLGA/Gelatin ratios of 1:1 (FGBM PHG2). The control groups included a blank group, a PLGA/nHA FGBM group (FGBM PH), and a Bio-Gide® group. The membranes (FGBM PH, FGBM PHG2, and Bio-Gide®) were cut into 5.0 mm diameter

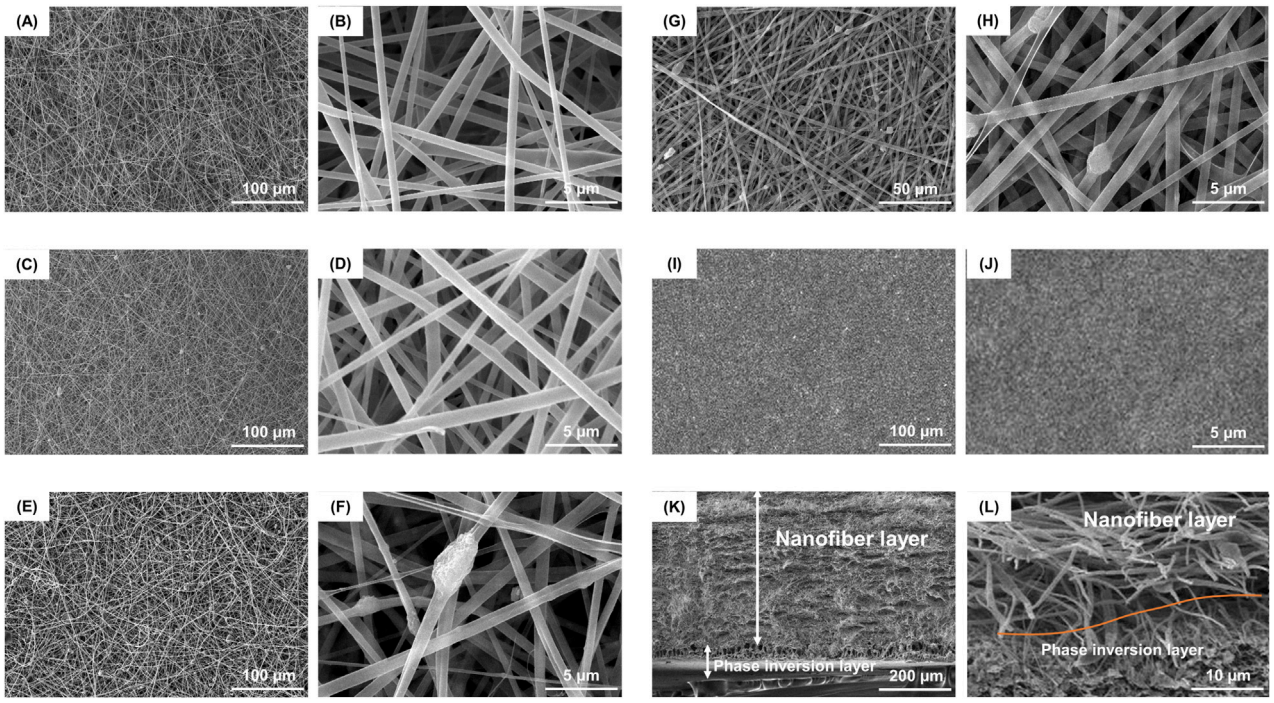

FIGURE 2
Representative SEM images of surface morphology and structure of different FGBMs. **(A, B)** FGBM PH. **(C, D)** FGBM PHG1. **(E, F)** FGBM PHG2. **(G, H)** FGBM PHG3. **(I, J)** The dense surface of PIM. **(K)** The cross-sectional thickness of the FGBM was about 600 μm, in which the phase inversion layer was about 100 μm and the nanofiber layer was about 500 μm. **(L)** The red curve indicated the boundary between the phase inversion layer and the nanofiber layer. The interlayer was tightly bonded.

circular pieces and applied to cover the bone defects. The blank controls had no membrane coverage. Following the application of sutures to the periosteum and scalp, the rats resumed normal activity following the recovery period. At 4 and 8 weeks, the rats were euthanized, and the cranial areas were harvested and fixed with 10% formalin for subsequent analysis.

2.7.2 Micro-computed tomography (Micro-CT) measurement

Micro-CT (SCAN CO, Switzerland) was used to monitor the healing of the bone defect area and to quantitatively assess the volume of regenerated bone. A simultaneous 3D reconstruction was performed through scanning with standardized segmentation parameters (sigma: 0.8, threshold value: 220–1,000). Circular contour lines, excluding the adjacent native bone, were delineated around the 5 mm diameter defect area. The machine's built-in software generated 3D reconstructed images from 2D slices. Quantitative outcomes were expressed as a percentage of bone volume to tissue volume.

2.7.3 Histological and histomorphometric observation

Specimens underwent decalcification using 20% EDTA for a period of 3 months. Following gradient dehydration in ethanol, the samples were embedded in paraffin and sectioned in a coronal plane, producing slices with a thickness of 5 μm. The specimens were subjected to Hematoxylin-Eosin staining (H&E) and microscopically observed to assess the regenerated bone.

2.8 Statistical analysis

All experiments were repeated three times, and the data obtained were expressed as the mean ± standard deviation (SD). Overall, the statistically significant values were estimated using two-sided Student's t-tests and one-way analysis of variance (ANOVA) tests. Statistical analyses were performed using SPSS 19.0 software (SPSS, Chicago, IL, United States). A P-value less than 0.05 was considered statistical significance. In the figures, letters were used to show statistical differences, and values with dissimilar letters are significantly different from each other ($p < 0.05$).

3 Results

3.1 Morphology observation of FGBMs

PLGA/nHA/Gelatin FGBM was successfully prepared (Supplementary Figure S1). The surface morphology of FGBM was examined using environmental scanning electron microscopy (ESEM) and transmission electron microscopy (TEM). The SEM images indicated the porous interconnected fibrous structures of nanofiber layers (Figures 2A–H). The TEM observations showed that the PLGA/nHA/Gelatin fibers had a smooth and continuous appearance, as well as a uniform distribution of nHA particles without any discernible defects (Supplementary Figure S2A, B). The energy-dispersive X-ray (EDX) spectrum and elemental mapping image of PLGA/

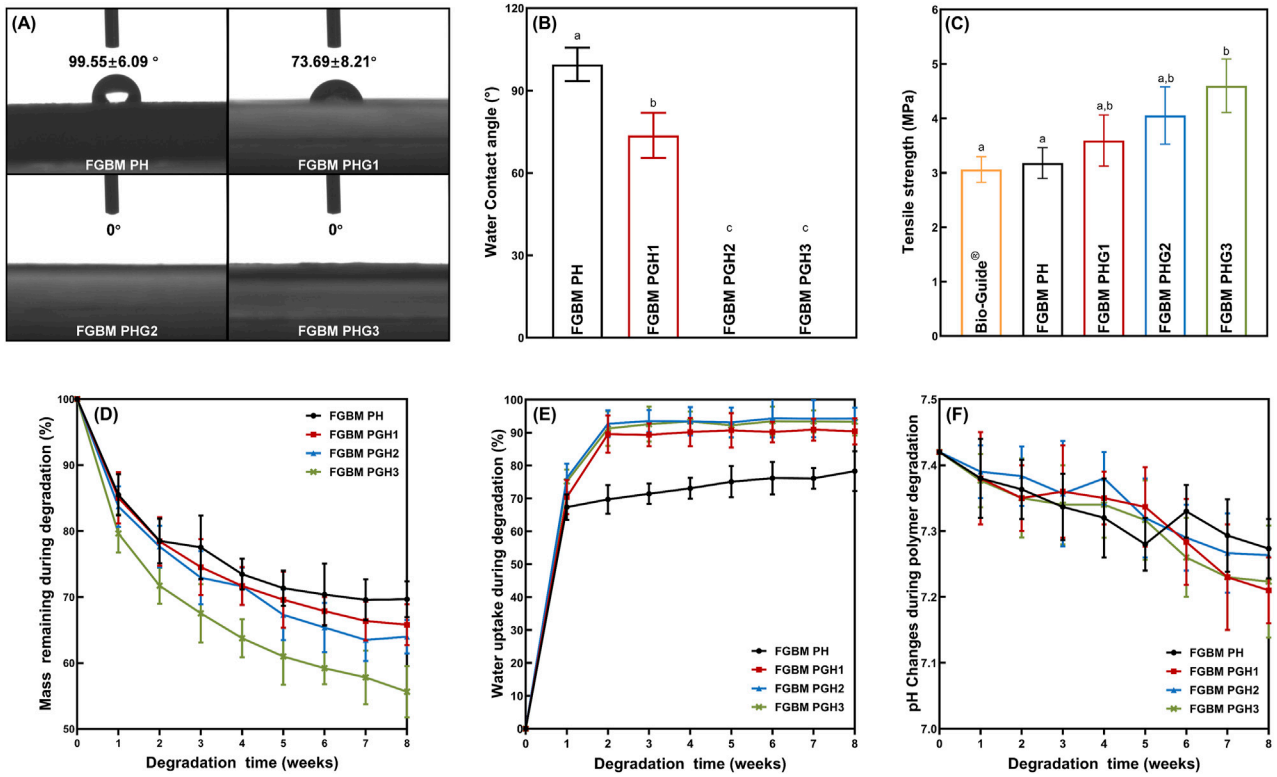

FIGURE 3
In vitro evaluation of physicochemical properties. **(A, B)** The water contact angle of the fiber surface of four groups of the FGBMs. **(C)** Means (Standard deviations) of tensile strength of Bio-Gide® (commercial control) and four groups of FGBM with different compositions. **(D)** Mass remaining during degradation (%) of the FGBMs with different compositions. **(E)** Water uptake during degradation (%) of the FGBMs with different compositions. **(F)** pH changes during polymer degradation of the FGBMs with different compositions. Different letters above the bar graph represent statistically significant differences among groups ($P < 0.05$).

nHA/Gelatin nanofiber layer displayed the proportion and distribution of phosphorus (P) and calcium (Ca), indicating the uniform dispersion of nHA on the FGBM (Supplementary Figure S2C). The fiber diameters for FGBM PH, FGBM PHG1, FGBM PHG2, and FGBM PHG3 were 1,145 ± 450 nm, 763 ± 267 nm, 653 ± 416 nm, and 922 ± 584 nm, respectively. Post gelatin incorporation, fiber diameters decreased compared to FGBM PH, subsequently increasing with higher gelatin proportions. nHA was evenly distributed on the fiber surface, forming protuberant structures locally due to nanoparticle aggregation, which increased with higher gelatin proportions. The individual phase inversion membrane (PIM) exhibited an asymmetric structure comprising a dense outer smooth surface and a porous inner rough surface (Figures 2I, J, S3).

Figures 2K, L illustrates the cross-sectional morphology of FGBM PHG3, resembling that of other FGBM. The cross-sectional thickness of FGBM measured approximately 600 μm, comprising a 100 μm phase inversion layer and a 500 μm nanofiber layer. In Figure 2K, both the dense layer and porous layer belonging to the phase inversion layer. The red curve depicted in Figure 2L indicates the interface between the phase inversion layer and the nanofiber layer, tightly bonded. The PLGA/nHA transition fiber layer bridged the phase inversion layer and electrospun fiber layer without obvious boundaries.

3.2 Contact angle analysis of FGBMs

The contact angle is a common index used to measure the hydrophilicity of materials. As depicted in Figures 3A,B, after incorporating gelatin into the fiber layer, water droplets spread out immediately upon contact with the fiber surface, and the water contact angle significantly reduced compared to that of the fiber without gelatin, reaching 0° ($P< 0.05$). With the increase in gelatin content, the water contact angle decreased noticeably. In the FGBM PHG2 and FGBM PHG3 groups, water droplets disappeared completely upon contact with the membranes, resulting in contact angles of 0° for both groups. These results were notably different from the FGBM PHG1 group.

3.3 Mechanical properties of FGBMs

FIGURE 3C illustrates the tensile strength of four types of PLGA/nHA/Gelatin FGBM and commercial collagen membranes. The tensile strength of the FGBM increased with the rise in gelatin content. FGBM PHG3 exhibited the highest tensile strength, measuring 4.60 Mpa, with statistically significant differences compared to FGBM PH (3.18 Mpa) and Bio-Gide® (3.06 Mpa) ($P< 0.05$). Conversely, no statistically significant differences were

10.3389/fphar.2024.1453036

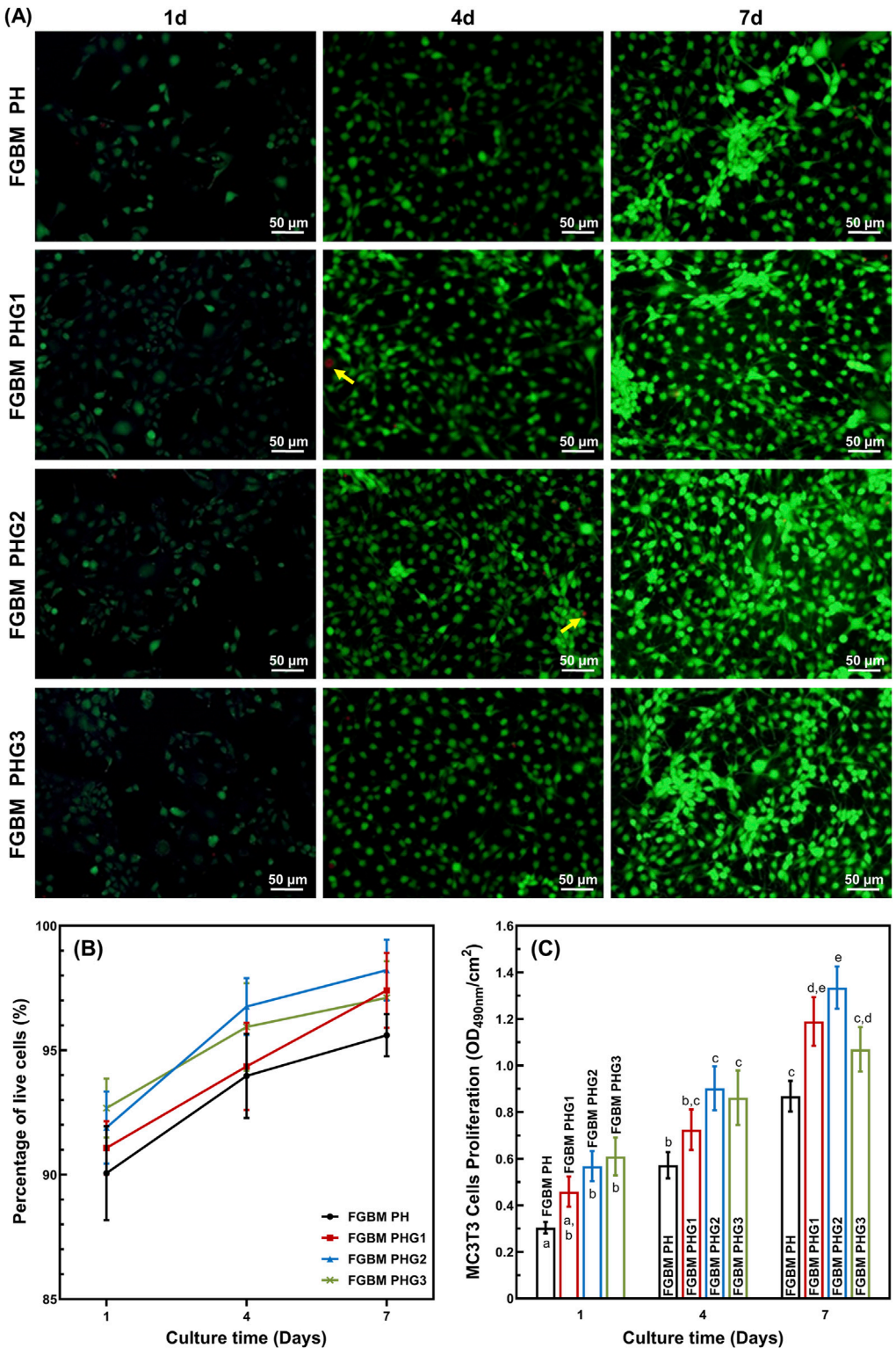

FIGURE 4
In vitro cellular proliferation activity of MC3T3-E1 cells on the electrospun fiber layers of the FGBMs. **(A)** Live/dead staining results of MC3T3-E1 cells of the four groups of FGBM at 1, 4 and 7 days. Green fluorescence is indicative of live cells, whereas red fluorescence (yellow arrows) is indicative of dead cells. **(B)** Percentage of live cells on the FGBM of the four groups. **(C)** Proliferative activity of MC3T3-E1 cells on FGBM of the four groups Different letters above the bar graph represent statistically significant differences among groups ($P < 0.05$).

observed between FGBM PHG1 (3.59 Mpa) and FGBM PHG2 (4.05 Mpa) ($P > 0.05$).

3.4 *In vitro* biodegradation of PLGA/nHA/gelatin FGBM

FIGURE 3D-F depicts the *in vitro* biodegradation results of four types of FGBM during the degradation period. The mass remaining increased at each time point, with FGBM PHG3 degrading the fastest (Figure 3D). By the 8th week, the mass of FGBM PHG3 had decreased by nearly half of its initial weight, yet the membrane morphology remained intact due to the support of the phase inversion layer. The performance and rate of water uptake of the gelatin-containing membranes increased significantly (Figure 3E). Within the first 2 weeks, the water uptake percentage of the membranes rapidly reached approximately 90%, followed by a gradual increase over the subsequent period. In contrast, the water uptake percentage of FGBM PH, the membrane without gelatin, was close to 70% at 2 weeks and increased slowly thereafter. The pH values of all four types of FGBM experienced a slight decrease at 8 weeks, yet they remained within the neutral range (Figure 3F).

3.5 *In vitro* barrier function of phase inversion membrane to L929 cells

The barrier effect of the PIM on L929 cells was evaluated *in vitro*. Supplementary Figure S4 illustrates the infiltration of L929 cells cultured on the smooth side (inside) of the phase inversion membrane to the other side of the membrane (outside). During the 1-day and 3-day incubation periods, the number of cells on the smooth side of the membrane increased, while only a minimal number of cells migrated into the medium under the membrane. This indicated that the PIM exhibited a superior barrier effect on L929 cells.

3.6 *In vitro* cell adhesion on the FGBM

The fluorescence micrographs of the early adhesion of MC3T3-E1 cells on the electrospun fiber layer of FGBM after cultured for 4 h are illustrated in Supplementary Figure S5A–D. Quantitative analysis of cell density (Supplementary Figure S5E) showed that the cells adhered on the surface of FGBM PHG2 and FGBM PHG3 were significantly more than the other two groups ($P < 0.05$), indicating that gelatin promoted the adhesion of osteoblasts on the membrane surface.

3.7 *In vitro* cell proliferation on the FGBM

The cell proliferation behavior of MC3T3-E1 cells on the electrospun fiber layer of FGBM are illustrated in Figure 4. Fluorescence micrographs of live and dead cell staining are presented in Figure 4A. Notably, the number of live cells (green fluorescence) increased significantly with prolonged culture time, with scattered dead cells (red fluorescence) observed. The percentages of live cells in all groups were consistently high, particularly in the FGBM groups containing gelatin. Cell viability increased with culture time. From 1 to 7 days during the culture period, the percentage of live cells in each group was higher than 90% with no statistical difference among the groups. Specifically, at 7 days, the number of live cells on FGBM PHG2 and FGBM PHG3 was significantly higher than that on FGBM PH and FGBM PHG1 (Figure 4B).

MTT assay of MC3T3-E1 cells was employed to evaluate cell viability. The results of the MTT assay indicated that cell viability of each group increased significantly during the culture period from the 1st to the 7th day (Figure 4C). At all time points during the culture period, the control group without gelatin incorporation was significantly lower than those of the other groups ($P < 0.05$). These findings suggest that PLGA/nHA/Gelatin composite fibers exhibit good cytocompatibility, and the introduction of gelatin can promote the proliferation of MC3T3-E1 cells.

3.8 *In vitro* cell differentiation on the FGBM

The effects of four types of FGBM on the differentiation of MC3T3-E1 cells are depicted in Figure 5. ALP is an early marker of osteoblast differentiation. Figure 5B shows the ALP activity measured after 1 and 14 days of MC3T3-E1 cell culture on PLGA/nHA/Gelatin FGBM. As observed, the ALP activity was at a similar level among the groups on the 1st day. After being cultured for 14 days, the ALP activity increased significantly ($P < 0.05$) in each group compared to the 1st day, indicating the excellent osteogenic effect of FGBM. During the culture period, with the increase of gelatin content, the ALP secretion increased at first and then decreased. Additionally, the ALP activity of the FGBM PHG2 group was significantly higher than that of the other three groups ($P < 0.05$).

For cytosolic mineral deposition of cells, ARS and the corresponding semi-quantitative method were used to assess the ability of four types of FGBM to induce osteogenic differentiation and mineral deposition. As shown in Figure 5A, there was an apparent deposition of calcium salt on all PLGA/nHA/Gelatin fibers at 14 days. Furthermore, the evaluation of calcium salt deposition confirmed the microscopic ARS staining results, with the FGBM PHG2 group exhibiting the highest cell mineral concentration, whereas the FGBM PHG3 group showed the lowest (Figure 5C).

3.9 Micro-computed tomography (Micro-CT) measurement

Micro-CT was employed to assess the impact of the prepared FGBM on bone defect regeneration. As shown in Figure 6A, at 4 and 8 weeks, the FGBM PHG2 group exhibited the greatest regenerated bone area. At 4 weeks, the FGBM PHG2 group exhibited a regenerated new bone volume of approximately 12%, which was significantly greater than that observed in the blank control and FGBM PH groups (Figure 6B). At 8 weeks, only a trace bone formation was observed at the edge of the defect area in the

10.3389/fphar.2024.1453036

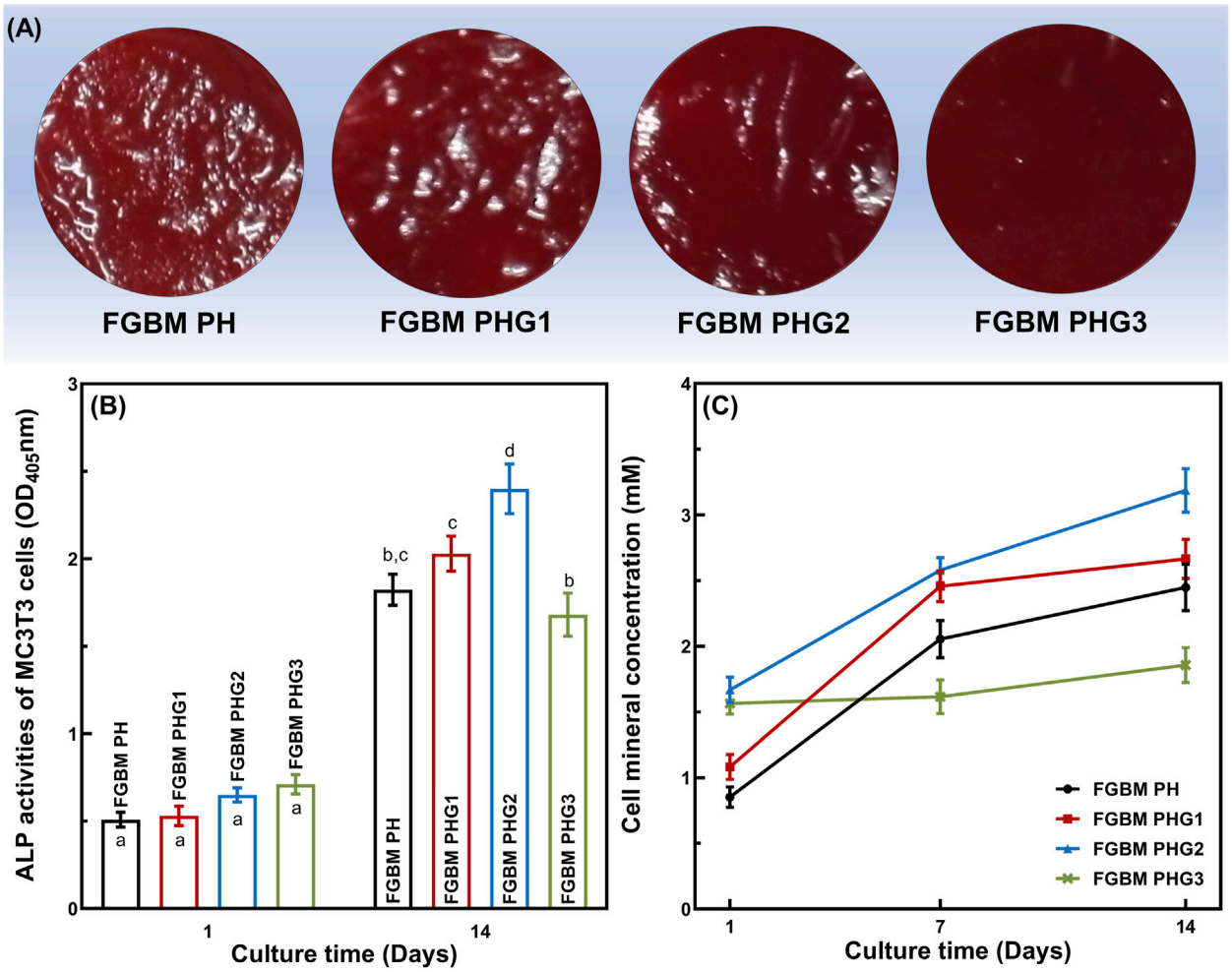

FIGURE 5
In vitro cellular differentiation activity of MC3T3-E1 cells on the electrospun fiber layer of the FGBMs. **(A)** The alizarin red S staining results of MC3T3-E1 cells at 14 days, respectively. **(B)** ALP activity of MC3T3-E1 cells on the FGBM at 1 and 14 days. **(C)** Quantitative analysis of cell mineral concentration of MC3T3-E1 cells on the FGBM of the four groups at 1, 7, and 14 days. Different letters above the bar graph represent statistically significant differences among groups ($P < 0.05$).

blank control group. When compared to the blank control group, the extent of the defect areas was significantly reduced in the three membrane-covered groups. Among the groups, the FGBM PHG2 group exhibited the highest bone volume of regenerated new bone, reaching nearly 30%. This value was significantly higher than that observed in the other groups ($P< 0.05$) (Figure 6C).

3.10 Histological observation

Histological images depicting the cranial defect area with H&E staining are illustrated in Figure 7. At the 4-week point (Figure 7A), the observation revealed the emergence of woven bone and fibrous connective tissue in the bone defect area across all groups. In the blank control group, limited new bone formation occurred at the defect area's edge, accompanied by a sparse distribution of osteoblasts. Complete infiltration of fibrous connective tissue was evident within the defect area. Notably, the FGBM PH group exhibited a visibly thicker membrane in the defect area compared to the FGBM PHG2 group. The PLGA/nHA/Gelatin FGBM was observed within a fibrous connective tissue cyst, maintaining its original morphology and providing a conducive environment for new bone formation. The osteoblasts surrounding the new bone and osteocytes scattered in the new bone matrix were observed in the membrane-covered groups. Notably, the FGBM PHG2 group displayed the highest number of osteoblasts and the largest volume of newly-formed unmineralized bone matrix, indicative of superior osteogenic performance.

Advancing to the 8-week point (Figure 7B), remnant membranes were still discernible in the defect areas of the FGBM PH and FGBM PHG2 groups, retaining much of their original morphology despite advanced degradation. In contrast, the Bio-Gide® group exhibited complete membrane degradation, with the defect area connected by fibrous connective tissue. Inflammatory cell infiltration around the FGBMs was notably less severe in the FGBM PHG2 group compared to the FGBM PH group. Relative to the 4-week assessment, a substantial increase in the volume of newly formed bone was evident in the membrane-covered groups.

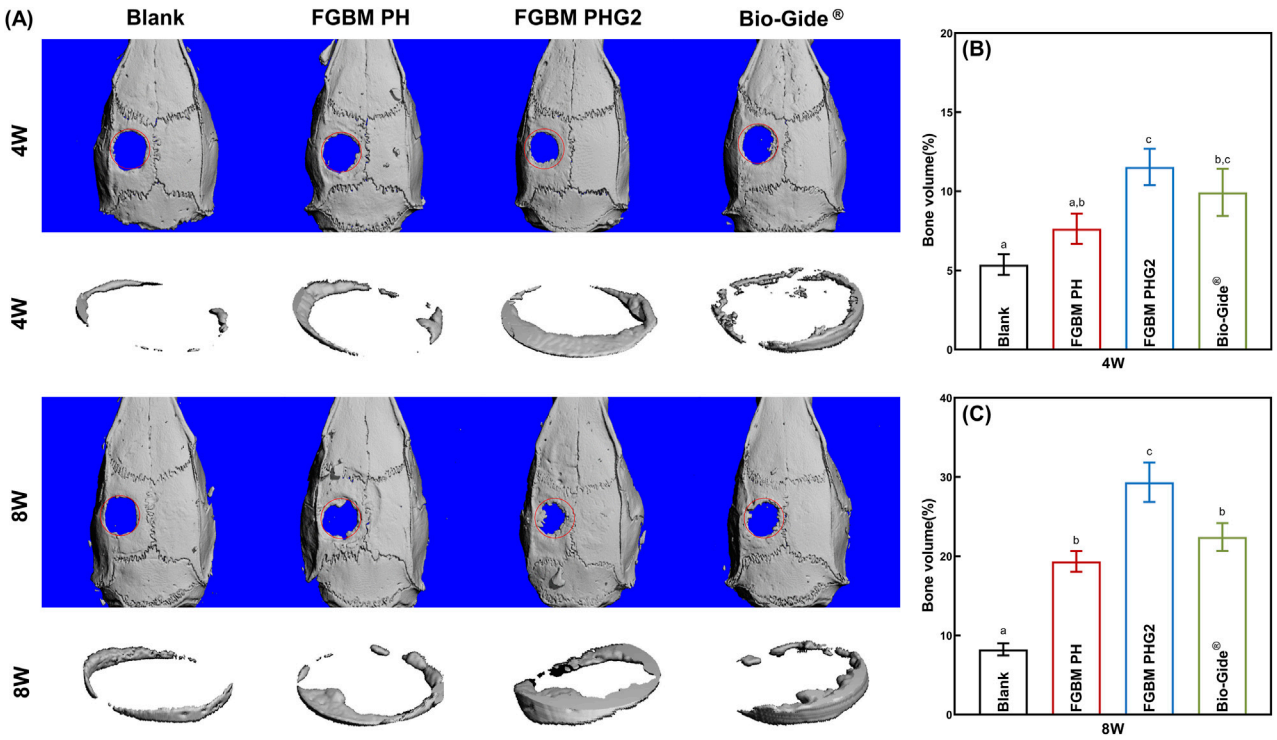

FIGURE 6
Micro-CT analysis of the bone defect areas after 4 and 8 weeks of implantation of FGBMs and commercial collagen membrane in rat cranial defect models. **(A)** Three-dimensional reconstructed images of micro-CT of the cranial defect area of rat models: new bone formation in the bone defect after 4–8-week implantation of the membranes. **(B)** The volume of bone regeneration in the defect area the of the rat models after 4-week implantation of the membranes. **(C)** The volume of bone regeneration in the defect area of the rat models after 8-week implantation of the membranes. Different letters above the bar graph represent statistically significant differences among groups ($P < 0.05$).

Conversely, the blank control group exhibited minimal change, with the defect area entirely connected by fibrous connective tissue. Within the FGBM PHG2 group, the newly formed bone appeared more mature, marked by the highest count of osteoblasts and the largest volume of newly-formed unmineralized bone matrix among the groups. Although the pace of advancement had decelerated compared to the earlier stage, it underscored a noteworthy and sustained osteogenic effect.

4 Discussion

4.1 Characterization and physicochemical properties

In this study, we successfully developed a functionally graded biomaterial membrane (FGBM) with excellent properties. Building upon the previously established bilayer structure consisting of a dense smooth phase inversion layer and a rough nanofiber layer, we incorporated a PLGA/nHA nanofiber layer into the FGBM structure to facilitate the transition between the PLGA/nHA phase inversion layer and the PLGA/nHA/Gelatin nanofiber layer, thereby promoting interlayer bonding. The incorporation of gelatin into scaffold materials can improve biocompatibility, and provide integrin-binding sites to promote cellular adhesion and proliferation (Fraioli et al., 2016). However, brittle texture, water solubility, and poor mechanical strength limit its use as a scaffold material alone (Zhang et al., 2020; Peng et al., 2021). In view of the complementary properties of polymers and gelatin, the electrospun PLGA/gelatin hybrid fibers had been widely investigated. It had been reported that electrospun fibers could be successfully prepared with PLGA/gelatin ratios of 9/1, 7/3, 5/5 and 3/7, etc. (Zheng et al., 2014; Gil-Castell et al., 2020). Nevertheless, whether the changes of PLGA/gelatin ratio have significant influence on bone tissue regeneration still lacks evidences. Based on previous studies, three different PLGA/gelatin ratios (7/3, 5/5, 3/7) were set up in this study to explore their effects on physicochemical properties and osteogenic properties of the membrane.

During synthesis, considering HFIP's low surface tension, low boiling point, and sufficiently high dielectric constant, it was selected as an ideal solvent for electrospinning (Pérez-Nava et al., 2022). However, the presence of fluorinated alcohols can induce phase separation between PLGA and gelatin, adversely affecting fiber morphology and the electrospinning process, and accelerating polymer degradation (Shalumon et al., 2010; Feng et al., 2012). Studies have shown that acetic acid effectively addresses phase separation issues in various polymer systems. The incorporation of acetic acid modulates the conductivity and volatility of the electrospinning solution, prevents phase separation, and simplifies the electrospinning process (Feng et al., 2012; Jing et al., 2014; Gil-Castell et al., 2018). Adding a 2‰ (volume/volume) concentration of acetic acid to the PLGA/Gelatin

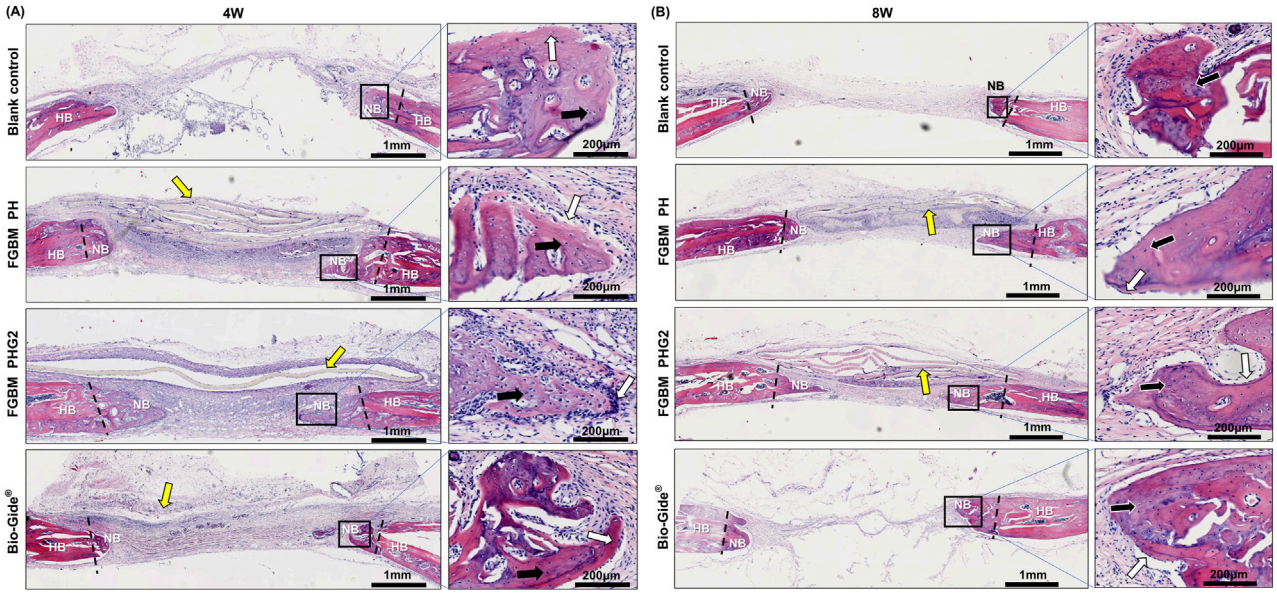

FIGURE 7
Representative H&E staining images of the bone defect areas after 4 and 8 weeks of implantation of FGBMs and commercial collagen membrane in rat cranial defect models. **(A, B)** H&E staining images of regenerated bone tissue after **(A)** 4-week and **(B)** 8-week implantation of the membranes. The periosteum side is on top, and the dura mater side is on the bottom (left part of **(A, B)**, scale bar = 1 mm), respectively. The black rectangle areas were magnified on the right (right part of **(A, B)**, scale bar = 200 μm), respectively. The boundary between the new bone and the host bone is marked by black dotted lines, the yellow arrows indicate the undegraded membranes, the white arrows indicate the osteoblasts, and the black arrows indicate the osteocytes. (HB: host bone, NB: new bone).

electrospinning solution rapidly transformed the opaque solution into a transparent and uniform state. Moreover, acetic acid volatilized quickly during the electrospinning process, preserving the composition, structure, and properties of the nanofiber layer (Li et al., 2016).

Subsequent SEM and TEM observations revealed excellent surface morphology and structure of the phase inversion layer and electrospun nanofiber layer of PLGA/nHA/Gelatin FGBM. The phase inversion layer exhibited an asymmetric surface structure with one smooth and dense side and one rough and porous side. The rough surface allowed for the formation of stable bonds during subsequent electrostatic spinning on it. The nanofiber layer structure closely resembled the osteoblastic extracellular matrix (ECM), providing a favorable microenvironment for osteoblast growth. According to our observations, an increase in fiber diameter with higher gelatin content. Previous studies have reported that higher gelatin content leads to increased fiber diameter, primarily due to changes in the properties of the electrospinning solution, such as shear viscosity, surface tension, and conductivity (Howard et al., 2023). An appropriate ratio of PLGA/nHA/Gelatin electrospinning solution improved viscosity and conductivity, facilitating the formation of smooth and homogeneous nanoscale fibers.

The hydrophilic properties of biomaterial surfaces significantly influence cell adhesion, with water contact angle being a crucial indicator of surface physicochemical properties. Incorporating gelatin into the electrospun fiber layer transitions the surface from hydrophobic to hydrophilic, attributed to the microstructure of the composite fiber and the hydrophilic polar groups on the gelatin molecular chain (Ravichandran et al., 2011; Feng et al., 2012; Pozzobon et al., 2021). Although hydrophilicity improved, the water contact angle of FGBM PHG1 remained significantly higher than that of FGBM PHG2 and FGBM PHG3, indicating that most gelatin components were embedded in the continuous phase of PLGA. Increased gelatin content led to the appearance of bicontinuous phases between gelatin and PLGA, facilitating water penetration through micro-pores. Additionally, hydrogen bonding between gelatin and HFIP, along with the volatilization of HFIP during the electrospinning process, caused the migration of gelatin polar groups to the fiber surface, significantly enhancing membrane hydrophilicity, cell adhesion, and metabolic substance exchange.

Adequate tensile strength is essential for an ideal GBRM to maintain sufficient space for bone regeneration. The mechanical test results revealed a significant increase in the tensile strength of all FGBM PHG groups compared to the others, attributed to the synthesis process. To enhance interlayer bonding in FGBM, a PLGA/nHA electrospun nanofiber layer was incorporated as a transition between the phase inversion layer and the PLGA/nHA/Gelatin nanofiber layer. Due to their similar composition, the PLGA/nHA electrospun nanofiber is tightly coupled with the rough surface of the phase inversion layer (Fu et al., 2017). Furthermore, the PLGA/nHA nanofiber layer and the PLGA/nHA/Gelatin nanofiber layer share the same fiber structure, with the fibers overlapping and interweaving to form a strong bond. Additionally, we crosslinked the membrane with glutaraldehyde steam to improve the biological stability of the materials. Our study aligns with previous findings suggesting that increasing gelatin content initially enhances the tensile strength of fiber scaffolds, with a subsequent decrease. This correlation is consistent with

studies such as Lee et al. (Lee et al., 2008). We suspect that this effect is mainly related to the cross-linking of fibers, where the formation of cross-linked networks between the gelatin molecular chains after cross-linking increases intermolecular forces, enhancing the tensile strength.

4.2 *In vitro* biodegradation properties

As a potential resorbable GBRM, it is necessary to consider the degradation performance of FGBM, as it directly impacts the barrier function and spatial maintenance capacity of the membrane. The degradation evaluation results of this study demonstrated an accelerated membrane degradation with an increase in gelatin content. With the increased proportion of gelatin, it became more exposed to the fiber surface. Despite cross-linking, a significant amount of dissolution occurred within 1 week of degradation due to the inherent hydrophilicity of gelatin. If the FGBM were implanted in the body, gelatin would degrade faster in the presence of macrophages, free radicals, and enzymes accumulate (Tracy et al., 1999). However, in this study, the FGBM remained intact for 8 weeks because of the support of the phase inversion layer. Although the electrospun fiber layer degraded rapidly, the FGBM could still provide sufficient time and space for the regeneration of bone tissue. Regarding the persistence of the *in vitro* degradation period of the phase inversion layer, this observation may be attributed to the specific ratio (75/25) of lactic and glycolic acids in PLGA, as well as the incorporation of nHA (Díaz et al., 2017). The water uptake performance and rate of the membranes with gelatin-containing increased significantly, indicating that the incorporation of gelatin would facilitate the cellular affinity of the membranes *in vivo*.

4.3 *In vitro* cells behaviors

The biocompatibility is significant for implantable biomaterials. In this study, osteoblast cells demonstrated enhanced adhesion and proliferation activities on gelatin-rich membranes, while the fibroblasts were effectively blocked from the outside of phase inversion layer. The gradual increase in cells and good cellular activity observed in each group throughout the culture period indicated that the FGBMs were cytocompatible. The early adhesion behavior of MC3T3-E1 cells on FGBM PHG2 and FGBM PHG3 nanofiber layers was notably more active. This was believed to be related to the higher hydrophilicity of FGBM PHG2 and FGBM PHG3, which was derived from gelatin, allowing osteoblasts to spread more easily on the surface of the nanofiber layers. Furthermore, the RGD peptide chains presented in gelatin could be recognized by integral protein receptors on cells. The polar groups on gelatin enhanced their interaction with negatively charged cells, thereby playing a role in the targeting of cells during the early adhesion and proliferation processes (Fraioli et al., 2016; Cai et al., 2020). However, compared to the other groups, the proliferation viability of cells in the FGBM PHG3 group exhibited a decline at 7 days. This decline could be attributed to the rapid degradation of gelatin, the principal component of the FGBM PHG3 membrane, and the disruption of the fibrous structure under cell culture conditions. It is essential to acknowledge potential challenges, such as the cytotoxicity of calcium phosphate particles, especially at the nanoscale to submicron scale, as the nHA particles in FGBM PHG2 were uniformly dispersed and increased fiber roughness (Sun et al., 1998; Chen et al., 2019). Further investigation into potential cytotoxic effects is therefore warranted. In contrast, the FGBM PHG2 group exhibited the highest cellular activity during the culture period, indicating that the PLGA and gelatin formed a double continuous phase interwoven structure. The hydrophobic interaction between PLGA and gelatin limited a significant amount of gelatin leaching. Even with gelatin degradation, the continuous PLGA phase was able to maintain the fiber structure stability. Furthermore, it had been demonstrated that fiber diameter influences cell adhesion, proliferation, and differentiation to some extent. The smaller the diameter of the fibers, the more cells adhered and the more spread out the cell morphology (Tian et al., 2008; Christopherson et al., 2009). The fibers with the smallest diameter were observed in FGBM PHG2, which might also contribute to their highest cell viability.

ALP is an extracellular enzyme secreted by osteoblasts and serves as a key marker of osteoblast differentiation (Li et al., 2019; Liu et al., 2021). In this study, the relevance between ALP activity and gelatin proportions was demonstrated through measurements taken at 1 and 14 days of MC3T3-E1 cell culture. Notably, the FGBM PHG2 group exhibited the highest ALP activity, whereas the FGBM PHG3 group demonstrated the lowest activity. Consistent findings were observed in ARS staining, confirming variations in cell mineral concentration between these two groups. The findings in the FGBM PHG3 group suggest that the degradation of gelatin and the lysis of nHA contributed to damage in the structure and composition of the electrospun fiber layer. This, in turn, led to a reduction in the number of cells and a decrease in the differentiation activity of individual cells. These insights underscore the importance of maintaining the stability of the fibrous structure for optimal osteogenic differentiation.

4.4 *In vivo* osteogenesis assessments

The *in vitro* assessments of FGBM revealed favorable mechanical properties, an appropriate biodegradation rate, and satisfactory *in vitro* biocompatibility and osteogenic ability. The FGBM PHG2 group demonstrated optimal overall *in vitro* performance, particularly in terms of osteogenic ability. Therefore, the FGBM PHG2 group was chosen as the test group to evaluate its bone regenerative ability and tissue compatibility *in vivo*. The commercial collagen membrane, Bio-Gide®, is a representative example and has been widely used in clinical practice (Zhang et al., 2019). Micro-CT assessments demonstrated that the FGBM PHG2 group significantly enhanced bone regeneration compared to the FGBM PH group and the commercial product (Bio-Gide®). Specifically, the FGBM PHG2 group had the highest bone volume of regenerated new bone (nearly 30%) to quantify the observed improvements in bone regeneration. A histological assessment of the bone defect

area was performed to further investigate the mechanism by which FGBM PHG2 regenerated a significant amount of bone. Histological assessments, conducted through H&E staining, revealed that the *in vivo* degradation rate of FGBM was notably slower compared to Bio-Gide®. Although partial degradation was observed, FGBMs retained their original morphology even after 8 weeks of implantation, suggesting the robustness of the phase inversion layer in maintaining mechanical properties *in vivo*. The adequate tensile strength and cellular barrier function of the phase inversion layer of FGBM PHG2 prevented fibroblasts on the soft tissue side from growing into the bone defect area, and the reasonable degradation rate of FGBM created a protective environment for bone tissue regeneration. The selection of an optimal gelatin content was a critical determinant in achieving the observed positive outcomes. This nuanced choice significantly contributed to the overall success of FGBM PHG2. The relatively rapid degradation of PLGA/nHA/Gel FGBM with this specific gelatin content accelerated the release of nHA particles, thereby promoting further *in vivo* osteogenic mineralization (Wang et al., 2023). This nuanced choice in composition contributed significantly to the overall success of FGBM PHG2. Calcium ions in the degraded and released nHA particles exchanged with carboxylic acids in PLGA and gelatin, maintaining the stability of the osteogenic microenvironment and reducing the inflammatory response (Li et al., 2014). Meanwhile, the degradation-induced exposure of the intrinsic RGD peptide chain on gelatin played a pivotal role in facilitating osteogenesis. This exposure, by promoting the adhesion and proliferation of integrin-mediated osteoblast-related cells and inducing extracellular matrix (ECM) mineralization, significantly contributed to the observed positive outcomes in osteogenesis (Hsiong et al., 2009; Amjadian et al., 2016; Cai et al., 2020). Amino acids, the degradation product of gelatin, provided cellular nutrients for the local osteogenic microenvironment and facilitated osteoblast proliferation (Gu et al., 2018). The findings indicated that the FGBM PHG2 group exhibited a faster rate and greater efficacy in promoting *in vivo* osteogenesis in comparison to the FGBM PH group. This was evidenced by the FGBM PHG2 group exhibiting the largest number of osteoblasts and the largest volume of the newly-formed unmineralized bone matrix. Local inflammation in the defect area was reduced in the FGBM PHG2 group compared to the FGBM PH group. This is likely due to the incorporation of gelatin, which improves the hydrophilicity and *in vivo* biocompatibility of the FGBM. Overall, the FGBM PHG2 demonstrated excellent comprehensive performance *in vitro* and *in vivo*.

5 Conclusion

This study developed a novel PLGA/nHA/Gelatin functionally graded bilayer membrane through the integration of phase inversion and electrospinning methods. The investigation focused on assessing its physicochemical and biological properties and examining its impact on osteogenesis and tissue compatibility in an animal model. Results revealed that the addition of gelatin did not affect the electrospinning performance of the solution. Moreover, the resulting electrospun fiber layer tightly integrated with the phase inversion layer, displaying enhanced hydrophilic, mechanical, and biodegradation properties.

The PLGA/nHA/Gelatin FGBM with an asymmetric structure exhibited excellent tissue barrier function due to the presence of the smooth phase inversion layer. Furthermore, the nanofiber layer effectively mimicked the extracellular matrix of natural osteoblasts, which facilitated osteoblast proliferation and differentiation. Particularly, the PLGA/nHA/Gelatin FGBM with a PLGA/Gelatin mass ratio of 1:1 (FGBM PHG2) exhibited optimal osteoconductive and osteoinductive activities both *in vitro* and *in vivo*. These findings suggest its potential application in bone regeneration treatments.

Data availability statement

The raw data supporting the conclusions of this article will be made available by the authors, without undue reservation.

Ethics statement

The animal study was approved by the Animal Experimentation Ethics Committee of the Stomatology School of Jilin University. The study was conducted in accordance with the local legislation and institutional requirements.

Author contributions

JL: Writing–review and editing, Writing–original draft, Methodology, Investigation, Formal Analysis, Data curation, Conceptualization. JD: Writing–review and editing, Validation, Methodology, Investigation, Data curation. TZ: Writing–review and editing, Validation, Methodology, Investigation, Data curation. BL: Writing–review and editing, Resources, Data curation. JW: Writing–review and editing, Methodology, Investigation. HW: Formal Analysis, Writing–review and editing, Writing–original draft, Project administration, Investigation, Data curation. LF: Resources, Writing–review and editing, Writing–original draft, Project administration, Methodology, Investigation, Data curation, Conceptualization.

Funding

The authors declare that financial support was received for the research, authorship, and/or publication of this article. This work was supported by Scientific Research Projects for Oral Implantology of China Oral Health Foundation (COHF ZZZX202401).

Acknowledgments

Figure 1 was modified from Servier Medical Art (http://smart.servier.com/), licensed under a Creative Common Attribution 4.0 unported License (https://creativecommons.org/licenses/by/4.0/).

Conflict of interest

The authors declare that the research was conducted in the absence of any commercial or financial relationships that could be construed as a potential conflict of interest.

Publisher's note

All claims expressed in this article are solely those of the authors and do not necessarily represent those of their affiliated organizations, or those of the publisher, the editors and the reviewers. Any product that may be evaluated in this article, or claim that may be made by its manufacturer, is not guaranteed or endorsed by the publisher.

Supplementary material

The Supplementary Material for this article can be found online at: https://www.frontiersin.org/articles/10.3389/fphar.2024.1453036/full#supplementary-material

References

Abe, G. L., Sasaki, J.-I., Katata, C., Kohno, T., Tsuboi, R., Kitagawa, H., et al. (2020). Fabrication of novel poly(lactic acid/caprolactone) bilayer membrane for GBR application. *Dent. Mater.* 36 (5), 626–634. doi:10.1016/j.dental.2020.03.013

Aldana, A. A., and Abraham, G. A. (2017). Current advances in electrospun gelatin-based scaffolds for tissue engineering applications. *Int. J. Pharm.* 523 (2), 441–453. doi:10.1016/j.ijpharm.2016.09.044

Amjadian, S., Seyedjafari, E., Zeynali, B., and Shabani, I. (2016). The synergistic effect of nano-hydroxyapatite and dexamethasone in the fibrous delivery system of gelatin and poly(l-lactide) on the osteogenesis of mesenchymal stem cells. *Int. J. Pharm.* 507 (1), 1–11. doi:10.1016/j.ijpharm.2016.04.032

Bee, S.-L., and Hamid, Z. A. A. (2022). Asymmetric resorbable-based dental barrier membrane for periodontal guided tissue regeneration and guided bone regeneration: a review. *J. Biomed. Mater. Res. Part B Appl. Biomaterials* 110 (9), 2157–2182. doi:10.1002/jbm.b.35060

Buser, D., Urban, I., Monje, A., Kunrath, M. F., and Dahlin, C. (2023). Guided bone regeneration in implant dentistry: basic principle, progress over 35 years, and recent research activities. *Periodontol 2000* 93 (1), 9–25. doi:10.1111/prd.12539

Cai, S., Wu, C., Yang, W., Liang, W., Yu, H., and Liu, L. (2020). Recent advance in surface modification for regulating cell adhesion and behaviors. *Nanotechnol. Rev.* 9 (1), 971–989. doi:10.1515/ntrev-2020-0076

Chen, F., Wang, M., Wang, J., Chen, X., Li, X., Xiao, Y., et al. (2019). Effects of hydroxyapatite surface nano/micro-structure on osteoclast formation and activity. *J. Mater. Chem. B* 7 (47), 7574–7587. doi:10.1039/C9TB01204D

Christopherson, G. T., Song, H., and Mao, H.-Q. (2009). The influence of fiber diameter of electrospun substrates on neural stem cell differentiation and proliferation. *Biomaterials* 30 (4), 556–564. doi:10.1016/j.biomaterials.2008.10.004

Dahlin, C., Linde, A., Gottlow, J., and Nyman, S. (1988). Healing of bone defects by guided tissue regeneration. *Plast. Reconstr. Surg.* 81 (5), 672–676. doi:10.1097/00006534-198805000-00004

Díaz, E., Puerto, I., Ribeiro, S., Lanceros-Mendez, S., and Barandiarán, J. M. (2017). The influence of copolymer composition on PLGA/nHA scaffolds' cytotoxicity and *in vitro* degradation. *Nanomaterials* 7 (7), 173. doi:10.3390/nano7070173

Elgali, I., Omar, O., Dahlin, C., and Thomsen, P. (2017). Guided bone regeneration: materials and biological mechanisms revisited. *Eur. J. Oral Sci.* 125 (5), 315–337. doi:10.1111/eos.12364

Feng, B., Tu, H., Yuan, H., Peng, H., and Zhang, Y. (2012). Acetic-acid-mediated miscibility toward electrospinning homogeneous composite nanofibers of GT/PCL. *Biomacromolecules* 13 (12), 3917–3925. doi:10.1021/bm3009389

Fraioli, R., Dashnyam, K., Kim, J.-H., Perez, R. A., Kim, H.-W., Gil, J., et al. (2016). Surface guidance of stem cell behavior: chemically tailored co-presentation of integrin-binding peptides stimulates osteogenic differentiation *in vitro* and bone formation *in vivo*. *Acta Biomater.* 43, 269–281. doi:10.1016/j.actbio.2016.07.049

Fu, L., Wang, Z., Dong, S., Cai, Y., Ni, Y., Zhang, T., et al. (2017). Bilayer poly(lactic-co-glycolic acid)/nano-hydroxyapatite membrane with barrier function and osteogenesis promotion for guided bone regeneration. *Mater. (Basel)* 10 (3), 257. doi:10.3390/ma10030257

Gautam, S., Sharma, C., Purohit, S. D., Singh, H., Dinda, A. K., Potdar, P. D., et al. (2021). Gelatin-polycaprolactone-nanohydroxyapatite electrospun nanocomposite scaffold for bone tissue engineering. *Mater. Sci. Eng. C* 119, 111588. doi:10.1016/j.msec.2020.111588

Gil-Castell, O., Badia, J. D., Ontoria-Oviedo, I., Castellano, D., Sepúlveda, P., and Ribes-Greus, A. (2020). Polycaprolactone/gelatin-based scaffolds with tailored performance: *in vitro* and *in vivo* validation. *Mater. Sci. Eng. C* 107, 110296. doi:10.1016/j.msec.2019.110296

Gil-Castell, O., Badia, J. D., and Ribes-Greus, A. (2018). Tailored electrospun nanofibrous polycaprolactone/gelatin scaffolds into an acid hydrolytic solvent system. *Eur. Polym. J.* 101, 273–281. doi:10.1016/j.eurpolymj.2018.02.030

Gu, Y., Bai, Y., and Zhang, D. (2018). Osteogenic stimulation of human dental pulp stem cells with a novel gelatin-hydroxyapatite-tricalcium phosphate scaffold. *J. Biomed. Mater. Res. Part A* 106 (7), 1851–1861. doi:10.1002/jbm.a.36388

Howard, C. J., Paul, A., Duruanyanwu, J., Sackho, K., Campagnolo, P., and Stolojan, V. (2023). The manufacturing conditions for the direct and reproducible formation of electrospun PCL/gelatine 3D structures for tissue regeneration. *Nanomaterials* 13 (24), 3107. doi:10.3390/nano13243107

Hsiong, S. X., Boontheekul, T., Huebsch, N., and Mooney, D. J. (2009). Cyclic arginine-glycine-aspartate peptides enhance three-dimensional stem cell osteogenic differentiation. *Tissue Eng. Part A* 15 (2), 263–272. doi:10.1089/ten.tea.2007.0411

Ji, W., Yang, F., Seyednejad, H., Chen, Z., Hennink, W. E., Anderson, J. M., et al. (2012). Biocompatibility and degradation characteristics of PLGA-based electrospun nanofibrous scaffolds with nanoapatite incorporation. *Biomaterials* 33 (28), 6604–6614. doi:10.1016/j.biomaterials.2012.06.018

Jin, S., Sun, F., Zou, Q., Huang, J., Zuo, Y., Li, Y., et al. (2019). Fish collagen and hydroxyapatite reinforced poly(lactide-co-glycolide) fibrous membrane for guided bone regeneration. *Biomacromolecules* 20 (5), 2058–2067. doi:10.1021/acs.biomac.9b00267

Jin, S., Xia, X., Huang, J., Yuan, C., Zuo, Y., Li, Y., et al. (2021). Recent advances in PLGA-based biomaterials for bone tissue regeneration. *Acta Biomater.* 127, 56–79. doi:10.1016/j.actbio.2021.03.067

Jing, X., Salick, M. R., Cordie, T., Mi, H.-Y., Peng, X.-F., and Turng, L.-S. (2014). Electrospinning homogeneous nanofibrous poly(propylene carbonate)/gelatin composite scaffolds for tissue engineering. *Industrial and Eng. Chem. Res.* 53 (22), 9391–9400. doi:10.1021/ie500762z

Lee, J., Tae, G., Kim, Y. H., Park, I. S., Kim, S.-H., and Kim, S. H. (2008). The effect of gelatin incorporation into electrospun poly(l-lactide-co-ε-caprolactone) fibers on mechanical properties and cytocompatibility. *Biomaterials* 29 (12), 1872–1879. doi:10.1016/j.biomaterials.2007.12.029

Li, D., Chen, W., Sun, B., Li, H., Wu, T., Ke, Q., et al. (2016). A comparison of nanoscale and multiscale PCL/gelatin scaffolds prepared by disc-electrospinning. *Colloids Surf. B Biointerfaces* 146, 632–641. doi:10.1016/j.colsurfb.2016.07.009

Li, D., Sun, H., Jiang, L., Zhang, K., Liu, W., Zhu, Y., et al. (2014). Enhanced biocompatibility of PLGA nanofibers with gelatin/nano-hydroxyapatite bone biomimetics incorporation. *ACS Appl. Mater. and Interfaces* 6 (12), 9402–9410. doi:10.1021/am5017792

Li, N., Zhou, L., Xie, W., Zeng, D., Cai, D., Wang, H., et al. (2019). Alkaline phosphatase enzyme-induced biomineralization of chitosan scaffolds with enhanced osteogenesis for bone tissue engineering. *Chem. Eng. J.* 371, 618–630. doi:10.1016/j.cej.2019.04.017

Li, P., Li, Y., Kwok, T., Yang, T., Liu, C., Li, W., et al. (2021). A bi-layered membrane with micro-nano bioactive glass for guided bone regeneration. *Colloids Surfaces B Biointerfaces* 205, 111886. doi:10.1016/j.colsurfb.2021.111886

Lian, M., Han, Y., Sun, B., Xu, L., Wang, X., Ni, B., et al. (2020). A multifunctional electrowritten bi-layered scaffold for guided bone regeneration. *Acta Biomater.* 118, 83–99. doi:10.1016/j.actbio.2020.08.017

Lian, M., Sun, B., Qiao, Z., Zhao, K., Zhou, X., Zhang, Q., et al. (2019). Bi-layered electrospun nanofibrous membrane with osteogenic and antibacterial properties for guided bone regeneration. *Colloids Surfaces B Biointerfaces* 176, 219–229. doi:10.1016/j.colsurfb.2018.12.071

Lin, X., Patil, S., Gao, Y.-G., and Qian, A. (2020). The bone extracellular matrix in bone formation and regeneration. *Front. Pharmacol.* 11, 757. doi:10.3389/fphar.2020.00757

Liu, W., Dong, X., Qin, H., Sui, L., and Wang, J. (2021). Three-dimensional porous reduced graphene oxide/hydroxyapatite membrane for guided bone regeneration. *Colloids Surfaces B Biointerfaces* 208, 112102. doi:10.1016/j.colsurfb.2021.112102

Liu, Y., and Li, W. (2019). Nature-Inspired multifunctional bilayer architecture advances bone defect repair. *Chem* 5 (10), 2515–2517. doi:10.1016/j.chempr.2019.09.004

Mizraji, G., Davidzohn, A., Gursoy, M., Gursoy, U. K., Shapira, L., and Wilensky, A. (2023). Membrane barriers for guided bone regeneration: an overview of available biomaterials. *Periodontol 2000* 93 (1), 56–76. doi:10.1111/prd.12502

Naenni, N., Stucki, L., Hüsler, J., Schneider, D., Hämmerle, C. H. F., Jung, R. E., et al. (2021). Implants sites with concomitant bone regeneration using a resorbable or non-resorbable membrane result in stable marginal bone levels and similar profilometric outcomes over 5 years. *Clin. Oral Implants Res.* 32 (8), 893–904. doi:10.1111/clr.13764

Nahid, R., Bansal, M., and Pandey, S. (2022). Horizontal bone augmentation using two membranes at dehisced implant sites: a randomized clinical study. *J. Oral Biol. Craniofacial Res.* 12 (5), 487–491. doi:10.1016/j.jobcr.2022.06.003

Naik, A., Shepherd, D. V., Shepherd, J. H., Best, S. M., and Cameron, R. E. (2017). The effect of the type of HA on the degradation of PLGA/HA composites. *Mater. Sci. Eng. C* 70, 824–831. doi:10.1016/j.msec.2016.09.048

Omar, O., Elgali, I., Dahlin, C., and Thomsen, P. (2019). Barrier membranes: more than the barrier effect? *J. Clin. Periodontology* 46 (S21), 103–123. doi:10.1111/jcpe.13068

Patil, S., Bhandi, S., Bakri, M. M. H., Albar, D. H., Alzahrani, K. J., Al-Ghamdi, M. S., et al. (2023). Evaluation of efficacy of non-resorbable membranes compared to resorbable membranes in patients undergoing guided bone regeneration. *Heliyon* 9 (3), e13488. doi:10.1016/j.heliyon.2023.e13488

Peng, T., Zhu, J., Huang, T., Jiang, C., Zhao, F., Ge, S., et al. (2021). Facile preparation for gelatin/hydroxyethyl 2 composite aerogel with good mechanical strength, heat insulation, and water resistance. *J. Appl. Polym. Sci.* 138 (23), 50539. doi:10.1002/app.50539

Pérez-Nava, A., Reyes-Mercado, E., and González-Campos, J. B. (2022). Production of chitosan nanofibers using the HFIP/acetic acid mixture as electrospinning solvent. *Chem. Eng. Process. - Process Intensif.* 173, 108849. doi:10.1016/j.cep.2022.108849

Pozzobon, L. G., Sperling, L. E., Teixeira, C. E., Malysz, T., and Pranke, P. (2021). Development of a conduit of PLGA-gelatin aligned nanofibers produced by electrospinning for peripheral nerve regeneration. *Chemico-Biological Interact.* 348, 109621. doi:10.1016/j.cbi.2021.109621

Qin, X., Pan, H., Yang, K., Xie, W., Yang, G., and Wang, J. (2023). Biodegradable and biocompatible alginate/gelatin/MXene composite membrane with efficient osteogenic activity and its application in guided bone regeneration. *J. Biomaterials Sci.* 34, 1843–1857. doi:10.1080/09205063.2023.2187987

Ravichandran, R., Ng, C. C. H., Liao, S., Pliszka, D., Raghunath, M., Ramakrishna, S., et al. (2011). Biomimetic surface modification of titanium surfaces for early cell capture by advanced electrospinning. *Biomed. Mater.* 7 (1), 015001. doi:10.1088/1748-6041/7/1/015001

Retzepi, M., and Donos, N. (2010). Guided Bone Regeneration: biological principle and therapeutic applications. *Clin. Oral Implants Res.* 21 (6), 567–576. doi:10.1111/j.1600-0501.2010.01922.x

Rider, P., Kačarević, Ž. P., Elad, A., Tadic, D., Rothamel, D., Sauer, G., et al. (2022). Biodegradable magnesium barrier membrane used for guided bone regeneration in dental surgery. *Bioact. Mater.* 14, 152–168. doi:10.1016/j.bioactmat.2021.11.018

Salhotra, A., Shah, H. N., Levi, B., and Longaker, M. T. (2020). Mechanisms of bone development and repair. *Nat. Rev. Mol. Cell Biol.* 21 (11), 696–711. doi:10.1038/s41580-020-00279-w

Shah, A. T., Zahid, S., Ikram, F., Maqbool, M., Chaudhry, A. A., Rahim, M. I., et al. (2019). Tri-layered functionally graded membrane for potential application in periodontal regeneration. *Mater. Sci. Eng. C* 103, 109812. doi:10.1016/j.msec.2019.109812

Shalumon, K. T., Anulekha, K. H., Girish, C. M., Prasanth, R., Nair, S. V., and Jayakumar, R. (2010). Single step electrospinning of chitosan/poly(caprolactone) nanofibers using formic acid/acetone solvent mixture. *Carbohydr. Polym.* 80 (2), 413–419. doi:10.1016/j.carbpol.2009.11.039

Sheikh, Z., Qureshi, J., Alshahrani, A. M., Nassar, H., Ikeda, Y., Glogauer, M., et al. (2017). Collagen based barrier membranes for periodontal guided bone regeneration applications. *Odontology* 105 (1), 1–12. doi:10.1007/s10266-016-0267-0

Shi, J.-Y., Montero, E., Wu, X.-Y., Palombo, D., Wei, S.-M., and Sanz-Sánchez, I. (2022). Bone preservation or augmentation simultaneous with or prior to dental implant placement: a systematic review of outcomes and outcome measures used in clinical trials in the last 10 years. *Clin. Oral Implants Res.* 34 (S25), 68–83. doi:10.1111/clr.13953

Sun, J.-S., Liu, H.-C., Hong-Shong Chang, W., Li, J., Lin, F.-H., and Tai, H.-C. (1998). Influence of hydroxyapatite particle size on bone cell activities: an *in vitro* study. *J. Biomed. Mater. Res.* 39 (3), 390–397. doi:10.1002/(SICI)1097-4636(19980305)39:3<390::AID-JBM7>3.0.CO;2-E

Testori, T., Weinstein, T., Scutellà, F., Wang, H. L., and Zucchelli, G. (2018). Implant placement in the esthetic area: criteria for positioning single and multiple implants. *Periodontol 2000* 77 (1), 176–196. doi:10.1111/prd.12211

Tian, F., Hosseinkhani, H., Hosseinkhani, M., Khademhosseini, A., Yokoyama, Y., Estrada, G. G., et al. (2008). Quantitative analysis of cell adhesion on aligned micro- and nanofibers. *J. Biomed. Mater. Res. Part A* 84A (2), 291–299. doi:10.1002/jbm.a.31304

Tracy, M. A., Ward, K. L., Firouzabadian, L., Wang, Y., Dong, N., Qian, R., et al. (1999). Factors affecting the degradation rate of poly(lactide-co-glycolide) microspheres *in vivo* and *in vitro*. *Biomaterials* 20 (11), 1057–1062. doi:10.1016/S0142-9612(99)00002-2

Wang, H., Li, X., Lai, S., Cao, Q., Liu, Y., Li, J., et al. (2023). Construction of vascularized tissue engineered bone with nHA-coated BCP bioceramics loaded with peripheral blood-derived MSC and EPC to repair large segmental femoral bone defect. *ACS Appl. Mater. and Interfaces* 15 (1), 249–264. doi:10.1021/acsami.2c15000

Xiang, J., Li, Y., Ren, M., He, P., Liu, F., Jing, Z., et al. (2022). Sandwich-like nanocomposite electrospun silk fibroin membrane to promote osteogenesis and antibacterial activities. *Appl. Mater. Today* 26, 101273. doi:10.1016/j.apmt.2021.101273

Xu, C., Liu, Z., Chen, X., Gao, Y., Wang, W., Zhuang, X., et al. (2024). Bone tissue engineering scaffold materials: fundamentals, advances, and challenges. *Chin. Chem. Lett.* 35 (2), 109197. doi:10.1016/j.cclet.2023.109197

Yoshimoto, I., Sasaki, J.-I., Tsuboi, R., Yamaguchi, S., Kitagawa, H., and Imazato, S. (2018). Development of layered PLGA membranes for periodontal tissue regeneration. *Dent. Mater.* 34 (3), 538–550. doi:10.1016/j.dental.2017.12.011

Zhang, K.-R., Gao, H.-L., Pan, X.-F., Zhou, P., Xing, X., Xu, R., et al. (2019). Multifunctional bilayer nanocomposite guided bone regeneration membrane. *Matter* 1 (3), 770–781. doi:10.1016/j.matt.2019.05.021

Zhang, L., Dong, Y., Zhang, N., Shi, J., Zhang, X., Qi, C., et al. (2020). Potentials of sandwich-like chitosan/polycaprolactone/gelatin scaffolds for guided tissue regeneration membrane. *Mater. Sci. Eng. C* 109, 110618. doi:10.1016/j.msec.2019.110618

Zheng, M., Wang, X., Yue, O., Hou, M., Zhang, H., Beyer, S., et al. (2021). Skin-inspired gelatin-based flexible bio-electronic hydrogel for wound healing promotion and motion sensing. *Biomaterials* 276, 121026. doi:10.1016/j.biomaterials.2021.121026

Zheng, R., Duan, H., Xue, J., Liu, Y., Feng, B., Zhao, S., et al. (2014). The influence of Gelatin/PCL ratio and 3-D construct shape of electrospun membranes on cartilage regeneration. *Biomaterials* 35 (1), 152–164. doi:10.1016/j.biomaterials.2013.09.082

frontiers | Frontiers in Pharmacology

TYPE Original Research
PUBLISHED 12 November 2024
DOI 10.3389/fphar.2024.1476255

OPEN ACCESS

EDITED BY
Jie Fang,
Sichuan University, China

REVIEWED BY
Li Xiao,
Sichuan Academy of Medical Sciences and Sichuan Provincial People's Hospital, China
Vineet Mahajan,
University of Pittsburgh, United States
Yueying Zhou,
Central South University, China

*CORRESPONDENCE
Hongyi Zhu,
420308955@qq.com
Junhui Yin,
yinjunhui1429@126.com

†These authors have contributed equally to this work

RECEIVED 05 August 2024
ACCEPTED 25 October 2024
PUBLISHED 12 November 2024

CITATION
Gao Y, Wei H, Peng X, Wang C, Zhu H and Yin J (2024) ER stress-induced YAP upregulation leads to chondrocyte phenotype loss in age-related osteoarthritis.
Front. Pharmacol. 15:1476255.
doi: 10.3389/fphar.2024.1476255

ER stress-induced YAP upregulation leads to chondrocyte phenotype loss in age-related osteoarthritis

Yanchun Gao[1†], Haifeng Wei[1†], Xiaoyuan Peng[1], Chenchen Wang[2], Hongyi Zhu[1*] and Junhui Yin[1*]

[1]Department of Orthopaedic Surgery, Shanghai Sixth People's Hospital Affiliated to Shanghai Jiao Tong University School of Medicine, Shanghai, China, [2]Department of Orthopedics Surgery, Shanghai Sixth People's Hospital Affiliated to Shanghai Jiao Tong University School of Medicine, Shanghai, China

Background: Osteoarthritis (OA) is a common degenerative joint disease, leading to pain and restricted mobility. Age-related endoplasmic reticulum (ER) stress has been implicated in the pathogenesis of OA, but the underlying mechanisms remain unclear. This study aims to explore the relationship between age-related ER stress, YAP overexpression, and chondrocyte phenotype loss in the development of OA.

Methods: Cartilage samples were collected from patients undergoing amputation, and age-related ER stress markers and YAP expression were assessed using immunohistochemical staining and qPCR. Transgenic mice with cartilage-specific YAP overexpression (YAP^{OE}) were created, and Pamrevlumab was administered to evaluate its therapeutic effects.

Results: Higher expression of ER stress markers and YAP were showed in aged tissues compared to younger tissues. YAP overexpression led to decreased levels of cartilage phenotype markers and increased osteogenesis-related proteins. *In vivo*, YAP^{OE} mice exhibited OA-like cartilage degeneration, which was mitigated by Pamrevlumab treatment.

Conclusion: Age-related ER stress induces YAP overexpression, contributing to OA pathogenesis. Pamrevlumab effectively prevents this phenotype loss in YAP^{OE} mice, suggesting its potential as a therapeutic agent for OA. These findings provide new insights into the molecular mechanisms of OA and highlight the importance of targeting the ER stress-YAP-CTGF signaling pathway in OA treatment and prevention.

KEYWORDS

er stress, YAP, ctgf, pamrevlumab, degeneration, chondrocyte

1 Introduction

Osteoarthritis (OA) is the most common joint disease in adults worldwide, characterized by the degenerative destruction of articular cartilage. The pathological changes in OA-affected joints manifest as pain and restricted mobility, leading to a significant decline in the quality of life for those affected (Litwic et al., 2013; Martel-Pelletier et al., 2016). The financial and social burdens induced by OA are increasingly severe, particularly in the older population (Adebayo et al., 2017). Despite treatments such as joint replacement and specific medications, the pathogenesis of OA remains unclear (Baldini et al., 2015; Marshall et al., 2014; McAlindon et al., 2014).

Age is a significant factor influencing the prevalence of knee and hip osteoarthritis in the elderly (Prieto-Alhambra et al., 2014; Long et al., 2022; GBD, 2021 Other Musculoskeletal Disorders Collaborators, 2023). Data from the Johnson County Osteoarthritis Project showed that the prevalence of radiographic knee osteoarthritis increased from 26.2% in the 55–64 age group to nearly 50% in the 75+ age group. Similarly, the prevalence of symptomatic hip osteoarthritis rose from 5.9% in the 45–54 age group to 17% in the 75+ age group (Ambrose et al., 2024). While many studies have focused on clinical evidence of age as a factor in OA prevalence, further research is needed to elucidate the pathogenesis of age-induced osteoarthritis (Hou et al., 2018; Liu et al., 2023). Age-related activation of endoplasmic reticulum (ER) stress is strongly associated with the development of several age-related diseases (Liu et al., 2018; Taylor, 2016; Pinky et al., 2023; Garcia et al., 2023).

Age-related activation of endoplasmic reticulum (ER) stress is strongly associated with the development of several age-related diseases (Liu et al., 2018; Taylor, 2016; Pinky et al., 2023; Garcia et al., 2023). Numerous studies have described a link between ER stress and OA (Li et al., 2016; Takada et al., 2011; Rellmann et al., 2021). In chondrocytes from OA patients of different ages, there is evidence of age-dependent ER stress and the unfolded protein response (UPR). Aged articular cartilage chondrocytes exhibit decreased expression of calnexin and increased immunohistochemical staining for ER stress markers, suggesting that reduced expression of molecular chaperones during aging induces ER stress (Tan et al., 2020). Recent research has indicated that ER stress can contribute to various diseases through the activation of the YAP pathway (Liu et al., 2021; Panda et al., 2022; Anerillas et al., 2023; Wang et al., 2022).

The Hippo/YAP pathway is critically involved in cartilage development and plays a key role in cell fate and tissue regeneration (Yang et al., 2017; Hansen et al., 2015), and finally leads to Osteoarthritis (Sun et al., 2023). Increasing evidence has indicated that the Hippo/YAP pathway is also tightly involved in cartilage development (Karystinou et al., 2015), YAP was found as a negative regulator of chondrocyte differentiation as it promotes early chondrocyte proliferation via binding TEADs for direct upregulation of Sox6 but inhibits subsequent chondrocyte hypertrophy and maturation (Deng et al., 2016). Connective tissue growth factor (CTGF), a significant downstream protein of YAP, is abundantly expressed in chondrocytes of patients with severe osteoarthritis (Shome et al., 2020; Dudek et al., 2021; MacDonald et al., 2021; Tang et al., 2018). It is suggested that the activity of YAP-CTGF is tightly related to the OA progression (Zhang et al., 2020).

This study aims to investigate the relationship between ER stress and YAP signaling in the context of cartilage phenotype loss in OA. By providing an in-depth analysis of the pathogenesis of osteoarthritis, we aim to propose a new direction for future research based on our findings.

2 Results

2.1 Age-related ER stress in chondrocytes

Immunohistochemical staining of cartilage tissue revealed the expression of ER stress-related proteins BIP, XBP1s, ATF4, and CHOP. Quantitative analysis of these results showed that ER stress-related proteins were highly expressed in the Aged Group (Figures 1A–H). Cartilage tissues were extracted from SD rats at different ages (4, 20, 36, 52, and 68 weeks) and subjected to qPCR. The results indicated that the mRNA expression levels of XBP1, ATF4, and CHOP increased with age (Figures 1I–K).

2.2 YAP expression and cartilage phenotype changes in aging

Immunohistochemical staining showed higher YAP expression in the Aged Group (Figures 2A,B). qPCR analysis of cartilage from rats of different ages demonstrated that mRNA expression levels of YAP and Col I increased with age (Figures 2C,D), whereas the expression levels of Col II, Aggrecan, and SOX9 decreased, indicating a degenerative cartilage phenotype with age (Figures 2E–G). Human chondrocytes were treated with TM (an ER stress inducer) and 4-PBA (an ER stress inhibitor). As demonstrated by Western blot analysis TM induces endoplasmic reticulum (ER) stress, leading to increased phosphorylation of PERK and IRE, and elevated expression of ER stress-related proteins such as ATF4, XBP1s, and CHOP. In contrast, 4-PBA can mitigate these changes. Correspondingly, ER stress activation results in the upregulation of YAP, while inhibition of ER stress reduces YAP expression (Figure 2H).

2.3 Overexpression of YAP leads to cartilage phenotype loss and upregulation of osteogenesis-related proteins

Overexpression of YAP in chondrocytes via lentivirus transfection resulted in increased expression of CTGF and decreased levels of SOX9, Col II, and Aggrecan, as shown by Western blot (Figure 3A). qPCR analysis showed similar trends (Figure 3B). Immunofluorescent staining indicated decreased SOX9 and Aggrecan and increased osteogenesis-related proteins ALP and RUNX2 in YAP-overexpressing chondrocytes (Figure 3C. These *in vitro* results suggest that increased YAP expression leads to the loss of cartilage phenotype and upregulation of osteogenesis-related proteins.

Western blot analysis showed that CTGF knockdown rescued the reduction of Col II, SOX9, and Aggrecan in YAP-overexpressing chondrocytes (Figure 3D). Treatment with varying concentrations of CTGF led to decreased expression of Col II, Aggrecan, and SOX9 (Figure 3E). Immunofluorescent staining confirmed the downregulation of SOX9 and Aggrecan and upregulation of osteogenesis-related proteins ALP and RUNX2 after CTGF stimulation (Figure 3F). Increased CTGF levels induced the loss of cartilage phenotypes and upregulation of osteogenic phenotypes.

2.4 YAP^{OE} induces osteoarthritis in a transgenic mouse model

Overexpression of YAP in cartilage-specific transgenic mice resulted in irregular cartilage morphology and decreased cartilage thickness, as shown by Alcian blue and Safranin-O and Fast green staining (Figures 4A,B). Mankin's Score and ORASI Score were significantly higher in the YAP^{OE} group compared to the control,

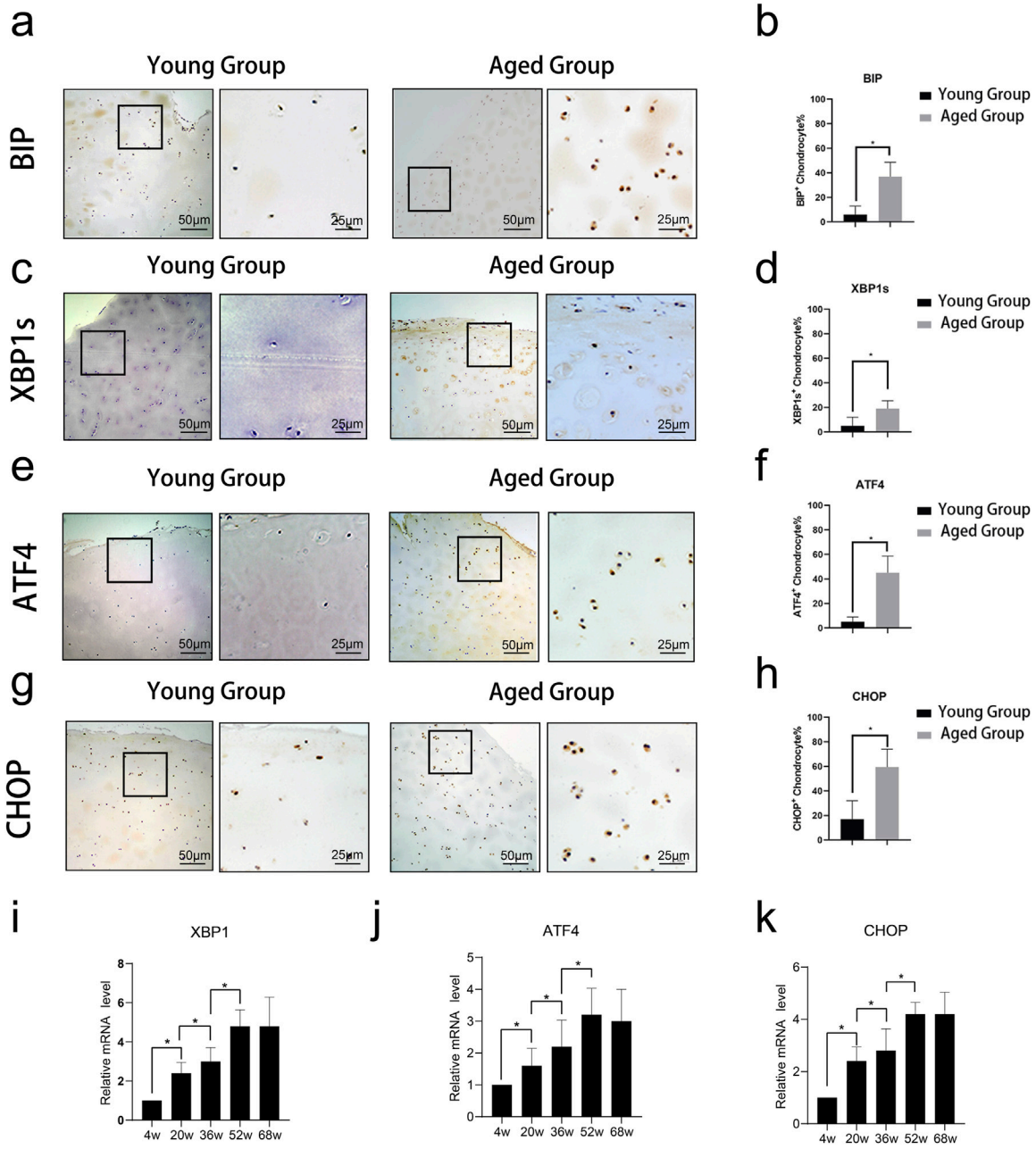

FIGURE 1
Expression of ER stress-related proteins in cartilage tissue across different age groups. Immunohistochemical staining of cartilage tissue revealed the expression of ER stress-related proteins BIP, XBP1s, ATF4, and CHOP. **(A–D)** Representative images of immunohistochemical staining for ER stress-related proteins BIP, XBP1s, ATF4, and CHOP in cartilage tissue from young (4w, 20w) and aged (52w, 68w) rats. Staining intensity and the number of positive cells were notably higher in the aged groups compared to the young groups, indicating increased expression of these proteins with age. **(E-H)** Quantitative analysis of the percentage of BIP, XBP1s, ATF4, and CHOP-positive chondrocytes in young and aged rats. Data shows significantly higher expression levels of all four proteins in the aged group (*$p < 0.05$). **(I-K)** Quantitative analysis of relative mRNA expression levels of XBP1s, ATF4, and CHOP in cartilage tissue from rats at 4, 20, 36, 52, and 68 weeks. The results demonstrate a gradual increase in mRNA expression with age, highlighting age-associated upregulation of ER stress-related gene expression. Statistical significance is denoted by *$p < 0.05$.

indicating a stronger tendency toward osteoarthritis (Figures 4C,D). Immunohistochemical staining showed lower Col II and higher CTGF expression, indicating cartilage phenotype loss following YAP activation (Figures 4E,F). A significant reduction in Col II + cells and an increase in CTGF + chondrocytes were observed in the YAP^{OE} group (Figure 4G). These results demonstrate that YAP overexpression induces osteoarthritis in the transgenic mice model.

2.5 Pamrevlumab rescued YAP overexpression-induced cartilage phenotype loss in vitro

Pamrevlumab treatment rescued the downregulation of Col II, SOX9, and Aggrecan caused by YAP overexpression, as shown by Western blot (Figure 4H). Immunofluorescent staining confirmed

10.3389/fphar.2024.1476255

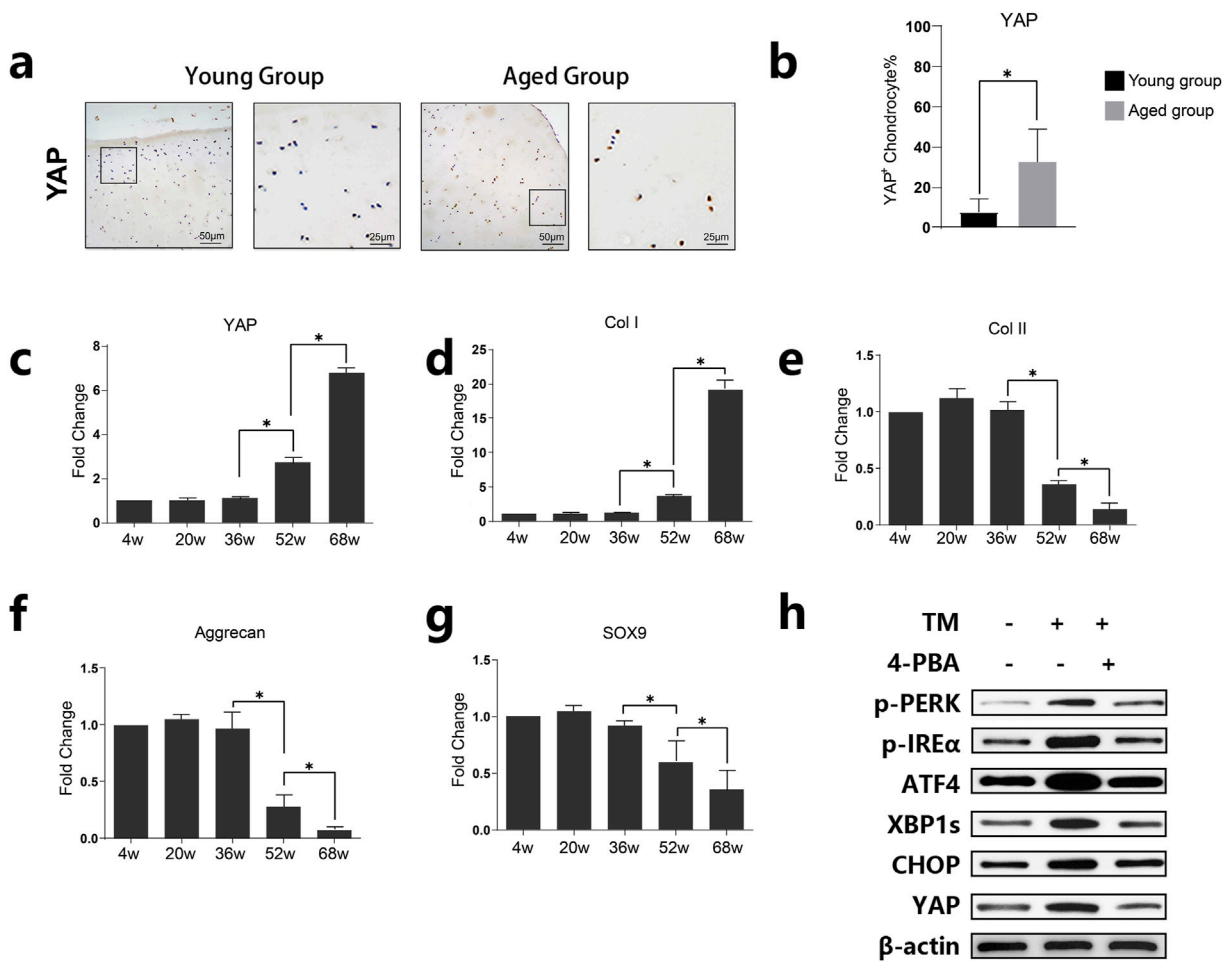

FIGURE 2
Expression of YAP and its association with age-related changes in cartilage tissue. **(A)** Representative images of immunohistochemical staining for YAP in cartilage tissues from young and aged groups. Increased staining in the aged group suggests higher YAP expression in older cartilage. **(B)** Quantitative analysis of YAP-positive chondrocytes in young and aged groups. Data are presented as mean ± SD, showing significantly elevated levels of YAP in the aged group (*$p < 0.05$). **(C–G)** Quantitative analysis of relative mRNA levels of YAP, Col I, Col II, Aggrecan, and SOX9 across different age groups (4w, 20w, 36w, 52w, 68w). The results show age-dependent changes, with YAP and Col I expression increasing, while Aggrecan and SOX9 decrease with age, indicating cartilage degeneration with age **(H)** Western blot analysis showing the expression levels of YAP, p-PERK, p-IREα, ATF4, XBP1s, and CHOP in the presence or absence of tunicamycin (TM) and 4-phenylbutyric acid (4-PBA). The results demonstrate ER stress upregulated YAP whereas inhibition of ER stress reduced YAP expression.

that Pamrevlumab rescued the reduction of SOX9 and Aggrecan, while osteogenesis-related proteins ALP and RUNX2 decreased (Figure 4I). Thus, Pamrevlumab can rescue YAP^{OE}-induced chondrocyte phenotype loss.

2.6 Amrevlumab rescues YAP overexpression-induced osteoarthritis in vivo

Intra-articular injection of Pamrevlumab into YAPOE-induced mice showed a protective effect, as demonstrated by chemical staining with Alcian blue, Toluidine blue, and Safranin-O and Fast green (Figure 5A). Pamrevlumab treatment rescued the low expression of Col II and high expression of Col I observed in YAPOE mice (Figure 5B). The percentage of Collagen II + cells increased in Pamrevlumab-treated transgenic mice (Figure 5C). Mankin's score and ORASI Score were significantly lower in Pamrevlumab-treated YAP^{OE} mice (Figures 5D,E). These findings illustrate that YAP-CTGF signaling regulates osteoarthritis pathogenesis and that Pamrevlumab can mitigate YAP^{OE}-induced osteoarthritis.

3 Discussion

In this study, using knee cartilage samples from rats and humans of different ages, we demonstrated that age-related ER stress-induced YAP overexpression leads to the loss of chondrocyte phenotypes. After confirming through *in vitro* experiments that YAP overexpression is a key factor in chondrocyte phenotype loss, we developed a transgenic mouse model with YAP overexpression specifically in the knee joint. This mouse model spontaneously exhibited signs of osteoarthritis without requiring osteoarthritis induction. Through both *in vivo* and *in vitro* experiments,

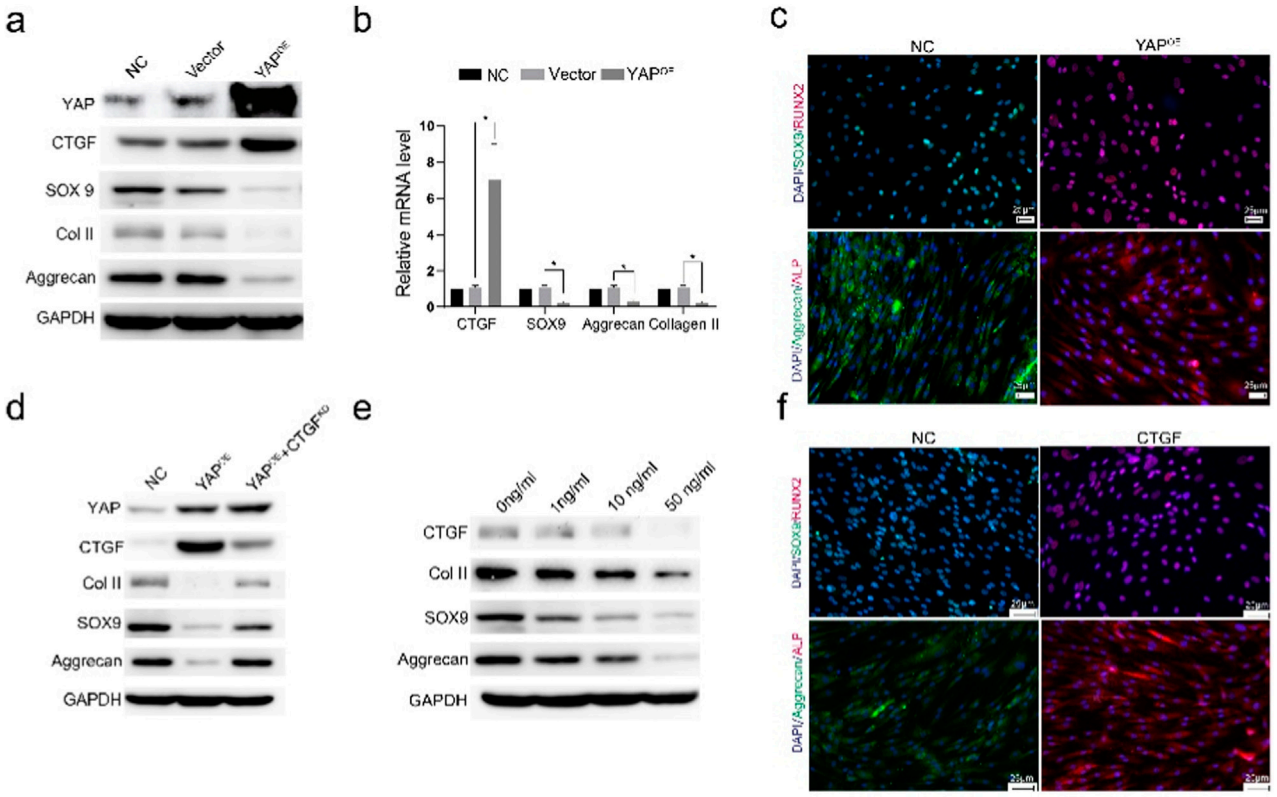

FIGURE 3
YAP overexpression leads to cartilage phenotype loss and upregulation of osteogenic-related proteins. **(A)** Western blot analysis showing the expression levels of YAP, CTGF, SOX9, COL II, and Aggrecan in cells with YAP overexpression. The results indicate that YAP overexpression promotes the upregulation of CTGF and downregulation of cartilage-specific proteins. **(B)** Quantitative analysis of mRNA expression levels of CTGF, SOX9, Aggrecan, and COL II under different treatment conditions. Data suggest a significant increase in CTGF and a reduction in cartilage markers with YAP overexpression (*$p < 0.05$). **(C)** Immunofluorescence staining for SOX9 and Aggrecan (cartilage markers), and ALP and RUNX2 (osteogenesis-related proteins) in control (NC) and YAP-overexpressing (YAP^{OE}) groups. YAP overexpression decreases cartilage markers while increasing osteogenesis-related markers, indicating a shift toward an osteogenic phenotype. **(D)** Western blot analysis of COL II, SOX9, and Aggrecan in different groups, including NC, YAP^{OE}), and YAP^{OE} with CTGF knockdown (YAP^{OE} + $CTGF^{KD}$). The results show that CTGF knockdown partially rescues the cartilage phenotype loss induced by YAP overexpression. **(E)** Western blot analysis of COL II, SOX9, and Aggrecan treated with varying concentrations of CTGF (0, 1, 10, 50 ng/mL). Increasing CTGF concentrations leads to the reduction of cartilage markers, supporting its role in the loss of cartilage phenotype. **(F)** Immunofluorescence staining of SOX9/Aggrecan (cartilage markers) and ALP/RUNX2 (osteogenesis-related proteins) with or without CTGF stimulation. The presence of CTGF maintains cartilage markers and reduces the expression of osteogenesis-related markers, indicating its involvement in the cartilage-to-bone phenotype transition.

Pamrevlumab was proven effective in preventing osteoarthritis. We propose a novel conclusion that aging-induced ER stress activation triggers YAP-CTGF signaling, causing chondrocyte phenotype loss and leading to osteoarthritis. This conclusion offers a new research direction in the pathogenesis of osteoarthritis for future studies.

ER stress is involved in the development of several aging-related diseases and is an important target for the study of degenerative diseases (Chen et al., 2023; Gao et al., 2018). Researchers have pointed out that age-related increases in ER stress are significant triggers for the development of osteoarthritis (Dreier et al., 2022). Several studies have suggested that activation of ER stress is involved in the pathophysiologic process of osteoarthritis by causing chondrocyte death (Li et al., 2016; Rellmann et al., 2021; Tan et al., 2020; Yang et al., 2020). Furthermore, as an essential physiological process regulating cellular function, ER stress is involved in regulating various cellular phenotypes (Raines et al., 2022; He et al., 2021; Aghadi et al., 2022; Chen and Cubillos-Ruiz, 2021; Gao et al., 2020). Dibyendu K et al. pointed out that PERK-mediated phosphorylation of eIF2α drives the selective translation of ATF4 and CHOP, enhancing YAP expression (Panda et al., 2022). Wu et al. (Wu et al., 2015) demonstrated in a study on liver cancer that the PERK kinase-eIF2α axis can activate Yap, while prolonged ER stress can create a negative feedback loop to inhibit Yap and promote apoptosis. Another study showed that in gastric cancer, YAP may regulate ER stress by activating the ERK signaling pathway (Liu et al., 2019). Additionally, as a key downstream protein of the IRE1a signaling axis, XBP1s is also considered to participate in the regulation of the YAP/TAZ signaling pathway (Fan et al., 2020). In our study, we have identified for the first time the interaction between YAP activation and ER stress in osteoarthritis, which is completely different from previous research. Based on existing studies (Takaguri et al., 2017; Yap et al., 2021; Yap et al., 2020), we speculate that signaling molecules such as PERK and IRE1 must play a crucial role. Moving forward, we will continue to investigate the effects of the three classical downstream pathways of ER stress

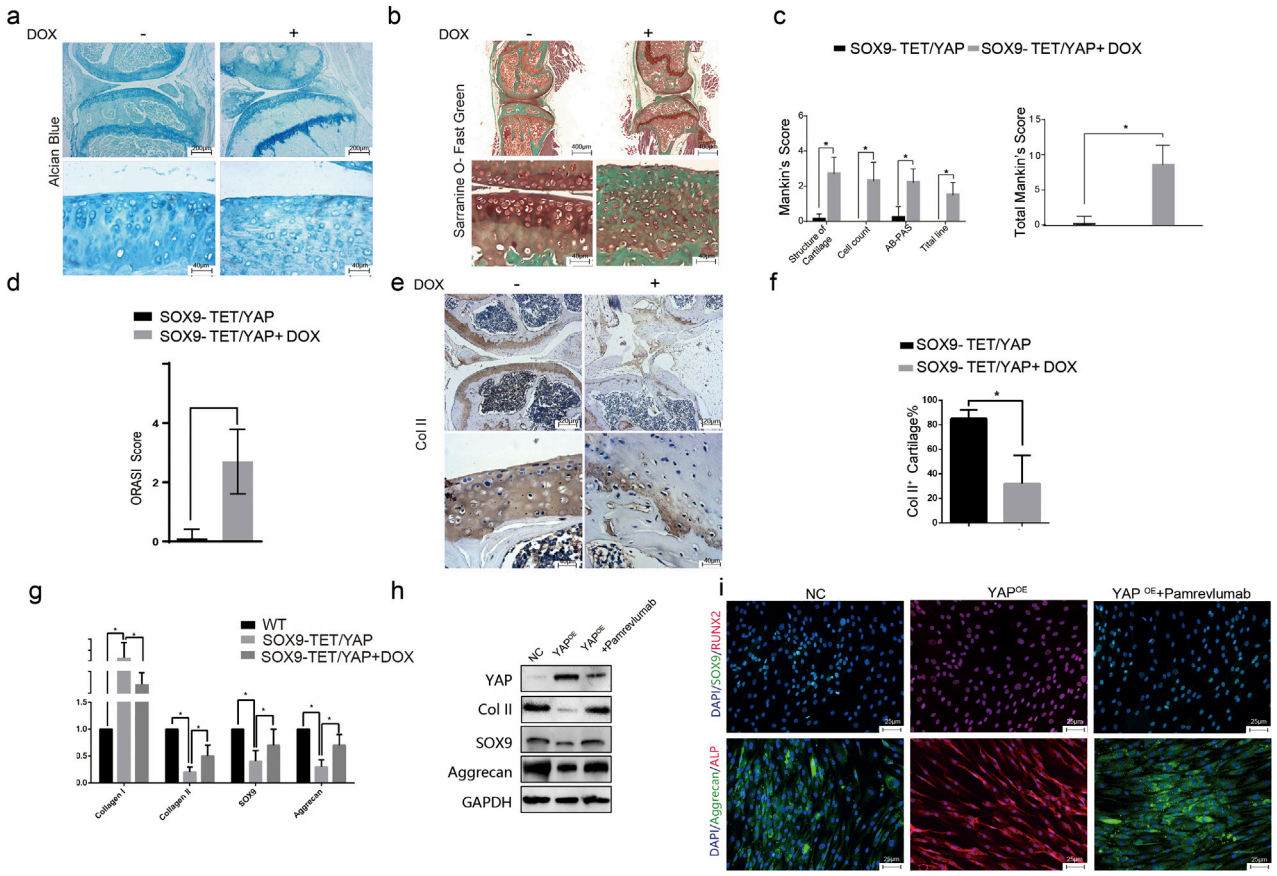

FIGURE 4
YAP overexpression induces osteoarthritis-like changes in a transgenic mouse model. **(A)** Representative images of Alcian blue staining of knee joints in transgenic mice with YAP^{OE}. The staining indicates a reduction in cartilage matrix components in the YAP^{OE} mice, suggesting cartilage degradation. **(B)** Representative images of Safranin-O and Fast Green staining of knee joints in transgenic mice with YAP^{OE}. The images show cartilage deterioration and decreased proteoglycan content in the presence of YAP overexpression. **(C–D)** Quantitative assessment using Mankin's score and Osteoarthritis Research Society International (ORASI) score to evaluate cartilage damage in YAP^{OE} transgenic mice with or without DOX administration. YAP overexpression (induced by DOX) significantly increases cartilage degeneration scores (*$p < 0.05$). **(E–F)** Immunohistochemical staining and quantitative analysis of COL II in YAP^{OE} transgenic mice, showed decreased COL II expression in the YAP^{OE} group, indicating loss of cartilage integrity. **(G)** Relative mRNA expression levels of cartilage-associated genes (COL I, COL II, SOX9, and Aggrecan) across NC, YAP^{OE}, and YAP^{OE} treated with Pamrevlumab groups. Pamrevlumab treatment partially restores cartilage gene expression, counteracting the effects of YAP overexpression. **(H)** Western blot analysis showing the protein levels of YAP, COL II, SOX9, and Aggrecan in control and YAP^{OE} mice, with and without Pamrevlumab treatment. The data indicate that Pamrevlumab reduces YAP-induced downregulation of cartilage markers. **(I)** Immunofluorescence staining for cartilage-specific proteins (SOX9, Aggrecan) and osteogenesis-related markers (ALP, RUNX2) in control, YAP^{OE}, and YAP^{OE} + Pamrevlumab-treated groups. Pamrevlumab treatment appears to mitigate the YAP-induced increase in osteogenic markers, supporting its protective role against cartilage degradation.

on the YAP signaling axis to clarify the specific mechanisms involved in osteoarthritis. Our study suggests that ER stress regulates chondrocyte phenotypes through the activation of the YAP pathway. Research on downstream signaling pathways following ER stress in chondrocytes is still ongoing.

The YAP signaling pathway plays an essential role in cell aging (Sladitschek-Martens et al., 2022). It is regarded as an age-related protein, upregulated in various cells, and is associated with a wide variety of degenerative diseases, including cardiogenesis, skeletal muscle aging, vascular senescence, macular degeneration, and hair cell regeneration (Monroe et al., 2019; Setiawan et al., 2021; Pan et al., 2021; Rudolf et al., 2020). Maintaining YAP function can rejuvenate old cells, while YAP overexpression can lead to a series of aging symptoms (Zhang et al., 2018; Cha et al., 2022). These studies confirm the correlation between the YAP pathway and age-related diseases. In this study, we also found a close correlation between YAP and aging in young and old human samples, as well as in rats of different ages, which is consistent with most research findings. Additionally, YAP-related proteins and pathways have been shown to have significant associations with osteoarthritis (OA) in numerous previous studies (Zhang et al., 2011). Recent studies indicate its critical role in the pathogenesis of osteoarthritis. Gong et al. found an evident association between increased total expression of YAP and degenerative cartilage from OA patients (Gong et al., 2019). YAP was markedly upregulated both in mRNA and protein levels in OA mice (Zhang et al., 2019). The activation of YAP is thought to cause the phenotypic loss of chondrocytes, contributing to osteoarthritis development. Conditional knockout of YAP in mice preserves collagen II expression and protects cartilage from degeneration in osteoarthritis models (Zhang et al., 2020). As a degenerative disease, osteoarthritis is closely related to endochondral bone formation, cartilage degeneration, and

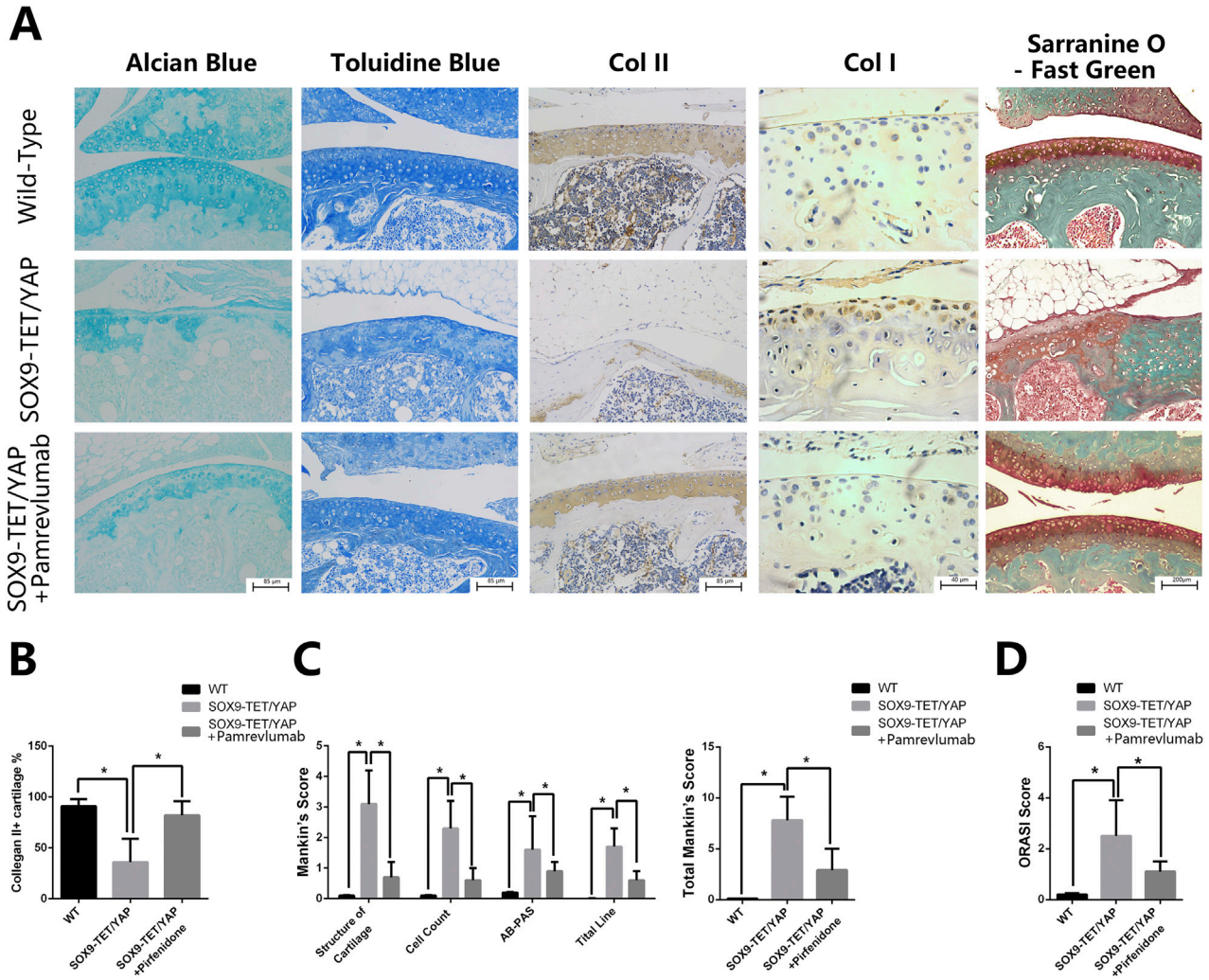

FIGURE 5
Pamrevlumab rescued YAP overexpression-induced osteoarthritis *in vivo*. **(A)** Representative images of chemical staining (Alcian Blue, Toluidine Blue, and Safranin O-Fast Green) from cartilage tissue of Wild-Type (WT), YAP^{OE}, and YAP^{OE} + Pamrevlumab-treated mice. The YAP^{OE} group exhibits significant cartilage degradation, while Pamrevlumab treatment improves cartilage integrity, resembling the WT condition. **(B)** Immunohistochemical staining for COL II and COL I in cartilage tissues from WT, YAP^{OE}, and YAP^{OE} + Pamrevlumab groups. The results show reduced COL II and increased COL I expression in the SOX9-TET/YAP group, indicative of cartilage loss and osteoarthritis, whereas Pamrevlumab treatment partially restores COL II levels. **(C)** Quantitative analysis of COL II-positive cartilage percentage across the three groups. Pamrevlumab significantly increases COL II presence compared to untreated SOX9-TET/YAP mice (*$p < 0.05$). **(D)** Mankin's score analysis of cartilage structure, cell count, AB-PAS staining, and tidemark integrity. The YAP^{OE} group shows elevated scores (indicative of cartilage degradation), while Pamrevlumab reduces these scores, suggesting cartilage preservation. **(E)** Osteoarthritis Research Society International (ORASI) score comparing WT, YAP^{OE}, and YAP^{OE} + Pamrevlumab mice. Pamrevlumab significantly lowers ORASI scores in YAP overexpression models, demonstrating its potential protective effect against YAP-induced osteoarthritis.

structural disorganization of subchondral bone (Cox et al., 2013; Hosaka et al., 2013; Saito et al., 2010). In osteoarthritis, MSCs show disordered chondrogenic differentiation. Recent studies found that chondrocytes and osteoblasts are not independent lineages. In the pathological process of osteoarthritis, hypertrophic chondrocytes survive the cartilage-to-bone transition and become osteogenic cells, explaining both cartilage degeneration and endochondral bone formation (Yang et al., 2014; Zhou et al., 2014; Staines et al., 2013).

CTGF is identified as a direct YAP target gene important for cell growth (Fan et al., 2013; Chan et al., 2011; Zhao et al., 2008). The YAP-CTGF signaling axis plays an indispensable role in endochondral ossification in osteoarthritis (Delve et al., 2020). Although research on this signaling axis in the field of osteoarthritis is relatively limited, it has been well studied in the fields of fibrosis and cancer, and may be mediated by TEAD (Qing et al., 2022; Li et al., 2022; Gabdulkhakova et al., 2023). According to previous research, when the Hippo pathway is activated, MST1/2 activates LATS1/2. The LATS1/2 kinase phosphorylates YAP at the Ser127 site. Phosphorylated YAP binds to 14-3-3 proteins, leading to its retention in the cytoplasm and preventing it from functioning as a transcriptional co-activator. Additionally, phosphorylated YAP is more prone to ubiquitination and degradation, which further reduces the level of active YAP. Thus, YAP phosphorylation plays a role in the negative regulation of YAP (Mannaerts et al., 2015; Li et al., 2024). YAP chondrocyte nuclear translocation is regulated by differential phosphorylation in response to anabolic and catabolic stimuli and

contribute to reduced anabolic activity and promotion of further cartilage loss (Cui et al., 2023). Some studies have manipulated the YAP signaling axis by inhibiting or increasing YAP phosphorylation (Zhang et al., 2024). In this study, we used Pamrevlumab to directly inhibit CTGF, and therefore did not address the impact of YAP phosphorylation on this pathway.

Previous studies show its contribution to joint homeostasis and osteoarthritis by controlling matrix sequestration. The deletion of CTGF increased the thickness of the articular cartilage and protected mice from osteoarthritis (Tang et al., 2018). Pamrevlumab, a humanized anti-CTGF antibody, has been tested in clinical trials for muscular dystrophy, pancreatic cancer, liver fibrosis, idiopathic pulmonary fibrosis, and type 1 and 2 diabetes (Ramazani et al., 2018). In this study, Pamrevlumab was effective in preventing cartilage phenotype loss and osteoarthritis-like lesions caused by YAP overexpression. Despite the complex mechanism of osteoarthritis, it remains a potential medication for treating and preventing osteoarthritis (Kaplon and Reichert, 2021; Xie et al., 2021).

This study still has some limitations. First, we proposed that aging establishes a connection with the YAP-CTGF signaling axis through endoplasmic reticulum stress. However, it is undeniable that there are likely many interactions involving other signaling pathways. YAP is not the only protein associated with the development of osteoarthritis, but we believe our research introduces a new direction, providing a foundation for future basic research and targeted therapeutic drug development. Second, due to the limitations of experimental conditions, the sample size in the study is relatively small. A smaller sample size and manual analysis of images may lead to bias in the experimental results. However, we believe that these limited samples can still yield valid experimental results. In this study, we did not perform large-scale RNA sequencing analysis, But the results from existing literature related to RNA sequencing data support our view (Ji et al., 2019; Pemmari et al., 2020; Soul et al., 2018). Third, although the research on this drug shows promising prospects, there is still a long way to go before it can be applied clinically. Further exploration is needed regarding its long-term therapeutic effects, potential side effects, and optimal dosage.

4 Materials and methods

4.1 Patients and specimens

Human cartilage samples were obtained from 20 patients following amputation, as described by Battistelli (Battistelli et al., 2005). Patients were divided into two age groups: <50 years (young group) and >50 years (aged group) (Copp et al., 2023; Kim et al., 2024). This study was approved by the Ethics Committee of Shanghai Sixth People's Hospital and complies with the Declaration of Helsinki.

4.2 Rats at different ages

All animal experiments were approved by the Animal Care and Use Committee of Shanghai Sixth People's Hospital. Female SD rats of different ages (2 weeks, 18 weeks, 34 weeks, 50 weeks, 66 weeks) were obtained, with each age group containing five rats. They were maintained for 2 weeks, then euthanized, and cartilage tissues from their limbs were collected for subsequent PCR quantification experiments.

4.3 Establishment of the YAP^{OE} transgenic mice models and treatment

Ten mice were used: five wild-type and five YAP^{OE} transgenic mice. Wild-type C57BL/6 mice served as the control group. The gain-of-function transgenic Tet-On-YAP1 mice line was created by microinjection of C57BL/6 fertilized eggs with the pRP (Exp)-TRE3G > YAP1 mutation > IRES/EGFP plasmid. Transgene PCR primers were: Transgene PCR primer F: CGGGGCTAAAGTGCA TCTCG. Transgene PCR primer R: CCAGGCCACATATGATTA GTTCCAGG. The sequence of SOX9rtTA was obtained from the pRP (Exp)-sox9Promoter > Tet3G/IRES/tTS plasmid. Transgene PCR primer F: GGAAGCTGCCCGACTCCTTCTT. Transgene PCR primer R: CCTGCCATGTTGTTGTCTGATCGATG. SOX9rtTA was crossed with Tet-On-YAP1 mice. To induce YAP expression in chondrocytes, eight-week-old SOX9rtTA/Tet-On-YAP1 mice were treated with 2 mg/mL doxycycline in drinking water for 8 weeks. This established a transgenic mice model overexpressing YAP in chondrocytes.

To verify the protective effect of Pamrevlumab in YAP^{OE} mice, 60 mice were included: 20 wild-type and 40 YAP^{OE} transgenic mice. 20 of the transgenic mice served as positive controls and 20 were treated with Pamrevlumab. In the negative and positive control groups, saline was injected intra-articularly and periarticularly twice a week from 2 weeks before to the end of doxycycline administration. The treatment group received Pamrevlumab (40 mg/kg) injections twice a week over the same period. Randomization was not used to allocate experimental units. No unscheduled animal deaths occurred before completing the experiments. Randomization was not used to allocate experimental units. No unscheduled animal deaths occurred before completing the experiments.

4.4 Cell culture, treatment

Primary chondrocytes were isolated from cartilage fragments dissected from the femoral heads, femoral condyles, and tibial plateaus of C57BL/6 mice or humans. Articular cartilage was cut into small pieces and digested with 0.25% trypsin at 37°C for 30 min. After washing three times with PBS, the pieces were digested with 0.25% collagenase II at 37°C for 8 h. The cell suspension was filtered using a 70 μm cell strainer and centrifuged at 1,000 rpm for 5 min to collect primary chondrocytes. The chondrocytes were plated at a density of 0.15×10^5 cells/mL in DMEM with penicillin (100 U/mL), streptomycin (100 μg/mL), and 10% fetal bovine serum (Gibco, Grand Island, NY, United States), and cultured at 37°C in a humidified 5% CO_2 atmosphere. Pamrevlumab (Selleck, China) was administered at a concentration of 100 μM 2 days before lentiviral transfection.

4.5 Lentivirus transfection

For protein overexpression and knockdown, targeted sequences were designed (Gene Pharma, Shanghai, China). Lentiviral vectors for YAP and CTGF were constructed by inserting the genes' coding sequences (CDSs) into the pLenti vector. Virus packaging was conducted according to the VSVG-delta 8.9 system. Target sites in human genes included: $shYAP^{OE}$: 5′-CTCAGGATGGAGAAA TTTA-3′. $shCTGF^{KD}$: 5′-GCTGACCTGGAAGAGAACATT-3′. After 72 h of infection, the infection efficiency was assessed through Western blot analysis.

4.6 Western blot analysis

Cells were harvested and lysed with cell lysis buffer supplemented with protease and phosphatase inhibitors (Sigma-Aldrich, St. Louis, MO) on ice for 15 min. Protein concentrations were diluted 1:5 with protein loading buffer (Transgen Biotech, Beijing, China). A total of 30 μg of protein was subjected to SDS-PAGE after denaturation at 95°C for 5 min. Cell lysates were analyzed on a 10% Tris-HCl gel under reducing conditions. Proteins were transferred to 0.22-μm PVDF membranes (MERCK, Darmstadt, Germany) and blocked with 5% non-fat dry milk at 4°C overnight. Membranes were incubated for 2 h at 37°C with anti-SOX9 (Abcam, Cambridge, MA), anti-YAP, anti-aggrecan, anti-collagen II (Col II), and anti-GAPDH (Cell Signaling Technology, Danvers, MA). Secondary antibodies (Cell Signaling Technology, Danvers, MA) were used for 1 h at 37°C. After washing with tris buffered saline with Tween, membranes were exposed to an ECL substrate in a darkroom and analyzed with the FluorChem M system (ProteinSimple, San Jose, CA, United States). Results were quantified using Quantity One software (Bio-Rad Laboratories, Hercules, CA, United States).

4.7 Quantitative real-time polymerase chain reaction (qRT-PCR)

Full-thickness cartilage was collected from the knees of various aged SD rats. After excising the subchondral bone, the cartilage was chopped and homogenized with Trizol (Transgen Biotech, Beijing, China). cDNA synthesis was performed using TransScript® All-in-One First-Strand cDNA Synthesis SuperMix for qPCR (Transgen Biotech). qPCR was performed with TransStart® Top Green qPCR SuperMix (Transgen Biotech), using β-actin for normalization.

4.8 Immunohistochemistry and immunohistochemistry staining

Knees and articular cartilage were harvested and fixed in 4% formaldehyde for 48 h. Femoral condyles were decalcified in EDTA for 28 days, then dehydrated in graded ethanol, and made transparent with xylene. Specimens were embedded in paraffin and sectioned into 5 μm slices. Toluidine blue staining evaluated cartilage degeneration and calcium deposition (Shepard and Mitchell, 1976; Sridharan and Shankar, 2012). Safranin-O and fast green staining assessed matrix proteoglycan and joint morphology. Osteoarthritis progression was evaluated using the modified Mankin's score and OARSI system (Chen et al., 2023; Zhang et al., 2020). Immunohistochemistry was performed to evaluate ER stress and chondrocyte phenotype, using primary antibodies for type II collagen, type I collagen, BIP, XBP1s, ATF4, CHOP, YAP, and CTGF (all from Abcam, 1:100).

4.9 Statistical methods

One-way analysis of variance (ANOVA) was used to compare the means of multiple groups. Fisher's exact test compared disease incidence between groups. Independent-sample t-tests compared means between two groups. Statistical analysis was conducted using SPSS 20.0 (IBM Corp, Armonk, NY, United States). P values <0.05 were considered statistically significant.

5 Conclusion

This study found that the YAP-CTGF axis, activated by age-related ER stress, causes the loss of the chondrocyte phenotype. We established a transgenic mice model with YAP overexpressed in cartilage and observed osteoarthritis-like pathological changes in the knee tissue of the mice. Pamrevlumab inhibited this loss of chondrocyte phenotype due to YAP overexpression and prevented osteoarthritis development *in vivo*. This study suggests an important role for ER stress-induced YAP upregulation in degenerative knee diseases and provides new possibilities for the pharmacological prevention of osteoarthritis.

Data availability statement

The original contributions presented in the study are included in the article/Supplementary Material, further inquiries can be directed to the corresponding authors.

Ethics statement

The studies involving humans were approved by the Research Ethics Committee of Shanghai Sixth People's Hospital Affiliated to Shanghai Jiao Tong University School of Medicine (protocol code 2024-YS-107, approval date 2024) and conducted in accordance with the Declaration of Helsinki and local legislation. Written informed consent for participation in this study was provided by the participants' legal guardians/next of kin. The animal studies were approved by the same committee (protocol code DWLL 2019-0284, approval date 2019) and conducted according to local legislation.

Author contributions

YG: Writing–original draft, Writing–review and editing, Conceptualization, Data curation, Investigation. HW: Investigation, Writing–original draft, Methodology, Software. XP: Methodology, Project administration, Writing–review and editing. CW: Writing–review and editing, Resources, Validation. HZ:

Validation, Writing–review and editing, Funding acquisition, Supervision, Writing–original draft. JY: Funding acquisition, Writing–original draft, Writing–review and editing, Project administration, Visualization.

Funding

The author(s) declare that financial support was received for the research, authorship, and/or publication of this article. This research was funded by the Interdisciplinary Program of Shanghai Jiao Tong University, grant number YG2021QN98 and Shanghai Sixth People's Hospital Cultivation Project, ynms202108.

Acknowledgments

The authors greatly acknowledge the financial support from the Interdisciplinary Program of Shanghai Jiao Tong University (YG2021QN98), Shanghai Sixth People's Hospital Cultivation Project (ynms202108).

Conflict of interest

The authors declare that the research was conducted in the absence of any commercial or financial relationships that could be construed as a potential conflict of interest.

Publisher's note

All claims expressed in this article are solely those of the authors and do not necessarily represent those of their affiliated organizations, or those of the publisher, the editors and the reviewers. Any product that may be evaluated in this article, or claim that may be made by its manufacturer, is not guaranteed or endorsed by the publisher.

References

Adebayo, O. O., Ko, F. C., Wan, P. T., Goldring, S. R., Goldring, M. B., Wright, T. M., et al. (2017). Role of subchondral bone properties and changes in development of load-induced osteoarthritis in mice. *Osteoarthr. Cartil.* 25, 2108–2118. doi:10.1016/j.joca.2017.08.016

Aghadi, M., Elgendy, R., and Abdelalim, E. M. (2022). Loss of FOXA2 induces ER stress and hepatic steatosis and alters developmental gene expression in human iPSC-derived hepatocytes. *Cell Death Dis.* 13, 713. doi:10.1038/s41419-022-05158-0

Ambrose, K. R., Huffman, K. F., Odom, E. L., Foster, A. L., Turkas, N., and Callahan, L. F. (2024). A public health approach to osteoarthritis in the United States. *Osteoarthr. Cartil.* 32, 406–410. doi:10.1016/j.joca.2023.12.004

Anerillas, C., Mazan-Mamczarz, K., Herman, A. B., Munk, R., Lam, K. G., Calvo-Rubio, M., et al. (2023). The YAP-TEAD complex promotes senescent cell survival by lowering endoplasmic reticulum stress. *Nat. Aging* 3, 1237–1250. doi:10.1038/s43587-023-00480-4

Baldini, A., Castellani, L., Traverso, F., Balatri, A., Balato, G., and Franceschini, V. (2015). The difficult primary total knee arthroplasty: a review. *Bone Jt. J.* 97-B, 30–39. doi:10.1302/0301-620X.97B10.36920

Battistelli, M., Borzi, R. M., Olivotto, E., Vitellozzi, R., Burattini, S., Facchini, A., et al. (2005). Cell and matrix morpho-functional analysis in chondrocyte micromasses. *Microsc. Res. Tech.* 67, 286–295. doi:10.1002/jemt.20210

Cha, S., Wang, J., Lee, S. M., Tan, Z., Zhao, Q., and Bai, D. (2022). Clock-modified mesenchymal stromal cells therapy rescues molecular circadian oscillation and age-related bone loss via miR142-3p/Bmal1/YAP signaling axis. *Cell Death Discov.* 8, 111. doi:10.1038/s41420-022-00908-7

Chan, S. W., Lim, C. J., Chong, Y. F., Pobbati, A. V., Huang, C., and Hong, W. (2011). Hippo pathway-independent restriction of TAZ and YAP by angiomotin. *J. Biol. Chem.* 286, 7018–7026. doi:10.1074/jbc.C110.212621

Chen, X., and Cubillos-Ruiz, J. R. (2021). Endoplasmic reticulum stress signals in the tumour and its microenvironment. *Nat. Rev. Cancer* 21, 71–88. doi:10.1038/s41568-020-00312-2

Chen, X., Shi, C., He, M., Xiong, S., and Xia, X. (2023). Endoplasmic reticulum stress: molecular mechanism and therapeutic targets. *Signal Transduct. Target Ther.* 8, 352. doi:10.1038/s41392-023-01570-w

Copp, M. E., Shine, J., Brown, H. L., Nimmala, K. R., Hansen, O. B., Chubinskaya, S., et al. (2023). Sirtuin 6 activation rescues the age-related decline in DNA damage repair in primary human chondrocytes. *Aging (Albany NY)* 15, 13628–13645. doi:10.18632/aging.205394

Cox, L. G., van Donkelaar, C. C., van Rietbergen, B., Emans, P. J., and Ito, K. (2013). Alterations to the subchondral bone architecture during osteoarthritis: bone adaptation vs endochondral bone formation. *Osteoarthr. Cartil.* 21, 331–338. doi:10.1016/j.joca.2012.10.013

Cui, Y., Miao, M. Z., Wang, M., Su, Q. P., Qiu, K., Arbeeva, L., et al. (2023). Yes-associated protein nuclear translocation promotes anabolic activity in human articular chondrocytes. *Osteoarthr. Cartil.* 31, 1078–1090. doi:10.1016/j.joca.2023.04.006

Delve, E., Co, V., Regmi, S. C., Parreno, J., Schmidt, T. A., and Kandel, R. A. (2020). YAP/TAZ regulates the expression of proteoglycan 4 and tenascin C in superficial-zone chondrocytes. *Eur. Cell Mater* 39, 48–64. doi:10.22203/eCM.v039a03

Deng, Y., Wu, A., Li, P., Li, G., Qin, L., Song, H., et al. (2016). Yap1 regulates multiple steps of chondrocyte differentiation during skeletal development and bone repair. *Cell Rep.* 14, 2224–2237. doi:10.1016/j.celrep.2016.02.021

Dreier, R., Ising, T., Ramroth, M., and Rellmann, Y. (2022). Estradiol inhibits ER stress-induced apoptosis in chondrocytes and contributes to a reduced osteoarthritic cartilage degeneration in female mice. *Front. Cell Dev. Biol.* 10, 913118. doi:10.3389/fcell.2022.913118

Dudek, M., Angelucci, C., Pathiranage, D., Wang, P., Mallikarjun, V., Lawless, C., et al. (2021). Circadian time series proteomics reveals daily dynamics in cartilage physiology. *Osteoarthr. Cartil.* 29, 739–749. doi:10.1016/j.joca.2021.02.008

Fan, R., Kim, N. G., and Gumbiner, B. M. (2013). Regulation of Hippo pathway by mitogenic growth factors via phosphoinositide 3-kinase and phosphoinositide-dependent kinase-1. *Proc. Natl. Acad. Sci. U. S. A.* 110, 2569–2574. doi:10.1073/pnas.1216462110

Fan, S., Price, T., Huang, W., Plue, M., Warren, J., Sundaramoorthy, P., et al. (2020). PINK1-Dependent mitophagy regulates the migration and homing of multiple myeloma cells via the MOB1B-mediated hippo-YAP/TAZ pathway. *Adv. Sci. (Weinh)* 7, 1900860. doi:10.1002/advs.201900860

Gabdulkhakova, A., Krutsenko, Y., Zhu, J., Liu, S., Poddar, M., Singh, S., et al. (2023). Loss of TAZ after YAP deletion severely impairs foregut development and worsens cholestatic hepatocellular injury. *Hepatol. Commun.* 7, e0220. doi:10.1097/HC9.0000000000000220

Gao, Y., Zhu, H., Wang, Q., Feng, Y., and Zhang, C. (2020). Inhibition of PERK signaling prevents against glucocorticoid-induced endotheliocyte apoptosis and osteonecrosis of the femoral head. *Int. J. Biol. Sci.* 16, 543–552. doi:10.7150/ijbs.35256

Gao, Y., Zhu, H., Yang, F., Wang, Q., Feng, Y., and Zhang, C. (2018). Glucocorticoid-activated IRE1α/XBP-1s signaling: an autophagy-associated protective pathway against endotheliocyte damage. *Am. J. Physiol. Cell Physiol.* 315, C300–C309. doi:10.1152/ajpcell.00009.2018

Garcia, G., Zhang, H., Moreno, S., Tsui, C. K., Webster, B. M., Higuchi-Sanabria, R., et al. (2023). Lipid homeostasis is essential for a maximal ER stress response. *Elife* 12, e83884. doi:10.7554/eLife.83884

GBD 2021 Other Musculoskeletal Disorders Collaborators (2023). Global, regional, and national burden of other musculoskeletal disorders, 1990-2020, and projections to 2050: a systematic analysis of the Global Burden of Disease Study 2021. *Lancet Rheumatol.* 5, e670–e682. doi:10.1016/S2665-9913(23)00232-1

Gong, Y., Li, S. J., Liu, R., Zhan, J. F., Tan, C., Fang, Y. F., et al. (2019). Inhibition of YAP with siRNA prevents cartilage degradation and ameliorates osteoarthritis development. *J. Mol. Med. Berl.* 97, 103–114. doi:10.1007/s00109-018-1705-y

Hansen, C. G., Moroishi, T., and Guan, K. L. (2015). YAP and TAZ: a nexus for Hippo signaling and beyond. *Trends Cell Biol.* 25, 499–513. doi:10.1016/j.tcb.2015.05.002

He, S., Fu, T., Yu, Y., Liang, Q., Li, L., Liu, J., et al. (2021). IRE1α regulates skeletal muscle regeneration through Myostatin mRNA decay. *J. Clin. Invest.* 131, e143737. doi:10.1172/JCI143737

Hosaka, Y., Saito, T., Sugita, S., Hikata, T., Kobayashi, H., Fukai, A., et al. (2013). Notch signaling in chondrocytes modulates endochondral ossification and osteoarthritis development. *Proc. Natl. Acad. Sci. U. S. A.* 110, 1875–1880. doi:10.1073/pnas.1207458110

Hou, A., Chen, P., Tang, H., Meng, H., Cheng, X., Wang, Y., et al. (2018). Cellular senescence in osteoarthritis and anti-aging strategies. *Mech. Ageing Dev.* 175, 83–87. doi:10.1016/j.mad.2018.08.002

Ji, Q., Zheng, Y., Zhang, G., Hu, Y., Fan, X., Hou, Y., et al. (2019). Single-cell RNA-seq analysis reveals the progression of human osteoarthritis. *Ann. rheumatic Dis.* 78, 100–110. doi:10.1136/annrheumdis-2017-212863

Kaplon, H., and Reichert, J. M. (2021). Antibodies to watch in 2021. *MAbs* 13, 1860476. doi:10.1080/19420862.2020.1860476

Karystinou, A., Roelofs, A. J., Neve, A., Cantatore, F. P., Wackerhage, H., and De Bari, C. (2015). Yes-associated protein (YAP) is a negative regulator of chondrogenesis in mesenchymal stem cells. *Arthritis Res. Ther.* 17, 147. doi:10.1186/s13075-015-0639-9

Kim, M. S., Choi, K. Y., Cho, R. K., Jang, H. J., Kwak, D. H., Yang, S. C., et al. (2024). The collagen-augmented chondrogenesis technique demonstrates superior cartilage repair compared to microfracture for cartilage defects of the knee joint, regardless of age. *Knee Surg. Sports Traumatol. Arthrosc.* doi:10.1002/ksa.12500

Li, L., Li, R., and Wang, Y. (2022). Identification of Small-molecule YAP-TEAD inhibitors by High-throughput docking for the Treatment of colorectal cancer. *Bioorg Chem.* 122, 105707. doi:10.1016/j.bioorg.2022.105707

Li, M., Zhang, F. J., and Bai, R. J. (2024). The hippo-YAP signaling pathway in osteoarthritis and rheumatoid arthritis. *J. Inflamm. Res.* 17, 1105–1120. doi:10.2147/JIR.S444758

Li, Y. H., Tardif, G., Hum, D., Kapoor, M., Fahmi, H., Pelletier, J. P., et al. (2016). The unfolded protein response genes in human osteoarthritic chondrocytes: PERK emerges as a potential therapeutic target. *Arthritis Res. Ther.* 18, 172. doi:10.1186/s13075-016-1070-6

Litwic, A., Edwards, M. H., Dennison, E. M., and Cooper, C. (2013). Epidemiology and burden of osteoarthritis. *Br. Med. Bull.* 105, 185–199. doi:10.1093/bmb/lds038

Liu, H., Mei, D., Xu, P., Wang, H., and Wang, Y. (2019). YAP promotes gastric cancer cell survival and migration/invasion via the ERK/endoplasmic reticulum stress pathway. *Oncol. Lett.* 18, 6752–6758. doi:10.3892/ol.2019.11049

Liu, H., Zhai, L., Liu, Y., Lu, D., VanderArk, A., Yang, T., et al. (2023). The histone demethylase KDM5C controls female bone mass by promoting energy metabolism in osteoclasts. *bioRxiv* 9, eadg0731. doi:10.1126/sciadv.adg0731

Liu, Y., Chang, J. C., Hon, C. C., Fukui, N., Tanaka, N., Zhang, Z., et al. (2018). Chromatin accessibility landscape of articular knee cartilage reveals aberrant enhancer regulation in osteoarthritis. *Sci. Rep.* 8, 15499. doi:10.1038/s41598-018-33779-z

Liu, Y., Molchanov, V., and Yang, T. (2021). Enzymatic machinery of ubiquitin and ubiquitin-like modification systems in chondrocyte homeostasis and osteoarthritis. *Curr. Rheumatol. Rep.* 23, 62. doi:10.1007/s11926-021-01022-w

Long, H., Liu, Q., Yin, H., Wang, K., Diao, N., Zhang, Y., et al. (2022). Prevalence trends of site-specific osteoarthritis from 1990 to 2019: findings from the global burden of disease study 2019. *Arthritis Rheumatol.* 74, 1172–1183. doi:10.1002/art.42089

MacDonald, I. J., Huang, C. C., Liu, S. C., Lin, Y. Y., and Tang, C. H. (2021). Targeting CCN proteins in rheumatoid arthritis and osteoarthritis. *Int. J. Mol. Sci.* 22, 4340. doi:10.3390/ijms22094340

Mannaerts, I., Leite, S. B., Verhulst, S., Claerhout, S., Eysackers, N., Thoen, L. F., et al. (2015). The Hippo pathway effector YAP controls mouse hepatic stellate cell activation. *J. Hepatol.* 63, 679–688. doi:10.1016/j.jhep.2015.04.011

Marshall, D. A., Pykerman, K., Werle, J., Lorenzetti, D., Wasylak, T., Noseworthy, T., et al. (2014). Hip resurfacing versus total hip arthroplasty: a systematic review comparing standardized outcomes. *Clin. Orthop. Relat. Res.* 472, 2217–2230. doi:10.1007/s11999-014-3556-3

Martel-Pelletier, J., Barr, A. J., Cicuttini, F. M., Conaghan, P. G., Cooper, C., Goldring, M. B., et al. (2016). Osteoarthritis. *Nat. Rev. Dis. Prim.* 2, 16072. doi:10.1038/nrdp.2016.72

McAlindon, T. E., Bannuru, R. R., Sullivan, M. C., Arden, N. K., Berenbaum, F., Bierma-Zeinstra, S. M., et al. (2014). OARSI guidelines for the non-surgical management of knee osteoarthritis. *Osteoarthr. Cartil.* 22, 363–388. doi:10.1016/j.joca.2014.01.003

Monroe, T. O., Hill, M. C., Morikawa, Y., Leach, J. P., Heallen, T., Cao, S., et al. (2019). YAP partially reprograms chromatin accessibility to directly induce adult cardiogenesis *in vivo*. *Dev. Cell* 48, 765–779. doi:10.1016/j.devcel.2019.01.017

Pan, X., Wu, B., Fan, X., Xu, G., Ou, C., and Chen, M. (2021). YAP accelerates vascular senescence via blocking autophagic flux and activating mTOR. *J. Cell Mol. Med.* 25, 170–183. doi:10.1111/jcmm.15902

Panda, D. K., Bai, X., Zhang, Y., Stylianesis, N. A., Koromilas, A. E., Lipman, M. L., et al. (2022). SCF-SKP2 E3 ubiquitin ligase links mTORC1/ER stress/ISR with YAP activation in murine renal cystogenesis. *J. Clin. Invest.* 132, e153943. doi:10.1172/JCI153943

Pemmari, A., Leppänen, T., Hämäläinen, M., Moilanen, T., Vuolteenaho, K., and Moilanen, E. (2020). Widespread regulation of gene expression by glucocorticoids in chondrocytes from patients with osteoarthritis as determined by RNA-Seq. *Arthritis Res. and Ther.* 22, 1–13. doi:10.1186/s13075-020-02289-7

Pinky, N., Salman, M., Kumar, P., Khan, M. A., Jamal, A., Parvez, S., et al. (2023). Age-related pathophysiological alterations in molecular stress markers and key modulators of hypoxia. *Ageing Res. Rev.* 90, 102022. doi:10.1016/j.arr.2023.102022

Prieto-Alhambra, D., Judge, A., Javaid, M. K., Cooper, C., Diez-Perez, A., and Arden, N. K. (2014). Incidence and risk factors for clinically diagnosed knee, hip and hand osteoarthritis: influences of age, gender and osteoarthritis affecting other joints. *Ann. Rheum. Dis.* 73, 1659–1664. doi:10.1136/annrheumdis-2013-203355

Qing, J., Ren, Y., Zhang, Y., Yan, M., Zhang, H., Wu, D., et al. (2022). Dopamine receptor D2 antagonism normalizes profibrotic macrophage-endothelial crosstalk in non-alcoholic steatohepatitis. *J. Hepatol.* 76, 394–406. doi:10.1016/j.jhep.2021.09.032

Raines, L. N., Zhao, H., Wang, Y., Chen, H. Y., Gallart-Ayala, H., Hsueh, P. C., et al. (2022). PERK is a critical metabolic hub for immunosuppressive function in macrophages. *Nat. Immunol.* 23, 431–445. doi:10.1038/s41590-022-01145-x

Ramazani, Y., Knops, N., Elmonem, M. A., Nguyen, T. Q., Arcolino, F. O., van den Heuvel, L., et al. (2018). Connective tissue growth factor (CTGF) from basics to clinics. *Matrix Biol.* 68-69, 44–66. doi:10.1016/j.matbio.2018.03.007

Rellmann, Y., Eidhof, E., and Dreier, R. (2021). Review: ER stress-induced cell death in osteoarthritic cartilage. *Cell Signal* 78, 109880. doi:10.1016/j.cellsig.2020.109880

Rudolf, M. A., Andreeva, A., Kozlowski, M. M., Kim, C. E., Moskowitz, B. A., Anaya-Rocha, A., et al. (2020). YAP mediates hair cell regeneration in balance organs of chickens, but LATS kinases suppress its activity in mice. *J. Neurosci.* 40, 3915–3932. doi:10.1523/JNEUROSCI.0306-20.2020

Saito, T., Fukai, A., Mabuchi, A., Ikeda, T., Yano, F., Ohba, S., et al. (2010). Transcriptional regulation of endochondral ossification by HIF-2alpha during skeletal growth and osteoarthritis development. *Nat. Med.* 16, 678–686. doi:10.1038/nm.2146

Setiawan, I., Sanjaya, A., Lesmana, R., Yen, P. M., and Goenawan, H. (2021). Hippo pathway effectors YAP and TAZ and their association with skeletal muscle ageing. *J. Physiol. Biochem.* 77, 63–73. doi:10.1007/s13105-021-00787-z

Shepard, N., and Mitchell, N. (1976). Simultaneous localization of proteoglycan by light and electron microscopy using toluidine blue O. A study of epiphyseal cartilage. *J. Histochem Cytochem* 24, 621–629. doi:10.1177/24.5.132503

Shome, D., von Woedtke, T., Riedel, K., and Masur, K. (2020). The HIPPO transducer YAP and its targets CTGF and Cyr61 drive a paracrine signalling in cold atmospheric plasma-mediated wound healing. *Oxid. Med. Cell Longev.* 2020, 4910280. doi:10.1155/2020/4910280

Sladitschek-Martens, H. L., Guarnieri, A., Brumana, G., Zanconato, F., Battilana, G., Xiccato, R. L., et al. (2022). YAP/TAZ activity in stromal cells prevents ageing by controlling cGAS-STING. *Nature* 607, 790–798. doi:10.1038/s41586-022-04924-6

Soul, J., Dunn, S. L., Anand, S., Serracino-Inglott, F., Schwartz, J.-M., Boot-Handford, R. P., et al. (2018). Stratification of knee osteoarthritis: two major patient subgroups identified by genome-wide expression analysis of articular cartilage. *Ann. rheumatic Dis.* 77, 423. doi:10.1136/annrheumdis-2017-212603

Sridharan, G., and Shankar, A. A. (2012). Toluidine blue: a review of its chemistry and clinical utility. *J. Oral Maxillofac. Pathol.* 16, 251–255. doi:10.4103/0973-029X.99081

Staines, K. A., Pollard, A. S., McGonnell, I. M., Farquharson, C., and Pitsillides, A. A. (2013). Cartilage to bone transitions in health and disease. *J. Endocrinol.* 219, R1–R12. doi:10.1530/JOE-13-0276

Sun, K., Guo, J., Guo, Z., Hou, L., Liu, H., Hou, Y., et al. (2023). The roles of the Hippo-YAP signalling pathway in Cartilage and Osteoarthritis. *Ageing Res. Rev.* 90, 102015. doi:10.1016/j.arr.2023.102015

Takada, K., Hirose, J., Senba, K., Yamabe, S., Oike, Y., Gotoh, T., et al. (2011). Enhanced apoptotic and reduced protective response in chondrocytes following endoplasmic reticulum stress in osteoarthritic cartilage. *Int. J. Exp. Pathol.* 92, 232–242. doi:10.1111/j.1365-2613.2010.00758.x

Takaguri, A., Kubo, T., Mori, M., and Satoh, K. (2017). The protective role of YAP1 on ER stress-induced cell death in vascular smooth muscle cells. *Eur. J. Pharmacol.* 815, 470–477. doi:10.1016/j.ejphar.2017.09.033

Tan, L., Register, T. C., and Yammani, R. R. (2020). Age-related decline in expression of molecular chaperones induces endoplasmic reticulum stress and chondrocyte apoptosis in articular cartilage. *Aging Dis.* 11, 1091–1102. doi:10.14336/AD.2019.1130

Tang, X., Muhammad, H., McLean, C., Miotla-Zarebska, J., Fleming, J., Didangelos, A., et al. (2018). Connective tissue growth factor contributes to joint homeostasis and osteoarthritis severity by controlling the matrix sequestration and activation of latent TGFβ. *Ann. Rheum. Dis.* 77, 1372–1380. doi:10.1136/annrheumdis-2018-212964

Taylor, R. C. (2016). Aging and the UPR(ER). *Brain Res.* 1648, 588–593. doi:10.1016/j.brainres.2016.04.017

Wang, J., Chen, M., Wang, M., Zhao, W., Zhang, C., Liu, X., et al. (2022). The novel ER stress inducer Sec C triggers apoptosis by sulfating ER cysteine residues and

degrading YAP via ER stress in pancreatic cancer cells. *Acta Pharm. Sin. B* 12, 210–227. doi:10.1016/j.apsb.2021.07.004

Wu, H., Wei, L., Fan, F., Ji, S., Zhang, S., Geng, J., et al. (2015). Integration of Hippo signalling and the unfolded protein response to restrain liver overgrowth and tumorigenesis. *Nat. Commun.* 6, 6239. doi:10.1038/ncomms7239

Xie, J., Wang, Y., Lu, L., Liu, L., Yu, X., and Pei, F. (2021). Cellular senescence in knee osteoarthritis: molecular mechanisms and therapeutic implications. *Ageing Res. Rev.* 70, 101413. doi:10.1016/j.arr.2021.101413

Yang, B., Sun, H., Song, F., Yu, M., Wu, Y., and Wang, J. (2017). YAP1 negatively regulates chondrocyte differentiation partly by activating the β-catenin signaling pathway. *Int. J. Biochem. Cell Biol.* 87, 104–113. doi:10.1016/j.biocel.2017.04.007

Yang, H., Wen, Y., Zhang, M., Liu, Q., Zhang, H., Zhang, J., et al. (2020). MTORC1 coordinates the autophagy and apoptosis signaling in articular chondrocytes in osteoarthritic temporomandibular joint. *Autophagy* 16, 271–288. doi:10.1080/15548627.2019.1606647

Yang, L., Tsang, K. Y., Tang, H. C., Chan, D., and Cheah, K. S. (2014). Hypertrophic chondrocytes can become osteoblasts and osteocytes in endochondral bone formation. *Proc. Natl. Acad. Sci. U. S. A.* 111, 12097–12102. doi:10.1073/pnas.1302703111

Yap, J., Chen, X., Delmotte, P., and Sieck, G. C. (2020). TNFα selectively activates the IRE1α/XBP1 endoplasmic reticulum stress pathway in human airway smooth muscle cells. *Am. J. Physiology-Lung Cell. Mol. Physiology* 318, L483–L493. doi:10.1152/ajplung.00212.2019

Yap, K. N., Yamada, K., Zikeli, S., Kiaris, H., and Hood, W. R. (2021). Evaluating endoplasmic reticulum stress and unfolded protein response through the lens of ecology and evolution. *Biol. Rev.* 96, 541–556. doi:10.1111/brv.12667

Zhang, C., Wang, F., Xie, Z., Chen, L., Sinkemani, A., Yu, H., et al. (2018). Dysregulation of YAP by the Hippo pathway is involved in intervertebral disc degeneration, cell contact inhibition, and cell senescence. *Oncotarget* 9, 2175–2192. doi:10.18632/oncotarget.23299

Zhang, H., Pasolli, H. A., and Fuchs, E. (2011). Yes-associated protein (YAP) transcriptional coactivator functions in balancing growth and differentiation in skin. *Proc. Natl. Acad. Sci. U. S. A.* 108, 2270–2275. doi:10.1073/pnas.1019603108

Zhang, Q., Fang, X., Zhao, W., and Liang, Q. (2019). The transcriptional coactivator YAP1 is overexpressed in osteoarthritis and promotes its progression by interacting with Beclin-1. *Gene* 689, 210–219. doi:10.1016/j.gene.2018.11.068

Zhang, X., Cai, D., Zhou, F., Yu, J., Wu, X., Yu, D., et al. (2020). Targeting downstream subcellular YAP activity as a function of matrix stiffness with Verteporfin-encapsulated chitosan microsphere attenuates osteoarthritis. *Biomaterials* 232, 119724. doi:10.1016/j.biomaterials.2019.119724

Zhang, Y., Tan, Y., Yuan, J., Tang, H., Zhang, H., Tang, Y., et al. (2024). circLIFR-007 reduces liver metastasis via promoting hnRNPA1 nuclear export and YAP phosphorylation in breast cancer. *Cancer Lett.* 592, 216907. doi:10.1016/j.canlet.2024.216907

Zhao, B., Ye, X., Yu, J., Li, L., Li, W., Li, S., et al. (2008). TEAD mediates YAP-dependent gene induction and growth control. *Genes Dev.* 22, 1962–1971. doi:10.1101/gad.1664408

Zhou, X., von der Mark, K., Henry, S., Norton, W., Adams, H., and de Crombrugghe, B. (2014). Chondrocytes transdifferentiate into osteoblasts in endochondral bone during development, postnatal growth and fracture healing in mice. *PLoS Genet.* 10, e1004820. doi:10.1371/journal.pgen.1004820

frontiers | Frontiers in Pharmacology

TYPE Review
PUBLISHED 07 January 2025
DOI 10.3389/fphar.2024.1501590

OPEN ACCESS

EDITED BY
Rain L. Wong,
University of North Carolina at Chapel Hill, United States

REVIEWED BY
Milind Ratnaparkhe,
ICAR Indian Institute of Soybean Research, India
Ismail Hadisoebroto Dilogo,
University of Indonesia, Indonesia

*CORRESPONDENCE
Kai Zhou,
zhoukai_wchp@wchscu.cn
Zongke Zhou,
zhouzongke@scu.edu.cn

RECEIVED 25 September 2024
ACCEPTED 09 December 2024
PUBLISHED 07 January 2025

CITATION
Tang H, Ling T, Zhao E, You M, Chen X, Chen G, Zhou K and Zhou Z (2025) The efficacy of core decompression combined with regenerative therapy in early femoral head necrosis: a systematic review and meta-analysis involving 954 subjects.
Front. Pharmacol. 15:1501590.
doi: 10.3389/fphar.2024.1501590

The efficacy of core decompression combined with regenerative therapy in early femoral head necrosis: a systematic review and meta-analysis involving 954 subjects

Haiwei Tang, Tingxian Ling, Enze Zhao, Mingke You, Xi Chen, Gang Chen, Kai Zhou* and Zongke Zhou*

Department of Orthopedics, West China Hospital, Sichuan University, Chengdu, Sichuan, China

Background: The debate continues on whether combining core decompression (CD) with regenerative therapy provides a more effective treatment for early femoral head necrosis than CD alone. This systematic review and meta-analysis endeavored to assess its efficacy.

Methods: We systematically searched PubMed, Web of Science, and Cochrane Library through July 2024 for RCTs and cohort studies evaluating the impact of core decompression (CD) with regenerative therapy versus CD alone in early-stage osteonecrosis (ARCO I, II or IIIa or Ficat I or II) of the femoral head (ONFH). Bias was evaluated using the Cochrane ROB 2.0 for RCTs and the Newcastle-Ottawa Scale (NOS) for cohort studies. The primary outcome was disease progression, measured by the incidence of staging advancement and total hip arthroplasty (THA) conversion. Clinical outcomes, including VAS, HHS, WOMAC, and Lequesne index, were secondary measures. Subgroup analyses were performed for variables such as age, BMI, follow-up period, and dosage in the bone marrow aspirate concentrate (BMAC) group, with results depicted in forest plots.

Results: This study represented a total of seven RCTs (mean follow-up time 36.57 months) and eight cohort trials (mean follow-up time 74.18 months) involving 954 hips. CD, when combined with agents, exhibited considerably enhanced efficacy over CD alone (risk ratio (RR) = 0.55 (95% CI 0.39–0.77), $p < 0.001$, $I^2 = 54\%$) and 0.59 (95% CI 0.43–0.81), $p = 0.001$, $I^2 = 51\%$), respectively). However, a significant difference was exclusive to the CD combined with BMAC group in terms of stage progression outcomes (stage progression, RR = 0.47 (95% CI 0.28–0.78), $p = 0.004$, $I^2 = 67\%$); THA conversions, RR = 0.41 (95% CI 0.32–0.52), $p < 0.001$, $I^2 = 43\%$). Secondary outcomes (VAS,

Abbreviations: ONFH, osteonecrosis of the femoral head; THA, total hip arthroplasty; CD, core decompression; BMAC, bone marrow aspirate concentrate; BMPs, bone morphogenetic proteins; PRP, platelet-rich plasma; BMSCs, bone mesenchymal stem cells; OB, osteoblasts; VAS, visual analog scale; HHS, Harris Hip Score; WOMAC, Western Ontario and McMaster Universities Osteoarthritis Index.

HHS, WOMAC score and Lequesne index) showed improved results when CD was combined with other regenerative agents, such as bone mesenchymal stem cells (BMSCs) and bone morphogenetic proteins (BMPs), etc. In the reported data, the regenerative group demonstrated significantly higher rates of subjective improvement in pain and functional outcomes compared to those in the CD group (71.74% (66/92) vs. 56.38% (53/94). Subgroup analysis revealed superior outcomes in the low-dose (less than 20 mL) BMAC group and patients aged under 40 years old in stage progression rate and THA conversion rate.

Conclusion: CD, when combined with regenerative therapy, can diminish hip pain and enhance functionality, but its ability to slow disease progression remains uncertain. BMAC presents a more substantiated efficacy evidence than other agents, with low-doses of BMAC in patients under 40 years potentially slowing ONFH progression. Nonetheless, the high heterogeneity and relatively short follow-up time of these studies make it difficult to draw accurate conclusions, which necessitates verification through future trials comparing CD versus CD combined with regenerative therapy, with a focus on extended follow-up periods.

Systematic Review Registration: identifier CRD42023467873.

KEYWORDS

osteonecrosis of the femoral head, core decompression, regenerative therapy, joint preservation surgery, meta-analysis

Introduction

Osteonecrosis of the femoral head (ONFH) is a pathological condition characterized by the localized demise of osteocytes and bone marrow elements, attributable to compromised arterial perfusion, venous stasis, or structural disruption of the femoral head (Wen et al., 2022). As a common and refractory disease in orthopedics, ONFH results in a huge economic burden worldwide. In the United States, the condition affects over 10,000 new patients annually and contributes to 10% of all hip arthroplasty (THA) (Mont et al., 2015). In Japan, the annual incidence rate was 1.91 per 100,000, which was estimated that there were around 2,400 cases per year from 2010 to 2013 (Ikeuchi et al., 2015). And the cumulative number of ONFH patients up to 8.12 million in 2013 in China (Zhao et al., 2015). The etiology of ONFH is multifactorial and individual-specific, which can be divided into two major categories: traumatic and nontraumatic. Major etiological factors of traumatic ONFH include femoral neck fracture, acetabular fracture, femoral head dislocation, and severe hip sprain or contusion, while nontraumatic ONFH is triggered by application of corticosteroid (the most common type), excessive alcohol consumption, decompression sickness, hemoglobin disease, autoimmune diseases (like systematic lupus erythematosus) and idiopathic diseases (Mont et al., 2020; Zhao et al., 2020; Zheng et al., 2022). Thus, heavy corticosteroid use and alcohol abuse are risk factors for ONFH. Additionally, smoking and obesity are also associated with an increased risk (Cao et al., 2016; Takahashi et al., 2012). While THA is the prevalent treatment for ONFH, there has been a notable shift towards head-preserving procedures, particularly core decompression (CD), especially favored for younger and more active demographics due to the anticipated need for a minimum of one revision post-THA, aseptic loosening and prosthesis wear (Mont et al., 2020; Ng et al., 2023). The fundamental rationale behind CD is to alleviate intramedullary pressure and bolster blood circulation, thereby fostering revascularization and osteogenesis at the affected site (Liu et al., 2018). Despite a consensus from a handful of small-scale randomized trials suggesting the superiority of CD over nonoperative interventions (Mont et al., 2020), the literature is replete with conflicting reports questioning the efficacy of CD in preventing femoral head collapse (Yoon et al., 2018; Chughtai et al., 2017). In a study of 1,206 hips CD patients, Mont et al. discovered that the necrosis of 36% of the cases continued to progress following CD alone (Mont et al., 1996). Hua et al. (2019) and Goodman (2000) also contended that mere CD is insufficient to halt the progression of ONFH, asserting that robust support for the subchondral bone is imperative. Moreover, CD's success is significantly higher in Ficat stages I and II than in stage III, underscoring its applicability primarily in the early phases of ONFH (Hua et al., 2019).

Given the potential for iatrogenic collapse in the drilled region following CD, it is imperative to consider robust support mechanisms (Hua et al., 2019; Goodman, 2000). Due to the limited availability of autologous or allogeneic bone grafts, as well as concerns regarding donor complications and immune rejection, there is a pressing need for innovative methodologies (Tang et al., 2024). Hernigou et al. (1999) demonstrated that both the quantity and functionality of bone mesenchymal stem cells (BMSCs) were diminished in patients with ONFH, thereby offering novel insights for researchers aiming to adjust the pathological microenvironment and facilitate bone regeneration through exogenous supplementation of these cells, ultimately providing necessary support. In 2004, A seminal study by Gangji et al. (2004) compared the standalone efficacy of CD to CD combined with bone marrow aspirate concentrate (BMAC), revealing that the latter combination was more effective in preventing collapse and ameliorating symptoms, which aroused wide concern. Therefore, BMAC may enhance the efficacy of CD by enhancing osteogenic ability and regulating the bone marrow

microenvironment (Calori et al., 2017). Recently, the advent of regenerative therapies such as BMSCs, bone morphogenetic proteins (BMPs), platelet-rich plasma (PRP), and osteoblasts (OB) has spurred the integration of these modalities with CD, presenting a promising strategy for ONFH management. However, the synergistic effects of combining CD with regenerative therapies are still under scrutiny, with diverse treatment agents yielding varied outcomes (Wang et al., 2024; Hu et al., 2023; Liu et al., 2021; Wang et al., 2023).

This systematic review and meta-analysis aims to critically assess the efficacy of combining CD with regenerative therapies versus CD alone in the prevention of femoral head collapse and alleviation of symptoms in patients with precollapsing or mild collapsed ONFH (ARCO stage I, II and IIIa or Ficat stage I and II). Additionally, we seek to identify patient characteristics that may predict a favorable response to CD combined with regenerative therapies through subgroup analysis. We hypothesize that the cohort receiving CD in conjunction with a regenerative agent will demonstrate improved therapeutic outcomes, particularly in terms of disease stage progression and clinical manifestations. We anticipate that younger individuals with lower body mass indices (BMIs) will derive greater benefits from this combined therapeutic approach.

Materials and methods

The present meta-analysis was conducted in adherence to the Preferred Reporting Items for Systematic Reviews and Meta-analysis (PRISMA) guidelines (Page et al., 2021) and Assessing of Multiple Systematic Reviews (AMSTAR) criteria (Shea et al., 2017). This study protocol was registered with PROSPERO (ID number: CRD42023467873), ensuring transparency and protocol adherence.

Search strategy

A comprehensive literature searched was performed in PubMed, Web of Science, and the Cochrane Library databases from their inception through 19 July 2024. The search strategy incorporated the following search terms: "osteonecrosis of the femoral head," "femoral head necrosis, " "femur head necrosis," "avascular necrosis in femoral head," "avascular necrosis of the femoral head," "cell therapy," "regenerative therapy," "regenerative therapies," "regeneration therapy," "BMAC," "bone marrow aspirate concentrate," "BMSCs," "bone mesenchymal stem cells," "MSCs," "mesenchymal stem cells," "PRP," "platelet-rich plasma," "OB," "osteoblasts," "core decompression," and "CD." No language restrictions were applied to the search.

Eligibility criteria

Study selection was based on a thorough review of abstracts and full texts. Inclusion criteria were as follows: 1) Population: Patients with nontraumatic femoral head necrosis in the ARCO stage I, II and IIIa or Ficat stage I and II, aged 18 years or older; 2) Intervention: Patient receiving CD combined with any regenerative treatment; 3) Comparator: Patients received CD alone; 4) Outcomes: Primary outcomes included the number of progressions to severe collapse (defined as progressive collapse of ≥2 mm within the follow-up period) (Osawa et al., 2021) and THA conversion; secondary outcomes included clinical outcomes [visual analog scale (Li et al., 2013) score, Harris Hip Score [HHS] score, Western Ontario and McMaster Universities Osteoarthritis Index [WOMAC] score and Lequesne Index (Lequesne et al., 1987)]. 5) Study design: Randomized controlled trials (RCTs) or cohort studies with a control group were included. Exclusion criteria were: 1) Patients with traumatic femoral head necrosis or in a severe collapsed (>2 mm) phase; 2) Animal studies; 3) Noncomparative studies, case reports, and case series; 4) Nonoriginal research such as reviews and technical reports; 5) Studies from which relevant data could not be extracted, and those that did not respond to requests for data from the original authors.

Data extraction

Data from eligible studies were extracted by two independent reviewers. The extracted data included the first author, publication year, study type, number of hips, patient characteristics, type of regenerative therapy, dosage of agents, follow-up duration, disease stage, and outcomes (number of hips progressing to collapse and THA conversion, VAS score, HHS score, WOMAC score, and Lequesne Index), excluding the late-stage cases (ARCO stage IIIb or IV). If the original text does not explicitly specify the precise value, specific data is extracted using Origin 2021 software from image. Graphical data were quantified using Plot Digitizer software (Version 2.6.8, Joseph Huwaldt and Scott Steinhorst) (Jelicic Kadic et al., 2016).

Quality assessment

The risk of bias in RCTs was assessed using the revised Cochrane risk of bias tool for randomized trials (RoB 2.0) (Sterne et al., 2019) which evaluates randomization process, deviations from intended interventions, missing outcome data, measurement of the outcome, selection of the reported result and overall bias. For non-RCT trials, six additional criteria based on NOS scale were used to assess the potential of bias: selection bias, detection bias, comparability, bias in measurement of outcomes, bias due to missing data, and adequacy of follow-up.

Outcome measures

In these included literature, the patients were all clinical visits during follow-up, and the researchers were responsible for data collection. The primary outcomes were the number of hips progressing to collapse and conversion to THA. Secondary outcomes included clinical outcomes. Subgroup analysis was conducted based on the type of regenerative agent, patient age, BMI, BMAC dosage, and mean follow-up duration (based on the mean statistical characteristics and follow-up time of the patients). Following Mao et al. (2020), patients were divided into subgroups based on age (under 40 years old being the ideal age group for stem

cell therapy). Additionally, based on a retrospective study (Pan et al., 2020), patients were categorized based on BMI (greater than 24 years old being associated with a higher risk of joint-preservation failure). BMAC dosage were artificially divided into three groups: low (less than 20 mL), medium (20–40 mL), and high (more than 40 mL), considering the approximate volume of ARCO stage III or IV femoral head necrosis (22 cm^3) (Hu et al., 2015). The mean follow-up duration was categorized into three subgroups: less than 24 months, 24–60 months, and more than 60 months.

Statistical analysis

All statistical analyses were performed using RevMan 5.4.1 software. Continuous data were presented as mean difference (MD) with 95% confidence interval (CI), while binary data were presented as risk ratio (RR) with 95% CI. Heterogeneity was assessed using the I^2 statistic with a value of 50% or higher indicating higher significant heterogeneity. The random effects model assumes that not only the effects vary across different studies, but also that their underlying true effects are drawn from a specific distribution. Consequently, it is capable of accommodating variations both within and between studies (Halme et al., 2023). Thus, the random effect model was used for $I^2 > 50\%$, and the fixed effect model was used for $I^2 < 50\%$. Subgroup analyses were conducted to compare efficacy of different BMAC dosage, age groups, BMIs and follow-up durations. Funnel plots were used to detect publication bias, and a $p < 0.05$ was considered statistically significant.

Results

Selection of included studies

The systematic search yielded a total of 830 articles, comprising 352 from the PubMed database and 478 from other databases, with duplicate articles subsequently removed. A total of 603 irrelevant articles were removed after the title and abstract were checked. Finally, 15 publications were eventually included in the study after the full-text reviews. The included studies compared CD alone versus CD combined with various regenerative therapies, including BMAC (Gangji et al., 2004; Boontanapibul et al., 2021; Cruz-Pardos et al., 2016; Gangji et al., 2011; Hernigou et al., 2018; Pepke et al., 2016; Tabatabaee et al., 2015), BMSCs (Kang et al., 2018; Nally et al., 2018), PRP (Aggarwal et al., 2021) and OB ect. (Jayankura et al., 2023; Liang et al., 2023; Martinot et al., 2020). Additionally, two studies compared CD combined with BMAC versus OB (Gangji et al., 2016; Hauzeur et al., 2020). In two of these studies, bone plugs were employed to seal the inlet of the pipe subsequent to injection in order to avert leakage of the regenerated agent (Tabatabaee et al., 2015; Aggarwal et al., 2021). To ensure the reliability of the results, we conducted subgroup analyses of regenerative agent therapies utilizing this specific approach as opposed to conventional regenerative agent therapies for the purpose of evaluating efficacy; Additionally, there was a study that incorporated regeneration agents with iliac bone particles into the channel, and thus it was excluded (Fu et al., 2022). Tables 1, 2 illustrate the characteristics of the included studies, and the study selection process is depicted in Figure 1.

Study characteristics

Our meta-analysis encompassed 15 studies that evaluated the efficacy of CD versus CD combined with regenerative therapies in 954 hip lesions. The majority of the studies involved sample sizes exceeding 20 hips (Boontanapibul et al., 2021; Cruz-Pardos et al., 2016; Gangji et al., 2011; Hernigou et al., 2018; Pepke et al., 2016; Tabatabaee et al., 2015; Kang et al., 2018; Nally et al., 2018; Aggarwal et al., 2021; Jayankura et al., 2023; Liang et al., 2023; Martinot et al., 2020; Gangji et al., 2016; Hauzeur et al., 2020), with a minimum follow-up of 12 months, an average patient age of 41.20 ± 11.13 and a mean BMI of 26.08 ± 4.60 kg/m^2. No significant differences between patients receiving CD alone versus those receiving CD combined with regenerative therapies. Staging systems varied across studies, with four utilizing Ficat staging (Cruz-Pardos et al., 2016; Nally et al., 2018; Aggarwal et al., 2021; Martinot et al., 2020), and the remaining eleven employing ARCO staging (Gangji et al., 2004; Boontanapibul et al., 2021; Gangji et al., 2011; Hernigou et al., 2018; Pepke et al., 2016; Tabatabaee et al., 2015; Kang et al., 2018; Jayankura et al., 2023; Liang et al., 2023; Gangji et al., 2016; Hauzeur et al., 2020). Clinical outcomes are assessed using the number of hips with stage progression and THA conversion, as well as the Visual Analog Scale (VAS), Harris Hip Score (HHS), Western Ontario and McMaster Universities Osteoarthritis Index (WOMAC) and Lequesne Index. Detailed study characteristics are summarized in Table 1, with two rows allocated to one study (Martinot et al., 2020) that utilized two comparison groups.

Assessment for risk of bias

Among the enrolled RCTs, two studies explicitly described the method of randomized sequence generation (Pepke et al., 2016; Hauzeur et al., 2020), while the remaining studies did not reported on this, but based on the ROB 2.0 tool algorithm, the randomization is low risk (Gangji et al., 2011; Tabatabaee et al., 2015; Aggarwal et al., 2021; Jayankura et al., 2023; Gangji et al., 2016). Allocation concealment was implemented in three studies (Tabatabaee et al., 2015; Jayankura et al., 2023; Hauzeur et al., 2020). Blinding of participants and personnel was conducted in three studies (Gangji et al., 2011; Tabatabaee et al., 2015; Jayankura et al., 2023), with one study not employing blinding (Hauzeur et al., 2020). In terms of blinding of outcome assessment, just one study was deemed to have a unclear risk of bias and its overall risk is moderate (Tabatabaee et al., 2015). All studies provided complete outcome reports and data, with no apparent sources of bias identified. Among the non-RCTs, only one study explicitly mentioned blinding of assessors (Gangji et al., 2004), leading to an unclear risk of bias for the remaining studies (Boontanapibul et al., 2021; Cruz-Pardos et al., 2016; Kang et al., 2018; Nally et al., 2018; Liang et al., 2023; Martinot et al., 2020). Three studies had unclear selection bias (Gangji et al., 2004; Cruz-Pardos et al., 2016; Liang et al., 2023). The risk of bias summary for the included studies is presented in Figures 2, 3. One RCT (Tabatabaee et al., 2015) was deemed to be of low quality due to

TABLE 1 Characteristics of included studies.

Study	Design	Level of evidence[a]	Intervention	Control (Drill diameter)	Dosage of agents	NO. of Hips (C/T)	Age (C/T) (SD)	BMI (Kg/m^2) (C/T) (SD)	Follow-up (month)	Disease Stage	Outcomes Primary	Secondary
Gangji et al. (2011)	Prospective, RCT	Ib	CD + BMAC	CD (NR)	49.7 mL	11/13	45.7 (2.8)/ 42.2 (2.6)	NR	60 m	ACRO I/II	Progression to collapse, THA conversion	VAS, Lequesne Index
Tabatabaee et al. (2015)	Prospective RCT	Ib	CD + BMAC (bone plugs)	CD (2.7 mm)	58 mL	9/12	26.8 (5.8)/ 31 (11.4)	NR	24 m	ACRO I/II	Progression to collapse, THA conversion	VAS, WOMAC
Pepke et al. (2016)	Prospective RCT	Ib	CD + BMAC	CD (5 mm)	10 mL	14/11	44.5 (3.3)/ 44.3 (3.4)	NR	24 m	ACRO I/II	THA conversion	VAS HHS
Aggarwal et al. (2021)	Prospective RCT	Ib	CD + PRP (bone plugs)	CD (10 mm)	8 mL	28/25	35.2 (12.5)/ 38.2 (10.4)	NR	64 m	Ficat I/II	Progression to collapse, THA conversion	HHS
Jayankura et al. (2023)	Prospective RCT	Ib	CD + OB	CD (NR)	5 mL	29/25	45 (10)/ 46 (10)	NR	12 m	ACRO I/II	Progression to collapse, THA conversion	HHS
Hauzeur et al. (2020)	Prospective RCT	Ib	CD + OB	CD + BMAC (3 mm)	40 mL	26/27	50 (12)/ 51 (10)	27 (5)/26 (5)	36 m	ACRO I/II	Progression to collapse, THA conversion	—
Gangji et al. (2016)	Prospective RCT	Ib	CD + OB	CD + BMAC (NR)	41 mL	30/30	50.6 (11.8)/ 50.6 (11.8)	NR	36 m	ACRO I/II	Progression to collapse	—
Boontanapibul et al. (2021)	Retrospective cohort	IIb	CD + BMAC	CD (3.2 mm)	5 mL	33/50	43 (10)/ 38 (13)	28 (6)/27 (5)	36 m	ACRO I/II/IIIa	Progression to collapse, THA conversion	—
Hernigou et al. (2018)	Prospective cohort	IIb	CD + BMAC	CD (4 mm)	20 mL	125/125	36 (7)/ 36 (7)	NR	300 m	ACRO I/II	Progression to collapse, THA conversion	VAS, HHS, WOMAC
Cruz-Pardos et al. (2016)	Retrospective cohort	IIb	CD + BMAC	CD (4 mm)	20 mL	19/41	38.9 (13)/ 43.3 (10.8)	NR	45 m	Ficat I/II	Progression to collapse, THA conversion	—

(Continued on following page)

10.3389/fphar.2024.1501590

TABLE 1 (*Continued*) Characteristics of included studies.

Study	Design	Level of evidence[a]	Intervention	Control (Drill diameter)	Dosage of agents	NO. of Hips (C/T)	Age (C/T) (SD)	BMI (Kg/m^2) (C/T) (SD)	Follow-up (month)	Disease Stage	Outcomes Primary	Secondary
Gangji et al. (2004)	Prospective cohort	IIb	CD + BMAC	CD (3 mm)	51 mL	8/10	48.8 (11.2)/ 40.9 (9.8)	NR	24 m	ACRO I/II	Progression to collapse, THA conversion	VAS, WOMAC, Lequesne Index
Kang et al. (2018)	Retrospective cohort	IIb	CD + BMSCs	CD (NR)	15 mL	30/30	47.3 (9.7)/ 46.0 (9.3)	24.0 (4.1)/ 23.8 (3.7)	51.36 m	ACRO I/II	Progression to collapse, THA conversion	—
Nally et al. (2018)	Retrospective cohort	IIb	CD + BMSCs	CD (7 mm)	NR	47/16	38.9 (10.1)/ 40.4 (12.8)	NR	72 m	Ficat I/II	THA conversion	—
Liang et al. (2023)	Retrospective cohort	IIb	CD + BMMC + PRP	CD (3 mm)	7 mL	20/24	37.5 (5.3)/ 36.4 (5.3)	25.59 (3.43)/ 25.11 (2.89)	41.1 m	ACRO I/II/IIIa	Progression to collapse, THA conversion	VAS, HHS
Martinot et al. (2020)	Retrospective cohort	IIb	CD + BM	CD (4.3 mm)	NR	23/40	41.06 (9.53)/ 43.23 (10.97)	26.27 (3.78)/ 27.24 (4.13)	24 m	Ficat I/II	THA conversion	HHS
Martinot et al. (2020)	Retrospective cohort	IIb	CD + BM + BMP	CD (4.3 mm)	NR	23/23	41.06 (9.53)/ 37.47 (10.10)	26.27 (3.78)/ 25.31 (4.17)	24 m	Ficat I/II	THA conversion	HHS

T, intervention group; C, control group; RCT, randomized clinical trial; CD, core decompression; BMAC, bone marrow aspirate concentrate; PRP, platelet-rich plasma; OB, osteoblast; BMSCs, bone marrow mesenchymal stem cells; BMMC, bone marrow mononuclear cell; BM, bone marrow; BMP, bone-morphogenetic protein; VAS, visual analog scale; HHS, harris hip score; WOMAC, Western Ontario and McMaster Universities Osteoarthritis Index; ARCO, association research circulation osseous; NR, not report.

[a]Oxford Centre for Evidence-based Medicine.

10.3389/fphar.2024.1501590

TABLE 2 Details of the outcomes of CD + BMAC vs. CD.

Outcomes	No. of studies	No. of hips	Statistical method	Pooled method	I^2	Effect size	*p*
Staging advancement							
1 Progression to collapse							
1.1 BMAC dose							
High dose	31 (Takahashi et al., 2012; Gangji et al., 2011; Tabatabaee et al., 2015)	63 (35 vs. 28)	RR (95% CI)	Fix, M-H	0%	0.19 [0.08, 0.46]	<0.001
Medium dose	2 (Cruz-Pardos et al., 2016; Hernigou et al., 2018)	310 (166 vs. 144)	RR (95% CI)	Random, M-H	90%	0.62 [0.24, 1.59]	0.320
Low dose	1 (Boontanapibul et al., 2021)	83 (50 vs. 33)	RR (95% CI)	Fix, M-H	NA	0.56 [0.34, 0.92]	0.020
Overall	6 (Gangji et al., 2004; Boontanapibul et al., 2021; Cruz-Pardos et al., 2016; Gangji et al., 2011; Hernigou et al., 2018; Tabatabaee et al., 2015)	456 (251 vs. 205)	RR (95% CI)	Random, M-H	67%	0.47 [0.28, 0.78]	0.004
1.2 Age							
Age >40	3 (Gangji et al., 2004; Cruz-Pardos et al., 2016; Gangji et al., 2011)	102 (64 vs. 38)	RR (95% CI)	Random, M-H	71%	0.47 [0.15, 1.46]	0.190
Age <40	3 (Boontanapibul et al., 2021; Hernigou et al., 2018; Tabatabaee et al., 2015)	354 (187 vs. 167)	RR (95% CI)	Fix, M-H	44%	0.40 [0.31, 0.52]	<0.001
Overall	6 (Gangji et al., 2004; Boontanapibul et al., 2021; Cruz-Pardos et al., 2016; Gangji et al., 2011; Hernigou et al., 2018; Tabatabaee et al., 2015)	456 (251 vs. 205)	RR (95% CI)	Random, M-H	67%	0.47 [0.28, 0.78]	0.004
1.3 Follow-up time							
<24 months	2 (Gangji et al., 2004; Tabatabaee et al., 2015)	39 (22 vs. 17)	RR (95% CI)	Fix, M-H	0%	0.10 [0.02, 0.50]	0.005
24–60 months	3 (Boontanapibul et al., 2021; Cruz-Pardos et al., 2016; Gangji et al., 2011)	167 (104 vs. 63)	RR (95% CI)	Random, M-H	61%	0.63 [0.35, 1.14]	0.130
>60 months	1 (Hernigou et al., 2018)	250 (125 vs. 125)	RR (95% CI)	Fix, M-H	NA	0.39 [0.29, 0.53]	<0.001
Overall	6 (Gangji et al., 2004; Boontanapibul et al., 2021; Cruz-Pardos et al., 2016; Gangji et al., 2011; Hernigou et al., 2018; Tabatabaee et al., 2015)	456 (251 vs. 205)	RR (95% CI)	Random, M-H	67%	0.47 [0.28, 0.78]	0.004
2 THA conversion							
2.1 BMAC dose							
High dose	3 (Gangji et al., 2004; Gangji et al., 2011; Tabatabaee et al., 2015)	63 (35 vs. 28)	RR (95% CI)	Fix, M-H	0%	0.35 [0.10, 1.23]	0.100
Medium dose	2 (Cruz-Pardos et al., 2016; Hernigou et al., 2018)	310 (166 vs. 144)	RR (95% CI)	Random, M-H	86%	0.50 [0.19, 1.35]	0.170
Low dose	2 (Boontanapibul et al., 2021; Pepke et al., 2016)	108 (61 vs. 47)	RR (95% CI)	Fix, M-H	0%	0.55 [0.35, 0.88]	0.010

(Continued on following page)

10.3389/fphar.2024.1501590

TABLE 2 (*Continued*) Details of the outcomes of CD + BMAC vs. CD.

Outcomes	No. of studies	No. of hips	Statistical method	Pooled method	I^2	Effect size	*p*
Overall	7 (Gangji et al., 2004; Boontanapibul et al., 2021; Cruz-Pardos et al., 2016; Gangji et al., 2011; Hernigou et al., 2018; Pepke et al., 2016; Tabatabaee et al., 2015)	481 (262 vs. 219)	RR (95% CI)	Fix, M-H	43%	0.41 [0.32, 0.52]	<0.001
2.2 Age							
Age >40	4 (Gangji et al., 2004; Cruz-Pardos et al., 2016; Gangji et al., 2011; Pepke et al., 2016)	127 (75 vs. 52)	RR (95% CI)	Fix, M-H	0%	0.73 [0.44, 1.22]	0.230
Age <40	3 (Boontanapibul et al., 2021; Hernigou et al., 2018; Tabatabaee et al., 2015)	354 (187 vs. 167)	RR (95% CI)	Fix, M-H	0%	0.35 [0.26, 0.46]	<0.001
Overall	7 (Gangji et al., 2004; Boontanapibul et al., 2021; Cruz-Pardos et al., 2016; Gangji et al., 2011; Hernigou et al., 2018; Pepke et al., 2016; Tabatabaee et al., 2015)	481 (262 vs. 219)	RR (95% CI)	Fix, M-H	43%	0.41 [0.32, 0.52]	<0.001
2.3 Follow-up time							
<24 months	3 (Gangji et al., 2004; Pepke et al., 2016; Tabatabaee et al., 2015)	64 (33 vs. 31)	RR (95% CI)	Fix, M-H	0%	0.55 [0.23, 1.33]	0.190
24–60 months	3 (Boontanapibul et al., 2021; Cruz-Pardos et al., 2016; Gangji et al., 2011)	167 (104 vs. 63)	RR (95% CI)	Fix, M-H	0%	0.61 [0.41, 0.90]	0.010
>60 months	1 (Hernigou et al., 2018)	250 (125 vs. 125)	RR (95% CI)	Fix, M-H	NA	0.32 [0.23, 0.44]	<0.001
Overall	7 (Gangji et al., 2004; Boontanapibul et al., 2021; Cruz-Pardos et al., 2016; Gangji et al., 2011; Hernigou et al., 2018; Pepke et al., 2016; Tabatabaee et al., 2015)	481 (262 vs. 219)	RR (95% CI)	Fix, M-H	43%	0.41 [0.32, 0.52]	<0.001
2.4 BMI							
BMI >24	3 (Boontanapibul et al., 2021; Liang et al., 2023; Martinot et al., 2020)	236 (137 vs. 99)	RR (95% CI)	Fix, M-H	0%	0.55 [0.38, 0.77]	<0.001
BMI <24	1 (Kang et al., 2018)	60 (30 vs. 30)	RR (95% CI)	Fix, M-H	NA	0.40 [0.18, 0.89]	0.020
Overall	4 (Boontanapibul et al., 2021; Kang et al., 2018; Liang et al., 2023; Martinot et al., 2020)	296 (167 vs. 129)	RR (95% CI)	Fix, M-H	0%	0.51 [0.37, 0.71]	<0.001
Clinical outcomes							
1 VAS score							
CD + BMAC	4 (Gangji et al., 2004; Gangji et al., 2011; Hernigou et al., 2018; Pepke et al., 2016)	317 (159 vs. 158)	MD (95% CI)	Random, I-V	91%	−15.87 [−24.43, −7.31]	<0.001
CD + BMSCs	2 (Tabatabaee et al., 2015; Kang et al., 2018)	81 (42 vs. 39)	MD (95% CI)	Random, I-V	96%	−7.23 [−24.97,10.50]	0.420

(Continued on following page)

10.3389/fphar.2024.1501590

TABLE 2 (*Continued*) Details of the outcomes of CD + BMAC vs. CD.

Outcomes	No. of studies	No. of hips	Statistical method	Pooled method	I^2	Effect size	*p*
CD + BMMC + PRP	1 (Liang et al., 2023)	44 (24 vs. 20)	MD (95% CI)	Fix, I-V	NA	−12.00 [−21.67, −2.33]	0.020
Overall	7 (Gangji et al., 2004; Gangji et al., 2011; Hernigou et al., 2018; Pepke et al., 2016; Tabatabaee et al., 2015; Kang et al., 2018; Liang et al., 2023)	442 (225 vs.217)	MD (95% CI)	Random, I-V	91%	−12.86 [−18.36, −7.36]	<0.001
2 HHS score							
CD + BMAC	2 (Hernigou et al., 2018; Pepke et al., 2016)	275 (136 vs. 139)	MD (95% CI)	Random, I-V	72%	8.99 [4.08, 13.90]	<0.001
CD + PRP	1 (Aggarwal et al., 2021)	53 (25 vs.28)	MD (95% CI)	Fix, I-V	NA	14.30 [8.42, 20.19]	<0.001
CD + BMMC + PRP	1 (Liang et al., 2023)	44 (24 vs. 20)	MD (95% CI)	Fix, I-V	NA	5.73 [1.60, 9.86]	0.007
Overall	4 (Hernigou et al., 2018; Pepke et al., 2016; Aggarwal et al., 2021; Liang et al., 2023)	372 (185 vs. 187)	MD (95% CI)	Random, I-V	72%	9.19 [5.69, 12.70]	<0.001
3 WOMAC score							
CD + BMAC	3 (Gangji et al., 2004; Hernigou et al., 2018; Tabatabaee et al., 2015)	289 (147 vs. 142)	MD (95% CI)	Random, I-V	98%	−10.78 [−21.08, −0.47]	0.040
CD + OB	1 (Jayankura et al., 2023)	44 (21 vs. 23)	MD (95% CI)	Fix, I-V	NA	4.00 [−11.09, 19.09]	0.600
Overall	4 (Gangji et al., 2004; Hernigou et al., 2018; Tabatabaee et al., 2015; Jayankura et al., 2023)	333 (168 vs. 165)	MD (95% CI)	Random, I-V	97%	−8.34 [−17.66, 0.98]	0.080
4 Lequesne Index							
CD + BMAC	2 (Gangji et al., 2004; Gangji et al., 2011)	42 (23 vs. 19)	MD (95% CI)	Random, I-V	63%	−3.39 [−4.96, −1.83]	<0.001

CD, core decompression; BMAC, bone marrow aspirate concentrate; PRP, platelet rich plasma; OB, osteoblast; BMSCs, bone marrow mesenchymal stem cells; BMMC, bone marrow mononuclear cell; VAS, visual analog scale; HHS, harris hip score; WOMAC, Western Ontario and McMaster Universities Osteoarthritis Index; CI, confidence interval; RR, relative risk; MD, mean difference; I–V, Inverse–Variance; M–H, Mantel–Haenszel. NA, not applicable.

10.3389/fphar.2024.1501590

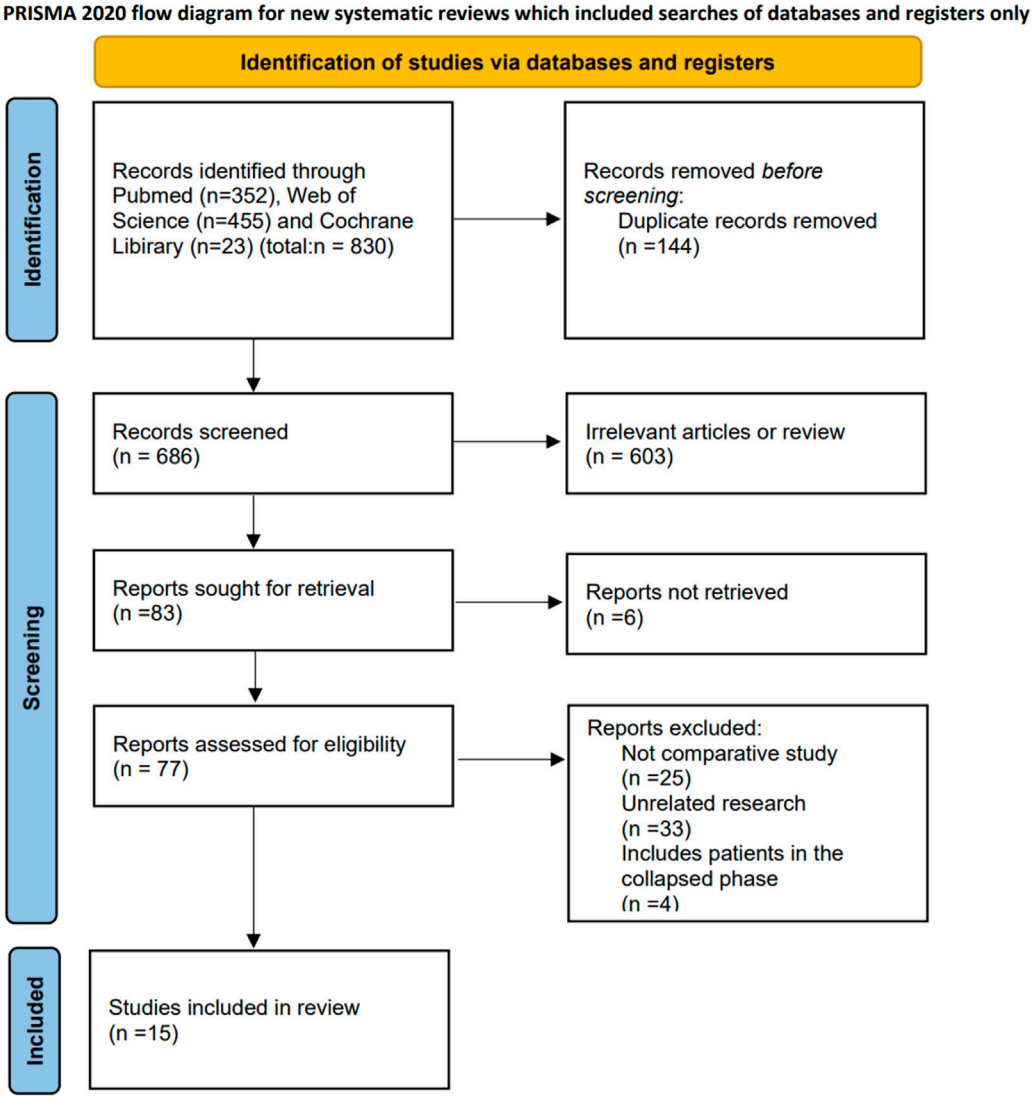

FIGURE 1
Flow chart of the search and search results.

its uncertain overall risk and two cohort studies (Cruz-Pardos et al., 2016; Liang et al., 2023) were also considered low-quality because of more than two uncertain risk assessments.

CD vs. CD combined with regenerative therapies outcomes

Stage advancement outcomes

Ten studies reported the number of hips that progressed to collapse (Gangji et al., 2004; Boontanapibul et al., 2021; Cruz-Pardos et al., 2016; Gangji et al., 2011; Hernigou et al., 2018; Tabatabaee et al., 2015; Kang et al., 2018; Aggarwal et al., 2021; Jayankura et al., 2023; Liang et al., 2023), and 14 studies reported the number of hips that underwent THA conversion (Gangji et al., 2004; Boontanapibul et al., 2021; Cruz-Pardos et al., 2016; Gangji et al., 2011; Hernigou et al., 2018; Pepke et al., 2016; Tabatabaee et al., 2015; Kang et al., 2018; Nally et al., 2018; Aggarwal et al., 2021; Jayankura et al., 2023; Liang et al., 2023; Martinot et al., 2020). The forest plots are displayed in Figures 4, 5. The pooled analysis indicated that CD combined with regenerative therapies demonstrated a significant improvement in efficacy compared to CD alone, with both progression (risk ratio (RR) = 0.55, 95% CI 0.39 to 0.77, $p < 0.001$, $I^2 = 54\%$) and THA conversion (RR = 0.59, 95% CI 0.43 to 0.81, $p = 0.001$, $I^2 = 51\%$) showing statistical significance. Given the uniqueness of the two studies (Tabatabaee et al., 2015; Aggarwal et al., 2021), bone plugs were employed to seal the entrance of the pipeline to avoid the leakage of the regeneration agent, which could potentially impact the test results. Consequently, we performed a subgroup analysis regarding the use of bone suppositories, and the outcomes still indicated that CD combined with the regeneration preparation was superior to CD alone, with both progression (RR = 0.57, 95% CI 0.40 to 0.81, $p = 0.002$, $I^2 = 59\%$) and THA conversion (RR = 0.60, 95% CI 0.42 to 0.87, $p =$

FIGURE 2
Risk of bias summary of RCTs: low risk of bias in green; some concerns of bias in yellow; high risk of bias in red.

0.007, I^2 = 61%) showing statistical significance (Supplementary Figures 4, 5). Then we conducted subgroup analysis of different regenerative agents, which revealed that only the CD combined with BMAC group exhibited a statistically significant improvement in efficacy for both outcomes, with RR = 0.47 (95% CI 0.28 to 0.78, p = 0.004, I^2 = 67%) and RR = 0.41 (95% CI 0.32 to 0.52, p < 0.001, I^2 = 43%), respectively. A funnel plot indicated the presence of significant publication bias (Supplementary Figures 2, 3). After excluding the three low-quality studies, the findings continued to demonstrate that CD combined regeneration therapy was superior to CD alone, in terms of progression (RR = 0.47, 95% CI 0.38 to 0.59, p < 0.001, I^2 = 37%) and THA conversion (RR = 0.59, 95% CI 0.41 to 0.86, p = 0.005, I^2 = 57%). Subgroup analysis also showed that only the BMAC group showed a statistically significant improvement with RR = 0.40 (95% CI 0.32 to 0.52, p < 0.001, I^2 = 0%) and RR = 0.37 (95% CI 0.29 to 0.48, p < 0.001, I^2 = 23%), respectively (Supplementary Figures 6, 7).

In the subgroup analysis of CD combined with BMAC, significant differences were observed between low- and high-dose groups in the number of hips progressing to collapse with RR = 0.56 (95% CI 0.34 to 0.92, p = 0.020, I^2 = 0%) and RR = 0.23 (95% CI 0.10 to 0.56, p = 0.001, I^2 = 0%). However, only the low-dose group showed statistically significant reductions in THA conversions (RR = 0.55, 95% CI 0.35 to 0.88, p = 0.010, I^2 = 0%). After removed the low-quality studies, both the low- and medium-dose group showed satisfactory efficacy (Supplementary Figures 13, 15). Furthermore, statistically significant differences in both staging progression and THA conversion were observed when the patient population was younger than 40 years old (RR = 0.40, 95% CI 0.31 to 0.52, p < 0.001, I^2 = 44% and RR = 0.35, 95% CI 0.26 to 0.46, p < 0.001, I^2 = 0%, respectively). Although there were no statistical differences in the two subgroups in staging progression after excluding the low-quality studies, only the patients who younger than 40 years old showed significant differences in THA conversion rate (RR = 0.35, 95% CI 0.26 to 0.46, p < 0.001, I^2 = 46%) (Supplementary Figures 17, 19). In the follow-up time subgroup, a statistically significant difference in the two primary outcomes was noted when the follow-up exceeded 60 months (RR = 0.47, 95% CI 0.28 to 0.78, p < 0.001, I^2 = 0%) and 0.41 (95% CI 0.32 to 0.52, p < 0.001, I^2 = 0%). However, when considering BMI, the difference was statistically significant regardless of whether BMI exceeded 24, with an overall RR of 0.51 (95% CI 0.37 to 0.71, p < 0.001, I^2 = 0%). After sensitivity analysis, the results of these two subgroups did not change (Table 2).

Clinical outcomes

Seven studies reported the VAS score, revealing a statistically significant difference favoring CD combined with regenerative therapies over CD alone. The CD alone group exhibited 12.86 points higher VAS scores than the CD combined with regenerative therapies group (95% CI -18.36 to −7.36, p < 0.001, I^2 = 91%). Four studies reported the HHS score, with a statistically significant difference observed between the two groups. The CD alone group had 9.19-point lower HHS score compared to the CD

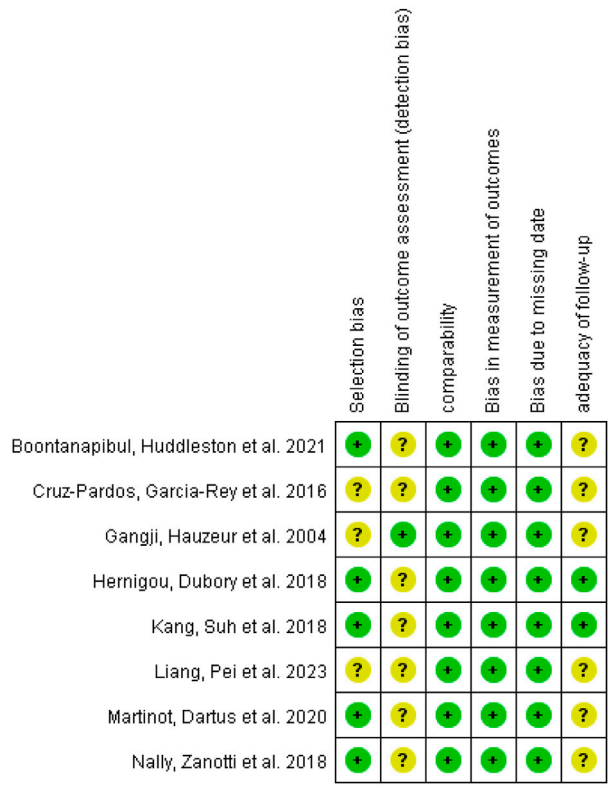

FIGURE 3
Risk of bias summary of non-RCTs: low risk of bias in green; unclear risk of bias in yellow; high risk of bias in red.

combined with regenerative therapies group (95% CI 5.69 to 12.70, $p < 0.001$, $I^2 = 72\%$). Four studies reported the WOMAC score, with no statistically significant difference found between CD alone and CD combined with regenerative therapies (mean difference, 8.34; 95% CI -17.66 to 0.98, $p = 0.080$, $I^2 = 97\%$). However, the CD combined with BMAC group had a 10.78-point lower than the CD group, which was statistically significant (95% CI 0.47 to 21.08, $p = 0.040$, $I^2 = 98\%$). The Lequesne Index was reported by two studies, both in the CD combined with BMAC group. The CD group had a 3.39-point higher Lequesne Index than the CD combined with BMAC group, with a statistically significant difference (95% CI -4.96 to −1.83, $p < 0.001$, $I^2 = 63\%$). After the three low-quality studies were removed, the results remain the same as before (Table 2).

CD combined with BMAC vs. CD combined with OB outcomes

Two studies reported the number of staging progressions, with a statistically significant difference favoring CD combined with OB (RR = 2.29, 95% CI 1.29 to 4.06, $p = 0.005$, $I^2 = 0\%$). Only one study reported the number of THA conversions, with no statistically significant difference observed (RR = 2.34, 95% CI 0.82 to 6.66, $p = 0.110$, $I^2 = 0\%$). One study reported the VAS score, with no statistically significant difference found between the CD combined with BMAC group and CD combined with OB group, despite a11.00-point lower VAS score in the former (95% CI -31.75 to 9.75, $p = 0.300$, $I^2 = 0\%$) (Table 3).

Discussion

ONFH is a prevalent condition that often leads to the dysfunction or functional loss of the hip joint in young individuals. While THA is the gold standard for treating end-stage ONFH, it is not ideal for younger individuals due to the risk of postoperative complications and limited durability (Zhao and Ma, 2020). Consequently, joint-preservation treatments are of significant value, especially for this demographic (Mont et al., 2020). However, the applicability of joint-preservation procedures is not uniform across all ONFH cases. A meta-analysis by Hua et al. highlighted the variability in success rates of CD at different stages of ONFH, with a notably low success rate of 27.44% in Ficat stage III (Hua et al., 2019). Similarly, Yuan's mid-to long-term cohort study reported a modest success rate of 33.33% for avascular fibular grafting in ARCO stage IIIb, in contrast to the 79.49% success rate observed in stages II and IIIa (Yuan et al., 2021). These findings suggest that joint-preservation procedures may be efficacious primarily in the early or mildly collapsed stages of the disease.

The landscape of joint-preservation surgical techniques is varied and includes CD, tantalum rods implantation, and both vascularized and nonvascularized bone grafts. Despite their availability, their efficacy remains a subject of debate. Porous tantalum rods were once considered an optimal mechanical substitute post-CD due to their superior strength, fatigue resistance, and biocompatibility (Zhang et al., 2013). However, due to suboptimal success rates and an increased risk of THA-related complications upon failure, their use has been phased out (Cheng et al., 2018; Olsen et al., 2016; Shuler et al., 2007; Tanzer et al., 2008). Bone graft offer an alternative form of support, with vascularized bone grafts providing the additional benefit of promoting healing through the reestablishment of blood supply (Kim et al., 2005). A network meta-analysis conducted by Hu et al. (2023) demonstrated the effectiveness of all bone grafting treatments. Nonetheless, the high technical demands and potential harvest-site morbidities, with prevalence rates of 13%–20%, limit their widespread adoption (Houdek et al., 2017; Barla et al., 2017).

In recent years, regenerative therapies, such as BMSCs and PRP, have gained prominence (Rodeo, 2023). BMSCs contribute to regeneration through direct differentiation and paracrine effects (Chang et al., 2021), while PRP significantly enhances the concentration and release of growth and differentiation factors at the site of damage, thus accelerating the body's natural healing process (Qian et al., 2020). These orthobiologics are straightforward to prepare and administer, prompting researchers to explore their combination with CD to enhance treatment efficacy. Li et al. (2024) conducted a network meta-analysis that subdivided regenerative agents into 6 types, revealing that only BMAC and BMSCs demonstrated superior efficacy. However, the BMAC study referenced in this article included only 245 hips and did not assess variations in BMAC dosage, hip functionality, or pain levels. Compared with this article, we further evaluated the most appropriate dose of BMAC, the age of the appropriate population, BMI, and its long-term efficacy. In addition, the sample size of the BMAC group was increased to 481 hips and the quality of life of patients was evaluated by VAS, HHS, and WOMAC scores. In two other meta-analysis, researchers also confirmed the effectiveness of cell therapy in enhancing the efficacy of CD (Li et al., 2023; Saini et al., 2023). However, in these two articles, several studies included

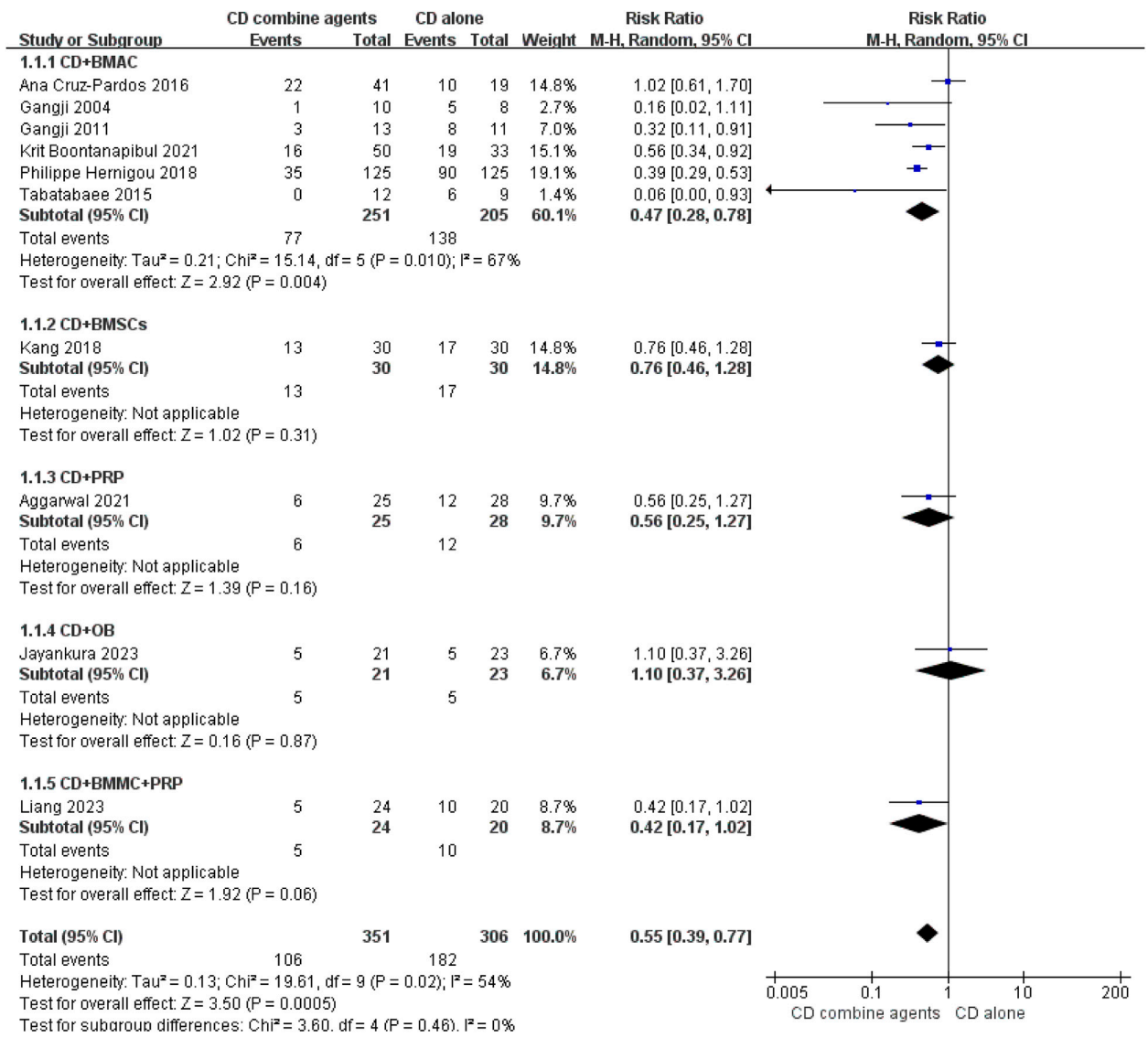

FIGURE 4
Efficacy of CD alone versus CD combined with agents. Outcome: stage progression.

utilized cell therapy in conjunction with bone grafts to provide mechanical support, which may compromise the comparability among studies. Furthermore, the inclusion of patients with ARCO stage III and IV in certain studies also undermined the reliability of their conclusions. In our studies, we only included patients in the early stage of ONFH, and excluded studies combined with bone grafting, which increased the reliability of the conclusion.

The collapse of the femoral head is a critical factor in determining the suitability of head preservation therapy for ONFH patients (Kuroda et al., 2019). We assessed the efficacy of specific treatment regimens using the number of hips that progressed to collapse and required THA as primary outcome indicators. A Study had suggested that CD combined with BMSCs or BMAC is more effective than CD alone (Wang et al., 2019a). Another systematic review by Han et al. published in 2020 found that PRP could improve treatment outcomes for patients with early-stage ONFH, both in combination with CD and other regimens (Han et al., 2020). However, recent research had not observed any additional benefits from combining CD with OB (Jayankura et al., 2023). Our results indicated that CD combined with BMAC group exhibited significant efficacy, with other regenerative therapies, such as BMSCs and PRP, failing to demonstrate satisfactory outcomes. The discrepancy may be attributed to the complex cellular composition of BMAC, which includes macrophages known to enhance MSC osteogenic differentiation (Kim and Hematti, 2009; Loi et al., 2016; Lu et al., 2017). The reference to BMAC as BMSCs may not be entirely accurate (Jeyaraman et al., 2021). Additionally, the limited number of studies and small sample sizes may have hindered the ability to draw accurate conclusions regarding the combination of CD with other regenerative agents. As noted previously, two articles employed bone plugs to seal the pipeline (Tabatabaee et al., 2015;

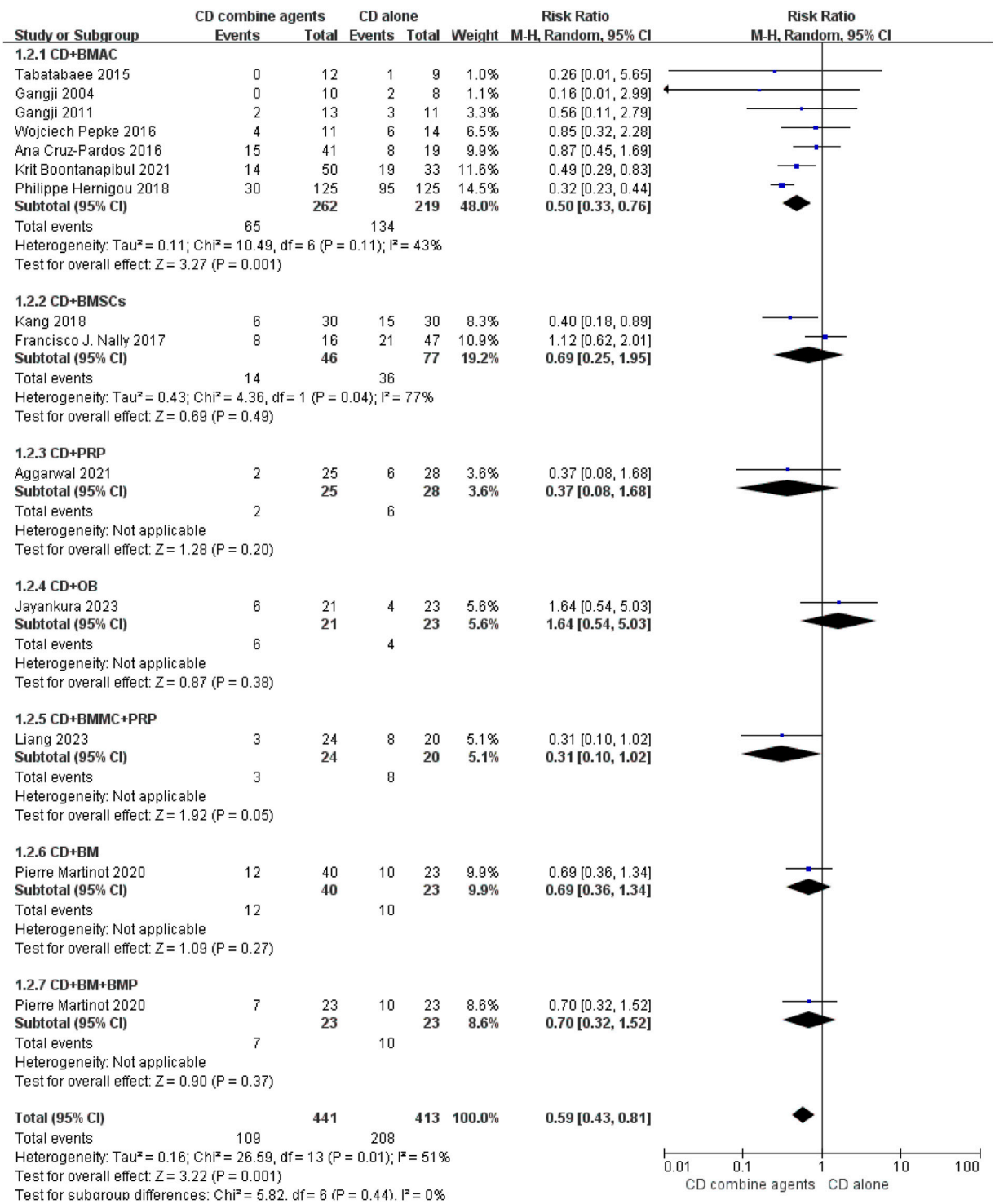

FIGURE 5
Efficacy of CD alone versus CD combined with agents, Outcome: Hip Number of THA conversion.

Aggarwal et al., 2021), which might have an impact on the accuracy of the results. Hence, a subgroup analysis was conducted. The subgroup analysis indicated that conventional regenerative therapy still demonstrated superior efficacy. However, the efficacy of the two studies involving the addition of bone suppositories remained ambiguous, potentially due to the small sample size. Interestingly, the article using bone plugs was deleted in the sensitivity analysis of BMAC, and the results did not change significantly. Therefore, bone plugs might only serve the function of preventing the extravasation of regenerative agents, and their supporting effect could be limited. The use of bone plugs in subsequent clinical practice is controversial, as the relationship

TABLE 3 Details of the outcomes of CD + BMAC vs. CD + OB.

Outcomes	No. of studies	No. of hips	Statistical method	Pooled method	I^2	Effect size	*p*
Staging advancement							
1 Progression to collapse	2 (Gangji et al., 2016; Hauzeur et al., 2020)	113 (56 vs. 57)	RR (95% CI)	Fix, M-H	0%	2.29 [1.29, 4.06]	0.005
2 THA conversion	1 (Hauzeur et al., 2020)	53 (26 vs. 27)	RR (95% CI)	Fix, M-H	NA	2.34 [0.82, 6.66]	0.110
Clinical outcomes							
1 VAS score	1 (Hauzeur et al., 2020)	53 (26 vs. 27)	MD (95% CI)	Fix, I-V	NA	−11.00 [−31.75, 9.75]	0.300

CD, core decompression; BMAC, bone marrow aspirate concentrate; OB, osteoblast; VAS, visual analog scale; CI, confidence interval; RR, relative risk; MD, mean difference; I-V, Inverse–Variance; M-H, Mantel–Haenszel; NA, not applicable.

between their benefits and the risk of complications remains uncertain.

The comparison between BMAC and OB did not yield a clear advantage for OB, with a 2023 RCT recommending against their combined use in ONFH treatment due to a lack of observed benefits (Jayankura et al., 2023). Despite decreased osteoblast activity being a pathological feature of ONFH (Maestro-Paramio et al., 2021), direct supplementation of osteoblasts has not proven feasible. Unfortunately, there are few studies that directly compare the efficacy of BMAC with other regenerative agents. Although they possess certain capacity for tissue repair, the majority of regenerating agents are not directly replenished by BMSCs, which may contribute to their failure. Thus, BMAC is considered a reliable regenerative therapy, but further trials are needed to confirm the effectiveness of other regenerative agents. Limitations in BMAC include variability in preparation techniques and a lack of consensus on optimal dosages. The ideal patient population for BMAC treatment remains undefined, as host factors such as age and BMI can influence the efficacy of regenerative therapeutics (Mao et al., 2020; Pan et al., 2020). To better define the optimal population and treatment efficacy, we conducted subgroup analyses based on BMAC dosage, age, BMI, and follow-up duration.

Given that the average necrotic volume for stage III femoral head necrosis is approximately 22 mL Hu et al. (2015), the injected dose should ideally be less than this volume to avoid increased pressure in the bone marrow cavity and potential leakage Our analysis stratified the BMAC dosage into three groups based on 20 mL increments. A study published latest suggested that a 20 mL BMAC dosage may yield better results (Wang et al., 2023), but it its inclusion of bone grafts alongside other studies introduces a confounding factor, leading to less robust conclusions. Our findings indicate that the low-dose BMAC group (less than 20 mL) exhibited a more favorable effect in mitigating the progression of femoral head necrosis. The determination of the optimal BMAC dosage necessitates further trials, and we propose that administering less than 20 mL of BMAC may be a prudent strategy. Moreover, MSC function is influenced by numerous factors, including the obese environment and host age, with a reduction in MSC function and quantity observed in both obese and older patients (Carvalho et al., 2021; Pham et al., 2023). A meta-analysis has identified patients under 40 years of age as an ideal population for stem cell treatments (Mao et al., 2020). Studies have also implicated a BMI exceeding 30 as an independent risk factor for imaging progression and THA conversion following CD plus BMAC (Hoogervorst et al., 2022). with a BMI over 24 conferring a 2.58-fold increased risk of joint preservation failure compared to patients with a BMI under 24 (Pan et al., 2020). Our subgroup analysis of age and BMI corroborated the enhanced efficacy of CD plus BMAC in patients under 40. However, no significant efficacy difference was noted for patients with a BMI over 24, possibly due to the majority of patients having a BMI above 24 but not meeting the obesity threshold (BMI >28), and the small sample size's potential influence on the outcomes. A study by Hernigou et al. (2018) with a follow-up of up to 25 years, demonstrated that CD plus BMAC improved disease prognosis (Osawa et al., 2021). Our findings align with this conclusion, although the efficacy of CD plus BMAC did not differ significantly in studies with follow-up periods of less than 24 months. This may indirectly suggest that CD

alone has improved the near-term prognosis of femoral head necrosis, offering a modestly meaningful effect.

PRP is a concentrated preparation of autologous plasma that not only encompasses a diverse array of growth factors conducive to bone induction and tissue regeneration, but also effectively eliminates inflammatory mediators to alleviate pain. Its elevated concentration of growth factors can stimulate the proliferation of osteoblasts and chondrocytes, while also facilitating neovascularization in necrosis regions to enhance blood supply. Consequently, PRP may represent a promising therapeutic approach for the management of ONFH (Su et al., 2022; Tong et al., 2018). However, the literature on PRP's use in ONFH is scarce, with only a few studies suggesting its potential in delaying ONFH progression. The small sample sizes in these studies preclude the drawing of definitive conclusions. Moreover, similar to BMAC, the lack of detailed reporting on PRP formulations hampers a comprehensive assessment of its efficacy (Chahla et al., 2017). Further research is imperative to establish the role of PRP in ONFH, with a need for clarification on PRP compositions. Osteoblasts play a crucial role in the formation of new bone, as they not only directly promote osteogenesis but also modulate osteoclast activity and angiogenesis in areas of necrosis (Chen et al., 2018). Preliminary studies have indicated that enhancing osteoblast function via upstream signaling pathways can ameliorate femoral head necrosis (Wang et al., 2019b; Tian et al., 2020). However, clinical applications remain relatively constrained. Future research ought to focus on conducting high-quality, large-scale studies to validate the efficacy of regenerative agents.

In terms of hip pain and function, our study's findings, in concordance with the majority of previous studies (Wang et al., 2023; Wang et al., 2019a), indicate that the combination of CD with regenerative therapies significantly improves hip pain and function metrics (VAS, HHS, WOMAC, and Lequesne Index). This suggests that the integration of regenerative therapies with CD is likely effective in enhancing hip pain and function. However, the lack of statistical significance in certain subgroups may be attributable to small sample sizes. A 2020 study by Hauzeur et al. comparing VAS scores between CD combined with BMAC and CD combined with OB found no significant difference, implying that OB does not offer additional benefits over BMAC in terms of hip pain and function (Hauzeur et al., 2020).

Besides, we performed a sensitivity analysis due to the heterogeneity of this study. There were no significant changes in the results of the two primary outcome measures and various hip functional scores after excluding the three low-quality studies. In the BMAC subgroup, after sensitivity analysis, the heterogeneity of the study was reduced but the conclusions did not change, indicating the reliability of the results. The only difference is that, following sensitivity analysis, moderate doses of BMAC also appear to exhibit some therapeutic effectiveness. This may be attributed to the limited number of studies, leading to conflicting results. Therefore, the optimal therapeutic dose of BMAC remains uncertain, but small doses of BMAC (less than 20 mL) are seemingly recommended.

In terms of safety, postoperative complications were reported in eight of all the included studies (Gangji et al., 2004; Gangji et al., 2011; Pepke et al., 2016; Tabatabaee et al., 2015; Jayankura et al., 2023; Martinot et al., 2020; Hauzeur et al., 2020; Fu et al., 2022). Among 311 hip joints, 26 patients expressed complaints of pain (8.36%), 2 patients presented with hematoma (0.64%), 8 patients experienced transient fever (2.57%), 2 patients had positive bone marrow bacterial culture but no infection (0.64%), and 1 patient suffered from postoperative fracture (0.32%). And there was no significant difference between the CD group and the CD combined regeneration therapy group. Additionally, among a total of 88 cases of hip joint in the BMAC-related study, 3 patients experienced pain (3.41%), 2 patients had positive bone marrow bacteriological culture but were not infected (2.27%), and 2 patients had hematoma (2.27%). These results indicate that both CD combined regenerative therapies and CD + BMAC possess a considerable safety profile, at least without elevating the risk of postoperative complications related to CD alone.

The strength of our meta-analysis lies in its comprehensive comparison of different regenerative therapies based on all available RCTs and cohort studies, providing an evidence-based foundation for the application of CD combined with regenerative therapies. Nevertheless, several limitations exist. The scarcity of research on CD combined with regenerative therapies other than BMAC prevents definitive conclusions. Variations in the type of regenerative agents, regenerative therapy preparation method, dose, and cell count, as well as large differences in the number of patients and baseline data from each study, make this study highly heterogeneous and may affect the reliability of the results, even though using random effects model. Future trials should standardize these variables. Additionally, the lack of data precluded an assessment of prognostic factors such as preoperative femoral head necrosis volume, etiologies, and gender. Subgroup analyses of these factors are necessary to guide clinical applications effectively. More clinical trials are warranted to identify independent risk factors affecting the prognosis of CD in early-stage ONFH patients and to further refine clinical practices. Finally, because there are few studies with long-term follow-up, relatively short follow-up times can also make conclusions unreliable. Longer follow-up studies are needed.

Conclusion

Our analysis of various randomized controlled trials and cohort studies suggests the combination of CD and regenerative therapies, particularly BMAC, can enhance pain relief and functional improvement in ONFH patients. However, current evidence suggests that only BMAC shows potential to delay the progression of ONFH. A low dosage of BMAC (less than 20 mL) for patients who under 40 may yield the most considerable efficacy. Similar future studies should focus on longer follow-up durations, the comparative analysis of efficacy variations across different doses or cell concentrations of regenerative agents, and the establishment of standardized procedures for regenerative preparation.

Author contributions

HT: Methodology, Conceptualization, Data curation, Formal Analysis, Writing–original draft. TL: Writing–original draft, Project administration, Software, Validation. EZ: Formal Analysis, Investigation, Visualization, Writing–original draft. MY: Project

administration, Resources, Supervision, Writing–original draft. XC: Conceptualization, Investigation, Resources, Writing–original draft. GC: Methodology, Resources, Writing–review and editing. KZ: Formal Analysis, Funding acquisition, Methodology, Validation, Writing–review and editing. ZZ: Funding acquisition, Methodology, Writing–review and editing.

Funding

The author(s) declare that financial support was received for the research, authorship, and/or publication of this article. The authors would like to thank the following funding sources: The National Natural Science Foundation of China (82002304, 82172394, U22A20280), The National Key Research and Development Program of China (2022YFC2503100 and 2022YFC2503104), 1.3.5 project for disciplines of excellence, West China Hospital, Sichuan University (2023HXFH012), Sichuan Science and Technology Department Key Research Projects (22ZDYF2639), Health Commission of Sichuan Province Program (21PJ038) and Sichuan University-Dazhou Municipal People's Government School-city Cooperation Special Fund Project (2022CDDZ-21).

Conflict of interest

The authors declare that the research was conducted in the absence of any commercial or financial relationships that could be construed as a potential conflict of interest.

Publisher's note

Supplementary material

The Supplementary Material for this article can be found online at: https://www.frontiersin.org/articles/10.3389/fphar.2024.1501590/full#supplementary-material

References

Aggarwal, A. K., Poornalingam, K., Jain, A., and Prakash, M. (2021). Combining platelet-rich plasma instillation with core decompression improves functional outcome and delays progression in early-stage avascular necrosis of femoral head: a 4.5- to 6-year prospective randomized comparative study. *J. arthroplasty* 36 (1), 54–61. doi:10.1016/j.arth.2020.07.010

Barla, M., Polirsztok, E., Peltié, E., Jouve, J. L., Legré, R., Dautel, G., et al. (2017). Free vascularised fibular flap harvesting in children: an analysis of donor-site morbidity. *Orthop. & traumatology, Surg. & Res. OTSR* 103 (7), 1109–1113. doi:10.1016/j.otsr.2017.05.009

Boontanapibul, K., Huddleston, J. I., 3rd, Amanatullah, D. F., Maloney, W. J., and Goodman, S. B. (2021). Modified kerboul angle predicts outcome of core decompression with or without additional cell therapy. *J. arthroplasty* 36 (6), 1879–1886. doi:10.1016/j.arth.2021.01.075

Calori, G. M., Mazza, E., Colombo, A., Mazzola, S., and Colombo, M. (2017). Core decompression and biotechnologies in the treatment of avascular necrosis of the femoral head. *EFORT open Rev.* 2 (2), 41–50. doi:10.1302/2058-5241.2.150006

Cao, H., Guan, H., Lai, Y., Qin, L., and Wang, X. (2016). Review of various treatment options and potential therapies for osteonecrosis of the femoral head. *J. Orthop. Transl.* 4, 57–70. doi:10.1016/j.jot.2015.09.005

Carvalho, M. S., Alves, L., Bogalho, I., Cabral, J. M. S., and da Silva, C. L. (2021). Impact of donor age on the osteogenic supportive capacity of mesenchymal stromal cell-derived extracellular matrix. *Orig. Res.* 9, 747521. doi:10.3389/fcell.2021.747521

Chahla, J., Cinque, M. E., Piuzzi, N. S., Mannava, S., Geeslin, A. G., Murray, I. R., et al. (2017). A call for standardization in platelet-rich plasma preparation protocols and composition reporting: a systematic review of the clinical orthopaedic literature. *J. bone Jt. Surg. Am. volume* 99 (20), 1769–1779. doi:10.2106/jbjs.16.01374

Chang, C., Yan, J., Yao, Z., Zhang, C., Li, X., and Mao, H. Q. (2021). Effects of mesenchymal stem cell-derived paracrine signals and their delivery strategies. *Adv. Healthc. Mater.* 10 (7), e2001689. doi:10.1002/adhm.202001689

Chen, X., Wang, Z., Duan, N., Zhu, G., Schwarz, E. M., and Xie, C. (2018). Osteoblast–osteoclast interactions. *Connect. Tissue Res.* 59 (2), 99–107. doi:10.1080/03008207.2017.1290085

Cheng, Q., Tang, J. L., Gu, J. J., Guo, K. J., Guo, W. S., Wang, B. L., et al. (2018). Total hip arthroplasty following failure of tantalum rod implantation for osteonecrosis of the femoral head with 5- to 10-year follow-up. *BMC Musculoskelet. Disord.* 19 (1), 289. doi:10.1186/s12891-018-2219-z

Chughtai, M., Piuzzi, N. S., Khlopas, A., Jones, L. C., Goodman, S. B., and Mont, M. A. (2017). An evidence-based guide to the treatment of osteonecrosis of the femoral head. *bone & Jt. J.* 99-b (10), 1267–1279. doi:10.1302/0301-620x.99b10.Bjj-2017-0233.R2

Cruz-Pardos, A., Garcia-Rey, E., Ortega-Chamarro, J. A., Duran-Manrique, D., and Gomez-Barrena, E. (2016). Mid-term comparative outcomes of autologous bone-marrow concentration to treat osteonecrosis of the femoral head in standard practice. *Hip Int. J. Clin. Exp. Res. hip pathology Ther.* 26 (5), 432–437. doi:10.5301/hipint.5000366

Fu, D., Qin, K., Yang, S., Lu, J., and Zhao, D. (2022). Autologous stem cells combined with core decompression on patients with osteonecrosis of the femoral head. Article. *Acta Medica Mediterr.* 38 (4), 2849–2858. doi:10.19193/0393-6384_2022_4_425

Gangji, V., De Maertelaer, V., and Hauzeur, J. P. (2011). Autologous bone marrow cell implantation in the treatment of non-traumatic osteonecrosis of the femoral head: five year follow-up of a prospective controlled study. *Bone* 49 (5), 1005–1009. doi:10.1016/j.bone.2011.07.032

Gangji, V., Hauzeur, J. P., Matos, C., De Maertelaer, V., Toungouz, M., and Lambermont, M. (2004). Treatment of osteonecrosis of the femoral head with implantation of autologous bone-marrow cells: a pilot study. Journal article. *J. bone Jt. Surg. Am. volume* 86 (6), 1153–1160. doi:10.2106/00004623-200406000-00006

Gangji, V., Toungouz, M., Lechanteur, C., Beguin, Y., Baudoux, E., Malaise, M., et al. (2016). Autologous osteoblastic cells versus concentrated bone marrow implantation in osteonecrosis of the femoral head: a randomized controlled single blind study. Journal article; Conference proceeding. *Ann. rheumatic Dis.* 75, 387. doi:10.1136/annrheumdis-2016-eular.1502

Goodman, S. B. (2000). Survival analysis of hips treated with core decompression or vascularized fibular grafting because of avascular necrosis. *J. bone Jt. Surg. Am. volume* 82 (2), 289.

Halme, A. L. E., McAlpine, K., and Martini, A. (2023). Fixed-effect versus random-effects models for meta-analyses: random-effects models. *Eur. Urol. focus* 9 (5), 693–694. doi:10.1016/j.euf.2023.10.023

Han, J., Gao, F., Li, Y., Ma, J., Sun, W., Shi, L., et al. (2020). The use of platelet-rich plasma for the treatment of osteonecrosis of the femoral head: a systematic review. *BioMed Res. Int.* 2020, 2642439. doi:10.1155/2020/2642439

Hauzeur, J. P., Lechanteur, C., Baudoux, E., De Maertelaer, V., Pather, S., Katz, R., et al. (2020). Did osteoblastic cell therapy improve the prognosis of pre-fracture osteonecrosis of the femoral head? A randomized, controlled trial. *Clin. Orthop. Relat. Res.* 478 (6), 1307–1315. doi:10.1097/corr.0000000000001107

Hernigou, P., Beaujean, F., and Lambotte, J. C. (1999). Decrease in the mesenchymal stem-cell pool in the proximal femur in corticosteroid-induced osteonecrosis. *J. bone Jt. Surg. Br.* 81 (2), 349–355. doi:10.1302/0301-620x.81b2.8818

Hernigou, P., Dubory, A., Homma, Y., Guissou, I., Flouzat Lachaniette, C. H., Chevallier, N., et al. (2018). Cell therapy versus simultaneous contralateral decompression in symptomatic corticosteroid osteonecrosis: a thirty year follow-up prospective randomized study of one hundred and twenty five adult patients. *Int. Orthop.* 42 (7), 1639–1649. doi:10.1007/s00264-018-3941-8

Hoogervorst, P., Campbell, J. C., Scholz, N., and Cheng, E. Y. (2022). Core decompression and bone marrow aspiration concentrate grafting for osteonecrosis

of the femoral head. *J. Bone Jt. Surg. Am.* 104 (Suppl. 2), 54–60. doi:10.2106/jbjs.20.00527

Houdek, M. T., Bayne, C. O., Bishop, A. T., and Shin, A. Y. (2017). The outcome and complications of vascularised fibular grafts. *bone & Jt. J.* 99-b (1), 134–138. doi:10.1302/0301-620x.99b1.Bjj-2016-0160.R1

Hu, L., Deng, X., Wei, B., Wang, J., and Hou, D. (2023). Comparative analysis of surgical interventions for osteonecrosis of the femoral head: a network meta-analysis of randomized controlled trials. *J. Orthop. Surg. Res.* 18 (1), 965. doi:10.1186/s13018-023-04463-4

Hu, L. B., Huang, Z. G., Wei, H. Y., Wang, W., Ren, A., and Xu, Y. Y. (2015). Osteonecrosis of the femoral head: using CT, MRI and gross specimen to characterize the location, shape and size of the lesion. *Br. J. radiology* 88 (1046), 20140508. doi:10.1259/bjr.20140508

Hua, K. C., Yang, X. G., Feng, J. T., Wang, F., Yang, L., Zhang, H., et al. (2019). The efficacy and safety of core decompression for the treatment of femoral head necrosis: a systematic review and meta-analysis. *J. Orthop. Surg. Res.* 14 (1), 306. doi:10.1186/s13018-019-1359-7

Ikeuchi, K., Hasegawa, Y., Seki, T., Takegami, Y., Amano, T., and Ishiguro, N. (2015). Epidemiology of nontraumatic osteonecrosis of the femoral head in Japan. *Mod. Rheumatol.* 25 (2), 278–281. doi:10.3109/14397595.2014.932038

Jayankura, M., Thomas, T., Seefried, L., Dubrana, F., Günther, K. P., Rondia, J., et al. (2023). Does adjunction of autologous osteoblastic cells improve the results of core decompression in early-stage femoral head osteonecrosis? A double-blind, randomized trial. Article. *Clin. Orthop. Relat. Res.* 481 (8), 1527–1540. doi:10.1097/corr.0000000000002610

Jelicic Kadic, A., Vucic, K., Dosenovic, S., Sapunar, D., and Puljak, L. (2016). Extracting data from figures with software was faster, with higher interrater reliability than manual extraction. *J. Clin. Epidemiol.* 74, 119–123. doi:10.1016/j.jclinepi.2016.01.002

Jeyaraman, M., Muthu, S., Jain, R., and Khanna, M. (2021). Autologous bone marrow derived mesenchymal stem cell therapy for osteonecrosis of femoral head: a systematic overview of overlapping meta-analyses. *J. Clin. Orthop. trauma* 13, 134–142. doi:10.1016/j.jcot.2020.11.015

Kang, J. S., Suh, Y. J., Moon, K. H., Park, J. S., Roh, T. H., Park, M. H., et al. (2018). Clinical efficiency of bone marrow mesenchymal stem cell implantation for osteonecrosis of the femoral head: a matched pair control study with simple core decompression. *Stem cell Res. & Ther.* 9 (1), 274. doi:10.1186/s13287-018-1030-y

Kim, J., and Hematti, P. (2009). Mesenchymal stem cell-educated macrophages: a novel type of alternatively activated macrophages. *Exp. Hematol.* 37 (12), 1445–1453. doi:10.1016/j.exphem.2009.09.004

Kim, S. Y., Kim, Y. G., Kim, P. T., Ihn, J. C., Cho, B. C., and Koo, K. H. (2005). Vascularized compared with nonvascularized fibular grafts for large osteonecrotic lesions of the femoral head. *J. bone Jt. Surg. Am. volume* 87 (9), 2012–2018. doi:10.2106/jbjs.D.02593

Kuroda, Y., Tanaka, T., Miyagawa, T., Kawai, T., Goto, K., Tanaka, S., et al. (2019). Classification of osteonecrosis of the femoral head. *Bone Jt. Res.* 8 (10), 451–458. doi:10.1302/2046-3758.810.Bjr-2019-0022.R1

Lequesne, M. G., Mery, C., Samson, M., and Gerard, P. (1987). Indexes of severity for osteoarthritis of the hip and knee. Validation--value in comparison with other assessment tests. *Scand. J. rheumatology Suppl.* 65, 85–89. doi:10.3109/03009748709102182

Li, H., Usas, A., Poddar, M., Chen, C. W., Thompson, S., Ahani, B., et al. (2013). Platelet-rich plasma promotes the proliferation of human muscle derived progenitor cells and maintains their stemness. *PloS one* 8 (6), e64923. doi:10.1371/journal.pone.0064923

Li, M., Chen, D., Ma, Y., Zheng, M., and Zheng, Q. (2023). Stem cell therapy combined with core decompression versus core decompression alone in the treatment of avascular necrosis of the femoral head: a systematic review and meta-analysis. *J. Orthop. Surg. Res.* 18 (1), 560. doi:10.1186/s13018-023-04025-8

Li, Y., Ma, X., Dong, B., Li, Y., and Liang, Z. (2024). Network meta-analysis of invasive treatment for early-stage osteonecrosis of the femoral head. *J. Orthop. Surg. Res.* 19 (1), 30. doi:10.1186/s13018-023-04513-x

Liang, D., Pei, J., Zhang, X., and Chen, X. (2023). Clinical outcomes of autologous platelet-rich plasma and bone marrow mononuclear cells grafting combined with core decompression for Association Research Circulation Osseous II-IIIA stage non-traumatic osteonecrosis of the femoral head. *Int. Orthop.* 47 (9), 2181–2188. doi:10.1007/s00264-023-05779-w

Liu, L., Gao, F., Sun, W., Wang, Y., Zhang, Q., Wang, B., et al. (2018). Investigating clinical failure of core decompression with autologous bone marrow mononuclear cells grafting for the treatment of non-traumatic osteonecrosis of the femoral head. *Int. Orthop.* 42 (7), 1575–1583. doi:10.1007/s00264-018-3918-7

Liu, Q., Guo, W., Li, R., and Lee, J. H. (2021). Efficacy of various core decompression techniques versus non-operative treatment for osteonecrosis of the femoral head: a systemic review and network meta-analysis of randomized controlled trials. *BMC Musculoskelet. Disord.* 22 (1), 948. doi:10.1186/s12891-021-04808-2

Loi, F., Córdova, L. A., Zhang, R., Pajarinen, J., Lin, T. h., Goodman, S. B., et al. (2016). The effects of immunomodulation by macrophage subsets on osteogenesis *in vitro*. *Stem cell Res. & Ther.* 7, 15. doi:10.1186/s13287-016-0276-5

Lu, L. Y., Loi, F., Nathan, K., Lin, T. H., Pajarinen, J., Gibon, E., et al. (2017). Pro-inflammatory M1 macrophages promote Osteogenesis by mesenchymal stem cells via the COX-2-prostaglandin E2 pathway. *J. Orthop. Res. official Publ. Orthop. Res. Soc.* 35 (11), 2378–2385. doi:10.1002/jor.23553

Maestro-Paramio, L., García-Rey, E., Bensiamar, F., and Saldaña, L. (2021). Osteoblast function in patients with idiopathic osteonecrosis of the femoral head: implications for a possible novel therapy. *Bone Jt. Res.* 10 (9), 619–628. doi:10.1302/2046-3758.109.Bjr-2021-0016.R1

Mao, L., Jiang, P., Lei, X., Ni, C., Zhang, Y., Zhang, B., et al. (2020). Efficacy and safety of stem cell therapy for the early-stage osteonecrosis of femoral head: a systematic review and meta-analysis of randomized controlled trials. *Stem cell Res. & Ther.* 11 (1), 445. doi:10.1186/s13287-020-01956-5

Martinot, P., Dartus, J., Leclerc, J. T., Putman, S., Girard, J., and Migaud, H. (2020). Hip survival after plain core decompression alone versus bone morphogenetic protein and/or bone marrow reinjection with core decompression for avascular osteonecrosis of the femoral head: a retrospective case control study in ninety two patients. *Int. Orthop.* 44 (11), 2275–2282. doi:10.1007/s00264-020-04692-w

Mont, M. A., Carbone, J. J., and Fairbank, A. C. (1996). Core decompression versus nonoperative management for osteonecrosis of the hip. *Clin. Orthop. Relat. Res.* 324, 169–178. doi:10.1097/00003086-199603000-00020

Mont, M. A., Cherian, J. J., Sierra, R. J., Jones, L. C., and Lieberman, J. R. (2015). Nontraumatic osteonecrosis of the femoral head: where do we stand today? A ten-year update. *J. bone Jt. Surg. Am. volume* 97 (19), 1604–1627. doi:10.2106/jbjs.O.00071

Mont, M. A., Salem, H. S., Piuzzi, N. S., Goodman, S. B., and Jones, L. C. (2020). Nontraumatic osteonecrosis of the femoral head: where do we stand today? a 5-year update. *J. bone Jt. Surg. Am. volume* 102 (12), 1084–1099. doi:10.2106/jbjs.19.01271

Nally, F. J., Zanotti, G., Buttaro, M. A., Diaz Dilernia, F., Mansilla, I. G., Comba, F. M., et al. (2018). THA conversion rate comparing decompression alone, with autologous bone graft or stem cells in osteonecrosis. *Hip Int. J. Clin. Exp. Res. hip pathology Ther.* 28 (2), 189–193. doi:10.5301/hipint.5000552

Ng, M. K., Gordon, A. M., Piuzzi, N. S., Wong, C. H. J., Jones, L. C., and Mont, M. A. (2023). Trends in surgical management of osteonecrosis of the femoral head: a 2010 to 2020 nationwide study. *J. arthroplasty* 38 (7s), S51–s57. doi:10.1016/j.arth.2023.03.071

Olsen, M., Lewis, P. M., Morrison, Z., McKee, M. D., Waddell, J. P., and Schemitsch, E. H. (2016). Total hip arthroplasty following failure of core decompression and tantalum rod implantation. *bone & Jt. J.* 98-b (9), 1175–1179. doi:10.1302/0301-620x.98b9.37252

Osawa, Y., Seki, T., Takegami, Y., Makida, K., Ochiai, S., and Imagama, S. (2021). Collapse progression or cessation affects the natural history of contralateral osteonecrosis of the femoral head. *J. arthroplasty* 36 (12), 3839–3844. doi:10.1016/j.arth.2021.08.005

Page, M. J., McKenzie, J. E., Bossuyt, P. M., Boutron, I., Hoffmann, T. C., Mulrow, C. D., et al. (2021). The PRISMA 2020 statement: an updated guideline for reporting systematic reviews. *Int. J. Surg. Lond. Engl.* 88, 105906. doi:10.1016/j.ijsu.2021.105906

Pan, J., Ding, Q., Lv, S., Xia, B., Jin, H., Chen, D., et al. (2020). Prognosis after autologous peripheral blood stem cell transplantation for osteonecrosis of the femoral head in the pre-collapse stage: a retrospective cohort study. *Stem cell Res. & Ther.* 11 (1), 83. doi:10.1186/s13287-020-01595-w

Pepke, W., Kasten, P., Beckmann, N. A., Janicki, P., and Egermann, M. (2016). Core decompression and autologous bone marrow concentrate for treatment of femoral head osteonecrosis: a randomized prospective study. *Orthop. Rev.* 8 (1), 6162. doi:10.4081/or.2016.6162

Pham, D.-V., Nguyen, T.-K., and Park, P.-H. (2023). Adipokines at the crossroads of obesity and mesenchymal stem cell therapy. *Exp. & Mol. Med.* 55 (2), 313–324. doi:10.1038/s12276-023-00940-2

Qian, Z., Wang, H., Bai, Y., Wang, Y., Tao, L., Wei, Y., et al. (2020). Improving chronic diabetic wound healing through an injectable and self-healing hydrogel with platelet-rich plasma release. *ACS Appl. Mater Interfaces* 12 (50), 55659–55674. doi:10.1021/acsami.0c17142

Rodeo, S. A. (2023). Orthobiologics: current status in 2023 and future outlook. *Future Outlook* 31 (12), 604–613. doi:10.5435/jaaos-d-22-00808

Saini, U., Jindal, K., Rana, A., Aggarwal, S., Kumar, P., and Sharma, S. (2023). Core decompression combined with intralesional autologous bone marrow derived cell therapies for osteonecrosis of the femoral head in adults: a systematic review and meta-analysis. *Surg. J. R. Coll. Surg. Edinb. Irel.* 21 (3), e104–e117. doi:10.1016/j.surge.2022.04.010

Shea, B. J., Reeves, B. C., Wells, G., Thuku, M., Hamel, C., Moran, J., et al. (2017). AMSTAR 2: a critical appraisal tool for systematic reviews that include randomised or non-randomised studies of healthcare interventions, or both. *BMJ Clin. Res. ed* 358, j4008. doi:10.1136/bmj.j4008

Shuler, M. S., Rooks, M. D., and Roberson, J. R. (2007). Porous tantalum implant in early osteonecrosis of the hip: preliminary report on operative, survival, and outcomes results. *J. arthroplasty* 22 (1), 26–31. doi:10.1016/j.arth.2006.03.007

Sterne, J. A. C., Savović, J., Page, M. J., Elbers, R. G., Blencowe, N. S., Boutron, I., et al. (2019). RoB 2: a revised tool for assessing risk of bias in randomised trials. *BMJ Clin. Res. ed* 366, l4898. doi:10.1136/bmj.l4898

Su, C. A., Jildeh, T. R., Vopat, M. L., Waltz, R. A., Millett, P. J., Provencher, M. T., et al. (2022). Current state of platelet-rich plasma and cell-based therapies for the treatment of osteoarthritis and tendon and ligament injuries. *J. bone Jt. Surg. Am. volume* 104 (15), 1406–1414. doi:10.2106/jbjs.21.01112

Tabatabaee, R. M., Saberi, S., Parvizi, J., Mortazavi, S. M., and Farzan, M. (2015). Combining concentrated autologous bone marrow stem cells injection with core decompression improves outcome for patients with early-stage osteonecrosis of the femoral head: a comparative study. *J. arthroplasty* 30 (9 Suppl. l), 11–15. doi:10.1016/j.arth.2015.06.022

Takahashi, S., Fukushima, W., Kubo, T., Iwamoto, Y., Hirota, Y., and Nakamura, H. (2012). Pronounced risk of nontraumatic osteonecrosis of the femoral head among cigarette smokers who have never used oral corticosteroids: a multicenter case-control study in Japan. *J. Orthop. Sci. official J. Jpn. Orthop. Assoc.* 17 (6), 730–736. doi:10.1007/s00776-012-0293-x

Tang, H., Zhao, E., Lai, Y., Chen, A., Chen, X., Zeng, W., et al. (2024). 3D bioprinting techniques and hydrogels for osteochondral integration regeneration. *Int. J. Bioprint.* 0, 4472. doi:10.36922/ijb.4472

Tanzer, M., Bobyn, J. D., Krygier, J. J., and Karabasz, D. (2008). Histopathologic retrieval analysis of clinically failed porous tantalum osteonecrosis implants. *J. bone Jt. Surg. Am. volume* 90 (6), 1282–1289. doi:10.2106/jbjs.F.00847

Tian, L., Sun, S., Li, W., Yuan, L., and Wang, X. (2020). Down-regulated microRNA-141 facilitates osteoblast activity and inhibits osteoclast activity to ameliorate osteonecrosis of the femoral head via up-regulating TGF-β2. *Cell cycleGeorget. Tex* 19 (7), 772–786. doi:10.1080/15384101.2020.1731053

Tong, S., Yin, J., and Liu, J. (2018). Platelet-rich plasma has beneficial effects in mice with osteonecrosis of the femoral head by promoting angiogenesis. *Exp. Ther. Med.* 15 (2), 1781–1788. doi:10.3892/etm.2017.5655

Wang, C., Sun, W., Ling, S., Wang, Y., Wang, X., Meng, H., et al. (2019b). AAV-Anti-miR-214 prevents collapse of the femoral head in osteonecrosis by regulating osteoblast and osteoclast activities. *Mol. Ther. Nucleic acids* 18, 841–850. doi:10.1016/j.omtn.2019.09.030

Wang, J., Xu, P., and Zhou, L. (2023). Comparison of current treatment strategy for osteonecrosis of the femoral head from the perspective of cell therapy. *Front. cell Dev. Biol.* 11, 995816. doi:10.3389/fcell.2023.995816

Wang, X., Hu, L., Wei, B., Wang, J., Hou, D., and Deng, X. (2024). Regenerative therapies for femoral head necrosis in the past two decades: a systematic review and network meta-analysis. *Stem cell Res. & Ther.* 15 (1), 21. doi:10.1186/s13287-024-03635-1

Wang, Z., Sun, Q. M., Zhang, F. Q., Wang, L. G., and Wang, W. J. (2019a). Core decompression combined with autologous bone marrow stem cells versus core decompression alone for patients with osteonecrosis of the femoral head: a meta-analysis. *Int. J. Surg. Lond. Engl.* 69, 23–31. doi:10.1016/j.ijsu.2019.06.016

Wen, Z., Li, Y., Cai, Z., Fan, M., Wang, J., Ding, R., et al. (2022). Global trends and current status in osteonecrosis of the femoral head: a bibliometric analysis of publications in the last 30 years. *Orig. Res.* 13, 897439. doi:10.3389/fendo.2022.897439

Yoon, B.-H., Lee, Y.-K., Kim, K.-C., Ha, Y.-C., and Koo, K.-H. (2018). No differences in the efficacy among various core decompression modalities and non-operative treatment: a network meta-analysis. *Int. Orthop.* 42 (12), 2737–2743. doi:10.1007/s00264-018-3977-9

Yuan, P., Liu, X., Du, B., Sun, G. Q., Wang, X., and Lin, X. Y. (2021). Mid-to long-term results of modified avascular fibular grafting for ONFH. *J. hip Preserv. Surg.* 8 (3), 274–281. doi:10.1093/jhps/hnab046

Zhang, Y., Li, L., Shi, Z. J., Wang, J., and Li, Z. H. (2013). Porous tantalum rod implant is an effective and safe choice for early-stage femoral head necrosis: a meta-analysis of clinical trials. *Eur. J. Orthop. Surg. & traumatology Orthop. traumatologie* 23 (2), 211–217. doi:10.1007/s00590-012-0962-7

Zhao, D., and Ma, Z. (2020). Application of biomaterials for the repair and treatment of osteonecrosis of the femoral head. *Regen. Biomater.* 7 (1), 1–8. doi:10.1093/rb/rbz048

Zhao, D., Zhang, F., Wang, B., Liu, B., Li, L., Kim, S. Y., et al. (2020). Guidelines for clinical diagnosis and treatment of osteonecrosis of the femoral head in adults (2019 version). *J. Orthop. Transl.* 21, 100–110. doi:10.1016/j.jot.2019.12.004

Zhao, D. W., Yu, M., Hu, K., Wang, W., Yang, L., Wang, B. J., et al. (2015). Prevalence of nontraumatic osteonecrosis of the femoral head and its associated risk factors in the Chinese population: results from a nationally representative survey. *Chin. Med. J.* 128 (21), 2843–2850. doi:10.4103/0366-6999.168017

Zheng, Y., Zheng, Z., Zhang, K., and Zhu, P. (2022). Osteonecrosis in systemic lupus erythematosus: systematic insight from the epidemiology, pathogenesis, diagnosis and management. *Autoimmun. Rev.* 21 (2), 102992. doi:10.1016/j.autrev.2021.102992

frontiers | Frontiers in Pharmacology

TYPE Review
PUBLISHED 03 February 2025
DOI 10.3389/fphar.2025.1532629

OPEN ACCESS

EDITED BY
Lufei Wang,
Guangxi Medical University, China

REVIEWED BY
Christian Kweku Adokoh,
University of Cape Coast, Ghana
Zhen Yang,
Peking University People's Hospital, China
Yongdi Li,
Guizhou Provincial People's Hospital, China

*CORRESPONDENCE
Yushu Bai,
spinebaiys@163.com
Xianzhao Wei,
weixianzhao@126.com
Xiaoyi Zhou,
13818909826@163.com

†These authors share first authorship

RECEIVED 22 November 2024
ACCEPTED 13 January 2025
PUBLISHED 03 February 2025

CITATION
Zhang H, Li X, Jia Z, Jiao K, Liu C, Deng Z, Bai Y, Wei X and Zhou X (2025) Bioprinted hydrogels in bone regeneration: a bibliometric analysis. *Front. Pharmacol.* 16:1532629. doi: 10.3389/fphar.2025.1532629

Bioprinted hydrogels in bone regeneration: a bibliometric analysis

Huijie Zhang[1†], Xiaoyu Li[1†], Zhenyu Jia[2†], Kun Jiao[1,3], Chen Liu[1,4], Zixiang Deng[1], Yushu Bai[1*], Xianzhao Wei[1*] and Xiaoyi Zhou[1*]

[1]Department of Orthopedics, Shanghai Changhai Hospital, Shanghai, China, [2]Department of Orthopedics, General Hospital of Southern Theater Command, Guangzhou, China, [3]Department of Orthopedics, Shanghai Changzheng Hospital, Shanghai, China, [4]Department of Outpatient Service, Military District Shenyang No. 1 Retreat Center for Separated Cadres, Liaoning, China

Background: The application of bioprinted hydrogels in the field of bone regeneration is garnering increasing attention. The objective of this study is to provide a comprehensive overview of the current research status, hotspots and research directions in this field through bibliometric methods, and to predict the development trend of this field.

Methods: A search was conducted on 27 December 2024, for papers published on the Web of Science from 2010 to 2025. We used the bibliometrix package in the software program R to analyze the retrieved data and VOSviewer and CiteSpace to visualize hotspots and research trends in bioprinted hydrogels for bone regeneration.

Results: We identified and reviewed 684 articles published in this field between 2010 and 2025. A total of 811 institutions and 1,166 researchers from 41 countries/regions contributed to these publications. Among them, China led in terms of the number of articles published, single-country publications (SCP), and multi-country publications (MCP). Our bibliometric-based visualization analysis revealed that the mechanical properties and osteogenic differentiation capacity of biomaterials have been a focal research topic over the past decade, while emerging research has also concentrated on the *in vitro* fabrication of stem cells for bone regeneration and osteogenic differentiation, particularly the precise application of *in situ* stem cell-loaded bioprinted organoids.

Conclusion: This study provides an in-depth analysis of the research trajectory in the application of bioprinted hydrogels for bone regeneration. The number of research papers in this field is increasing annually, and the main research hotspots include bone regeneration, 3D printing, scaffolds, and hydrogels. Future research directions may focus on gelatin, additive manufacturing, and growth factors. Additionally, international collaboration is essential to enhance the effectiveness of bioprinted hydrogels in bone regeneration applications.

KEYWORDS

bibliometric, bone regeneration, tissue engineering, hydrogel, bioprinting

Abbreviations: SCP, Single-country Publications; MCP, Multi-country Publications; CaP, Calcium Phosphate; 3D, Three-dimensional; 4D, Four-dimensional; SCU, Sichuan University; SJTU, Shanghai Jiao Tong University; MSCs, Mesenchymal Stem Cells; ECM, Extracellular Matrix.

1 Introduction

The skeleton is a critical organ that provides structural support and facilitates movement within the body (Song et al., 2024). The primary etiologies of bone defects are fractures resulting from accidents and sports activities, resection of osseous tumors, and revision of prosthetic devices (Song et al., 2024). With the development of biomedical engineering, scientists are gradually focusing on treating bone defects through bone tissue engineering. An increasing number of researchers have conducted multidimensional studies on the human skeleton to identify effective therapeutic strategies for bone defects (Rosset et al., 2014), such as autologous bone grafting, allogeneic bone grafting, and a the use of artificial bone scaffolds (Zhu et al., 2017). Currently, autologous bone grafting is considered the "gold standard" for treating bone defects (Keating et al., 2005). However, autologous bone grafting is limited by bone volume, risk of infection, potential for secondary injury, and chronic pain (García-Gareta et al., 2015). Allogeneic bone grafts are also associated with complications such as infection and immune rejection (McEwan et al., 2018). Therefore, a less invasive treatment strategy that can consistently support bone regeneration over time is needed. Bone tissue engineering encompasses the application of *in vitro* cultured cells or growth factors onto biocompatible scaffolds, which are then deployed to target bone defects. This approach facilitates the release of cells and growth factors, promoting osteoblast proliferation and bone tissue regeneration (Shan and Wu, 2024). The selection of biomaterials, such as polymer scaffolds, bioactive glass, and hydrogels, is crucial for the success rate in healing bone defects. Key properties include excellent biocompatibility, biodegradability, high mechanical strength, and the ability to support cell adhesion and growth (Albrektsson and Johansson, 2001). Regarding the materials used for bone generation, the current focus is on metal, bioceramic, and polymer scaffolds (Wang et al., 2020). Metallic materials such as stainless steel, cobalt-chromium alloys, and titanium alloys are widely used in orthopedics and dentistry due to their exceptional mechanical strength (Iatecola et al., 2021); however, their poor biodegradability prevents them from being used as carriers of cells or growth factors in the field of bone regeneration (Tzagiollari et al., 2022). Bioceramic scaffolds, such as calcium phosphate (CaP), calcium sulfate, and calcium silicate (Wang et al., 2020), have entered the orthopedic field owing to their good biocompatibility, corrosion resistance, and low cost. Nevertheless, their inadequate fatigue resistance prevents them from serving as long-term bone tissue support within the human body. Therefore, hydrogels stand out among many biomaterials owing to their cell-loaded and tunable mechanical properties (Yue et al., 2020), and they have emerged as a significant component in regenerative medicine (Liu and Hsu, 2018).

Hydrogel is a polymer with a three-dimensional mesh structure, and its properties such as biocompatibility, nontoxicity, and degradability have led to a wide range of biomedical applications, such as wound dressings, contact lenses, and biosensors (Ortega et al., 2023; Cao et al., 2021). Polymer networks can be molded into three-dimensional structures with different porosities; therefore, they can provide constructive microenvironments suitable for controlled cell growth (Muir and Burdick, 2021; Zhang Y. et al., 2020; Oliva et al., 2021). Hydrogels have become excellent bioinks for bioprinting because of their high water content and three-dimensional mesh structure, which minimizes the shear stress on cells (Bertsch et al., 2023). Moreover, the high water content makes hydrogels highly permeable and porous, enabling the rapid diffusion of balanced oxygen and nutrients (Chimene et al., 2016). The tunable properties of hydrogels permit the adjustment of their mechanical strength to align with the specific demands of the target tissue (Li et al., 2018), enhancing applicability. Bioprinted hydrogels have become an important technology in the field of bone regeneration because their internal network structure can be modulated by changing the external geometry and volume of the scaffold to achieve dynamic drug delivery and fostering osteoblast development within the human body (Wan et al., 2020). As Figure 1 shows, hydrogels have a wide variety of applications in the bone regeneration field (Nie et al., 2019). With fractures, hydrogel scaffolds accelerate bone healing by releasing growth factors and have emerged as bone graft substitutes (Chen L. et al., 2023; Kolambkar et al., 2011). Hydrogels can utilize their degradation properties for the sustained release of drugs to enhance patients' bone density and treat osteoporosis symptoms (Gong et al., 2022; Ding et al., 2023). Hydrogels serve as joint lubricants, effectively treating conditions such as osteoarthritis (Vinikoor et al., 2023; Duan et al., 2023). In minimally invasive surgery, hydrogels can be administered via injection to completely fill and address bone defect cavities (Ghandforoushan et al., 2023). Moreover, hydrogels are important for targeted drug delivery to inflammatory bone lesions (Xie et al., 2022; Kuo et al., 2023). With the rapid development of printing technology, bioprinting hydrogel combines cells with hydrogel ink to create tissue-like structures through 3D printing technology, providing a good environment for human tissues and cells to grow and develop (Zhu et al., 2022). Although hydrogels are somewhat uncontrollable in terms of degradation properties, drug release rate and mechanical properties, researchers in various fields are constantly trying new syntheses to achieve the stability of various properties of hydrogels. Currently, bioprinted hydrogels are predominantly utilized in the fields of skin tissue engineering (Zhou et al., 2020), cardiovascular tissue engineering (Sousa et al., 2021) and bone tissue engineering (Zhang J. et al., 2020). Among them, in order to achieve high mineralization of bone tissue and proliferation of cellular diversity. Researchers are also continuously developing hydrogel bioinks that can match the biological properties of bone tissue. Tavares et al., 2021 used a GelMA/MSN CaP Dex hydrogel as a bioink to fabricate three-dimensional bone tissue containing osteogenic tissue using extrusion-based 3D printing technology. Cidonio et al. (2020) accomplished the *in vitro* and *in vivo* growth of bone mineral tissue by utilizing Laponite®-alginate-methylcellulose casting of human bone marrow stromal cells as a biocarrier. Yuan et al. (2021) used photo-crosslinked methacrylated gelatin in combination with silica nanoparticles to achieve rapid diffusion of internal stem cells and improve the osteogenic efficiency of stem cells. With the rapid development of the additive manufacturing industry, the high resolution of bioprinting has led to it becoming the dominant manufacturing technology in the medical field (Mandrycky et al., 2016). This technique is extensively utilized in bone tissue engineering, regenerative medicine, and medical device applications (Wan et al., 2020). Three-dimensional (3D) bioprinting

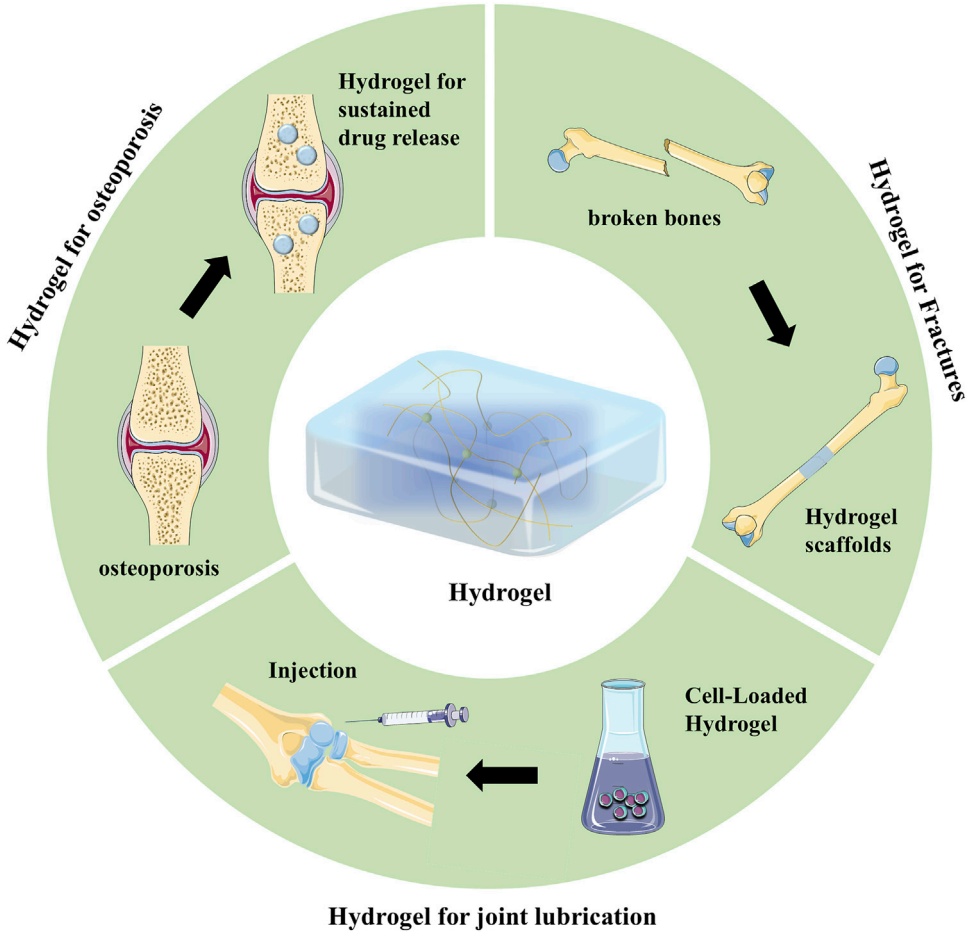

FIGURE 1
Hydrogels in bone regeneration.

for treating bone defects has been the focus in the field (Zhang et al., 2019a). Furthermore, with the development of bioprinting technology, four-dimensional (4D) bioprinting has also been developed, which adds a temporal dimension to 3D bioprinting. Specifically, in 4D bioprinting, changes in temperature or pH over time stimulate the print (Kang et al., 2022), altering its mechanical properties to accommodate the growth patterns of autogenous bone (Suo et al., 2018), thereby offering new possibilities for the fabrication of irregular bone constructs in clinics (Murphy and Atala, 2014).

The discipline of bibliometrics is widely used to predict the direction of development and research patterns in a particular field (González-Alcaide et al., 2017). It employs different methods to assess research trends and helps researchers identify influential articles in the field, thereby contributing to continuously optimize research innovations (Bertsch et al., 2023; Zhang et al., 2024; Chen S. et al., 2023). By analyzing data such as the number of publications and the number of citations, it provides a reference basis for researchers who are about to enter the field to formulate their research plans. Through analyzing the cooperation network between countries and organizations, it assists researchers in the rational allocation of resources. Meanwhile, the construction of a knowledge map can help scholars quickly grasp the hot topics and research directions (Figure 2). In recent years, there has been a steady increase in the number of researchers focusing on bioprinted hydrogels for bone regeneration. However, There is a significant gap in the quantitative analysis of scientific results in this field, particularly concerning research trends, research quality, and the identification of interdisciplinary research gaps from a historical perspective. The objective of this paper is to evaluate the research articles on the application of bioprinted hydrogels in bone regeneration worldwide over the past 15 years by using the Web of Science core database and bibliometric tools to assess the current state of research, collaborative development paths, leading countries and institutions, cited literature, and future development trends according to the information on the distribution of publications by country, authors, journals, and impact. It is expected to help the subsequent researchers to understand the current research status in this field, formulating the systematic research strategy, and fostering the rapid development of bioprinted hydrogels in bone tissue engineering. These findings may assist subsequent researchers in understanding the current research landscape in this field, formulating systematic research strategies, and fostering the rapid advancement of bioprinted hydrogels in bone tissue engineering.

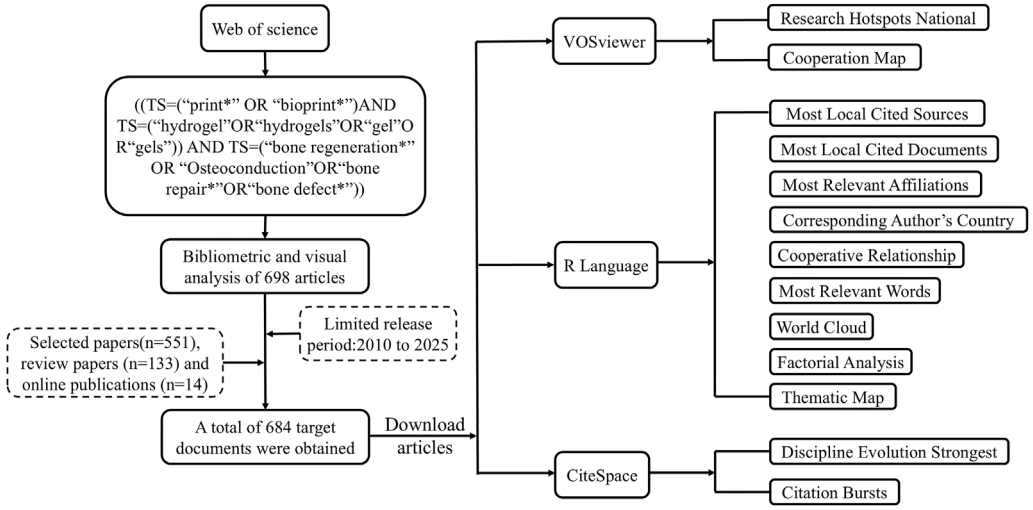

FIGURE 2
Graphical summary.

2 Materials and methods

2.1 Search strategies

The Web of Science database covers the largest amount of literature in the medical field and is frequently utilized in bibliometric studies (Wang et al., 2022). We collected relevant literature from this database, focusing on the application of bioprinted hydrogels for bone regeneration. To ensure accuracy and consistency, we conducted a systematic search on 27 December 2024, for relevant literature included in the Web of Science database between January 2010 and March 2025. All retrievals were performed on the same day to prevent data bias due to updates in the Web of Science. Based on the previous statistics, we set the search strategy as follows: [(TS=("print*" OR "bioprint*") AND TS=("hydrogel"OR"hydrogels"OR"gel"OR"gels")) AND TS=("bone regeneration*" OR "Osteoconduction"OR"bone repair*"OR"bone defect*")]. Removing conference abstracts, book chapters, and reviews, we retrieved a total of 684 related papers.

2.2 Data collection and statistics

684 articles were imported into VOSviewer (1.6.19) and bibliometric analysis was performed using the bibliometrix package (4.1.3) in R (4.3.0). We used tools such as CiteSpace (6.3.1), VOSviewer (1.6.19), the bibliometrix package (4.1.3) in R (4.3.0), and PS (2020) to process, visualize, and analyze the data of the 684 documents collected from the Web of Science database. The counting method used for all analyses was full count. In addition, an online bibliometric analysis platform (https://bibliometric.com) was used to assist in the analysis of the intensity of cooperation between countries.

CiteSpace (6.3.1) is an analytical software program developed for bibliometrics that employs algorithms to automatically extract and analyze key information in a research area. The tool analyzes the scope and hotspots of research in a given field and identifies trends for improvement in related disciplines (Cheng et al., 2022). We used this tool to obtain citation biplot overlays to analyze keywords, references, clusters, and collaborative relationships between countries and institutions. We used the burst detector option to detect the first 30 keywords. VOSviewer (1.6.19) systematically collects and organizes basic information, including countries, institutions, authors, journal publications, and collaborative networks, and visualizes and analyzes the data (van Eck and Waltman, 2010). This software can extract the key information that researchers require from a wide range of literature to create co-citation and co-authorship networks (Chen et al., 2021). We used software to explore the temporal distribution and dynamic variability of keywords in the field and accurately reveal the evolutionary trends of hotspots in the research area. In order to analyze the research hotspots, the type of analysis was selected as co-occurrence, the unit of analysis was selected as keywords, and the analysis was carried out using the full count method.

The bibliometrix package (version 4.1.3) in R is a mapping tool designed for systematic analysis (Aria et al., 2021) that enables the mapping and analysis of country distribution maps, author publications, and keyword development. It also facilitates the identification of trending themes and milestones in the literature for publications in related research areas. The most relevant affiliations should be selected as options during the analysis. Thematic maps and factor analysis are employed to elucidate the components of the constitutional structure.

3 Results

3.1 Analysis of most locally cited documents and sources in the field

3.1.1 Most locally cited sources

The 684 collected documents were analyzed in depth, which cited a total of 4,444 journals and were ranked according to the number of papers and the number of journals. The top ten journals

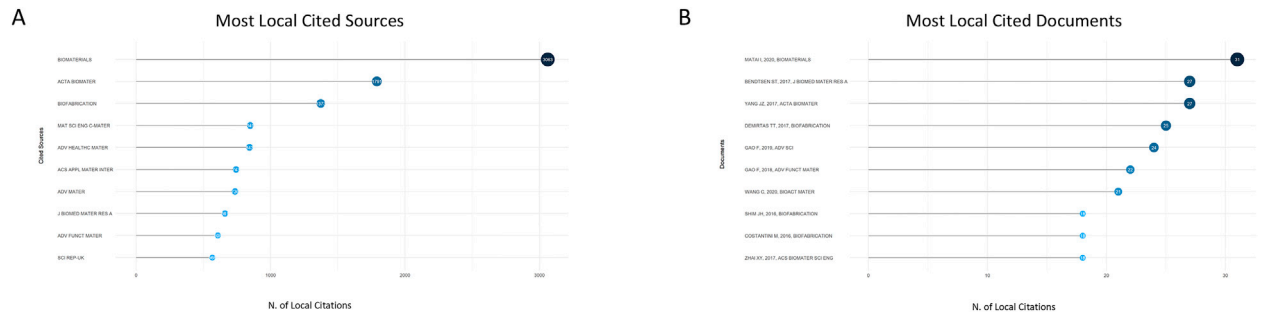

FIGURE 3
(A) The number of citations and the top ten highly cited journals in this field from 2006 to 2024. **(B)** The number of citations of highly cited documents in this field and the top ten articles from 2006 to 2024.

TABLE 1 Top 10 most relevant affiliations.

Rank	Institution	Contribution (%)	Country
1	Sichuan University	13.4	China
2	Shanghai Jiao Tong University	12.1	China
3	Zhejiang University	7.4	China
4	Chinese Academy of Sciences	7.1	China
5	Jilin University	5.8	China
6	South China University of Technology	5.1	China
7	Nanjing Medical University	4.8	China
8	Shandong University	4.5	China
9	China Medical University Taiwan	3.9	China
10	Jinan University	3.9	China

in terms of the number of articles are shown in Figure 3A, with the most-cited journal being *Biomaterials* (3,488), which had far more citations than any other journal. This demonstrates that *Biomaterials* holds an authoritative position in the field of medical bioprinted hydrogels for bone regeneration and plays a significant role as trendsetters in the field.

3.1.2 Most locally cited documents

The most locally cited literature can help researchers who are new to the field quickly select the best literature to read. The author rankings were based on the number of citations in the literature on bone regeneration with bioprinted hydrogel. Figure 3B illustrates the top ten cited papers in the field. TURNBULL G et al., 's 2020 article in *Bioactive Materials*, "3D bioactive composite scaffolds for bone tissue engineering" was ranked first in citations and cited 38 times in this research area, with a total of cited 914 times.

3.2 Analysis of affiliations and countries

3.2.1 Most relevant affiliation

A total of 811 research institutions, including universities, contributed to the literature published in the field. Table 1 lists the top 10 institutions in terms of the number of papers published, along with the name of the country where each institution is located. Supplementary Table S1 lists the top 10 authors with publications in the field. Sichuan University (SCU) in China ranked first with 92 research papers related to the application of bioprinted hydrogels in bone regeneration, followed by Shanghai Jiao Tong University (SJTU), also in China, with 53 papers. This demonstrates the outstanding research achievements of SCU and SJTU in the field of bioprinted hydrogels. The top 10 research institutions in this field are all affiliated with China, suggesting that Asia may be at a higher level of research in this field.

3.2.2 Corresponding Author's country

For single-country publications (SCPs), all authors of an article are all from the same country, whereas for multi-country publications (MCPs), the authors of an article are from more than one country, indicating international collaboration. As shown in Figure 4A, we analyzed the SCPs and MCPs of the top 20 countries. An analysis of the statistics on the nationalities of the corresponding authors of the relevant literature shows that China dominates this research field, with the United States ranking second. Among them, China's SCP value has a clear gap with the United States, while China ranks first for MCPs. These data

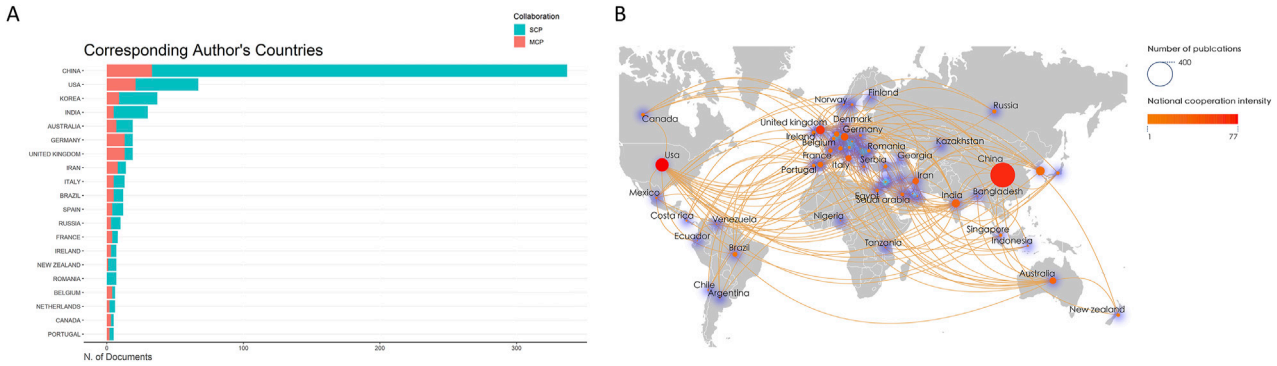

FIGURE 4
(A) Top 20 most productive countries. **(B)** Cooperation networks in countries around the world.

suggest that China is capable of conducting research in this field relatively independently and possesses a strong capacity for international cooperation. This result also corroborates those for major research institutions with the most relevant affiliations, with countries with a higher number of major research institutions also having more corresponding authors than other countries.

3.2.3 Analysis of the cooperative relationship between countries

We filtered and visualized international cooperation based on the number of publications, constructing a network of cooperation based on the number of publications and relationships between countries. As shown in Figure 4B, the size of the circle radius indicates the country's contribution to the number of papers in the field, the color of the circle indicates the intensity of the country's cooperation, and the density of the lines around the circle indicates the number of collaborations between that country and other countries. The highest density of the lines indicates that the country is at the center of research in this field. Close cooperation has occurred between China and the United States, the United Kingdom, and Germany, while the United States has also engaged in productive cooperation with South Korea, the United Kingdom, and Iran, in addition to more cooperation with China.

3.3 Analysis of keywords and research hotspots

Keyword analysis can outline the research object, content, and hotspots within a research field by identifying the most frequent words in the field, which are central to academic papers. Supplementary Table S2 lists the top 10 keywords with the highest frequency in this field, and among the extensive literature, "bone regeneration", "3D printing", "scaffold" and "hydrogel" are the keywords that appear more frequently (Figure 5), indicating that bioprinted hydrogel scaffolds are the current research hotspot in the field of bone regeneration.

We analyzed the titles, subject headings, and abstracts of 684 papers to identify common phrases and determine their frequency of occurrence. As shown in Figure 6A, "scaffolds" (138) appears most frequently, which is consistent with the results of the word cloud search.

The keywords in the field were categorized into five clusters using VOSviewer, as shown in Figure 6B. Cluster 1 focuses on the development of 3D-printed hydrogel scaffolds in additive manufacturing. Cluster 2 mainly includes the application of cellular scaffolds in bone tissue engineering. Cluster 3 focuses on bio-inks such as hydrogels and the effects of biomaterials on cells in the microenvironment. Cluster 4 investigates the application of growth factors in the field of bone regeneration. Cluster 5 provides an overview of the current state-of-the-art research on 4D printing in the field of biomedical sciences.

We then further used VOSviewer to color-code all keywords based on the average publication year, revealing trends in the field over time and exploring upcoming innovation directions. By analyzing the keyword sequencing map (Figure 6C), we found that osteogenesis, microenvironment, hydrogel, and 4D printing are relatively novel and promising areas in the field of bone regeneration. Recently, researchers have combined bioprinted hydrogel technology with cell-loaded scaffolds to advance the field of bone regeneration by restoring microenvironmental homeostasis at bone defect sites.

Keyword clustering analysis reveals the main themes and development states of a particular research area (Zhong et al., 2020). CiteSpace was used to divide the keywords into 19 sets and generate a clustering timeline. As shown in Figure 6D, the keywords included "#0 3 d printing""#1 alginate fiber""#2 3d bioactive composite scaffold""#3 3d-printed barium strontium""#4 stem cell function""#5 topical review""#6 inert dental glass-ceramics""#7 cell-patterned construct""#8 vivo repair""#9 enhanced toughness""#10 organ engineering""#11 beta tri-calcium phosphate""#12 bactericidal activity""#13 bone tissue""#14 3 d-bioprinted osteoblast-laden nanocomposite hydrogel construct""#15 injectable bmp2""#16 nitride-based hybrid aerogel membrane""#17 dicalcium phosphates bioceramics"and"#18 recent advancement". That the result shows that "3D printing" is the most important research area for hydrogels in bone tissue engineering. To further confirm the accuracy of our results, we conducted a thematic analysis of keyword trends using R (Figure 6E). Keywords such as "microenvironment" "defect" "biomaterials" "cells" "osteogenesis" "scaffolds" have been

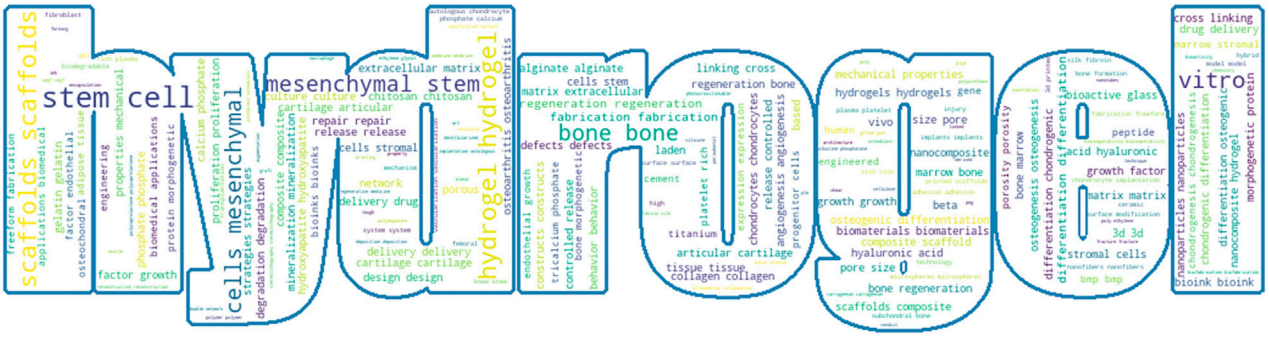

FIGURE 5
Wordcloud of the collection of literature keywords included in the study.

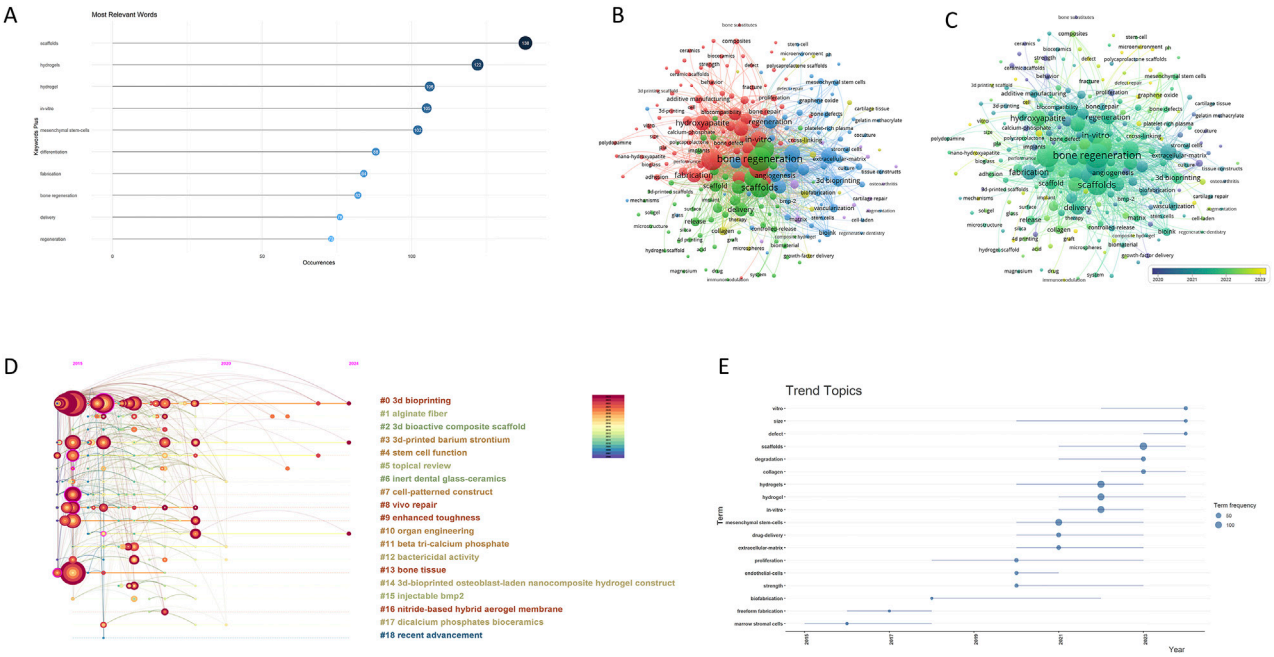

FIGURE 6
Analysis of keywords and Research Hotspots. **(A)** Top 10 most relevant words. **(B)** The keywords related to the application of bioprinted hydrogels in bone regeneration are divided into X clusters according to different colors. The size of the circle represents the frequency with which keywords appear. **(C)** The distribution of keywords is presented according to the average time of appearance. Purple keywords appear earlier than yellow keywords. **(D)** The timeline of clustering for keywords. **(E)** Map of keywords trend topics.

emerging in the field recently, indicating their importance. In addition, "scaffolds" "mesenchymal stem-cells" " vitro" "hyaluronic-acid hydrogels" and "biofabrication" are important parts of bone tissue engineering in long-term studies. The evolutionary trend of these themes is consistent with the results of our analysis above.

3.4 Thematic map

Each quadrant on the thematic map has a specific meaning. The horizontal axis (*X*-axis) indicates centrality, and the vertical axis (*Y*-axis) indicates density. Regarding the quadrant distribution plotted in this study (Figure 7), the first quadrant (upper right) focuses on the optimization of hydrogel scaffolds, suggesting a promising future for this area. The second quadrant (upper left) shows the preparation of hydroxyapatite, the mechanical properties of biomaterials and the study of composite scaffolds, suggesting that this topic is well-developed but less important in the field of bone regeneration. The third quadrant (lower left) focuses on the imminent rapid surge or imminent slow disappearance of the controlled release of nanoparticles. Finally, the fourth quadrant (lower right) is dedicated to *in vitro* manufacturing of stem cells for bone regeneration and osteogenic differentiation. While these directions have not yet achieved mature research results, they hold an important position in the field of bone regeneration and may become a hot research area in the future.

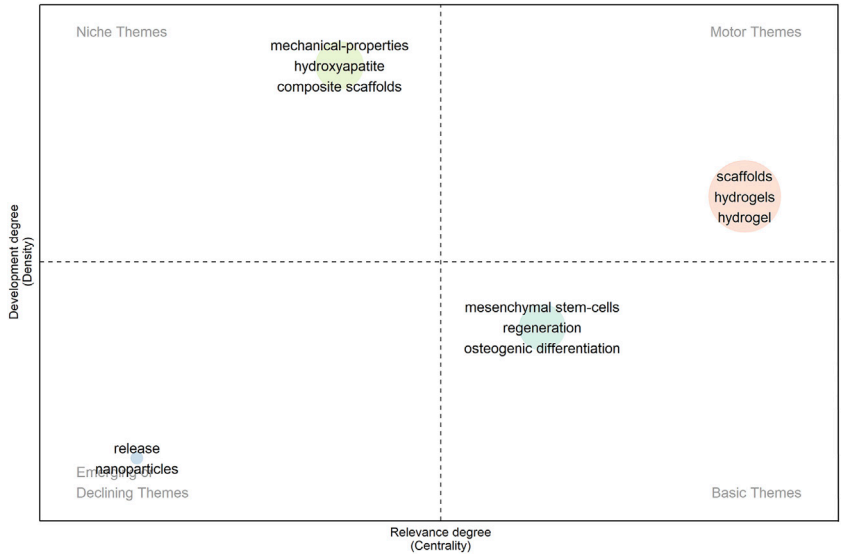

FIGURE 7
Strategic theme map.

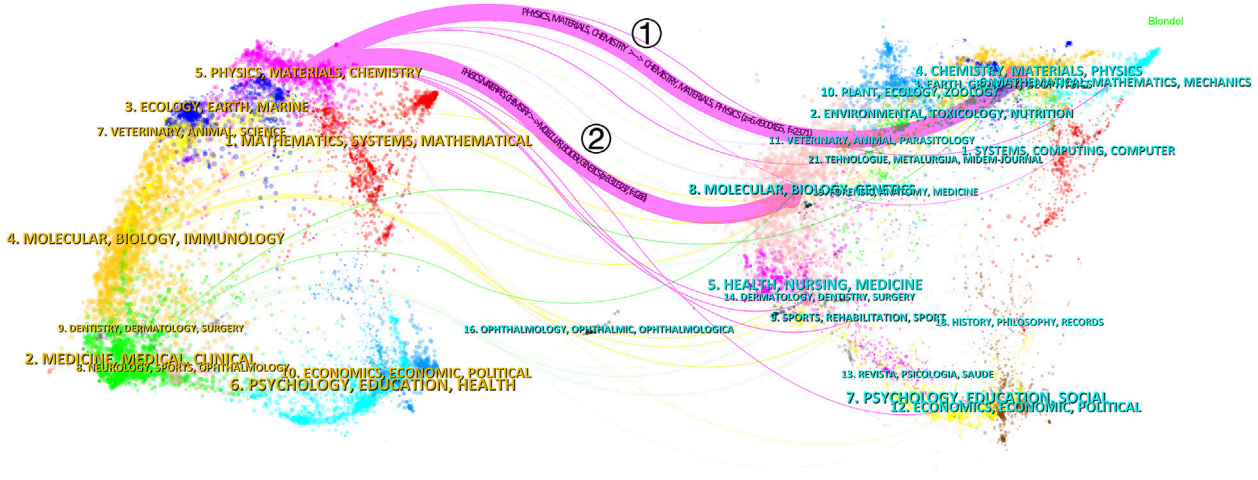

FIGURE 8
The dual-map overlay of journals related to applications of bioprinted hydrogels in bone regeneration.

3.5 Trends in discipline evolution

The dual-map overlay of journals illustrates the citation relationships between journals and cited journals, with cited journals on the left and cited sources on the right. As shown in Figure 8, two primary and several secondary paths are displayed. Path ① indicates that literature published in CHEMISTRY, MATERIALS, and PHYSICS journals is mainly cited by other literature in PHYSICS, MATERIALS, and CHEMISTRY journals. Path ② indicates that literature published in MOLECULAR, BIOLOGY, and GENETICS journals is primarily cited by papers in PHYSICS, MATERIALS, and CHEMISTRY journals. The top 10 most cited articles in this field are shown in Supplementary Table S3, in which "Three-dimensional (3D) printed scaffold and material selection for bone repair" published by Zhang et al. (2019b) in Acta Biomaterialia in 2019, ranked first with 52 citations.

3.6 Factorial analysis and keywords bursts

3.6.1 Factorial analysis

We used factorial analysis to identify 6 distinct clusters. As shown in Figure 9A, the categories of bone. regeneration, delivery, hydrogel, stem cells, differentitation, regeneration, Mechanical. properties, scaffolds, *in vitro*, fabrication, hydroxyapatite, tissue, biomaterials, hydrogel, Mesenchymal Stem Cells were not mutually exclusive, with overlap occurring between categories.

A

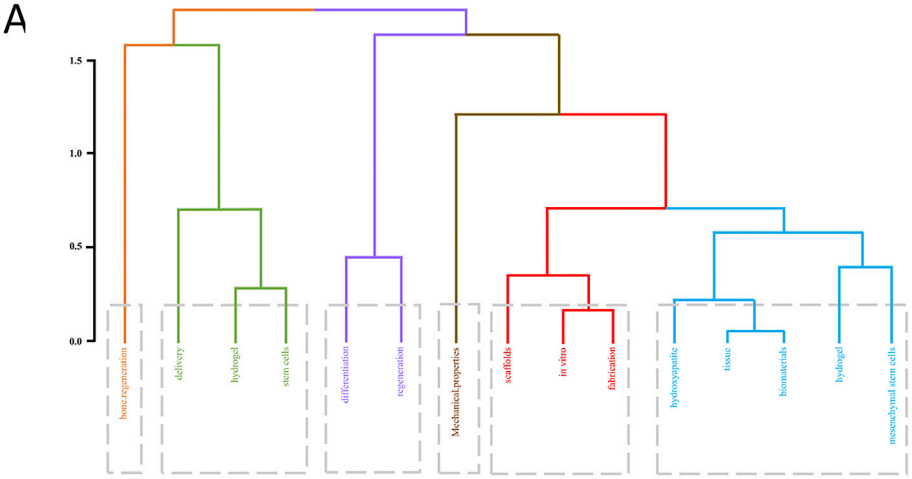

B

Top 30 Keywords with the Strongest Citation Bursts

Keywords	Year	Strength	Begin	End	2015 - 2024
growth factor delivery	2015	2.29	**2015**	2017	
marrow stromal cells	2015	1.96	**2015**	2019	
freeform fabrication	2015	1.94	**2015**	2018	
proliferation	2015	1.93	**2015**	2018	
mechanical properties	2015	1.73	**2015**	2017	
bone repair	2016	2.54	**2016**	2021	
phosphate	2016	1.99	**2016**	2020	
morphogenetic protein 2	2015	2.77	**2017**	2021	
biocompatibility	2017	2.2	**2017**	2020	
therapy	2017	1.81	**2017**	2019	
stromal cells	2017	1.81	**2017**	2019	
activation	2018	2.04	**2018**	2019	
endothelial cells	2017	2.93	**2019**	2020	
vegf	2019	2.38	**2019**	2021	
calcium phosphate	2016	2.97	**2020**	2021	
tissue	2015	2.85	**2020**	2022	
chitosan	2018	2.53	**2020**	2021	
gelatin	2017	4.23	**2021**	2024	
composite scaffolds	2015	3.08	**2021**	2022	
osteogenic differentiation	2017	2.91	**2021**	2022	
controlled release	2015	2.66	**2021**	2022	
cartilage	2015	2.41	**2021**	2022	
in vitro	2015	2.35	**2021**	2022	
additive manufacturing	2015	1.87	**2021**	2024	
3d printed scaffolds	2019	1.67	**2021**	2022	
design	2015	3.04	**2022**	2024	
cells	2015	2.33	**2022**	2024	
graphene oxide	2018	2.11	**2022**	2024	
alginate	2019	1.81	**2022**	2024	
growth factor	2018	1.74	**2022**	2024	

FIGURE 9
(A) The dendrogram shows the most extensive evolution of bioprinted hydrogels in the discipline of bone regeneration. **(B)** Top 30 Keywords with the Strongest Citation Bursts.

3.6.2 Citation burst analysis

We used CiteSpace to generate the top 30 keywords. As shown in Figure 9B, the start and end times of sudden keyword bursts can be visualized, with the shortest yearly interval being 1.67 years. Over the past 15 years, the keywords that have received the most attention for the longest period are "bone repair" (22,016–2021), "phosphate" (2016–2020) and "morphogenetic protein" (2017–2020), all of which have been hotspots for hydrogel applications in bone regeneration. In contrast, keywords that received less attention were "activation" (2018–2019), "endothelial cells" (2019–2020), "composite scaffolds" (2021–2022), "osteogenic differentiation" (2021–2022), "controlled release" (2021–2022) and "*in vitro*" (2021–2022). "gelatin" (2021–2024), "additive manufacturing" (2021–2024), "design" (2022–2024), "cells" (2022–2024), "graphene oxide" (2022–2024), "alginate" (2022–2024) and "growth factor" (2022–2024) are keywords that have been used with high frequency in recent years, suggesting that these aspects may be the focus of research on the application of hydrogels in the bone regeneration field, which has high potential.

4 Discussion

Bibliometric analysis is a discipline that responds to the status and trends of research (Chen et al., 2014; Chen et al., 2012). This study provides the first comprehensive analysis of the use of bioprinted hydrogels for bone regeneration and offers statistics on the major journals and organizations in this field.

4.1 Research status

Bone is a tissue that can be sustainably regenerated (Dimitriou et al., 2011) and is the hardest organ in the human body. The treatment of both direct and indirect fractures involves bone regeneration. Bone defects not only cause an imbalance in the body, but more importantly, disturb the adaptive system within the bone, limiting its ability to regenerate. The three important processes in bone regeneration are osteoinduction, osteoconduction, and osteointegration (Albrektsson and Johansson, 2001). Osteoinduction refers to the formation of undifferentiated cells for osteogenesis through the aggregation of mesenchymal stem cells (Lewallen et al., 2015), osteoconduction refers to providing an environment for osteoblast growth (Weber, 2019), and osteointegration is the seamless integration of bone tissue with an implant (Morandini Rodrigues et al., 2022). After a patient undergoes trauma and inflammation sets in, mesenchymal stem cells (MSCs) aggregate at the trauma site to form fragile tissue, followed by angiogenesis, which promotes the hardening of soft tissue into hard bone tissue, and finally, osteoclasts and osteoblasts undergo superimposed replacement. Osteoblasts and osteoclasts are key factors involved in the bone regeneration process (Salhotra et al., 2020a). Osteoblasts are mainly derived from stem cells, and MSCs have become common stem cells in the field of bone tissue engineering owing to their proliferative properties (Tsiapalis and O'Driscoll, 2020). Since the internal pore size of the bone varies and is stepped from the inside to the outside, only a suitable pore size can ensure optimal cell adhesion. It has been the most clinically used treatment modality for autologous bone grafting (Dimitriou et al., 2011) because it lacks the risk of immune rejection and retains the same plasticity as living bone (Pereira et al., 2020); however, the limited amount of bone and donor site complications cannot be ignored. Allogeneic grafts have a large numerical advantage but their integration is less efficient (Ehrler and Vaccaro, 2000). Theoretically, allogeneic grafts can achieve the same effects as isografts; however, their use in treatment has not yet been standardized. Artificial bone grafts have become the focus of researchers and are mainly categorized as metals (Lu et al., 2023), bioceramics (Zhao et al., 2022) and polymers (Bharadwaz and Jayasuriya, 2020). However, bone tissue reconstruction with biologically inert metals often leads to secondary surgical repair because of the wear and tear susceptibility of the material (Salhotra et al., 2020b). Compared to other pure bioscaffold materials, hydrogel materials possess unique application potential in the field of bone regeneration.

Hydrogel is a hydrophilic polymer with a three-dimensional network structure, mainly classified as natural (e.g., collagen, hyaluronic acid, chitosan, and alginate) and synthetic (Zhu and Marchant, 2011). The excellent biocompatibility, high mechanical properties, adjustability and cell-carrying properties of hydrogels enable them to better adapt to the geometry and microenvironment of the bone defect sites, while the biodegradable nature of hydrogels avoids the risk of secondary surgeries for patients. Although the excellent biocompatibility of natural hydrogels places them in a high position in the field of regenerative medicine, their potential uncontrollability is an issue that researchers cannot ignore. Synthetic hydrogels lack biological activity, although they exhibit strong mechanical properties. Consequently, researchers are constantly searching for hydrogel materials that can carry cells. Saravanan et al. (Saravanan et al., 2018) indicated that CS/GP/GO hydrogels have better biocompatibility with MSCs and can promote osteogenesis, while Liu et al. (Liu et al., 2020) indicated that CD/HA/PVA hydrogels can support the proliferation and differentiation of MSCs *in vivo*.

Recently, bioprinting technology, which enables the construction of 3D structures using cells, proteins, and biomaterials, has been applied in the field of bone regeneration (Dimitriou et al., 2011) and offers a possibility for bone regeneration therapy. Multi-layer stacked printing can simulate the internal complexity of natural bone tissue, individualize the geometry of the area to be filled with bone defects, and adjust the hydrogel properties to match the mechanical strength of natural bone. Breakthroughs have been made in 3D bioprinting technology (Daly et al., 2017), and cell-loaded bioprinting has been realized (Yang et al., 2017). Bioprinted structures can change the internal spatial structure at different stimuli, enabling a high degree of control over mesenchymal stem cells. However, owing to the limitations of 3D bioprinting in personalizing the treatment of bone defects, 4D bioprinting was developed. This technology can change over time in response to stimuli such as pH, temperature, and is well adapted to the microenvironmental reconstruction of irregular bone defect sites (Zhang et al., 2019a). It can fulfill the functional transformation between organisms and hydrogel materials. In addition, bioprinted hydrogel scaffolds enable controlled release of bioactive molecules to induce vascularization and nerve regeneration in regenerated bone. Currently, bioprinted hydrogel scaffolds applied in the field of bone regeneration have been able to achieve good physical support from the macroscopic structure, but how to change the bionic properties of the microstructure of the hydrogel material to match different functional characteristics is the current challenge. So bioprinting of in situ-loaded stem cell bone-like organs may be the future development direction.

The results of the Most Relevant Affiliations indicate that research on the application of bioprinted hydrogels in bone regeneration is still in its initial stage, proving the great potential of research in this field. The results of the analysis of cooperation between institutions and countries show that although the cooperation between China and the United States is closer, which provides favorable conditions for technological exchanges between the two countries. However, the cooperation network between China and other countries is relatively weaker. The cross-regional and cross-institutional cooperation needs to be strengthened, therefore, institutions of various countries should quickly establish excellent academic cooperation in order to promote the rapid development of bioprinting hydrogel technology in the field of bone regeneration.

4.2 Research hotspots and prospects

Biomaterials science combined with stem cell therapy and tissue engineering techniques are the basis of regenerative medicine. Bone regenerative medicine is a research area that focuses on bioprinted hydrogels. Compared with traditional techniques, bioprinted hydrogels can maximize the filling of space at the fracture site while simultaneously guaranteeing the stability of their mechanical properties. In recent years, research has shown on the development of cell-loaded hydrogels for the reconstruction of bone tissue for vascularization and nerve regeneration (Ashammakhi et al., 2019). However, the desirable decellularized extracellular matrix (ECM) of bone tissue has special mechanical structure and biochemical signals that can support cell adhesion and proliferation, Therefore, achieving the structural stability and signal maintenance of the ECM during decellularization in bioprinted hydrogels is the direction of scholars' further research. Additionally, exosome hydrogels should also be capable of promoting new vessel generation and tissue regeneration *in vivo*, as well as inhibiting local tissue fibrosis.

In addition, 3D bioprinting enables the control of hydrogel structure and function, while 4D bioprinting further alters the morphology of the hydrogel over time. Future research on bioprinting will focus on the spatial equilibrium of MSCs with hydrogel scaffolds and osteogenic transformations (Benning et al., 2017). Bioprinting is a relatively recent technology (Kumar Gupta et al., 2022). Although bioprinting technology has been widely used in the field of biomedical engineering, bioprinted hydrogels have certain limitations in terms of computer program settings, large-scale production, and cell-carrying efficiency. To prevent the reduction of cell viability in printed hydrogels, the release of alkaline ions (Heid and Boccaccini, 2020) to prevent local pH increases or to optimize the thickness of the hydrogel coating (Ringeisen et al., 2004) can be considered. Bioprinting can improve the precision of personalized treatment for bone defects to a certain extent. However, printing standardization needs further exploration. To ensure the sustainable development of this technology in the medical field, future restrictions need to be strengthened in terms of the relevant requirements of regulatory authorities, demonstration of safety and efficacy, and translation of results. The stability and safety of hydrogels for bioprinting have to be demonstrated in a variety of animal models to further characterize their physicochemical properties such as degradability and mechanical properties. Additionally, qualified materials and standardized manufacturing lines during clinical translation are prerequisites for avoiding immune response. There is an immediate demand for further biological optimization of the materials and standard safe operating procedures. Basic research is the cornerstone of the development of bone regeneration technology, and translating the results is the key to clinical treatment. Reducing the cost of bioprinting, improving hydrogel cell-carrying technology, and shortening the time required for bone regeneration will promote the application of alternative hydrogel bone grafts in clinical treatment in the field of bone regeneration in the future.

5 Conclusion

Over the past 15 years, the use of bioprinted hydrogels in the field of bone regeneration has continued to attract attention. In this study, 684 documents collected from the Web of Science database were processed and visualized for data analysis using bibliometric tools. The numerous articles will be analyzed objectively, systematically, and comprehensively to enhance the reader's perspective on the field as a whole. The study shows that the main institutions involved in the field of bone regeneration globally are concentrated in China and the United States. China ranks first in the field of bone regeneration in terms of the number of publications and the number of SCPs, with close cooperation between China and the United States. The journal of *Biomaterials* is the most published journal in this field, and the article "3D bioactive composite scaffolds for bone tissue engineering" by TURNBULL G et al. in *Bioactive Materials* is the most cited article in the field. These studies provide a rapid and precise orientation for researchers who are about to carry out studies in this field. At the same time, they provide a reference for future interdisciplinary collaborations. In addition, these findings can help policymakers in the industry to take a comprehensive and systematic view of the field's growth prospects. However, this study, which is based on previous research with a certain lag, has some limitations. We only collected published papers, not those that will be published or are still undergoing research, ignoring some potentially valuable papers.

Author contributions

HZ: Formal Analysis, Investigation, Writing–original draft, Writing–review and editing. XL: Formal Analysis, Investigation, Methodology, Writing–review and editing. ZJ: Formal Analysis, Investigation, Writing–review and editing. KJ: Writing–review and editing. CL: Writing–review and editing. ZD: Writing–review and editing. YB: Conceptualization, Resources, Supervision, Writing–review and editing. XW: Conceptualization, Resources, Supervision, Writing–review and editing. XZ: Conceptualization, Resources, Supervision, Writing–review and editing.

Funding

The author(s) declare that financial support was received for the research, authorship, and/or publication of this article. This study

was supported by "YuanHang Talent Project" of Naval Medical University.

Acknowledgments

We sincerely acknowledge Yushu Bai, Xianzhao Wei and Xiaoyi Zhou for their guidance, support and encouragement throughout the research process. Second, we would like to acknowledge every researcher in the team for their work on this paper, and last but not least, we would like to appreciate the valuable comments and suggestions from the reviewers and the editorial board, which greatly improved the quality of this manuscript.

Conflict of interest

The authors declare that the research was conducted in the absence of any commercial or financial relationships that could be construed as a potential conflict of interest.

Generative AI statement

The author(s) declare that no Generative AI was used in the creation of this manuscript.

Publisher's note

Supplementary material

The Supplementary Material for this article can be found online at: https://www.frontiersin.org/articles/10.3389/fphar.2025.1532629/full#supplementary-material

References

Albrektsson, T., and Johansson, C. (2001). Osteoinduction, osteoconduction and osseointegration. *Eur. Spine J.* 10 (Suppl. 2), S96–S101. doi:10.1007/s005860100282

Aria, M., Alterisio, A., Scandurra, A., Pinelli, C., and D'Aniello, B. (2021). The scholar's best friend: research trends in dog cognitive and behavioral studies. *Anim. Cogn.* 24 (3), 541–553. doi:10.1007/s10071-020-01448-2

Ashammakhi, N., Hasan, A., Kaarela, O., Byambaa, B., Sheikhi, A., Gaharwar, A. K., et al. (2019). Advancing frontiers in bone bioprinting. *Adv. Healthc. Mater* 8 (7), e1801048. doi:10.1002/adhm.201801048

Benning, L., Gutzweiler, L., Tröndle, K., Riba, J., Zengerle, R., Koltay, P., et al. (2017). Cytocompatibility testing of hydrogels toward bioprinting of mesenchymal stem cells. *J. Biomed. Mater Res. A* 105 (12), 3231–3241. doi:10.1002/jbm.a.36179

Bertsch, P., Diba, M., Mooney, D. J., and Leeuwenburgh, S. C. G. (2023). Self-healing injectable hydrogels for tissue regeneration. *Chem. Rev.* 123 (2), 834–873. doi:10.1021/acs.chemrev.2c00179

Bharadwaz, A., and Jayasuriya, A. C. (2020). Recent trends in the application of widely used natural and synthetic polymer nanocomposites in bone tissue regeneration. *Mater Sci. Eng. C Mater Biol. Appl.* 110, 110698. doi:10.1016/j.msec.2020.110698

Cao, H., Duan, L., Zhang, Y., Cao, J., and Zhang, K. (2021). Current hydrogel advances in physicochemical and biological response-driven biomedical application diversity. *Signal Transduct. Target Ther.* 6 (1), 426. doi:10.1038/s41392-021-00830-x

Chen, C., Dubin, R., and Kim, M. C. (2014). Emerging trends and new developments in regenerative medicine: a scientometric update (2000 - 2014). *Expert Opin. Biol. Ther.* 14 (9), 1295–1317. doi:10.1517/14712598.2014.920813

Chen, C., Hu, Z., Liu, S., and Tseng, H. (2012). Emerging trends in regenerative medicine: a scientometric analysis in CiteSpace. *Expert Opin. Biol. Ther.* 12 (5), 593–608. doi:10.1517/14712598.2012.674507

Chen, L., Yu, C., Xiong, Y., Chen, K., Liu, P., Panayi, A. C., et al. (2023a). Multifunctional hydrogel enhances bone regeneration through sustained release of Stromal Cell-Derived Factor-1α and exosomes. *Bioact. Mater* 25, 460–471. doi:10.1016/j.bioactmat.2022.07.030

Chen, S., Sun, D., Wang, N., Fang, X., Xi, Z., Wang, C., et al. (2023b). Current status and trends in quantitative MRI study of intervertebral disc degeneration: a bibliometric and clinical study analysis. *Quant. Imaging Med. Surg.* 13 (5), 2953–2974. doi:10.21037/qims-22-1219

Chen, Y., Cheng, L., Lian, R., Song, Z., and Tian, J. (2021). COVID-19 vaccine research focusses on safety, efficacy, immunoinformatics, and vaccine production and delivery: a bibliometric analysis based on VOSviewer. *Biosci. Trends* 15 (2), 64–73. doi:10.5582/bst.2021.01061

Cheng, K., Guo, Q., Yang, W., Wang, Y., Sun, Z., and Wu, H. (2022). Mapping knowledge landscapes and emerging trends of the links between bone metabolism and diabetes mellitus: a bibliometric analysis from 2000 to 2021. *Front. Public Health* 10, 918483. doi:10.3389/fpubh.2022.918483

Chimene, D., Lennox, K. K., Kaunas, R. R., and Gaharwar, A. K. (2016). Advanced bioinks for 3D printing: a materials science perspective. *Ann. Biomed. Eng.* 44 (6), 2090–2102. doi:10.1007/s10439-016-1638-y

Cidonio, G., Glinka, M., Kim, Y. H., Kanczler, J. M., Lanham, S. A., Ahlfeld, T., et al. (2020). Nanoclay-based 3D printed scaffolds promote vascular ingrowth *ex vivo* and generate bone mineral tissue *in vitro* and *in vivo*. *Biofabrication* 12, 035010. doi:10.1088/1758-5090/ab8753

Daly, A. C., Freeman, F. E., Gonzalez-Fernandez, T., Critchley, S. E., Nulty, J., and Kelly, D. J. (2017). 3D bioprinting for cartilage and osteochondral tissue engineering. *Adv. Healthc. Mater* 6 (22). doi:10.1002/adhm.201700298

Dimitriou, R., Jones, E., McGonagle, D., and Giannoudis, P. V. (2011). Bone regeneration: current concepts and future directions. *BMC Med.* 9, 66. doi:10.1186/1741-7015-9-66

Ding, W., Zhou, Q., Lu, Y., Wei, Q., Tang, H., Zhang, D., et al. (2023). ROS-scavenging hydrogel as protective carrier to regulate stem cells activity and promote osteointegration of 3D printed porous titanium prosthesis in osteoporosis. *Front. Bioeng. Biotechnol.* 11, 1103611. doi:10.3389/fbioe.2023.1103611

Duan, W. L., Zhang, L. N., Bohara, R., Martin-Saldaña, S., Yang, F., Zhao, Y. Y., et al. (2023). Adhesive hydrogels in osteoarthritis: from design to application. *Mil. Med. Res.* 10 (1), 4. doi:10.1186/s40779-022-00439-3

Ehrler, D. M., and Vaccaro, A. R. (2000). The use of allograft bone in lumbar spine surgery. *Clin. Orthop. Relat. Res.* 371 (371), 38–45. doi:10.1097/00003086-200002000-00005

García-Gareta, E., Coathup, M. J., and Blunn, G. W. (2015). Osteoinduction of bone grafting materials for bone repair and regeneration. *Bone* 81, 112–121. doi:10.1016/j.bone.2015.07.007

Ghandforoushan, P., Alehosseini, M., Golafshan, N., Castilho, M., Dolatshahi-Pirouz, A., Hanaee, J., et al. (2023). Injectable hydrogels for cartilage and bone tissue regeneration: a review. *Int. J. Biol. Macromol.* 246, 125674. doi:10.1016/j.ijbiomac.2023.125674

Gong, Y., Bu, Y., Li, Y., Hao, D., He, B., Kong, L., et al. (2022). Hydrogel-based delivery system applied in the local anti-osteoporotic bone defects. *Front. Bioeng. Biotechnol.* 10, 1058300. doi:10.3389/fbioe.2022.1058300

González-Alcaide, G., Peris, J., and Ramos, J. M. (2017). Areas of research and clinical approaches to the study of liver abscess. *World J. Gastroenterol.* 23 (2), 357–365. doi:10.3748/wjg.v23.i2.357

Heid, S., and Boccaccini, A. R. (2020). Advancing bioinks for 3D bioprinting using reactive fillers: a review. *Acta Biomater.* 113, 1–22. doi:10.1016/j.actbio.2020.06.040

Iatecola, A., Longhitano, G. A., Antunes, L. H. M., Jardini, A. L., Miguel, E. d. C., Béreš, M., et al. (2021). Osseointegration improvement of Co-Cr-Mo alloy produced by additive manufacturing. *Pharmaceutics* 13 (5), 724. doi:10.3390/pharmaceutics13050724

Kang, X., Zhang, X. B., Gao, X. D., Hao, D. J., Li, T., and Xu, Z. W. (2022). Bioprinting for bone tissue engineering. *Front. Bioeng. Biotechnol.* 10, 1036375. doi:10.3389/fbioe.2022.1036375

Keating, J. F., Simpson, A. H., and Robinson, C. M. (2005). The management of fractures with bone loss. *J. Bone Jt. Surg. Br.* 87 (2), 142–150. doi:10.1302/0301-620x.87b2.15874

Kolambkar, Y. M., Dupont, K. M., Boerckel, J. D., Huebsch, N., Mooney, D. J., Hutmacher, D. W., et al. (2011). An alginate-based hybrid system for growth factor delivery in the functional repair of large bone defects. *Biomaterials* 32 (1), 65–74. doi:10.1016/j.biomaterials.2010.08.074

Kumar Gupta, D., Ali, M. H., Ali, A., Jain, P., Anwer, M. K., Iqbal, Z., et al. (2022). 3D printing technology in healthcare: applications, regulatory understanding, IP repository and clinical trial status. *J. Drug Target* 30 (2), 131–150. doi:10.1080/1061186X.2021.1935973

Kuo, C. Y., Lin, T. Y., and Yeh, Y. C. (2023). Hydrogel-based strategies for the management of osteomyelitis. *ACS Biomater. Sci. Eng.* 9 (4), 1843–1861. doi:10.1021/acsbiomaterials.2c01057

Lewallen, E. A., Riester, S. M., Bonin, C. A., Kremers, H. M., Dudakovic, A., Kakar, S., et al. (2015). Biological strategies for improved osseointegration and osteoinduction of porous metal orthopedic implants. *Tissue Eng. Part B Rev.* 21 (2), 218–230. doi:10.1089/ten.TEB.2014.0333

Li, X., Sun, Q., Li, Q., Kawazoe, N., and Chen, G. (2018). Functional hydrogels with tunable structures and properties for tissue engineering applications. *Front. Chem.* 6, 499. doi:10.3389/fchem.2018.00499

Liu, L., Yang, B., Wang, L. Q., Huang, J. P., Chen, W. Y., Ban, Q., et al. (2020). Biomimetic bone tissue engineering hydrogel scaffolds constructed using ordered CNTs and HA induce the proliferation and differentiation of BMSCs. *J. Mater Chem. B* 8 (3), 558–567. doi:10.1039/c9tb01804b

Liu, Y., and Hsu, S. H. (2018). Synthesis and biomedical applications of self-healing hydrogels. *Front. Chem.* 6, 449. doi:10.3389/fchem.2018.00449

Lu, Y., Wang, X., Chen, H., Li, X., Liu, H., Wang, J., et al. (2023). Metal-bone scaffold for accelerated peri-implant endosseous healing. *Front. Bioeng. Biotechnol.* 11, 1334072. doi:10.3389/fbioe.2023.1334072

Mandrycky, C., Wang, Z., Kim, K., and Kim, D. H. (2016). 3D bioprinting for engineering complex tissues. *Biotechnol. Adv.* 34 (4), 422–434. doi:10.1016/j.biotechadv.2015.12.011

McEwan, J. K., Tribe, H. C., Jacobs, N., Hancock, N., Qureshi, A. A., Dunlop, D. G., et al. (2018). Regenerative medicine in lower limb reconstruction. *Regen. Med.* 13 (4), 477–490. doi:10.2217/rme-2018-0011

Morandini Rodrigues, L., Lima Zutin, E. A., Sartori, E. M., Rizzante, F. A. P., Mendonça, D. B. S., Krebsbach, P. H., et al. (2022). Nanoscale hybrid implant surfaces and Osterix-mediated osseointegration. *J. Biomed. Mater Res. A* 110 (3), 696–707. doi:10.1002/jbm.a.37323

Muir, V. G., and Burdick, J. A. (2021). Chemically modified biopolymers for the formation of biomedical hydrogels. *Chem. Rev.* 121 (18), 10908–10949. doi:10.1021/acs.chemrev.0c00923

Murphy, S. V., and Atala, A. (2014). 3D bioprinting of tissues and organs. *Nat. Biotechnol.* 32 (8), 773–785. doi:10.1038/nbt.2958

Nie, J., Pei, B., Wang, Z., and Hu, Q. (2019). Construction of ordered structure in polysaccharide hydrogel: a review. *Carbohydr. Polym.* 205, 225–235. doi:10.1016/j.carbpol.2018.10.033

Oliva, N., Shin, M., and Burdick, J. A. (2021). Editorial: special issue on advanced biomedical hydrogels. *ACS Biomater. Sci. Eng.* 7 (9), 3993–3996. doi:10.1021/acsbiomaterials.1c01059

Ortega, M. A., De Leon-Oliva, D., Boaru, D. L., Fraile-Martinez, O., García-Montero, C., Diaz, R., et al. (2023). Unraveling the new perspectives on antimicrobial hydrogels: state-of-the-art and translational applications. *Gels* 9 (8), 617. doi:10.3390/gels9080617

Pereira, H. F., Cengiz, I. F., Silva, F. S., Reis, R. L., and Oliveira, J. M. (2020). Scaffolds and coatings for bone regeneration. *J. Mater Sci. Mater Med.* 31 (3), 27. doi:10.1007/s10856-020-06364-y

Ringeisen, B. R., Kim, H., Barron, J. A., Krizman, D. B., Chrisey, D. B., Jackman, S., et al. (2004). Laser printing of pluripotent embryonal carcinoma cells. *Tissue Eng.* 10 (3-4), 483–491. doi:10.1089/107632704323061843

Rosset, P., Deschaseaux, F., and Layrolle, P. (2014). Cell therapy for bone repair. *Orthop. Traumatol. Surg. Res.* 100 (1 Suppl. l), S107–S112. doi:10.1016/j.otsr.2013.11.010

Salhotra, A., Shah, H. N., Levi, B., and Longaker, M. T. (2020a). Mechanisms of bone development and repair. *Nat. Rev. Mol. Cell Biol.* 21 (11), 696–711. doi:10.1038/s41580-020-00279-w

Salhotra, A., Shah, H. N., Levi, B., and Longaker, M. T. (2020b). Mechanisms of bone development and repair. *Nat. Rev. Mol. Cell Biol.* 21, 696–711. doi:10.1038/s41580-020-00279-w

Saravanan, S., Vimalraj, S., and Anuradha, D. (2018). Chitosan based thermoresponsive hydrogel containing graphene oxide for bone tissue repair. *Biomed. Pharmacother.* 107, 908–917. doi:10.1016/j.biopha.2018.08.072

Shan, B. H., and Wu, F. G. (2024). Hydrogel-based growth factor delivery platforms: strategies and recent advances. *Adv. Mater* 36 (5), e2210707. doi:10.1002/adma.202210707

Song, Q., Wang, D., Li, H., Wang, Z., Sun, S., Wang, Z., et al. (2024). Dual-response of multi-functional microsphere system to ultrasound and microenvironment for enhanced bone defect treatment. *Bioact. Mater* 32, 304–318. doi:10.1016/j.bioactmat.2023.10.007

Sousa, C. F. V., Saraiva, C. A., Correia, T. R., Pesqueira, T., Patrício, S. G., Rial-Hermida, M. I., et al. (2021). Bioinstructive layer-by-layer-coated customizable 3D printed perfusable microchannels embedded in photocrosslinkable hydrogels for vascular tissue engineering. *Biomolecules* 11, 863. doi:10.3390/biom11060863

Suo, H., Zhang, D., Yin, J., Qian, J., Wu, Z. L., and Fu, J. (2018). Interpenetrating polymer network hydrogels composed of chitosan and photocrosslinkable gelatin with enhanced mechanical properties for tissue engineering. *Mater Sci. Eng. C Mater Biol. Appl.* 92, 612–620. doi:10.1016/j.msec.2018.07.016

Tavares, M. T., Gaspar, V. M., Monteiro, M. V., S Farinha, J. P., Baleizão, C., and Mano, J. F. (2021). GelMA/bioactive silica nanocomposite bioinks for stem cell osteogenic differentiation. *Biofabrication* 13, 035012. doi:10.1088/1758-5090/abdc86

Tsiapalis, D., and O'Driscoll, L. (2020). Mesenchymal stem cell derived extracellular vesicles for tissue engineering and regenerative medicine applications. *Cells* 9 (4), 991. doi:10.3390/cells9040991

Tzagiollari, A., McCarthy, H. O., Levingstone, T. J., and Dunne, N. J. (2022). Biodegradable and biocompatible adhesives for the effective stabilisation, repair and regeneration of bone. *Bioeng. (Basel)* 9 (6), 250. doi:10.3390/bioengineering9060250

van Eck, N. J., and Waltman, L. (2010). Software survey: VOSviewer, a computer program for bibliometric mapping. *Scientometrics* 84 (2), 523–538. doi:10.1007/s11192-009-0146-3

Vinikoor, T., Dzidotor, G. K., Liu, Y., Kan, H. M., Barui, S., Chorsi, M. T., et al. (2023). Injectable and biodegradable piezoelectric hydrogel for osteoarthritis treatment. *Nat. Commun.* 14 (1), 6257. doi:10.1038/s41467-023-41594-y

Wan, Z., Zhang, P., Liu, Y., Lv, L., and Zhou, Y. (2020). Four-dimensional bioprinting: current developments and applications in bone tissue engineering. *Acta Biomater.* 101, 26–42. doi:10.1016/j.actbio.2019.10.038

Wang, C., Ye, X., Zhao, Y., Bai, L., He, Z., Tong, Q., et al. (2020). Cryogenic 3D printing of porous scaffolds for *in situ* delivery of 2D black phosphorus nanosheets, doxorubicin hydrochloride and osteogenic peptide for treating tumor resection-induced bone defects. *Biofabrication* 12 (3), 035004. doi:10.1088/1758-5090/ab6d35

Wang, J., Chi, Y., Yang, B., Zhang, Q., Wang, D., He, X., et al. (2022). The application of biomaterials in osteogenesis: a bibliometric and visualized analysis. *Front. Bioeng. Biotechnol.* 10, 998257. doi:10.3389/fbioe.2022.998257

Weber, F. E. (2019). Reconsidering osteoconduction in the era of additive manufacturing. *Tissue Eng. Part B Rev.* 25 (5), 375–386. doi:10.1089/ten.TEB.2019.0047

Xie, X., Wei, J., Zhang, B., Xiong, W., He, Z., Zhang, Y., et al. (2022). A self-assembled bilayer polypeptide-engineered hydrogel for spatiotemporal modulation of bactericidal and anti-inflammation process in osteomyelitis treatment. *J. Nanobiotechnology* 20 (1), 416. doi:10.1186/s12951-022-01614-3

Yang, J., Zhang, Y. S., Yue, K., and Khademhosseini, A. (2017). Cell-laden hydrogels for osteochondral and cartilage tissue engineering. *Acta Biomater.* 57, 1–25. doi:10.1016/j.actbio.2017.01.036

Yuan, W., Wang, H., Fang, C., Yang, Y., Xia, X., Yang, B., et al. (2021). Microscopic local stiffening in a supramolecular hydrogel network expedites stem cell mechanosensing in 3D and bone regeneration. *Mat. Horiz.* 8, 1722–1734. doi:10.1039/d1mh00244a

Yue, S., He, H., Li, B., and Hou, T. (2020). Hydrogel as a biomaterial for bone tissue engineering: a review. *Nanomater. (Basel)* 10 (8), 1511. doi:10.3390/nano10081511

Zhang, J., Wehrle, E., Adamek, P., Paul, G. R., Qin, X. H., Rubert, M., et al. (2020b). Optimization of mechanical stiffness and cell density of 3D bioprinted cell-laden scaffolds improves extracellular matrix mineralization and cellular organization for bone tissue engineering. *Acta Biomater.* 114, 307–322. doi:10.1016/j.actbio.2020.07.016

Zhang, L., Yang, G., Johnson, B. N., and Jia, X. (2019a). Three-dimensional (3D) printed scaffold and material selection for bone repair. *Acta Biomater.* 84, 16–33. doi:10.1016/j.actbio.2018.11.039

Zhang, L., Yang, G., Johnson, B. N., and Jia, X. (2019b). Three-dimensional (3D) printed scaffold and material selection for bone repair. *Acta Biomater.* 84, 16–33. doi:10.1016/j.actbio.2018.11.039

Zhang, X., Yi, K., Xu, J. G., Wang, W. X., Liu, C. F., He, X. L., et al. (2024). Application of three-dimensional printing in cardiovascular diseases: a bibliometric analysis. *Int. J. Surg.* 110 (2), 1068–1078. doi:10.1097/JS9.0000000000000868

Zhang, Y., Yu, T., Peng, L., Sun, Q., Wei, Y., and Han, B. (2020a). Advancements in hydrogel-based drug sustained release systems for bone tissue engineering. *Front. Pharmacol.* 11, 622. doi:10.3389/fphar.2020.00622

Zhao, C., Liu, W., Zhu, M., Wu, C., and Zhu, Y. (2022). Bioceramic-based scaffolds with antibacterial function for bone tissue engineering: a review. *Bioact. Mater* 18, 383–398. doi:10.1016/j.bioactmat.2022.02.010

Zhong, D., Luo, S., Zheng, L., Zhang, Y., and Jin, R. (2020). Epilepsy occurrence and circadian rhythm: a bibliometrics study and visualization analysis via CiteSpace. *Front. Neurol.* 11, 984. doi:10.3389/fneur.2020.00984

Zhou, Y., Yue, Z., Chen, Z., and Wallace, G. (2020). 3D coaxial printing tough and elastic hydrogels for tissue engineering using a catechol functionalized ink system. *Adv. Healthc. Mat.* 9, e2001342. doi:10.1002/adhm.202001342

Zhu, H., Monavari, M., Zheng, K., Distler, T., Ouyang, L., Heid, S., et al. (2022). 3D bioprinting of multifunctional dynamic nanocomposite bioinks incorporating Cu-doped mesoporous bioactive glass nanoparticles for bone tissue engineering. *Small* 18, e2104996. doi:10.1002/smll.202104996

Zhu, J., and Marchant, R. E. (2011). Design properties of hydrogel tissue-engineering scaffolds. *Expert Rev. Med. Devices* 8 (5), 607–626. doi:10.1586/erd.11.27

Zhu, Y., Zhang, K., Zhao, R., Ye, X., Chen, X., Xiao, Z., et al. (2017). Bone regeneration with micro/nano hybrid-structured biphasic calcium phosphate bioceramics at segmental bone defect and the induced immunoregulation of MSCs. *Biomaterials* 147, 133–144. doi:10.1016/j.biomaterials.2017.09.018

frontiers | Frontiers in Pharmacology

TYPE Review
PUBLISHED 31 March 2025
DOI 10.3389/fphar.2025.1484437

OPEN ACCESS

EDITED BY
Lufei Wang,
Guangxi Medical University, China

REVIEWED BY
Jinfang Gao,
Shanxi Medical University, China
Shulong Wang,
Beijing University of Chinese Medicine, China
Fanfan Wang,
Anhui University of Chinese Medicine, China

*CORRESPONDENCE
Rui Fang,
xjfrdoctor@163.com

RECEIVED 21 August 2024
ACCEPTED 19 March 2025
PUBLISHED 31 March 2025

CITATION
Zhang WH, Xiang WY, Yi L and Fang R (2025) The status and hotspot analysis of research on extracellular vesicles and osteoarthritis: a bibliometric analysis.
Front. Pharmacol. 16:1484437.
doi: 10.3389/fphar.2025.1484437

The status and hotspot analysis of research on extracellular vesicles and osteoarthritis: a bibliometric analysis

Wen Hao Zhang[1], Wen Yuan Xiang[1,2,3,4], Lin Yi[1,2,3,4] and Rui Fang[1,2,3,4]*

[1]The Fourth Clinical College of Xinjiang Medical University, Urumqi, China, [2]Department of Orthopaedic, Institute of Traditional Chinese Medicine Hospital of Xinjiang Uygur Autonomous Region, Urumqi, China, [3]Department of Orthopaedic, Xinjiang Uygur Autonomous Region Institute of Traditional Chinese Medicine, Urumqi, China, [4]Department of orthopaedic, The Fourth Affiliated Hospital of Xinjiang Medical University, Urumqi, China

Background: Degenerative joint disease, known as osteoarthritis (OA), is characterized by pain, swelling, and decreased mobility. The illness has a major negative influence on patients' quality of life and is common around the world, especially among older people. Nevertheless, there are insufficient possibilities for early diagnosis and therapy. Extracellular vesicles, or EVs, control the immune response, tissue healing, and cellular communication.

Methods: This work offers a bibliometric representation of the areas of focus and correlations between extracellular vesicles and osteoarthritis. We searched for osteoarthritis and extracellular vesicles in publications in the Web of Science Core Collection (WoSCC) database. Bibliometrics, an R package, CiteSpace 6.1. R2, and VOSviewer 1.6.17 were used to perform bibliometric analyses of concentration fields, trends, and relevant factors.

Results: 944 papers from 59 nations were published; the countries that contributed the most to the field were China, the USA, and Italy. Professors Laura and Enrico are the top contributors. Sichuan University, Istituto Ortopedico Galeazzi, and Shanghai Jiao Tong University are the top three universities. The International Journal of Molecular Sciences is an excellent publication. Exosome, expression, knee osteoarthritis, extracellular vesicle, mesenchymal stem cell, osteoarthritis, and inflammation are the most often occurring keywords.

Conclusion: These results suggest areas of interest and focus for future research on EVs and OA. This trend suggests that the volume of literature on OA and EVs will continue to rise, with more research being published in the future. This study helps scholars understand current research hotspots in the field and may inspire future research.

KEYWORDS

osteoarthritis, extracellular vesicles, bibliometric, hotspots, mesenchymal stem cell

1 Introduction

Osteoarthritis OA is a degenerative disease of the bones and joints that can be recognized by inflammation of the synovium, secondary osteophytes, and loss of articular cartilage. The most common clinical manifestations include stiffness, discomfort, edema, and dysfunction (Hunter, 2015; Sharma, 2021). With an approximate global burden of 16%, the prevalence of OA has dramatically increased due to the growing number of elderly and obese people (Cui et al., 2020). In China, the prevalence of OA exceeds 50% in people with knee pain over the age of 65, and the prevalence of OA exceeds 80% in those over the age of 75 with knee pain (Tang et al., 2016).

OA has a long disease progression period and is strongly associated with older age, gender, overweight, residential environment, and genetic predisposition (Di et al., 2024; Georgiev and Angelov, 2019; Simão et al., 2019). It also has a lengthy progression time. OA may result in decreased quality of life, disability, loss of joint function, and higher medical costs for patients (Ali et al., 2017). Patients with KOA are often assessed using the Kellgren-Lawrence (K-L) classification. Total knee arthroplasty (TKA) and unicompartmental knee arthroplasty (UKA) are frequently utilized for patients with grade III or IV K-L classification (Mancuso et al., 2016; Yao et al., 2023; Zhao et al., 2022).

However, there are issues related to high surgical costs, infections, blood embolism, implant lifespan, and longevity (Gililland et al., 2012; Sloan and Lee, 2021). Patients with early OA, such as those classified as grade I or II in the K-L grading system, are frequently treated with PRP (platelet-rich plasma), sodium hyaluronate, and non-steroidal anti-inflammatory medicines (NSAIDs) (Feng et al., 2023; Sánchez et al., 2021; Su et al., 2018). However, most of these treatments only moderate its symptoms of OA and do not fundamentally reverse its pathological changes. Therefore, exploring treatment modalities for OA is a worthwhile topic for in-depth investigation.

Stem cell therapy has become available as an experimental and clinical treatment option for adolescent OA. However, there are risks, such as safety and potential tumour differentiation (Damjanov and Andrews, 2016). EVs, a type of cell-free therapy, have been extensively studied for their advantages in regeneration, immunomodulation, and inflammation modulation by researchers (Liu et al., 2023; Lv et al., 2020). EVs are membrane structures that frequently originate from cells and have a diameter that ranges from 100 nm to 1 μm. Initially thought to be primarily metabolic waste products by researchers, EVs now represent a broad category of substances (Vandergriff et al., 2018; Andaloussi et al., 2013). All prokaryotic and eukaryotic cells studied to date produce and release phospholipid bilayer biovesicles known as EVs, containing abundant lipids, protein, ribonucleic acid, and other physiologically active substances. EVs are typically classified based on their vesicle diameter into apoptotic bodies, microvesicles, microparticles (Bheri et al., 2020; Andaloussi et al., 2013), and nano-vesicles (Zhang et al., 2021; Pang et al., 2023).

Apoptotic bodies are vesicles released by apoptotic cells containing intracellular proteins and nucleic acids (Xu et al., 2019). Microvesicles are small membranous vesicles secreted by microorganisms, containing proteins and lipids from the microorganism's surface (Wang X. et al., 2022). Small vesicles with membranes called microvesicles can get into cells and deliver lipids, proteins, and genetic information (Xie et al., 2016). EVs have shown promising results in treating conditions such as myocardial infarction (Nian and Fu, 2023), spinal cord injury (Fan et al., 2022), tumors (Shao et al., 2022), diabetes (Sun et al., 2021), and others in previous studies.

Bibliometrics is an essential tool for research assessment, systematically analyzing literature to provide researchers with comprehensive insights into data and trends (Zhang et al., 2023a; Zhang et al., 2023b). It provides a comprehensive overview of research trends, hotspots, and developmental behaviors within a particular field or matter. Bibliometrics helps assess the quantity and quality of publications on current topics, institutions, and regions. It also forecasts future research directions and guides research trends (Zhou et al., 2023; Hu et al., 2023). While studies on EVs and OA are present in existing bibliographic analyses, fewer studies have focused on bibliometric analyses specifically.

Using the WoSCC database, bibliometric tools like CiteSpace and VOSviewer, and websites like bibliometric.com, this study provides a bibliometric analysis of documents about EVs and OA. The analysis covers aspects such as country, institution, authors, journals, highly cited publications, and keywords. The study sheds light on hotspots, research trends, and upcoming advancements in EVs and OA.

2 Materials and methods

2.1 Data collection

This study employed the Web of Science Core Collection (WoSCC), a globally indexed scientific database. To ensure data accuracy, searches were conducted, data downloaded, and data analysis performed on 1 January 2025. The search covered publications from 1 January 2000 to 31 December 2024, with the following Boolean query: *TS=(Osteoarthritis OR Osteoarthritides OR Osteoarthrosis OR Osteoarthroses) AND TS=(Exosomes OR Extracellular Vesicles OR Secretory Vesicles OR Cell-Derived Microparticles)*. The search adhered strictly to the predefined keywords, and retrieved records underwent systematic analysis. Full-record datasets, including abstracts and citations, were exported and processed as outlined in Figure 1 (data extraction workflow).

3 Results

3.1 Trend analysis of publications

By conducting a keyword-based search in the Web of Science Core Collection (WoSCC) database, a total of 944 research articles related to extracellular vesicles (EVs) and osteoarthritis (OA) were identified. The first study exploring the relationship between EVs and OA dates back to 2000. From 2000 to 2015, the number of publications in this field remained relatively low (as shown in Figure 2), indicating limited academic attention during this period. Starting in 2016, the annual number of publications

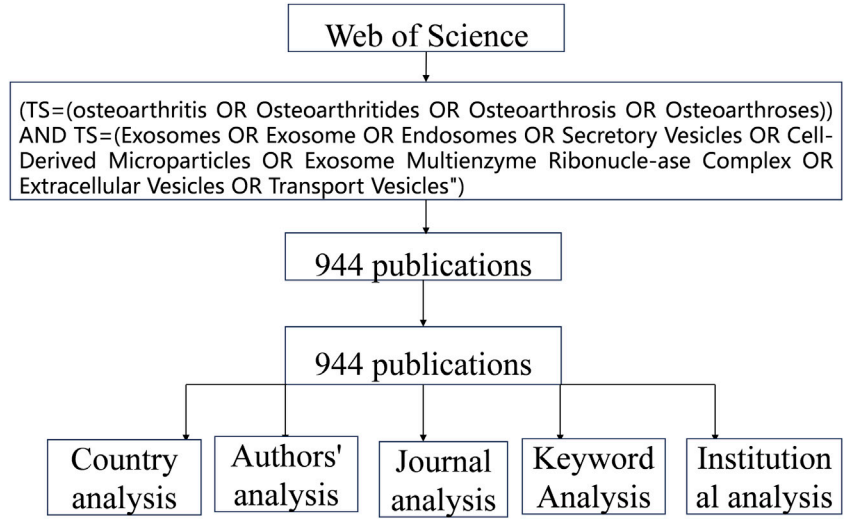

FIGURE 1
Flow diagram of the include articles.

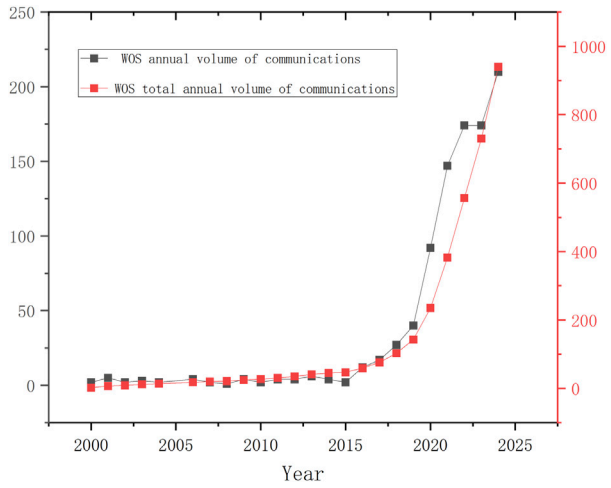

FIGURE 2
A Treands in total annual number of publications related to EVs and OA publications.

surpassed double digits for the first time, with 12 papers published that year.

Between 2016 and 2019, the number of publications continued to grow, reflecting a significant increase in research output. In 2021, the number of publications exceeded 100 (reaching 147), and by 2024, it peaked at 210. Although there was a slight decline in the number of publications in 2023 compared to 2022, the overall trend remained highly productive. As illustrated in Figure 2, research on EVs in OA has shown a consistent upward trajectory over the past 5 years, gradually emerging as an important and rapidly growing field. This trend is further supported by the increasing proportion of original research articles compared to review articles, highlighting the growing focus on the therapeutic, diagnostic, and mechanistic roles of EVs in OA. The substantial and valuable research output in this field underscores its potential for further exploration and development.

3.2 Countries/regions analysis

A visual analysis of the 944 publications from 2000 to 2024, focusing on the countries and regions involved, was conducted using VOSviewer software. When the threshold was set to one publication, 59 countries met this criterion; when the threshold was increased to four publications, 32 countries qualified.

As shown in Figure 3A, five clusters were identified, with the largest cluster comprising China and the United States. This cluster includes China, the United States, Japan, and Australia, encompassing 683 articles, which account for 72.35% of the total publications (Table 1). China leads with 518 articles, representing 54.87% of the total, and has garnered 15,077 citations, with an average of 29.11 citations per article and an H-index of 52. The total link strength of 82 highlights China's prominent position in this research field and its extensive international collaborations, as illustrated in Figures 3B, C.

The United States ranks second with 124 articles, accounting for 13.14% of the total. Its H-index is 30, and its publications have received 5,838 citations, with an average of 47.08 citations per article. Although the United States has fewer publications and a lower H-index compared to China, its higher average citation count reflects the broader recognition and impact of its research. Among the top ten countries, Germany stands out with 27 articles and the highest average citation count (62.84 per article), indicating the high quality and recognition of its research in this field.

Since 2017, China's research output has grown consistently, particularly after 2020, when its annual publications accounted for more than half of the total in this field. Both China and the United States serve as key nodes connecting other countries, driving significant advancements and collaborations in the field

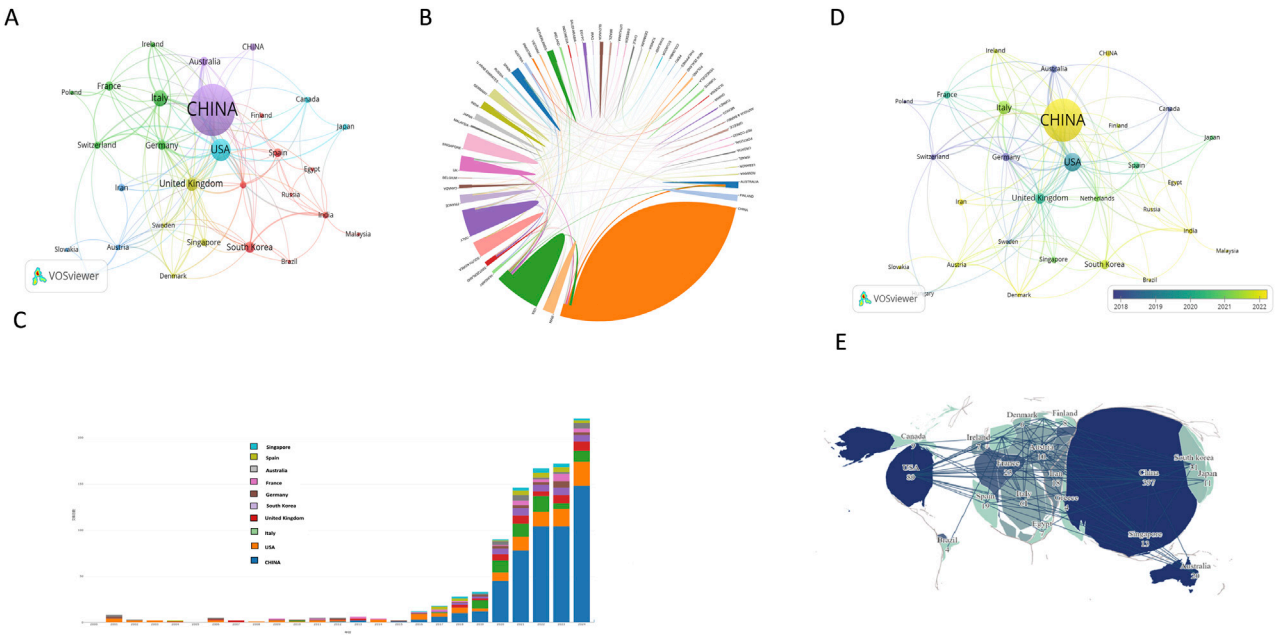

FIGURE 3
National collaborative analysis of extracellular vesicles and osteoarthritis **(A)** Collaboration between countries or regions based on VOSviewer; **(B)** The coauthorship network map of countries; **(C)** Annual number of publications in different countries **(D)** Map of the network of countries working together in time; **(E)** The coauthorship network map of countries.

TABLE 1 Top 10 countries in terms of the number of published papers.

Rank	Country	Record	Citations	Total link strength	Average citations	H-index
1	China	518	15077	82	29.11	52
2	United States of America	124	5,838	112	47.08	30
3	Italy	73	1741	53	23.85	23
4	United Kingdom	52	901	67	17.33	14
5	South Korea	41	924	22	22.54	13
6	Germany	31	1948	44	62.84	16
7	Australia	30	1,268	22	42.27	15
8	France	27	1,458	43	54.00	13
9	Spain	26	800	16	30.77	10
10	Iran	21	470	7	22.38	9

(Figures 3D, E). Over the past 3 years, China has been the most active country in terms of research and publications, demonstrating strong support and keen interest from scholars in this area.

3.3 Authors and co-cited authors analysis

A visual analysis of the authors included in the publications was conducted using VOSviewer software. When the publication threshold was set to one, 5,166 authors were identified as contributing to this research field; when the threshold was increased to five, 75 authors met this criterion. As shown in Figure 4A, the authors were grouped into distinct clusters based on their research areas and affiliated institutions.

The largest cluster comprises nine authors, primarily including Professor Laura de Girolamo and Professor Alessandra Colombini from Italy. The second-largest cluster consists of Professor Li Duan, Professor Li Xingfu, Professor Liang Yujie, Professor Wang Daping, Professor Xia Jiang, Professor Xiao Yin, Professor Xu Limei, and Professor Xu Xiao from Shenzhen University in China. Notably, these authors exhibit strong collaborative ties, making significant contributions to the advancement of the field (Figure 4A). Based on publication counts, Professor Laura de Girolamo and Professor Enrico Ragni from IRCCS Istituto Ortopedico Galeazzi in Italy

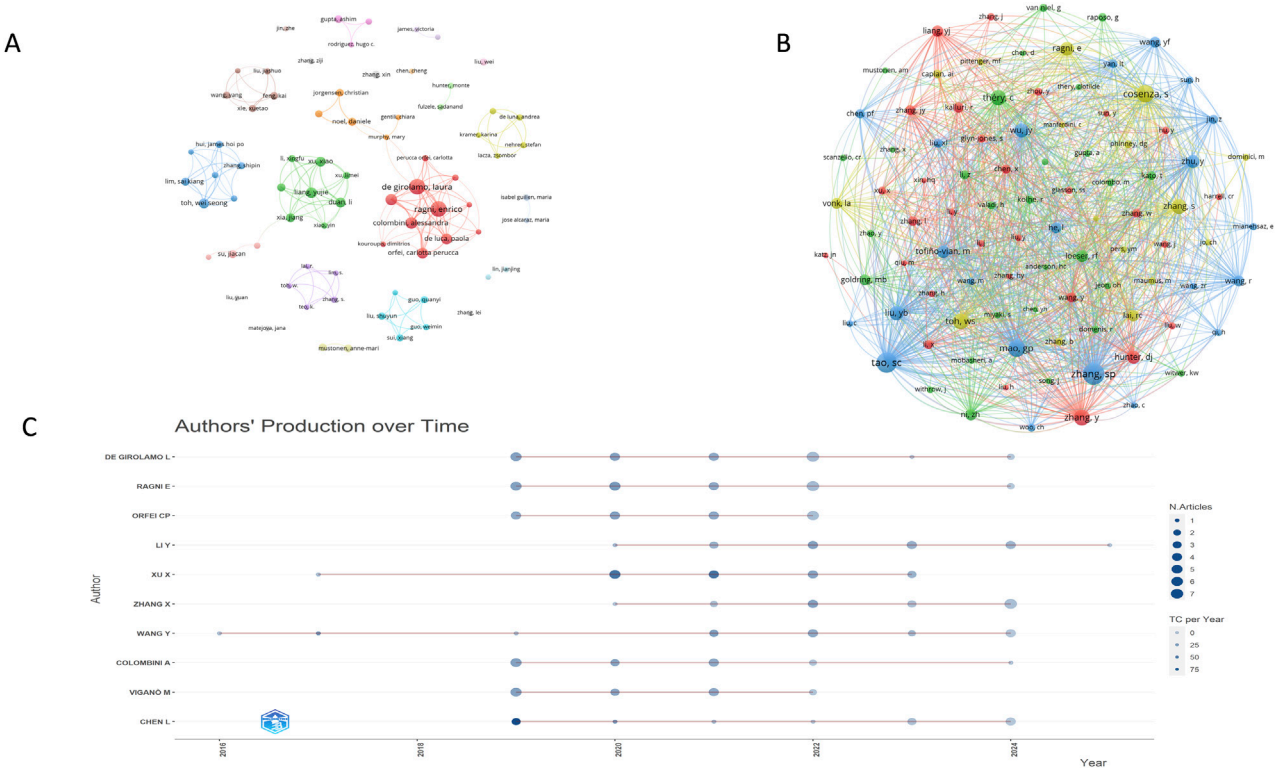

FIGURE 4
Analysis of author collaboration on extracellular vesicles and osteoarthritis. **(A)** Collaboration between authors based on VOSviewer; **(B)** Author co-citation coupling map; **(C)** Annual volumeof publications by top 10 authors.

TABLE 2 Top 10 authors in terms of the number of published papers.

Rank	Author	Country	Record	Citations	Average citations	Total link strength	H-index
1	De Girolamo, Laura	Italy	23	500	21.74	134	13
2	Ragni, Enrico	Italy	23	532	23.13	122	13
3	Colombini, Alessandra	Italy	15	457	30.47	89	12
4	Vigano, Marco	Italy	14	454	32.43	83	11
5	Orfei, Carlotta Perucca	Italy	13	365	28.08	80	11
6	Liang, Yujie	China	13	769	59.15	78	9
7	Duan, Li	China	13	313	24.08	72	8
8	De Luca, Paola	Italy	12	736	61.33	74	9
9	Xu, Xiao	China	12	1,567	130.58	59	9
10	Toh, Wei Seong	Singapore	12	765	63.75	74	9

have the highest number of publications, with 23 each (Table 2). It is worth noting that the top five authors by publication volume are all from Italy, highlighting the high level of collaboration and productivity among Italian scholars in this field. Chinese scholars Professor Liang Yujie and Professor Li Duan rank sixth. Professor SP Zhang from Singapore and Professor Tao SC from China are the most co-cited authors, with 350 and 329 co-citations, respectively (Table 3). In Figure 4B, the node size represents the co-citation count, and the line thickness indicates the co-citation strength between cited references. This visualization underscores the high recognition of authors such as Zhang SP, Tao SC, Alessandra Colombini, and Marco Viganò, reflecting the quality and academic impact of their work.

Among the top ten authors by publication volume, Professor Xu Xiao from Shenzhen University leads with an average of 130.58 citations per article, followed by Professor

TABLE 3 Top 10 Co-cited authors in terms of the number of published papers.

Rank	Author	Country	Citations	Total link strength	H-index
1	Zhang, Sp	China	350	6,205	6
2	Tao, Sc	China	329	6,371	2
3	Cosenza, S	France	260	5,065	3
4	Mao, Gp	China	247	5,692	4
5	Zhang, Y	China	229	4,070	10
6	Toh, Ws	Singapore	225	3,595	1
7	Théry, C	France	217	3,533	1
8	Zhang, S	China	201	3,829	1
9	Wu, Jy	China	196	4,035	3
10	Liu, Yb	China	191	4,145	2

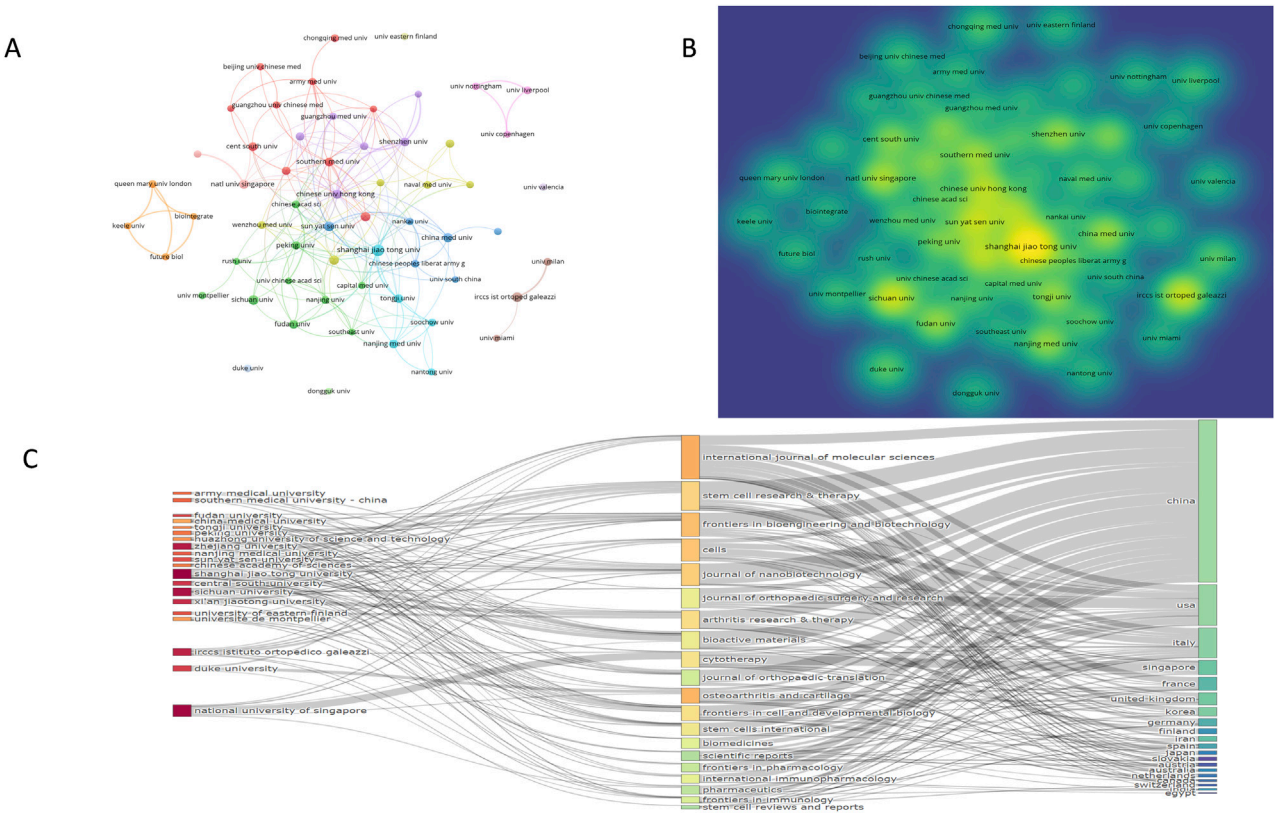

FIGURE 5
Analysis of institutional cooperation between extracellular vesicles and osteoarthritis **(A)** Collaboration between institution based on VOSviewer; **(B)** Hot spot distribution map of institutional issues; **(C)** Three plot map of institutions-journals-countries.

Toh Wei Seong and Professor De Luca Paola, with 63.75 and 61.33 citations per article, respectively. Figure 4C shows that most of these leading authors began their research around 2019, a year that marked a significant increase in the volume of publications in this field. This growth has continued through 2024, indicating that the field still holds substantial untapped potential.

3.4 Analysis of institution and research areas

A visual analysis of institutions involved in the included literature was conducted using VOSviewer software. When the publication threshold was set at 1, 1,214 institutions were identified as active in this research field, while increasing the threshold to five reduced the number to 97 qualifying

TABLE 4 Top 10 Institutional in terms of the number of published papers.

Rank	Institutiona	Country	Record	Citations	Average citations	Total link strength
1	Shanghai Jiao Tong University	China	48	1783	Cosenza et al. (2017)	36
2	Sichuan University	China	27	574	21.26	5
3	IRCCS Istituto Ortopedico Galeazzi	Italy	26	582	22.38	9
4	Sun Yat-sen University	China	23	1,113	48.39	22
5	Zhejiang University	China	22	1,197	54.41	13
6	Chinese University of Hong Kong	China	21	1759	83.76	42
7	National University of Singapore	Singapore	21	2,322	110.57	14
8	China Medical University	China	19	739	38.89	11
9	Huazhong University of Science and Technology	China	19	288	15.16	7
10	Fudan University	China	18	381	21.17	14

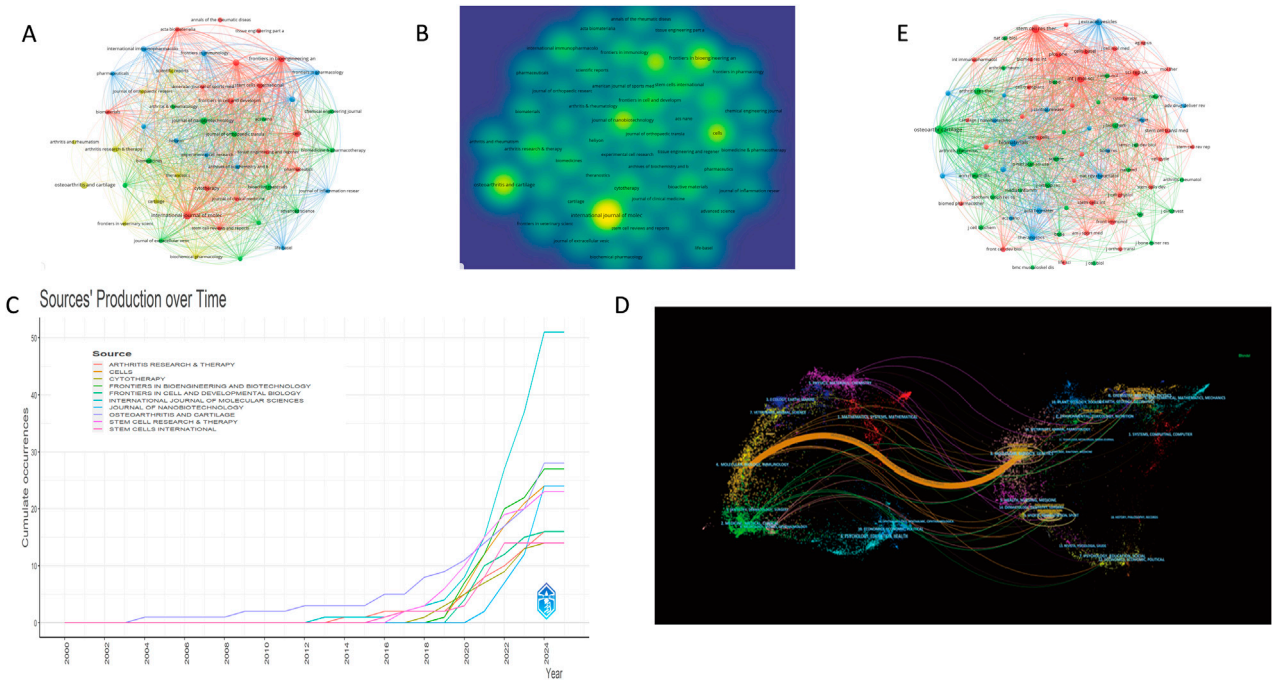

FIGURE 6
Journal collaboration analysis of extracellular vesicles and osteoarthritis. **(A)** Collaboration between journal based on VOSviewer. **(B)** Hot spot distribution map of journal issues; **(C)** Top 10 journals in terms of annual number of publications. **(D)** The dual-map overlay of journals contributed to publications. **(E)** Journal co-citation collaboration network mapping.

institutions. Figure 5A demonstrates distinct clustering patterns formed by authors from different research fields and institutions. These 76 institutions were organized into 5 clusters, with prominent representation from Chinese and American institutions in the larger clusters. Notably, institutions such as Zhejiang University, Sichuan University, Shanghai Jiao Tong University, and Shenzhen University demonstrated significant contributions (Figures 5A, B).

As shown in Table 4, Shanghai Jiao Tong University leads with 48 publications (5.08% of total publications), receiving 1,783 citations (37.15 citations per article). This is followed by Italy's Sichuan University with 27 publications (2.86% of total), receiving 574 citations (21.26 per article), and subsequently IRCCS Istituto Ortopedico with 26 publications (2.75% of total) and 582 citations (22.38 per article). Both Figure 5C and Table 4 reveal that Chinese institutions occupy 8 of the top 10 positions by publication volume. This highlights China's substantial engagement and contributions in this field, reflecting its growing recognition and institutional support within the research community.

TABLE 5 Top 10 Journal in terms of the number of published papers.

Rank	Journal	Country	Record	Citations	Average citations	H-index	Impact factor (2024)
1	International Journal of Molecular Sciences	Switzerland	51	757	14.84	11	3.7
2	Osteoarthritis and Cartilage	United Kingdom	28	742	26.50	14	5.1
3	Frontiers in Bioengineering and Biotechnology	Switzerland	27	680	25.19	11	4.5
4	Cells	Switzerland	24	412	17.17	16	5.3
5	Journal of Nanobiotechnology	United Kingdom	24	587	24.46	9	7.4
6	Stem Cell Research & Therapy	United Kingdom	23	2050	89.13	8	6.5
7	Arthritis Research & Therapy	United Kingdom	16	708	44.25	9	4.5
8	Frontiers in Cell and Developmental Biology	Switzerland	16	414	25.88	8	4.3
9	Cytotherapy	United Kingdom	14	93	6.64	9	4.4
10	Stem Cells International	United States of America	14	287	20.50	6	3.7

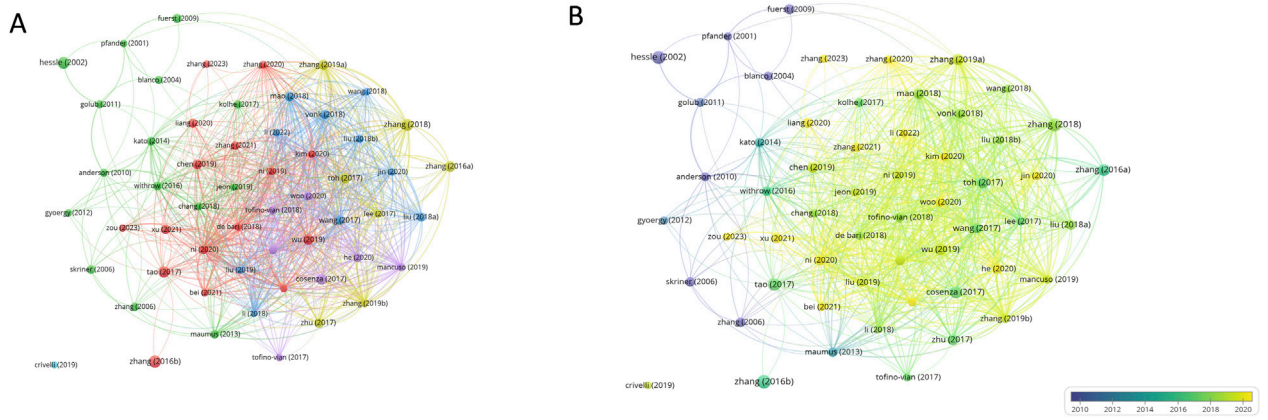

FIGURE 7
(A, B) Collaboration between publications based on VOSviewer.

3.5 Analysis of journals and research areas

A visual analysis of journals in this field from 2000 to 2024 was conducted using VOSviewer software. When the publication threshold was set to one, 315 journals were identified as contributing to this research area; when the threshold was increased to five, 49 journals met this criterion. Figures 6A, B reveal that *Frontiers in Bioengineering and Biotechnology*, *International Journal of Molecular Sciences*, *Cells*, and *Stem Cell Research & Therapy* form the largest clusters, indicating their prominent role and high activity in publishing articles within this field. As shown in Table 5, the *International Journal of Molecular Sciences* leads with 51 articles, accumulating 757 citations and an average of 14.84 citations per article, alongside a 2024 impact factor of 3.7. Notably, the *Stem Cell Research & Therapy* published 23 articles, which received 2,050 citations with an average of 89.13 citations per article, demonstrating the highest average citation rate in this research domain. Figure 6C illustrates that publication numbers were relatively low between 2000 and 2014, but a marked increase began in 2019 and continued to rise through 2024. Most top-ten journals reached their peak in 2022 followed by a slight decline, with 2020–2024 representing the most prolific period.

As shown in Figure 6D, the most frequently co-cited journals in bibliographic coupling analysis include *International Journal of Molecular Sciences*, *Stem Cell Research & Therapy*, *Biomaterials*, and *Osteoarthritis and Cartilage*. These journals have exerted significant influence on research and publications in this field, not only in terms of publication volume and co-citation frequency but also as critical channels for advancing scholarly discourse. Figure 6E presents a dual-map overlay of articles published between 2000 and 2024. Citation relationships are represented by colored lines on the right side (citing journals) and cited journals on the left. The analysis reveals a concentration of research in publications related to physics,

TABLE 6 Top 10 cited publications ranked in the field.

Rank	Author	years	Average citations	Total link strength	Journal	JCR (2022)	Title	Details
1	Zhang Y. et al. (2016)	2016	622	0	nature medicine	Q1	Implant-derived magnesium induces local neuronal production of CGRP to improve bone-fracture healing in rats	Magnesium transporter protein 1 (MAGT1)-dependent and transient receptor potential cation channels are induced by elevated magnesium, suggesting that magnesium plays a role in CGRP-mediated osteogenic differentiation
2	Zhang et al. (2018)	2018	568	175	Biomaterials	Q1	MSC exosomes mediate cartilage repair by enhancing proliferation, attenuating apoptosis and modulating immune reactivity	By activating the AKT and ERK signalling pathways, exosomal CD73 facilitates cell proliferation and infiltration in cartilage repair. In contrast, inhibiting these signalling pathways decreases cell proliferation and migration without impacting matrix production
3	Tao et al. (2017)	2017	475	212	Theranostics	Q1	Exosomes derived from miR-140-5p-overexpressing human synovial mesenchymal stem cells enhance cartilage tissue regeneration and prevent osteoarthritis of the knee in a rat model	While SMSC-140-Exos effectively prevented OA in a rat model *in vivo*, it improved the migration and proliferation of ACs *in vitro* without affecting ECM secretion
4	Zhang S. et al. (2016)	2016	454	156	osteoarthritis and cartilage	Q1	exosomes derived from human embryonic mesenchymal stem cells promote osteochondral regeneration	The first evidence of human embryonic MSC exosomes' efficacy in cartilage regeneration and their availability as a cell-free, off-the-shelf therapeutic alternative
5	Stefancin and Parker (2007)	2017	404	180	Scientific Reports	Q2	Mesenchymal stem cells derived exosomes and microparticles protect cartilage and bone from degradation in osteoarthritis	Exosomes and microvesicles/ microparticles both prevent mice from developing OA *in vivo* and exhibit comparable chondroprotective and anti-inflammatory properties *in vitro*
6	Toh et al. (2017)	2017	321	123	Seminars in Cell & Developmental Biology	Q1	MSC exosome as a cell-free MSC therapy for cartilage regeneration: Implications for osteoarthritis treatment	This study offers fresh insights into the development of off-the-shelf, cell-free MSC therapeutics. It addresses the potential mechanisms of action of MSC exosomes in cartilage regeneration within the framework of their immunomodulatory and regenerative potential
7	Zhang et al. (2019)	2019	318	127	Biomaterials	Q1	MSC exosomes alleviate temporomandibular joint osteoarthritis by attenuating inflammation and restoring matrix homeostasis	MSC exosomes reduce IL-1β-induced nitric oxide and MMP13 production and increase s-GAG synthesis that IL-1β blocks

(Continued on following page)

TABLE 6 (*Continued*) Top 10 cited publications ranked in the field.

Rank	Author	years	Average citations	Total link strength	Journal	JCR (2022)	Title	Details
8	Wu et al. (2019)	2019	318	157	Biomaterials	Q1	miR-100-5p-abundant exosomes derived from infrapatellar fat pad MSCs protect articular cartilage and ameliorate gait abnormalities *via* inhibition of mTOR in osteoarthritis	Exosomes derived from infrapatellar fat pad (IPFP) MSCs regulate the mTOR-autophagy pathway through miR100-5p, preserving cartilage homeostasis and shielding articular cartilage from harm
9	Mao et al. (2018)	2018	288	144	Stem Cell Research & Therapy	Q1	Exosomes derived from miR-92a-3p-overexpressing human mesenchymal stem cells enhance chondrogenesis and suppress cartilage degradation *via* targeting WNT5A	Exosomal miR-92a-3p targets WNT5A to regulate cartilage growth and homeostasis; exosomal miR-92a-3p may function as a Wnt inhibitor
10	Zhu et al. (2017)	2017	283	125	Stem Cell Research & Therapy	Q1	Comparison of exosomes secreted by induced pluripotent stem cell-derived mesenchymal stem cells and synovial membrane-derived mesenchymal stem cells for the treatment of osteoarthritis	In mice OA models, injections of both iMSC-Exos and SMMSC-Exos reduce OA; however, iMSC-Exos has more therapeutic efficacy than SMMSC-Exos

TABLE 7 Top 10 keywords in the list by frequency.

Rank	Keywords	Frequency	Centrality
1	extracellular vesicle	302	0.03
2	mesenchymal stem cell	253	0.02
3	osteoarthriti	179	0.04
4	exosm	165	0.03
5	expression	113	0.12
6	knee osteoarthriti	106	0.03
7	inflammation	104	0.04
8	knee	95	0.04
9	proliferation	86	0.03
10	cartilage	85	0.09

materials science, chemistry, immunology, molecular biology, medicine, and clinical studies. Most cited journals originate from disciplines such as sports science, rehabilitation, materials science, chemistry, genetics, molecular biology, and physics. The interdisciplinary networks and collaborations reflect current developments and emerging areas of interest across these domains.

3.6 Analysis of references

As shown in Figures 7A, B, the studies were collectively analyzed based on their citations. Using VOSviewer, publications with ≥100 citations were analyzed, revealing the top-cited works. The leading study, *"Implant-Derived Magnesium Induces Local Neuronal CGRP Production to Promote Fracture Healing in Rats"* (Zhang Y. et al., 2016). Published in *Nature Medicine*, has accumulated 622 citations (an average of 77.75 citations per year). This groundbreaking research demonstrates that magnesium ions enhance calcitonin gene-related peptide (CGRP)-mediated osteogenic differentiation by activating the MAGT1-dependent transient receptor potential cation channel, Table 6.

Ranking second is *"Mesenchymal Stem Cell-Derived Exosomes Mediate Cartilage Repair by Enhancing Proliferation, Inhibiting Apoptosis, and Modulating Immune Responses"* (Zhang et al., 2018), with 568 citations (an average of 94.67 citations per year). This study highlights the molecular mechanism by which exosomal CD73 promotes cell proliferation and infiltration during cartilage regeneration through the activation of the AKT and ERK signaling pathways. Notably, it was the first to reveal that inhibiting this pathway does not affect matrix synthesis but significantly reduces cell migration and proliferation. In third place is *"Exosomes Derived from miR-140-5p-Overexpressing Synovial Mesenchymal Stem Cells Enhance Cartilage Regeneration and Prevent Osteoarthritis in Rat Knees"* (Tao et al., 2017), published in *Theranostics*, with 475 citations (an average of 67.86 citations per year). This study systematically demonstrates that SMSC-140-Exos simultaneously promote the migration, proliferation, and extracellular matrix (ECM) secretion of articular chondrocytes (ACs) *in vitro*, while also validating their therapeutic potential in preventing osteoarthritis (OA) in a rat model. The academic influence of these highly cited studies underscores their significant value in advancing the field.

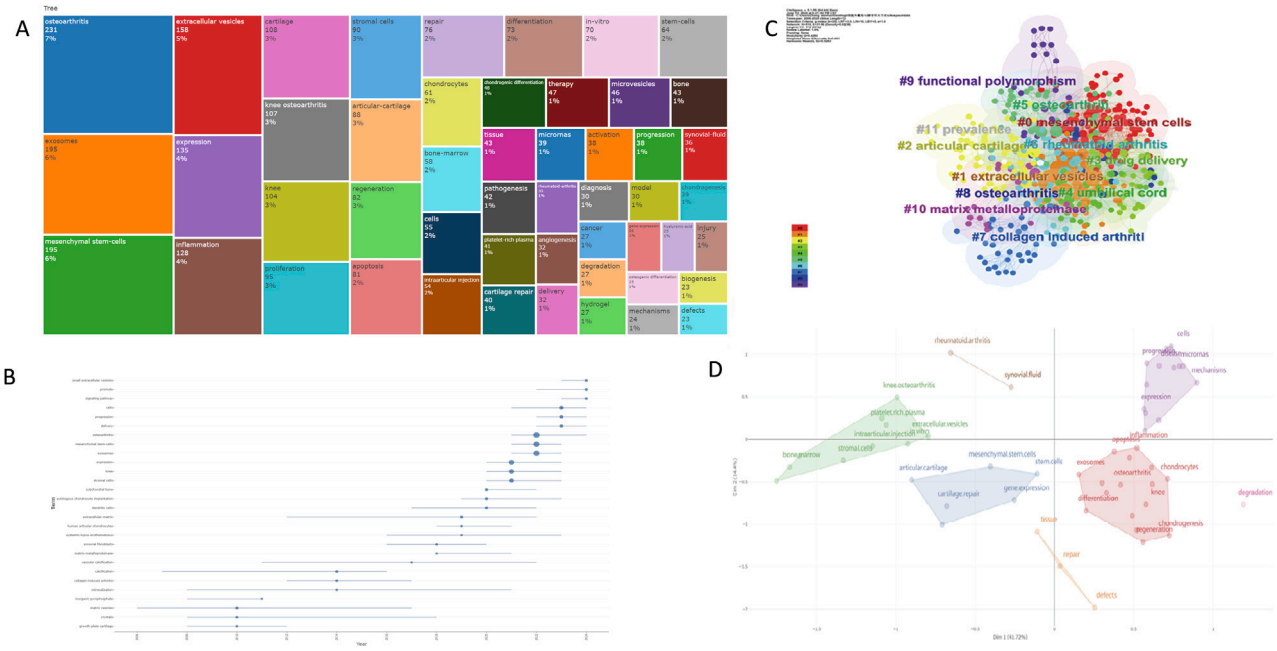

FIGURE 8
Keyword analysis of extracellular vesicles and osteoarthritis **(A)** Keyword Frequency Map **(B)** Keyword trend **(C)** and **(D)** Keywords clustering influencing factors analysis map and keyword clustering.

3.7 Analysis of Keywords

Keyword analysis is a critical tool for identifying the research focus of publications. Keywords appearing ≥100 times include *extracellular vesicle* (302 times), *mesenchymal stem cell* (253 times), *osteoarthritis* (179 times), *exosomes* (165 times), *expression* (113 times), *knee osteoarthritis* (106 times), and *inflammation* (104 times). Table 7 lists the top 20 keyword frequencies related to extracellular vesicles (EVs) in arthritis. In Figure 8A, larger squares represent higher keyword frequencies, while smaller squares indicate lower frequencies.

These keywords were organized into 10 clusters: #0 mesenchymal stem cells, #1 extracellular vesicles, #2 articular cartilage, #3 drug delivery, #4 umbilical cord, #5 osteoarthritis, #6 rheumatoid arthritis, #7 collagen-induced arthritis, #8 functional polymorphism, and #9 matrix metalloproteinase. These clusters encapsulate the research hotspots and focal areas of EVs in arthritis, as illustrated in Figures 8B–D. The thematic grouping of keywords further enhances the clarity and organization of research priorities in the study of EVs in osteoarthritis (OA).

4 Discussion

4.1 General information

From 2000 to 2024, the period from 2016 to 2024 marked a phase of rapid development in this field, with a significant increase in the number of publications. During this dynamic decade, researchers from China and the United States made substantial contributions to the field. China ranked first with 518 publications, 15,077 citations, an average of 29.11 citations per publication, and an H-index of 52. The United States ranked second with 124 publications, 5,838 citations, an average of 47.08 citations per publication, and an H-index of 30. Italy ranked third with 73 publications, an H-index of 23, and 1,741 citations (averaging 23.85 citations per publication). These countries demonstrated strong collaborative relationships and collectively advanced the development of this research field.

Professors De Girolamo, Laura and Ragni, Enrico each published 23 articles, ranking first with H-indices of 13 and average citation rates of 21.74 and 37.15 per article, respectively. Between 2020 and 2022, the top ten authors exhibited significant publication output, averaging at least three articles per year (Figure 4). In the institutional analysis, Shanghai Jiao Tong University led with 48 publications, an average of 37.5 citations per article, and a total link strength of 36. Sichuan University ranked second with 27 publications, an average of 21.26 citations per article, and a total link strength of 5. IRCCS Istituto Ortopedico Galeazzi ranked third, with 26 publications, an average of 22.38 citations per article, and a total link strength of 9.

These institutions, including Zhejiang University and Shenzhen University (SZU), exhibit close collaboration and have driven significant advancements in the field (Figure 5). In the journal analysis, *Frontiers in Bioengineering and Biotechnology*, *International Journal of Molecular Sciences*, *Cells*, and *Stem Cell Research & Therapy* rank as the top four journals, each publishing over 20 articles, reflecting their strong engagement and high publication frequency in this domain. A distinct clustering phenomenon is observed among these journals, with the largest cluster highlighted in red in the visualization.

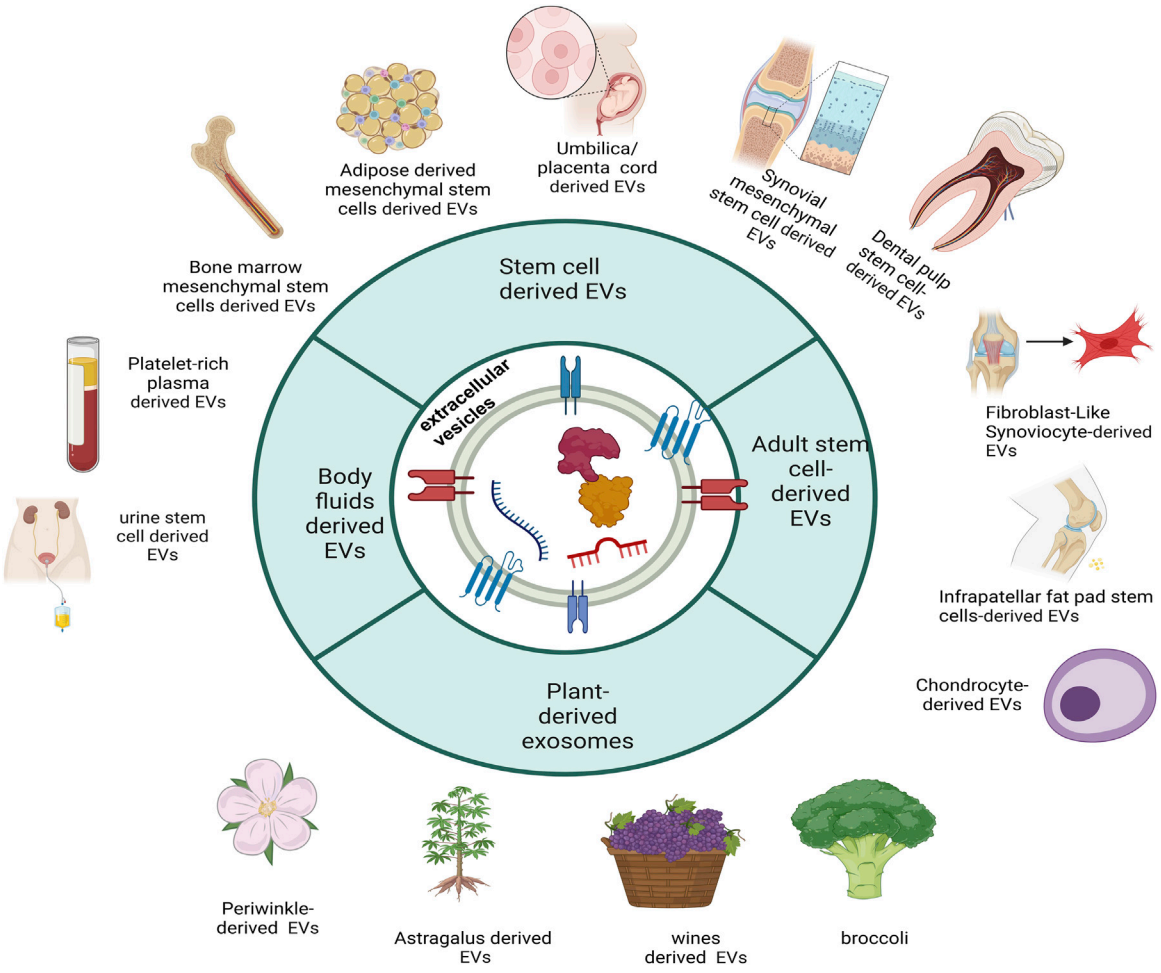

FIGURE 9
Evs from different sources play different roles in the treatment of OA (Chen et al., 2022; Yıldırım et al., 2024; Sarasati et al., 2023; Liu et al., 2024; Wang et al., 2021; Zhou et al., 2022; Sánchez et al., 2021; Meng et al., 2023; Kim et al., 2016; Gupta et al., 2021).

4.2 Hotspots and trends

Cluster analysis in keyword analysis effectively summarizes research hotspots and trends. Key terms such as #0 mesenchymal stem cells and #1 extracellular vesicles are pivotal in extracellular vesicle (EV) research. These EVs are categorized into non-plant-derived and plant-derived EVs based on their origins, reflecting the diversity and scope of research in this field (Lv et al., 2020; Qiu et al., 2023).

4.3 Relationship between non-plant-derived EVs and OA

Non-plant-derived EVs and plant-derived EVs, have garnered significant research interest for their therapeutic potential in OA. Bone marrow mesenchymal stem cell (BMSC)-derived EVs are among the earliest and most extensively studied strategies, demonstrating efficacy in chondrocyte proliferation, anabolism, and apoptosis inhibition, Figure 9 (Pittenger et al., 1999).

Exosomes from BMSCs treated with decellularized extracellular matrix (dECM-BMSC-Exos) enhance cartilage repair *via* miR-3473b-mediated PTEN/AKT pathway activation (Zhang B. et al., 2023). In monosodium iodoacetate (MIA)-induced OA models, BMSC-derived exosomes upregulate collagen II and MMP13 expression (He et al., 2020), while TUC339-enriched exosomes promote macrophage polarization to the anti-inflammatory M2 phenotype, mitigating joint injury (Shen et al., 2023). BMSCs further regulate immunomodulation through autotaxin-YAP pathway modulation (Wang et al., 2021). Dental pulp stem cells (DPSCs), sharing surface marker similarities with BMSCs but exhibiting superior proliferative capacity, enhance chondrocyte repair *via* intra-articular exosome delivery. These exosomes suppress TRPV4-mediated osteoclast activity, reducing subchondral bone remodeling and cartilage degradation in murine OA models (Fu et al., 2023). Adipose-derived stem cells (ADSCs), prized for their abundance and accessibility, secrete exosomes (ADSC-Exos) that promote cartilage regeneration and reduce inflammation. Elastogen (TE) pretreatment amplifies ADSC-Exo secretion and upregulates miR-451-5p, enhancing chondrocyte

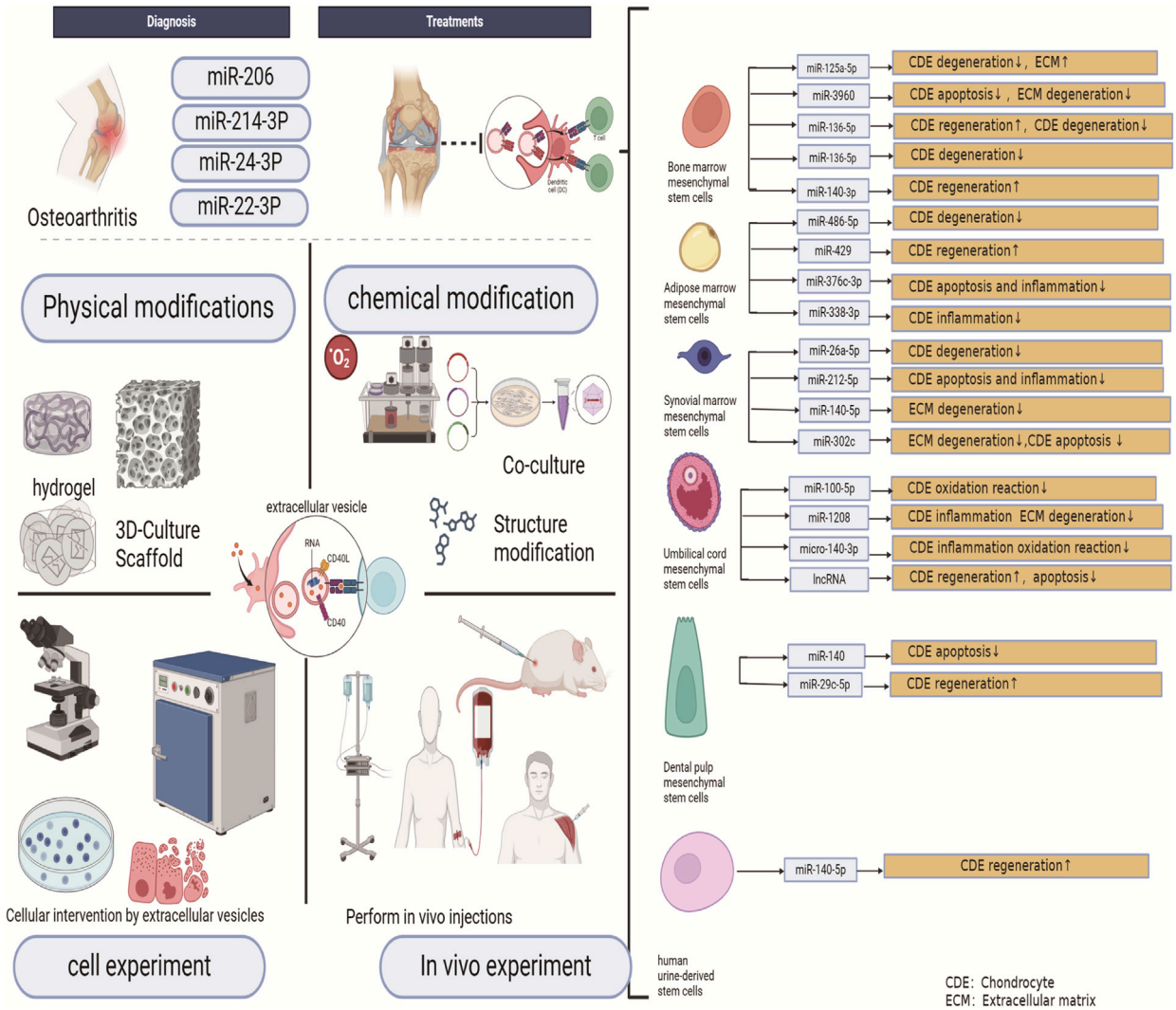

FIGURE 10
Role of different sources of evs and carrying miRNAs in diagnosis and treatment in OA (Gupta et al., 2021; Sánchez et al., 2021; Wan et al., 2023; Wang et al., 2021; Xu et al., 2023; Zhang et al., 2020; Zhou et al., 2022; Zhou et al., 2020; Zou et al., 2023).

matrix synthesis and repair in anterior cruciate ligament transection (ACLT) models (Meng et al., 2023).

Clinical translation efforts include chemically defined medium (CDM)-cultured small EVs (CDM4-sEVs), which exhibit high purity and stimulate chondrocyte proliferation, migration, and differentiation. CDM4-sEVs inhibit osteochondral degeneration *in vivo*, underscoring their therapeutic potential (Hanai et al., 2023). Synovial MSC-derived exosomes (SMSC-Exos) drive chondrocyte migration and collagen synthesis *via* Wnt5a/5b-YAP signaling, albeit at the expense of SOX9-dependent extracellular matrix production (Park et al., 2015; Liu and Lefebvre, 2015). SMSC-Exos also mitigate IL-1β-induced cartilage degradation through NRP1 targeting and miR-485-3p-mediated PI3K/Akt suppression (Qiu et al., 2024). Umbilical cord-derived MSC exosomes (hucMSC-EVs), aligned with keyword cluster #4 ("umbilical cord"), demonstrate chondroprotective effects by enhancing COL2A1 and aggrecan expression while suppressing ADAMTS5 and MMP13. METTL3-mediated NLRP3 m6A methylation reduction underlies their anti-inflammatory action (Zhou et al., 2022; Jin et al., 2021).

Exosomes that overexpress miR-92a-3p in MSCs promote matrix gene expression and cartilage growth. On the other hand, exosomes that block miR-92a-3p decrease chondrogenic differentiation and upregulate WNT5A expression, which reduces the formation of cartilage matrix. WNT5A is the direct target of miR-92a-3p, which inhibits its activity. Exosomes overexpressing miR-92a-3p could potentially serve as inhibitors of the Wnt signalling pathway and may be developed as therapeutic agents to modify the disease process in OA (Mao et al., 2018). However, more investigation is required to clarify the underlying mechanisms in more depth. Perinatal stem cells, including embryonic MSCs (EMSCs) and amniotic membrane MSCs (hAMSCs), balance extracellular matrix synthesis and degradation. EMSC-EVs preserve chondrocyte phenotype under inflammatory conditions (Wang et al., 2017), while

hAMSCs outperform ADSCs in modulating synovial macrophage polarization and glycosaminoglycan preservation (Topoluk et al., 2018).

Amniotic fluid stem cell exosomes (AFSC-Exos) deliver immunomodulatory factors (e.g., TGF, HGF) to attenuate inflammation and fibrosis (Beretti et al., 2018). hUSC-140-Exos further promote cartilage regeneration *via* VEGFA signaling (Liu et al., 2022). Collectively, these findings highlight MSC-EVs as versatile tools for OA intervention, though deeper mechanistic insights are needed to optimize clinical applications (Figures 9, 10) (Cheng et al., 2023; Yu et al., 2022; Kim et al., 2020; Wang S. et al., 2022).

4.4 Relationship between plant-derived EVs and OA

Plant extracellular vesicles (PELNs), secreted by most plant cells, share compositional similarities with animal-derived exosomes but exhibit distinct molecular profiles influenced by plant species, environmental factors, and isolation methods. These vesicles carry diverse bioactive molecules, including proteins, lipids, and nucleic acids, with demonstrated therapeutic potential in OA. Notably, Yıldırım et al. (Yıldırım et al., 2024) reported that tomato-derived EVs significantly upregulated chondrogenic markers—aggrecan, SRY-box transcription factor 9 (SOX9), and cartilage oligomeric matrix protein (COMP)—in human chondrocytes, thereby enhancing cartilage regeneration. Mechanistically, T-EVs facilitated growth factor delivery to chondrocytes, creating a pro-regenerative microenvironment that supports neo-cartilage formation and maturation.

Complementing these findings, Chen et al. (2022) engineered spinach-derived EVs functionalized with chondrocyte membrane fragments. Upon light exposure, these hybrid vesicles elevated intracellular adenosine triphosphate (ATP) and reduced nicotinamide adenine dinucleotide phosphate (NADPH) levels in degenerated chondrocytes. This metabolic reprogramming enhanced anabolic activity, restored cartilage homeostasis, and attenuated OA progression in a murine model. Together, these studies highlight the species-specific bioactivity of plant-derived EVs and their potential as tunable nanotherapeutics for OA intervention (Figure 9) (Chen et al., 2022; Yıldırım et al., 2024; Sarasati et al., 2023; Liu et al., 2024; Wang et al., 2021; Zhou et al., 2022; Sánchez et al., 2021; Meng et al., 2023; Kim et al., 2016; Gupta et al., 2021).

4.5 Relationship between EVs of body fluid origin and OA

Exosomes generated by somatic sources, like platelet-rich plasma-derived exosomes (PRP-Exos) (Zhang et al., 2022), are also very important. PRP-Exos decreases apoptosis, encourages chondrocyte migration and proliferation, and blocks the release of the inflammatory cytokine TNF-α. They mitigate the advancement of OA by reversing the effects of IL-1β on essential protein expression in the Wnt/β-catenin signalling pathway (Liu et al., 2019). It found that SDF-1 in PRP-Exo mediates the migration of bone marrow mesenchymal stem cells (mBMSCs) to the injury site *via* the CXCR4 receptor. Concurrently, TGF-β1 activates the Smad2/3 pathway, promoting their differentiation into chondrocytes by inducing Smad2/3 phosphorylation, upregulating the expression of SOX9 and COL II, and driving chondrogenic differentiation of mBMSCs. PRP-Exo inhibits IL-1β-induced phosphorylation of p65 (a subunit of NF-κB) and STAT3, thereby reducing the expression of MMP13 and COL X, which suppresses cartilage matrix degradation and chondrocyte hypertrophy. Additionally, PDGF-BB and TGF-β1 block the pro-inflammatory cytokine cascade by inhibiting IKKα and STAT signaling pathways (Figures 9, 10) (Zhang et al., 2022).

4.6 Relationship with OA after chemical modification of EVs

Another approach to enhance the functionality of non-plant-derived EVs involves modifying donor cells to improve their biochemical properties, thereby increasing their clinical applicability. One method includes genetic modification, where stem cells or EVs are engineered to overexpress specific miRNAs, circRNAs, or lncRNAs to achieve targeted effects (Huang et al., 2022; Wang et al., 2023). Likewise, lncRNA MEG-3-modified BMSCs-EVs slow down the advancement of OA by reducing IL-1β-induced chondrocyte senescence and apoptosis (Jin et al., 2021). Furthermore, it was discovered that TNF-α-induced exosomes improved HUVEC cell motility, invasion, and angiogenesis *via* the miR-200a-3p/KLF6/VEGFA axis (Zhang et al., 2023c). Another method to modify donor cells involves cell co-culture. Curcumin, the primary biological component of turmeric, has been utilized to treat MSCs, resulting in exosomes that reduce DNA methylation in the promoter regions of miR-143 and miR-124, thereby increasing their expression. Additionally, binding sites for miR-143 and miR-124 are found in the 3′untranslated region (3′UTR) of NF-kB and ROCK1, respectively, indicating that these miRNAs can directly target NF-kB and ROCK1. As a result, exosomal therapy considerably slows the advancement of OA 70 by restoring normal NF-kB and ROCK1 expression (Qiu et al., 2020). Controlling the concentration of oxygen is another strategy. It has been demonstrated that hypoxia preserves the characteristics of stem cell development, impacting their phenotypic and function and boosting the therapeutic potential of stem cells and the EVs they produce. EVs produced from umbilical cord stem cells (USC-EVs) under hypoxic settings were found to be far more effective in promoting chondrocyte migration and proliferation than EVs produced under normoxic conditions. The enhancement was made possible by using USC-EVs to transfer miR-26a-5p to chondrocytes (Wan et al., 2022), Figure 10 (Gupta et al., 2021; Sánchez et al., 2021; Wan et al., 2023; Wang et al., 2021; Xu et al., 2023; Zhang et al., 2020; Zhou et al., 2022; Zhou et al., 2020; Zou et al., 2023).

4.7 Relationship with OA after physical modification of EVs

Physical interventions to engineer EVs offer innovative strategies for OA treatment, encompassing 3D culture systems,

biomaterial encapsulation, and targeted drug delivery. Compared to conventional 2D methods, 3D culture techniques—such as spinner flasks, hanging droplets, and pellet systems—significantly enhance MSC exocytosis efficiency, amplifying paracrine therapeutic effects (Lee and Lee, 2022). Chen et al. (2019) developed a 3D-printed scaffold integrating cartilage extracellular matrix (ECM), gelatin methacrylate (GelMA), and exosomes, which facilitated cartilage regeneration by promoting chondrocyte migration and polarizing synovial macrophages toward the anti-inflammatory M2 phenotype.

Hydrogel-based EV delivery outperforms other biomaterials, enhancing bone marrow MSC (BMSC) migration, proliferation, and differentiation to accelerate cartilage repair and ECM remodeling. MSC-derived nano-vacuoles (MSC-NVs) encapsulated in hydrogels exhibit superior mechanical stability and biocompatibility. In murine OA models, hydrogel-loaded MSC-NVs improved matrix synthesis, reduced catabolic factor secretion, and attenuated disease severity, while GelMA-NVs suppressed inflammation *via* M2 macrophage polarization (Zhang et al., 2021; Pang et al., 2023). Wan et al. (2023) advanced this approach with a photocrosslinkable spherical GelMA hydrogel encapsulating cartilage-targeting exosomes (W-Exo@GelMA), which enhanced joint retention and chondrocyte specificity, effectively delaying OA progression through dual anabolic promotion and catabolic inhibition.

Integrating hydrogels with 3D-printed scaffolds provides tailored mechanical support and joint-mimetic microenvironments, optimizing EV release kinetics and joint homeostasis (Vijayavenkataraman et al., 2018; Sun et al., 2023). Li et al. (2023) engineered a biomimetic double-network hydrogel scaffold incorporating adipose MSC-derived exosomes and decellularized ECM, which enhanced BMSC adhesion, differentiation, and osteochondral regeneration in rat OA models. Rat BMSCs displayed improved adhesion, spreading, migration, proliferation, and chondrogenic and osteogenic differentiation *in vitro* with the help of this scaffold. It successfully promoted cartilage and subchondral bone tissue regeneration in a rat model of OA. EVs serve as versatile carriers for diverse therapeutics, including antisense oligonucleotides (Yang et al., 2021), mRNA (Bu et al., 2021), siRNA (Huang et al., 2021), protein/peptide drugs (Yang et al., 2018; Wu et al., 2023), and curcumin (Sun et al., 2010). For instance, Xu et al. (2021) engineered exosomes to deliver kartogenin (KGN), boosting intracellular concentrations and chondrogenesis in synovial fluid MSCs, demonstrating efficacy *in vitro* and *in vivo*. These advancements underscore the potential of physically engineered EVs to revolutionize OA therapy through precision targeting, controlled release, and enhanced regenerative outcomes.

4.8 Relationship with arthritis after physical modification of EVs

EVs, particularly exosomes, have emerged as pivotal players in the pathophysiology, diagnosis, and treatment of rheumatoid arthritis (RA) and OA. Both conditions share common features, including cartilage degeneration, synovial inflammation, structural bone alterations, pain, and functional impairment. EVs, with their stability in circulation and minimally invasive sampling, offer a promising avenue for early disease detection and intervention, potentially improving patient outcomes (Liu et al., 2023).

In OA, reduced expression of miR-193b-3p in plasma exosomes correlates with inflammatory activity and joint degradation, positioning it as a potential biomarker for early disease detection and monitoring (Meng et al., 2018; Wang et al., 2012). Exosomal miRNAs, such as miR-let-7b, modulate inflammatory responses by targeting Toll-like receptors (TLRs) and promoting M1 macrophage polarization, leading to the secretion of pro-inflammatory cytokines like IL-1, IL-6, and TNF (Kim et al., 2016).

Conversely, MSC-derived EVs exhibit immunomodulatory effects, suppressing T cell proliferation, enhancing regulatory T cells (Tregs), and ameliorating inflammation in arthritic models (Cosenza et al., 2018). Despite their therapeutic potential, the precise mechanisms by which EVs influence OA progression—through inflammatory modulation, cellular senescence, and metabolic regulation—remain incompletely understood. The complexity of OA pathogenesis necessitates a multifaceted diagnostic and therapeutic approach, as reliance on single biomarkers is insufficient for comprehensive disease management. EVs represent a promising cell-free therapeutic platform, with significant potential for drug delivery and targeted therapy. However, critical questions regarding exosome sourcing, quality, dosage, and functional mechanisms require further exploration. Future research should focus on optimizing EV-based strategies to fully harness their diagnostic and therapeutic potential, ultimately advancing the management of RA and OA.

4.9 Advantages and limitations of research

In contrast to traditional literature reviews, bibliometric visualisation and analysis using software such as CiteSpace, VOSviewer, and the R package bibliometrics can effectively demonstrate the research hotspots and critical areas in the field, giving scholars valuable references and guiding future research directions more comprehensively.

However, this study has several limitations that should be acknowledged. Firstly, it relies solely on the Web of Science (WOS) core database, which may introduce biases and errors in understanding the overall trends and scope of publications. Secondly, due to the multidisciplinary nature of the field involving various research aspects, some publications related to EVs in the diagnosis and treatment of OA may not be fully captured, potentially limiting the scope of this study.

Furthermore, the study did not provide a complete assessment of the research focus and quality of each retrieved article. However, it provides novel possibilities for this field's future study directions. It is advised that various databases should be integrated to progress in the future, and different analysis techniques should be used to investigate more extensive and in-depth study avenues. This approach could enhance our understanding of EVs' role in OA diagnosis and treatment and contribute to the progression of research in this critical area.

5 Conclusion

This comprehensive bibliometric analysis evaluated global research trends on EVs in OA from 2000 onward, revealing

sustained growth in annual publication rates. China emerged as the leading contributor, followed by the United States. Prof. Laura Girolamo ranked as the most prolific and cited author. The study systematically investigated EVs' dual role in OA pathogenesis and therapy. Mechanistic insights highlighted their potential as early diagnostic biomarkers *via* high-expression factors and as pathogenic drivers *versus* regenerative agents influencing chondrocyte integrity. Furthermore, EVs demonstrated therapeutic modulation through cargo delivery and synergistic integration with biomaterials or genetic engineering, offering avenues to attenuate OA progression. This synthesis underscores EVs' multifaceted impact on OA diagnostics and targeted intervention strategies.

Author contributions

WZ: Conceptualization, Data curation, Formal Analysis, Writing–original draft, Funding acquisition, Investigation, Methodology, Project administration, Resources, Software, Supervision, Validation, Visualization, Writing–review and editing. WX: Data curation, Formal Analysis, Validation, Visualization, Writing–original draft, Writing–review and editing. LY: Data curation, Methodology, Supervision, Writing–original draft, Writing–review and editing. RF: Conceptualization, Data curation, Formal Analysis, Writing–original draft.

Funding

The author(s) declare that financial support was received for the research and/or publication of this article. Funding was provided by the National Natural Science Foundation of China (number: 82360934;82405423) and; Natural Science Foundation of Xinjiang Uygur Autonomous Region (2022D01C170, 2022D01C171, 2023D01C145); Xinjiang Uygur Autonomous Region Science and Technology Innovation Leading Talent Programme (2022TSYCLJ0007, 2023TSYCQNTJ0050); Xinjiang Uygur Autonomous Region Key research and development task special projects (2021B03006).

Conflict of interest

The authors declare that the research was conducted in the absence of any commercial or financial relationships that could be construed as a potential conflict of interest.

Publisher's note

References

Ali, A., Rosenberger, L., Weiss, T. R., Milak, C., and Perlman, A. I. (2017). Massage therapy and quality of life in osteoarthritis of the knee: a qualitative study. *Pain Med.* 18, 1168–1175. doi:10.1093/pm/pnw217

Andaloussi, S. E. L., Mäger, I., Breakefield, X. O., and Wood, M. J. (2013). Extracellular vesicles: biology and emerging therapeutic opportunities. *Nat. Rev. Drug Discov.* 12, 347–357. doi:10.1038/nrd3978

Beretti, F., Zavatti, M., Casciaro, F., Comitini, G., Franchi, F., Barbieri, V., et al. (2018). Amniotic fluid stem cell exosomes: therapeutic perspective. *Biofactors* 44, 158–167. doi:10.1002/biof.1407

Bheri, S., Hoffman, J. R., Park, H. J., and Davis, M. E. (2020). Biomimetic nanovesicle design for cardiac tissue repair. *Nanomedicine (Lond).* 15, 1873–1896. doi:10.2217/nnm-2020-0097

Bu, T., Li, Z., Hou, Y., Sun, W., Zhang, R., Zhao, L., et al. (2021). Exosome-mediated delivery of inflammation-responsive Il-10 mRNA for controlled atherosclerosis treatment. *Theranostics* 11, 9988–10000. doi:10.7150/thno.64229

Chen, P., Liu, X., Gu, C., Zhong, P., Song, N., Li, M., et al. (2022). A plant-derived natural photosynthetic system for improving cell anabolism. *Nature* 612, 546–554. doi:10.1038/s41586-022-05499-y

Chen, P., Zheng, L., Wang, Y., Tao, M., Xie, Z., Xia, C., et al. (2019). Desktop-stereolithography 3D printing of a radially oriented extracellular matrix/mesenchymal stem cell exosome bioink for osteochondral defect regeneration. *Theranostics* 9, 2439–2459. doi:10.7150/thno.31017

Cheng, C., Wu, Y., Huang, Y., Xue, Q., Wang, Y., Liao, F., et al. (2023). Epigenetic modification and exosome effects on autophagy in osteoarthritis. *Biochem. Pharmacol.* 218, 115930. doi:10.1016/j.bcp.2023.115930

Cosenza, S., Ruiz, M., Maumus, M., Jorgensen, C., and Noël, D. (2017). Pathogenic or therapeutic extracellular vesicles in rheumatic diseases: role of mesenchymal stem cell-derived vesicles. *Int. J. Mol. Sci.* 18, 889. doi:10.3390/ijms18040889

Cosenza, S., Toupet, K., Maumus, M., Luz-Crawford, P., Blanc-Brude, O., Jorgensen, C., et al. (2018). Mesenchymal stem cells-derived exosomes are more immunosuppressive than microparticles in inflammatory arthritis. *Theranostics* 8, 1399–1410. doi:10.7150/thno.21072

Cui, A., Li, H., Wang, D., Zhong, J., Chen, Y., and Lu, H. (2020). Global, regional prevalence, incidence and risk factors of knee osteoarthritis in population-based studies. *EClinicalMedicine* 29-30, 100587. doi:10.1016/j.eclinm.2020.100587

Damjanov, I., and Andrews, P. W. (2016). Teratomas produced from human pluripotent stem cells xenografted into immunodeficient mice - a histopathology atlas. *Int. J. Dev. Biol.* 60, 337–419. doi:10.1387/ijdb.160274id

Di, J., Bai, J., Zhang, J., Chen, J., Hao, Y., Bai, J., et al. (2024). Regional disparities, age-related changes and sex-related differences in knee osteoarthritis. *BMC Musculoskelet. Disord.* 25, 66. doi:10.1186/s12891-024-07191-w

Fan, L., Liu, C., Chen, X., Zheng, L., Zou, Y., Wen, H., et al. (2022). Exosomes-loaded electroconductive hydrogel synergistically promotes tissue repair after spinal cord injury via immunoregulation and enhancement of myelinated axon growth. *Adv. Sci. (Weinh)* 9, e2105586. doi:10.1002/advs.202105586

Feng, T., Wang, X., Jin, Z., Qin, X., Sun, C., Qi, B., et al. (2023). Effectiveness and safety of manual therapy for knee osteoarthritis: an overview of systematic reviews and meta-analyses. *Front. Public Health* 11, 1081238. doi:10.3389/fpubh.2023.1081238

Fu, Y., Cui, S., Zhou, Y., and Qiu, L. (2023). Dental pulp stem cell-derived exosomes alleviate mice knee osteoarthritis by inhibiting TRPV4-mediated osteoclast activation. *Int. J. Mol. Sci.* 24, 4926. doi:10.3390/ijms24054926

Georgiev, T., and Angelov, A. K. (2019). Modifiable risk factors in knee osteoarthritis: treatment implications. *Rheumatol. Int.* 39, 1145–1157. doi:10.1007/s00296-019-04290-z

Gililland, J. M., Anderson, L. A., Sun, G., Erickson, J. A., and Peters, C. L. (2012). Perioperative closure-related complication rates and cost analysis of barbed suture for closure in TKA. *Clin. Orthop. Relat. Res.* 470, 125–129. doi:10.1007/s11999-011-2104-7

Gupta, A., Maffulli, N., Rodriguez, H. C., Mistovich, R. J., Delfino, K., Cady, C., et al. (2021). Cell-free stem cell-derived extract formulation for treatment of knee osteoarthritis: study protocol for a preliminary non-randomized, open-label, multi-center feasibility and safety study. *J. Orthop. Surg. Res.* 16, 514. doi:10.1186/s13018-021-02672-3

Hanai, H., Hart, D. A., Jacob, G., Shimomura, K., Ando, W., Yoshioka, Y., et al. (2023). Small extracellular vesicles derived from human adipose-derived mesenchymal stromal cells cultured in a new chemically-defined contaminate-free media exhibit enhanced

biological and therapeutic effects on human chondrocytes *in vitro* and in a mouse osteoarthritis model. *J. Extracell. Vesicles* 12, e12337. doi:10.1002/jev2.12337

He, L., He, T., Xing, J., Zhou, Q., Fan, L., Liu, C., et al. (2020). Bone marrow mesenchymal stem cell-derived exosomes protect cartilage damage and relieve knee osteoarthritis pain in a rat model of osteoarthritis. *Stem Cell Res. Ther.* 11, 276. doi:10.1186/s13287-020-01781-w

Hu, X., Wang, B., Hu, L., Han, D., and Wu, J. (2023). Bibliometric analysis of global trends in remimazolam-related research over the past 15 Years: compared with propofol. *Drug Des. Devel Ther.* 17, 2119–2135. doi:10.2147/dddt.S411829

Huang, W., Qu, M., Li, L., Liu, T., Lin, M., and Yu, X. (2021). SiRNA in MSC-derived exosomes silences CTGF gene for locomotor recovery in spinal cord injury rats. *Stem Cell Res. Ther.* 12, 334. doi:10.1186/s13287-021-02401-x

Huang, Y., Liu, Y., Huang, Q., Sun, S., Ji, Z., Huang, L., et al. (2022). TMT-based quantitative proteomics analysis of synovial fluid-derived exosomes in inflammatory arthritis. *Front. Immunol.* 13, 800902. doi:10.3389/fimmu.2022.800902

Hunter, D. J. (2015). Viscosupplementation for osteoarthritis of the knee. *N. Engl. J. Med.* 372, 1040–1047. doi:10.1056/NEJMct1215534

Jin, Y., Xu, M., Zhu, H., Dong, C., Ji, J., Liu, Y., et al. (2021). Therapeutic effects of bone marrow mesenchymal stem cells-derived exosomes on osteoarthritis. *J. Cell Mol. Med.* 25, 9281–9294. doi:10.1111/jcmm.16860

Kim, S. J., Chen, Z., Essani, A. B., Elshabrawy, H. A., Volin, M. V., Volkov, S., et al. (2016). Identification of a novel toll-like receptor 7 endogenous ligand in rheumatoid arthritis synovial fluid that can provoke arthritic joint inflammation. *Arthritis Rheumatol.* 68, 1099–1110. doi:10.1002/art.39544

Kim, Y. G., Choi, J., and Kim, K. (2020). Mesenchymal stem cell-derived exosomes for effective cartilage tissue repair and treatment of osteoarthritis. *Biotechnol. J.* 15, e2000082. doi:10.1002/biot.202000082

Lee, S. Y., and Lee, J. W. (2022). 3D spheroid cultures of stem cells and exosome applications for cartilage repair. *Life (Basel)* 12, 939. doi:10.3390/life12070939

Li, Q., Yu, H., Zhao, F., Cao, C., Wu, T., Fan, Y., et al. (2023). 3D printing of microenvironment-specific bioinspired and exosome-reinforced hydrogel scaffolds for efficient cartilage and subchondral bone regeneration. *Adv. Sci. (Weinh)* 10, e2303650. doi:10.1002/advs.202303650

Liu, B., Xian, Y., Chen, X., Shi, Y., Dong, J., Yang, L., et al. (2024). Inflammatory fibroblast-like synoviocyte-derived exosomes aggravate osteoarthritis via enhancing macrophage glycolysis. *Adv. Sci. (Weinh)* 11, e2307338. doi:10.1002/advs.202307338

Liu, C. F., and Lefebvre, V. (2015). The transcription factors SOX9 and SOX5/SOX6 cooperate genome-wide through super-enhancers to drive chondrogenesis. *Nucleic Acids Res.* 43, 8183–8203. doi:10.1093/nar/gkv688

Liu, X., Wang, L., Ma, C., Wang, G., Zhang, Y., and Sun, S. (2019). Exosomes derived from platelet-rich plasma present a novel potential in alleviating knee osteoarthritis by promoting proliferation and inhibiting apoptosis of chondrocyte via Wnt/β-catenin signaling pathway. *J. Orthop. Surg. Res.* 14, 470. doi:10.1186/s13018-019-1529-7

Liu, Y., Zeng, Y., Si, H. B., Tang, L., Xie, H. Q., and Shen, B. (2022). Exosomes derived from human urine-derived stem cells overexpressing miR-140-5p alleviate knee osteoarthritis through downregulation of VEGFA in a rat model. *Am. J. Sports Med.* 50, 1088–1105. doi:10.1177/03635465221073991

Liu, Z., Zhuang, Y., Fang, L., Yuan, C., Wang, X., and Lin, K. (2023). Breakthrough of extracellular vesicles in pathogenesis, diagnosis and treatment of osteoarthritis. *Bioact. Mater* 22, 423–452. doi:10.1016/j.bioactmat.2022.10.012

Lv, L., Sheng, C., and Zhou, Y. (2020). Extracellular vesicles as a novel therapeutic tool for cell-free regenerative medicine in oral rehabilitation. *J. Oral Rehabil.* 47 (Suppl. 1), 29–54. doi:10.1111/joor.12885

Mancuso, F., Hamilton, T. W., Kumar, V., Murray, D. W., and Pandit, H. (2016). Clinical outcome after UKA and HTO in ACL deficiency: a systematic review. *Knee Surg. Sports Traumatol. Arthrosc.* 24, 112–122. doi:10.1007/s00167-014-3346-1

Mao, G., Zhang, Z., Hu, S., Zhang, Z., Chang, Z., Huang, Z., et al. (2018). Exosomes derived from miR-92a-3p-overexpressing human mesenchymal stem cells enhance chondrogenesis and suppress cartilage degradation via targeting WNT5A. *Stem Cell Res. Ther.* 9, 247. doi:10.1186/s13287-018-1004-0

Meng, F., Li, Z., Zhang, Z., Yang, Z., Kang, Y., Zhao, X., et al. (2018). MicroRNA-193b-3p regulates chondrogenesis and chondrocyte metabolism by targeting HDAC3. *Theranostics* 8, 2862–2883. doi:10.7150/thno.23547

Meng, S., Tang, C., Deng, M., Yuan, J., Fan, Y., Gao, S., et al. (2023). Tropoelastin-Pretreated exosomes from adipose-derived stem cells improve the synthesis of cartilage matrix and alleviate osteoarthritis. *J. Funct. Biomater.* 14, 203. doi:10.3390/jfb14040203

Nian, W., and Fu, C. (2023). Exosomes in myocardial infarction: therapeutic potential and clinical application. *J. Cardiovasc Transl. Res.* 16, 87–96. doi:10.1007/s12265-022-10284-3

Pang, L., Jin, H., Lu, Z., Xie, F., Shen, H., Li, X., et al. (2023). Treatment with mesenchymal stem cell-derived nanovesicle-containing gelatin methacryloyl hydrogels alleviates osteoarthritis by modulating chondrogenesis and macrophage polarization. *Adv. Healthc. Mater* 12, e2300315. doi:10.1002/adhm.202300315

Park, H. W., Kim, Y. C., Yu, B., Moroishi, T., Mo, J. S., Plouffe, S. W., et al. (2015). Alternative Wnt signaling activates YAP/TAZ. *Cell* 162, 780–794. doi:10.1016/j.cell.2015.07.013

Pittenger, M. F., Mackay, A. M., Beck, S. C., Jaiswal, R. K., Douglas, R., Mosca, J. D., et al. (1999). Multilineage potential of adult human mesenchymal stem cells. *Science* 284, 143–147. doi:10.1126/science.284.5411.143

Qiu, B., Xu, X., Yi, P., and Hao, Y. (2020). Curcumin reinforces MSC-derived exosomes in attenuating osteoarthritis via modulating the miR-124/NF-kB and miR-143/ROCK1/TLR9 signalling pathways. *J. Cell Mol. Med.* 24, 10855–10865. doi:10.1111/jcmm.15714

Qiu, F. S., Wang, J. F., Guo, M. Y., Li, X. J., Shi, C. Y., Wu, F., et al. (2023). Rgl-exomiR-7972, a novel plant exosomal microRNA derived from fresh Rehmanniae Radix, ameliorated lipopolysaccharide-induced acute lung injury and gut dysbiosis. *Biomed. Pharmacother.* 165, 115007. doi:10.1016/j.biopha.2023.115007

Qiu, M., Xie, Y., Tan, G., Wang, X., Huang, P., and Hong, L. (2024). Synovial mesenchymal stem cell-derived exosomal miR-485-3p relieves cartilage damage in osteoarthritis by targeting the NRP1-mediated PI3K/Akt pathway: exosomal miR-485-3p relieves cartilage damage. *Heliyon* 10, e24042. doi:10.1016/j.heliyon.2024.e24042

Sánchez, M., Jorquera, C., Sánchez, P., Beitia, M., García-Cano, B., Guadilla, J., et al. (2021). Platelet-rich plasma injections delay the need for knee arthroplasty: a retrospective study and survival analysis. *Int. Orthop.* 45, 401–410. doi:10.1007/s00264-020-04669-9

Sarasati, A., Syahruddin, M. H., Nuryanti, A., Ana, I. D., Barlian, A., Wijaya, C. H., et al. (2023). Plant-derived exosome-like nanoparticles for biomedical applications and regenerative therapy. *Biomedicines* 11, 1053. doi:10.3390/biomedicines11041053

Shao, X., Hua, S., Feng, T., Ocansey, D. K. W., and Yin, L. (2022). Hypoxia-regulated tumor-derived exosomes and tumor progression: a focus on immune evasion. *Int. J. Mol. Sci.* 23, 11789. doi:10.3390/ijms231911789

Sharma, L. (2021). Osteoarthritis of the knee. *N. Engl. J. Med.* 384, 51–59. doi:10.1056/NEJMcp1903768

Shen, X., Qin, J., Wei, Z., and Liu, F. (2023). Bone marrow mesenchymal stem cell exosome-derived lncRNA TUC339 influences the progression of osteoarthritis by regulating synovial macrophage polarization and chondrocyte apoptosis. *Biomed. Pharmacother.* 167, 115488. doi:10.1016/j.biopha.2023.115488

Simão, A. P., Mendonça, V. A., Avelar, N. C. P., da Fonseca, S. F., Santos, J. M., de Oliveira, A. C. C., et al. (2019). Whole body vibration training on muscle strength and brain-derived neurotrophic factor levels in elderly woman with knee osteoarthritis: a randomized clinical trial study. *Front. Physiol.* 10, 756. doi:10.3389/fphys.2019.00756

Sloan, M., and Lee, G. C. (2021). Is conversion TKA a primary or revision? Clinical course and complication risks approximating revision TKA rather than primary TKA. *J. Arthroplasty* 36, 2685–2690.e1. doi:10.1016/j.arth.2021.03.034

Stefancin, J. J., and Parker, R. D. (2007). First-time traumatic patellar dislocation: a systematic review. *Clin. Orthop. Relat. Res.* 455, 93–101. doi:10.1097/BLO.0b013e31802eb40a

Su, X., Li, C., Liao, W., Liu, J., Zhang, H., Li, J., et al. (2018). Comparison of arthroscopic and conservative treatments for knee osteoarthritis: a 5-year retrospective comparative study. *Arthroscopy* 34, 652–659. doi:10.1016/j.arthro.2017.09.023

Sun, D., Zhuang, X., Xiang, X., Liu, Y., Zhang, S., Liu, C., et al. (2010). A novel nanoparticle drug delivery system: the anti-inflammatory activity of curcumin is enhanced when encapsulated in exosomes. *Mol. Ther.* 18, 1606–1614. doi:10.1038/mt.2010.105

Sun, T., Feng, Z., He, W., Li, C., Han, S., Li, Z., et al. (2023). Novel 3D-printing bilayer GelMA-based hydrogel containing BP,β-TCP and exosomes for cartilage-bone integrated repair. *Biofabrication* 16, 015008. doi:10.1088/1758-5090/ad04fe

Sun, Y., Tao, Q., Wu, X., Zhang, L., Liu, Q., and Wang, L. (2021). The utility of exosomes in diagnosis and therapy of diabetes mellitus and associated complications. *Front. Endocrinol. (Lausanne)* 12, 756581. doi:10.3389/fendo.2021.756581

Tang, X., Wang, S., Zhan, S., Niu, J., Tao, K., Zhang, Y., et al. (2016). The prevalence of symptomatic knee osteoarthritis in China: results from the China health and retirement longitudinal study. *Arthritis Rheumatol.* 68, 648–653. doi:10.1002/art.39465

Tao, S. C., Yuan, T., Zhang, Y. L., Yin, W. J., Guo, S. C., and Zhang, C. Q. (2017). Exosomes derived from miR-140-5p-overexpressing human synovial mesenchymal stem cells enhance cartilage tissue regeneration and prevent osteoarthritis of the knee in a rat model. *Theranostics* 7, 180–195. doi:10.7150/thno.17133

Toh, W. S., Lai, R. C., Hui, J. H. P., and Lim, S. K. (2017). MSC exosome as a cell-free MSC therapy for cartilage regeneration: implications for osteoarthritis treatment. *Semin. Cell Dev. Biol.* 67, 56–64. doi:10.1016/j.semcdb.2016.11.008

Topoluk, N., Steckbeck, K., Siatkowski, S., Burnikel, B., Tokish, J., and Mercuri, J. (2018). Amniotic mesenchymal stem cells mitigate osteoarthritis progression in a synovial macrophage-mediated *in vitro* explant coculture model. *J. Tissue Eng. Regen. Med.* 12, 1097–1110. doi:10.1002/term.2610

Vandergriff, A., Huang, K., Shen, D., Hu, S., Hensley, M. T., Caranasos, T. G., et al. (2018). Targeting regenerative exosomes to myocardial infarction using cardiac homing peptide. *Theranostics* 8, 1869–1878. doi:10.7150/thno.20524

Vijayavenkataraman, S., Yan, W. C., Lu, W. F., Wang, C. H., and Fuh, J. Y. H. (2018). 3D bioprinting of tissues and organs for regenerative medicine. *Adv. Drug Deliv. Rev.* 132, 296–332. doi:10.1016/j.addr.2018.07.004

Wan, J., He, Z., Peng, R., Wu, X., Zhu, Z., Cui, J., et al. (2023). Injectable photocrosslinking spherical hydrogel-encapsulated targeting peptide-modified engineered exosomes for osteoarthritis therapy. *J. Nanobiotechnology* 21, 284. doi:10.1186/s12951-023-02050-7

Wan, S., Bao, D., Li, J., Lin, K., Huang, Q., Li, Q., et al. (2022). Extracellular vesicles from hypoxic pretreated urine-derived stem cells enhance the proliferation and migration of chondrocytes by delivering miR-26a-5p. *Cartilage* 13, 19476035221077401. doi:10.1177/19476035221077401

Wang, C., He, Y., Zheng, J., Wang, X., and Chen, S. (2023). Dissecting order amidst chaos of programmed cell deaths: construction of a diagnostic model for KIRC using transcriptomic information in blood-derived exosomes and single-cell multi-omics data in tumor microenvironment. *Front. Immunol.* 14, 1130513. doi:10.3389/fimmu.2023.1130513

Wang, H. J., Zhang, P. J., Chen, W. J., Feng, D., Jia, Y. H., and Xie, L. X. (2012). Four serum microRNAs identified as diagnostic biomarkers of sepsis. *J. Trauma Acute Care Surg.* 73, 850–854. doi:10.1097/TA.0b013e31825a7560

Wang, S., Lei, B., Zhang, E., Gong, P., Gu, J., He, L., et al. (2022). Targeted therapy for inflammatory diseases with mesenchymal stem cells and their derived exosomes: from basic to clinics. *Int. J. Nanomedicine* 17, 1757–1781. doi:10.2147/ijn.S355366

Wang, Y., Yu, D., Liu, Z., Zhou, F., Dai, J., Wu, B., et al. (2017). Exosomes from embryonic mesenchymal stem cells alleviate osteoarthritis through balancing synthesis and degradation of cartilage extracellular matrix. *Stem Cell Res. Ther.* 8, 189. doi:10.1186/s13287-017-0632-0

Wang, Y., Zhao, M., Li, W., Yang, Y., Zhang, Z., Ma, R., et al. (2021). BMSC-derived small extracellular vesicles induce cartilage reconstruction of temporomandibular joint osteoarthritis via autotaxin-YAP signaling Axis. *Front. Cell Dev. Biol.* 9, 656153. doi:10.3389/fcell.2021.656153

Wang X., X., Xu, X., Zhang, Y., An, X., Zhang, X., Chen, G., et al. (2022). Duo cadherin-functionalized microparticles synergistically induce chondrogenesis and cartilage repair of stem cell aggregates. *Adv. Healthc. Mater* 11, e2200246. doi:10.1002/adhm.202200246

Wu, J., Kuang, L., Chen, C., Yang, J., Zeng, W. N., Li, T., et al. (2019). miR-100-5p-abundant exosomes derived from infrapatellar fat pad MSCs protect articular cartilage and ameliorate gait abnormalities via inhibition of mTOR in osteoarthritis. *Biomaterials* 206, 87–100. doi:10.1016/j.biomaterials.2019.03.022

Wu, Q., Fu, X., Li, X., Li, J., Han, W., and Wang, Y. (2023). Modification of adipose mesenchymal stem cells-derived small extracellular vesicles with fibrin-targeting peptide CREKA for enhanced bone repair. *Bioact. Mater* 20, 208–220. doi:10.1016/j.bioactmat.2022.05.031

Xie, L., Mao, M., Zhou, L., and Jiang, B. (2016). Spheroid mesenchymal stem cells and mesenchymal stem cell-derived microvesicles: two potential therapeutic strategies. *Stem Cells Dev.* 25, 203–213. doi:10.1089/scd.2015.0278

Xu, C., Mi, Z., Dong, Z., Chen, X., Ji, G., Kang, H., et al. (2023). Platelet-derived exosomes alleviate knee osteoarthritis by attenuating cartilage degeneration and subchondral bone loss. *Am. J. Sports Med.* 51, 2975–2985. doi:10.1177/03635465231188122

Xu, X., Lai, Y., and Hua, Z. C. (2019). Apoptosis and apoptotic body: disease message and therapeutic target potentials. *Biosci. Rep.* 39. doi:10.1042/bsr20180992

Xu, X., Liang, Y., Li, X., Ouyang, K., Wang, M., Cao, T., et al. (2021). Exosome-mediated delivery of kartogenin for chondrogenesis of synovial fluid-derived mesenchymal stem cells and cartilage regeneration. *Biomaterials* 269, 120539. doi:10.1016/j.biomaterials.2020.120539

Yang, J., Luo, S., Zhang, J., Yu, T., Fu, Z., Zheng, Y., et al. (2021). Exosome-mediated delivery of antisense oligonucleotides targeting α-synuclein ameliorates the pathology in a mouse model of Parkinson's disease. *Neurobiol. Dis.* 148, 105218. doi:10.1016/j.nbd.2020.105218

Yang, Y., Hong, Y., Cho, E., Kim, G. B., and Kim, I. S. (2018). Extracellular vesicles as a platform for membrane-associated therapeutic protein delivery. *J. Extracell. Vesicles* 7, 1440131. doi:10.1080/20013078.2018.1440131

Yao, L., Jia, Q., Wu, J., Chai, Y., Gao, C., Wang, Y., et al. (2023). Assessing perceived participation among older adults total hip arthroplasty and total knee arthroplasty patients six months post-surgery: a cross-sectional study. *Front. Public Health* 11, 1282461. doi:10.3389/fpubh.2023.1282461

Yıldırım, M., Ünsal, N., Kabataş, B., Eren, O., and Şahin, F. (2024). Effect of Solanum lycopersicum and citrus limon-derived exosome-like vesicles on chondrogenic differentiation of adipose-derived stem cells. *Appl. Biochem. Biotechnol.* 196, 203–219. doi:10.1007/s12010-023-04491-0

Yu, H., Huang, Y., and Yang, L. (2022). Research progress in the use of mesenchymal stem cells and their derived exosomes in the treatment of osteoarthritis. *Ageing Res. Rev.* 80, 101684. doi:10.1016/j.arr.2022.101684

Zhang, B., Gu, J., Wang, Y., Guo, L., Xie, J., and Yang, M. (2023d). TNF-α stimulated exosome derived from fibroblast-like synoviocytes isolated from rheumatoid arthritis patients promotes HUVEC migration, invasion and angiogenesis by targeting the miR-200a-3p/KLF6/VEGFA axis. *Autoimmunity* 56, 2282939. doi:10.1080/08916934.2023.2282939

Zhang, F. X., Liu, P., Ding, W., Meng, Q. B., Su, D. H., Zhang, Q. C., et al. (2021). Injectable Mussel-Inspired highly adhesive hydrogel with exosomes for endogenous cell recruitment and cartilage defect regeneration. *Biomaterials* 278, 121169. doi:10.1016/j.biomaterials.2021.121169

Zhang, J., Rong, Y., Luo, C., and Cui, W. (2020). Bone marrow mesenchymal stem cell-derived exosomes prevent osteoarthritis by regulating synovial macrophage polarization. *Aging (Albany NY).* 12, 25138–25152. doi:10.18632/aging.104110

Zhang, S., Chu, W. C., Lai, R. C., Lim, S. K., Hui, J. H., and Toh, W. S. (2016). Exosomes derived from human embryonic mesenchymal stem cells promote osteochondral regeneration. *Osteoarthr. Cartil.* 24, 2135–2140. doi:10.1016/j.joca.2016.06.022

Zhang, S., Chuah, S. J., Lai, R. C., Hui, J. H. P., Lim, S. K., and Toh, W. S. (2018). MSC exosomes mediate cartilage repair by enhancing proliferation, attenuating apoptosis and modulating immune reactivity. *Biomaterials* 156, 16–27. doi:10.1016/j.biomaterials.2017.11.028

Zhang, S., Teo, K. Y. W., Chuah, S. J., Lai, R. C., Lim, S. K., and Toh, W. S. (2019). MSC exosomes alleviate temporomandibular joint osteoarthritis by attenuating inflammation and restoring matrix homeostasis. *Biomaterials* 200, 35–47. doi:10.1016/j.biomaterials.2019.02.006

Zhang, Y., Jia, Z., Xia, X., and Wang, J. (2023a). Knowledge mapping of COVID-19 and autoimmune diseases: a visual and bibliometric analysis. *Clin. Exp. Med.* 23, 3549–3564. doi:10.1007/s10238-023-01089-y

Zhang, Y., Peng, Y., and Xia, X. (2023b). Autoimmune diseases and gut microbiota: a bibliometric and visual analysis from 2004 to 2022. *Clin. Exp. Med.* 23, 2813–2827. doi:10.1007/s10238-023-01028-x

Zhang, Y., Qi, G., Yan, Y., Wang, C., Wang, Z., Jiang, C., et al. (2023c). Exosomes derived from bone marrow mesenchymal stem cells pretreated with decellularized extracellular matrix enhance the alleviation of osteoarthritis through miR-3473b/phosphatase and tensin homolog axis. *J. Gene Med.* 25, e3510. doi:10.1002/jgm.3510

Zhang, Y., Wang, X., Chen, J., Qian, D., Gao, P., Qin, T., et al. (2022). Exosomes derived from platelet-rich plasma administration in site mediate cartilage protection in subtalar osteoarthritis. *J. Nanobiotechnology* 20, 56. doi:10.1186/s12951-022-01245-8

Zhang, Y., Xu, J., Ruan, Y. C., Yu, M. K., O'Laughlin, M., Wise, H., et al. (2016). Implant-derived magnesium induces local neuronal production of CGRP to improve bone-fracture healing in rats. *Nat. Med.* 22, 1160–1169. doi:10.1038/nm.4162

Zhao, J., Dong, X., Zhang, Z., Gao, Q., Zhang, Y., Song, J., et al. (2022). Association of use of tourniquets during total knee arthroplasty in the elderly patients with post-operative pain and return to function. *Front. Public Health* 10, 825408. doi:10.3389/fpubh.2022.825408

Zhou, H., Shen, X., Yan, C., Xiong, W., Ma, Z., Tan, Z., et al. (2022). Extracellular vesicles derived from human umbilical cord mesenchymal stem cells alleviate osteoarthritis of the knee in mice model by interacting with METTL3 to reduce m6A of NLRP3 in macrophage. *Stem Cell Res. Ther.* 13, 322. doi:10.1186/s13287-022-03005-9

Zhou, Q., Cai, Y., Jiang, Y., and Lin, X. (2020). Exosomes in osteoarthritis and cartilage injury: advanced development and potential therapeutic strategies. *Int. J. Biol. Sci.* 16, 1811–1820. doi:10.7150/ijbs.41637

Zhou, W., Hu, S., Wu, Y., Xu, H., Zhu, L., Deng, H., et al. (2023). A bibliometric analysis of mesenchymal stem cell-derived exosomes in acute lung injury/acute respiratory distress syndrome from 2013 to 2022. *Drug Des. Devel Ther.* 17, 2165–2181. doi:10.2147/dddt.S415659

Zhu, Y., Wang, Y., Zhao, B., Niu, X., Hu, B., Li, Q., et al. (2017). Comparison of exosomes secreted by induced pluripotent stem cell-derived mesenchymal stem cells and synovial membrane-derived mesenchymal stem cells for the treatment of osteoarthritis. *Stem Cell Res. Ther.* 8, 64. doi:10.1186/s13287-017-0510-9

Zou, J., Yang, W., Cui, W., Li, C., Ma, C., Ji, X., et al. (2023). Therapeutic potential and mechanisms of mesenchymal stem cell-derived exosomes as bioactive materials in tendon-bone healing. *J. Nanobiotechnology* 21, 14. doi:10.1186/s12951-023-01778-6

Frontiers in Pharmacology

Explores the interactions between chemicals and living beings

The most cited journal in its field, which advances access to pharmacological discoveries to prevent and treat human disease.

Discover the latest Research Topics

See more →

Frontiers

Avenue du Tribunal-Fédéral 34
1005 Lausanne, Switzerland
frontiersin.org

Contact us

+41 (0)21 510 17 00
frontiersin.org/about/contact